Targeting Immune Checkpoints in Breast Cancer

Nicola Gaynor B.Sc.

Thesis submitted for the award of Ph.D.

National Institute for Cellular Biotechnology
School of Biotechnology
Dublin City University

Supervised by: Dr. Denis Collins

Co. Supervisor: Professor John Crown
St. Vincent's University Hospital

March 2019

I hereby certify that this material, which I now submit for assessment on the programme of study leading to the award of Ph.D. degree is entirely my own work, that I have exercised reasonable care to ensure that the work is original, and does not to the best of my knowledge breach any law of copyright, and has not been taken from the work of others save and to the extent that such work has been cited and acknowledged within the text of my work.

Signed: _____ (Candidate) ID No.: _____ Date: _____

Acknowledgements

I wish to thank my supervisor Dr. Denis Collins for his unfailing support over the course of my project. Thanks for being there for any help, advice or mockery that was needed, it was great to have you in my corner. Thank you to my co-supervisor Prof. John Crown whose continued support and guidance is immensely important in translating our research into a clinical benefit.

A huge thanks to Cancer Clinical Research Trust (CCRT) who generously funded my Ph.D. project and continue to do outstanding work for cancer research. I would also like to thank all of the patients and healthy volunteers who donated samples for my project, without whom the work would not have been possible.

Thanks to everybody in the NICB who create such a friendly environment to work in, particularly all of the past and present members of the Targeted Therapies group Norma, Alex, Naomi, Neil, Shannon, Sean, Alacoque, Deirdre, Fred, Alanna, Nupur, Alexandra, Laura, Trish, Karen and Thamir. Another thank you goes to all of the collaborators who helped during my Ph.D.; Stephen, Bruce, Sinead, John, Enda, Javier, Rob and Keith.

I would also like to thank everyone in the open office for all the chats, rants, rambling stories, games nights, food and Harry Potter appreciation we have shared over the last few years. Someday we will complete the movie marathon, and hopefully restart them all over again.

Thanks to my family and friends for all of their support throughout my Ph.D., questions of when I will be finished can now be satisfactorily answered. Finally thanks to Kevin for listening to my whinging and doing the washing up with minimal complaint, I couldn't have done it without your help.

Table of Contents

Abbreviations

7AAD	7-aminoactinomycin-D
ABCB1	ATP binding cassette subfamily B member 1
aCGH	Array comparative genomic hybridisation
ADCC	Antibody dependent cell-mediated cytotoxicity
AMP/DEL	Amplification/Deletion
APC	Antigen presenting cell
BCA	Bicinchoninic acid
BSA	Bovine serum albumin
cAMP	Cyclic adenosine mono-phosphate
CFSE	Carboxyfluorescein succinimidyl ester
cHL	Classical Hodgkin's lymphoma
CIT	Current immune targets
CLL	Chronic lymphocytic leukemia
CMV	Cytomeglovirus
CNV	Copy number variation
CR	Complete responder
CTLA4	Cytotoxic T-lymphocyte antigen 4
DAMPs	Damage associated molecular patterns
DMEM	Dulbecco's modified eagle medium
dMMR	Mismatch repair deficient
DMSO	Dimethyl sulfoxide
DNTP	Deoxyribonucleotide triphosphate
EBV	Epstein-Barr virus
EC	Effector cell
EDTA	Ethylenediaminetetraacetic acid
EGF	Epidermal growth factor
EMT	Epithelial to mesenchymal transition
ER	Estrogen receptor
FBS	Foetal bovine serum
FCG2A	Fc fragment of IgG receptor IIa
FCG2B	Fc fragment of IgG receptor IIb
FCG3A	Fc fragment of IgG receptor IIIa
HBSS	Hank's balanced salt solution
HBV	Hepatitis B virus
HCV	Hepatitis C virus
HER2	Human epidermal growth factor 2
HGNC	Hugo Gene Nomenclature Committee
HI FBS	Heat inactivated foetal bovine serum
HPV	Human papillomavirus
ICI	Immune checkpoint inhibitor
IL-2	Interleukin-2
Ig	Immunoglobulin
irAE	Immune-related adverse effect
IRIS	Immune response *in silico*

ITAMs	immune receptor tyrosine-based activation motifs
Kb	Kilobase
KLRK1	Killer cell lectin like receptor K1
LAG3	lymphocyte activation gene-3
LDH	Lactate dehydrogenase
MAF	Mutation annotation format
MALDI-TOF	matrix-assisted laser desorption ionization time-of-flight
MEM	Eagle's minimum essential medium
MMTV	Mouse mammary tumour virus
MSI-H	Microsatellite instablity-high
NEAA	Non-essential amino acids
NK cell	Natural killer cell
NR	Non-responder
NSCLC	Non-small cell lung cancer
ORR	Objective response rate
OS	Overall survival
PAMPs	Pathogen associated molecular patterns
PBMC	Peripheral blood mononuclear cell
PBS	Phosphate buffer saline
PCR	Polymerase chain reaction
PD-1	Programmed death-1
PD-L1	Programmed death-ligand 1
PD-L2	Programmed death-ligand 2
PFS	Progression free survival
PMSF	Phenylmethylsulfonyl fluoride
PR	Partial responder
RBC	Red blood cell
RCC	Renal cell carcinoma
RFS	Relapse free survival
RIPA	Radioimmunoprecipitation assay
RPM	Revolutions per minute
RPMI-1640	Roswell park memorial institute-1640
siRNA	Short interfering RNA
SNP	Single nucleotide polymorphism
SOC	Standard of care
SOP	Standard operating procedure
T-ADCC	Trastuzumab-mediated ADCC
TC	Target cell
TCDCC	Target cell dead cell control
TCR	T cell receptor
TIGIT	T cell immunoglobulin and ITIM domain
TIL	Tumour infiltrating lymphocyte
TIM3	T cell immunoglobulin-3
TKI	Tyrosine kinase inhibitor
TNBC	Triple negative breast cancer
TNF	Tumour necrosis factor
UC	Urothelial carcinoma
UNK	Unknown responder
VISTA	V-domain Ig suppressor of T cell activation
VCF	Variant call format

Targeting Immune Checkpoints in Breast Cancer **Nicola Gaynor**

Abstract

Immune checkpoints are regulators of immune activation that can be triggered to suppress the immune response against tumours. Immune checkpoint inhibitors (ICIs) have shown efficacy in a variety of cancer types, but in the majority of cancer types only a minority of patients respond. The aim of this Ph.D. was to examine mechanisms of immune response against breast cancer cells by examining immune relevant treatments.

The monoclonal antibody trastuzumab is approved to treat HER2+ breast cancer. Trastuzumab can engage certain cells of the immune system to kill cancer cells through antibody-dependent cell-mediated cytotoxicity (ADCC). The ability of cancer patients' immune cells to engage in trastuzumab-mediated ADCC was determined *in vitro* using peripheral blood mononuclear cell (PBMC) samples from the ICORG 10-05 clinical trial.

The PD-1 receptor and its cognate ligand PD-L1 are an immune checkpoint axis that is currently under investigation in the clinic. Protocols to examine the impact of ICIs *in vitro* are limited. An assay was developed using immune cell populations isolated from healthy volunteers that this sample cohort could be utilised for this purpose.

A link between EGFR and PD-L1 expression was discovered in a panel of HER2-targeted therapy resistant breast cancer cell lines. The molecular mechanisms underlying this link suggest that there is value in the rational combinations of EGFR/HER2 inhibitors and ICIs.

Adenosine is a metabolic checkpoint in the tumour microenvironment. Modulation of adenosine receptor 2A (A2AR) resulted in altered trastuzumab-mediated ADCC in treatment-naïve HER2+ breast cancer *in vitro*, suggesting a potential therapeutic role for A2AR modulation in breast cancer.

A hypothesis to explain the efficacy of ICIs in heavily pre-treated cancer patients was explored. The study suggests that immune-related gene sets have significantly lower rates of amplification and deletion and recurrent point mutation *versus* commonly targeted cancer-related genes. This suggests the targets of ICIs are more genetically stable than commonly targeted cancer-related pathways.

1. Introduction

1.1 Introduction

The immune surveillance hypothesis was developed more than 100 years ago and it states the incidence of cancer would be higher if not for the ability of the immune system to eliminate cancer cells before they form a tumour [1]. This hypothesis centres on the ability of the immune system to consistently recognise and destroy cells that have the potential to cause cancer. It also leads to the conclusion that any tumour that has developed has somehow managed to evade immune detection and/or destruction. The immune surveillance hypothesis naturally feeds into the concept of immunoediting as a means of cancer cell-mediated immune escape [2,3]. Immunoediting is the process of alteration of tumour immunogenicity patterns due to the pressure of the immune response against the tumour. There are three stages to immunoediting- elimination, equilibrium and escape. In the elimination stage, a competent immune system monitors and destroys any potentially cancerous cells [2,3]. In the equilibrium stage, cancer cells that have evaded destruction and have a non-immunogenic phenotype are selected for proliferation [2,3]. In the escape phase, the immune system is unable to suppress the growth of cancer cells and a tumour forms. There are a number of mechanisms the cancer cell can employ to circumvent the immune system, such as evasion of immune cell detection, increased resistance to cell death pathways, or by creating an immunosuppressive environment [2]. The ability of cancer cells to avoid immune-mediated destruction is now considered one of the hallmarks of cancer [4].

Numerous studies have provided evidence to support the theory of immune surveillance. One such study demonstrated a 3-fold increase in cancer risk for patients after organ transplant due to immunosuppression used to prevent organ rejection [5]. This led to malignancies being the main cause of death following a successfully grafted organ transplant [5]. Pre-clinical *in vivo* studies have shown an increase in cancer formation in immune-deficient mice, further supporting the immune surveillance hypothesis [6–10]. The tumours that developed in these immune-deficient mice were more immunogenic than the carcinogen-induced tumours developed in immune-competent mice as they were not under pressure to avoid immune-mediated destruction [6]. Within the immune equilibrium stage there is evidence of cytotoxic immune cells (natural killer cells (NK cells), CD8+ T cells and γδ T cells) being present in the microenvironment of dormant cancer cells with the balance of active cytotoxic immune cell populations switching to an immunosuppressive phenotype to allow for escape [11]. The immunosuppressive phenotype relies on loss of immunogenicity or an immunosuppressive microenvironment [12]. Loss of immunogenicity can occur by a decrease in specific antigen expression, down-regulation of MHC-class I or co-stimulatory molecules or by the expression of inhibitory receptors such as immune checkpoints [13]. The creation of an immunosuppressive microenvironment can occur through the release of cytokines such as IL-10 and TGF-β and the recruitment of immunosuppressive immune cells such as regulatory T cells (Tregs) [14–16]. Through these mechanisms, and many others, the cancer cell is now less immunogenic and can enter the immune escape phase

where tumour cells continue to proliferate without triggering an immune response or by having sufficiently dampened the immune system so there will be no effective immune response [12].

Targeting immunosuppression is now an established clinical strategy. Due to the heterogeneity of immune escape mechanisms there are now a range of immunotherapy strategies aimed at restoring the immune response. One class of immunotherapies are cancer vaccines, which aim to increase the antigen recognition of the immune system. Another is adoptive cell therapy, which replenishes cytotoxic immune cells to boost the anti-tumour immune response. This thesis focuses on immune checkpoint inhibitors (ICIs), immunomodulatory agents that aim to relieve tumour-mediated immune cell suppression [14].

1.2 Mechanisms of immune cell-mediated cytotoxicity

There are many mechanisms of immune cell-mediated cytotoxicity against cancer cells such as direct cell killing by cytotoxic cells, (e.g. CD8+ T cells and NK cells), phagocytosis mediated by macrophages or antibody dependent-cell mediated cytotoxicity (ADCC) effected by a range of immune cells, primarily NK cells.

1.2.1 Direct cytotoxicity- T cells

Naïve T cells are produced in the thymus. Dendritic cells, acting as antigen presenting cells (APCs), present non-self antigens to naïve T cells. The T cell then differentiates into an effector cell [17]. There are two main types of effector T cells; helper T cells (CD4+ T cells) and cytotoxic T cells (CD8+ T cells) [17]. The activity of the T cell is determined by the balance of co-stimulatory and co-inhibitory receptors on APCs (**Section 1.3**). Once sufficiently stimulated, helper CD4+ T cells modulate the behaviour and activity of other immune cell populations, such as B cells and monocytes [18]. CD4+ T cells also produce factors, such as IL-2 and CD40-L, which allow for activation and proliferation of CD8+ T cells [19]. Once activated, cytotoxic CD8+ T cells elicit antigen specific cytotoxic responses by binding to MHC class-I, which is stabilised by CD8, on infected or transformed cells [19]. There are three major mechanisms by which CD8+ T cells mediate cytotoxicity; i) by the interaction of Fas and Fas-L which leads to caspase activation and apoptosis within the tumour cell [20], ii) by the release of perforin and granzyme into the lytic synapse, where perforin forms lytic pores in the cell membrane which allows entry of granzyme into the cancer cell causing apoptosis [20,21] and iii) by cytokine release, such as TNF and IFN-γ, which can be mediated by CD4+ and CD8+ T cells and have direct anti-tumour effects [20] (**Figure 1.1**).

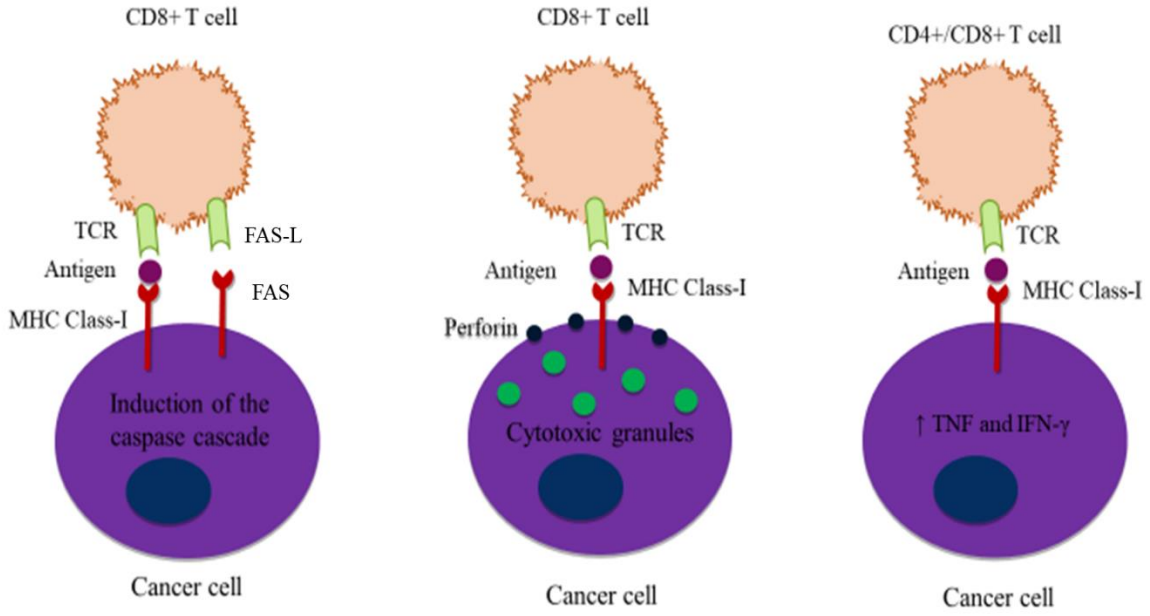

Figure 1.1: Mechanisms of T cell-mediated cytotoxicity by Fas-Fas-L interaction, perforin and granzyme release and by the release of anti-tumour cytokines.

1.2.2 Direct cytotoxicity- NK cells

NK cells form in the bone marrow and contain cytotoxic granules. NK cells can be activated by the presence of certain cytokines such as IL-2, IL-12, IL-15, IL-21, IFN-α and IFN-β [22]. NK cells recognise altered non-self- and stress-related proteins in infected or transformed cells but do not require antigen specific recognition to elicit cytotoxicity [22].

In normal cells, MHC class-I is recognised by inhibitory receptors, such as killer cell immunoglobulin-like receptors (KLRK), which balance activating (cytotoxic) signals [23],[22]. In transformed cells, MHC class-I is more likely to be absent and does not provide a signal for NK cell inhibition. In this case the NK cell is triggered by activating receptors, such as c-lectin family members like NKG2D. Stress-related proteins MICA and MICB are ligands for NKG2D which lead to NK cell activation [22,23] (**Figure 1.2**).

Once the NK cell has recognised a transformed or infected cell, they elicit cytotoxicity primarily by the perforin/granzyme system [21,22] (**Figure 1.2**). NK cells can also mediate cytotoxicity through Fas-L and other tumour necrosis family (TNF) signalling networks, such as TRAIL [22,24].

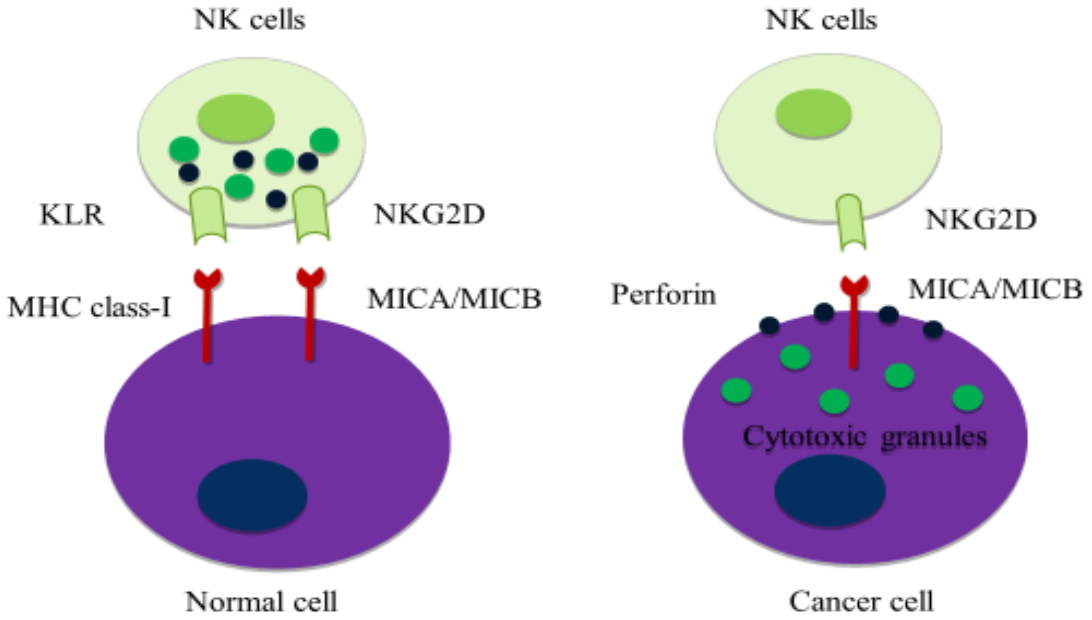

Figure 1.2: Inhibition of NK cell cytotoxicity against a normal cell by MHC class-I recognition by KLR receptors. Cytotoxicity elicited against a tumour cell by the recognition of MICA and MICB by NKG2D, in the absence of MHC class-I expression, causing the release of perforin and granzyme which trigger apoptosis in the cell.

1.2.3 Antibody dependent cell-mediated cytotoxicity

Fc receptors are antibody receptors involved in antigen recognition. ADCC is the process where Fc receptor bearing effector cells can recognise and kill an antibody-bound target cell. CD16 (FcγRIII, FCG3), CD32 (FcγRII, FCG2) or CD64 (FcγRI, FCG1) expressed on the immune cell can recognise and bind to the Fc portion of an immunoglobulin (Ig) and initiate ADCC, this primarily occurs through CD16 [25,26]. CD56+/CD16+ NK cells, CD16/CD32/CD64+ monocytes (e.g. CD14+ CD16+ monocytes [27]), specific CD16+ T cell subpopulations (e.g. γδ T cells [28]) and B cells are capable of eliciting ADCC [29–31]. To elicit ADCC, the antibody that has been produced by helper T cell-activated B cells (which become antibody-producing plasma cells) as part of the humoral immune response binds to the antigen [31]. ADCC-capable immune cells can trigger apoptosis in a target cell by interactions with the TNF family, such as Fas, and TRAIL, and by the perforin/granzyme system [32,33]. The perforin/granzyme system is the predominant mechanism employed in ADCC. Once the Fc receptor is bound to the antibody this triggers the phosphorylation of immune receptor tyrosine-based activation motifs (ITAMs) within the effector cell [32]. This triggers the exocytosis of cytotoxic granules, perforin and granzymes, into the lytic synapse, which as previously described, induces apoptosis (**Figure 1.3**) [34,35].

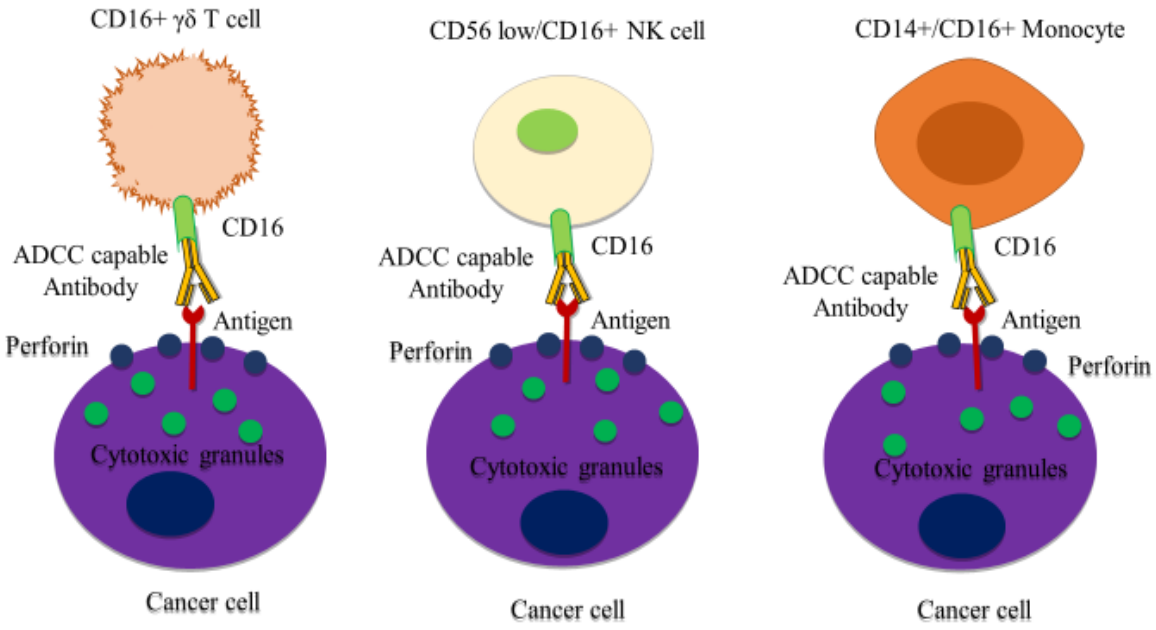

Figure 1.3: Antibody dependent cell-mediated cytotoxicity (ADCC) elicited by CD16+ NK cells, T cells and monocytes bound to an ADCC-capable monoclonal antibody which has recognised a specific antigen. Once this occurs, the immune cell can release perforin and cytotoxic granules into the lytic synapse which forms pores in the cancer cell membrane and leads to induction of apoptosis.

1.3 Immune checkpoint proteins

Immune checkpoint proteins can be expressed on the tumour cell and certain immune cell populations. Immune checkpoint proteins dampen the immune response by inactivating immune cells capable of tumour destruction [14]. Blockade of immune checkpoints has shown impressive results in a range of solid state cancers, particularly melanoma, non-small cell lung cancer (NSCLC) and renal cancer [36,37]. The potential benefit of this class of drugs is widespread across most cancer types and an unprecedented number of clinical studies are underway to examine the benefit of these agents.

Immune checkpoints are upregulated upon continued immune cell activation as a negative regulator of the immune response in order to prevent excess damage to peripheral tissues [14]. Upon activation of the checkpoint the immune cell is inhibited from eliciting a cytotoxic response [38,39]. These proteins are crucial in maintaining the balance between auto-immunity and self-tolerance [38,39]. However, the tumour can co-opt this network to gain a survival advantage. Immune checkpoint signalling can create an immunosuppressive environment allowing for the escape of the tumour cell from immune system-mediated destruction. There is strict regulation on activation of cytotoxic immune cells such as CD8+ T cells and NK cells. T cells, for example, require two sets of signals from an APC to become active. A T cell must receive an antigen presented by the MHC class-I complex on the APC recognised by the T cell receptor (TCR). It must also receive a co-stimulatory signal from CD28, expressed on T cells,

binding to CD80 or CD86, expressed on APCs [40] (**Figure 1.4**). Immune checkpoint proteins can act as inhibitors, with exclusive signalling axes counteracting co-stimulatory signals (e.g. PD-1/PD-L1 [39]) or directly competing with co-stimulatory molecules (e.g. CTLA-4/CD28 competing for CD80/CD86 binding [41–43]) preventing T cell activation with continued immune checkpoint expression leading to T cell exhaustion also referred to as anergy [40,41,43] (**Figure 1.4**). There are a range of immune checkpoint proteins that have been targeted in cancer, the most clinically developed of these are anti- CTLA4, PD-1 and PD-L1 therapies [14].

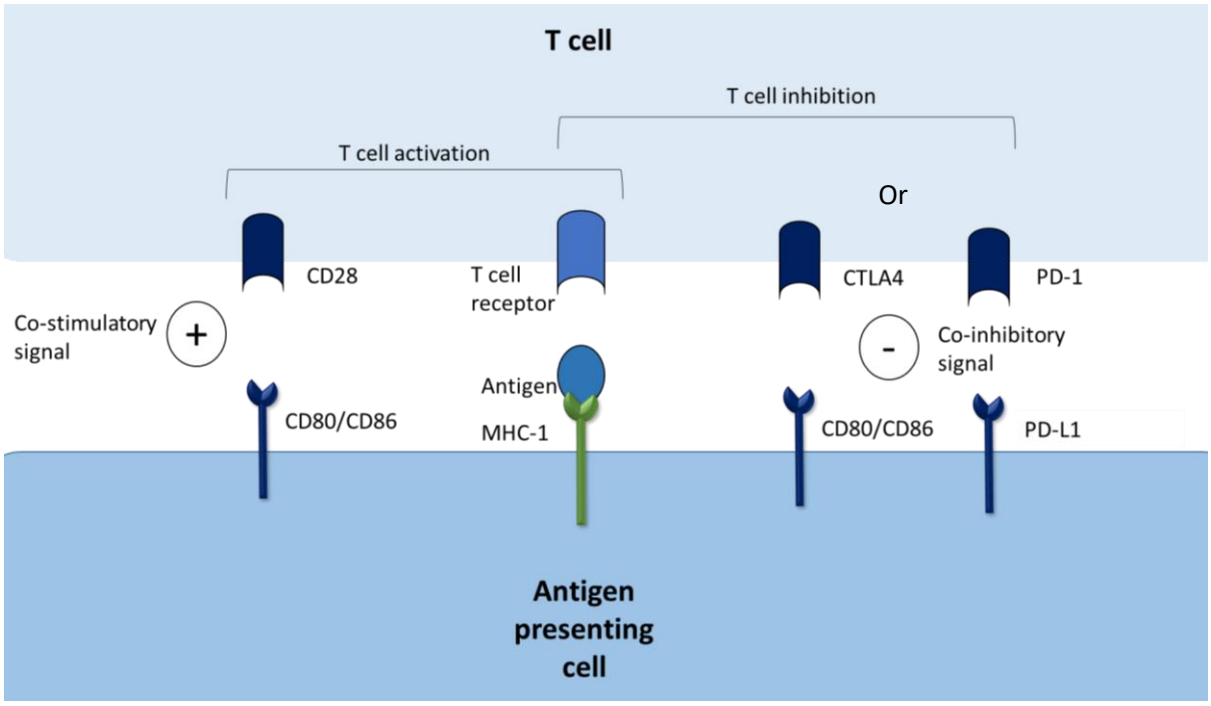

Figure 1.4: T cell activation as shown by co-stimulatory signalling by CD28 associating with CD80/CD86 after TCR recognition of MHC class-I bound antigen. T cell inhibition shown by co-inhibitory signalling by CTLA4 binding with CD80/CD86 or PD-1 binding to PD-L1.

1.3.1 CTLA4

Cytotoxic T-lymphocyte antigen 4 (CTLA4), also known as CD152, is an immune checkpoint protein. CTLA4 is expressed on regulatory T cells (Treg) and anergic T cells [44]. CTLA4 is a transmembrane protein with an extracellular surface receptor with a similar structure to CD28 to allow for competitive binding [45]. CTLA4 also contains a cytoplasmic domain containing two tyrosine-based motifs used for signal transduction [45]. CTLA4 is responsible for regulating T cell function and limiting excessive immune cell-mediated damage [44]. CTLA4 is contained within micro-vesicles in the cytoplasm. When a TCR becomes activated, CTLA4 is trafficked to the cell membrane by T cell interacting molecule (TRIM) [41,43]. CTLA4 is phosphorylated at Y201VKM (by Lck, Fyn, and Rlk) and phosphorylated CTLA4 remains cell surface bound [41,43]. CTLA4 then competes with its homolog CD28 for ligands

CD80 and CD86, preventing CD28 acting as a co-stimulator for T cell activation [41–43]. CTLA4 also interacts with PI3K, GRB2, filamin A, PKCθ, ZAP70 and phosphatases such as PTPN11 and PP2A to initiate an inhibitory response within the T cell [43]. Dephosphorylation of CTLA4 allows for reinternalization of the protein into endosomes and lysosomes which can be recycled upon further T cell activation [43].

1.3.1.1 Ipilimumab

Ipilimumab (Yervoy ®) was the first immune checkpoint inhibitor to gain FDA approval after trials in metastatic melanoma in 2011 [46]. Ipilimumab is a fully human IgG1 monoclonal antibody, which targets CTLA4 [46]. Ipilimumab blocks CTLA4 interaction with CD80 and CD86 on APCs or T cells, preventing the inhibitory effect of CTLA4, allowing CD28 to bind to CD80/CD86 and activate the T cell. Ipilimumab acts primarily by affecting intra-immune cell interactions to allow continued T cell activation, rather than tumour-immune cell interactions [46].

In a phase III study, patients with previously treated metastatic melanoma were randomised to receive either ipilimumab, a gp100 peptide vaccine or a combination of both [47]. The gp100 vaccine uses the melanoma enriched glycoprotein 100 as an antigen to target melanoma for immune-mediated destruction [47]. Patients that received the gp100 vaccine alone had a median overall survival of 6.4 months, patients who received ipilimumab and the gp100 vaccine had a median overall survival of 10 months, while patients who received ipilimumab alone had a median overall survival of 10.1 months [47]. These results led to FDA approval for ipilimumab in previously treated, unresectable metastatic melanoma. In 2015, ipilimumab was also approved for adjuvant treatment of stage III melanoma after a phase III trial on 951 patients revealed an increase in recurrence free survival when treated with ipilimumab versus placebo [48]. At 3 years, the recurrence free survival rate for ipilimumab treated patients was 46.5 % versus 34.8 % for placebo [48].

Ipilimumab is also approved for use in combination with nivolumab, a PD-1 inhibitor, to treat advanced treatment naive renal cell carcinoma (RCC) and metastatic microsatellite instability high (MSI-h) or mismatch repair deficient (dMMR) colorectal cancer which has progressed on previous treatment (**Further discussed in Table 1.2**). Over 100 clinical trials are currently ongoing to further demonstrate the potential benefits of ipilimumab treatment [49].

1.3.1.2 Tremelimumab

Tremelimumab is a human IgG2 monoclonal antibody directed against CTLA4. It has a similar mechanism of action to ipilimumab, blocking the interaction between CTLA4 and CD28, therefore preventing CTLA4-mediated immune cell inactivation [50]. Tremelimumab has received orphan drug

designation for the treatment of malignant mesothelioma following modest clinical efficacy in a phase IIb trial [50]. When further examined in the phase IIb trial "Determine", tremelimumab did not meet its trial endpoints for the treatment of second or third line unresectable malignant mesothelioma [51]. Tremelimumab is currently being examined in combination with other immunomodulatory agents in approximately 50 clinical trials to determine whether this drug may have a clinical benefit in other cancer types [49].

1.3.2 PD-1

Programmed death-1 (PD-1), or CD279, a member of the CD28 family is expressed on lymphoid cells including T cells, B cells and NK cells and myeloid cells [46]. PD-1 is a transmembrane protein with a single extracellular IgV domain [52]. The cytoplasmic domain of PD-1 contains an immune receptor tyrosine-based inhibitory motif and an immune receptor tyrosine-based switch motif [52].

Programmed death-ligand 1 (PD-L1), or CD274, is a ligand for PD-1. Upon PD-L1 binding to PD-1 in the presence of the TCR signalling complex, PD-1 delivers a co-inhibitory signal [53]. This interaction leads to phosphorylation of PD-1, the recruitment of PTPN11 (SHP2) [53] which dephosphorylates ZAP70, PCKθ and CD3ζ, ending the TCR/CD28 signal [54,55]. PD-1/PD-L1 interaction leads to reduced proliferation of T cells, cytokine production, such as IL-2, IL-10 and IFN-γ, and T cell-mediated cytolysis [39,54,56]. Prolonged immune activity leads to continuous PD-1 activation which is associated with T cell anergy [57]. PD-1 expression has also been shown to negatively impact the cytotoxic capacity of NK cells, as well as inhibiting cytokine production [58]. PD-1 expression has also been shown to have inhibitory effects on myeloid-derived cells such as monocytes and macrophages [59,60].

The second ligand of PD-1 is programmed death-ligand 2 (PD-L2) or CD273. PD-L2 expression is restricted to APCs. PD-L2 is also thought to cause T cell suppression in a PD-1-dependent manner but to a lesser degree than the effect seen with PD-L1 [61–64]. There are also indications that PD-L2 may have a PD-1 independent role which is present in tumour rejection [61,62]. More investigation is needed to determine the true role of PD-L2 as an immune checkpoint protein.

1.3.2.1 Targeting PD-1

As of yet Nivolumab and pembrolizumab are the only clinically approved PD-1 inhibitors. Nivolumab and pembrolizumab have vastly altered the treatment of many advanced, metastatic and unresectable cancer types. These treatments appear to show durable effects in a wide variety of malignancies, and the number of clinical trials being conducted with these agents is staggering. More than 600 clinical trials involving PD-1 inhibition are supported by the National Cancer Institute [49]. Both nivolumab and pembrolizumab bind to PD-1 with high affinity. Both antibodies are IgG4 antibodies which have low

affinity for complement and Fc receptors [65]. This minimises the host effector cell/immune engagement function of these antibodies ensuring they elicit their effects primarily due to inhibition of PD-1:PD-L1 interactions by direct occupancy and steric blockade of the PD-L1 binding site of PD-1. Both antibodies are very similar in terms of structure, the only significant difference is in the antigen binding component of the variable domain of the antibody [66,67]. Both antibodies have shown similar efficacy and mechanisms of action in *in vitro* assays involving T cells and in *in vivo* murine studies [65]. Both antibodies also show a similar side effect profile and similar dosing levels [65].

1.3.2.2 Pembrolizumab

Pembrolizumab (Keytruda ®) is a fully human IgG4 monoclonal antibody targeted at PD-1. It blocks the interaction of PD-1 and its ligands, preventing immune cell deactivation and suppression. Pembrolizumab is also approved to treat a wide variety of cancer types which are detailed more thoroughly in **Table 1.1**.

Pembrolizumab was the first PD-1 targeted therapy to gain approval, and the first immune checkpoint inhibitor to be approved as a first line treatment, both following trials in melanoma [68,69]. Pembrolizumab is also the first ever anti-cancer treatment to be approved in all cancer types based on a biomarker; pembrolizumab is approved to treat any MSI-h or dMMR cancer [70]. Trials with pembrolizumab were often conducted primarily with PD-L1+ patients [71–74]. As a consequence, a number of pembrolizumab's approvals are within a PD-L1+ population. However, in NCSLC, head and neck cancer, classical Hodgkin's lymphoma (cHL) and urothelial carcinoma PD-L1 expression did not affect response to pembrolizumab [75–78]. Monotherapy response rates to pembrolizumab occur in a minority of patients, marking a need for response prediction markers and viable combination options. Pembrolizumab is currently involved in almost 400 NCI-supported trials as a monotherapy and in combination with other therapies across a range of cancer types [49].

Table 1.1 Key clinical trials for approval of pembrolizumab.

Cancer type	Treatment setting	FDA approved	Trial name	Sample size	Comparison treatment	OS	PFS	ORR	PD-L1 correlation	Ref
Melanoma	Metastatic melanoma that progressed after ipilimumab (and vemurafanib if BRAF+)	Accelerated approval 2014	Keynote-001	173	-	60.5 % at 12 months	57 % at 6 months	26 %	Not stated	68
Melanoma	First line treatment of metastatic or unresectable melanoma	2015	Keynote-006	834	Ipilimumab	71.3 *vs.* 58.2 % at 12 months	47.3 *vs.* 46.4 % at 6 months	33.3 *vs.* 11.9 %	Inconclusive	69
NSCLC	Advanced NSCLC which progressed on platinum-based chemotherapy	Accelerated approval 2015	Keynote-001	61	-	Not stated	Between 2.1 and 9.1 months	41 %	All patients examined >50 % PD-L1 +	71
NSCLC	First line treatment of PD-L1+ metastatic NSCLC with no EGFR or ALK mutations	2016	Keynote-024	305	Platinum-based chemotherapy	80.2 *vs.* 76.4 % at 6 months	Median of 10.3 *vs.* 6.7 months	44.8 *vs.* 27.8 %	All patients examined >50 % PD-L1 +	72
NSCLC	First line treatment of metastatic non-squamous NSCLC in combination with pemetrexed and carboplatin, regardless of PD-L1 expression	Accelerated approval 2017	Keynote-021	123	Pemetrexed and carboplatin	93 *vs.* 81 % at 6 months	13 *vs.* 8.9 months	55 *vs.* 29 %	Increased response rates correlated with PD-L1 + patients	79

OS- Overall survival, PFS-Progression free survival, ORR-Objective response rate, cHL-Classic Hodgkin's lymphoma, UC-Urothelial carcinoma, MSI-h-Microsatellite instability high, dMMR-Mismatch repair deficient.

NSCLC	First line treatment of metastatic non-squamous NSCLC in combination with pemetrexed and platinum-based chemotherapy, regardless of PD-L1 expression	Expanded approval 2018	Keynote-189	616	Pemetrexed and platinum containing chemotherapy	69.2 *vs.* 49.4 %	8.8 *vs*. 4.9 months	48 *vs.* 19 %	Benefit was seen regardless of PD-L1 expression	76
Head and neck squamous cancer	Recurrent or metastatic head and neck cancer after disease progression on platinum containing chemotherapy	Accelerated approval 2016	Keynote-012	192	-	Median of 8.5 months	24.9 % at 6 months	17.7 %	Benefit was seen regardless of PD-L1 expression	77
cHL	Adult and paediatric patients with refractory cHL or patients who have recurrent cHL following at least three lines of prior therapy	Accelerated approval 2017	Keynote-087	210	-	Not stated	Median duration of response 11.1 months	69 %	Most patients PD-L1 high, but benefit seen regardless of expression	78
UC	Locally advanced or metastatic UC in the first line if ineligible or have progression on platinum-containing chemotherapy	Accelerated approval 2017	Keynote-045	370	Chemotherapy	10.3 vs. 7.4 months (platinum failure)	2.1 *vs*. 3.3 months (platinum failure)	29 % (cisplatin ineligible) 21 *vs.* 11 % (platinum failure)	Benefit was seen regardless of PD-L1 expression	75

OS- Overall survival, PFS-Progression free survival, ORR-Objective response rate, cHL-Classic Hodgkin's lymphoma, UC-Urothelial carcinoma, MSI-h-Microsatellite instability high, dMMR-Mismatch repair deficient.

MSI-h, dMMR cancer	Any solid tumour that is MSI-h or dMMR who have progressed on treatment or have no other treatment option	Accelerated approval 2017 (Priority review)	Keynote-016/164/001/028/158	149	-	Not stated	78 % of responders at 6 months	39.6 %	Not stated	70
Gastric, gastricoesphageal junction cancer	PD-L1 + patients with recurrent or locally advanced or metastatic gastric or gastroesophageal junction adenocarcinoma	Accelerated approval 2017	Keynote-059	259 (143 PD-L1 +)	-	Not stated	26 % at 12 months	13.3 % (PD-L1 +)	Response occurred in PD-L1 + patients	73
Cervical cancer	PD-L1 + recurrent or metastatic cervical cancer patients who have progressed on or after chemotherapy	Accelerated approval 2018	Keynote-158	98 (77 PD-L1 +)	-	Not stated	91 % at 6 months	14.3 % (PD-L1 +)	Response occurred in PD-L1 + patients	74
B cell lymphoma	Refractory primary mediastinal large B-cell lymphoma or have relapsed after two or more prior lines of therapy	Accelerated approval 2018	Keynote-170	49	-	Not stated	1.1 to 19.2 months for responders	45 %	Potential correlation between response and PD-L1 +	80

OS- Overall survival, PFS-Progression free survival, ORR-Objective response rate, cHL-Classic Hodgkin's lymphoma, UC-Urothelial carcinoma, MSI-h-Microsatellite instability high, dMMR-Mismatch repair deficient.

1.3.2.3 Nivolumab

Nivolumab (Opdivo ®) is a fully human IgG4 PD-1 antibody that blocks the interaction of PD-1 with PD-L1 and PD-L2. This disrupts the ability of PD-1 to negatively regulate T-cell activation and proliferation [81]. Nivolumab is FDA-approved to treat a wide range of cancer types with and without ipilimumab. This is detailed further in Table 1.2.

Nivolumab has shown a relatively durable response in heavily pre-treated, highly mutated cancer types, particularly in melanoma and non-small cell lung cancer (NSCLC) [82–87]. However, this response occurs in a minority of patients with nivolumab monotherapy. Although this is still impressive in these settings, it appears combination therapy may improve response rates to nivolumab treatment further [85,88]. PD-L1 expression appears to correlate to response and overall benefit to nivolumab in melanoma and non-squamous NSCLC [82,84,85,87]. There does not seem to be a correlation between PD-L1 expression and response to nivolumab treatment in RCC, cHL, urothelial carcinoma, hepatocellular carcinoma and head and neck cancer as there was clinical benefit seen regardless of PD-L1 expression level [86,88–93]. There is still a clinically unmet need to find a method of predicting response to nivolumab treatment. Nivolumab is currently involved in almost 300 NCI supported clinical trials [49].

Table 1.2: Key clinical trials for approval of nivolumab.

Cancer type	Treatment setting	FDA approved	Trial	Sample size	*Vs.* treatment	OS	PFS	ORR	PD-L1 correlation	Ref
Melanoma	Unresectable metastatic melanoma that progressed on the first line treatment, BRAF WT	Accelerated approval 2014	Checkmate-066	418	Decarbazine	72.9 *vs.* 42.1 % at 12 months	5.1 *vs.* 2.2 months	40 *vs.* 13.9 %	Correlation with increased survival in nivolumab treated PD-L1+ patients	82
Melanoma	Unresectable metastatic melanoma across BRAF status in combination with ipilimumab	Accelerated approval 2016	Checkmate-067	945	Ipilimumab	Not reported	11.5 (N+I) *vs.* 6.9 (N) *vs.* 2.9 (I) months	57.6 (N+I) *vs.* 43.7 (N) *vs.* 19 (I) %	Correlation with increased PFS in nivolumab treated PD-L1+ patients	85
Melanoma	Adjuvant nivolumab in melanoma with lymph node involvement or metastatic disease	2017	Checkmate-238	906	Ipilimumab	66 *vs.* 54.5 % at 18 months	66.4 *vs.* 52.7 %	Not reported	Correlation with increased PFS in nivolumab treated PD-L1+ patients	84
Squamous-NSCLC	Advanced/metastatic squamous NSCLC with progression on platinum-based chemotherapy	2015	Checkmate-017	272	Docetaxel	42 *vs.* 24 % at 12 months	3.5 *vs.* 2.8 months	20 *vs.* 9 %	No correlation with PD-L1 expression	86

OS- Overall survival, PFS- Progression free survival, ORR-Objective response rate, WT- Wild type, SCLC- Small cell lung cancer, RCC- Renal cell carcinoma, cHL- Classical Hodgkin's lymphoma, UC- Urothelial carcinoma, MSI-h- Microsatellite instability high, dMMR- mismatch repair deficient, SOC-Standard of Care.

Non-squamous NSCLC	Advanced or metastatic non-squamous NSCLC with progression on platinum-based chemotherapy	2015	Checkmate-057	582	Docetaxel	51 *vs*. 39 % at 12 months	19 and 8 % at 12 months	19 *vs*. 12 %	Correlation with all endpoints in nivolumab treated PD-L1+ patients	87
SCLC	SCLC which has progressed on platinum containing chemotherapy and one other line of treatment	Accelerated approval 2018	Checkmate-032	109	-	Not reported	Among responders 17.9 months	12 %	Inconclusive	94
RCC	RCC which had progressed on anti-angiogenic therapy	2015	Checkmate-025	821	Everolimus	Median of 25 *vs*. 19.6 months	4.6 *vs*. 4.4 months	25 *vs*. 5 %	No correlation with PD-L1 expression	89
RCC	RCC previously untreated with an intermediate or poor risk in combination with ipilimumab	2018	Checkmate-214	1096	Sunitinib	75 *vs*. 60 %	11.6 *vs*. 8.4 months	42 *vs*. 27 %	Benefit seen regardless of PD-L1 expression	88
cHL	cHL which has progressed after autologous stem cell transplant and brentuximab/vedotin or progressed after three lines of treatment	Break-through approval 2016	Checkmate-205	80	-	Not reported	Not reported	66.3 %	Not reported	95

OS- Overall survival, PFS- Progression free survival, ORR-Objective response rate, WT- Wild type, SCLC- Small cell lung cancer, RCC- Renal cell carcinoma, cHL- Classical Hodgkin's lymphoma, UC- Urothelial carcinoma, MSI-h- Microsatellite instability high, dMMR- mismatch repair deficient, SOC-Standard of Care.

UC	Locally advanced or metastatic UC which has progressed on platinum-based therapy	Accelerated approval 2017	Checkmate-275	270	-	Median of 7 months	Not reported	19.6 %	Benefit seen regardless of PD-L1 expression	90
Colorectal cancer	MSI-h or dMMR metastatic colorectal cancer if the cancer had progressed on fluoropyrimidine, oxaliplatin, and irinotecan	Accelerated approval 2017	Checkmate-142	74	-	Not reported	Not reported	31.1 %	Not reported	96
Hepatocellular carcinoma	Hepatocellular carcinoma which progressed on sorafenib treatment	Accelerated approval 2017	Checkmate-040	154	-	Not reported	Among responders response was from 3.2 to 38.2 + months	14.3 %	Benefit seen across range of PD-L1 expression	93
Head and Neck	Metastatic or recurrent squamous cell carcinoma of the head and neck after progression on platinum-based therapy	2017	Checkmate-141	361	Methotrexate, docetaxel, or cetuximab (SOC)	Median of 7.5 *vs.* 5.1 months (SOC)	13.3 *vs.* 5.8 % (SOC)	At 6 months 19.7 *vs*. 9.9 % (SOC)	Longer overall survival regardless of PD-L1 status	92

OS- Overall survival, PFS- Progression free survival, ORR-Objective response rate, WT- Wild type, SCLC- Small cell lung cancer, RCC- Renal cell carcinoma, cHL- Classical Hodgkin's lymphoma, UC- Urothelial carcinoma, MSI-h- Microsatellite instability high, dMMR- mismatch repair deficient, SOC-Standard of Care.

1.3.3 PD-L1

PD-L1 is a type 1 transmembrane protein which is widely expressed, due its role in attenuating the immune response to infection to avoid prolonged tissue damage [14]. This is a normal process to avoid auto-immune damage [14]. PD-L1 expression has been found in many tumour types, such as melanoma, ovarian, lung, squamous cell carcinoma, colon adenocarcinoma and breast adenocarcinoma [46]. PD-L1 expression can be constitutive or induced. Constitutive PD-L1 expression is associated with oncogenic mutation [97,98]. PD-L1 expression can be induced through inflammation by IFN-γ TNFα, IL-1α, and IL-1β as well as the infiltration of tumour-associated lymphocytes [99–101]. PD-L1 is glycosylated with N-linked glycoproteins in the endoplasmic reticulum and Golgi apparatus, before being trafficked to the cell membrane to act as a ligand for PD-1. Glycosylation of PD-L1 stabilises expression and increases resistance to degradation [102]. Expression of PD-L1 can be exploited by tumour cells to evade immune-mediated destruction. PD-L1 binding to PD-1 results in immunosuppression by inhibiting T cell proliferation, activation, cytokine release and overall cell survival [103].

As well as binding to PD-1, PD-L1 can also act as a ligand to CD80 relaying an inhibitory signal to T cells [104,105]. This effect has the potential to limit T cell proliferation and cytokine production [104,105]. The binding affinity of CTLA4 to CD80 is stronger than that between PD-L1 and CD80, with the binding affinity of PD-L1 for PD-1 also higher than that of its interaction with CD80 [105]. The interaction of PD-L1 with CD80 warrants further investigation.

PD-L1 can also exist in a soluble form mainly produced by monocytes, macrophages and dendritic cells [106]. Soluble PD-L1 can still act as a ligand for PD-1 to mediate its immunosuppressive effects. The process of the release of PD-L1 from the membrane is not yet fully characterised, but matrix metalloproteases have been implicated in the process [107]. Soluble PD-L1 levels have provisionally been linked to poorer overall survival in the plasma of diffuse large cell B cell lymphoma patients (n=288) [106] and increased likelihood of metastasis in the serum of breast cancer patients (n=70) [108].

1.3.3.1 Atezolizumab

Atezolizumab (Tecentriq ®) is a human IgG1 monoclonal antibody against PD-L1 [109]. Atezolizumab was the first FDA approved PD-L1 inhibitor. Atezolizumab is engineered with a modification in its Fc domain preventing antibody dependent cell-mediated cytotoxicity (ADCC) engagement [109]. This modification was made due to the expression of PD-L1 on immune cells which could lead to an anti-immune cell immune response, which would have a negative impact on the anti-tumour immune response [110]. Atezolizumab is approved to treat urothelial carcinoma (UC) and NSCLC, details of approval are in Table 1.3. Atezolizumab is currently being evaluated in more than 100 clinical trials as a monotherapy and in combination with other therapies across a range of cancer types [49].

1.3.3.2 Avelumab

Avelumab is a human IgG1 monoclonal antibody, unlike many of the other immune checkpoint inhibitors, avelumab can induce ADCC as a part of its mechanism of action [111]. This is another mechanism by which avelumab can elicit an immune response against the tumour, but this is reliant on PD-L1 expression being present on the tumour rather than on immune cells. The other immune checkpoint inhibitors described do not have the capacity to induce ADCC. This was a proactive action taken to avoid immune checkpoint expressing immune cells being targeted by the ADCC response. Mechanisms of avoiding induction of ADCC are by being a member of the IgG4 subclass or by mutating the Fc portion of the antibody. Avelumab has received FDA approval for the treatment of UC and metastatic Merkel cell carcinoma [112,113]. This is the first FDA-approved treatment for metastatic Merkel cell carcinoma. Details of the FDA approvals for avelumab are detailed in Table 1.3. Avelumab is currently being investigated in approximately 50 clinical trials for its efficacy in a range of malignancies [49].

1.3.3.3 Durvalumab

Durvalumab is an IgG1 anti-PD-L1 monoclonal antibody which is not capable of eliciting ADCC due to Fc modification [67]. Durvalumab is currently FDA-approved to treat UC and NSCLC patients [114,115]. Details of the indications for which durvalumab is approved are listed in **Table 1.3**. Durvalumab is currently being investigated in approximately 100 clinical trials over a range of cancer types [49].

1.3.3.4 Targeting PD-L1

Inhibition of PD-L1 has been shown to be a viable treatment strategy with successes of three different antibodies in UC, NSCLC and Merkel cell carcinoma [112–119]. Detectable PD-L1 membrane expression does not appear to be necessary for response to PD-L1 targeted antibodies, however in most cases response rates were increased in PD-L1+ patients [112,116,118]. There are not as many indications for PD-L1 inhibitors as the PD-1 inhibitors nivolumab and pembrolizumab, but there is no appropriate comparison of clinical benefit as of yet. Further clinical trials will further investigate the potential of PD-L1 inhibition *vs.* PD-1 inhibition.

Table 1.3: Key clinical trials for approval of PD-L1 targeted therapies.

Drug	Cancer type	Treatment setting	FDA approved	Trial	Sample size	*Vs.* treatment	OS	PFS	ORR	PD-L1 correlation	Ref
Atezolizumab	UC	UC that has progressed on platinum-based chemotherapy	Priority review and accelerated approval 2016	IMvigor210	310	-	Not stated	84 % of responders at 11.7 months	15 %	Greater effect in PD-L1 + population	116
Atezolizumab	UC	UC patients ineligible for platinum-based chemotherapy	Accelerated approval 2017	IMvigor210	119	-	Median of 15.9 months	Median of 2.7 months	23.5 %	Responders seen across all PD-L1 expression ranges	117
Atezolizumab	NSCLC	NSCLC that progressed on platinum-based chemotherapy and targeted therapy	2016	OAK and POPLAR trials	1225 (OAK) 144 (POPLAR)	Docetaxel	13.8 *vs*. 9.6 months (OAK) 12.6 *vs*. 9.7 months (POPLAR)	Not stated	Not stated	Potential increased benefit in PD-L1 + patients but responders seen across all expression ranges (OAK and POPLAR)	118,119
Atezolizumab	TNBC	First line Metastatic TNBC in combination with nab-paclitaxel	Pending approval	IMpassion-310	910	SOC	Median 21.3 *vs.*17.6 months	Not stated	56 *vs.* 46 %	Higher ORR and OS to combination in PD-L1+ patients	120

OS-Overall survival, PFS-Progression free survival, ORR-Objective response rate, TNBC- Triple negative breast cancer, SOC-Standard of care, UC-Urothelial carcinoma.

Avelumab	UC	Locally advanced or metastatic UC that has progressed on platinum-containing chemotherapy	Accelerated approval 2017	JAVELIN	249	-	Not stated	Not stated	16.1 %	Not stated	113
Avelumab	Merkel cell carcinoma	Metastatic Merkel cell carcinoma	Accelerated approval 2017	JAVELIN	88	-	52 % at 12 months	30 % at 12 months	33 %	Higher probability of response if PD-L1 + but responses seen across all PD-L1 subgroups	112
Durvalumab	UC	Locally advanced/ metastatic UC that progressed on platinum-based chemotherapy	Accelerated approval 2017	NCT-01693562	191	-	Median of 18.2 month	Median of 1.5 months	17.8 %	Responses seen regardless of PD-L1 expression	114
Durvalumab	NSCLC	Unresectable stage III NSCLC which has not progressed on chemo-radiation therapy	2018	PACIFIC	709	Placebo	Not stated	16.8 *vs.* 5.6 months	28.4 *vs.* 16 %	Responses seen regardless of PD-L1 expression	115

OS-Overall survival, PFS-Progression free survival, ORR-Objective response rate, TNBC- Triple negative breast cancer, SOC-Standard of care, UC-Urothelial carcinoma.

1.3.4 Immune-related adverse events

The adverse effects experienced due to immune checkpoint inhibition are termed immune-related adverse events (irAE). irAEs are ranked from grade 1-5 using Common Terminology Criteria for Adverse Events (CTCAE) grade 1 = mild, grade 2 = moderate, grade 3 = severe, grade 4 = life threatening, and grade 5 = death related to toxicity [121].

irAEs occur in 70-88 % of patients treated with ipilimumab [47,122]. irAEs related to ipilimumab are dermatitis, enterocolitis, endocrinopathies, liver abnormalities (elevated serum liver tests, hepatitis), and uveitis [47,48,123]. Grade 3 and above irAEs occur in 10-27 % of patients on ipilimumab treatment [47,122,123]. These effects are primarily due to inflammatory T cell infiltration of organs and increased serum inflammatory cytokines [46]. These effects are dose-related and can be treated with high dose steroids. However the irAEs do lead to cessation of ipilimumab treatment and in rare incidences can cause morbidity [124]. In the only phase III trial run with ipilimumab, there was a 2.1 % death rate caused by treatment [47]. In pre-clinical models, CTLA-4 knockout mice die 2-3 weeks after birth due to hyperproliferation of lymphocytes which infiltrate organs causing them to fail [125]. This may also be an indication of the tolerability of CTLA-4 inhibition.

The most commonly reported adverse event reported associated with PD-1 and PD-L1 inhibition is fatigue. This occurs in 16-37 % of patients being treated with an anti-PD-1 antibody and 12-24 % of patients receiving an anti-PD-L1 antibody [126]. Other adverse effects associated with PD-1 blockade include rash, diarrhoea and colitis [127]. These occur in 57-85 % of patients, 12-20 % of patients had grade 3-4 irAEs with PD-1 blockade [126]. These adverse effects are also largely managed with steroid treatment. Serious cases of pneumonitis and myocarditis have been observed after PD-1 blockade, proving fatal in some cases, although these events are relatively rare [127,128]. In pre-clinical studies PD-1 knockout mice show spontaneous autoimmune disorders and have increased tissue damage upon infection [129]. PD-L1 knockout is not fatal in mice and displays no obvious phenotype until challenged with an infection [103].

Immune checkpoint inhibition can elicit a wide range of irAEs which are largely managed through steroidal treatment. However, some patients are particularly susceptible to an adverse reaction. These include patients with pre-existing auto-immune disorders, the elderly and patients who have received stem cell therapy [130]. Both nivolumab and pembrolizumab are approved for the treatment of lymphoma after stem cell treatment relapse which requires particular monitoring of the irAEs including graft vs. host disease [78,80,95].

Anti-PD-1 therapy has overtaken anti-CTLA-4 therapy as a preferred immune checkpoint inhibitor. This may be due in part to a lower range of irAEs seen with anti-PD-1 therapy most likely due to the stage of the immune response the different drugs target. CTLA-4 is crucial in early stages of T cell

development and expansion [130,131]. PD-1 and PD-L1 are involved later in the life cycle of the T cell, limiting immune-mediated damage to normal tissue in the periphery. This localises PD-1/PD-L1 expression to the site of inflammation or in the case of cancer, at the tumour, and may cause less systemic irAE than inhibition of CTLA4 [130,131]. The irAEs associated with PD-1 and PD-L1 treatment are still serious and have to be considered in cancers with low response rates to immune checkpoint inhibitors. The irAEs alone indicate a clear need for methods to identify patients who will benefit from receiving immune checkpoint inhibitors to allow stratification of patient populations prior to receiving immune checkpoint inhibitors. The health economic implications also need to be considered.

1.3.5 Challenges associated with immune checkpoint inhibitors

As well as the irAEs, there are also a number of other challenges associated with immune checkpoint inhibition. A minority of patients respond to immune checkpoint inhibition and the cost of treatment with pembrolizumab or nivolumab ranges from €50,000 to €100,000 *per annum* [132,133]. There is a need to predict those patients who will respond to immune checkpoint inhibition to minimise unnecessary treatment of patients with expensive and difficult to tolerate treatments. To date, there is no conclusive biomarker of response to treatment with immune checkpoint inhibitors, but a number of candidate biomarkers are under investigation.

1.3.5.1 PD-L1 as a biomarker

Tumour PD-L1 expression has been of prime interest in the search for a biomarker of response to anti-PD-1 checkpoint inhibitors. PD-L1 expression does correlate with the likelihood of receiving benefit from anti-PD-1 or anti-PD-L1 treatment in some cancers, particularly melanoma and non-squamous NSCLC [73,74,79,82,84–86]. Pembrolizumab is approved alongside a companion diagnostic which measures tumour PD-L1 expression (PD-L1 IHC 22C3 pharmDx) for NSCLC, gastric cancer, cervical cancer and urothelial cancer [71–75]. This is due to pembrolizumab being approved only in PD-L1 + patient populations. This means that all patients receiving pembrolizumab in these settings must be PD-L1+ by PD-L1 IHC 22C3 pharmDx [71–75]. SP142 (Ventana), SP263 (Ventana) and 22C3 (Dako) are also clinically approved tests to determine PD-L1 expression [134]. However, the majority of trials show PD-L1 negative patients still respond to approved anti-PD-1 and anti-PD-L1 antibodies and there are also many PD-L1+ patients who do not respond to therapy [75–78,88,90,92,93,115,117]. This indicates that PD-L1 is not a definitive biomarker for PD-1 and PD-L1-targeted therapies.

There may be many reasons for the lack of correlation of PD-L1 expression with response. The nature of PD-L1 expression may affect its use as a marker. PD-L1 expression can be constitutive or induced and PD-L1 undergoes glycosylation post-translationally [99–101]. Therefore, the manner by which PD-L1 is expressed may affect duration of expression and tumour heterogeneity. Also there may be

mechanisms other than PD-1 engagement by tumour PD-L1 that are responsible for immunosuppression, such as soluble PD-L1 or PD-L2 expression [64]. There may also be issues with the method for determining PD-L1 expression between trials. Different antibodies and tests are used to measure PD-L1 expression, along with different cut- offs for classifying expression. Trials have used greater than 1 %, 5 %, 10 %, 25 % and 50 % PD-L1 expression as PD-L1+ [71–75]. Also some trials measure tumour expressing PD-L1 only, whereas some trials assess PD-L1 expression on tumour cells and immune cell infiltrate [71–75]. This leaves room for discordant results regarding PD-L1 status and response to treatment.

1.3.5.2 Tumour mutational burden as a biomarker

Tumour mutational burden (TMB) is being investigated as another biomarker of response to immunotherapies. TMB can be measured by next generation sequencing or whole exome sequencing of the tumour [135]. Goodman *et al.*[136] examined TMB retrospectively in 151 patients treated with immune checkpoint inhibition across a range of cancers. They found that patients with more than 20 mutations/megabase had a better objective response rate, progression free survival and over survival [136]. Rizvi *et al.* [135] showed that a TMB greater than the 50th percentile correlated with an increased durable clinical benefit to PD-1 or PD-L1 inhibition in 49 NSCLC patients. Kowanetz *et al.* [137] also showed an increased response rate, progression free survival and overall survival rate when treated with atezolizumab in NSCLC patients with a high percentile TMB. This method used selective gene sequencing of Foundation 1 (FM1) genes which is a panel of 315 cancer-related genes developed by Roche Foundation Medicine and used for the detection of genomic alterations in cancer [137].

ICIs appear to be beneficial across a range of different cancer types, which is extremely unusual for targeted therapies. The TMB hypothesis is based on tumours with a higher mutation rate having higher levels of neo-antigens, protein products of mutated genes, which are recognised as non-self by the immune system leading to a greater chance of immune response initiation [14]. This idea was supported by Herbst *et al.*, who showed a potential correlation between mutation rate and response to immune checkpoint inhibition in lung cancer patients who smoked but not in those who did not smoke [109]. Further support for the importance of TMB in response to ICIs comes from tumours that are MSI-h or dMMR tumours [70]. Both MSI-h and dMMR tumours exhibit lack of DNA mismatch repair which leads to a high mutation rate [70]. Conversely, response rates to ICIs in microsatellite stable and mismatch repair proficient colorectal cancer were close to 0 % [138]. Examining the level of mutational burden and neoantigen load may be beneficial as an indicator of patients that are likely to respond to treatment.

1.3.5.2 Tumour infiltrating lymphocytes (TILs) as biomarkers

The "inflamed" tumour phenotype, also termed "hot" tumours, show the best response to immune checkpoint inhibition [46]. Hot tumours are PD-L1+ and tumour infiltrating lymphocyte (TIL) + [46]. Patients negative for PD-L1 and TILs have a lower response rate to ICIs [46]. The composition of the TILs also appears to impact on the response to immune checkpoint inhibition. Having a tumour infiltrate positive for Th1 CD4+ cells, cytotoxic CD8+ T cells, NK cells, dendritic cells and M1 macrophages indicates a better clinical outcome [139]. The presence of memory and effector T cells are also indicators of a better prognosis. Galon *et al.* observed a lower rate of metastasis in human colorectal cancer tumours with memory and effector T cells [140]. This formed the basis of the Immunoscore, which measures tumour infiltration and status of T cells to predict recurrence in colorectal cancer [141]. Chemokines can also be used to determine the nature of the TILs. CX3CL1, CXCL9 and CXCL10 expression act as immune cell recruiters and appear to be a marker of "good" immune cell infiltrate [142–144]. M2 macrophages, myeloid-derived suppressor cells (MDSCs), neutrophils, Th2 and Th17 CD4+ T cells and Treg cells appear to be predictors of a worse prognosis when present in tumours [142,145]. The immune landscape of the tumour is therefore of critical importance when considering the value of tumour PD-L1 expression as a biomarker of response.

Current data suggests that a combination of markers creating an immune profile (PD-L1, markers of TILs, TMB, inflammation markers and inhibitory and stimulatory cytokines) for each patient may be required to provide the best predictive value for immune checkpoint inhibitor response.

1.3.5.4 Pre-clinical examination of immune checkpoint inhibitors

Due to the success of ICIs in the clinic, trials are progressing rapidly to examine the effects of these drugs in many cancers. Further pre-clinical work on ICIs is needed to understand these drugs but appropriate pre-clinical models are required. Most pre-clinical evidence of the efficacy of ICIs is seen in syngeneic mouse models [146]. Syngeneic mice possess a functional murine immune response which can act against an implanted murine tumour [146]. This requires a murine tumour with the same genetic background as the mouse strain, which limits the flexibility of the experiment [146]. Human tumours can also be co-implanted into immunodeficient mice with human immune cells. This allows for immunotherapies to be examined in a humanised system, however, this process is expensive and only allows for a short duration of the experiment due to eventual graft *vs.* host disease [146,147].

In vitro pre-clinical tests can examine the effect of ICIs on immune cells, for instance effects on T cell activation, proliferation, exhaustion, chemotaxis, cytokine response and ICI binding [148–150]. Luciferase reporter assays can be used to examine the effects of ICIs on the interactions between immune cells and cancer cells *in vitro* [151,152]. In such a model, luminescence can be detected upon a specified event taking

place, such as the interaction of an immune cell and a tumour cell, or an ICI and an immune cell. The level of luminescence detected correlates with the level of interaction. FACS models which co-incubate immune cells and cancer cells and use viability dyes to determine cell death are beginning to emerge as a mechanism of examining ICIs *in vitro* [105,153]. This allows for single cell analysis of the cancer cells and measurement of cancer cell death due to specific treatment conditions. There is no consensus on the best method of analysis of ICIs *in vitro*, all proposed methods show limitations which need to be considered when developing the pre-clinical models to be used.

1.3.6 Novel immune checkpoint targets

1.3.6.1 Inhibitory immune checkpoints

Novel inhibitory immune checkpoint proteins being investigated include lymphocyte activation gene-3 (LAG-3), T cell immunoglobulin-3 (TIM-3), T cell immunoglobulin and ITIM domain (TIGIT), V-domain Ig suppressor of T cell activation (VISTA) and B7-H3 [154] (**Figure 1.5**).

LAG3 or CD233 is expressed on activated T cells, NK cells, B cells and plasmacytoid dendritic cells and is capable of eliciting a negative effect on the function of these cells [154]. LAG3 binds to MHC class-II and maintains T cell exhaustion and limits T cell proliferation, as well as regulating the maturation and activation of dendritic cells [155,156]. IMP321 is a recombinant LAG3-Ig fusion protein which binds to MHC class-II and activates APCs and CD8+ T cell activity [157]. LAG525 and BMS-986016 are IgG4 monoclonal antibodies which block the interaction of LAG3 with MHC-class II [158,159]. IMP321, LAG525 and BMS-986016 are currently in clinical trials [160].

TIM-3 is expressed on T cells, NK cells and macrophages. TIM3 expression often occurs on dysfunctional and anergic T cells. TIM3 has four known ligands galectin-9 (Gal-9), high mobility group protein B1 (HMGB1), carcinoembryonic antigen cell adhesion molecule 1 (Ceacam-1), and phosphatidylserine [161].TIM3 induces peripheral tolerance by regulating T cell proliferation and cytokine production. TIM-3 induces expansion of immunosuppressive myeloid-derived suppressor cells [162]. MBG453 is a monoclonal antibody targeting TIM3 that is in clinical trial [163].

TIGIT is an immunoreceptor which is part of the CD28-like family receptors. TIGIT binds to CD115 and CD112 to blocking the stimulatory pathways activated through their interaction with CD266 and LFA-1 respectively [164]. TIGIT is immunosuppressive to T cells and NK cells, increases immunosuppressive cytokine production, decreases IFN-γ and IL-17, and prevents maturation of dendritic cells [165,166]. OMP-31M32 is monoclonal antibody that targets TIGIT and is in clinical trials[160].

VISTA, or programmed death-1 homolog, regulates the immune response to protect against an excessive auto-immune response [167]. VISTA is primarily expressed on T cells and CD11b+ myeloid

cells which acts as an immunosuppressor to the T cell response upon binding to its receptor, which is as yet unknown [167]. JNJ-61610588 is an IgG1 monoclonal antibody targeted at VISTA [160]. CA-170 is an orally available dual small molecule inhibitor of VISTA and PD-L1 [160,168]. JNJ-61610588 and CA-170 are both being examined in clinical trials [160].

B7-H3 or CD276 is an immune checkpoint protein which is a member of the B7-CD28 family which plays a complex and not fully understood role in regulating the innate immune response [169]. B7-H3 is expressed across a range of tissues as well as APCs, NK cells, B cells and T cells. B7-H3 is highly expressed on tumour cells in a wide range of cancer types where it can inhibit TIL infiltration, T cell activity and cytokine release [169]. Enoblituzumab is an Fc humanised IgG1 monoclonal antibody targeted at B7-H3 [170]. MGD009 is a dual affinity re-targeting protein which binds to CD3 and B7-H3 to recruit T cells to the tumour microenvironment while relieving B7-H3-mediated immunosuppression [171]. 8H9 is an antibody coupled with radioactive iodine, which promotes cancer cell death on internalisation to the tumour cell [172]. Enoblituzumab, MGD009 and 8H9 are being examined in clinical trials [154].

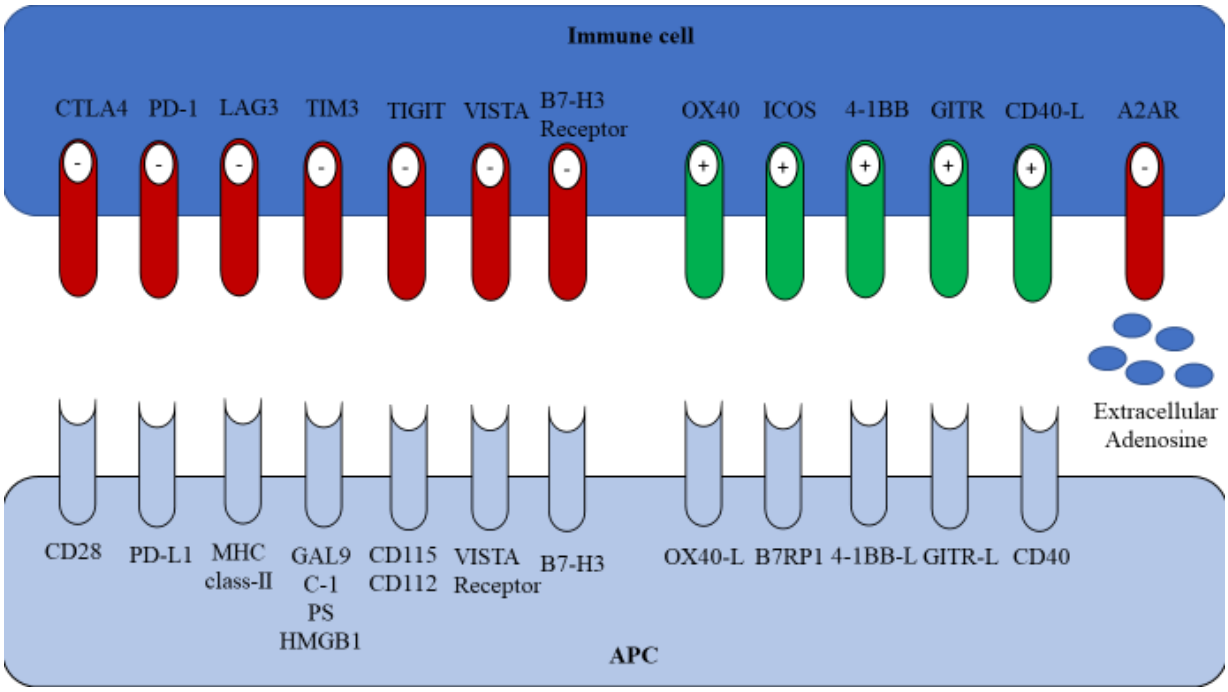

Figure 1.5: Current and novel immune checkpoint targets discussed in this study including inhibitory receptors (shown in red) CTLA4, PD-1, PD-L1, LAG3, TIM3, TIGIT, VISTA, B7-H3 and A2AR and stimulatory checkpoints (shown in green) OX40, ICOS, 4-1BB, GITR and CD40.

1.3.6.2 Stimulatory immune checkpoints

Immune-stimulatory checkpoint pathways being investigated include OX40, Inducible co-simulator (ICOS), GITR, 4-1BB and CD40 (**Figure 1.5**). OX40 (CD134) is a member of the TNF receptor family and is expressed by activated T cells, Tregs, neutrophils and NK cells. Once bound to its ligand (OX40L), OX40 plays a pivotal role in activation, proliferation, and survival of T cells and modulation of NK cell function [160]. MEDI6383, MEDI0562, MEDI6469, INCAGN01949, and GSK3174998 are monoclonal antibodies capable of activating OX40 which are being investigated in early stage clinical trials [160]. ICOS is a T cell co-stimulatory molecule in the CD28 family which is expressed on T cells. Once ligated by B7RP1, ICOS stimulates proliferation and cytokine production of T cells [160]. JTX-2011 is an agonistic monoclonal antibody of ICOS being examined in clinical trials [173]. GSK3359609 is a humanized IgG4 monoclonal agonistic antibody of ICOS that is undergoing clinical investigation [174]. As well as MEDI-570, an agonist monoclonal IgG1 targeted at ICOS in early stage clinical trials [160]. Glucocorticoid-induced TNF receptor family-related protein (GITR) is a co-stimulatory receptor expressed by T cells and NK cells. Its ligand (GITRL), is expressed by APCs and endothelial cells. Signalling upon ligation of GITR appears to have a role in upregulating the immune system, leukocyte adhesion, and migration [163]. TRX-518, BMS-986156 and AMG228 are agonist monoclonal antibodies targeted at GITR which are currently being investigated in clinical trials [175–177]. 4-1BB (CD137) is a member of the TNF family. Ligation of 4-1BB by 4-1BB-L induces activation of cytotoxic T cells and NK cells [178]. This results in increased pro-inflammatory cytokine secretion, cytolytic function, and ADCC [178]. Utomilumab and Urelumab are agonist monoclonal antibodies for 4-1BB which are in clinical examination [179,180]. CD40 is another member of the TNF receptor family, CD40 is expressed by APCs and B cells. CD40-L, the ligand for CD40, is expressed by activated T cells, ligation of CD40 stimulates cytokines secretion and T cell activation [181]. There are many agents that target the stimulation of the CD40 signalling pathway, with eight molecules under clinical investigation (CP-870893, APX005M, ADC-1013, lucatumumab, Chi Lob 7/4, dacetuzumab, SEA-CD40, and RO7009789) [160].

1.3.6.3 A2AR as an immune checkpoint in the tumour microenvironment

The tumour microenvironment has become an important target in modulating the immune response. It is important in both regulating immune cell infiltration, regulation of signalling pathways and regulation of tumour growth and metastasis. Molecules targeting tumour microenvironment components, such as adenosine signalling through A2AR, are under clinical investigation (**Figure 1.5**) [182].

Adenosine signalling through A2AR has been highlighted as a key mediator of immunosuppression to the extent that it has now labelled as a metabolic immune checkpoint [183]. Adenosine tri-phosphate (ATP) is released into the tumour microenvironment under hypoxic conditions (average cancer tumour oxygen

level of 1-2 % *vs.* 5-10 % in non-cancerous tissues) [184,185]. Extracellular ATP is hydrolysed to generate Adenosine di-phosphate (ADP) then Adenosine mono-phosphate (AMP) by the ectonucleotidase CD39. In hypoxic conditions, AMP is dephosphorylated by another ectonucleotidase CD73, which leads to the formation of adenosine [186]. Adenosine kinase, which is responsible for adenosine breakdown, is also decreased in hypoxic conditions [187]. This leads to an accumulation of adenosine in the tumour microenvironment (**Figure 1.6**).

Adenosine can bind to 4 G-protein coupled receptors which are all part of the ADORA family; A1R (ADORA1), A2AR (ADORA2A), A2BR (ADORA2B) and A3R (ADORA3). The ADORA family have diverse multifunctional roles in the body from the cardiovascular system and neurological function to hormonal and immune regulation [188]. A1R signalling inhibits adenylate cyclase and leads to decreased cyclic AMP (cAMP) levels while increasing phospholipase C activity. This is important in regulating the cardiovascular system, neurological function and detoxification [189]. A3R also inhibits adenylate cyclase, increases phospholipase C activity and increases calcium mobility. A3R activation is involved in cardioprotective functions and inhibition of neutrophil-mediated tissue injury [189]. Adenosine can bind to the A2AR or A2BR and form a negative feedback immunosuppressive system that limits tissue damage during the immune response. Tumours can benefit from this immunosuppression, particularly through A2AR signalling (**Figure 1.6**) [190].

The A2A receptor is expressed on T cells, NK cells, monocytes, macrophages and dendritic cells. Adenosine-mediated activation of the A2 receptors causes increased adenylyl cyclase activity which converts ATP to cAMP. Increased cAMP activity can then trigger the expression of a range of immunosuppressive mediators, such as PD-1, CTLA4, TGF-ß and IL-10 (**Figure 1.6**) [191]. A2AR signalling is also involved in inhibition of TCR signalling through blocking activation of ZAP70, suppressing MAPK and protein kinase C signalling and inhibiting NFκB activation in T cells and reducing IL-2 secretion which dampens expression of CD28 [192–194]. In CD8+ T cells, A2AR inhibits proliferation and cytokine production [195], while also increasing the suppressive function of Tregs through increased FOXP3 expression [196]. Ligation of A2AR decreases the expression of co-stimulatory molecule CD40L and increases the expression of inhibitory molecules CTLA4, PD-1 and LAG3 on T cells [197,198]. This suggests that blocking adenosine- mediated tumour suppression in the tumour microenvironment may be beneficial to the anti-tumour immune response.

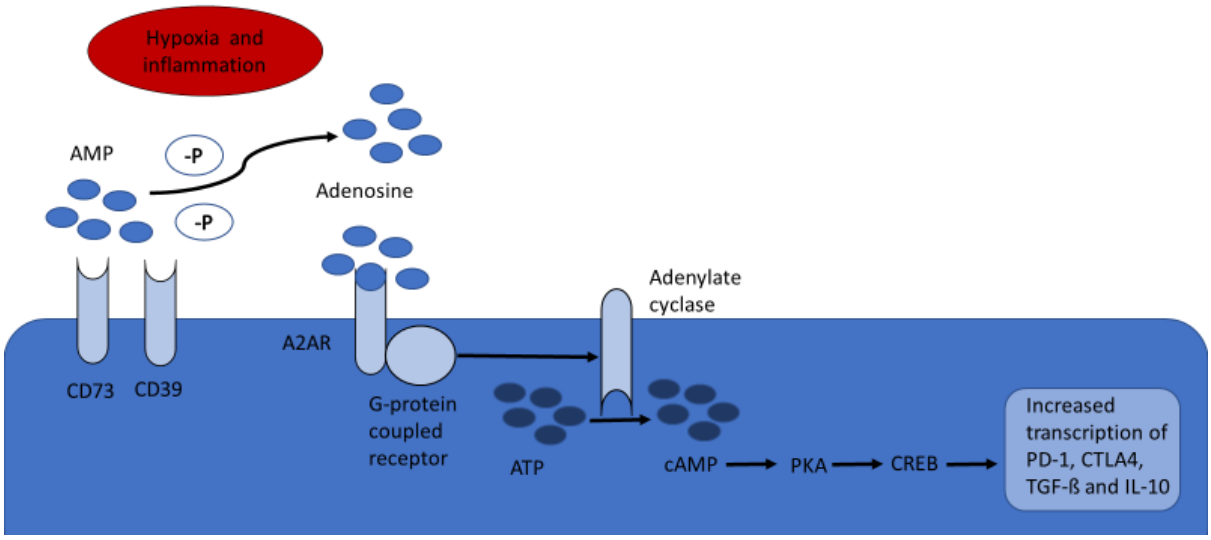

Figure 1.6: Adenosine formation through dephosphorylation of AMP by CD39 and CD73 leading to A2AR activation which initiates adenylate cyclase-mediated conversion of ATP to cAMP. cAMP increases transcription of PD-1, CTLA4, TGF-ß and IL-10.

1.3.6.3.1 Pre-clinical studies on adenosine

The role of adenosine in tumour immunosuppression has been investigated pre-clinically. A2AR-deficient and wild type (WT) mice were challenged with melanoma and lymphoma tumours [199]. A2AR-deficient mice were capable of spontaneous tumour regression in approximately 60 % of cases, this was not seen in the WT mice. When NK cells and T cells were attenuated, tumours did not regress to the same extent in the A2AR-deficient mice. The same study showed tumour growth and metastasis was also attenuated with A2AR antagonist treatment through increased cytotoxicity of CD8+ T cells [199]. Targeting CD73 and CD39 has also shown promise in pre-clinical studies. CD73 inhibition caused a decrease in tumour growth and metastasis in models of melanoma, lymphoma and mammary tumours *in vivo* [200]. Inhibition of CD39 showed similar effects by reducing tumour growth and metastasis in murine melanoma and colon cancer models [201].

1.3.6.3.2 Clinical investigation of A2AR inhibitors

A2AR inhibition is currently being investigated in four phase I clinical trials. These trials are all using an A2AR antagonist in combination with either PD-1 or PD-L1 inhibition [202]. NCT02403193 is a phase I/Ib trial examining A2AR antagonist PBF-509 and a novel PD-1 inhibitor (PDR001) in patients with NSCLC. NCT03099161 is a phase I trial examining the A2AR antagonist MK-3814 (preladenant) in combination with pembrolizumab in patients with advanced tumours. NCT02740985 is a phase I trial examining AZD4635, an A2AR antagonist, in combination with durvalumab in advanced solid

malignancies. These trials have not reported results to date [202]. In the phase Ia/Ib NCT02655822 trial, anti-A2AR agent CPI-444 is being trialled in combination with atezolizumab in advanced melanoma, NSCLC, TNBC and RCC. 48 patients were treated and the disease control rate (CR/PR or stable disease) was 45 % across all tumour types, with higher rates in NSCLC (50 %) and RCC (86 %) [203]. For the 50 % of patients on this trial that had received prior PD-1/PD-L1 therapy, there was a significantly higher tumour expression of A2AR, CD73 and CD39, which may indicate adenosine-mediated immune evasion following a non-response to PD-1/PD-L1 treatment [203].

Inhibition of A2AR appears to be beneficial in relieving immunosuppression in pre-clinical models and has progressed to early stage clinical trials with promising results. These results are supporting evidence for the role of adenosine as an immune checkpoint inhibitor and suggest it may be a promising target in a range of solid tumours in combination with immunomodulatory treatments.

1.3.6.4 Resistance to immune checkpoint inhibitors

The more mutations the cancer cell develops to give it a survival advantage, the more likely the immune system is to recognise it as non-self. Maintaining an ever-present, stable immune response to eliminate mutated cells is essential but as explained previously, is also circumvented in cancer. There is emerging evidence of patients with innate resistance to immune checkpoint inhibition. The underlying mechanisms are incompletely understood at present. Acquired resistance is thought to occur due to tumour-mediated mechanisms of evasion. These include altered neoantigen formation/ presentation/processing and alterations to cellular signalling pathways whose cell surface receptors interact with cytotoxic immune cells [204]. There are also tumour extrinsic approaches to mediate resistance to immune checkpoint inhibition. These include alterations to the microenvironment, such as increased recruitment of MDSCs which generate oxidative stress, depleting nutrients for lymphocytes and enhancing immunosuppression of Tregs [204,205]. Stromal cells can also act as another tumour extrinsic mechanism. Increases in cancer-associated fibroblasts alter T cell infiltration via FAK signalling [204,206]. Immune checkpoint inhibitors have elicited durable responses in cancers with a high tumour mutational burden. Immune cells are not expected to harbour mutations but cognate ligands and receptors on tumour cells must remain functional to allow the immune system to be re-activated by immunotherapy. A hypothesis to explain this could be that immune-related genes are less likely to mutate, providing a genetically stable target within the tumour. This could be investigated using publicly available datasets.

1.4 Rationale for immune checkpoint inhibition in breast cancer

1.4.1 Breast cancer

Breast cancer is the second most prevalent cancer in women in Ireland [207]. Breast cancer affects approximately 3000 women and 20 men every year in Ireland [207]. Breast cancer is divided into three clinical subtypes. Human epidermal growth factor receptor 2/c-neu/HER2 + accounts for approximately 20 % of breast cancers [208,209]. Oestrogen receptor (ER) + (with or without progesterone receptor (PR) expression) accounts for approximately 70 % of breast malignancies, with triple negative breast cancer (TNBC) (HER2-, ER-, PR-) tumours accounting for approximately 10 % of breast cancers [209,210]. Genomic analysis has identified further molecular subsets of breast cancer: Luminal A, Luminal B, HER2-enriched, basal-like and normal-like [211]. Within ER+ tumours there are luminal A and luminal B tumours [211]. Luminal A tumours usually express high levels of ER, and have a better prognosis [211]. Luminal B tumours have lower levels of ER and express EGFR and HER2 [211]. HER2-enriched tumours can be ER- or ER+. HER2+/ER+ tumours tend be similar to luminal B subtypes, whereas HER2+/ER- tumours tend to be similar to basal-like tumours [211].

1.4.2 Rationale for immune checkpoint inhibition in TNBC

1.4.2.1 TNBC

TNBC is characterised by the absence of HER2, ER or PR overexpression and no driver mutations have been identified across TNBC [212]. TNBCs are treated with traditional cytotoxic chemotherapies including anthracyclines, taxanes and cyclophosphamide as there are no targeted therapies available [213]. TNBC is associated with a high risk of relapse, a short progression free survival and overall survival with approximately 50 % of patients diagnosed with stage I-III TNBC experiencing disease recurrence (5 year survival rate is 63 %) [213].

1.4.2.2 Immune response to TNBC

In TNBC, the ECOG E2197 and E1199 trials showed a significant correlation between high TILs and better prognosis in 481 patients [214]. This effect was also seen in non-HER2-amplified breast cancer. The finHER trial reported a correlation between high infiltration of TILs and a lower risk of distant recurrence in 778 patients [215]. These findings suggest that the presence of a tumour-specific immune response is beneficial in TNBC. TNBC may benefit from the addition of immunomodulatory agents which further prime the anti-tumour immune response in patients with high TILs or could be used as a mechanism to create an immune-rich environment in immunologically “cold” tumours.

There is also a high level of PD-L1 expression in TNBC cell line models at a protein and RNA level [216,217]. Mittendorf *et al*. [216] examined PD-L1 expression in TNBC using the TCGA dataset where they found that 20 % of TNBC tumours were positive for PD-L1 expression using a cut off of greater than 5 % membranous PD-L1 staining. Studies in other cancer types have used cut-offs of 1 % PD-L1 staining which may result in higher levels of PD-L1 being reported in TNBC [218]. It was also shown that PD-L1 expression was significantly higher in TNBC than the other breast cancer subtypes at the transcript level [216].

Shah *et al.* [219] demonstrated a high level of somatic mutation, and in particular variation in mutations, in 104 early TNBC patients using transcriptome sequence data. The TMB and neo-antigen formation level is high in TNBC, which has been shown to have a positive correlation with response to immune checkpoint inhibition [220].

1.4.3 Rationale for immune checkpoint inhibition in HER2+ breast cancer

1.4.3.1 HER2+ breast cancer

The ErbB family of genes contains four members, EGFR, ErbB2 (HER2), ErbB3 (HER3) and ErbB4 (HER4) [221]. Each member of the family is a receptor tyrosine kinase comprising of an extracellular domain, a transmembrane region and an intracellular tyrosine kinase domain [221]. The receptors form homo- and hetero-dimers upon activation [221]. EGFR, HER3 and HER4 are activated by interaction with ligands, whereas HER2 resides in a permanent, ligand-independent open conformation which allows it to homo- or heterodimerise [222]. HER2+ breast cancer is characterised by amplification of the 17q ErbB amplicon leading to overexpression of the HER2 protein [223]. This leads to increased activation of cell growth and proliferation pathways (e,g. PI3K and MAPK pathways) [224]. HER2+ breast tumours are highly proliferative and aggressive and had a poor prognosis before the advent of HER2 targeted therapies [225].

HER2+ breast cancer is treated with chemotherapy and targeted therapies. Trastuzumab (Herceptin ®) and pertuzumab (Perjeta ®) are monoclonal antibodies which target the extracellular portion of the HER2 receptor. Trastuzumab is an IgG1 monoclonal antibody targeted at the domain IV extracellular portion of HER2. Once bound, trastuzumab can supress HER2 intracellular signalling as well as eliciting ADCC [226,227]. Trastuzumab is approved for the treatment of early stage and metastatic HER2+ breast cancer [228]. Pertuzumab is also an IgG1 monoclonal antibody, but pertuzumab is targeted at domain II of the HER2 extracellular domain, effectively preventing HER2 heterodimerization as well as halting HER2 signalling and eliciting ADCC [229,230]. Pertuzumab is approved to treat early stage and metastatic HER2+ breast cancer in combination with trastuzumab [231,232]. TDM-1 (Kadcyla®), is an

antibody-drug conjugate which comprises of trastuzumab linked to the cytotoxic agent emtansine [210]. TDM-1 is approved to treat second line HER2+ breast cancer which is refractory to trastuzumab [233].

Tyrosine kinase inhibitors (TKI) lapatinib, an EGFR/HER TKI, and neratinib, a pan-HER family TKI, are also approved as targeted therapy for HER2+ breast cancer. Lapatinib is approved for use in combination with capecitabine as second-line therapy for metastatic HER2+ breast cancer that is refractory to trastuzumab [234]. Lapatinib is also approved to treat advanced breast cancer in combination with trastuzumab, or an aromatase inhibitor if hormone receptor +, if the patient has progressed on trastuzumab and chemotherapy regimens. Neratinib is approved for the treatment of early-stage HER2+ breast cancer following adjuvant trastuzumab treatment [235].

Response rates in early stage HER2+ breast cancer are high at 80-90 % , however patients do relapse and acquired resistance is a major clinical issue [236]. Patients with metastatic and advanced HER2+ breast cancer have a worse prognosis with overall advanced or metastatic breast cancer 5 year survival at approximately 22 % [237].

1.4.3.2 Immune response to HER2+ breast cancer

HER2+ breast cancer is classed as an immunologic breast cancer subtype [238]. A meta-analysis of 5 trials involving neo-adjuvant treatment of HER2+ breast cancer with trastuzumab and chemotherapy (n=1256) showed a significant correlation between a high level of TILs and an increased likelihood of a pathological complete response [217]. This effect was also seen in advanced HER2+ breast cancer with 427 patients shown to have a more favourable response to trastuzumab and lapatinib when higher tumour infiltration of CD8+ T cells was present [239]. This suggests that the presence of a tumour-specific immune response is beneficial in response to treatment in HER2+ breast cancer.

PD-L1 expression has been observed in tumour samples from HER2+ breast cancer patients. Kim *et al.* demonstrated that 81 HER2+ breast cancer patients out of 167 (48.5%) had detectable levels of PD-L1 expression on their tumour cells by IHC [240]. Of those 81 PD-L1+ patients, 53.1 % (n=43) exhibited PD-L1 expression on their TILs in comparison to the 9.3 % (8) patients who had PD-L1 negative tumour cells and PD-L1+ TILs [240]. With the use of immunomodulatory agents, it may therefore be possible to increase treatment benefit in HER2+ breast tumours with a high TIL level, or to induce a tumour phenotype/microenvironment conducive to an improved immune response in tumours without a high TIL level.

As previously discussed, tumour mutational burden and the generation of neo-epitopes have been associated with immunogenicity and potential response to ICIs in several tumour types. Thomas *et al.* investigated tumour mutational burden in 930 patients across the breast cancer subtypes using the TCGA and Metabric databases [241]. A higher tumour mutational burden was seen in HER2+ breast cancer

as opposed to ER+ breast cancer [241]. This may also predispose patients with HER2+ breast cancer to a better response to immune checkpoint inhibition.

1.4.4 Rationale for immune checkpoint inhibition in hormone receptor+ breast cancer

1.4.4.1 ER+ breast cancer

Oestrogen receptor positive (ER+) breast cancer is characterised by expression of oestrogen receptor with or without progesterone receptor expression (PR). Upon binding of oestrogen to the oestrogen receptor, the receptor translocates to the nucleus and acts as transcription factors to oestrogen response elements which lead to increased growth and proliferation [242]. Progesterone receptors are upregulated in the presence of progesterone. Progesterone binds to these receptors which again translocate to the nucleus to initiate transcription of growth and proliferation-based proteins [242]. Hormone-dependent cancers are typically treated with endocrine therapy, such as receptor antagonists (e.g. tamoxifen or fulvestrant) and aromatase inhibitors (anastrazole or letrazole), with or without chemotherapy [210].

1.4.4.2 Immune response in ER+ breast cancer

ER+ breast cancer is not traditionally seen as an immunogenic cancer type compared with HER2+ breast cancer and TNBC [243,244]. There is no conclusive evidence of clinical relevance of TILs in ER+ breast cancer [243,244]. Cimino-Mathews *et al.* [245] showed luminal breast cancers to have the lowest level of tumour PD-L1 expression compared with HER2+ and basal-like tumours across 26 primary cancer specimens. Basal-like tumours incorporates HER2+ and TNBC tumours, with 70 % of TNBC tumours being basal-like [246]. Xu *et al.* [247] demonstrated a lower level of tumour mutational burden in luminal A breast cancer tumours than HER2+ breast cancer tumours. These results indicate that ER+ breast cancer may not benefit from immune checkpoint inhibitor treatment as the other breast cancer subtypes. However, oestrogen has been linked to inflammation in the tumour microenvironment [248–250] and there are still a subset of patients with PD-L1+ tumours, so it is possible that a subset of ER+ patients may benefit from immune checkpoint inhibition.

1.5 Immune checkpoint inhibition in breast cancer

1.5.1 Immune checkpoint inhibition in TNBC

1.5.1.1 Targeting PD-1

The first trial of ICIs in breast cancer was the phase Ib Keynote-012 trial in 2014. PD-1 inhibition was investigated in 32 metastatic TNBC patients [251]. The patients included in the trial were all PD-L1+ and treated with pembrolizumab [251]. The overall response rate was 16 %. The median overall survival rate was 10.2 months and at 12 months the overall survival was 41.1 %. Median progression free survival was 1.9 months and the 12-month progression free survival rate was 18.5 %. This is a positive result considering the heavily pre-treated nature of these patients with advanced disease and the current chemotherapy response rates which are low [251]. Liedtke *et al.* showed a pathological complete response rate of 15 % to a range of cytotoxic chemotherapy in neo-adjuvant chemotherapy in TNBC with a lower response rate in patients with metastatic disease [252]. A Phase II investigation of pembrolizumab is currently underway in metastatic TNBC patients (Keynote-086 trial). Provisional results from this trial show that there was an overall response rate of 5 % from 170 previously treated metastatic TNBC patients with 60 % of patients having PD-L1+ tumours [253]. In the PD-L1+ patient cohort overall response was 23 % with a manageable safety profile [254]. These findings indicate pembrolizumab may be beneficial in the treatment of PD-L1+ TNBC.

1.5.1.2 Targeting PD-L1

PD-L1-targeting antibodies are also being trialled in metastatic TNBC. Atezolizumab has been trialled in two phase I studies. Emens *et al.* showed that in a cohort of 21 PD-L1+ metastatic TNBC patients response to atezolizumab was 19 %, with 6 month progression free survival at 33 % [255]. Schmid *et al.* also trialled atezolizumab in metastatic TNBC (n=112) [256]. There was an overall response rate of 17 % in PD-L1-high patients with a response rate of 8 % in PD-L1-low patients. Median duration of response was 21.2 months [256]. The phase I JAVELIN trial examined avelumab in metastatic TNBC [257]. From this trial, 58 metastatic treatment-refractory TNBC patients received avelumab treatment alone. Overall response rate was 5.2 % in the cohort as a whole [257]. When examined by PD-L1 expression, patients with PD-L1+ tumour-associated immune cells had an overall response rate of 22.2 % in comparison to a response rate of 2.6 % in patients with PD-L1-negative tumour-associated immune cells [257]. These results indicate there is potential benefit from PD-L1 inhibition in metastatic TNBC, particularly in PD-L1+ patients.

Immune checkpoint inhibition strategies are particularly focused on TNBC due to the unmet clinical need in this setting and the immunogenicity of this breast cancer subtype [213]. There are currently three

phase III trials in TNBC investigating pembrolizumab in combination with chemotherapy, along with 6 phase III clinical trials in TNBC for atezolizumab in combination with chemotherapy [258].

1.5.2 Immune checkpoint inhibition in ER+ breast cancer

In the Keynote-028 phase Ib, 25 PD-L1+ metastatic ER+, HER2- breast cancer patients were treated with pembrolizumab. The overall response rate was 12 % with a median duration of response of 12 months and median overall survival of 8.6 months [259]. This shows there may be potential for immune checkpoint inhibition in metastatic PD-L1+ ER+ breast cancer.

1.5.3 Immune checkpoint inhibition in HER2+ breast cancer

The phase II Keynote-014 study examined pembrolizumab in advanced HER2+ breast cancer patients who had progressed on trastuzumab treatment. 40/52 patients had PD-L1 + tumours and in this cohort the response rate was 15.2 % with a median duration of disease control of 11.1 months. If PD-L1 status was combined with TIL status of greater than 5 %, the overall response rate was 39 %. No PD-L1-negative patients responded to treatment [260].

Other trials in the HER2+ breast cancer setting aim to combine ICIs with HER2-targeted therapies. This is particularly seen with PD-L1 inhibitor atezolizumab which is in a phase III trial with paclitaxel/trastuzumab/pertuzumab as first line therapy in metastatic HER2+ breast cancer (NCT03199885), a phase II study of TDM-1 with and without atezolizumab (KATE2, NCT02924883) and a phase Ib trial investigating atezolizumab, trastuzumab and pertuzumab/TDM-1 *versus* docetaxel, trastuzumab and pertuzumab (NCT02605915) [258]. Durvalumab and trastuzumab is also being examined in HER2+ breast cancer (NCT02649686) [258]. These trials are at early stages of development and have not yet reported results. Overall there appears to be a benefit of immune checkpoint inhibition in HER2+ breast cancer.

1.6 Rationale for combining immune checkpoint inhibition with HER family targeted therapies in breast cancer

1.6.1 HER2 and Trastuzumab

Trastuzumab is an IgG1 monoclonal antibody targeted at the extracellular domain of HER2. Trastuzumab blocks HER2 intracellular signalling pathways including MAPK and PI3K, inhibiting HER2 mediated cell growth as well as eliciting ADCC [261,262]. CD56low/CD16+ NK cells appear to be the main mediators of trastuzumab-mediated ADCC (T-ADCC) [29,263]. To elicit T-ADCC, trastuzumab

binds to the extracellular portion of the HER2 receptor. NK cells can trigger apoptosis in a target cell primarily by the perforin/granzyme system (**Figure 1.3**).

The ADCC response is critical in successful response to trastuzumab treatment. This has been demonstrated in a number of studies. Clynes *et al.* demonstrated severely reduced efficacy of trastuzumab in CD16-knockout mice, with mutation of the Fc region of trastuzumab reducing the anti-tumour effects of the antibody [26]. It has also been demonstrated in three *in vitro* studies that T-ADCC correlated with response to trastuzumab treatment using patient immune cells [263–265]. Beano *et al.* [265] showed a correlation between ADCC levels and long-term clinical response to trastuzumab treatment. ADCC levels were examined using circulating NK cells isolated from patients with metastatic HER2+ breast cancer after one round of neo-adjuvant trastuzumab and chemotherapy treatment [265]. Varchetta *et al.* [30] also demonstrated a partial correlation between ADCC levels and response to trastuzumab treatment. This study was performed using primary HER2+ breast cancer patient PBMC samples which were taken after the commencement of neo-adjuvant trastuzumab monotherapy [263]. They also showed the interaction of CD16 + NK cells and trastuzumab to be crucial in eliciting a positive response to trastuzumab [263]. Gennari *et al.* [264] found that a higher level of T-ADCC elicited by PBMCs, and a higher level of TIL infiltration, correlated with a positive clinical response to trastuzumab in patients with primary HER2+ breast cancer which had been treated with trastuzumab monotherapy.

These studies suggest that trastuzumab efficacy is closely linked to the anti-tumour immune response and that a functional immune response is beneficial to a response to trastuzumab in HER2+ breast cancer. ADCC capable cells, such as CD16+ NK cells, monocytes, T cells and B cells, can express PD-1 and PD-L1. ICIs may be beneficial in relieving PD-1/PD-L1 mediated immune suppression on cells capable of eliciting an ADCC response in the presence of trastuzumab.

The T-ADCC response and response to chemotherapy given with trastuzumab can be affected by germline single nucleotide polymorphisms (SNPs). Fc receptors, particularly CD16 (FcγRIII, FCG3) are essential for effector cell recognition of trastuzumab and the initiation of ADCC. Clynes *et al.* [26] demonstrated that Fcγ knockout mice and mice with mutated Fc domains were no longer capable eliciting ADCC with trastuzumab or the CD20-specific monoclonal antibody rituximab, severely impacting the antibodies ability to cause tumour rejection [26]. Musolino *et al.*[266] examined the effect of germline SNPs on response to trastuzumab and chemotherapy in 54 metastatic HER2+ breast cancer patients. They demonstrated that patients with a minor or heterozygous allele at amino acid 158 in FCG3 had a lower objective response rate and progression free survival when receiving trastuzumab therapy than those with a reference allele [266]. PBMCs from patients with a heterozygous or minor allele for FGG3 also elicited a lower level of T-ADCC *in vitro* [266].

As previously stated in Section 1.2.2, NKG2D, transcribed from the KLRK1 gene, is critical in NK cell-mediated cytotoxicity [267–269]. Furue *et al.* [270] showed that 379 colorectal cancer patients with a

RS1049174 SNP in KLRK1 had a higher proportion of NK cells which are capable of high levels of cytotoxicity *in vitro* (HNK1 *vs.* LNK1) and that this affected cancer risk and overall survival rates [270,271]. Espinoza *et al.* [271] showed that this was due to the SNP occurring in the targeting site of the negative regulatory miR-1245, allowing for the preferential formation of high activity NK cells in 123 Human Papilloma virus (HPV) infected cancers (cervical and anogenital cancers) [271].

Taxanes and anthracyclines, chemotherapies used to treat HER2+ breast cancer, are substrates for ABCB1 (P-glycoprotein, P-gp). [272]. ABCB1 SNPs have the ability to affect substrate chemotherapy bioavailability and mediate drug resistance to these drugs [273,274]. Madrid-Paredes *et al.* showed that the RS1045642 SNP in the ABCB1 gene was linked with a higher resistance to chemotherapy and trastuzumab treatment in 84 patients with HER2+ breast cancer [273]. Kim *et al.* [274] showed that a minor allele in ABCB1 in RS1045642 was shown to be detrimental to progression free survival and overall survival in 57 patients with metastatic HER2+ breast cancer [274]. SNPs present in a patients' germline may alter response to the treatment of HER2+ breast cancer due to their effects on the immune response and response to chemotherapeutic agents.

1.6.2 PD-L1 and EGFR

EGFR was found to be expressed in 18 % of 2567 breast cancer tumours with HER2+ breast cancers significantly more likely to express EGFR than other breast cancer subtypes [275]. This may contribute to the success of lapatinib (a dual EGFR/HER2 TKI) and neratinib (a pan-HER TKI) in HER2+ breast cancer. EGFR expression in TNBC has been associated with higher proliferation, higher levels of genomic instability, higher risk of relapse and a worse prognosis in the adjuvant setting [276]. Due to the lack of targeted therapies and the expression of EGFR in TNBC pre-clinical and clinical studies are currently ongoing to determine the potential efficacy of EGFR-targeted agents such as the monoclonal antibody cetuximab and TKIs erlotinib and getfitinib [277,278].

This is relevant to immune checkpoint inhibition as there may be a link between PD-L1 expression and EGFR activity which has been predominately reported in lung cancer to date. Akbay *et al.* found when EGFR activity is inhibited *in vitro* there is a decrease in PD-L1 expression [97]. Further circumstantial evidence was reported as a relative increase in the presence of exhausted T cells was found in malignancies with constitutively activated EGFR. Akbay *et al*. also reported a higher response rate to PD-1 inhibition in EGFR-overexpressing NSCLC tumours than non-EGFR over-expressing cancers in murine carcinogen-induced, immune proficient lung cancer models [97]. Azuma *et al.* quantified PD-L1 expression in 164 surgical resections of NSCLC using IHC and flow cytometry [98]. They found that PD-L1 expression was higher in tumours that had constitutively active EGFR versus wild type EGFR. They also found that higher EGFR expression levels were significantly associated with poorer overall survival [98]. Tang *et al.* showed similar results using formalin-fixed paraffin embedded tumour slides

stained for PD-L1 and EGFR in 170 patients with NSCLC. They saw an increase in PD-L1 expression when EGFR overexpression was present, the co-expression of both correlating with shorter overall survival [279]. This link has been provisionally examined in breast cancer with evidence for blocking EGFR destabilising PD-L1 expression in two TNBC cells lines (EGFR-amplified MDA-MB-468 and BT549)[102].

There is evidence emerging from clinical studies that the link between EGFR and PD-L1 may have impact when PD-1/PD-L1 immune checkpoint inhibition and EGFR-targeted therapies are used in combination. When nivolumab was used in combination with EGFR inhibitors, PD-L1+ patients were more sensitive to EGFR targeting TKIs such as gefitinib and erlotinib [280]. It was also found that patients had a higher response rate (61.2% versus 34.8%), a longer PFS (11.7 months versus 5.7 months) and a longer overall survival (21.9 months versus 12.5 months) on an EGFR TKI if they were PD-L1+ [280]. The evidence to date suggests there is a potential link between EGFR activity and PD-L1 expression, particularly in lung cancer. This link may be relevant to other cancer types, including breast cancer, and could support a rationale for combining EGFR inhibitors with PD-1/PD-L1 axis inhibition.

1.7 Summary

The immune response is often dysregulated during cancer development and progression. This can be caused by immunosuppression mediated by immune checkpoints. ICIs have been showing durable responses in a range of cancer types. However, the response rate to ICI monotherapy remains low. To maximise the benefits of ICIs, appropriate biomarkers to predict response are needed along with rational combination strategies.

ADCC is important in the response to trastuzumab in HER2+ breast cancer. PBMCs isolated from HER2+ breast cancer patients can allow for examination of factors affecting ADCC levels. It may also be beneficial to relieve PD-1-mediated immunosuppression when examining ADCC.

Pre-clinical models for examination of ICIs *in vitro* are lacking when it comes to examining the impact on effector cell cytotoxicity. Improved understanding of the mechanisms of these immune checkpoints may lead to improved patient stratification and increased response rates.

PD-L1 expression can have suppressive effects on the anti-tumour immune response. The link between EGFR and PD-L1 has been uncovered in lung cancer and a rationale exists for examining the link in breast cancer.

Immunosuppression also occurs in the tumour microenvironment through A2AR signalling. Inhibition of A2AR signalling may be beneficial in boosting the immune response against breast cancer.

In the clinic, ICIs are showing success in heavily pre-treated cancers which have failed multiple treatment lines. This indicates that the mechanisms in place to activate the immune response are still in place in advanced cancers. This may be due to a lower rate of mutation in immune-related genes in cancer.

1.8 Study Aims

The main objectives of this study were to

i) Determine the *in vitro* cytotoxic capabilities of circulating PBMCs from HER2+ breast cancer patients enrolled in the Phase II neo-adjuvant ICORG 10-05 clinical trial and assess the results in the context of:
   a. Treatment received
   b. Pathological complete response
   c. *In vitro* response to the anti-PD-1 therapy pembrolizumab
   d. Germline SNP variations in Fc receptors, NKG2D ligand KLRK1 and drug resistance transporter ABCB1.

ii) Develop an assay to examine the activity of anti-PD-1 and anti-PD-L1 ICIs *in vitro* using healthy volunteer PBMC samples.

iii) Investigate a potential link between EGFR activity and PD-L1 expression in models of HER2+ and TNBC to provide pre-clinical rationale for anti-EGFR/PDL1 treatment strategies.

iv) Model adenosine-mediated immunosuppression and its effect on T-ADCC *in vitro* to assess the potential for targeting the A2AR metabolic immune checkpoint in the presence of trastuzumab.

v) Using publicly available genomic datasets, examine the hypothesis that the ability of ICIs to display clinical activity in highly mutated and treatment-resistant cancers is due to a lower level of mutation in immune genes.

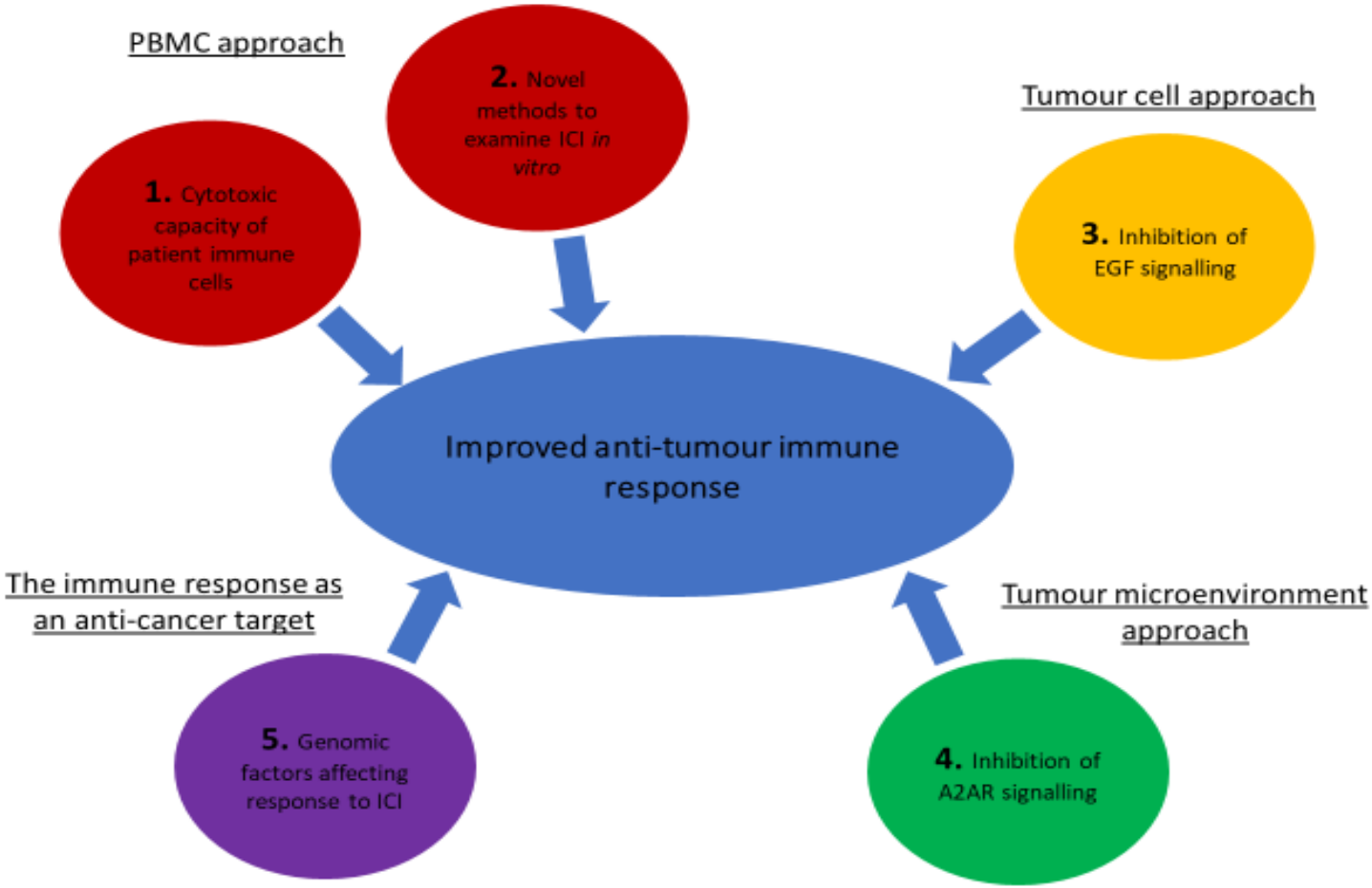

Figure 1.7: Different approaches to understanding and improving the anti-tumour immune response which were investigated in this thesis. Approaches include the use of patient and healthy volunteer PBMCs to develop assays to examine ICI efficacy *in vitro*, targeting EGFR on tumour cells to potentiate the immune response, targeting adenosine/A2AR signalling to relieve immunosuppression and exploring a hypothesis to explain the response to ICIs in heavily pre-treated cancers. ICI- Immune checkpoint inhibitor.

2. Materials and Methods

2.1 Cell lines in culture and reagents

A range of cell line panels from different cancers were used in this project. The cell lines in Table 2.1 were cultured for protein lysates, proliferation and immune cytotoxicity assays (**Table 2.1**). All culture conditions and cell culture medium used are listed below (**Table 2.1**). The majority of cell lines were cultured in media supplemented with heat inactivated foetal bovine serum (HI FBS) (Sigma Aldrich), as this serum is preferable for immunological work. Drug resistant cell lines were cultured in the FBS which was found to best maintain resistance. When used in direct comparison the corresponding parental cell lines were cultured in the same FBS as the resistant cell line. For the purposes of immune cytotoxicity assays and any work relevant to immune cytotoxicity assays all cell lines were switched to HI FBS before the assay commenced. All cell culture procedures were performed as per the guidelines set out in NICB SOP [#005, #006 and #007] and cell lines were mycoplasma tested at regular intervals.

Targeted therapy-, TKI- and chemotherapy-resistant cell lines were obtained from the NICB and Molecular Therapeutics for Cancer Ireland culture collections. The procedure used to generate each cell line and the individual responsible are listed in Table 2.2.
A list of the compounds used in this project, their source, stock concentration and storage conditions are listed in Table 2.3.

Table 2.1: The cell lines used in this project and the culture conditions required. Included are; Roswell Park Memorial Institute-1640 medium (RPMI-1640) (Sigma Aldrich), HI FBS (Sigma Aldrich), TNBC FBS (Gibco), FBS gold (Analab), Eagle's Minimum Essential Medium (MEM) (Sigma Aldrich), Dulbecco's Modified Eagle Medium (DMEM) (Sigma Aldrich), Non-Essential Amino Acids (NEAA) (Gibco).

Cell Line	Culture Medium	Culture Conditions
HER2+ breast cancer		
SKBR3	RPMI-1640 + 10 % HI FBS/FBS gold/TNBC FBS	37 ºC, 5 % CO2
BT474	RPMI-1640 + 10 % HI FBS/TNBC FBS	37 ºC, 5 % CO2
HCC1954	RPMI-1640 + 10 % HI FBS/TNBC FBS	37 ºC, 5 % CO2
HER2 low, ER+		
MCF7	MEM +10 % HI FBS	37 ºC, 5 % CO2
CAMA-1	MEM, 10 % HI FCS, NEAA,1 mM Na pyruvate, 2 mM L-glutamine	37 ºC, 5 % CO2
Triple negative breast cancer		
HCC1143	RPMI-1640 + 10 % HI FBS	37 ºC, 5 % CO2
MDA-MB-231	RPMI-1640 + 10 % HI FBS	37 ºC, 5 % CO2
Lung Cancer		
SK-LU-1	MEM, 1 % NEAA, 1 mM Na pyruvate, 2 mM L-glutamine, 5 % HI FCS	37 ºC, 5 % CO2
A549	DMEM/Ham's F-12, 5 % HI FCS	37 ºC, 5 % CO2
NCI-H460	RPMI-1640 + 10 % HI FBS	37 ºC, 5 % CO2
NCI-H82	RPMI-1640 + 10 % HI FBS	37 ºC, 5 % CO2
NCI-H69	RPMI 1640, 1 mM Na- pyruvate, 10 % HI FCS	37 ºC, 5 % CO2
DMS53	RPMI-1640 + 10 % HI FBS	37 ºC, 5 % CO2
NCI-H1229	RPMI 1640, 1 mM Na pyruvate, 5 % HI FCS	37 ºC, 5 % CO2
Drug resistant cell lines		
SKBR3-Lap	RPMI-1640 + 10 % TNBC FBS	37 ºC, 5 % CO2
SKBR3-Afa	RPMI-1640 + 10 % FBS gold/TNBC FBS	37 ºC, 5 % CO2
SKBR3-Tr	RPMI-1640 + 10 % TNBC FBS	37 ºC, 5 % CO2
SKBR3-TL	RPMI-1640 + 10 % TNBC FBS	37 ºC, 5 % CO2
BT474-Tr	RPMI-1640 + 10 % TNBC FBS	37 ºC, 5 % CO2

HCC1954-Lap	RPMI-1640 + 10 % TNBC FBS	37 ºC, 5 % CO2
HCC1954-Ner	RPMI-1640 + 10 % TNBC FBS	37 ºC, 5 % CO2
MCF7-TXT	RPMI-1640 + 5 % HI FBS	37 ºC, 5 % CO2
MCF7-CISP	RPMI-1640 + 5 % HI FBS	37 ºC, 5 % CO2
MCF-ADR	RPMI-1640 + 5 % HI FBS	37 ºC, 5 % CO2
A549-CPT	DMEM L-12 Ham's + 5 % HI FBS	37 ºC, 5 % CO2
SK-LU-1-TAX	MEM, 1 % NEAA, 1 mM Na pyruvate, 2 mM L-glutamine, 5 % HI FCS	37 ºC, 5 % CO2
	Controls	
Raji B	RPMI-1640 + 10 % HI FBS	37 ºC, 5 % CO2
K562	RPMI-1640 + 10 % HI FBS	37 ºC, 5 % CO2

Table 2.2: Description of TKI and therapy resistant cell lines used in this study.

Cell line	Method of resistant cell line generation	Generated by
SKBR3-Lap	Continuous exposure to 250 nM lapatinib for 6 months	Dr. Bridget Browne
SKBR3-Afa	Continuous exposure to 150 nM afatinib for at 6 months	Dr. Alexandra Canonici
SKBR3-Tr	Continuous exposure to 10 µg/mL trastuzumab for a minimum of 10 months	Dr. Bridget Browne
SKBR3-TL	Continuous exposure to combined trastuzumab (5 µg/mL (34 nM)) and lapatinib (100 nM)	Dr. Bridget Browne
BT474-Tr	Continuous exposure to 1.4 µM trastuzumab for a minimum of 10 months	Dr. Bridget Browne
HCC1954-Lap	Continuous exposure to 1 µM lapatinib for at 6 months	Dr. Martina McDermott
HCC1954-Ner	Continuous exposure to 150 nM neratinib for at 6 months	Dr. Susan Breslin
MCF7-TXT	Pulse selected cells (4 hrs/week) with docetaxel (6 pulses 50,10,10,13,13,13 ng/mL)	Dr. Yizheng Liang
MCF7-CISP	Pulse selected cells (4 hrs/week) with cisplatin (9 pulses 0.8,1,3,3,3,3,3,3.5,3.5 µg/mL)	Dr. Yizheng Liang
MCF-ADR	Pulse selected cells (4 hrs/week) with adriamycin (4 pulses 0.25,0.25,0.2,0.25 µg/mL)	Dr. Yizheng Liang
A549-CPT	Pulse selected cells (4 hrs/week) with carboplatin (10 pulses, 100 ug/mL)	Dr. Laura Breen
SK-LU-1-TAX	Pulse selected cells with paclitaxel (10 ng/mL, 10 pulses)	Dr. Laura Breen

Table 2.3: List of compounds used in this project, concentrations and storage conditions.

Compound	Supplier	Stock concentration	Short-term storage	Long-term storage
		Drugs		
Lapatinib (Tyverb ®)	Sequioa Research Products	10 mM in DMSO	Room Temperature	−20 ºC
Afatinib (Gilotrif ®)	Sequioa Research Products	10 mM in DMSO	Room Temperature	−20 ºC
Neratinib (Nerlynx ®)	Sequioa Research Products	10 mM in DMSO	Room Temperature	−20 ºC
Trastuzumab (Herceptin ®)	St. Vincent's Hospital	21 mg/mL	Refrigerated at 4 ºC	Refrigerated at 4 ºC
Rituximab (Rituxan ®)	St. Vincent's Hospital	10 mg/mL	Refrigerated at 4 ºC	Refrigerated at 4 ºC
Docetaxel (Taxotere®)	St. Vincent's Hospital	10 mg/mL	Room Temperature	Room Temperature
Cisplatin (Platinol-AQ®)	St. Vincent's Hospital	1 mg/mL	Room Temperature	Room Temperature
Adriamycin (Doxorubicin®)	St. Vincent's Hospital	2 mg/mL	Room Temperature	Room Temperature
Carboplatin (Paraplatin®)	St. Vincent's Hospital	10 mg/mL	Room Temperature	Room Temperature
Paclitaxel (Taxol®)	St. Vincent's Hospital	6 mg/mL	Room Temperature	Room Temperature
Pembrolizumab (Keytruda®)	St. Vincent's Hospital	10 mg/mL	Refrigerated at 4 º C	Refrigerated at 4 º C
Nivolumab (Opvido®)	St. Vincent's Hospital	10 mg/ml	Refrigerated at 4 º C	Refrigerated at 4 º C
Atezolizumab (Tecentriq®)	Roche	7 mg/mL	Refrigerated at 4 º C	−20 ºC
Saracatinib (AZD0530)	Selleckchem	10 mM in DMSO	Room Temperature	−20 ºC
SHP099	Selleckchem	10 mM in DMSO	Refrigerated at 4 ºC	−80 ºC
Preladenant (SCH 58261)	Sigma Aldrich	10 mM in DMSO	−20 ºC	−20 ºC

Non-drug cytokines, ligands and agonists				
IL-2	Peprotech	PBS containing 0.1% BSA protein carrier	−20 ºC	−20 ºC
EGF	Peprotech	PBS containing 0.1% BSA protein carrier	−20 ºC	−20 ºC
Adenosine	Sigma Aldrich	PBS	Refrigerated at 4 ºC	Refrigerated at 4 ºC
CGS21680	Sigma Aldrich	DMSO	−20 ºC	−20 ºC

2.2 Proliferation assays

Cells were seeded in 96 well plates at 100 µL/well at the densities listed in Table 2.4 After 24 hours, cells were treated with a drug or combination of drugs at a 2X concentration at 100 µL/well. The plates were then incubated for 5 days and proliferation was measured using an acid phosphatase assay. Media was removed from the plates and the cells were washed twice with PBS. One hundred µL of acid phosphatase substrate (10 mM p-nitrophenol phosphate (Sigma Aldrich)) in 0.1 M sodium acetate (Sigma Aldrich), 0.1 % Triton X-100 (BDH, pH 5.5) was added to each well and the plate was then incubated at 37 °C for a cell line-dependent period (60-120 minutes). The reaction was stopped with 50 µL of 0.1 M sodium hydroxide. The absorbance was then read at 405 nm and at 620 nm (reference wavelength) on a plate reader (Biotek) using Gen5 software. Percentage growth was calculated relative to an untreated control. All assays were performed in biological triplicate.

Table 2.4: Seeding density used for proliferation assays

Cell line	Cell seeding density (per well)
SKBR3-Par	3000
SKBR3-Afa	3000
HCC1954-Par	2500
HCC1954-Lap	2500
MCF7-Par	3000
MCF7-Txt	5000
MCF7-Cisp	5000
MCF-Adr	5000
A549-Par	3000
A549-Cpt	3000
SK-LU-1-Par	5000
SK-LU-1-Tax	5000

2.3 Preparation of lysates for immunoblotting

Cells were seeded in 100 mm petri dishes or 6 well plates achieving 70-80 % confluency at the time point scheduled for take down. At the scheduled time point the cells were washed twice with PBS. RIPA buffer (Sigma Aldrich) containing 100X protease inhibitor cocktail (Calbiochem), 2 mM PMSF (Sigma Aldrich), and 1 mM sodium orthovanadate (Sigma Aldrich) was added to the cells. Three hundred µL of RIPA buffer/100 mm petri dish and 100 µL RIPA buffer/well of a 6 well plate was added. The cells were incubated on ice for 20 minutes. Cells were scraped, and lysis buffer was collected. Lysates were sheared with a blunt 21 G needle and centrifuged at 14,000 R.P.M for 10 minutes at 4 ºC. Supernatant was collected and stored at -80 °C. Protein quantification was carried out using a bicinchoninic acid (BCA) quantification kit (Pierce). Pre-existing lysates generated using the same method as above were used to expand certain cell line panels to be examined by western blot (**Table 2.5**).

Table 2.5: Pre-existing lysates used for western blotting. HER2+ panel made by Dr. Alexandra Canonici and Dr. Neil Conlon, TNBC panel made by Dr. Patricia Guale, Melanoma panel made by Dr. Thamir Mahgoub.

Breast HER2+	Breast TNBC	Melanoma
UACC-732	MDAMB-468	Malme3M
EFM-192A	MDAMB-231	SK-MEL-2
MDA-MB-361	HCC1187	SK-MEL-5
JIMT-1	HCC1937	SK-MEL-28
MDA-MB-453	CAL-85-1	WM-115
HCC1954	HDQP-1	WM-266-4
	BT549	LOX-IMVI
	HCC70	
	CAL-120	
	BT20	

2.4 Western blotting

Samples were made up to 30 μg using PBS, loading buffer (4X) (ThermoFisher) and reducing agent (10X) (ThermoFisher). Samples were then electrophoretically resolved on Novex or Bolt 4-12 % gradient polyacrylamide gels (ThermoFisher). The proteins were then transferred to a nitrocellulose membrane using the iBlot 1(ThermoFisher), iBlot 2 (Thermo Fisher) or Trans-Blot Turbo (Bio-Rad) transfer systems. Ponceau S (Sigma Aldrich) was used to determine successful transfer of the protein to the membrane. The membrane was blocked in 1X NET buffer (1.5 M NaCl, 0.05 M EDTA, 0.5 M Tris pH 7.8, 0.5 % Triton X-100, 0.25 % w/v porcine gelatine) for 1 hour at room temperature. Primary antibodies used were made up in NET buffer and are listed below in Table 2.6. The membranes were then incubated in primary antibody overnight at 4 ºC with gentle rocking. The primary antibody was removed, and membranes were washed three times in NET buffer at room temperature for 10 minutes each. For dark room development, the membranes were incubated in secondary antibody (rabbit or mouse 1:1000, made up in NET) (Sigma Aldrich) for 1 hour. For development with the Licor Odyssey infrared imaging system, the membranes were incubated in fluorescent secondary antibody (rabbit or mouse 1:5000, made up in NET) (Licor). Three further ten minute washes were performed in NET at room temperature, the blots were washed in PBS and developed. Blots were developed in a dark room using ECL clarity (Bio-Rad) to induce chemi-luminescence and developed on CL Xposure film (Fisher Scientific). Alternatively, blots were developed using the Licor Odyssey infrared imaging system with Odyssey V2 software. Densitometry was performed the Total LabQuant program using biological triplicate blots. Alpha tubulin was used as a loading control for all western blots performed.

Table 2.6: Antibodies used for western blotting

Antibody	Dilution	Blotting Conditions	Secondary antibody	Positive control	Supplier	Cat. No.
Mouse Secondary	1:1000	NET	-	-	Sigma Aldrich	A6782
Rabbit Secondary	1:1000	NET	-	-	Sigma Aldrich	A6154
Fluorescent Mouse Secondary	1:5000	NET	-	-	Licor	92668070 -Red 92632210 -Green
Fluorescent Rabbit Secondary	1:5000	NET	-	-	Licor	92668021 -Red
Alpha tubulin	1:1000	NET	Mouse	-	Sigma Aldrich	T6199
PD-1	1:1000	NET	Rabbit	Activated T cells	Cell Signalling Technology	D4W2J
PD-L1	1:1000	NET	Rabbit	Raji B	Cell Signalling Technology	13684 (E1L3N)
EGFR	1:1000	NET	Mouse	MDA-MB-468	ThermoFisher	MS665
pEGFR Tyr 1068	1:1000	NET	Rabbit	MDA-MB-468	Millipore	07-818
AKT	1:1000	NET	Rabbit	HeLa	Cell Signalling Technology	4691
pAKT Ser473	1:1000	NET	Rabbit	PC-3	Cell Signalling Technology	4060
ERK 1/2	1:1000	NET	Rabbit	HeLa	Cell Signalling Technology	4695
pERK 1/2 y202/204	1:1000	NET	Rabbit	HeLa	Cell Signalling Technology	9101
PTPN11	1:1000	NET	Mouse	A431	Millipore	06-118
pPTPN11 Tyr542	1:1000	NET	Rabbit	C6	Cell Signalling Technology	3751

LCK	1:1000	NET	Rabbit	Activated T cells	Cell Signalling Technology	2752
pLCK Tyr 505	1:1000	NET	Rabbit	Activated T cells	Cell signalling Technology	2571
HER2	1:1000	NET	Mouse	SKBR3	EMD Millipore	OP15
A2AR	1:1000	NET	Rabbit	HeLa	Abcam	ab3461
MICA	1:1000	NET	Rabbit	MDA-MB-231	Abcam	ab93170
MHC class-I	1:1000	NET	Rabbit	Raji B	Abcam	ab52922
HLA-E	1:1000	NET	Mouse	human endothelial cell	Abcam	ab2216
NKTR	1:1000	NET	Rabbit	K562	Proteintech	19978-1-AP

2.5 Small interfering RNA (siRNA) transfection

HCC1954, MDA-MB-231 and SKBR3 cells were seeded in a 6 well plate to achieve 70-80 % confluency at 24 hours. The cell lines were separately transfected with PD-L1 siRNA (s26549) (ThermoFisher), a scrambled siRNA sequence (D-00180-10) (Millipore) and kinesin siRNA (Sigma Aldrich). The siRNAs were each diluted to a final concentration of 25 nM in 250 µL Opti-MEM reduced serum medium (Invitrogen) and 7.5 µL Trans-IT X2 transfection reagent (Mirus). The siRNA solutions were incubated at room temperature for 15 minutes then added drop-wise to different areas the relevant well of cells. The cells were incubated with the siRNA and transfection reagents for 48 hours then harvested for lysates and examined by western blotting as previously described (**Section 2.2 and 2.3**).

2.6 Deglycosylation of protein lysates

Protein lysates (excluding the addition of PMSF) were generated for HCC1954, MDA-MB-231, SKBR3-Par and SKBR3-Lap cell lines as previously described in Section 2.2. Proteins were deglycosylated using an N- and O-glycoprotein deglycosylation mix (New England BioLabs). One hundred µg of protein was diluted in 18 µL of UHP water. Two µL of 10X glycoprotein denaturing buffer was added before the sample was heated at 100 °C for 10 minutes. The sample was collected by brief centrifugation and chilled on ice. Five µL 10X glycobuffer 2, 5µL 10 % NP-40, 15 µL of UHP

water and 5 µL deglycosylation enzyme cocktail were added to the sample. Samples were incubated at 37 °C for 4 hours. Shifts in protein weight caused by deglycosylation were examined by western blot as previously described in Section 2.3.

2.7 Ethical approval and consent form for healthy volunteers

Ethical approval for the collection of whole blood was obtained from St. Vincent's University Hospital Research Ethics Committee and Dublin City University Research Ethics Committee in 2009 and from Dublin City University Research Ethics Committee in 2017.

Ethical approval for blood samples to be drawn from DCU staff was obtained from St. Vincent's University Hospital and DCU ethics committee by Dr. Denis Collins in 2009 (DCUREC/2009/063) to investigate "Cell-mediated cytotoxicity in response to trastuzumab exposure in non-HER2 amplified breast cancer cell lines".

In 2017 Biological safety approval was granted by the DCU Biological Safety Committee allowing for the safe handling of 20 mL healthy volunteer blood samples in the NICB as part of the "Human immune cell anti-cancer study". Ethical approval for the "Human immune cell anti-cancer study" was granted by the DCU research ethics committee (DCUREC/2017/116) for 20 mL blood samples to be drawn by a trained phlebotomist from healthy volunteer DCU staff and students. Participants were recruited through a mass email to DCU staff with information about the study and asking for volunteers. Individuals who were eligible for participation were contacted directly to organise their blood draw. Informed consent forms were signed, witnessed and dated before blood was drawn. Biological safety approval, ethical approval, plain language statement and informed consent forms are attached in Appendix 1.

2.8 Isolation of peripheral blood mononuclear cells (PBMCs) from whole blood

A 20 mL whole blood sample was taken under the approvals outlined in Section 2.7. The blood sample was diluted in a 1:1 ratio with Hanks Balanced Salt Solution (HBSS) (Sigma Aldrich) (containing 10 % HI FBS and 0.5 % pen/strep (Gibco)). Ficoll-Paque (VWR) was added to 4 X 30 mL sterilins. The blood sample was then layered slowly on top of the Ficoll-Paque in a 1:0.75 ratio (e.g. 10 mL whole blood: 7.5 mL Ficoll-Paque). The tubes were centrifuged at 1800 R.P.M. for 30 minutes at brake and acceleration set to 0. The sample separated into layers, with the buffy layer containing the peripheral blood mononuclear cells (PBMCs) in between the HBSS and Ficoll-Paque. The red blood cells (RBCs) accumulated in the bottom of the tube below the Ficoll-Paque. The top layer (HBSS) was removed and discarded. The PBMC layer was carefully removed with a Pasteur pipette, moving in a slow circular motion around the inside surface of the tube without disturbing the other layers. The collected PBMCs

from all tubes were diluted in 1:1 HBSS. The cells were then centrifuged at 1800 R.P.M. for 10 minutes with brake/accelerate set at 4. The supernatant was discarded, and the pellet was washed in 20 mL assay medium (filter sterilised RPMI, 10 % HI FBS, 0.5 % pen/strep (Gibco)), centrifuged at 1800 R.P.M. and re-suspended in 20 mL assay medium. Remaining PBMCs were cryoperseved at 1 x 10^7 cells/mL in HI FBS containing 5 % DMSO using a room temperature Mr. Frosty placed at -80 °C. After 48 hours the frozen PBMCs were transferred to liquid nitrogen for long term storage.

2.9 Frozen patient PBMC revival

Assay media was warmed to 37 ºC. The cryovials of frozen PBMCs were transferred from liquid nitrogen to a 37 ºC water bath. The cryovials were gently thawed and when a small crystal of ice remained, the vial was transferred to the biosafety laminar flow cabinet. One mL of warmed media was added dropwise to each cryovial and the cells were transferred to a 30 mL conical tube. One mL was added to each tube dropwise until each tube had a total of 10 mL. The tubes were centrifuged at 1100 R.P.M. for 10 minutes. The cells were re-suspended and washed in 5 mL warm RPMI and centrifuged again at 1100 R.P.M. for 10 minutes. The revived PBMCs were incubated at 37 ºC for 4-5 hours before starting the immune cytotoxicity assay.

2.10 Isolating NK cells and T cells from whole blood

NK cell negative selection magnetic beads kits (MACS) and T cell negative selection magnetic beads kits (MACS) were used to isolate NK cell and T cell populations from whole blood using a MACSxpress magnetic separator (MACS). The lyophilized magnetic beads pellet was reconstituted in 7.5 mL of buffer A. Equal parts of the reconstituted pellet and buffer B were mixed and added to whole blood at a 0.5:1 ratio. The blood with added magnetic beads was rotated for 5 minutes at 12 R.P.M. at room temperature. The cap was removed from the blood solution and placed in the MACSxpress magnet for 15 minutes. The cells of interest were then removed as shown below in Figure 2.1. The cells were then centrifuged at 1800 R.P.M. for 10 minute and re-suspended in assay medium.

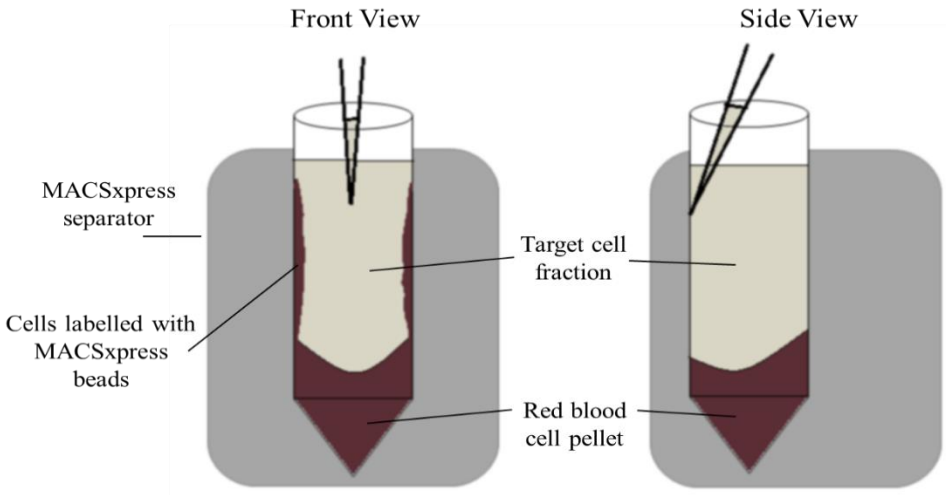

Figure 2.1: Isolation of immune cell population of interest using a negative selection magnetic beads kit and a MACSxpress magnetic separator. The pipette is placed along the front facing portion of the tube to remove cells without disturbing the positively selected cells collected by the magnet at the sides and back of the tube, while also not disturbing the RBC layer at the bottom of the tube.

2.11 Viability counting

One hundred and eighty µL of Guava Viacount (Merck Millipore) was added to each well of a 96 well round-bottomed plate in duplicate per sample. Twenty µL of a sample was added to duplicate wells of Viacount reagent. The plate was run on a Guava flow cytometer (Merck Millipore) using the Viacount software program. Populations were adjusted to ensure correct population positioning and the cell concentration and viability of each sample was recorded.

2.12 IL-2 stimulation of an enriched NK cell population

NK cells were isolated as described in Section 2.10 and counted as described in Section 2.11. The enriched NK cell population was seeded in a 1 mL suspension in a 12 well plate at 1 $x10^6$ cells/mL. Two hundred IU of IL-2 (Peprotech) were added per mL of cells. IL-2-stimulated NK cells attached to the well and were gently trypsonised when needed. Images of the enriched NK cell population were taken using a Leica DFC 500 microscope.

2.13 Activation and expansion of T cells using CD3/CD28 dynabeads

T cells were isolated as described in Section 2.10 and counted as described in Section 2.11. Cells were seeded in a 1 mL suspension in a 12 well plate at 1 x 10^6 cells/mL. CD3/CD28 dynabeads (Gibco) were washed in a PBS buffer containing 0.1 % BSA (Sigma Aldrich) and 2 mM EDTA (Sigma Aldrich) and re-suspended in assay media. Beads were added to the T cells at a 1:1 ratio. Thirty IU/mL of IL-2 was

added to each well to stimulate proliferation of the T cells [281]. Media on the T cells was replaced frequently, and T cells were sub-cultured when cell density exceeded 2.5 x 10^6 cells/mL. Images of the T cells were taken using a Leica DFC 500 microscope.

2.14 Flow cytometry analysis of markers expressed on NK cell and T cell populations

Flow cytometry was used to examine the activation status of cultured NK cell and T cell populations. The cells were counted as described in Section 2.11 and brought to 2.5 x 10^5 cells/mL. The cells were washed in an ice-cold PBS buffer containing 10 % HI FBS and 1 % sodium azide (Sigma Aldrich). Human Fc block (BD Biosciences) was added at 2.5 µg/mL then incubated for 10 minutes at room temperature. The appropriate titrated antibody volume was added to the cells and incubated for 30 minutes in the dark at room temperature (antibodies listed below Table 2.7). Cells were washed three times by centrifuging at 1400 R.P.M. for 5 minutes and re-suspending in the ice-cold PBS buffer. The cells were then analysed on the Guava flow cytometer using the Incyte program. Unstained cells were used as a control to determine percentage staining of the cell population.

Table 2.7: Antibodies used to examine markers expressed on T cells and NK cells.

Marker	Cell population	Flurochrome	Supplier	Catalogue no.
PD-1	T cell/NK cell	APC	BD Bioscience	558694
PD-L1	T cell/NK cell	Pe Cy7	BD Bioscience	558017
CD3	T cell	PerCp-Cy5.5	BD Bioscience	560835
CD8	T cell	APC-Cy7	BD Bioscience	557834
CD56	NK cell	FITC	BD Bioscience	562794
CD38	NK cell	FITC	BD Bioscience	555459
CD69	T cell	APC-Cy7	BD Bioscience	557756

2.15 Immune cytotoxicity assays

The immune cytotoxicity assays described are based on the protocol developed by Collins *et al.* 2012 [282]. Target cells (TC) were grown to 70-80 % confluency for use in the assay. Pre-treatment of TC if necessary, occurred 24 or 48 hours before set-up of the immune cytotoxicity assay. Effector cells (EC) were processed for the assay as described in Sections 2.8, 2.9, 2.10, 2.12 and 2.13. After the EC were processed, TC were washed in PBS and incubated in PBS containing 0.1 mM carboxyfluorescein succinimidyl ester (CFSE) (Sigma Aldrich) for 20 minutes. TC were then washed in PBS and incubated in 20 mL assay medium for 25 minutes to quench excess CFSE. Adherent TC were trypsinised and re-suspended in assay medium. TC were centrifuged and the cell pellets re-suspended. Cell viability of TC

and EC was determined using the Guava Viacount method (**Section 2.11**). All cells were brought to a concentration between 1.0 x 10^5 and 2.5 x 10^5 cells/mL depending on cell count and viability levels. Cells were divided and treated with a relevant drug or drug combination and plated in 96 well round bottom plates in duplicate or triplicate wells at a ratio of 1:1, 5:1 or 10:1 of EC: TC as appropriate (**Figure 2.8-2.14**). Control wells included basal cell death, 100 % dead cell controls (TCDCC), EC only and a negative control for ADCC (CD20-specific rituximab at 10 µg/mL). The plates were centrifuged at 500 R.P.M. for 3 minutes and incubated for an allotted time (4 hours frozen patient PBMCs, 12 hours healthy volunteer ECs). After the specified time period, 5 µL of triton-X (ThermoFisher) was added to the dead cell control wells and 40 µL of 35 µM 7-aminoactinomycin-D (7AAD) (Sigma Aldrich) was added to all wells. Following this, the plates were read on a Guava Easycyte flow cytometer using the Guava InCyte program (Merck Millipore) to determine the viability of the target cells in each condition (**Figure 2.15**).

Average basal cell death values were subtracted from the each corresponding sample where EC were present to determine direct cytotoxicity levels e.g. EC: TC control 10:1 – Average control EC: TC 0:1. When a drug capable of ADCC was present this method gave the overall cytotoxicity levels (direct cytotoxicity and ADCC) e.g. EC: TC trastuzumab 10:1 – Average EC: TC trastuzumab 0:1. To calculate ADCC levels the average of the relevant direct cytotoxicity condition was subtracted from the total cell kill with the ADCC capable drug present e.g. EC: TC 10:1 Trastuzumab – Average EC: TC 10:1 control.

TC only	TC 0:1 Control	TC 0:1 Control	TC 0:1 Control	TC 0:1 T	TC 0:1 T	TC 0:1 T
Sample 1	EC:TC 10:1 Control	EC:TC 10:1 Control	EC:TC 10:1 Control	EC:TC 10:1 T	EC:TC 10:1 T	EC:TC 10:1 T
Sample 2	EC:TC 10:1 Control	EC:TC 10:1 Control	EC:TC 10:1 Control	EC:TC 10:1 T	EC:TC 10:1 T	EC:TC 10:1 T
Sample 3	EC:TC 10:1 Control	EC:TC 10:1 Control	EC:TC 10:1 Control	EC:TC 10:1 T	EC:TC 10:1 T	EC:TC 10:1 T
Controls	TC 0:1 Ritux	TC 0:1 Ritux	TC 0:1 Ritux	TCDCC	TCDCC	TCDCC
Controls	EC:TC 10:1 Ritux	EC:TC 10:1 Ritux	EC:TC 10:1 Ritux	PBMC only	PBMC only	PBMC only

Figure 2.8: Representative plate layout for immune cytotoxicity assay using frozen patient PBMC samples to examine trastuzumab-mediated ADCC. Effector cell (EC): Target cell (TC) ratio of 10:1 was used. Cells were treated with and without trastuzumab (T). Rituxumab (Ritux) was used as an ADCC negative control. Target cell dead cell control (TCDCC) and PBMC only wells were also used as controls.

TC only	TC 0:1 Control	TC 0:1 Control	TC 0:1 Control	TC 0:1 T	TC 0:1 T	TC 0:1 T	TC 0:1 P	TC 0:1 P	TC 0:1 P	TC 0:1 T+P	TC 0:1 T+P	TC 0:1 T+P
Sample 1	EC:TC 10:1 Control	EC:TC 10:1 Control	EC:TC 10:1 Control	EC:TC 10:1 T	EC:TC 10:1 T	EC:TC 10:1 T	EC:TC 10:1 P	EC:TC 10:1 P	EC:TC 10:1 P	EC:TC 10:1 T+P	EC:TC 10:1 T+P	EC:TC 10:1 T+P
Sample 2	EC:TC 10:1 Control	EC:TC 10:1 Control	EC:TC 10:1 Control	EC:TC 10:1 T	EC:TC 10:1 T	EC:TC 10:1 T	EC:TC 10:1 P	EC:TC 10:1 P	EC:TC 10:1 P	EC:TC 10:1 T+P	EC:TC 10:1 T+P	EC:TC 10:1 T+P
Sample 3	EC:TC 10:1 Control	EC:TC 10:1 Control	EC:TC 10:1 Control	EC:TC 10:1 T	EC:TC 10:1 T	EC:TC 10:1 T	EC:TC 10:1 P	EC:TC 10:1 P	EC:TC 10:1 P	EC:TC 10:1 T+P	EC:TC 10:1 T+P	EC:TC 10:1 T+P
Controls	TC 0:1 Ritux	TC 0:1 Ritux	TC 0:1 Ritux	TCDCC	TCDCC	TCDCC						
Controls	EC:TC 10:1 Ritux	EC:TC 10:1 Ritux	EC:TC 10:1 Ritux	PBMC only	PBMC only	PBMC only						

Figure 2.9: Representative plate layout for immune cytotoxicity assay using frozen patient PBMC samples examining the effect of pembrolizumab (P) on trastuzumab (T)-mediated ADCC. Effector cell (EC): Target cell (TC) ratio of 10:1 was used. Cells were treated with and without T, P and P+T. Rituxumab (Ritux) was used as an ADCC negative control. Target cell dead cell control (TCDCC) and PBMC only wells were also used as controls.

TC only	TC 0:1 Control	TC 0:1 Control	TC 0:1 Control	TC 0:1 T	TC 0:1 T	TC 0:1 T	TC 0:1 P	TC 0:1 P	TC 0:1 P	TC 0:1 T+P	TC 0:1 T+P	TC 0:1 T+P
EC:TC Vol 1	EC:TC 10:1 Control	EC:TC 10:1 Control	EC:TC 10:1 Control	EC:TC 10:1 T	EC:TC 10:1 T	EC:TC 10:1 T	EC:TC 10:1 P	EC:TC 10:1 P	EC:TC 10:1 P	EC:TC 10:1 T+P	EC:TC 10:1 T+P	EC:TC 10:1 T+P
TC only	TC 0:1 N	TC 0:1 N	TC 0:1 N	TC 0:1 T+N	TC 0:1 T+N	TC 0:1 T+N	TC 0:1 A	TC 0:1 A	TC 0:1 A	TC 0:1 T+A	TC 0:1 T+A	TC 0:1 T+A
EC:TC Vol 1	EC:TC 10:1 N	EC:TC 10:1 N	EC:TC 10:1 N	EC:TC 10:1 T+N	EC:TC 10:1 T+N	EC:TC 10:1 T+N	EC:TC 10:1 A	EC:TC 10:1 A	EC:TC 10:1 A	EC:TC 10:1 T+A	EC:TC 10:1 T+A	EC:TC 10:1 T+A
Controls	TC 0:1 Ritux	TC 0:1 Ritux	TC 0:1 Ritux	TCDCC	TCDCC	TCDCC	PBMC P	PBMC P	PBMC P	PBMC N	PBMC N	PBMC N
Controls	EC:TC 10:1 Ritux	EC:TC 10:1 Ritux	EC:TC 10:1 Ritux	PBMC only	PBMC only	PBMC only	PBMC A	PBMC A	PBMC A			

Figure 2.10: Representative plate layout for immune cytotoxicity assay using healthy volunteer (vol) PBMC samples examining the effect of pembrolizumab (P), nivolumab (N) and atezolizumab (A) on direct cytotoxicity and on trastuzumab (T)-mediated ADCC. Effector cell (EC): Target cell (TC) ratio of 10:1 was used. Cells were treated with and without T, P, N, A, P+T, N+T and A+T. Rituxumab (Ritux) was used as an ADCC negative control. Target cell dead cell control (TCDCC) and PBMC only wells were also used as controls.

TC only	TC 0:1 Control	TC 0:1 Control	TC 0:1 Control	TC 0:1 T	TC 0:1 T	TC 0:1 T	TC 0:1 P	TC 0:1 P	TC 0:1 P	TC 0:1 T+P	TC 0:1 T+P	TC 0:1 T+P
EC:TC Vol 1	EC:TC 1:1 Control	EC:TC 1:1 Control	EC:TC 1:1 Control	EC:TC 1:1 T	EC:TC 1:1 T	EC:TC 1:1 T	EC:TC 1:1 P	EC:TC 1:1 P	EC:TC 1:1 P	EC:TC 1:1 T+P	EC:TC 1:1 T+P	EC:TC 1:1 T+P
TC only	TC 0:1 N	TC 0:1 N	TC 0:1 N	TC 0:1 T+N	TC 0:1 T+N	TC 0:1 T+N	TC 0:1 A	TC 0:1 A	TC 0:1 A	TC 0:1 T+A	TC 0:1 T+A	TC 0:1 T+A
EC:TC Vol 1	EC:TC 1:1 N	EC:TC 1:1 N	EC:TC 1:1 N	EC:TC 1:1 T+N	EC:TC 1:1 T+N	EC:TC 1:1 T+N	EC:TC 1:1 A	EC:TC 1:1 A	EC:TC 1:1 A	EC:TC 1:1 T+A	EC:TC 1:1 T+A	EC:TC 1:1 T+A
Controls	TC 0:1 Ritux	TC 0:1 Ritux	TC 0:1 Ritux	TCDCC	TCDCC	TCDCC	EC P	EC P	EC P	EC N	EC N	EC N
Controls	EC:TC 1:1 Ritux	EC:TC 1:1 Ritux	EC:TC 1:1 Ritux	EC only	EC only	EC only	EC A	EC A	EC A			

Figure 2.11: Representative plate layout for immune cytotoxicity assay using healthy volunteer (vol) NK and T cells examining the effect of pembrolizumab (P), nivolumab (N) and atezolizumab (A) on direct cytotoxicity and on trastuzumab (T)-mediated ADCC. Effector cell (EC): Target cell (TC) ratio of 1:1 was used. Cells were treated with and without T, P, N, A, P+T, N+T and A+T. Rituxumab (Ritux) was used as an ADCC negative control. Target cell dead cell control (TCDCC) and EC only wells were also used as controls.

TC only	TC 0:1 Control	TC 0:1 Control	TC 0:1 Control	TC 0:1 T	TC 0:1 T	TC 0:1 T	TC 0:1 A	TC 0:1 A	TC 0:1 A	TC 0:1 T+A	TC 0:1 T+A	TC 0:1 T+A
EC:TC Vol 1	EC:TC 5:1 Control	EC:TC 5:1 Control	EC:TC 5:1 Control	EC:TC 5:1 T	EC:TC 5:1 T	EC:TC 5:1 T	EC:TC 5:1 A	EC:TC 5:1 A	EC:TC 5:1 A	EC:TC 5:1 T+A	EC:TC 5:1 T+A	EC:TC 5:1 T+A
TC only **EGF pre-treated**	TC 0:1 Control	TC 0:1 Control	TC 0:1 Control	TC 0:1 T	TC 0:1 T	TC 0:1 T	TC 0:1 A	TC 0:1 A	TC 0:1 A	TC 0:1 T+A	TC 0:1 T+A	TC 0:1 T+A
EC:TC Vol 1 **TC EGF Pre-treated**	EC:TC 5:1 Control	EC:TC 5:1 Control	EC:TC 5:1 Control	EC:TC 5:1 T	EC:TC 5:1 T	EC:TC 5:1 T	EC:TC 5:1 A	EC:TC 5:1 A	EC:TC 5:1 A	EC:TC 5:1 T+A	EC:TC 5:1 T+A	EC:TC 5:1 T+A
Controls	TC 0:1 Ritux	TC 0:1 Ritux	TC 0:1 Ritux	TCDCC	TCDCC	TCDCC	EC A	EC A	EC A			
Controls	EC:TC 5:1 Ritux	EC:TC 5:1 Ritux	EC:TC 5:1 Ritux	EC only	EC only	EC only						

Figure 2.12: Representative plate layout for immune cytotoxicity assay using healthy volunteer (vol) PBMCs examining the effect of 10 ng/mL EGF pre-treatment of target cells (TC) for 24 hours on direct cytotoxicity and on trastuzumab (T)-mediated ADCC. Effector cell (EC): TC ratio of 5:1 was used. Cells were treated with and without T, A and A+T. Rituxumab (Ritux) was used as an ADCC negative control. Target cell dead cell control (TCDCC) and PBMC only wells were also used as controls.

TC only	TC 0:1 Control	TC 0:1 Control	TC 0:1 T	TC 0:1 T	TC 0:1 Ad	TC 0:1 Ad	TC 0:1 Ad+T	TC 0:1 Ad+T		
EC:TC Vol 1 1:1	TC 1:1 Control	TC 1:1 Control	TC 1:1 T	TC 1:1 T	TC 1:1 Ad	TC 1:1 Ad	TC 1:1 Ad+T	TC 1:1 Ad+T		
EC:TC Vol 1 5:1	TC 5:1 Control	TC 5:1 Control	TC 5:1 T	TC 5:1 T	TC 5:1 Ad	TC 5:1 Ad	TC 5:1 Ad+T	TC 5:1 Ad+T		
EC:TC Vol 1 10:1	TC 10:1 Control	TC 10:1 Control	TC 10:1 T	TC 10:1 T	TC 10:1 Ad	TC 10:1 Ad	TC 10:1 Ad+T	TC 10:1 Ad+T		
Controls	TC 0:1 Ritux	TC 0:1 Ritux	TC 1:1 Ritux	TC 1:1 Ritux	TC 5:1 Ritux	TC 5:1 Ritux	TC 10:1 Ritux	TC 10:1 Ritux	TCDCC	TCDCC

Figure 2.13: Representative plate layout for immune cytotoxicity assay using healthy volunteer (vol) PBMCs examining the effect of adenosine (Ad) on direct cytotoxicity and on trastuzumab (T)-mediated ADCC. Target cells (TC) were pre-treated with media, DMSO and 2 µM lapatinib for 48 hours. Plate layout was replicated/pre-treatment condition. Effector cell (EC): TC ratio of 1:1, 5:1 and 10:1 in duplicate wells was used. Cells were treated with and without T, Ad and Ad+T. Rituxumab (Ritux) was used as an ADCC negative control. Target cell dead cell control (TCDCC) and PBMC only wells were also used as controls.

TC only	TC 0:1 Control	TC 0:1 Control	TC 0:1 Control	TC 0:1 T	TC 0:1 T	TC 0:1 T	TC 0:1 CGS	TC 0:1 CGS	TC 0:1 CGS	TC 0:1 T+CGS	TC 0:1 T+CGS	TC 0:1 T+CGS
EC:TC Vol 1	EC:TC 1:1 Control	EC:TC 1:1 Control	EC:TC 1:1 Control	EC:TC 1:1 T	EC:TC 1:1 T	EC:TC 1:1 T	EC:TC 1:1 CGS	EC:TC 1:1 CGS	EC:TC 1:1 CGS	EC:TC 1:1 T+CGS	EC:TC 1:1 T+CGS	EC:TC 1:1 T+CGS
TC only	TC 0:1 Pr	TC 0:1 Pr	TC 0:1 Pr	TC 0:1 T+Pr	TC 0:1 T+Pr	TC 0:1 T+Pr	TC 0:1 CGS+Pr	TC 0:1 CGS+Pr	TC 0:1 CGS+Pr	TC 0:1 T+CGS+ Pr	TC 0:1 T+CGS+ Pr	TC 0:1 T+CGS+ Pr
EC:TC Vol 1	EC:TC 1:1 Pr	EC:TC 1:1 Pr	EC:TC 1:1 Pr	EC:TC 1:1 T+Pr	EC:TC 1:1 T+Pr	EC:TC 1:1 T+Pr	EC:TC 1:1 CGS+Pr	EC:TC 1:1 CGS+Pr	EC:TC 1:1 CGS+Pr	EC:TC 1:1 T+CGS+ Pr	EC:TC 1:1 T+CGS+ Pr	EC:TC 1:1 T+CGS+ Pr
Controls	TC 0:1 Ritux	TC 0:1 Ritux	TC 0:1 Ritux	TCDCC	TCDCC	TCDCC						
Controls	EC:TC 1:1 Ritux	EC:TC 1:1 Ritux	EC:TC 1:1 Ritux	EC only	EC only	EC only						

Figure 2.14: Representative plate layout for immune cytotoxicity assay using healthy volunteer (vol) NK cells examining the effect of CGS21680 (CGS) and Preladenant (Pr) on direct cytotoxicity and on trastuzumab (T)-mediated ADCC. Effector cell (EC): Target cell (TC) ratio of 1:1 was used. Cells were treated with and without T, CGS, Pr, T+CGS, T+Pr, CGS+Pr and T+CGS+Pr. Rituxumab (Ritux) was used as an ADCC negative control. Target cell dead cell control (TCDCC) and EC cell only wells were also used as controls.

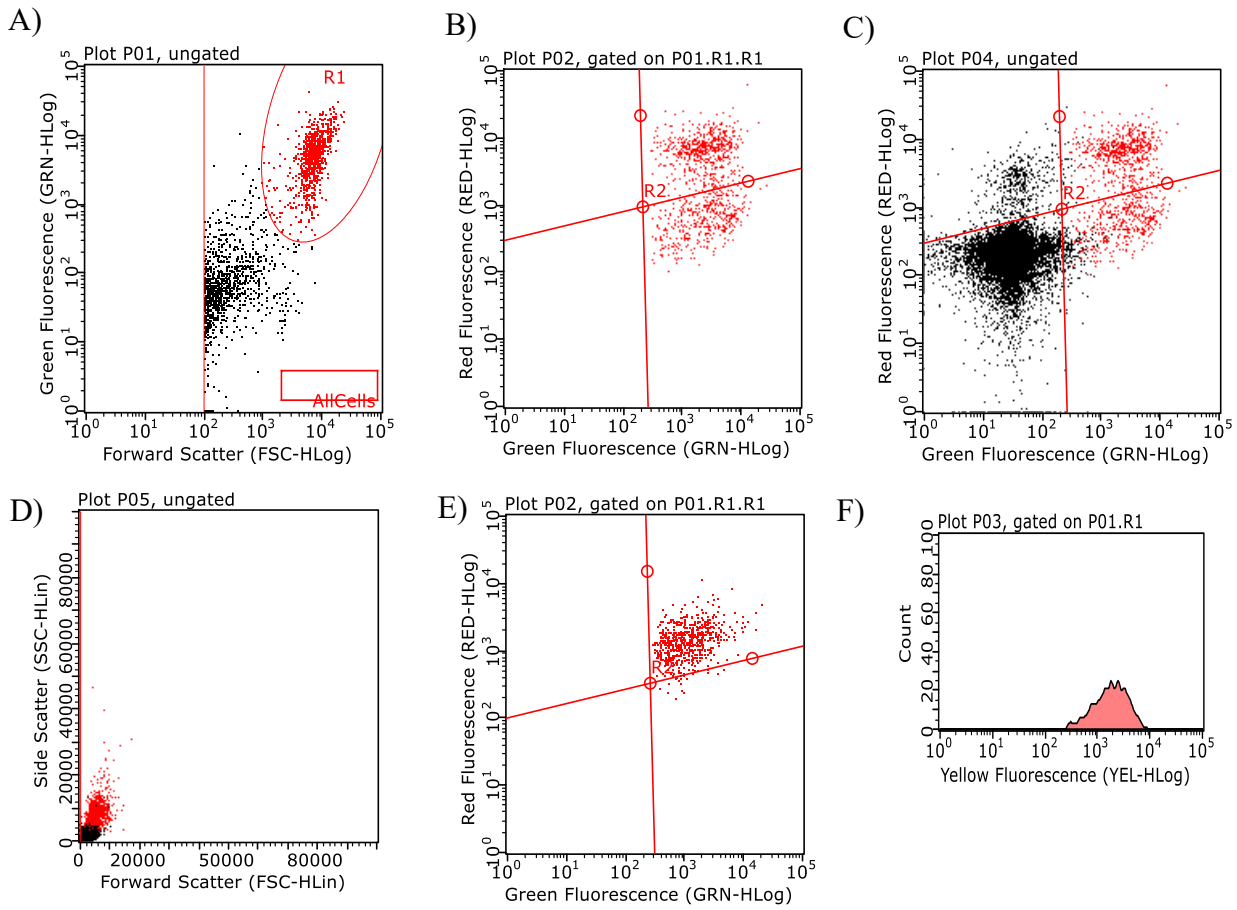

Figure 2.15: Representative Plots used for immune cytotoxicity assay analysis showing A) gating of target cells based on green fluorescence levels in a target cell (TC) only well. B) Plot gated on TC only showing live/dead cell balance based on red fluorescence levels. C) Ungated target cells and effector cells showing effector cells negative for green fluorescence and the live dead cell balance for both cell populations shown by red fluorescence levels. D) Side scatter *vs.* forward scatter for all cells in well to ensure all populations are accounted for. E) TCDCC levels showing 100 % dead cells, Allowing for quadrant placement for live/dead cell balance. F) Plot showing balance between fluorescence levels and cell event.

2.16 DNA Isolation from PBMC cell pellets

Patient PBMC samples remaining cells from ADCC assays were centrifuged and stored as a cell pellet at -80 °C. DNA was isolated using the PureLink genomic DNA kit (Invitrogen). The frozen cell pellet was re-suspended in 200 µL of sterile PBS. Twenty µL of Proteinase K and RNase A were added to the sample. The sample was briefly vortexed and incubated at room temperature for 2 minutes, and 200 µL of the PureLink genomic lysis/binding buffer was added to the sample. The sample was briefly vortexed and incubated at 55 °C for 10 minutes. Two hundred µL of 100% ethanol was added to the sample. The sample was then added to a PureLink spin column in a sterile collection tube. The sample was centrifuged at 10,000 R.P.M. for 1 minute. The spin column was placed in a new collection tube and washed with 500 µL of wash buffer 1 (prepared as per manual with 100 % ethanol) by centrifuging at 10,000 R.P.M. for 1 minute. The sample was washed with 500 µL wash buffer 2 (prepared as per manual with 100 % ethanol) and centrifuged at 14,000 R.P.M. for 3 minutes. The spin column was then placed in a sterile DNase free 1.5 mL microcentrifuge tube, and 50 µL of PureLink genomic elution buffer was added. The sample was incubated at room temperature for 1 minute then centrifuged at 14,000 R.P.M. for 1 minute. The elution process was repeated and the two samples containing the DNA were combined for DNA quantification. The DNA samples were quantified using the Qubit (ThermoFisher) and Qubit high sensitivity dsDNA quantification kit (ThermoFisher). One µL of DNA sample was added to a 199 µL of a master mix (Qubit 1X dsDNA buffer and 200X fluorescent DNA binding dye). Samples were prepared in thin walled 500 µL PCR tubes and fluorometrically scanned by the Qubit to determine DNA concentration. DNA samples were stored in PureLink DNA elution buffer at -20 °C for long-term storage.

2.17 SNP analysis of DNA isolated from patient PBMCs

To investigate the presence of SNPs, DNA (10 ng) was subjected to a mass spectroscopy-based SNP genotyping analysis by Dr. Sinead Toomey, RSCI. All primers were designed using Assay Design software from Agena Biosciences. Master mixes were prepared using 10X PCR buffer, MgCL2, DNTPs, Taq Polymerase, PCR Primer Mix and nuclease free water. Three µL of master mix was added to each well as appropriate, 2 µL of 5 ng/µL DNA was added as appropriate. PCR plates were briefly centrifuged, vortexed and briefly centrifuged again before loading into the thermal-cycler for amplification. PCR was run according to the program outlined in Table 2.8 below.

Table 2.8: PCR program

Stage	Temperature	Time	Stage description
Hold	94 °C	5 mins	Initial denaturation
45 Cycles	94 °C	20 secs	Denaturation
	56 °C	30 secs	Annealing
	72 °C	1 min	Extension
Hold	72 °C	3 mins	Final extension
Hold	4 °C	∞	Hold

To remove any unincorporated primers and dNTPs, and ExoSAP reaction was performed. SAP master mix was prepared (nuclease free water, SAP enzyme and SAP buffer). Two µL of SAP master mix was added to each well as appropriate. Plates were then briefly centrifuged, vortexed and briefly centrifuged again before loading into the thermal-cycler. The reaction was run according at 37 °C for 40 minutes, at 85 °C for 10 minutes and then at 4 degrees until the process is complete. Extension master mix was prepared using nuclease free water, 10X iPLEX Pro buffer Plus, iPLEX extension mix, Probe mix in 3 bins and iPLEX enzyme. Two µL of extension reaction master mix was added to each well as appropriate. Plates were then briefly centrifuged, vortexed and briefly centrifuged again before loading into the thermal-cycler. The reaction was run according to the program outlined in Table 2.9 below.

Table 2.9: Extension reaction program

Stage	Stage (2)	Temperature	Time	Stage description
Hold	N/A	94 °C	30 secs	Initial denaturation
40 Cycles	N/A	94 °C	5 secs	Denaturation
	5 Cycles*	52 °C	5 secs	Annealing
	N/A	80 °C	5 secs	Extension
Hold	N/A	72 °C	3 mins	Final extension
Hold	N/A	4 °C	∞	Hold

** 5 cycles sit within the 40 cycles*

Clean Resin (Sequenom) was spread on a clean, dry simple plate using a scraper plate so that the resin settled evenly into all wells and the plates were allowed to dry at room temperature for ten minutes. While the resin dried, 41 µL of HPLC-grade water was added to each well of the iPLEX Pro extension reaction product. Dried CLEAN resin was added to each well. This was performed by gently inverting the sample plate on top of the dimple plate, aligning the wells over the resin samples. Keeping the sample and dimple plates pressed together, both plates were inverted allowing the resin to fall into the sample wells. The plates were sealed and rotated for 30 minutes at room temperature. The plate was subsequently centrifuged at 3,200 g for 5 minutes to pellet the resin.

Ten nL of the desalted primer extension reactions were spotted onto Agena spectrochip II-G96 matrix chips using the Agena MassARRAY nanodispenser. Chips were run on an Agena MassArray matrix-assisted laser desorption/ionization (MALDI)-TOF MassArray system, and the MassArray Analyser 4 software was used to give a visual interpretation of the mass spectra data, which was inspected visually to ensure accurate recordings. Reactions where >15 % of the resultant mass ran in the mutant sites were scored as positive.

2.18 Gene list assembly

Cancer related gene lists and immune related gene lists with gene name, entrez number and description were assembled from the literature and online databases detailed in Table 2.10.

Table 2.10: Cancer and immune related gene lists assembled from literature and database searches.

Gene list	No. of genes	Rationale for using list	List assembly
Tumour Suppressors [283]	286	Commonly targeted cancer pathways associated with cancer development and progression	Genes from COSMIC database were listed as a tumour suppressor based on ratio of inactivating mutations to other mutations. Genes were listed as an oncogene if either two independent tumours had the same amino acid mutation or more than 4 different mutations were present
Oncogenes [283,284]	561		
PI3K [285]	238	Commonly mutated cancer pathways	KEGG pathway search for relevant pathway
MAPK [285]	256		
Cancer Hotspots	239	Genes with hotspot mutations present associated with cancer growth and progression	Curated from the TCGA dataset by Dr. Bruce Moran, UCD
Immunity genes [286]	1532	Included were complete genes with a functional transcript that demonstrates a defence characteristic	The gene list was curated by searching "common immunological terms" and literature searches followed by validation of the candidate genes
Innate GO [287]	780	Analyse specifically innate immune genes as classified by their gene ontology	Genes involved in the innate immune system only by Amigo Gene Ontology

IRIS [288]	1528	Immune genes expressed in immune cell populations. Immune cell specific expression is an indicator of importance in the function of the immune system	List was assembled from genome wide microarray expression profiling of immune cells
Current immune targets [14]	28	Genes are of relevance to clinical situation	Genes list assembled from currently used or prospective immune checkpoint targets
TCR [289]	248	T cell receptor genes included as a control of individual mutation rate	List compiled from TCR gene family using Hugo Gene Nomenclature Committee (HGNC)
IgG [289]	432	Immunoglobulin genes included as a control of individual mutation rate	List compiled from IgG gene family using HGNC
HLA [289]	45	HLA genes included as a control of individual mutation rate	List compiled from HLA gene family using HGNC
House Keeping [290]	407	Housekeeping genes included as a control for low promoter conservation levels	Used microarray and EST data to determine housekeeping genes across 18 human tissue types.
Transcription Factors [291–294]	812	Transcription factor genes included as a control for high promoter conservation levels	Literature search for lists of transcription factor or curation of transcription factor databases

2.19 Amplification/Deletion (AMP/DEL) study

Dr. Stephen Madden, RCSI, performed promoter conservation studies using the immune gene lists collated in section 2.18. Dr Madden determined the number of nucleotides conserved in the promoter region of each gene in the gene lists examined. The average number of conserved nucleotides for all genes within each gene list was used as a measure of promoter conservation rate. Dr. Madden downloaded publicly available aCGH data for 10 cancers from the gene expression omnibus. All data was analysed by Dr. Madden using R statistical programming, the Bioconductor package snapCGH was used to analyse the aCGH data (244A). The data was processed, and genomic breakpoints were detected using both the gain and loss of DNA (GLAD) and the DNAcopy methods. The aCGH analysis predicted regions of chromosomal amplification or deletion. This was then overlapped with our assembled gene lists. This was done on a sample by sample, cancer by cancer basis, where the average percentage overlap per cancer type was calculated for each gene list, by averaging the overlap of each individual sample within each cancer type. Statistical over/under representation was determined using a paired t-test by comparing the percentage overlap of each gene list versus a background of all other genes. All p-values were adjusted for multiple testing using the Benjamini and Hochberg method.

2.20 Point mutation study

Dr. Bruce Moran, UCD, carried out a study of the point mutation rate of the gene lists from the TCGA dataset. A manifest file containing the 33 available cancer-type MuTect2 MAF files from TCGA was downloaded. The associated compressed file was decompressed and converted to variant call format (VCF) using the 'maf2vcf.pl' tool and sorted by chromosome. Non-tumour samples were removed using 'SelectVariants' in GATK4 software. Each VCF was read into R (v3.4.4) using 'vcfRead' from the VariantAnnotation package and 'InputVcf' from the customProDB package. Variants in VCFs were annotated using biomaRt software to find chromosome name, start- and end-position, strand, external gene name, Ensembl gene ID and EntrezGene ID. Manually curated gene lists (**Table 2.10**) were read into R using 'read_tsv' from the Tidyverse. For each gene in a gene list, the number of variants per disease-type were calculated by a simple summing procedure. This integer value was then normalised to the gene length found in the annotation by dividing by total kilobase-pairs (Kb). This resulted in a set of Kb-normalised variant-counts per gene for each gene list. Randomly selected background or "bootstrap" gene lists were implemented to determine if the level of background mutations was significantly divergent from that of the gene list. To do this, a set of random genes found in the VCF and of equal size to the gene list had Kbp-normalised variant-counts per gene calculated. A Wilcoxon Rank Sum test was then performed against the gene list Kb-normalised variant-count data. Each bootstrap set and p-value were recorded and plotted.

2.21 Statistics

Unless otherwise stated p values were calculated using the student's t-test (two tailed with unequal variance) Tukey honest significance test, Mann Whitney test or Wilcoxon test as appropriate using Medcalc v18.6. Correlation analysis was calculated using Spearman Rho rank correlation using Medcalc v18.6. All statistical analysis was performed on biological triplicates or average values for grouped data and a cut off value of $p<0.05$ was considered significant. IC50 values were calculated using dose effect analyser Calcusyn (Biosoft, Version 1.1) and are representative of triplicate biological experiments.

3. Cytotoxicity profile of PBMCs isolated from HER2+ breast cancer patients on the TCHL clinical trial (ICORG10-05)

3.1 Introduction

ICORG10-05 was a neo-adjuvant phase II clinical trial which enrolled 88 HER2+ breast cancer patients. Treatment arms compared chemotherapy (docetaxel (Taxotere®) and carboplatin, (TC)) in combination with trastuzumab (Herceptin® (H)) alone (TCH), lapatinib (Tyverb® (L)) alone (TCL) or lapatinib with trastuzumab (TCHL). The TCL arm was terminated early due to the results of the ALTTO trial which showed lapatinib alone was inferior to trastuzumab [295]. As part of the translational element of the trial, blood samples were taken from patients before (pre-treatment) and after they received treatment (post-treatment). Post-treatment samples were taken before surgery. PBMCs were isolated from whole blood between 2011 and 2013 and frozen until needed for use in the assay. Immune cytotoxicity assays and SNP analysis were performed using the PBMCs from the trial. Direct cytotoxicity and T-ADCC against the SKBR3 cell line was measured. The overall cytotoxicity against the SKBR3 cell line was also determined, this is the cumulative cytotoxicity made up of direct cytotoxicity and T-ADCC. Direct cytotoxicity against the K562 HER2-, chronic myelogenous leukaemia cell line was also measured as these cells are particularly susceptible to immune cell-mediated cytotoxicity due to an absence of MHC class-I expression.

Matched pairs of pre- and post-treatment samples were used in immune cytotoxicity assays to examine the effect of treatment on the ability of PBMCs to elicit T-ADCC against the SKBR3 and K562 cell lines. Correlation of cytotoxicity levels with response to treatment (Complete responder (CR)/ Partial responder (PR)/Non-responder (NR)) was examined. CR was defined as having no residual invasive tumour in the breast or lymph nodes at surgery. PR was defined as a partial reduction in tumour burden which did not reach a complete response. NR was defined as showing no regression of tumour burden or tumour progression. Cytotoxicity levels were also examined in the context of treatment arm (TCHL, TCH and TCL). A subset of PBMC samples was used to determine the effect of the immune checkpoint inhibitor pembrolizumab on T-ADCC and direct cytotoxicity.

The patients' germline SNPs were analysed to determine any association with response to therapy or cytotoxicity levels elicited by patient PBMCs. The SNPs examined were selected as they have been linked to immune-mediated cytotoxicity and response to therapy in patients. Fc receptors are crucial in eliciting the trastuzumab-mediated immune response, this effect is also linked to patient outcome when receiving trastuzumab treatment [25,274,296]. KLRK1 is classically associated with NK cell-mediated cytotoxicity and has been previously linked to treatment outcome [273,274,297]. SNPs in the ABCB1 gene can affect the transport of chemotherapies commonly used in breast cancer, these effects have been shown to affect response to treatment [273,274,297]. The selected SNPs are associated with Fc receptors (RS10917661, RS1801274, RS396991 and RS428888), ABCB1 (RS1045642 and RS1128503) and KLRK1, a regulator of NK cell function (RS1049174 and RS2255336).

3.2 Characteristics of patient cohort

Table 3.1 and Table 3.2 details the PBMC samples revived from cryopreservation for use in this analysis along with treatment arm and response data for these patients. Samples from 51 patients which included matched pre-treatment and post-treatment pairs for 26 patients were used in this analysis.

Table 3.1: Complete set of patient samples from the TCHL trial revived for analysis in this study. Samples with an asterisk were included in matched pre- and post- treatment analysis. TCHL- Chemotherapy, trastuzumab and lapatinib, TCH- chemotherapy and trastuzumab, TCL- chemotherapy and lapatinib, CR- complete responder, PR- partial responder, NR- non-responder.

Patient Sample	Treatment Arm	Response
1	TCHL	PR
3*	TCL	NR
4*	TCHL	PR
5	TCHL	PR
6*	TCH	NR
7*	TCL	PR
8*	TCL	CR
9*	TCH	CR
11*	TCHL	PR
12*	TCL	NR
14*	TCH	CR
15*	TCL	CR
17	TCL	NR
18*	TCHL	PR
20*	TCHL	CR
21	TCHL	CR
22*	TCHL	PR
25	TCL	PR
26*	TCH	CR
29*	TCL	PR
31	TCHL	CR
32*	TCH	CR
33	TCH	PR

34*	TCH	CR
35	TCH	UNK
37	TCHL	PR
38	TCH	PR
41	TCHL	UNK
42*	TCHL	NR
43	TCH	CR
44	TCHL	CR
45	TCH	CR
46	TCH	PR
48	TCH	CR
49	TCHL	CR
50*	TCH	PR
51	TCHL	CR
52	TCH	CR
54*	TCHL	PR
56*	TCHL	PR
59*	TCH	CR
61*	TCHL	CR
62	TCHL	CR
64	TCHL	CR
72*	TCH	NR
75	TCHL	UNK
76	TCH	CR
82	TCHL	CR
84	TCHL	PR
87*	TCHL	PR
88*	TCHL	PR

Table 3.2: Revived patient cohort sample sizes including trial arm and response data for pre-treatment samples and pre- *vs.* post-treatment samples.

	TCHL			TCH			TCL		
	CR	PR	NR	CR	PR	NR	CR	PR	NR
Pre-treatment	10	12	1	11	4	2	2	3	3
Pre- *vs.* post-treatment	2	8	1	5	2	2	2	2	2

3.3 Pre-treatment patient samples

3.3.1 The impact of viability on PBMC activity

51 pre-treatment patient samples were revived from cryopreservation for analysis, and a range of viability levels in the PBMC samples was detected (0-98.7 %). Previous studies have shown the need for a viability cut off with cryopreserved PBMCs, as there can be correlation with increased activity at lower viability levels. A cut off point of 70 % viability or greater was used, as per Weinberg *et al.*[298]. 8 pre-treatment samples had a viability of less than 70 %. This left 43 pre-treatment samples for analysis (CR n=18, PR n=14, NR n=9 and UNK n=3). The cytotoxic capacity of the patient PBMCs were compared between response cohorts, there was insufficient data for unknown responders. There was no significant correlation between cytotoxicity and viability (**Table 3.3**).

Table 3.3: Viability and cytotoxicity correlations for pre-treatment samples using Spearman's coefficient of rank correlation (rho) test.

Response	Direct Cytotoxicity-SKBR3	T-ADCC-SKBR3	Direct Cytotoxicity-K562
CR (n=18)	-0.421 p=0.0817	-0.197 p=0.4328	-0.393 p=0.1640
PR (n=14)	-0.482 p=0.1334	0.412 p=0.1618	-0.505 p=0.0780
NR (n=9)	-0.200 p=0.6059	0.333 p=0.3807	-0.350 p=0.3558

3.3.2 Cytotoxicity levels elicited by PBMCs - pre-treatment

Cytotoxicity levels of patient PBMCs were determined to assess whether cytotoxic capacity was predictive of response to therapy. Using the Mann-Whitney test there was no significant difference between response cohorts (CR *vs.* PR *vs.* NR) in pre-treatment levels of direct cytotoxicity against the K562 cell line or overall cytotoxicity, direct cytotoxicity and T-ADCC levels against the SKBR3 cell line (**Table 3.4**). All response cohorts showed a significant increase in cytotoxicity with the addition of trastuzumab, shown by a significant increase from direct cytotoxicity to overall cytotoxicity, using the Wilcoxon rank test for paired samples (**Figure 3.1**).

Table 3.4: Average pre-treatment cytotoxicity levels for CR (n=18), PR (n=14) and NR (n=9) ± standard error of the mean.

	CR	**PR**	**NR**
Direct Cytotoxicity- K562	17.05 ± 2.6 %	13.36 ± 2.21 %	15.38 ± 1.88 %
Overall Cytotoxicity- SKBR3	23.15 ± 3.8 %	22.38 ± 4.14 %	23.28 ± 6.65 %
Direct Cytotoxicity- SKBR3	12. 47 ± 2.13 %	10.15 ± 2.42 %	12.26 ± 2.33 %
T-ADCC- SKBR3	10.86 ± 2.45 %	11.71 ± 3.09 %	10.71 ± 4.96 %

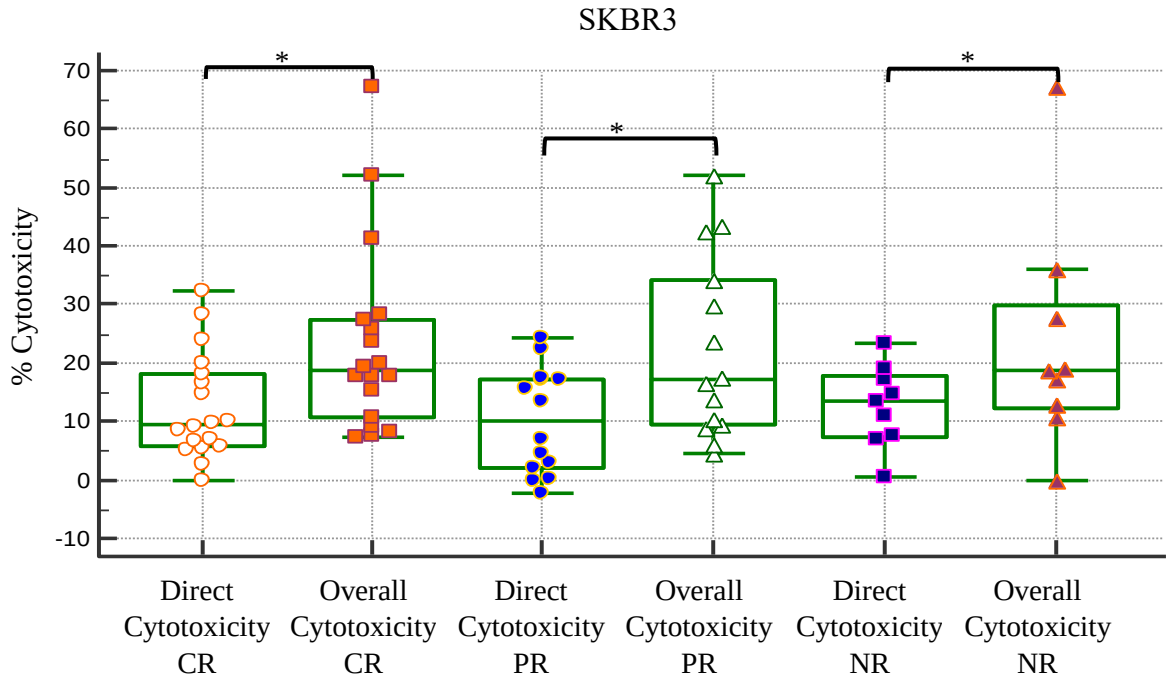

Figure 3.1: Box and whisker plot showing the cytotoxicity levels against the SKBR3 cell line with and without the addition of trastuzumab (10 µg/µL) in pre-treatment samples broken down by response type, CR (n=18), PR (n=14) NR (n=9). Significance was determined by Wilcoxon paired rank test. $p<0.05$ denoted by *.

3.3.3 Summary

There was no significant difference in cytotoxicity between responders in the pre-treatment setting (**Table 3.4)**. PBMCs were capable of eliciting an increased level of cytotoxicity in the presence of trastuzumab, independent of response to treatment (**Figure 3.1**).

3.4 Comparison of Cytotoxicity levels elicited by PBMCs with matched pre- and post-treatment samples

3.4.1 The impact of viability on PBMC cytotoxic capacity

Matched pre- and post-treatment PBMC samples were assessed to measure the impact of neo-adjuvant chemotherapy in an *in vitro* cytotoxicity capacity. 54 samples were revived for use in the immune cytotoxicity assay, 26 pre-treatment samples and 26 post-treatment samples (**Table 3.1**). There was a viability of less than 70 % in 3 pre-treatment and 4 post-treatment samples; which resulted in sample cohort of 19 paired pre-and post-treatment samples. These samples were primarily analysed within pre- and post-treatment cohorts. There was no correlation between viability and cytotoxicity levels (**Table 3.5**).

Table 3.5: Viability and cytotoxicity correlations for matched pre-treatment and post-treatment samples using Spearman's coefficient of rank correlation (rho) test.

Direct Cytotoxicity- K562		**Overall Cytotoxicity- SKBR3**		**Direct Cytotoxicity- SKBR3**		**T-ADCC-SKBR3**	
Pre	Post	Pre	Post	Pre	Post	Pre	Post
-0.317	-0.364	-0.058	-0.225	-0.248	-0.0895	0.175	-0.225
p=0.200	p=0.137	p=0.814	p=0.355	p=0.305	P=0.716	p=0.474	p=0.355

3.4.2 Cytotoxicity levels elicited by PBMCs – matched pre- and post-treatment

There was a significant decrease in direct cytotoxicity against the K562 cell line in the post-treatment samples (p=0.039) (**Table 3.6 and Figure 3.2**). There was no significant change in overall cytotoxicity or direct cytotoxicity against the SKBR3 cell line between pre- and post-treatment samples (**Table 3.5**). However, a significant decrease in T-ADCC in post-treatment samples compared to pre-treatment levels was detected (p=0.009) (**Table 3.6 and Figure 3.3**).

Table 3.6: Average cytotoxicity values for all matched pre- and post-treatment samples ± standard error of the mean. $p<0.05$ denoted by *.

	Pre-treatment	**Post-treatment**
Direct Cytotoxicity- K562	15.23 ± 1.78 %	11.46 ± 1.18 % *
Overall Cytotoxicity-SKBR3	24.27 ± 4.02 %	19.08 ± 2.11 %
Direct Cytotoxicity- SKBR3	11.3 ± 2.25%	13.79 ± 1.72 %
T-ADCC- SKBR3	13.46 ± 2.5 %	6.21 ± 1.37 % *

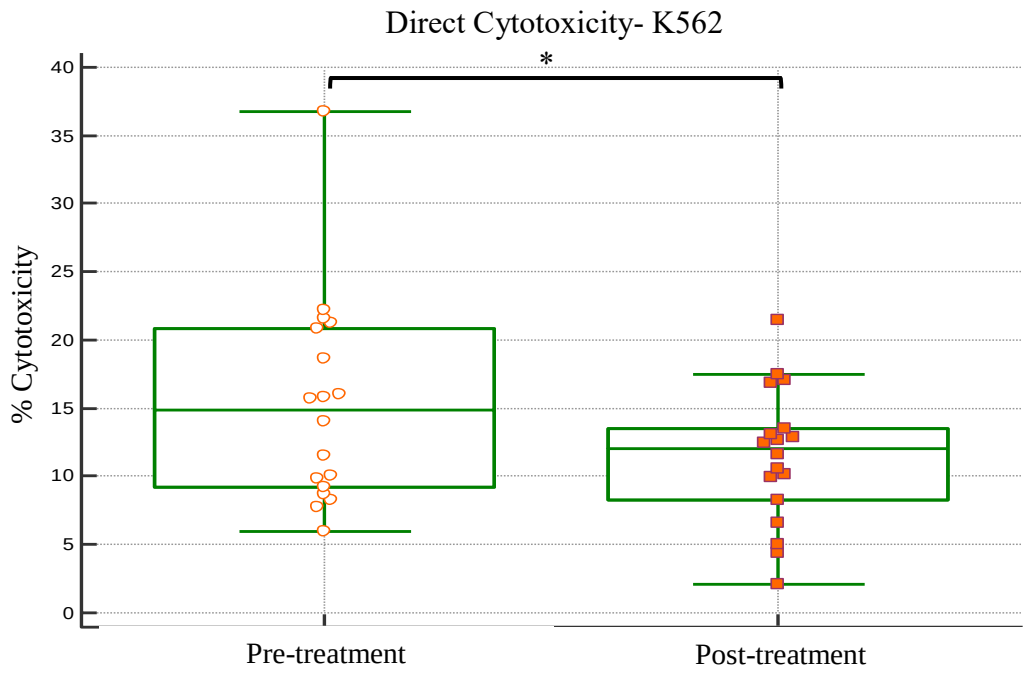

Figure 3.2: Box and whisker plot showing the direct cytotoxicity against the K562 cell line with pre- and post-treatment PBMCs (n=19). Wilcoxon paired rank test was used to measure significance. $p<0.05$ denoted by *.

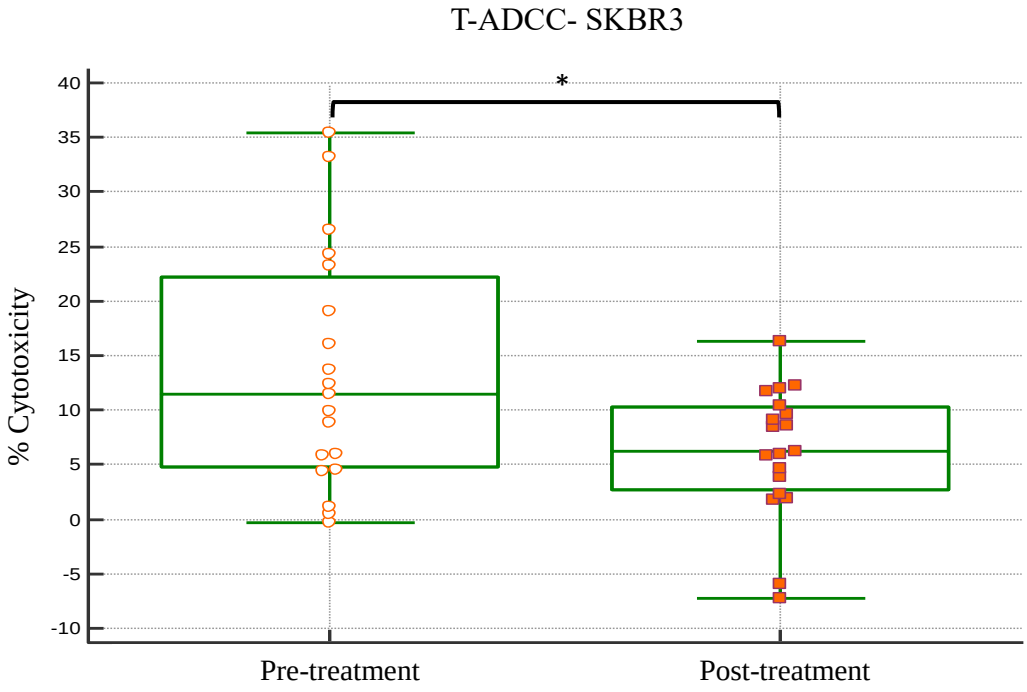

Figure 3.3: Box and whisker plot showing T-ADCC elicited by trastuzumab (10 µg/µL) against the SKBR3 cell line with pre- and post-treatment PBMCs (n=19). Wilcoxon paired rank test was used to measure significance. $p<0.05$ denoted by *.

3.4.3 Cytotoxicity levels elicited by PBMCs – matched pre- and post-treatment by response

To ascertain if the changes in *in vitro* PBMC cytotoxicity due to neo-adjuvant chemotherapy could be related to patient response to therapy, the data from Section 3.4.2 was broken down by patient response. Within the 19 matched pre- and post-treatment samples there were CR (n=8), PR (n=5) and NR (n=6). PR and NR patients were grouped in a Non-CR cohort to balance sample sizes (Non-CR n=11).

There was no change in direct cytotoxicity against the K562 cell line based on clinical response in pre- and post-treatment samples (**Table 3.7**).

Overall cytotoxicity levels against the SKBR3 cell line was decreased in post-treatment samples for CR (p=0.039). There was no significant difference in overall cytotoxicity between pre- and post-treatment samples for Non-CR (**Table 3.7 and Figure 3.4**).

There was no change in direct cytotoxicity against the SKBR3 cell line between CR and Non-CR patients pre- or post-treatment (**Table 3.7**).

Patients with a CR to treatment had a significantly lower level of T-ADCC against the SKBR3 cell line post-treatment (p=0.008). There was no significant change in T-ADCC between pre- and post-treatment samples for patients who had a Non-CR. PBMCs from Non-CR patients elicited a significantly higher level of T-ADCC post-treatment than CR patients (p=0.048) (**Table 3.7 and Figure 3.5**).

In order to assess the difference in cytotoxicity levels elicited by PBMCs with the addition of trastuzumab, direct cytotoxicity levels were compared to overall cytotoxicity levels. Cytotoxicity levels increased in pre-treatment samples with the addition of trastuzumab for both CR and Non-CR (p=0.009 and p=0.006 respectively) (**Table 3.7 and Figure 3.6**). In post-treatment samples cytotoxicity levels increased with the addition of trastuzumab for Non-CR (p=0.007) but not for CR (p=0.15) (**Table 3.7 and Figure 3.7**).

Table 3.7: Average cytotoxicity values ± standard error of the mean elicited by PBMCs pre- and post-treatment by CR (n=8) and Non-CR (n=11) patient cohorts. $p < 0.05$ denoted by *.

	Pre-treatment CR	Post-treatment CR	Pre-treatment Non-CR	Post-treatment Non-CR
Direct Cytotoxicity- K562	14.51 ± 3.87 %	8.77 ± 1.98 %	15.68 ± 1.75 %	13.17 ± 1.26 %
Overall Cytotoxicity- SKBR3	25 ± 7.88 %	15.56 ± 3.93 % *	23.74 ± 4.3 %	21.65 ± 2.1 %
Direct Cytotoxicity- SKBR3	10.57 ± 4.43 %	12.39 ± 2.94 %	11.83 ± 2.39 %	14.80 ± 2.14 %
T-ADCC- SKBR3	14.70 ± 3.83 %	3.67 ± 2.02 % *	12.56 ± 3.41 %	8.05 ± 1.72 %

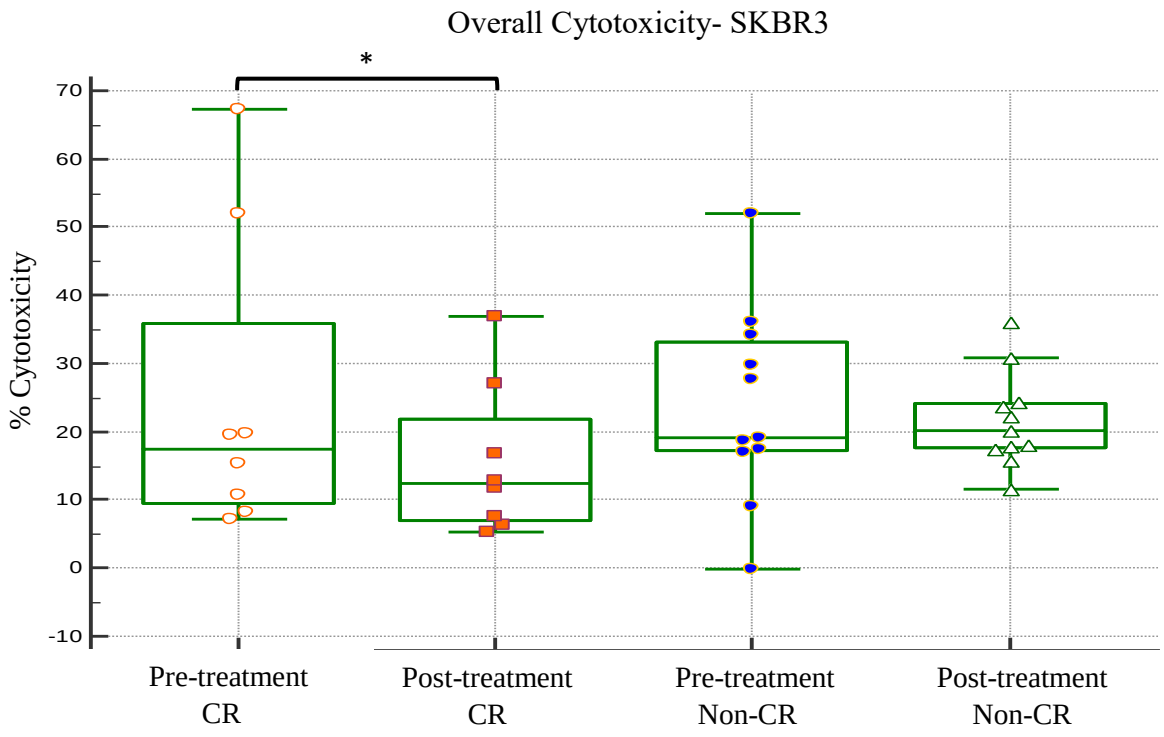

Figure 3.4: Box and whisker plot showing the overall cytotoxicity elicited in the presence of trastuzumab (10 µg/µL) by pre- and post-treatment PBMCs from CR and Non-CR patients against the SKBR3 cell line. Significance was determined by Wilcoxon paired rank test for paired samples. $p<0.05$ denoted by *.

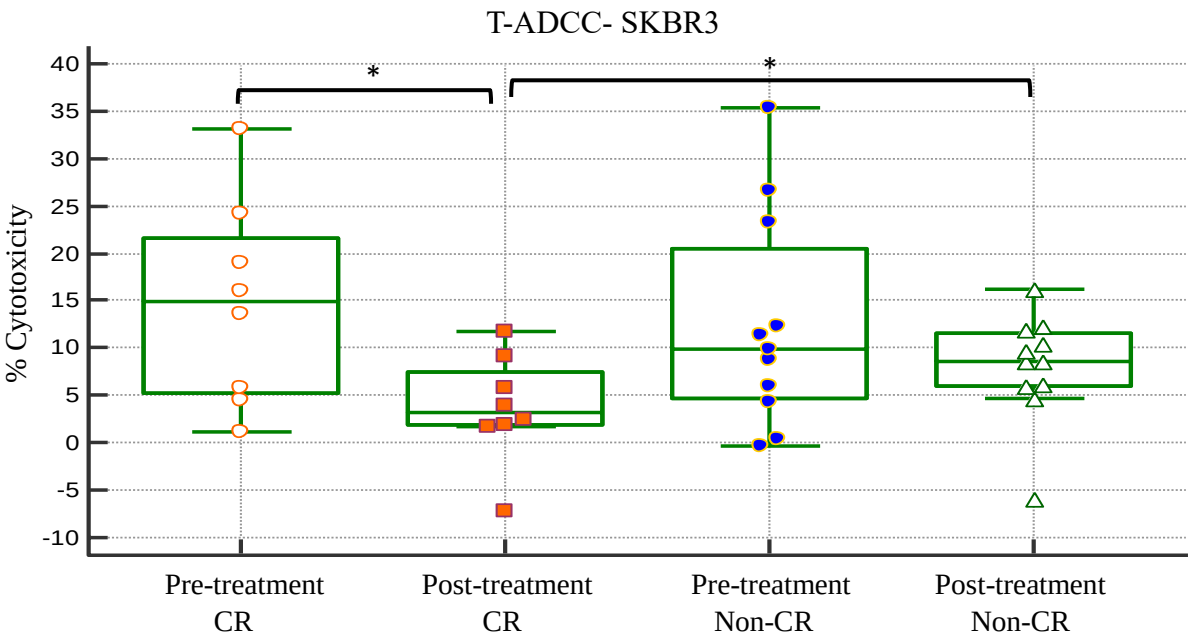

Figure 3.5: Box and whisker plot showing T-ADCC elicited in the presence of trastuzumab (10 µg/µL) by pre- and post-treatment PBMCs from CR and Non-CR patients against the SKBR3 cell line. Significance was determined by Wilcoxon paired rank test for paired samples and Mann-Whitney rank test for unpaired samples. $p<0.05$ denoted by *.

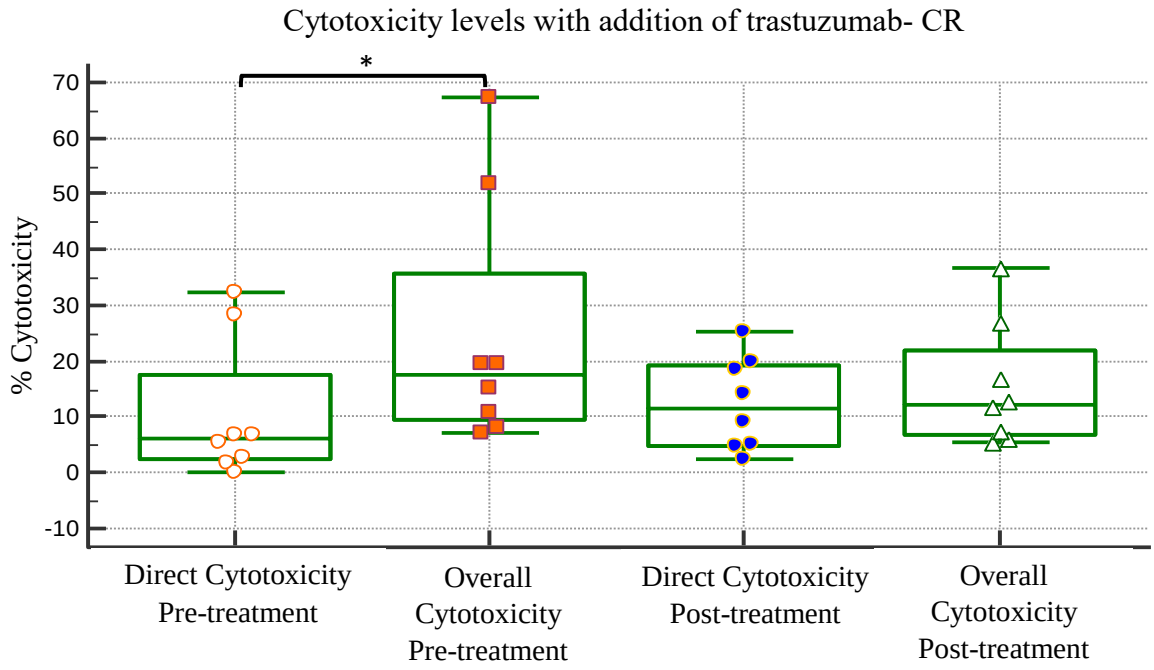

Figure 3.6: Box and whisker plot showing the cytotoxicity elicited against the SKBR3 cell line by pre- and post-treatment PBMCs from CR patients with and without trastuzumab treatment (10 µg/µL). Significance was determined by Wilcoxon paired rank test for paired samples. $p<0.05$ denoted by *.

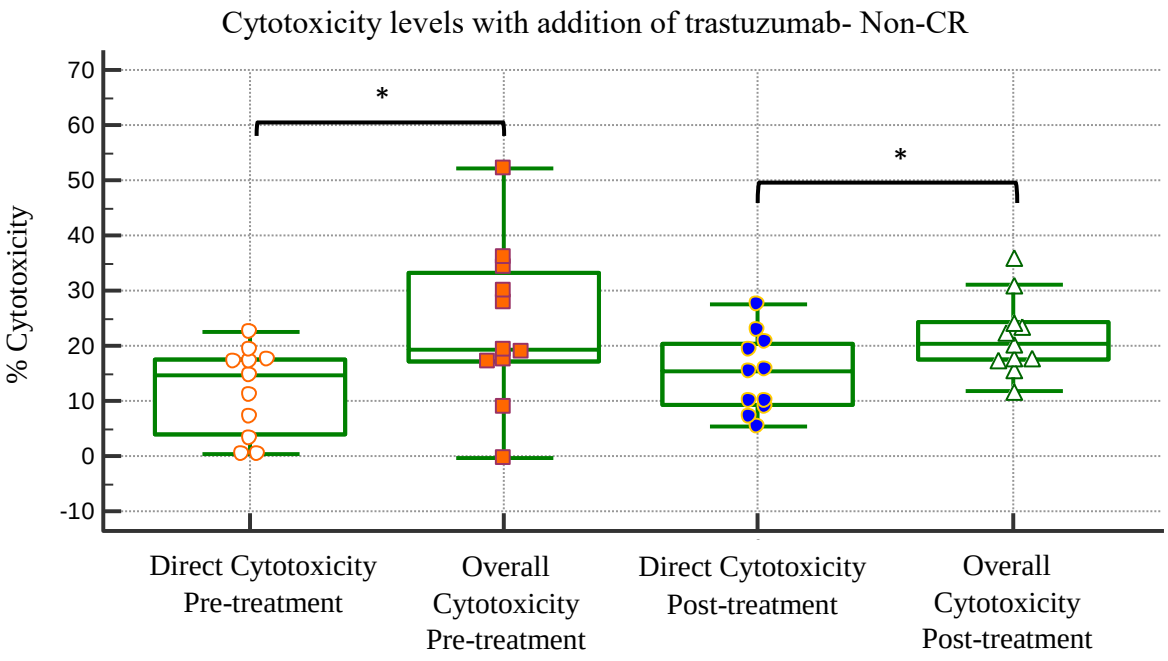

Figure 3.7: Box and whisker plot showing the cytotoxicity elicited against the SKBR3 cell line by pre- and post-treatment PBMCs from Non-CR patients with and without trastuzumab treatment (10 µg/µL). Significance was determined by Wilcoxon paired rank test for paired samples. $p<0.05$ denoted by *.

3.4.4 Cytotoxicity levels elicited by PBMCs – matched pre- and post-treatment by trial arm

To ascertain if the changes in *in vitro* PBMC cytotoxicity was due to neo-adjuvant chemotherapy received by the patients, the PBMCs from matched patient samples described in the data in Section 3.4.2 was broken down by trial arm.

Significant changes seen in Figures 3.8-3.10 need to be further investigated. Differences in pre-treatment levels of cytotoxicity between patient separated by trial arm lead to altered post-treatment levels between trial arms which are most likely artefacts of the dataset. Also, uneven distribution of response type (CR and Non-CR) within each trial arm have led to potential skewing of results (**Table 3.8**).

There was no significant difference in direct cytotoxicity against the K562 cell line in pre- *vs* post-treatment for patients enrolled on the TCHL, TCH or TCL trial arms measured by Wilcoxon paired rank test (**Table 3.9**).

There was no significant difference in overall cytotoxicity elicited against the SKBR3 cell line between pre-and post-treatments samples for patients enrolled on the TCHL, TCH or TCL trial arms measured by the Wilcoxon paired rank test (**Table 3.9**).

There was no difference in direct cytotoxicity against the SKBR3 cell line between pre- and post-treatment samples for patients enrolled on the TCHL or TCL trial arms measured by Wilcoxon paired rank test (**Table 3.9**). There was a significant increase in direct cytotoxicity in post-treatment samples from patients enrolled on the TCH arm when compared to pre-treatment levels (p=0.031) measured by Wilcoxon paired rank test. (**Figure 3.8 and Table 3.9**).

There was no significant change in T-ADCC between pre- and post-treatment samples for patients enrolled on the TCHL or TCH trial arms measured by Wilcoxon paired rank test (**Table 3.9**). There was a significant decrease in T-ADCC in post-treatment samples from patients enrolled on the TCL trial arm (p=0.013) measured by Wilcoxon paired rank test (**Figure 3.9 and Table 3.9**).

There was a significant increase in cytotoxicity level with the addition of trastuzumab in post-treatment samples on patients enrolled on the TCHL trial arm (p=0.004) (**Figure 3.10 and Table 3.9**). This difference was not significant for patients enrolled on the TCH or TCL trial arms (**Figure 3.10 and Table 3.9**).

Table 3.8: Matched pre- and post-treatment samples broken down by trial arm and response to treatment.

TCHL (n=9)	TCH (n=7)	TCL (n=3)
CR (n=2)	CR (n=4)	CR (n=2)
Non-CR (n=7)	Non-CR (n=3)	Non-CR (n=1)

Table 3.9: Average cytotoxicity values ± standard error of the mean elicited by PBMCs pre- and post-treatment by patients enrolled on the TCHL (n=9) and TCH (n=7) and TCL (n=3) trial arms. $p<0.05$ denoted by *.

	Pre-treatment TCHL	Post-treatment TCHL	Pre-treatment TCH	Post-treatment TCH	Pre-treatment TCL	Post-treatment TCL
Direct Cytotoxicity-K562	15.81 ± 2.15 %	12.94 ± 1.70 %	11.31 ± 1.48 %	9.32 ± 1.92 %	21.32 ± 7.81 %	11.28 ± 3.06%
Overall Cytotoxicity-SKBR3	30.14 ± 6.34 %	24.34 ± 2.89 %	13.55 ± 2.96 %	12.99 ± 2.26 %	31.69 ± 10.78 %	17.52 ± 5.66%
Direct Cytotoxicity-SKBR3	13.90 ± 3.33 %	14.40 ± 2.19 %	6.27 ± 2.35 %	12.68 ± 3.19 % *	15.22 ± 8.29 %	14.56 ± 6.19 %
T-ADCC-SKBR3	16.80 ± 4.33 %	10.19 ± 1.26 %	7.91 ± 2.74 %	2.46 ± 1.75 %	16.38 ± 4.46 %	3.01 ± 4.58 % *

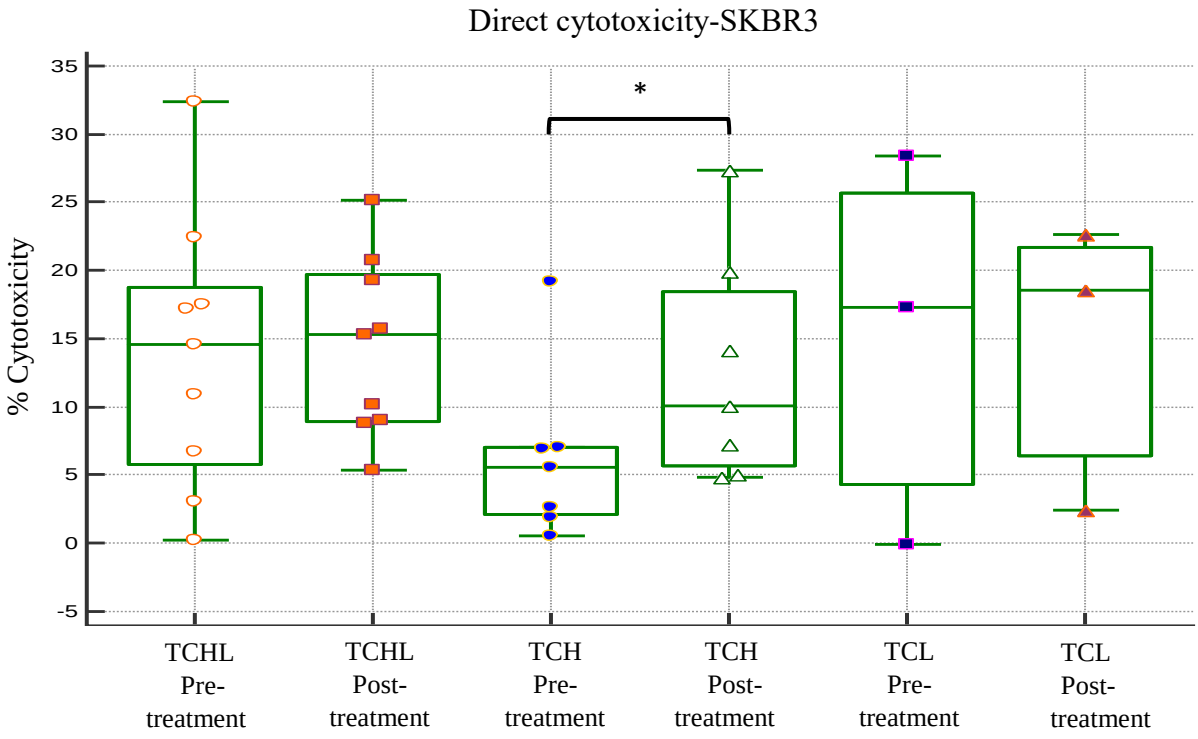

Figure 3.8: Box and whisker plot showing the direct cytotoxicity elicited against the SKBR3 cell line by pre- and post-treatment PBMCs from patients enrolled on the TCHL, TCH and TCL trial arms. Significance was determined by Wilcoxon paired rank test for paired samples. $p<0.05$ denoted by *.

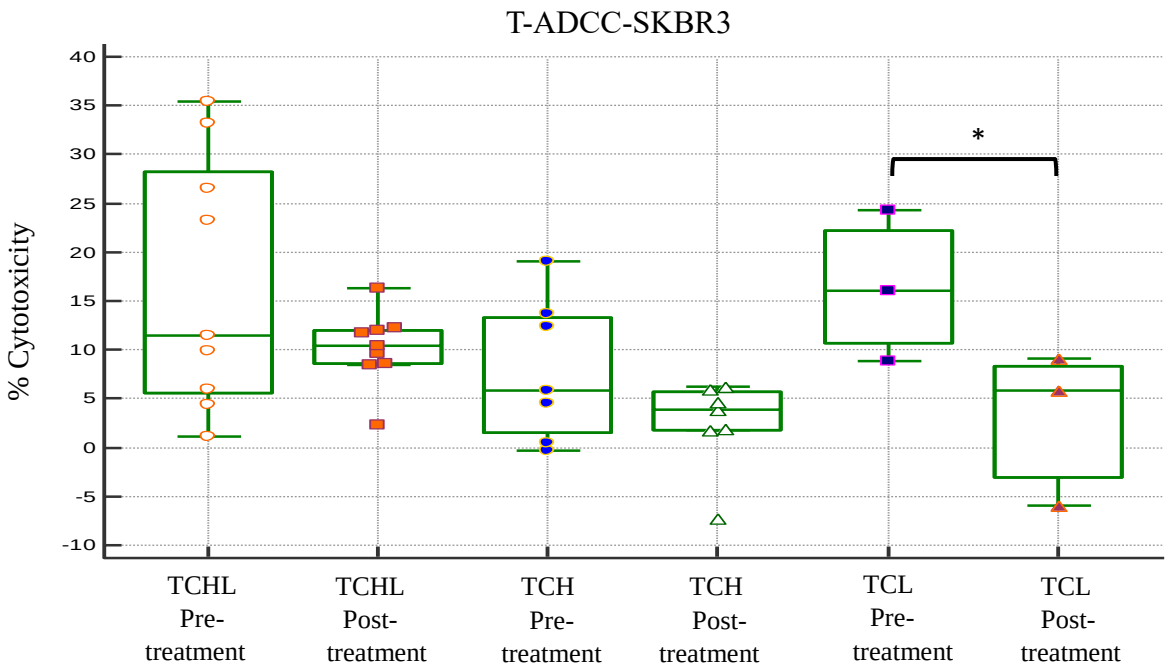

Figure 3.9: Box and whisker plot showing T-ADCC elicited by trastuzumab (10 µg/µL) against the SKBR3 cell line by pre- and post-treatment PBMCs from patients enrolled on the TCHL, TCH and TCL trial arms. Significance was determined by Wilcoxon paired rank test for paired samples. $p<0.05$ denoted by *.

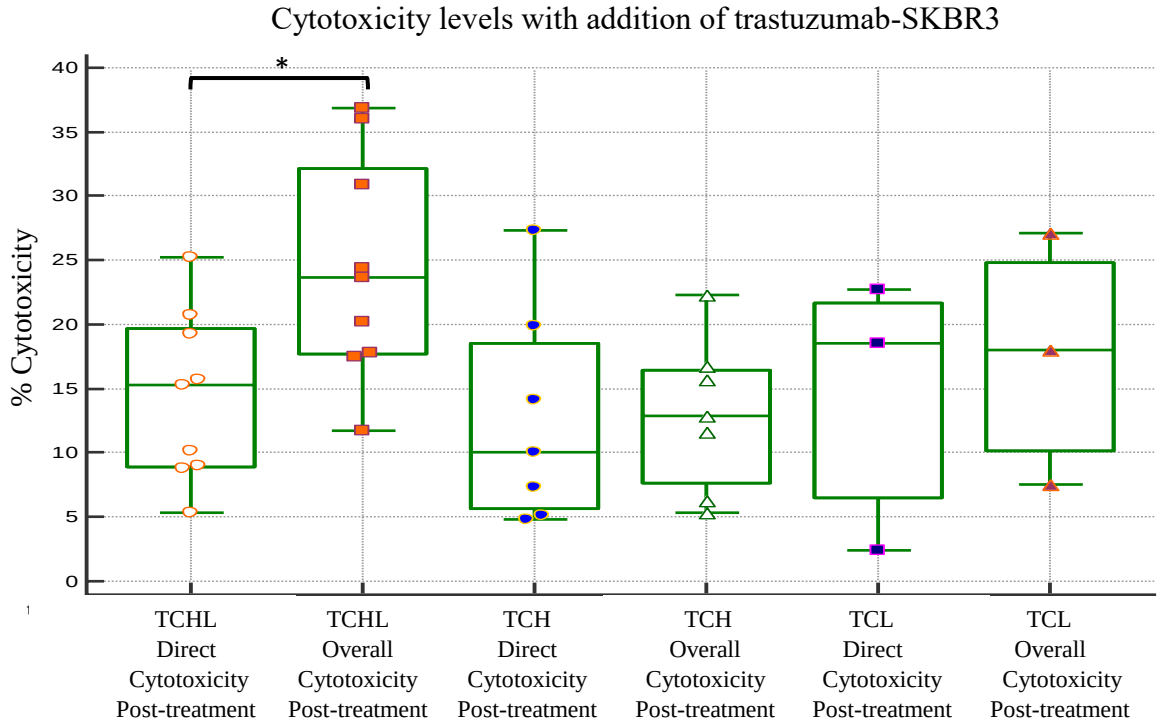

Figure 3.10: Box and whisker plot showing the cytotoxicity levels elicited with and without the addition trastuzumab (10 µg/µL) against the SKBR3 cell line by pre- and post-treatment PBMCs from patients enrolled on the TCHL, TCH and TCL trial arms. Significance was determined by Wilcoxon paired rank test for paired samples. $p<0.05$ denoted by *.

3.4.5 Summary

There was a decrease in the ability of PBMCs to elicit direct cytotoxicity and T-ADCC in post-treatment samples (**Section 3.4.2**). The decrease in T-ADCC in post-treatment samples was associated with a complete response to treatment, the CR cohort also showed a decreased level of overall cytotoxicity post-treatment (**Section 3.4.3**). Patients with a Non-CR did not show a significant decrease in T-ADCC or overall cytotoxicity post-treatment (**Section 3.4.3**). There were changes in cytotoxicity levels in post-treatment samples associated with treatment arm (**Section 3.4.4**). Direct cytotoxicity was increased in post-treatment samples for patients who received TCH treatment. Patients who received TCL treatment showed a decrease in T-ADCC post-treatment. Patients from the TCHL arm were the only trial arm to show an increase in cytotoxicity post-treatment with the addition of trastuzumab. These results will need to be further investigated as sample sizes were small and there was an uneven distribution of response cohorts.

3.5 The effect of the anti-PD-1 immune checkpoint inhibitor pembrolizumab on cytotoxicity elicited by patient PBMCs

3.5.1 The effect of pembrolizumab on pre-treatment PBMC cytotoxicity levels

To investigate if pembrolizumab could impact patient PBMC activity *in vitro*, 24 pre-treatment and 2 matched post-treatment samples (**Table 3.10**) were treated with trastuzumab in combination with pembrolizumab to determine the effect of inhibiting PD-1 on the cytotoxicity elicited by the patient PBMCs. All samples within this dataset had a viability of greater than 70 %. There was no correlation between viability and cytotoxicity (**Table 3.11**).

Table 3.10: Patient samples used to examine the effect of pembrolizumab on cytotoxicity elicited by patient PBMCs organised by response category (CR= pathological complete response, PR= partial response, NR= non-response, UNK= unknown).

Patient No.	Response	Patient No.	Response	Patient No.	Response	Patient No.	Response
21A	CR	1A	PR	3A	NR	35A	UNK
31A	CR	4A	PR	12A	NR	41A	UNK
49A	CR	5A	PR	17A	NR	75A	UNK
52A	CR	18A	PR	72A	NR		
62A	CR	33A	PR	72B	NR		
76A	CR	37A	PR				
82A	CR	38A	PR				
		84A	PR				
		87A	PR				
		88A	PR				
		88B	PR				

Table 3.11: Viability and cytotoxicity correlations for pre-treatment samples (n=24) using Spearman's coefficient of rank correlation (rho) test.

Direct Cytotoxicity-K562	Overall Cytotoxicity-SKBR3	Direct Cytotoxicity-SKBR3	T-ADCC-SKBR3
-0.360	-0.138	-0.403	0.337
p=0.09	p=0.529	p=0.060	p=0.156

When analysed together, there was no significant alteration to direct cytotoxicity elicited by the PBMCs against the SKBR3 or K562 cell lines in the presence of pembrolizumab (**Table 3.12**).

Across all 24 pre-treatment samples there was a significant increase in overall cytotoxicity elicited against the SKBR3 cell line when pembrolizumab was added to trastuzumab treatment (p=0.021). This was primarily due to a significant increase in T-ADCC in the presence of pembrolizumab (p=0.001). (**Table 3.21 and Figure 3.11**).

Table 3.12: Average direct cytotoxicity values ± standard error of the mean elicited by pre-treatment PBMCs +/- pembrolizumab (n=24). Significance denoted by *.

	Without pembrolizumab	**With pembrolizumab**
Direct Cytotoxicity-K562	14.50 ± 1.39 %	14.97 ± 1.52 %
Overall Cytotoxicity-SKBR3	17.23 ± 1.93 %	19.23 ± 1.94 % *
Direct Cytotoxicity-SKBR3	12.20 ± 1.74 %	11.24 ± 1.68 %
T-ADCC	4.68 ± 1.05 %	8.09 ± 1.21 % *

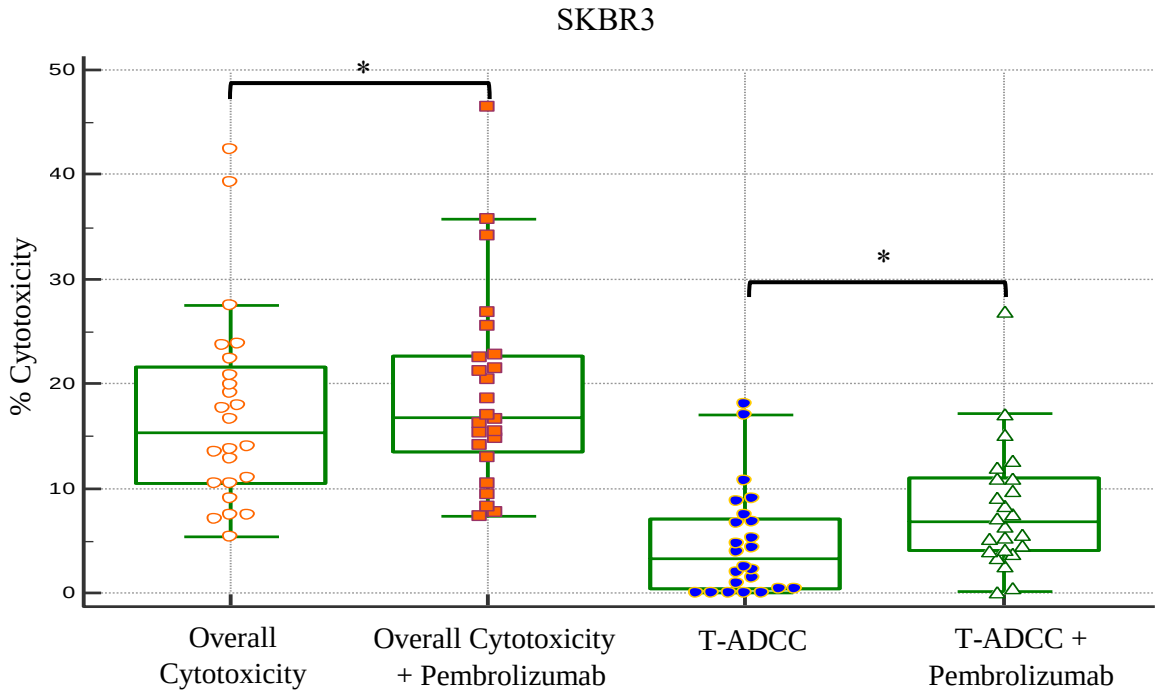

Figure 3.11: Box and whisker plot showing the overall cytotoxicity levels and T-ADCC in the presence of trastuzumab (10 µg/µL) elicited by pre-treatment PBMCs (n=24) with and without the addition of pembrolizumab treatment (10 µg/µL) elicited against the SKBR3 cell line. Significance was determined by the Wilcoxon rank paired test. * denotes p value of <0.05.

3.5.2 The effect of pembrolizumab on pre-treatment PBMC cytotoxicity levels when broken down by clinical response

Within the 24 pre-treatment patient samples used in this dataset, there were 7 CR, 14 Non-CR and 3 UNK (**Table 3.10**). When broken down by response to treatment 0/7 (0%) CR had a significant increase in T-ADCC with the addition of pembrolizumab (**Table 3.13 and Figure 3.12**). 4/10 PR and 3/4 NR (7/14, 50 % Non-CR) showed a significant increase in T-ADCC with the addition of pembrolizumab (**Table 3.13 and Figure 3.12**). This suggests that patients with a non-CR are more likely to have PBMCs that mediate increased T-ADCC in the presence of pembrolizumab.

This limited dataset suggests that this assay could act as a potential biomarker of response, identifying 50% (7/14) of patients that will have a non-CR to chemotherapy in the neo-adjuvant HER2+ breast cancer setting (**Patent application number GB 1811892.2**).

The ability of pembrolizumab to increase T-ADCC mediated by PBMCs suggests that the PBMCs isolated from the peripheral blood of partial responders contain ADCC-capable immune populations which are immunosuppressed through expression of PD-1, while the PBMCs of complete responders do not contain this PD-1 suppressed immune population. As this PD-1+/ADCC-capable immune cell type is present in the patient, it could also indicate that pembrolizumab treatment may be beneficial in increasing the immune response against the tumour in these patients.

Table 3.13: p values associated with increased T-ADCC with the addition of pembrolizumab for 21 pre-treatment samples with defined response data. p values were determined by unpaired Student's T test on data from triplicate wells for each sample. Significant p values are marked with an asterisk.

Patient No.	Response	p value for addition of pembrolizumab
21A	CR	0.227
31A	CR	0.571
49A	CR	0.163
52A	CR	0.970
62A	CR	0.880
76A	CR	0.082
82A	CR	0.341
1A	PR	0.605
4A	PR	0.003 *
5A	PR	0.201
18A	PR	0.178
33A	PR	0.091
37A	PR	0.008 *
38A	PR	0.790
84A	PR	0.009 *
87A	PR	0.072
88A	PR	0.011 *
3A	NR	0.002 *
12A	NR	0.637
17A	NR	0.031 *
72A	NR	0.011 *

A)

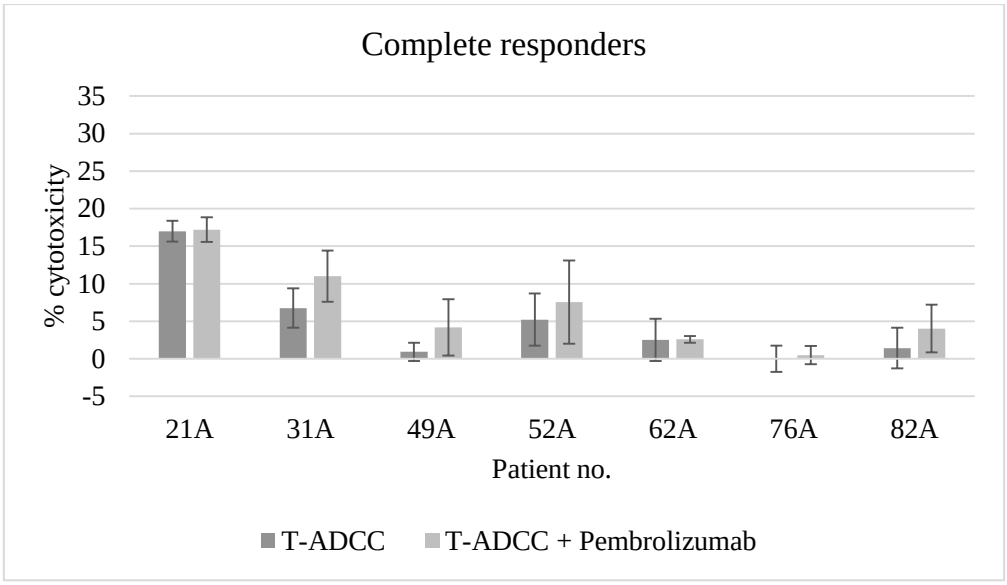

B)

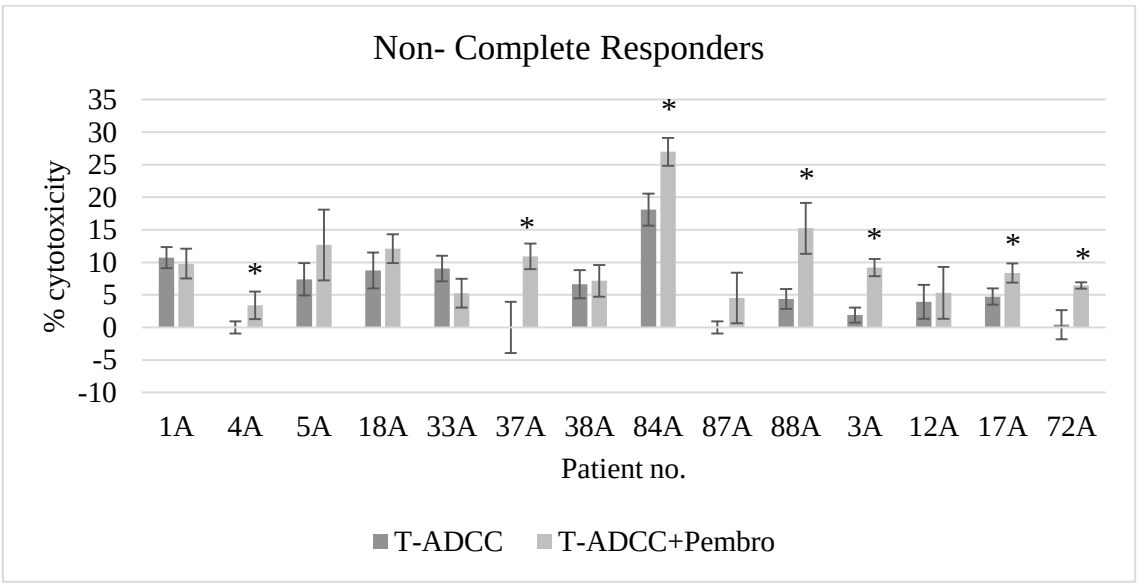

Figure 3.12: A) T-ADCC levels for CR (n=7) with and without the addition of pembrolizumab. **B)** T-ADCC levels for Non-CR (PR n=10, NR n=4) with and without the addition of pembrolizumab. Error bars represent values from triplicate wells. Significance was determined using the Student's T test. * denotes p value of <0.05.

3.5.3 The effect of pembrolizumab on matched pre- and post-treatment cytotoxicity levels

There were two matched pre- and post-treatment samples available for testing with the pembrolizumab/trastuzumab combination *in vitro*. The two sets of paired samples showed significant increases in T-ADCC with the addition of pembrolizumab in both pre-treatment samples (n=1 PR and n=1 NR), which was maintained in the post-treatment samples taken three months later (**Figure 3.13**). This demonstrates that the response to pembrolizumab may be sustained throughout treatment in the long-term.

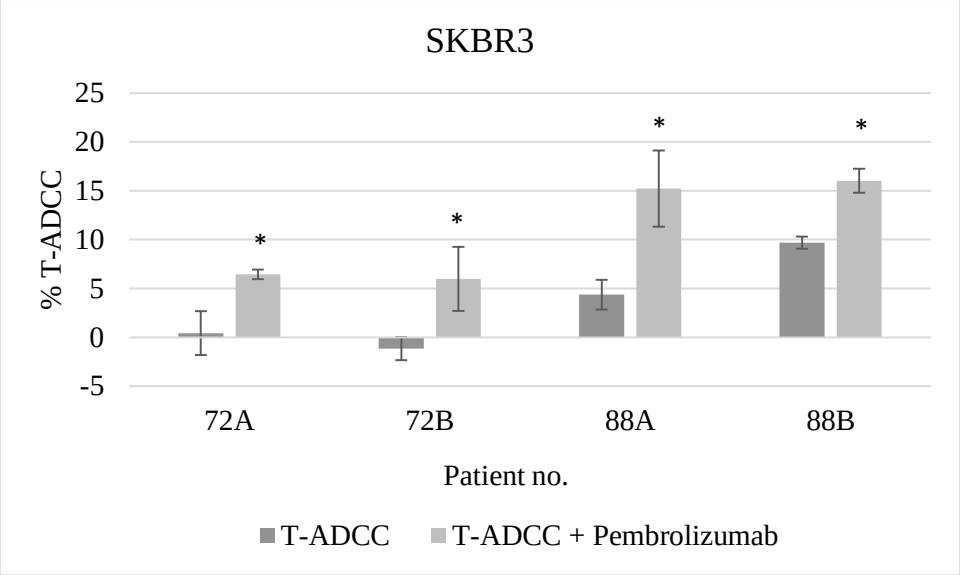

Figure 3.13: T-ADCC levels against SKBR3 cells for patient 72 and 88 pre- and post-treatment +/- pembrolizumab. Error bars represent values from triplicate wells. Student's T test was used to determine significance. * denotes p value of < 0.05.

3.5.4 TIL levels and the *in vitro* response to pembrolizumab

TIL levels were measured as part of the translational component of the ICORG 10-05 trial and are as yet unpublished. Corresponding TIL levels were available for 17/21 pre-treatment samples examined for response to pembrolizumab *in vitro*. Stromal and tumour infiltrating lymphocyte levels were investigated to see if they correlated with response to pembrolizumab *in vitro*.

There was no significant difference in TIL levels between CR (n=7) and Non-CR (n=10) patients examined in Section 3.5. This included TILs, stromal infiltrating lymphocytes (SILs) and combined TIL + SIL levels (**Figure 3.14 (A)**).

When the samples were broken down based on response to pembrolizumab *in vitro*, there were significantly more SILs in patients who did not respond to the addition of pembrolizumab (p=0.040). The combined level of TILs and SILs was also approaching significance (p=0.073) (**Figure 3.14 (B)**). When comparing immune cell levels for just the patients that responded in the assay to the immune cell levels in CR patients, there was significantly greater SILs and combined SIL + TIL levels for CR patients (p=0.025 and p=0.029 respectively) (**Figure 3.14 (C)**).

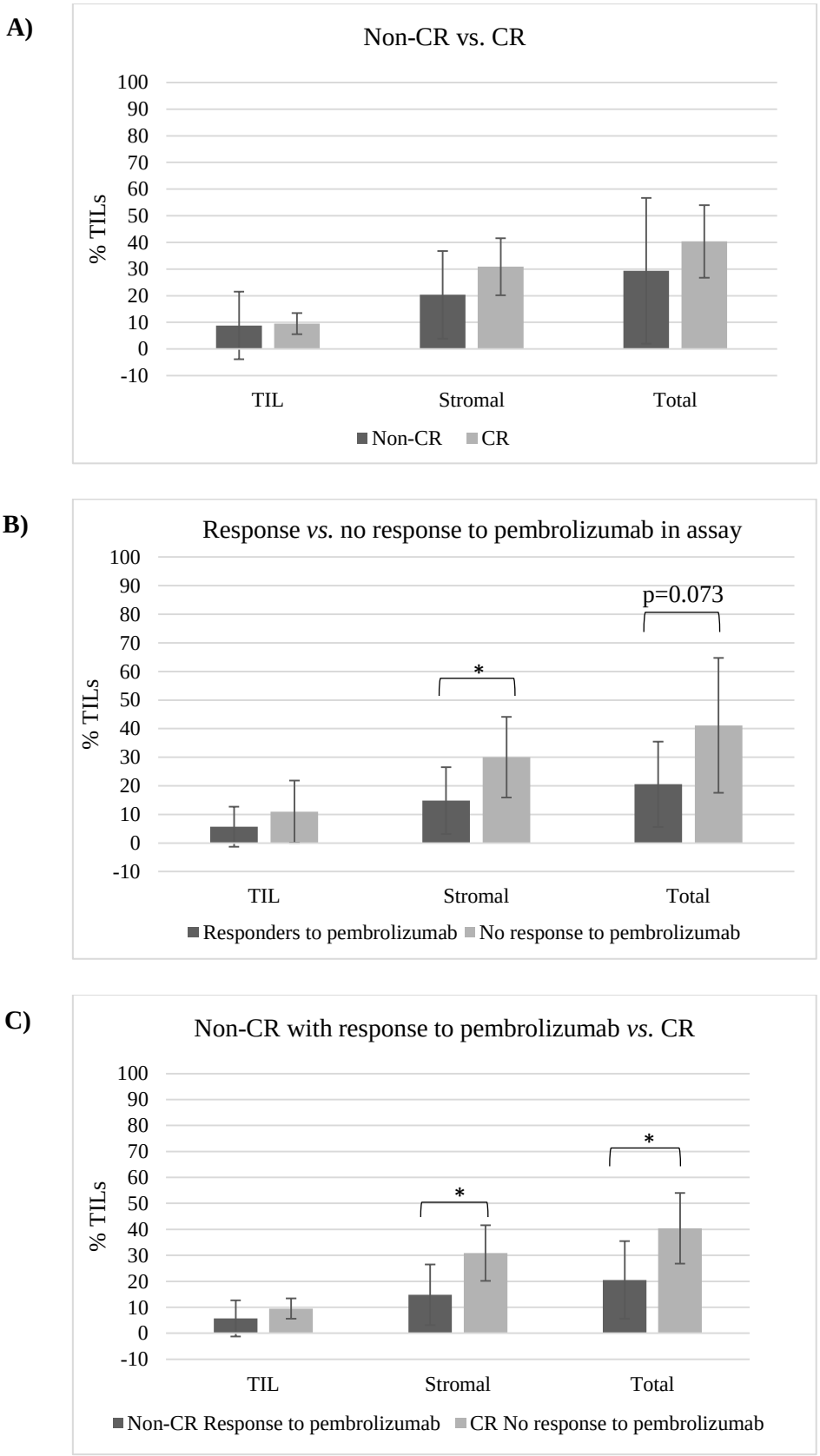

Figure 3.14: TIL, stromal TIL and total TIL levels associated with A) Non-CR (n=10) vs. CR (n=7) B) Assay responders (n=6) vs. Non-assay responders (n=11) C) Non-CR assay responders (n=6) vs. CR (n=7). Significance was determined by Student's T test. * denotes p value of <0.05.

3.5.5 Summary

This *in vitro* data suggests that pembrolizumab can enhance the immune response to trastuzumab using HER2+ breast cancer patient PBMCs through an increase in T-ADCC (**Section 3.5.1**). This is strong pre-clinical rationale for the combination of pembrolizumab and trastuzumab in the clinic. However, the study has also shown that patients with a Non-CR to neo-adjuvant chemotherapy are more likely to respond to pembrolizumab *in vitro* (**Section 3.5.2**). As this effect was not seen in any patients who had a CR, it indicates that;

1) A pembrolizumab/trastuzumab combination may only benefit some patients

2) This assay may be able to identify these patients (potentially a biomarker of response to pembrolizumab)

3) The assay may have the potential to predict response to current HER2-targeted therapy containing neo-adjuvant chemotherapy in HER2+ breast cancer.

One TCL patient showed a response to pembrolizumab in the *in vitro* assay which suggests the predictive potential of the assay is not confined to a trastuzumab-containing regimen. This response was maintained post-treatment in two matched pre- and post-treatment samples (**Section 3.5.3**). Patients who show a response to pembrolizumab *in vitro* show a decreased level of stromal lymphocyte infiltration compared with the CR cohort (**Section 3.5.4**).

3.6 The effect of SNPs on cytotoxicity elicited by PBMCs

Genetic factors such as single nucleotide polymorphisms (SNPs) can potentially influence immune cell activity and response to treatment. To examine the impact of natural variations in a drug resistance mechanism and receptors involved in the immune response to cancer, ABCB1, KLRK1 and Fc receptor polymorphisms were examined in the context of PBMC activity in the *in vitro* assays described in Sections 3.3 and 3.4.

The ABCB1 (P-gp) is a drug efflux pump associated with chemotherapy resistance [273,274]. The normal physiological role of ABCB1 is the excretion of harmful xenobiotics from the body in the gut and maintenance of the blood brain barrier [273,274]. Over-expression of ABCB1 in tumours can mediate resistance to chemotherapeutic agents [274]. SNP variations in ABCB1 can therefore impact bioavailability of substrate chemotherapeutics (docetaxel/paclitaxel/doxorubicin) and potentially alter tumour and immune cell susceptibility to these agents [273,274]. The NKG2D protein, from the KLRK1 gene, is important in regulating NK cell recognition of cells for elimination. Alterations in this protein can affect the NK cells ability to elicit cytotoxicity against cancer cells [297]. Alterations in Fc receptors

can also affect NK cells ability to bind to trastuzumab and elicit cytotoxicity against the cancer cell [25,274,296].

Germline DNA was available from 47 ICORG 10-05/TCHL patients through PBMCs while tumour DNA was extracted from 11 further ICORG 10-05 patients. The SNP status (homozygous for reference allele, heterozygous, homozygous for minor allele) for 58 patients was examined by the sequenom method and included in this analysis. Seven SNPs were examined; rs1045642, rs1049174, rs10917661, rs1128503, rs1801274, rs2255336, rs396991 and rs428888. The associated gene, proteins and function of these SNPs are characterised is Table 3.14.

Dr. Damien Cote, RCSI assessed the impact of the presence of these SNPs in the ICORG 10-05 *in vitro* cytotoxicity using the data generated in Sections 3.3 and 3.4. Pre- and post-treatment direct cytotoxicity (against SKBR3 and K562) and T-ADCC were categorised by patient SNP status. In addition, the absolute change/alteration between pre- and post-treatment levels (pre-treatment value – post-treatment value) was examined for direct cytotoxicity and T-ADCC as well, to provide a value associated with the impact of treatment. Significant alterations due to SNP status are presented.

Table 3.14: SNPs examined in this analysis.

rs ID	Associated Gene	Associated Protein	Function
rs1045642, rs1128503	ATP Binding Cassette Subfamily B Member 1 (ABCB1)	ABCB1	transport protein which can act as an efflux pump, associated with multi-drug resistance
rs1049174, rs2255336	Killer Cell Lectin Like Receptor K1 (KLRK1)	NKG2D	NKG2 family are relevant in regulating NK cell activity
rs10917661	Fc Fragment of IgG Receptor IIb (FCG2B)	FCG2B	IgG Fc receptor gene involved in the phagocytosis of immune complexes and in the regulation of antibody production by B-cells
rs1801274	Fc Fragment of IgG Receptor IIa (FCG2A)	FCG2A	IgG Fc receptor gene involved in the process of phagocytosis and clearing of immune complexes
rs396991, rs428888	Fc Fragment of IgG Receptor IIIa (FCG3A)	FCG3A	IgG Fc receptor gene involved in NK cell mediated ADCC response

3.6.1 SNPs in ABCB1 and cytotoxicity elicited by PBMCs

There was no difference in pre-treatment or post-treatment direct cytotoxicity against the K562 cell line associated with ABCB1 SNP status. However, the difference between pre- and post-treatment cytotoxicity levels was altered based on ABCB1 SNP status. Treatment received by the patients impacted the anti-K562 PBMC activity of patients with a heterozygous allele for the ABCB1 rs1045642 to a lesser extent than patients with a reference allele (p=0.011) or a minor allele (p=0.046) (**Figure 3.15**).

The minor allele for the ABCB1 rs1128503 SNP was associated with greater pre-treatment direct cytotoxicity against the SKBR3 cell line compared to patients with a heterozygous allele (p=0.050) (**Figure 3.16**). SNP status for ABCB1 did not produce a significant difference for PBMC-mediated cytotoxicity in any of the other assays examined.

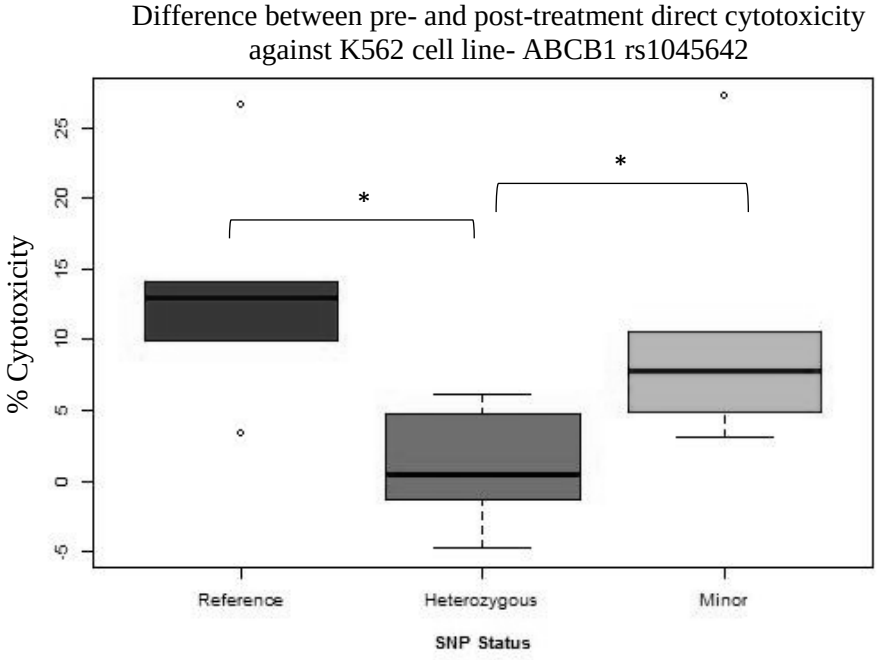

Figure 3.15: Box and whisker plot showing the reference (T/T) (n=5), heterozygous (C/T) (n=9) and minor (C/C) (n=5) SNP allele for ABCB1 rs1045642 for difference between pre- and post-treatment direct cytotoxicity against the K562 cell line. Significance determined by Tukey honest significant difference test. * denotes p value of <0.05.

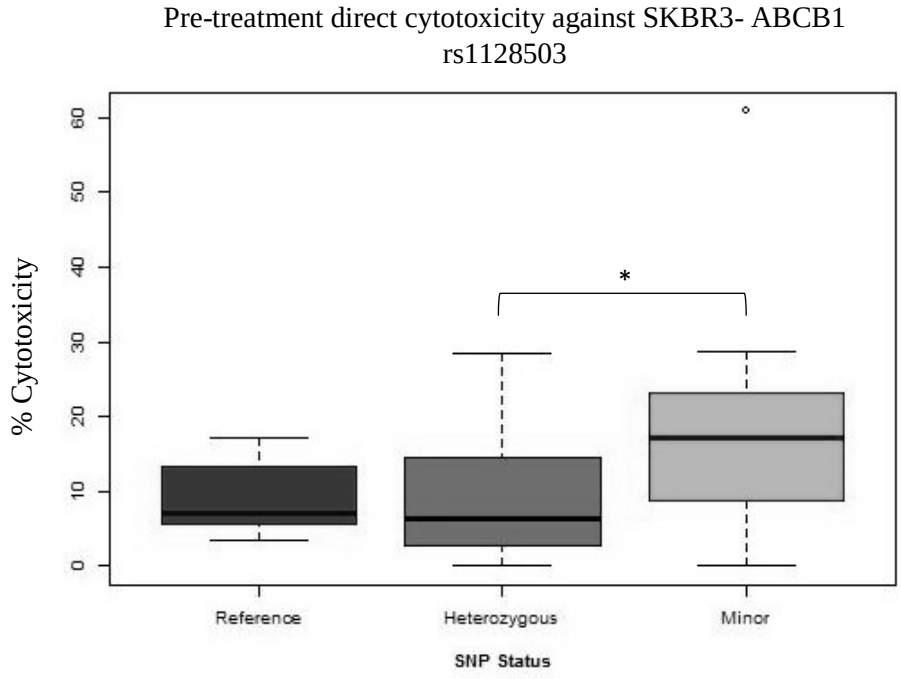

Figure 3.16: Box and whisker plot showing the reference (T/T) (n=7), heterozygous (C/T) (n=18) and minor (C/C) (n=16) SNP allele for RS1128503 for pre-treatment direct cytotoxicity against the SKBR3 cell line. Significance determined by Tukey honest significant difference test. * denotes p value of <0.05.

3.6.2 SNPs in KLRK1 and cytotoxicity elicited by PBMCs

Patients with a minor allele for the KLRK1 rs1049174 SNP showed a higher level of *in vitro* pre-treatment T-ADCC compared to patients with the reference or heterozygous allele (p=0.010 and p=0.003 respectively) (**Figure 3.17**). Treatment resulted in a significantly greater alteration in T-ADCC for patients with the minor allele compared to those with a heterozygous allele (p=0.048) (**Figure 3.18**).This effect was also seen for the KLRK1 rs2255336 SNP which showed higher pre-treatment T-ADCC in patients with the minor allele than those with the reference or heterozygous alleles (p=0.002 and p=0.008 respectively) (**Figure 3.19**). Treatment resulted in a greater alteration to the T-ADCC elicited by PBMCs with the minor allele of rs2255336 also, but the alteration did not reach significance versus the treatment induced changes in the heterozygous (p=0.077) and reference (p=0.092) allele samples. Further investigation the effect of treatment on T-ADCC regarding the rs1049174 SNP and the effects of the rs2255336 SNP on T-ADCC are required due to small sample size of the minor allele (n=2).

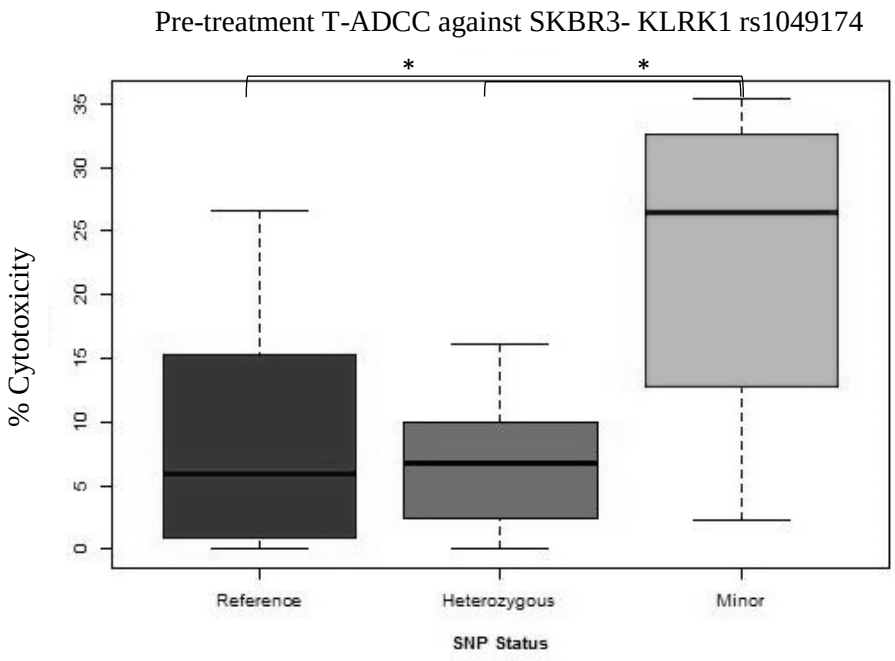

Figure 3.17: Box and whisker plot showing the reference (C/C) (n=19), heterozygous (C/G) (n=17) and minor (G/G) (n=4) SNP allele for KLRK1 rs1049174 for pre-treatment T-ADCC against the SKBR3 cell line. Significance determined by Tukey honest significant difference test. * denotes p value of <0.05.

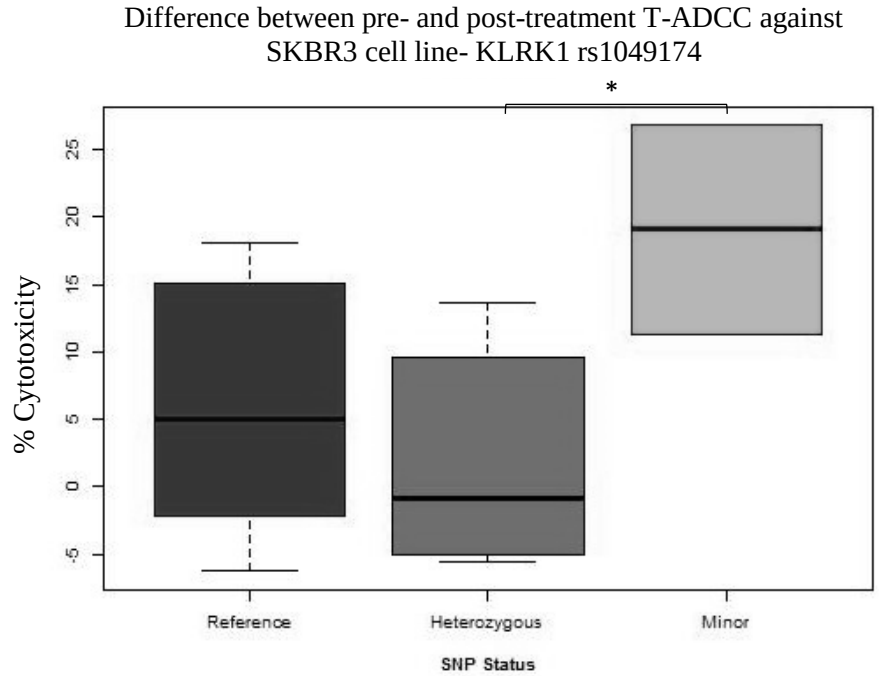

Figure 3.18: Box and whisker plot showing the reference (C/C) (n=9), heterozygous (C/G) (n=8) and minor (G/G) (n=2) SNP allele for KLRK1 rs1049174 for difference between pre- and post-treatment treatment T-ADCC against the SKBR3 cell line. Significance determined by Tukey honest significant difference test. * denotes p value of <0.05.

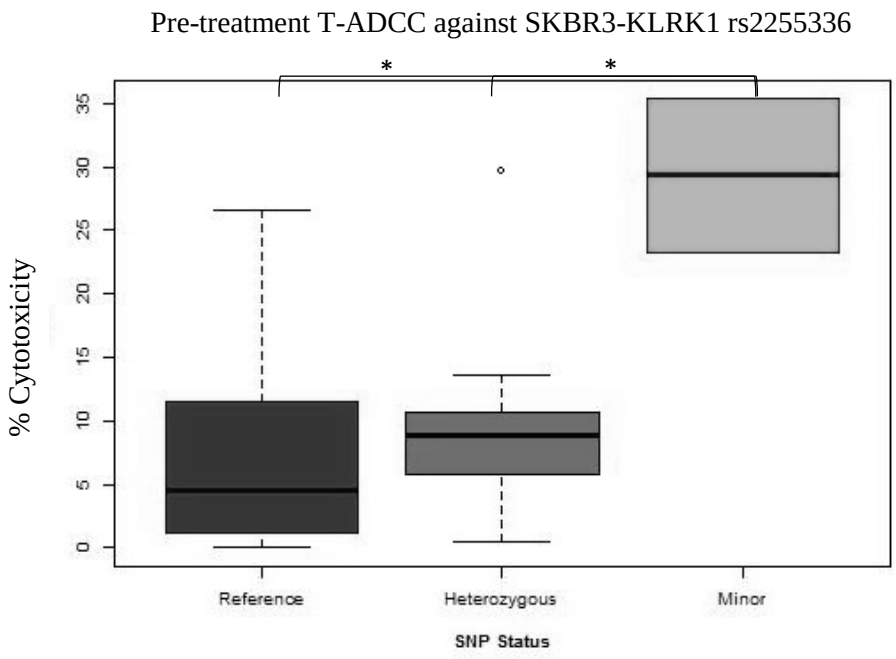

Figure 3.19: Box and whisker plot showing the reference (C/C) (n=28), heterozygous (C/T) (n=11) and minor (T/T) (n=2) SNP allele for KLRK1 rs2255336 for pre-treatment T-ADCC against the SKBR3 cell line. Significance determined by Tukey honest significant difference test. * denotes p value of <0.05.

3.6.3 SNPs in Fc receptors and cytotoxicity elicited by PBMCs

Treatment had significantly less impact on the *in vitro* capacity of PBMCs to kill SKBR3 cells for those patients with a minor allele for FCG3A rs396991 *vs.* patients with a heterozygous allele (p=0.025) and was approaching significance *vs.* patients with a reference allele (p=0.078) (**Figure 3.20**). Further samples will be required to further investigate this as the sample size is low (n=2). No significant changes were seen between FCG3A SNP groups when pre-treatment and post-treatment direct PBMC cytotoxicity against SKBR3 was examined.

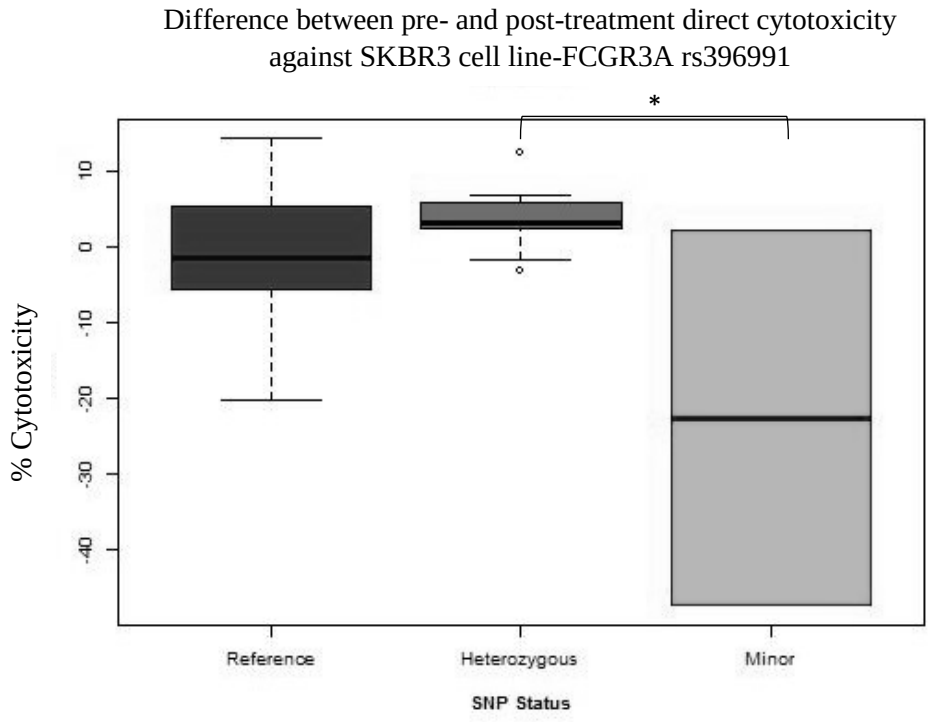

Figure 3.20: Box and whisker plot showing the reference (T/T) (n=9), heterozygous (C/T) (n=9) and minor (C/C) (n=2) SNP allele for FCG3A rs396991 for the difference between pre- and post-treatment direct cytotoxicity against the SKBR3 cell line. Significance determined by Tukey honest significant difference test. * denotes p value of <0.05.

3.6.4 Summary

SNPs in ABCB1, NKG2D and FCG3A affect the *in vitro* cytotoxicity levels elicited by HER2+ breast cancer patient PBMCs against cancer cells (**Section 3.6.1, 3.6.2 and 3.6.3**). The SNPs affect T-ADCC, direct cytotoxicity and can impact immune cell activity following neo-adjuvant therapy. Further investigation of these effects will need to be examined due to a small sample size for some allele types.

3.7 Summary

It has been reported that PBMC samples with a viability of less than 70 % are not suitable for *in vitro* assessment [298]. Therefore, only samples with a viability of greater than 70 % were included in this analysis.

There were no differences in *in vitro* cytotoxicity against K562, SKBR3 directly or T-ADCC between response cohorts in pre-treatment samples (**Section 3.3**).

When patients received neo-adjuvant chemotherapy (TCH, TCHL or TCL) there was a reduction in the ability of PBMCs to elicit direct cytotoxicity against K562 cells and T-ADCC against SKBR3 cells compared with pre-treatment levels (**Section 3.4.2**). When examined by response cohort, a decrease in T-ADCC post-treatment was associated with a pathological complete response to neo-adjuvant chemotherapy (**Section 3.4.3**). Patients who did not have a complete response did not show a decrease in T-ADCC or overall cytotoxicity (direct + T-ADCC) post-treatment (**Section 3.4.3**). There were also alterations present in PBMC-mediated cytotoxicity levels based on the treatment the patients received (TCHL, TCH or TCL) (**Section 3.4.4**)

Across all samples examined, the addition of pembrolizumab to trastuzumab significantly increased the level of T-ADCC and overall cytotoxicity that the PBMCs were capable of eliciting (**Section 3.5.1**). When broken down by response cohort, the patients that had significant increases in T-ADCC with the addition of pembrolizumab were all non-pathological complete responders (**Section 3.5.2**). This indicates that non-CR patients are more likely to have PD-1-immunosuppressed ADCC-capable immune cell subsets in their peripheral blood. This data suggests that testing the impact of an anti-PD-1 immune checkpoint inhibitor like pembrolizumab on the T-ADCC response elicited by HER2+ breast cancer patient PBMCs could be used to 1) predict response to neo-adjuvant chemotherapy, 2) identify patients that could benefit from anti-PD-1 therapy alone or combined trastuzumab/anti-PD-1 therapy.

This study also showed that SNPs in ABCB1 (rs1045642, rs1128503), NKG2D (rs1049174, rs2255336) and FCG3A (rs396991) affect the *in vitro* cytotoxic capacity of PBMCs (**Section 3.6**) and their response to neo-adjuvant chemotherapy.

3.8 Discussion

There are many methods of measuring ADCC *in vitro*. Traditionally the chromium release assay was the gold standard. Chromium-release assays use Chromium-51 loaded target cells. When the effector cells kill the target cell the chromium is released [299]. This can allow for measurement of cell death based on the levels of chromium isotope present. The Chromium-release assays give a measure of the cumulative cytotoxicity over a time-period. The main drawbacks of this assay are reproducibility, due to issues with chromium labelling and spontaneous release, as well as the need for radioactive components [299,300]. Another gold standard method of measuring ADCC is the lactate dehydrogenase (LDH) assay. LDH is a cytosolic enzyme present in most eukaryotic cells. When the target cell is lysed LDH is released into the culture media and can be detected colorimetrically through the reduction of NAD+ to NADH in the presence of lactate which can then be used as a measure of cell death [301]. The LDH assay also measures cumulative toxicity and is preferable to the chromium release assay due to the measurement of an endogenous factor rather than requiring the addition of radioactive chromium. The drawbacks to the LDH assay are again variability between replicates, which can be due to the effects of serum or serum starving, test drugs impacting lactate levels and potential contamination from dying immune cells which requires multiple stringent controls [301]. Using FACS analysis as a measure of ADCC is emerging as a more robust method of analysis [300]. Target cells are fluorescently labelled to differentiate them from the effector cells. Effector cells, target cells and antibodies are co-incubated at different ratios and treatment combinations with relevant controls. Viability dye is added allowing for differentiation of live/dead target cells and live/dead effector cells. A proportion of cells are then examined on a single cell basis to determine viability. With the appropriate use of controls the number of dead target cells which occurred due to T-ADCC can be determined [282,300]. This method allows for single cell analysis at a fixed time point to measure cell kill. This method is highly reproducible and extremely sensitive and allows for the direct evaluation of the death of target cells [300]. The assay does not provide a cumulative measure of cell death over a time period like the LDH and Chromium-release assays but it does provide a more sensitive and reproducible direct measure of the state of the target cell population that remains intact at assay takedown.

PBMC samples had to be frozen due to the number of patients involved in the study and the unpredictable timing of blood sample arrivals, as well as to allow analysis of matched pre- and post-treatment samples within the same assay. Viability and cell number of thawed PBMC samples was variable following freezing for up to 6 years. Data from the literature showed PBMC samples isolated and frozen by the same protocol could show a correlation between viability and functional activity. This effect was negated when samples with a viability of less than 70 % were excluded from analysis [298]. When samples with less than 70 % viability were excluded from this study, there were no significant

correlations seen between cytotoxicity and viability. This meant a reduced sample size but allowed for a more robust and dependable analysis.

3.8.1 Pre-treatment PBMC-mediated cytotoxicity does not correlate with response

There have been a number of studies which examine T-ADCC *in vitro* in breast cancer and its relationship with response to treatment. These studies have shown the importance of the ADCC response for effective trastuzumab treatment, and the relevance of measuring ADCC as an assessment of response in the clinic [30,264,265]. Beano *et al.* [265] used a chromium release assay to examine NK cell-mediated T-ADCC against K562 and SKBR3 cell lines. PBMCs were taken after one round of neo-adjuvant trastuzumab and chemotherapy (n=26). Using these samples they found that NK cell activity correlated with clinical response to trastuzumab [265]. Varchetta *et al.* [263] also used a chromium release assay to measure ADCC against the MDA-MB-361 cell line. They took PBMCs from patients before and after receiving four weeks of tri-weekly neo-adjuvant trastuzumab (n=18). They showed a partial correlation between T-ADCC and response in post-treatment samples. This effect was robust at high and low levels of T-ADCC but was less well defined at an intermediate level [263]. Gennari *et al.* examined T-ADCC elicited by pre- and post- neo-adjuvant tri-weekly trastuzumab-treated patient PBMCs against the HER2+ MDA-MB-361 cell line using the chromium release assay (n=11). A correlation between T-ADCC and response to treatment was seen in post-treatment samples [264]. Petricevic *et al.* [302] used a flow cytometry-based method to examine T-ADCC against the SKBR3 cell line elicited by PBMCs from patients with different breast cancer disease stages while on trastuzumab treatment (n=43). There was no correlation between T-ADCC and progression free survival in this study.

All patients examined within the TCHL study, regardless of clinical response (CR, PR, NR), showed a similar capacity to elicit ADCC in peripheral cells before receiving treatment (**Section 3.3.2**). All correlation seen between T-ADCC and response to therapy in the literature utilised post-treatment samples. In these studies pre-treatment T-ADCC levels were not reported to correlate with response to the respective neo-adjuvant treatment regimens [263–265]. *In vitro* measurement of pre-treatment levels of immune-mediated cytotoxicity and T-ADCC against the SKBR3 cell line was not predictive of patient response to neo-adjuvant chemotherapy in ICORG 10-05.

3.8.2 Decrease in T-ADCC post-treatment associated with complete response

Previous *in vitro* tests , such as those from Gennari *et al.* and Varchetta *et al.*, have shown an increase in T-ADCC capabilities of patient immune cells after receiving neo-adjuvant trastuzumab treatment alone [263,264]. Beano *et al.* demonstrated an increase in T-ADCC following one round of neo-adjuvant

chemotherapy and trastuzumab treatment [265]. Di Modica *et al.* [269] has also demonstrated an increase in T-ADCC following 4 rounds of docetaxel treatment using patient plasma combined with healthy volunteer NK cells, chromium release assay and HER2+ MDA-MB-361 and BT474 cell lines [269].

In the TCHL study, matched pre- and post-treatment samples were examined to determine the effect of treatment on PBMCs ability to elicit cytotoxicity and to determine if there were any features associated with response in a post-treatment setting. There was a significant decrease in the ability of PBMCs to elicit direct cytotoxicity against K562 cells and T-ADCC against SKBR3 cells post-treatment (**Section 3.4.2**). This shows that a downregulation in the cytotoxic capabilities of PBMCs after neo-adjuvant therapy. In studies performed by Varchetta *et al.* and Gennari *et al.*, T-ADCC was increased post-treatment, in these studies patients received trastuzumab treatment alone [30,264]. Di Modica *et al.* showed an increase in T-ADCC following docetaxel treatment, however this experimental set up used healthy volunteer NK cells as effector cells [269]. Differences in treatment regimen, duration of treatment alongside differences in method of determining T-ADCC may account for the differences T-ADCC patterns following neo-adjuvant treatment. This study shows a decrease in T-ADCC post-treatment, which indicates a downregulation of the immune response following this completion of 6 rounds of neo-adjuvant chemotherapy and trastuzumab treatment.

The studies described above have shown a positive correlation between response to treatment and T-ADCC levels following either neo-adjuvant trastuzumab-only therapy or one round of chemotherapy and trastuzumab [30,264,265]. In this analysis an inverse relationship in post-treatment T-ADCC between CR and Non-CR was observed (**Section 3.4.3**). This indicates that the immune response may be down regulated due to a complete response to treatment when ADCC levels are detected using a flow cytometry-based method after completion of 6 rounds of neo-adjuvant chemotherapy and trastuzumab treatment. Further investigation of the immune phenotype of these cells before and after treatment may elucidate the mechanisms behind this response.

In pre-clinical models lapatinib treatment has been shown to increase T-ADCC levels by stabilisation of HER2 on the cell surface [282,303]. While trastuzumab monotherapy leads to increased T-ADCC [30,264]. In the TCHL study there was an alteration in post-treatment cytotoxicity levels based on whether patients received trastuzumab or lapatinib in combination with chemotherapy. Patients who received both trastuzumab and lapatinib in combination with chemotherapy were the only treatment arm to show an increased level of *in vitro* overall cytotoxicity with the addition of trastuzumab post-treatment (**Section 3.4.4**). This indicates alterations in the post-treatment immune response depending on the HER2-targeted therapy received. Due to inadequate sample size and response distribution between treatment arms, greater numbers would be needed to examine the effects of treatment arm on cytotoxicity levels post-treatment.

3.8.3 Increase in T-ADCC with addition of pembrolizumab to trastuzumab treatment, which is associated with a non-complete response to neo-adjuvant treatment

Clinical trials examining the combination of ICI and trastuzumab are underway, with atezolizumab being close to receiving approval to treat TNBC [120]. Pembrolizumab is also showing modest but promising results in advanced breast cancer [258,260]. Taking all the samples examined in this study collectively, the addition of pembrolizumab to trastuzumab caused a general increase in the level of overall cytotoxicity (direct + T-ADCC) the PBMCs were capable of eliciting against the SKBR3 cell line, primarily through T-ADCC (**Section 3.5.1**).

When all samples examined in this study were broken down by response (CR *vs.* Non-CR), it was shown that 50 % (7/14) of patients with a Non-CR were the contributors to the pembrolizumab-related increase in overall cytotoxicity against the SKBR3 cell line (**Section 3.5.2**). This seems to suggest that a subset of patients that have a poor response to neo-adjuvant chemotherapy have circulating immune cells that are suppressed by the PD-1 axis and relief of this immunosuppression improves the anti-tumour immune response to trastuzumab *in vitro*. Also, patient samples that show a response to pembrolizumab *in vitro* show a decreased level of TIL infiltration compared with the CR cohort (**Section 3.5.4**). It is therefore possible that these PD-1-suppressed circulating immune cells could be related to the tumour and could be indicative of patients that will not benefit from current neo-adjuvant chemotherapy and may benefit from ICI treatment. This is discussed in detail below. For the 50 % (7/14) of Non-CR patient samples that did not respond to the addition of pembrolizumab *in vitro* (**Section 3.5.2**), they do not seem to have this particular PD-1-suppressed ADCC-capable immune cell subset. One could postulate that immunosuppressive features other than PD-1 could be present in these cells (e.g. CTLA-4, TIM-3) or other non-immune related mechanisms could have led to the unfavourable response to neo-adjuvant treatment. These patients did not have a significantly lower level of TILs than the CR patients, supporting the assertion that the immune response is not a contributing factor to response to chemotherapy in these patients (**Section 3.5.4**). Typically patients with higher levels of TILs show an increased response rate to ICI [46], in this incidence TILs were lower in patients who we predict may have a response to ICIs than patients with a complete response. This may indicate a stratification of TIL levels between complete responders to neoadjuvant chemotherapy, responders to ICIs and non-responders to ICI.

No patient who had a CR to neo-adjuvant therapy showed an increase in T-ADCC with the addition of pembrolizumab (0/7) (**Section 3.5.2**). These patients also had a higher level of TIL infiltration than Non-CR patients who responded to pembrolizumab (**Section 5.5.4**). This indicates that these patients do not possess circulating ADCC-capable immune cells which are suppressed by the PD-1 signalling axis. This correlates with data showing an active immune response to be beneficial in HER2+ breast cancer prognosis [217,238,239].

This data suggests that the presence of PD-1-suppressed ADCC-capable circulating immune cells and decreased TIL levels identifies certain HER2+ breast cancer patients that will not respond to neo-adjuvant chemotherapy. The assay responders contained two TCL patients, four TCHL and one TCH patients and so it cannot be stated that the assay identifies responders to trastuzumab-containing chemotherapy. Due to immune cells from these patients responding to an anti-PD-1 therapy *in vitro*, it is possible that these patients could potentially benefit from the addition of pembrolizumab to trastuzumab in the clinic. This treatment combination may be particularly beneficial in patients who would not have a CR to neo-adjuvant trastuzumab and chemotherapy alone.

NK cells are known to be the main mediators of ADCC in PBMCs and known to express PD-1 [227,304,305] making them the prime candidates for mediating the *in vitro* immune assay effects observed. A flow cytometry-based experiment to examine the composition of the PBMCs from TCHL patients in the samples examined in the immune cytotoxicity assays has been executed but is yet to be analysed. The expression of relevant immune markers, such as PD-1 and PD-L1 will be examined. This data should help identify the cell populations responsible for the responses in the *in vitro* assays.

3.8.4 Use of this model to predict response to treatment (Patent no. GB 1811892.2)

A major clinical goal is to identify patients who will benefit from chemotherapy those who will not. The recent publication of the final analysis of the TAILORx trial is a prime example of the potential power of biomarkers in the clinic. The molecular profiling test Oncotype DX uses a 21 gene panel to stratify ER+ breast cancer patients and has shown that 70% of ER+/HER2-negative/auxillary node negative patients (the most common type of breast cancer) can be spared the addition of chemotherapy to their hormone therapy as it adds no clinical benefit [306]. Characteristics of the immune response to cancer are also under investigation as potential prognostic biomarkers as exemplified by the Immunoscore in colon cancer [307].

Using the immune cytotoxicity assay, outlined in Section 2.15, 50 % of patients with a Non-CR to the neo-adjuvant treatment were detected. This indicates that this assay may have the potential to predict response to neo-adjuvant chemotherapy treatment of HER2+ breast cancer (and/or trastuzumab treatment) (**Section 3.5**). Using this approach to examine pre-treatment samples to predict response to treatment has not been shown previously. The use of the immune cytotoxicity assay for the prediction of response to neo-adjuvant chemotherapy and ICIs is the basis of patent application GB 1811892.2 (**Figure 3.21**).

Knowing a patient will not respond to therapy could be used to avoid unnecessary treatment and allow patients to progress to surgery sooner. An active immune response is a beneficial prognostic factor in breast cancer [239]. The immune cytotoxicity assay used in this thesis indicated response before the intervention of the therapy, showing it can act as a predictive factor for response to neo-adjuvant

chemotherapy. As the assay is immune-based, it may be predicting a predisposition present in the patient pre-treatment for the differential response of the immune system to chemotherapy, which may affect response to treatment. Chemotherapy can stimulate the immune response by killing cancer cells, releasing neo-antigens and disrupting the tumour micro-environment. This could potentially tip the balance in favour of the anti-cancer immune response [308]. A non-PD-1 immune-supressed patient may have a CR to neo-adjuvant chemotherapy due to an active immune response. A Non-CR patient suppressed by the PD-1 signalling axis may be prevented from achieving this response. This assay reveals the patients which are supressed by the PD-1 axis which may allow it to predict a Non-CR to neo-adjuvant chemotherapy. Patients who have a Non-CR but do not respond in the assay may possess other tumour-related factors which reduce the response to chemotherapy, such as hypoxic tumour environments, alternative immune checkpoint expression, drug access and bioavailability issues.

Alternatively, the immune cytotoxicity assay could identify patients that could benefit from the addition the addition of ICIs which may be successful in the neo-adjuvant setting, such as pembrolizumab. ICIs can have severe side effects. 90% of patients treated with anti-CTLA-4 and 70% treated with anti-PD-1/PD-L1 therapies display irAEs, with approximately 10% of irAEs presenting as life threatening [130,309]. ICIs are very expensive treatments with major health economic impacts (pembrolizumab -~50,000-100,000 Euro/annum in Ireland [132]). Multiple approaches are being pursued to identify biomarkers of response, with a liquid biopsy (blood sample-based) option remaining the most sought.

Currently there are a number of mechanisms being investigated for their use in predicting response to ICIs. Most commonly used is the determination of an "exhausted" immune cell/tumour microenvironment phenotype by measuring tumour and immune cell PD-L1 expression by IHC in tumour samples [310]. This method is clinically approved in indications where the ICI is only approved for use in PD-L1+ patients [71–74]. This method is subjective due to different tests and antibodies used as well as differences in PD-L1 positivity thresholds which leads to conflicting results on the use of PD-L1 as a biomarker. This method also relies on the presence of tumour sample which is invasive for the patient and may not allow for multiple testing during treatment or assessment following undetectable disease. Another method of predicting response to treatment is by using the tumour mutational burden as a biomarker [136–138,311]. This method has shown success in identifying patients who will respond to ICIs, although it again requires tumour samples and these samples need to be sequenced to assess the mutational burden which can be an expensive and time-consuming process.

The immune cytotoxicity assay relies on blood samples, which are easy to procure and relatively non-invasive for patients compared to tumour biopsies. Using blood samples also allows for repeat profiling of patients to monitor the immune profile following treatment or surgery. Blood samples do not require biopsies from patients who may have no residual disease or have multiple metastases that will not be undergoing surgery. The use of this assay as a long-term and reliable method of examining response is

supported by the two post-treatment samples which showed the same response to pembrolizumab in the assay as the pre-treatment samples taken approximately 3 months before (**Section 3.5.3**). This assay is versatile, and it is possible that it could be adapted with a range of ADCC capable monoclonal antibodies against a range of cancer cell line models from different cancer types. For full validation, the assay requires further examination in a larger patient cohort of neo-adjuvant HER2+ breast cancer patients to confirm the predictive value to current chemotherapy and in samples from patients who are receiving ICIs to examine its predictive value with regards ICIs.

As explained above, the presence of PD-1 responsive immune cells in nCR patient blood may identify patients that would benefit from pembrolizumab treatment (**Section 3.5.2**). Presuming the circulating cells are associated with the tumour, the relief of PD-1-mediated immunosuppression in these patients may facilitate the mounting of a cytotoxic antibody-mediated immune response against the tumour. The presence of anti-tumour antibodies in the patient's circulation is an area of study that would be worth pursuing: if ADCC capable immune cells are suppressed then perhaps anti-tumour antibodies are also present. In HER2+ breast cancer, trastuzumab could act as the anti-tumour antibody, therefore forming the rationale for the combination of trastuzumab and pembrolizumab for patients whose blood samples react in the *in vitro* immune cytotoxicity assay.

Ethical approval has been obtained from SVUH for pre-treatment blood samples to be taken from patients who have cancers for which ICI (melanoma, lung, kidney cancers) or monoclonal antibody therapy (HER2+ breast cancer, HER2+ gastric cancer, EGFR+, Ras WT colon cancer) is approved. PBMCs from these blood samples will be used to examine the effects of ICIs on direct PBMC-mediated cytotoxicity and T-ADCC against different cancer cell line models (WM115 (melanoma), NCI-H460 (lung cancer), SKBR3 and HCC1954 (HER2+ breast cancer)). 4 and 12 hour incubations will be used to examine variation in the predictive ability of the assay. Plasma samples will be used for cytokine analysis and FACS immunophenotyping. Response data for each patient sample will be obtained post-treatment to assess the predictive capacity of the test. This will be a measure of pathological complete response for patients receiving neo-adjuvant chemotherapy or progression-free survival. This will provide further information on the use of this test as a biomarker of response to treatment (chemotherapy and/or ICIs) in a larger patient cohort (n=120) and in different cancer types.

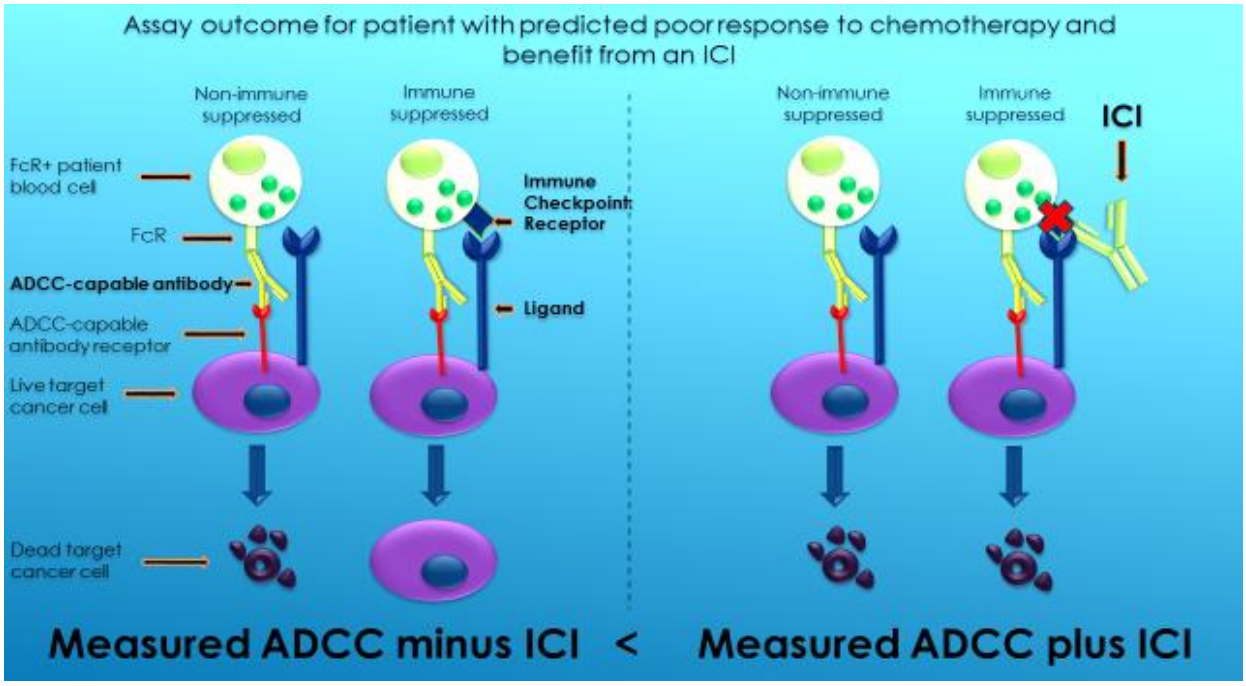

Figure 3.21: Depiction of the hypothesis underpinning the increase in T-ADCC caused by addition of pembrolizumab treatment. Patients with PD-1 mediated immunosuppression do not engage in T-ADCC without the addition of pembrolizumab. When PD-1 is blocked with pembrolizumab trastuzumab is capable of eliciting ADCC.

3.8.5 The effect of SNPs on PBMC-mediated cytotoxicity

Natural physiological variations in three genes were examined in this study. The SNP data was obtained primarily from analysis of germline DNA (n=47) from isolated PBMCs but the SNP status of eleven patients was determined from the tumour to increase the available dataset (Total n=58).

3.8.5.1 SNPs in ABCB1 gene affect direct PBMC-mediated cytotoxicity

The ABCB1 gene acts as a drug efflux pump with a major role in drug bioavailability, extruding harmful xenobiotics from healthy cells and is a mediator of multi-drug resistance when over-expressed [272–274]. Taxotere, one of the chemotherapy drugs given to all the ICORG 10-05 patients is a substrate for ABCB1. SNP variations can alter the ability of the ABCB1 gene protein product, P-gp, to transport substrate drugs affecting drug bioavailability and potency [272]. A homozygous or heterozygous (3435CC or 3435CT) in ABCB1 at rs1045642 (also known as C3435T) was shown to be detrimental to progression free survival and overall survival in patients with metastatic HER2+ breast cancer compared with the 3435TT genotype [274]. Docetaxel blood concentration was also higher for the 3435TT genotype. 3435CC has also been linked with a higher resistance to chemotherapy and trastuzumab treatment in HER2+ breast cancer [273]. In this study, patients with a heterozygous allele (CT) for ABCB1

rs1045642 did not have a reduction in direct cytotoxicity against K562 cells post-treatment (**Section 3.6.1**). This indicates that chemotherapy affected the ability of PBMCs to elicit direct cytotoxicity to a lesser degree in patients with a heterozygous allele (CT) *vs.* those with a homozygous allele for reference (TT) or mutant gene (CC). This suggests that patients with a heterozygous allele may have more protection from chemotherapy. A higher level of pre-treatment direct cytotoxicity was seen in patients with a minor allele (**Section 3.6.1**). This indicates that patients with SNPs in this gene may show alterations in their PBMCs ability to elicit direct cytotoxicity in the absence of chemotherapy.

These findings implicate an ABCB1 SNP as effecting the ability of PBMCs to elicit direct cytotoxicity and the effects of chemotherapy on this aspect of the immune response. These results merit further investigation in a larger neo-adjuvant and adjuvant patient cohort.

3.8.5.2 SNPs in KLRK1 gene affect T-ADCC

KLRK1 encodes the NKG2D protein. NKG2D contains a C-type lectin domain [22,23]. NKG2D is ligated by MICA, MICB and UL-16 binding proteins and is crucial in the recognition of stressed cells by the immune system. Ligation of NKG2D leads to activation of NK cells and T cells, which kill the targeted cell [22,23]. Other studies have shown that the activity of NKG2D is beneficial in NK cell mediated T-ADCC [267–269]. Studies have shown that the CG and GG rs1049174 variants leads to a higher proportion of NK cells which are capable of high levels of ADCC which can affect cancer risk and overall survival rates [270,271]. This is due to the SNP occurring in the targeting site of the negative regulatory miR-1245 [271]. CG and GG are associated with a lower risk of colon cancer [270]. In TCHL patients, those with a GG allele in the KLRK1 gene showed a higher level of pre-treatment T-ADCC (**Section 3.6.2**). This supports previous evidence of the rs1049174 SNP leading to more actively cytotoxic NK cells capable of increased levels of ADCC. This indicates that having a GG or CG genotype rs1049174 may be beneficial in eliciting a positive response to trastuzumab treatment.

3.8.5.3 SNPs in Fc receptors alter direct cytotoxicity

FCG1A (CD64), FCG2A (CD32), FCG2B (CD32), FCG3A (CD16) and FCG3B (CD16) are genes which belong to the immunoglobulin superfamily encoding for Fc gamma receptors [26]. Fc receptors are crucial for phagocytosis and ADCC. FCG3A is the main effector of T-ADCC. FCG3A can recognise the antigen bound antibody and stimulates the release of cytotoxic granules which trigger apoptosis in the marked cell [25,26]. Clynes *et al.* demonstrated that mutated Fc domains abrogated the ability of trastuzumab to cause tumour rejection [26]. Musolino *et al.*[266] demonstrated that in neo-adjuvant HER2+ breast cancer that patients with a minor or heterozygous allele (C/T or CC at rs396991) had a lower objective response rate and progression free survival when receiving trastuzumab therapy than those with a reference allele (TT at rs396991). Within adjuvant HER2+ breast cancer Hurvitz *et al.* [312] found

no significant difference in clinical response to trastuzumab when SNPs in the FCG3A receptor was examined (C/T, C/C, T/T at rs396991).

In the TCHL cohort, patients with a CC allele SNP in FCG3A (rs396991) showed alterations in direct cytotoxicity fold change between pre- and post-treatment, but no changes to T-ADCC levels (**Section 3.6.3**). This indicates that the ability of PBMCs to elicit direct cytotoxicity is affected differently by neo-adjuvant treatment in patients with a minor allele in FCG3A than patients with a heterozygous or homozygous allele. In this study, T-ADCC levels were not affected by SNPs in FCG3A as was shown in other neo-adjuvant studies but the numbers were small [266]. A larger sample cohort is needed to further examine the effects of SNPs in FCG3A on cytotoxicity elicited by PBMCs before and after chemotherapy and trastuzumab treatment.

4. The development of an assay to examine the effect of immune checkpoint inhibitors *in vitro* using immune cells isolated from healthy volunteers

4.1 Introduction

Immune checkpoint inhibitors (ICIs) are rapidly entering the clinic to treat a variety of cancer types (**Table 1.1, 1.2 and 1.3, Section 1.2**). Success has been demonstrated by these drugs; however, response often occurs only in a minority of patients (**Table 1.1, 1.2 and 1.3, Section 1.2**). Through pre-clinical examination of ICIs, it may be possible to determine which patients will benefit from ICIs or combination treatment strategies. Examining the effects of ICIs is difficult in a pre-clinical setting, as it generally accepted that it requires the presence of tumour-specific T cells [146]. Many studies use expensive mouse models to examine ICI activity [146]. There are some published *in vitro* models examining the impact of ICIs on proliferation of T cells, immune cell phenotype and expression of immunosuppressive markers but very few assays measure tumour cell death in the presence of ICIs and immune cells [148–150]. Tumour cell line -specific T cells are difficult to attain in large numbers and maintain long enough to carry out experiments.

As shown in Section 3.5, inhibition of PD-1 with pembrolizumab was capable of increasing T-ADCC elicited against a HER2+ cell line using a subset of patient PBMC samples. The T-ADCC function of PBMCs is measurable and a reflection of the potential impact of ICIs on one of the major processes involved in the adaptive immune response against tumour cells [313]. As patient samples are not always available, an assay which uses healthy volunteer samples would be preferable. This body of work is aimed at using a functional approach to develop an assay to examine the activity of ICIs *in vitro,* through the measurement of direct cytotoxicity and T-ADCC, using healthy volunteer immune cells.

NK cells have been identified as the main mediators of ADCC and direct cytotoxicity within the PBMC population and can express PD-1 [29]. Subset T cell populations e.g. γδ T cells or CD16+ T cells are also capable of eliciting a small amount of ADCC and can express PD-1. Anergic or exhausted, tumour-specific T cells are defined as the main targets of ICIs in the tumour microenvironment [14]. Given the responses of patient immune cells to pembrolizumab described in Chapter 3, we decided to examine the ability of healthy volunteer PBMCs, NK and T cells to respond to ICIs *in vitro.*

Five different cell populations (PBMCs/T cells/NK cells/exhausted T cells/exhausted NK cells) were examined for their ability to kill HER2+/PD-L1-low and HER2+/PD-L1-high breast cancer cell lines directly or by T-ADCC in the presence/absence of ICI. The K562 cell line was used as a HER2-null target cell line with particular susceptibility to direct cytotoxicity [282,314]. First, the cytotoxicity of a mixed population of PBMCs was examined. Then untreated, negatively selected T cells and NK cells were examined. Untreated, negatively selected, freshly isolated healthy volunteer T cells should be inactive and express very low levels of PD-1 and PD-L1. By activating the T cell population with CD3/CD28 it is possible to stimulate the proliferation of T cells and induce PD-1 and PD-L1 expression [315,316]. Freshly isolated healthy volunteer NK cells should also express very little PD-1 or PD-L1. A method

of culturing NK cells to exhaustion by continued stimulation with IL-2 was employed [317]. The ability of these exhausted NK and T cells to elicit an effect in the presence of an ICI in HER2+ breast cancer cell lines was examined. Two PD-1 targeted ICIs (pembrolizumab and nivolumab) and one PD-L1 targeted ICI (atezolizumab) were used in the assay and trastuzumab was used as the ADCC inducing antibody.

Direct cytotoxicity and T-ADCC elicited by the immune cell populations was measured to examine cytotoxicity levels. The overall cytotoxicity level elicited by the immune cell populations, which is a combination of direct cytotoxicity and T-ADCC, is also presented. Overall cytotoxicity demonstrates an increase in the overall cancer cell kill, rather than a shift in balance between direct cytotoxicity and T-ADCC.

4.2 Characterisation of target HER2+ breast cancer cell lines

4.2.1 PD-L1 and PD-1 expression

Two HER2+ breast cancer cell lines SKBR3 (HER2+/PD-L1 medium) and HCC1954 (HER2+ PD-L1 high) were selected for use in the assays. In order to develop an assay to examine the effect of inhibiting PD-1 and PD-L1, it was necessary to determine PD-1 and PD-L1 protein expression in the target cell lines. PD-1 and PD-L1 protein levels were examined in SKBR3 and HCC1954 cells by western blot. PD-L1 protein expression was detected in both HER2+ breast cancer cell lines examined. PD-L1 expression was significantly higher in the HCC1954 cell line when compared to the SKBR3 cell line ($p=9.30 \times 10^{-6}$) (**Figure 4.1**).

A very low expression double band was detectable in both cell lines at the PD-1 positive control molecular weight using the CST #D4W2J antibody **(Figure 4.1**). There was no significant change in expression between the SKBR3 or HCC1954 cell lines (**Figure 4.1**). PD-1 expression is unlikely to be present on tumour cells but as the specificity of the antibody was not tested, low-level, non-specific binding cannot be discounted.

SKBR3 and HCC1954 cell lines model HER2+ cell lines that expressed negligible levels of PD-1 and low versus high levels of tumour cell PD-L1 for use in the planned assays.

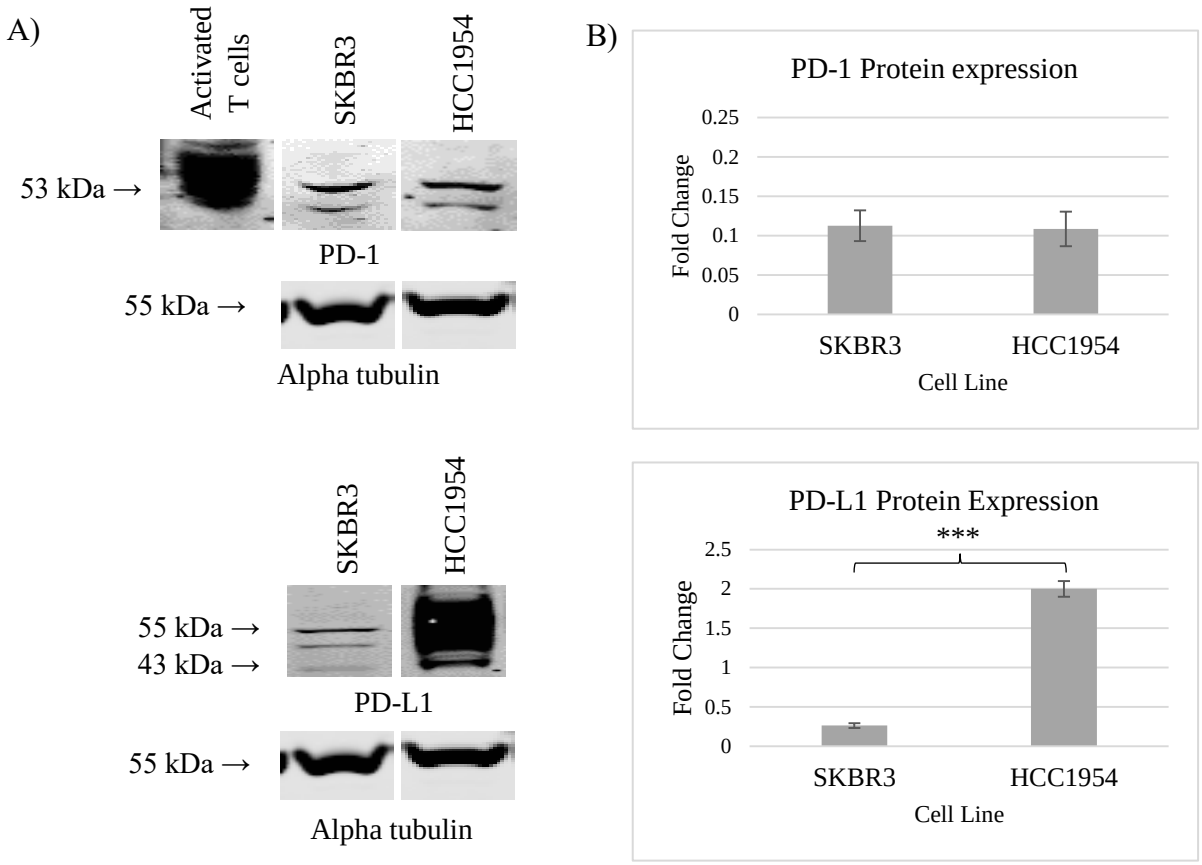

Figure 4.1: A) Western blotting for protein levels of PD-1 and PD-L1 in SKBR3 and HCC1954. Blots shown are representative images of triplicate blots. Expected weight of PD-1 antibody 52-65 kDa, expected weight of PD-L1 antibody 40-50 kDa. PD-L1 antibody validation in Section 4.1 **B)** Densitometry analysis of immunoblots of SKBR3 and HCC1954 cells for PD-1 and PD-L1. Error bars represent standard deviation of biological triplicate experiments. The Student's t test was used to determine statistical significance. * $p < 0.05$, ** $p < 0.01$ and *** $p < 0.001$.

4.2.2 The impact of direct ICI exposure on tumour cell proliferation

It was also necessary to examine whether there was a potential anti-proliferative effect elicited directly by pembrolizumab, nivolumab or atezolizumab against the HER2+ breast cancer cell lines alone or in combination with trastuzumab. SKBR3 cells showed on average a 40.76 +/- 2.06 % growth inhibition in the presence of trastuzumab (p=0.001). HCC1954 cells did not show a significant change in growth with trastuzumab treatment, consistent with its status as a trastuzumab resistant cell line [318]. The ICIs had no effect on HCC1954 proliferation (**Figure 4.2**). Only nivolumab significantly impacted SKBR3 proliferation, this effect was less than 10 % (6.89 ± 1.05 % (p=0.01)) (**Figure 4.2**). The ICIs had little or no effect on cell viability alone and did not impact the anti-proliferative effects of trastuzumab in combination.

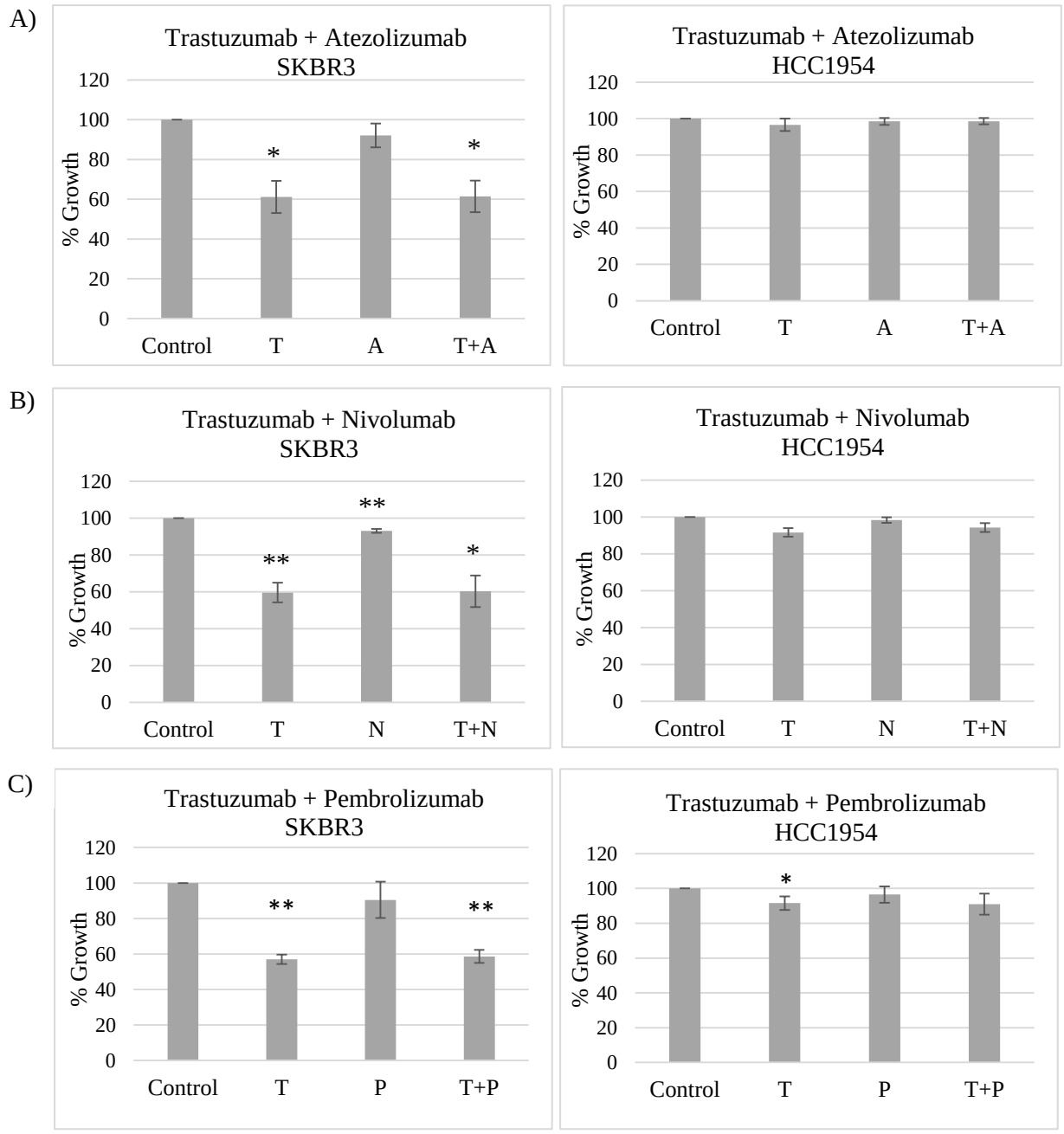

Figure 4.2: A) Proliferation of SKBR3 and HCC1954 cells following 5-day treatment with **A)** Trastuzumab (T) (10 µg/µL), atezolizumab (A) (10 µg/µL) and T+A combination. **B)** Trastuzumab (T) (10 µg/µL), nivolumab (N) (10 µg/µL) and T+N combination. **C)** Trastuzumab (T) (10 µg/µL), pembrolizumab (P) (10 µg/µL) and T+P combination. Percentage growth was calculated relative to untreated control and error bars represent standard deviation of biological triplicate experiments. The Student's t test was used to determine statistical significance. *p <0.05, **p <0.01 and *** p <0.001.

4.3 Healthy Volunteer sample breakdown

In total 10 blood samples were drawn to examine the cytotoxic capacity of immune cell populations in the presence of ICIs. Table 4.1 details the sex and age range of each healthy volunteer, as stated in their consent form, as well as the assay for which each blood sample was used. To improve comparison between the effector cell activities of each subset, where possible, NK cells and T cells were isolated from the same PBMC sample.

Table 4.1: Healthy volunteer information for samples used in this analysis.

Healthy volunteer	Sex	Age	Assay
Volunteer 1	Female	35-44	PBMC-mediated cytotoxicity
Volunteer 2	Female	25-34	PBMC-mediated cytotoxicity
Volunteer 3	Female	45-54	PBMC-mediated cytotoxicity
Volunteer 4	Female	55-64	Culturing experiment
Volunteer 5	Female	45-54	Un-activated/non-stimulated T cell and NK cell-mediated cytotoxicity
Volunteer 6	Female	25-34	Un-activated/non-stimulated T cell and NK cell-mediated cytotoxicity
Volunteer 7	Female	45-54	Un-activated/non-stimulated T cell and NK cell-mediated cytotoxicity
Volunteer 8	Female	25-34	Activated/Stimulated T cells and NK cell-mediated cytotoxicity
Volunteer 9	Female	45-54	Activated/Stimulated T cells and NK cell-mediated cytotoxicity
Volunteer 10	Female	34-45	Activated/Stimulated T cells and NK cell-mediated cytotoxicity

4.4 Analysis of functional capabilities of unstimulated PBMCs

A mixed PBMC population was isolated from whole blood samples from healthy volunteers 1, 2 and 3. These cells were run in an immune cytotoxicity assay with SKBR3 and HCC1954 cells, alone and in combination with atezolizumab, nivolumab or pembrolizumab, with or without trastuzumab (**Section 2.15, plate layout Figure 2.10**). After 12 hours, % cancer cell death was determined.

4.4.1 Impact of ICIs on PBMC-mediated cytotoxicity against the K562 cell line

Non-MHC class I-restricted K562 cells were used as a benchmark control to compare the cytotoxicity levels of PBMC samples from different individuals. Healthy volunteers 1, 2 and 3 had a range of cytotoxicity levels when assessed against the K562 cell line (30.57 ±1.75 %, 9.72 ± 1.48 % and 10.76 ± 0.64 % respectively) (**Table 4.2**). None of the ICIs examined had a consistent effect on cytotoxicity against the K562 cell line (**Table 4.2**).

Table 4.2: % direct cytotoxicity elicited against the K562 cell line. Significant alterations to cytotoxicity in the presence of atezolizumab, nivolumab and pembrolizumab are denoted with an arrow. NS=Not significant, - = No change. All antibodies were used at a concentration of 10 µg/µL.

Volunteer no.	% Cytotoxicity	Atezolizumab	Nivolumab	Pembrolizumab
Volunteer 1	30.57 ± 1.75 %	-	-	-
Volunteer 2	9.72 ± 1.48 %	-	↑	-
Volunteer 3	10.76 ± 0.64 %	-	↓	↓

4.4.2 Impact of ICIs on PBMC-mediated cytotoxicity against HER2+ breast cancer cell lines

4.4.2.1 SKBR3

The addition of ICIs Atezolizumab, nivolumab and Pembrolizumab caused a general trend of increased cytotoxicity.

Atezolizumab increased overall cytotoxicity induced by unstimulated PBMCs against SKBR3 for volunteer samples 2 (7.83 % (p=0.031)) and 3 (5.30 % (p=0.012)) (**Figure 4.3 and Table 4.3**).

The addition of nivolumab resulted in an increase in overall levels of cytotoxicity elicited by PBMCs against the SKBR3 cell line (Volunteer 1 5.29 % (p=0.033), Volunteer 2 10.10 % (p=0.008), Volunteer 3 6.45 % (p=0.006)) (**Figure 4.3 and Table 4.3**).

Pembrolizumab increased overall levels of cytotoxicity against the SKBR3 cell line with PBMCs from all three volunteers (Volunteer 1 5.29 % (p=0.036), Volunteer 2 9.77 % (p=0.007) and Volunteer 3 5.02 % (p=0.032)) (**Figure 4.3 and Table 4.3**).

There was a general increase in overall cytotoxicity elicited by unstimulated PBMCs with a combination of trastuzumab and an immune checkpoint inhibitor against the SKBR3 cells (**Table 4.3**). The increases in overall cytotoxicity in the SKBR3 cell line were most likely attributable to the significant increases in direct cytotoxicity with the addition of the immune checkpoint inhibitor (**Table 4.3**), as T-ADCC levels were unchanged with the addition of any of the ICIs examined (**Table 4.3**).

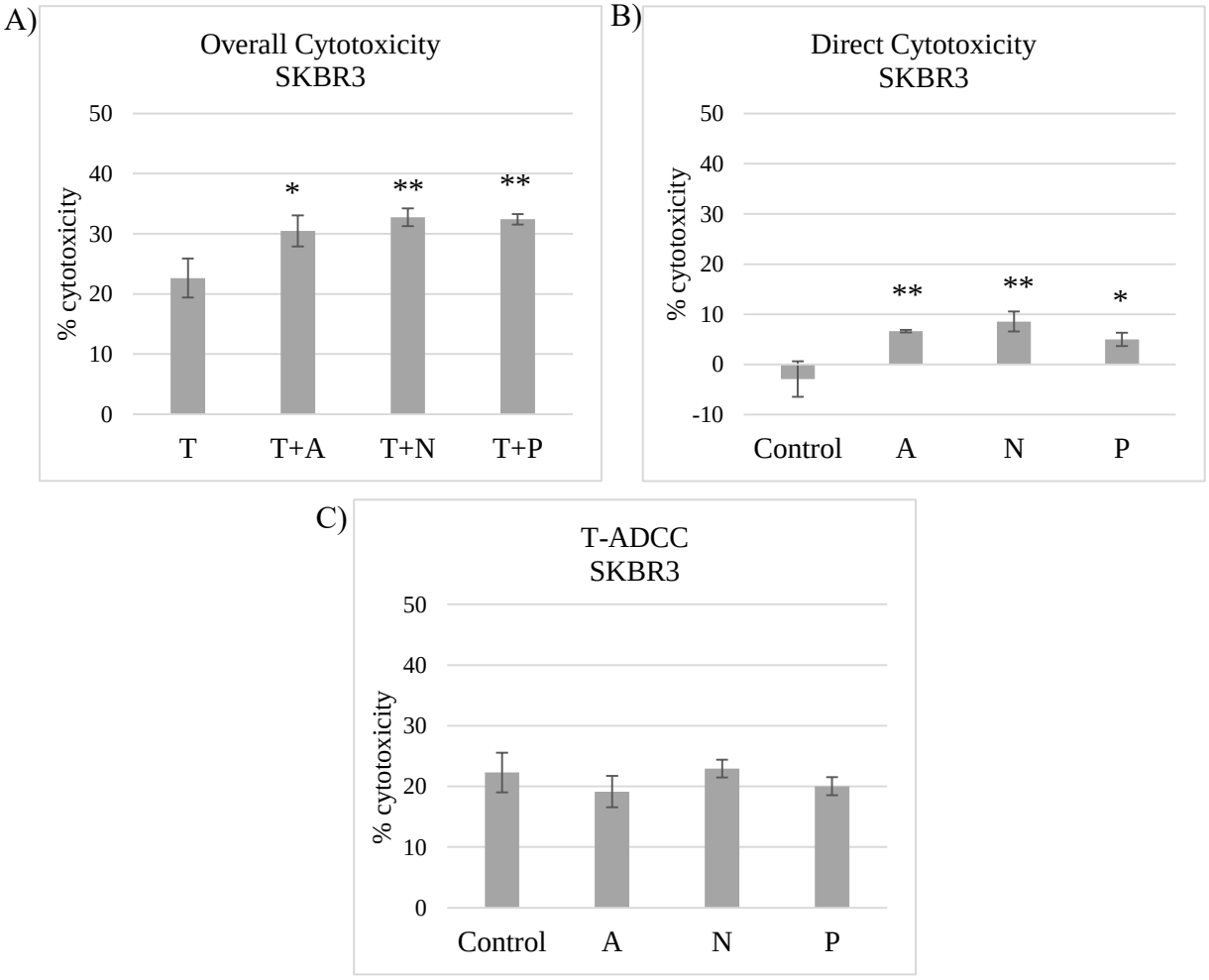

Figure 4.3: Unstimulated PBMC-mediated cytotoxicity against the SKBR3 cell line from a representative volunteer sample (Volunteer 2) A) Overall cytotoxicity **B)** Direct cytotoxicity **C)** T-ADCC. Error bars represent standard deviation of technical triplicate experiments. The Student's t test was used to determine statistical significance. * $p < 0.05$, ** $p < 0.01$ and *** $p < 0.001$. All antibodies were used at a concentration of 10 µg/µL.

Table 4.3: Unstimulated PBMC-mediated cytotoxicity against the SKBR3 cell line for all three volunteer samples A) Overall cytotoxicity **B)** Direct Cytotoxicity **C)** T-ADCC. Arrows denote statistically significant change in cytotoxicity levels. The Student's t test was used to determine statistical significance. NS= Not significant, - = No change. All antibodies were used at a concentration of 10 µg/µL.

A) Overall Cytotoxicity	**Atezolizumab**	**Nivolumab**	**Pembrolizumab**
Volunteer 1	-	↑	↑
Volunteer 2	↑	↑	↑
Volunteer 3	↑	↑	↑

B) Direct Cytotoxicity	**Atezolizumab**	**Nivolumab**	**Pembrolizumab**
Volunteer 1	-	-	-
Volunteer 2	↑	↑	↑
Volunteer 3	↑	↑	-

C) T-ADCC	**Atezolizumab**	**Nivolumab**	**Pembrolizumab**
Volunteer 1	-	-	-
Volunteer 2	-	-	-
Volunteer 3	↓	↓	↓

4.4.2.2 HCC1954

Overall cytotoxicity levels elicited by the PBMCs against the PD-L1-high HCC1954 cells were unchanged by the addition of ICIs, bar one instance where pembrolizumab increased overall cytotoxicity levels using volunteer sample 1 by 4.74 % (p=0.003), a result primarily attributable to an increase in T-ADCC levels of 4.26 % (p=0.006) (**Table 4.4**).

Atezolizumab increased direct cytotoxicity against the PD-L1+ HC1954 cell line in all three healthy volunteers by 1.91 % (p=0.046), 7.76 % (p=0.031) and 5.83 % (p=0.043) respectively (**Figure 4.4 and Table 4.4**). This increase did not affect overall cytotoxicity levels with the addition of trastuzumab. No consistent effect of nivolumab or pembrolizumab was seen across all three volunteer samples for direct cytotoxicity or T-ADCC (**Table 4.4**).

In summary, atezolizumab was capable of altering direct cytotoxicity against PD-L1+ HCC1954 elicited by unstimulated PBMCs in this assay. Unstimulated PBMCs did not produce a consistent change to T-ADCC levels or overall cytotoxicity levels in the presence of the three ICIs tested.

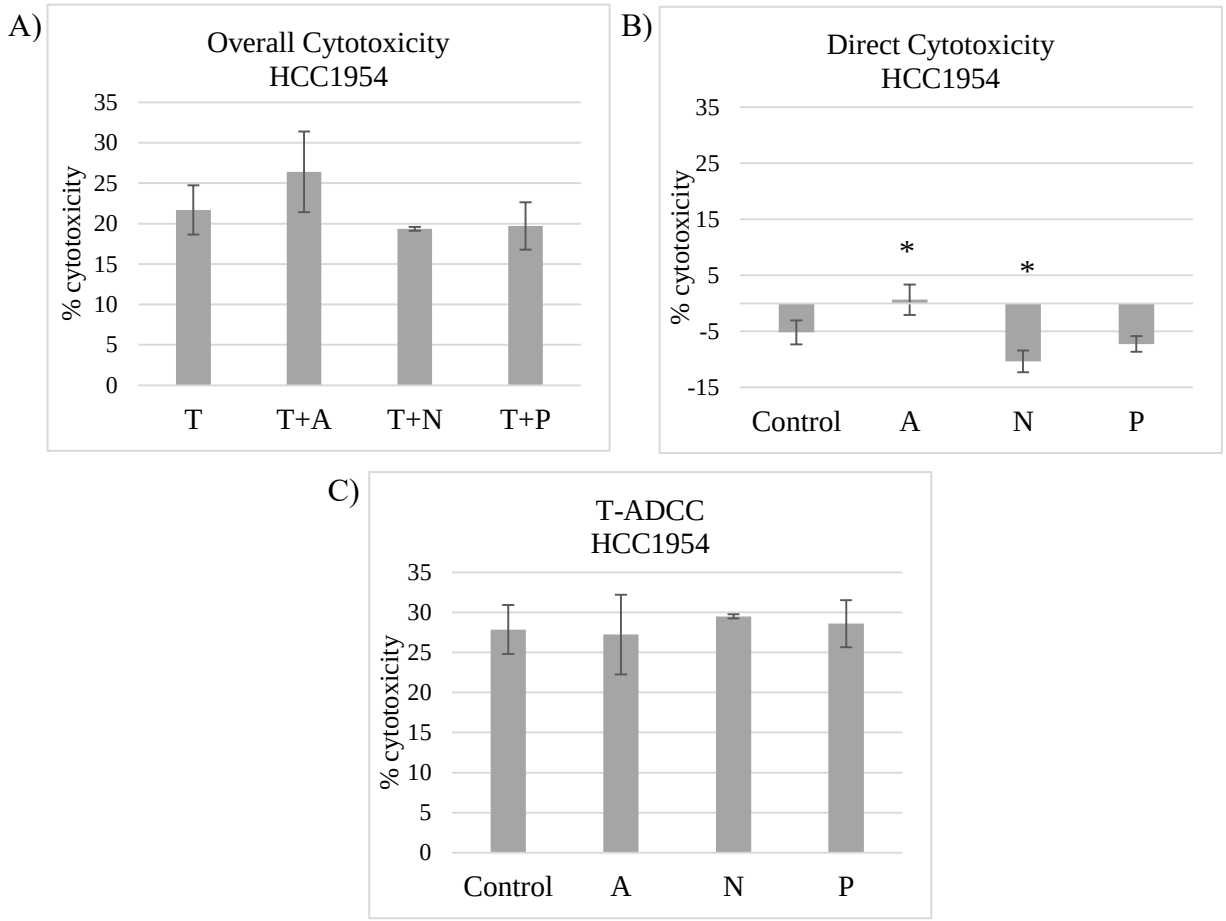

Figure 4.4: Unstimulated PBMC-mediated cytotoxicity against the HCC1954 cell line from a representative volunteer sample (Volunteer 3). A) Overall cytotoxicity **B)** Direct cytotoxicity **C)** T-ADCC. Error bars represent standard deviation of technical triplicate experiments. The Student's t test was used to determine statistical significance. * $p < 0.05$, ** $p < 0.01$ and *** $p < 0.001$. All antibodies were used at a concentration of 10 µg/µL.

Table 4.4: Unstimulated PBMC-mediated cytotoxicity against the HCC1954 cell line for all three volunteer samples A) Overall cytotoxicity **B)** Direct Cytotoxicity **C)** T-ADCC. Arrows denote statistically significant change in cytotoxicity levels. The Student's t test was used to determine statistical significance. NS= Not significant, - = No change. All antibodies were used at a concentration of 10 µg/µL.

A) Overall Cytotoxicity	Atezolizumab	Nivolumab	Pembrolizumab
Volunteer 1	-	-	↑
Volunteer 2	-	-	-
Volunteer 3	-	-	-

B) Direct Cytotoxicity	Atezolizumab	Nivolumab	Pembrolizumab
Volunteer 1	↑	-	-
Volunteer 2	↑	↑	↑
Volunteer 3	↑	↓	-

C) T-ADCC	Atezolizumab	Nivolumab	Pembrolizumab
Volunteer 1	-	-	↑
Volunteer 2	↓	-	↓
Volunteer 3	-	-	-

4.5 Analysis of functional capabilities of un-activated T cells

An enriched T cell population (T cells) was isolated from healthy volunteer blood samples to investigate the effect of ICI and trastuzumab treatment on the ability of T cells to elicit cytotoxicity against K562 cells and HER2+ breast cancer cell lines. T cells were selected for analysis as they play a major role in the anti-tumour immune response and can be suppressed by immune checkpoint expression, as well as eliciting low levels of T-ADCC. It was not expected that the un-activated T cell populations from healthy volunteers would result in substantial cytotoxicity as they are not primed for tumour cell killing and have low potential for inducing T-ADCC [319].

4.5.1 Impact of ICIs on un-activated T cell-mediated cytotoxicity against the K562 cell line

T cells were isolated from healthy volunteer blood samples 4, 5 and 6 and run in an assay as per Section 2.15, plate layout Figure 2.11. After a 12-hour incubation, the percentage cytotoxicity against cancer cells was determined using flow cytometry.

The average % cytotoxicity elicited against the K562 cells across healthy volunteer samples 4, 5 and 6 was -0.35 ± 1.41 % (**Table 4.5**). The ICIs examined had no consistent effects on cytotoxicity levels of the T cells against the K562 cell line, with only nivolumab causing an increase in one volunteer sample (**Table 4.5**).

Table 4.5: % direct cytotoxicity elicited by un-activated T cells against the K562 cell line. Significant alterations to cytotoxicity in the presence of atezolizumab, nivolumab and pembrolizumab are denoted with an arrow. NS=Not significant, - = No change. All antibodies were used at a concentration of 10 µg/µL.

Volunteer no.	% Cytotoxicity	Atezolizumab	Nivolumab	Pembrolizumab
Volunteer 4	-1.38 ± 1.13 %	-	-	-
Volunteer 5	1.25 ± 2.57 %	-	-	-
Volunteer 6	-0.92 ± 0.45 %	-	↑	-

4.5.2 Impact of ICIs on un-activated T cell-mediated cytotoxicity against HER2+ breast cancer cell lines

4.5.2.1 SKBR3

Overall cytotoxicity levels elicited by the freshly isolated un-activated T cells against SKBR3 cells was low (2.25 ± 5.74 %) and there were no consistent alterations to overall cytotoxicity levels with the addition of any of the ICIs examined (**Figure 4.5 and Table 4.6**).

The un-activated T cells elicited very low levels of direct cytotoxicity against SKBR3 cells with an average % direct cytotoxicity of 0.73 ± 4.26 % across the three volunteer samples used. This was not consistently altered by the addition of any of the ICIs examined (**Figure 4.5 and Table 4.6**).

Average T-ADCC levels against the SKBR3 cells were low, with an average of 0.38 ±1.21 % across the three volunteer samples used. There was a significant increase in T-ADCC against the SKBR3 cells with the addition of atezolizumab in volunteer samples 5 and 6 by 6.19 % ($p=0.011$) and 4.43 % ($p=0.028$) respectively. T-ADCC levels were also increased in the presence of pembrolizumab in volunteer 5 and 6 by 9.00 % ($p=0.005$) and 4.87 % ($p=0.083$) respectively (**Figure 4.5 and Table 4.6**).

Cytotoxicity elicited by un-activated isolated T cells was low in general, as expected. Neither direct cytotoxicity nor the overall level of cytotoxicity elicited by freshly isolated T cells were consistently affected by any of the ICIs examined. However, two volunteer samples did register minor, unexpected alterations to T-ADCC.

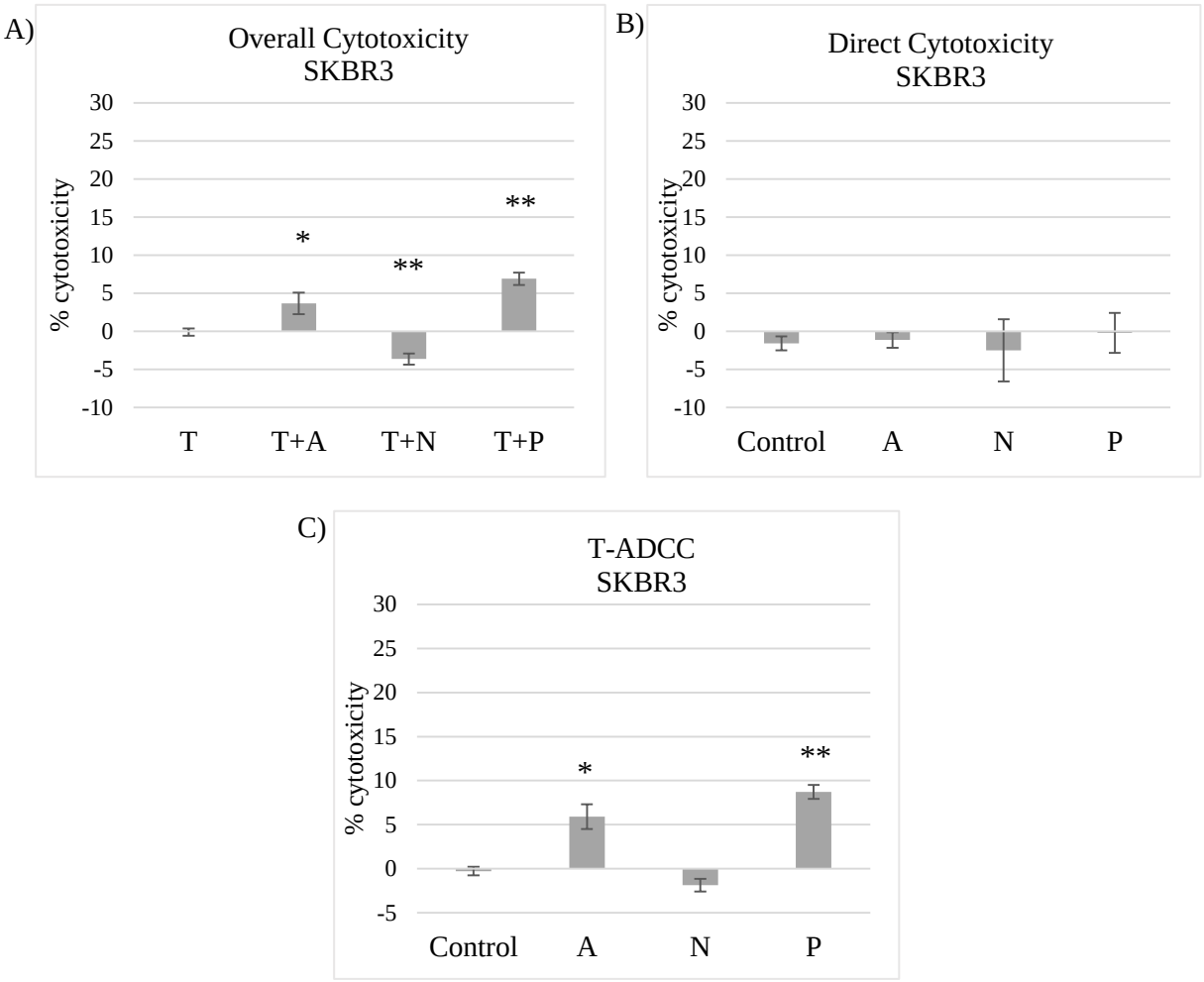

Figure 4.5: Un-activated T cell-mediated cytotoxicity against the SKBR3 cell line from a representative volunteer sample (Volunteer 5) A) Overall cytotoxicity **B)** Direct cytotoxicity **C)** T-ADCC. Error bars represent standard deviation of technical triplicate experiments. The Student's t test was used to determine statistical significance. * $p < 0.05$, ** $p < 0.01$ and *** $p < 0.001$. All antibodies were used at a concentration of 10 µg/µL.

Table 4.6: Un-activated T cell-mediated cytotoxicity against the SKBR3 cell line for all three volunteer samples A) Overall cytotoxicity **B)** Direct Cytotoxicity **C)** T-ADCC. Arrows denote statistically significant change in cytotoxicity levels. The Student's t test was used to determine statistical significance. NS = not significant, - = No change. All antibodies were used at a concentration of 10 µg/µL.

A) Overall Cytotoxicity	Atezolizumab	Nivolumab	Pembrolizumab
Volunteer 4	-	-	-
Volunteer 5	↑	↓	↑
Volunteer 6	↓	↓	-

B) Direct Cytotoxicity	Atezolizumab	Nivolumab	Pembrolizumab
Volunteer 4	-	-	-
Volunteer 5	-	-	-
Volunteer 6	↓	↓	-

C) T-ADCC	Atezolizumab	Nivolumab	Pembrolizumab
Volunteer 4	-	-	-
Volunteer 5	↑	-	↑
Volunteer 6	↑	-	-

4.5.2.2 HCC1954

Overall cytotoxicity levels elicited by un-activated T cells against HCC1954 were low (-1.71 ± 1.59 %) and levels remained unchanged with the addition of the ICI examined (**Figure 4.6 and Table 4.7**). The level of direct cytotoxicity elicited by un-activated T cells against the HCC1954 cells was an average of -4.29 ± 4.08 % across healthy volunteers 4, 5 and 6. The addition of ICI did not cause any consistent alteration to direct cytotoxicity mediated by the un-activated T cells against the HCC1954 cells (**Figure 4.6 and Table 4.7**). T-ADCC levels were low at an average of 0.28 ± 1.46 %, T-ADCC levels were also not affected by the addition of any of the ICI examined.

When used in this model, un-activated T cells elicit very low levels of cytotoxicity against the HCC1954 cell line and ICIs did not alter measured cytotoxicity.

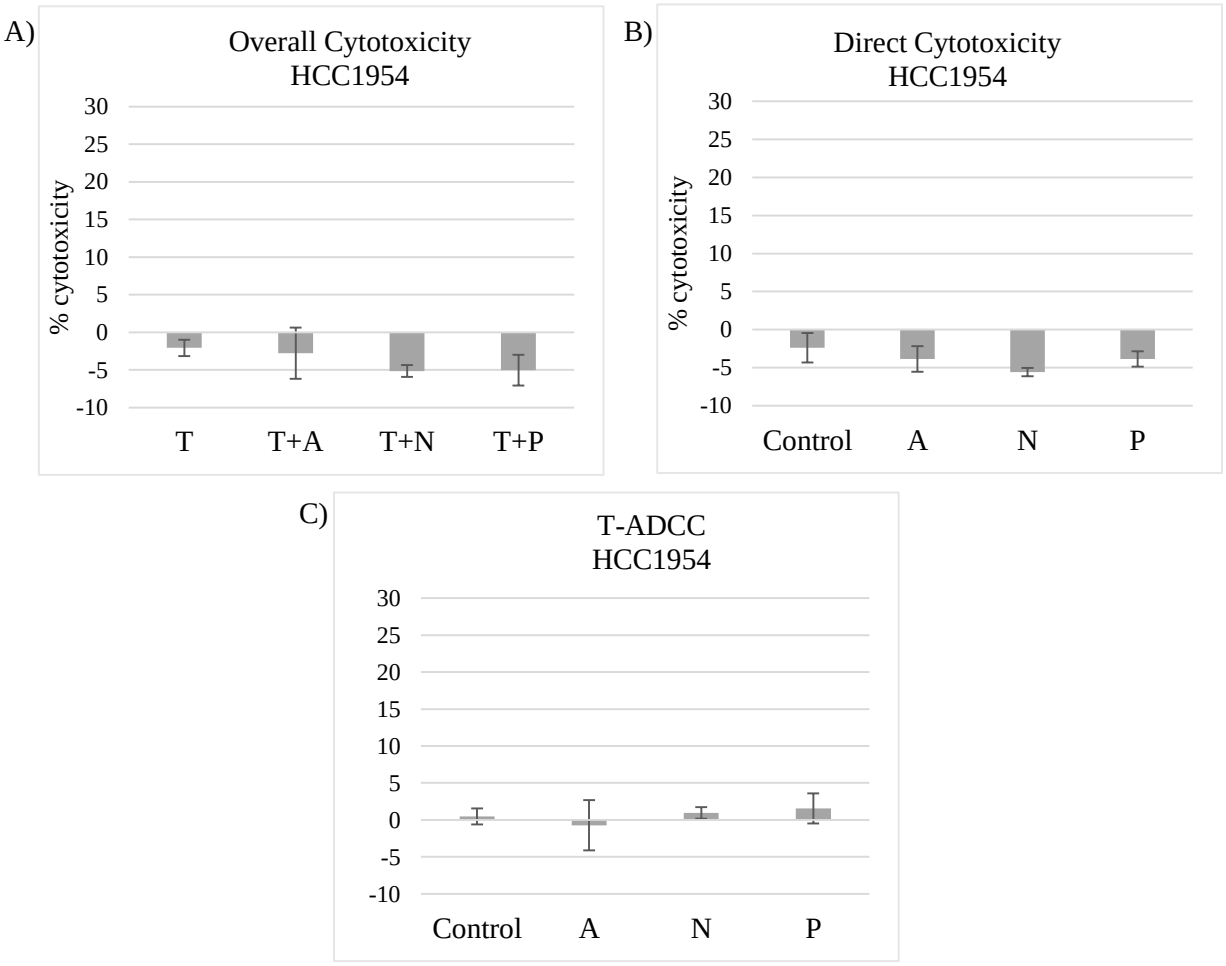

Figure 4.6: Un-activated T cell-mediated cytotoxicity against the HCC1954 cell line from a representative volunteer sample (Volunteer 5) A) Overall cytotoxicity **B)** Direct cytotoxicity **C)** T-ADCC. Error bars represent standard deviation of technical triplicate experiments. The Student's t test was used to determine statistical significance. * $p < 0.05$, ** $p < 0.01$ and *** $p < 0.001$. All antibodies were used at a concentration of 10 µg/µL.

Table 4.7: Un-activated T cell-mediated cytotoxicity against the HCC1954 cell line for all three volunteer samples A) Overall cytotoxicity **B)** Direct Cytotoxicity **C)** T-ADCC. Arrows denote statistically significant change in cytotoxicity levels. The Student's t test was used to determine statistical significance. NS= Not significant, - = No change. All antibodies were used at a concentration of 10 µg/µL.

A) Overall Cytotoxicity	Atezolizumab	Nivolumab	Pembrolizumab
Volunteer 4	↓	↓	-
Volunteer 5	-	-	-
Volunteer 6	-	-	-

B) Direct Cytotoxicity	Atezolizumab	Nivolumab	Pembrolizumab
Volunteer 4	↑	-	-
Volunteer 5	-	-	-
Volunteer 6	-	↑	-

C) T-ADCC	Atezolizumab	Nivolumab	Pembrolizumab
Volunteer 4	↓	↓	-
Volunteer 5	-	-	-
Volunteer 6	-	-	-

4.6 Analysis of functional capabilities of activated T cells

T cells were isolated from healthy volunteer samples 7, 8, 9 and 10. T cells from volunteer 7 were used to optimise a T cell activation protocol to be used in the immune cytotoxicity assay. T cells from volunteer 8, 9 and 10 were activated and used to assess the cytotoxicity levels elicited against K562 and HER2+ cell lines with and without the addition of trastuzumab and ICIs. The potential cytotoxicity of T cells in this setting is unknown.

4.6.1 Activation of T cells

T cells from volunteer 7 were cultured in the presence of CD3/CD28 dynabeads along with 30 IU of IL-2 for 8 days. The Gibco CD3/CD28 dynabeads protocol stated T cell exhaustion would occur within approximately 5-7 days of culturing (**Section 2.13**). On days 0, 1, 3, 6 and 8, cells were analysed by flow cytometry to examine activation status.

When the markers expressed on the T cells were examined, CD3 levels remained constant across all days examined at 76.49 ±8.64 % (**Figure 4.7**). CD69, a T cell activation marker, showed a low level expression in early culturing (day 0: 0.16 ± 0.07 %), with increased levels on day 6 (2.75 ± 1.60 %) (**Figure 4.7**). PD-1 and PD-L1 expression also increased on day 6 of culture (PD-1- day 0: 3.20 ± 0.27 %, day 6: 5.89 ± 0.09 %) (PD-L1– day 0: 3.24 ± 1.06 %, day 6: 14.20 ± 9.55 %) (**Figure 4.7**). Day 6 was picked as the optimum day to examine T cells as the population remained active (as characterised by CD69 expression) but were becoming anergic/exhausted as evidenced by increased PD-1 and PD-L1 expression.

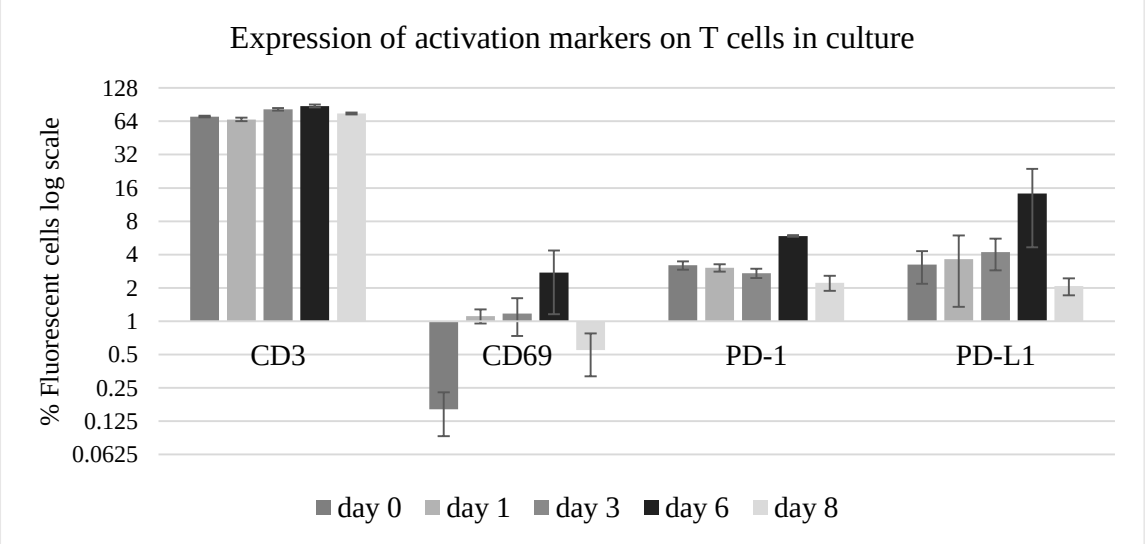

Figure 4.7: Expression of CD3, CD69, PD-1 and PD-L1 on T cells over 8 days of culture with CD3/CD28 dynabeads and IL-2. % fluorescent staining was relative to an unstained control. Error bars for days 0, 1 and 3 represent triplicate wells. Error bars for day 6 and 8 represent duplicate wells.

4.6.2 Morphology

The morphology of the T cells changed during culturing. They grew in size and became more irregular in shape. The T cells were also rapidly dividing and forming clusters of cells. These changes did not occur in the untreated T cell wells (**Figure 4.8**).

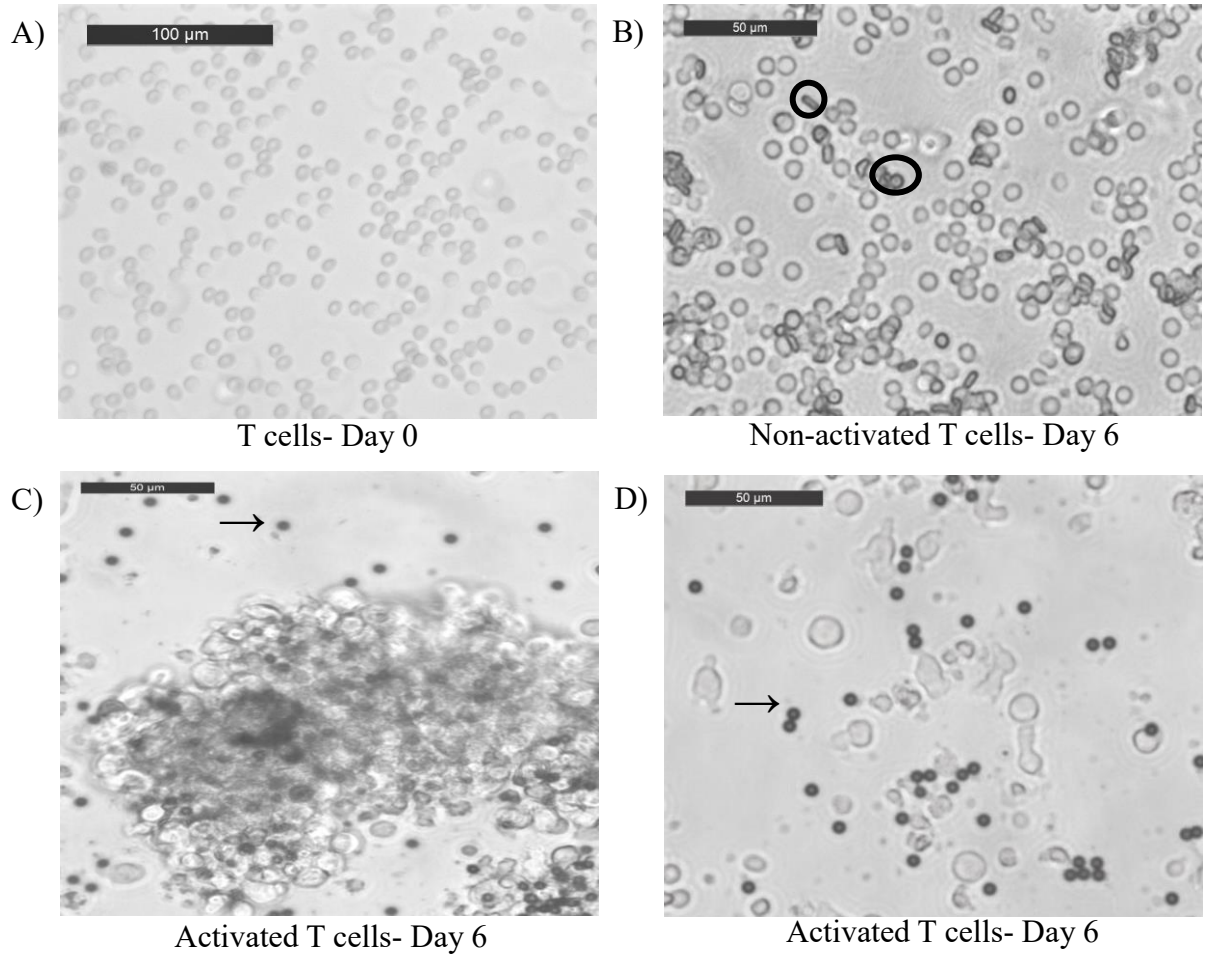

Figure 4.8: Volunteer 7 A) Un-activated T cells day 0. **B)** Un-activated T cells day 6 **C)** Cluster of activated T cells day 6. **D)** Singular activated T cells day 6. Circles mark red blood cell. Arrows marks CD3/CD28 dynabeads.

4.6.3 Impact of ICIs on activated T cell-mediated cytotoxicity against K562 cell line

Activated T cells were used in immune cytotoxicity assays against K562 using plate layout as per Section 2, Figure 2.11. After 12 hours incubation % tumour cell cytotoxicity was determined by flow cytometry.

Cytotoxicity levels elicited by the activated T cells against the K562 cell line were higher than un-activated T cells. Un-activated T cells elicited an average cytotoxicity level of 0.35 ± 1.41 % (**Table 4.5**) against the K562 cells. Activated T cells elicited an average cytotoxicity level of 13.87 ± 9.77 % (**Table 4.8**). The ICI examined did not cause any consistent changes in cytotoxicity elicited by the activated T cells (**Table 4.8**).

Table 4.8: % cytotoxicity elicited by activated T cells against the K562 cell line and significant alterations to cytotoxicity in the presence of atezolizumab, nivolumab and pembrolizumab. Arrows denote statistically significant change in cytotoxicity levels. The Student's t test was used to determine statistical significance. NS= Not significant, - = No change. All antibodies were used at a concentration of 10 µg/µL.

Volunteer no.	% Cytotoxicity	Atezolizumab	Nivolumab	Pembrolizumab
Volunteer 7	23.93 ± 0.97 %	-	-	-
Volunteer 8	4.43 ± 0.35 %	↑	-	-
Volunteer 9	13.24 ± 1.05 %	-	-	-

4.6.4 Impact of ICIs on activated T cell-mediated cytotoxicity against HER2+ breast cancer cell lines

Activated T cells were used in immune cytotoxicity assays against SKBR3 and HCC1954 using plate layout as per Section 2, Figure 2.11. After 12 hours incubation % tumour cell cytotoxicity was determined by flow cytometry.

4.6.4.1 SKBR3

There were no consistent changes to overall cytotoxicity levels elicited by activated T cells in the presence of trastuzumab and the ICIs examined (**Figure 4.9 and Table 4.9**).

Atezolizumab treatment resulted in small but significant increases in the level of direct cytotoxicity elicited by the activated T cells, 4.75 % p=0.013 and 2.6 % p=0.049 for volunteers 8 and 9 respectively

(**Figure 4.9 and Table 4.9**). Nivolumab also increased the level of direct cytotoxicity for volunteer 8 by 7.07 % which was approaching significance (p=0.059) (**Figure 4.9 and Table 4.9**). Pembrolizumab produced a 7.89 % increase in the level of direct cytotoxicity elicited by the activated T cells for volunteer 8 (p=0.005) against the SKBR3 cells (**Figure 4.9 and Table 4.9**).

T-ADCC levels against the SKBR3 cells were low with the activated T cells at an average of -2.95 ± 2.66 % across all three volunteers (**Figure 4.9**).

There was no persistent change to T-ADCC levels or overall cytotoxicity levels elicited by the activated T cells against SKBR3 cells in the presence of the ICIs examined. The ICIs were capable of increasing direct cytotoxicity elicited by activated T cells on some occasions, but this effect was not consistent

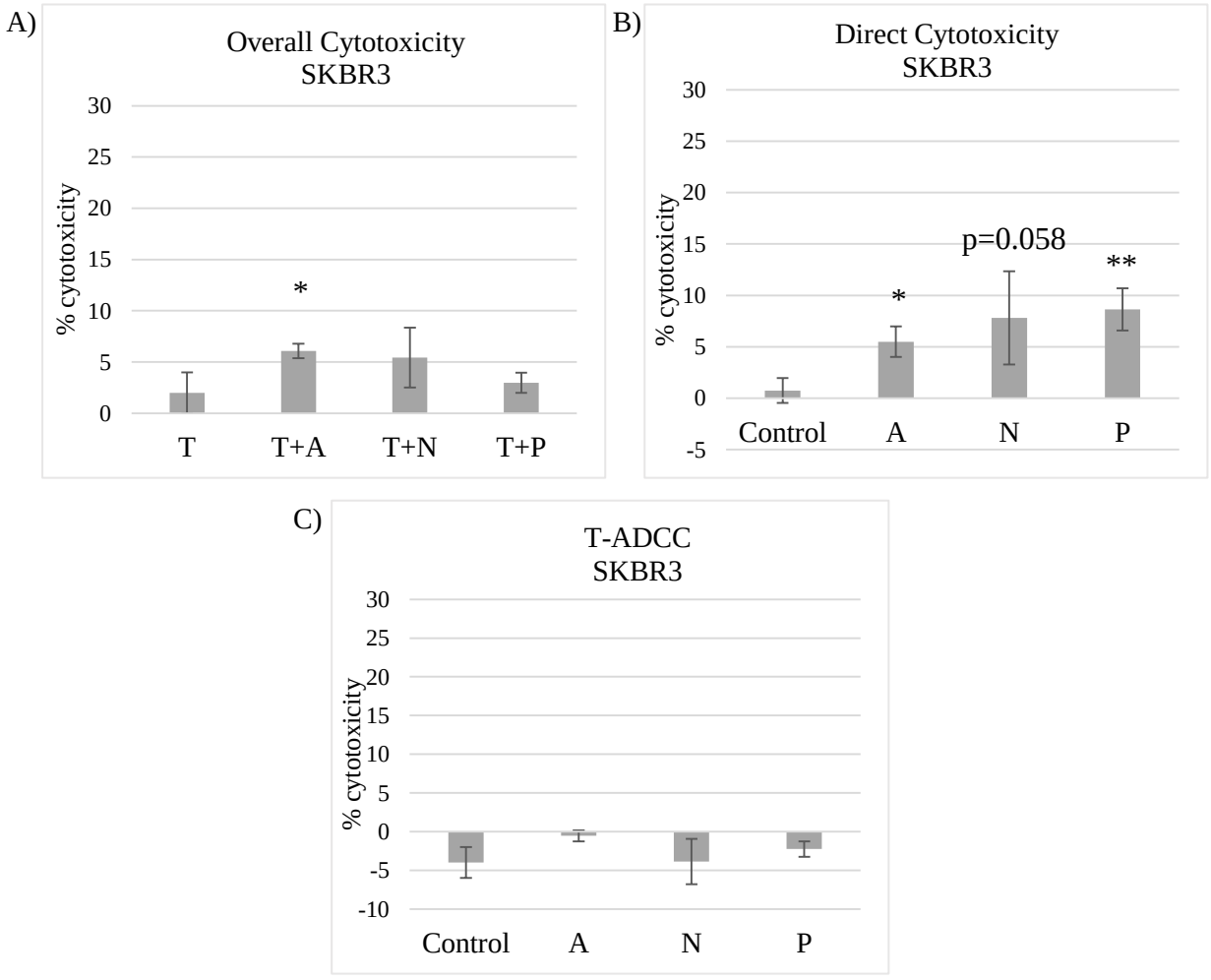

Figure 4.9: Activated T cell-mediated cytotoxicity against the SKBR3 cell line from a representative volunteer sample (Volunteer 8). A) Overall cytotoxicity **B)** Direct cytotoxicity **C)** T-ADCC. Error bars represent standard deviation of technical triplicate experiments. The Student's t test was used to determine statistical significance. * $p < 0.05$, ** $p < 0.01$ and *** $p < 0.001$. All antibodies were used at a concentration of 10 µg/µL.

Table 4.9: Activated T cell-mediated cytotoxicity against the SKBR3 cell line for all three volunteer samples A) Overall cytotoxicity **B)** Direct Cytotoxicity **C)** T-ADCC. Arrows denote statistically significant change in cytotoxicity levels. The Student's t test was used to determine statistical significance. NS=Not significant, - = No change. All antibodies were used at a concentration of 10 µg/µL.

A) Overall Cytotoxicity	**Atezolizumab**	**Nivolumab**	**Pembrolizumab**
Volunteer 8	↑	-	-
Volunteer 9	-	-	-
Volunteer 10	-	↑	-

B) Direct Cytotoxicity	**Atezolizumab**	**Nivolumab**	**Pembrolizumab**
Volunteer 8	↑	NS↑	↑
Volunteer 9	↑	-	NS↑
Volunteer 10	-	-	-

C) T-ADCC	**Atezolizumab**	**Nivolumab**	**Pembrolizumab**
Volunteer 8	-	-	-
Volunteer 9	-	-	-
Volunteer 10	↑	-	-

4.6.4.2 HCC1954

Overall cytotoxicity levels in the presence of trastuzumab were not consistently affected in conditions tested by the addition of any of the ICIs examined. There was an increase in overall cytotoxicity elicited by volunteer 8 in the presence of nivolumab (7.35 %, p=0.001) and pembrolizumab (7.01 %, p=0.055) (**Figure 4.10 and Table 4.10**).

Atezolizumab alone increased the direct cytotoxicity elicited by volunteer 10 (3.53 %, p=0.007). Nivolumab treatment produced a significant increase in direct cytotoxicity of 9.83 % (p=0.005) and 4.13 % (p=0.010) for volunteers 8 and 10. Pembrolizumab caused an increase of 8.11 % (p=0.022) and 5.43 % (p=0.012) in direct cytotoxicity for volunteers 8 and 10 (**Figure 4.10 and Table 4.10**).

As with SKBR3, T-ADCC was low with an average of -3.25 ± 2.70 % across all three volunteers. There was no consistent change to T-ADCC elicited by the activated T cells in the presence of the ICIs examined (**Table 4.10**).

The HCC1954 assay model showed that the ICIs examined were capable of inconsistently increasing the direct cytotoxicity elicited by activated T cells.

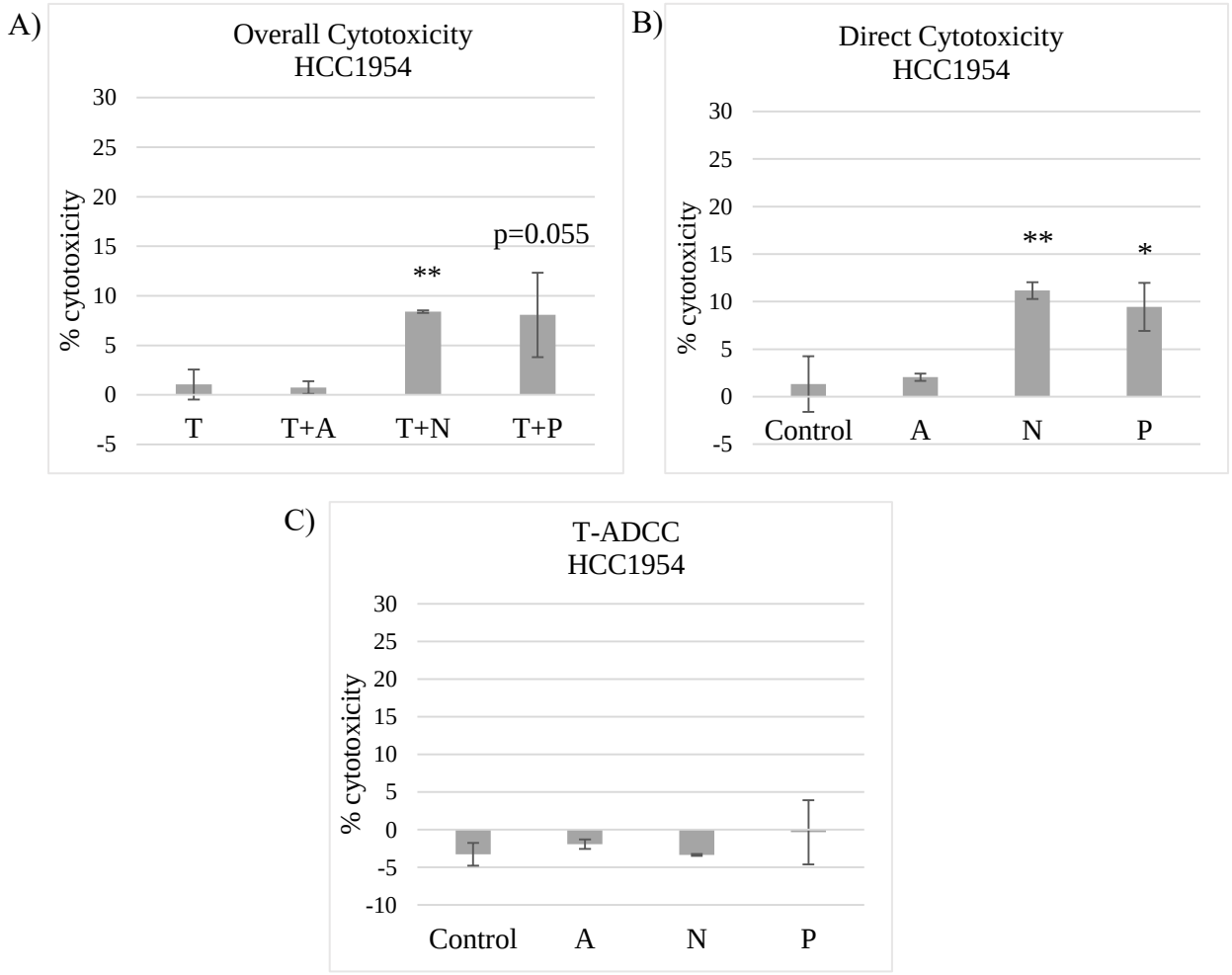

Figure 4.10: Activated T cell-mediated cytotoxicity against the HCC1954 cell line from a representative volunteer sample. (Volunteer 8). A) Overall cytotoxicity **B)** Direct cytotoxicity **C)** T-ADCC. Error bars represent standard deviation of technical triplicate experiments. The Student's t test was used to determine statistical significance. * $p < 0.05$, ** $p < 0.01$ and *** $p < 0.001$. All antibodies were used at a concentration of 10 µg/µL.

Table 4.10: Activated T cell-mediated cytotoxicity against the HCC1954 cell line for all three volunteer samples A) Overall cytotoxicity **B)** Direct Cytotoxicity **C)** T-ADCC. Arrows denote statistically significant change in cytotoxicity levels. The Student's t test was used to determine statistical significance. NS=Not significant, - = No change. All antibodies were used at a concentration of 10 µg/µL.

A) Overall Cytotoxicity	**Atezolizumab**	**Nivolumab**	**Pembrolizumab**
Volunteer 8	-	↑	NS↑
Volunteer 9	-	-	-
Volunteer 10	-	-	-

B) Direct Cytotoxicity	**Atezolizumab**	**Nivolumab**	**Pembrolizumab**
Volunteer 8	-	↑	↑
Volunteer 9	-	-	-
Volunteer 10	↑	↑	↑

C) T-ADCC	**Atezolizumab**	**Nivolumab**	**Pembrolizumab**
Volunteer 8	-	-	-
Volunteer 9	↑	-	-
Volunteer 10	-	-	-

4.7 Analysis of functional capabilities of unstimulated NK cells

An enriched NK cell population (NK cells) was isolated from healthy volunteer blood samples in order to investigate the effect of ICI and trastuzumab treatment on their ability to elicit cytotoxicity against HER2+ breast cancer cell lines. NK cells were selected for analysis as they are a prominent effector cell of ADCC and non-antigen specific direct cytotoxicity. Unstimulated NK cells were used in the ADCC assay against K562, SKBR3 and HCC1954 cell lines to determine any potential effects on cytotoxicity.

4.7.1 Impact of ICIs on unstimulated NK cell-mediated cytotoxicity against the K562 cell line

NK cells were isolated from healthy volunteers 4, 5, and 6 and used in immune cytotoxicity assays against K562, as per Section 2, Figure 2.11. After a 12-hour incubation, % tumour cell cytotoxicity was determined using flow cytometry.

The NK cells elicited an average cytotoxicity level of 11.26 ± 8.90 % across all three volunteers. The NK cells showed a range of cytotoxicity levels against the K562 cell line (**Table 4.11**). The ICIs examined had no significant effect on cytotoxicity elicited against the K562 cells (**Table 4.11**).

Table 4.11: % cytotoxicity elicited by freshly isolated NK cells against the K562 cell line and significant alterations to cytotoxicity in the presence of atezolizumab, nivolumab and pembrolizumab. Arrows denote statistically significant change in cytotoxicity levels. The Student's t test was used to determine statistical significance. NS= Not significant, - = No change. All antibodies were used at a concentration of 10 µg/µL.

Volunteer no.	% Cytotoxicity	Atezolizumab	Nivolumab	Pembrolizumab
Volunteer 4	2.06 ± 0.05 %	-	-	-
Volunteer 5	11.89 ± 1.10 %	-	-	-
Volunteer 6	19.83 ± 4.25 %	-	-	-

4.7.2 Impact of ICIs on unstimulated NK cell-mediated cytotoxicity against HER2+ breast cancer cell lines

NK cells were isolated from healthy volunteers 4, 5, and 6 and used in immune cytotoxicity assays against HER2+/PD-L1 low SKBR3 and HER2+/PD-L1 high HCC1954, as per Section 2, Figure 2.11. After a 12-hour incubation, % tumour cell death was determined using flow cytometry.

4.7.2.1 SKBR3

Overall cytotoxicity levels remained unchanged with the addition of any of the ICIs examined (**Figure 4.11 and Table 4.12**).

Atezolizumab increased direct cytotoxicity against SKBR3 cells by 20.33 % (p=0.002) for volunteer 6. Nivolumab increased direct cytotoxicity levels by 7.94 % (p=0.001) for volunteer 5 and by 25.13 % (p=0.002) for volunteer 6 (**Figure 4.11 and Tale 4.12**). Pembrolizumab increased direct cytotoxicity of NK cells from volunteer 6 by 15.9 % (p=0.025).

Atezolizumab increased T-ADCC levels for the volunteer 4 sample by 6.63 % (p=0.022) (**Figure 4.11 and Tale 4.12**). T-ADCC levels for the NK cells from volunteer 4 were increased by 10.43 % (p=0.018) in the presence of pembrolizumab (**Figure 4.11 and Tale 4.12**).

While there were volunteer-specific changes to direct cytotoxicity and T-ADCC elicited by unstimulated NK cells against SKBR3 cells in the presence of ICIs, these did not translate in to changes in overall cytotoxicity levels.

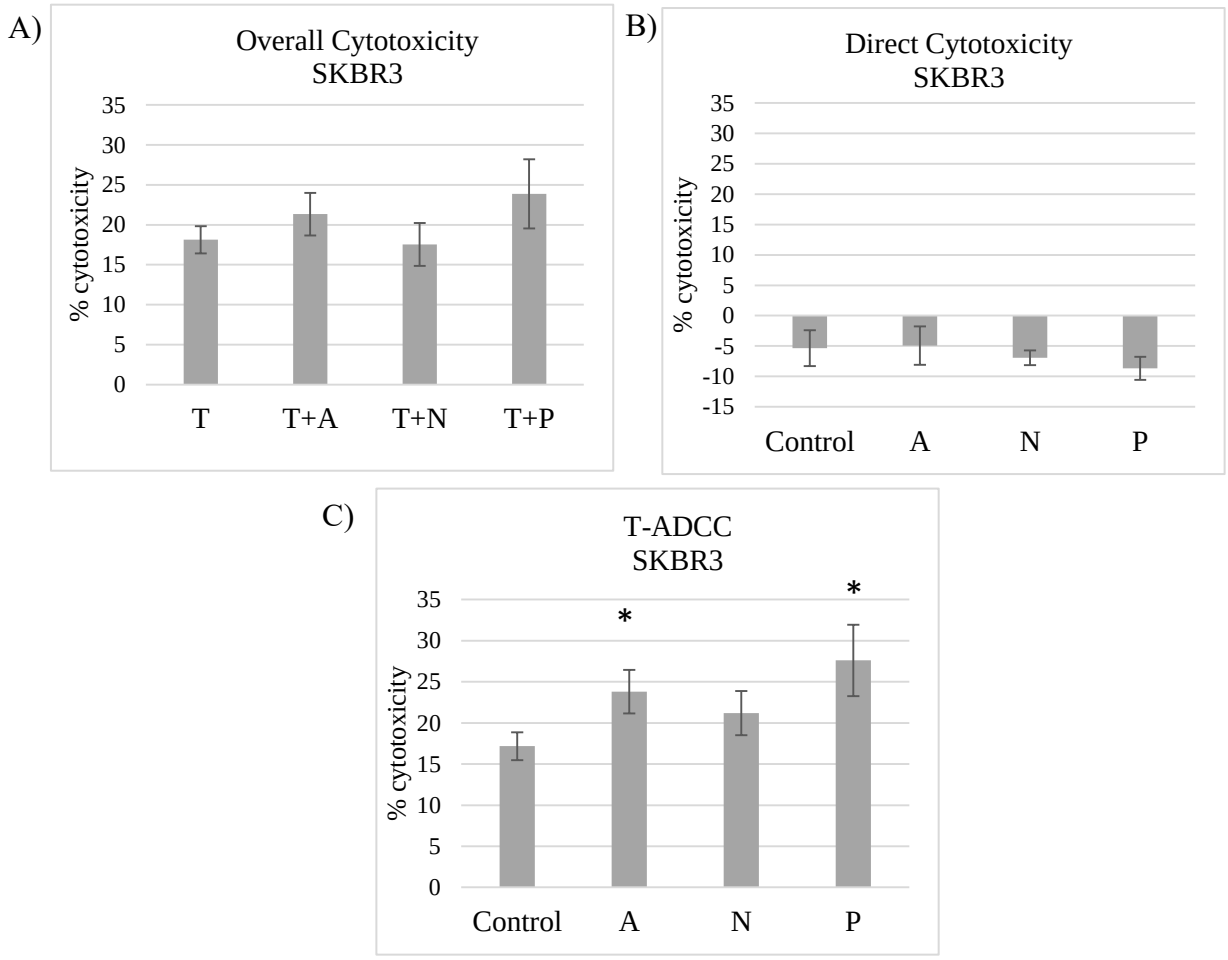

Figure 4.11: Unstimulated NK cell-mediated cytotoxicity against the SKBR3 cell line from a representative volunteer sample. (Volunteer 4). A) Overall cytotoxicity **B)** Direct cytotoxicity **C)** T-ADCC. Error bars represent standard deviation of technical triplicate experiments. The Student's t test was used to determine statistical significance. * $p < 0.05$, ** $p < 0.01$ and *** $p < 0.001$. All antibodies were used at a concentration of 10 µg/µL.

Table 4.12: Unstimulated NK cell-mediated cytotoxicity against the SKBR3 cell line for all three volunteer samples A) Overall cytotoxicity **B)** Direct Cytotoxicity **C)** T-ADCC. Arrows denote statistically significant change in cytotoxicity levels. The Student's t test was used to determine statistical significance. NS=Not significant, - = No change. All antibodies were used at a concentration of 10 µg/µL.

A) Overall Cytotoxicity	Atezolizumab	Nivolumab	Pembrolizumab
Volunteer 4	-	-	-
Volunteer 5	-	-	-
Volunteer 6	-	-	-

B) Direct Cytotoxicity	Atezolizumab	Nivolumab	Pembrolizumab
Volunteer 4	-	-	-
Volunteer 5	-	↑	-
Volunteer 6	↑	↑	↑

C) T-ADCC	Atezolizumab	Nivolumab	Pembrolizumab
Volunteer 4	↑	-	↑
Volunteer 5	-	-	-
Volunteer 6	-	-	-

4.7.2.2 HCC1954

Overall levels of cytotoxicity elicited by unstimulated NK cells against HCC1954 cells in the presence of trastuzumab were inconsistently affected by the addition of an ICI (**Figure 4.12 and Table 4.13**). An increase in overall cytotoxicity elicited by NK cells from volunteer 4 of 9.68 % was measured in the presence of pembrolizumab (p=0.002). Nivolumab increased overall cytotoxicity in the volunteer 5 sample by 11.61 % (p=0.034) (**Figure 4.12 and Table 4.13**).

Direct cytotoxicity of the volunteer 6 NK cells was increased by 3.5 % (p=0.015) in the presence of atezolizumab and 4.33 % (p=0.005) in the presence of nivolumab.

T-ADCC significantly decreased by 6.5 % (p=0.003) in the presence of nivolumab for the volunteer 6 sample and a 6.80 % (p=0.013) (**Figure 4.12 and Tale 4.13**). An increase of 6.8 % was measured in the presence of atezolizumab for volunteer 4 sample (p=0.013) (**Figure 4.12 and Tale 4.13**). Nivolumab increased T-ADCC in the volunteer 4 sample by 5.26 % (p=0.047) and an increase approaching significance of 9.80 % was seen in T-ADCC for volunteer 5 (p=0.054) (**Figure 4.12 and Tale 4.13**). In the presence of pembrolizumab, T-ADCC levels were increased by 12.63 % (p=0.001) using NK cells from volunteer 4 (**Figure 4.12 and Tale 4.13**).

ICIs were capable of altering direct cytotoxicity and T-ADCC mediated by unstimulated healthy volunteer NK cells on some occasions. However overall cytotoxicity levels were not consistently altered with the addition of any of the ICI examined.

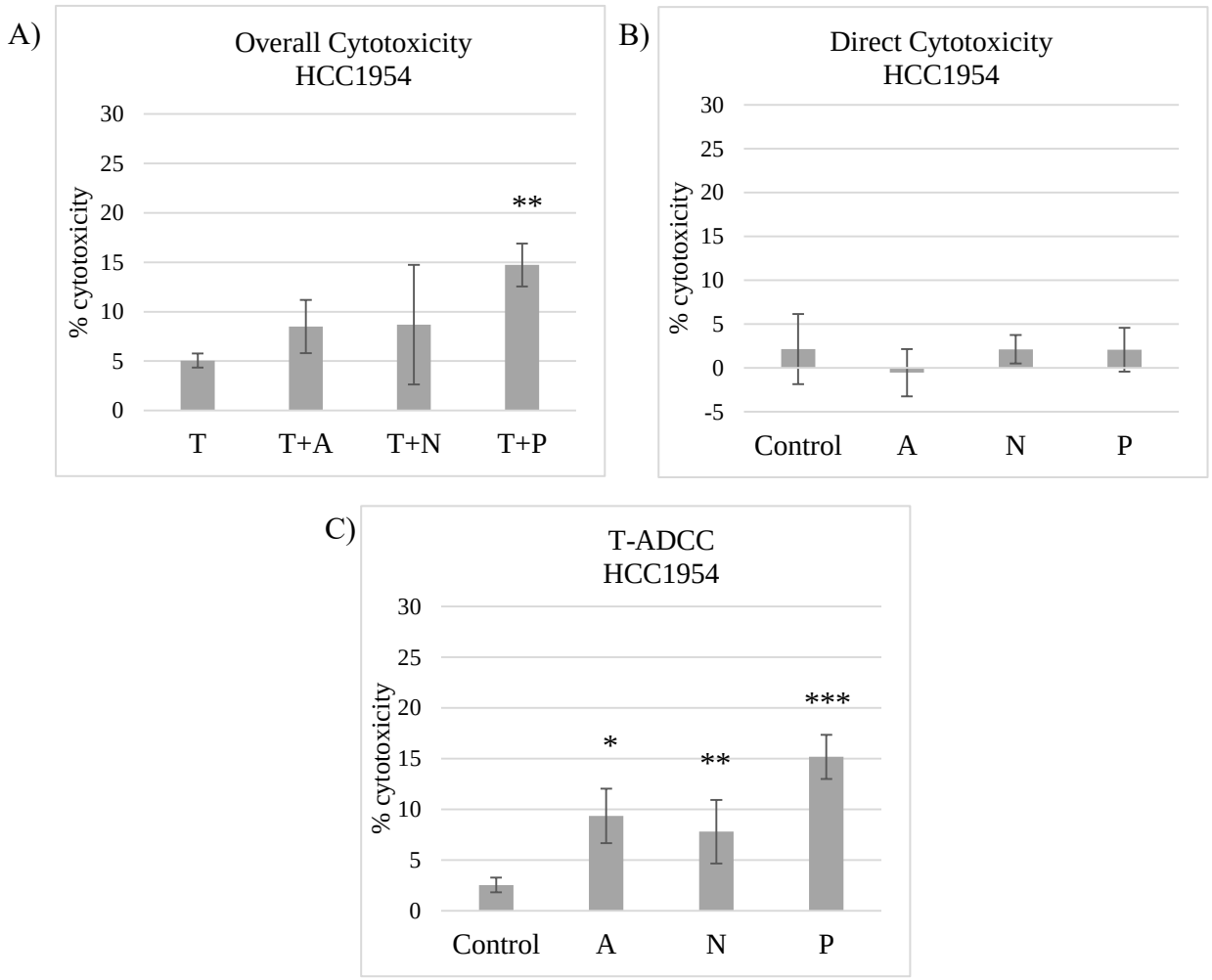

Figure 4.12: Unstimulated NK cell-mediated cytotoxicity against the HCC1954 cell line from a representative volunteer sample. (Volunteer 4). A) Overall cytotoxicity **B)** Direct cytotoxicity **C)** T-ADCC. Error bars represent standard deviation of technical triplicate experiments. The Student's t test was used to determine statistical significance. * $p < 0.05$, ** $p < 0.01$ and *** $p < 0.001$. All antibodies were used at a concentration of 10 µg/µL.

Table 4.13: Unstimulated NK cell-mediated cytotoxicity against the HCC1954 cell line for all three volunteer samples A) Overall cytotoxicity **B)** Direct Cytotoxicity **C)** T-ADCC. Arrows denote statistically significant change in cytotoxicity levels. The Student's t test was used to determine statistical significance. NS=Not significant, - = No change. All antibodies were used at a concentration of 10 µg/µL.

A) Overall Cytotoxicity	Atezolizumab	Nivolumab	Pembrolizumab
Volunteer 4	-	-	↑
Volunteer 5	-	↑	-
Volunteer 6	-	-	-

B) Direct Cytotoxicity	Atezolizumab	Nivolumab	Pembrolizumab
Volunteer 4	-	-	-
Volunteer 5	-	-	-
Volunteer 6	↑	↑	-

C) T-ADCC	Atezolizumab	Nivolumab	Pembrolizumab
Volunteer 4	↑	↑	↑
Volunteer 5	-	NS↑	-
Volunteer 6	-	↓	-

4.8 Analysis of functional capabilites of IL-2 stimulated NK cells

NK cells were isolated from healthy volunteers 7, 8, 9 and 10. NK cells from volunteer 7 were used to develop a method of stimulating NK cells *in vitro*. This method was then applied to samples 8, 9 and 10 to examine the effector capabilities of IL-2 stimulated NK cells against K562 and HER2+ breast cancer cell lines with and without the addition of trastuzumab and ICIs.

4.8.1 IL-2 stimulation of NK cells

NK cells were isolated from volunteer 7 in order to develop a NK cell stimulation protocol for further ADCC assays. The NK cells were cultured for 6 days in the presence of 200 IU of IL-2, on day 0, 1, 3 and 6 by flow cytometry. CD56 levels remained relatively constant throughout the 6 days at 29.06 ± 5.24 % with a spike present on day 3 at 61.72 ± 1.64 %. CD38, an activation marker for NK cells increased expression until day 3 when levels were at 76.27 ± 15.02 % following which, expression decreased to original levels on day 6 (27.03 ± 0.34 %). There was a small increase in PD-1 expression of 2.31 % and PD-L1 expression of 5.61 % on day 3, this was maintained for PD-L1 on day 6 (**Figure 4.13**).

Based on the alteration of in activation markers and immune checkpoint expression, Day 3 was chosen as the most appropriate day to use the stimulated NK cells in the assay.

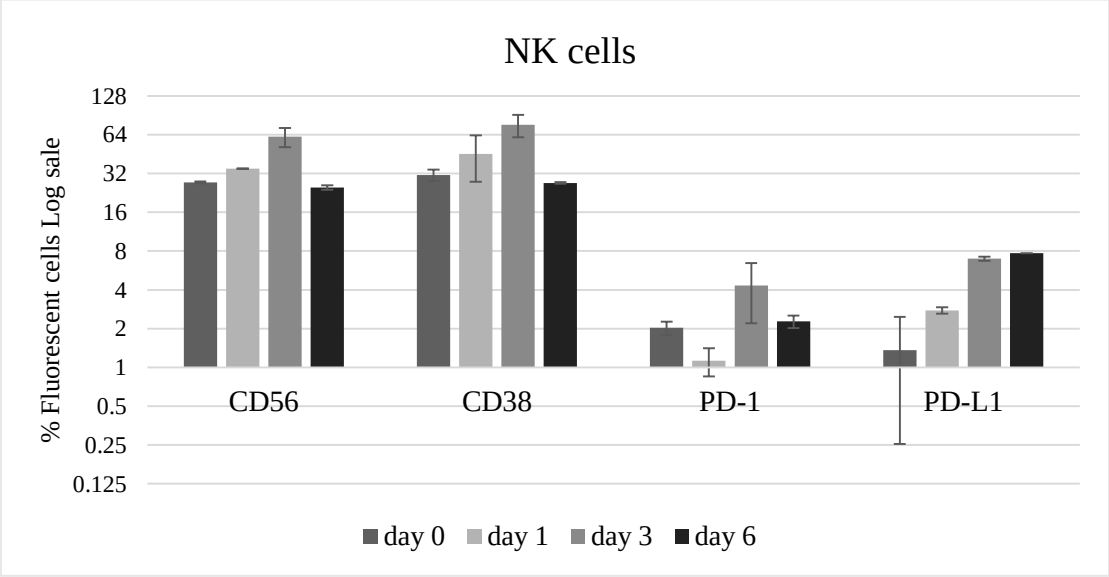

Figure 4.13: Expression of CD56, CD38, PD-1 and PD-L1 on NK cells over 6 days of culturing in the presence of IL-2. % fluorescent staining was relative unstained control. Fluorescence was examined on the Guava flow cytometer. Error bars represent duplicate wells.

4.8.2 Morphology

The morphology of the NK cells was monitored daily during the stimulation process. NK cells were small, spherical cells throughout culture, with no major changes in the size or shape. IL-2 stimulated NK cells began to loosely attach to the plate following approximately 24 hours of treatment.

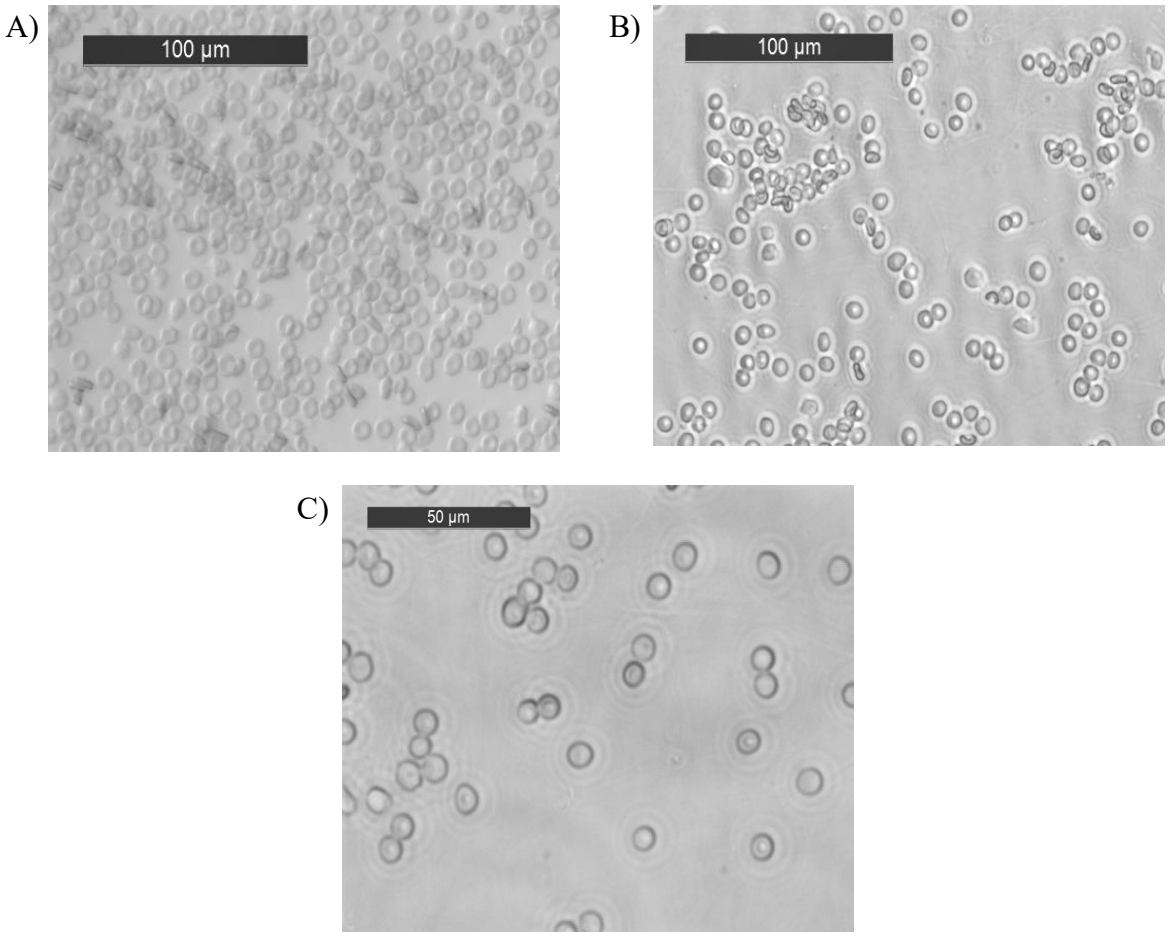

Figure 4.14: A) Non-activated NK cells isolated from healthy volunteer 7, day 0**. B)** IL-2 stimulated NK cells isolated from healthy volunteer 7, day 3 **C)** IL-2 stimulated NK cells from healthy volunteer 7, day 3 at increased magnification.

4.8.3 Impact of ICIs on IL-2 stimulated NK cell-mediated cytotoxicity against the K562 cell line

NK cells were isolated from blood samples from healthy volunteers 8, 9 and 10 and were cultured for 3 days in 200 IU of IL-2. NK cells were then used in an immune cytotoxicity assay with K562, SKBR3 and HCC1954 cell lines as per plate layout in Section 2 Figure 2.11. Tumour cell percentage cytotoxicity was measured by flow cytometry after a 12-hour incubation.

Cytotoxicity levels elicited by the stimulated NK cells against the K562 cells were much higher than unstimulated NK cells (11.26 ± 8.90 %, **Table 4.11**) at an average of 73.18 ± 7.83 % (**Table 4.13**). The ICIs examined did not alter cytotoxicity levels elicited by the stimulated NK cell population.

Table 4.13: % cytotoxicity elicited against the K562 cell line by NK cells and significant alterations to cytotoxicity in the presence of atezolizumab, nivolumab and pembrolizumab. Arrows denote statistically significant change in cytotoxicity levels. The Student's t test was used to determine statistical significance. NS=Not significant, - = No change. All antibodies were used at a concentration of 10 µg/µL.

Volunteer no.	% Cytotoxicity	Atezolizumab	Nivolumab	Pembrolizumab
Volunteer 1	77.63 ± 0.45 %	↓	↓	-
Volunteer 2	77.77 ± 4.44 %	-	-	-
Volunteer 3	64.14 ± 9.46 %	-	-	-

4.8.4 Impact of ICIs on IL-2 stimulated NK cell-mediated cytotoxicity against HER2+ breast cancer cell lines

4.8.4.1 SKBR3

Overall levels of cytotoxicity against SKBR3 cells were altered with the addition of an ICI to trastuzumab within certain samples. Atezolizumab treatment caused an 11.8 % increase in overall cytotoxicity elicited by NK cells isolated from volunteer 8 (p=0.009) (**Figure 4.15 and Table 4.14**). Nivolumab treatment caused a significant increase in overall cytotoxicity in volunteer samples 8 and 9 by 6.8 % (p=0.019) and 7.34 % ($p=1x10^{-4}$) respectively (**Figure 4.15 and Table 4.14**). Pembrolizumab treatment caused an increase in overall cytotoxicity in volunteer 8 by 7.70 % (p=0.073) and in volunteer 9 by 10.08 % ($p=3x10^{-4}$) (**Figure 4.15 and Table 4.14**).

There was a significant increase in direct cytotoxicity elicited by NK cells in the presence of atezolizumab in volunteer samples 9 by 21.06 % (p=0.001) and in volunteer sample 10 by 10.83 % (p=0.001) (**Figure 4.15 and Table 4.14**). Nivolumab increased direct cytotoxicity elicited by the NK cell population against SKBR3 cells for volunteer samples 8, 9 and 10 by 19.84 % (p=0.008), 25.65 % (p=0.001) and 15 % (p=0.003) respectively (**Figure 4.15 and Table 4.14**). Pembrolizumab elicited an increase in direct cytotoxicity in volunteer 9 by 9.49 % (p=0.011) and in volunteer 10 by 7.37 % (p=0.019) (**Figure 4.15 and Table 4.14**).

There was a significant increase in T-ADCC by 36.66 % (p=0.0009) in the presence of atezolizumab in volunteer sample 8 (**Figure 4.15 and Table 4.14**). Pembrolizumab caused an increase in T-ADCC in volunteer 8 by 29.46 % (p=0.001) and in volunteer 9 by 2.61 % (p=0.049) (**Figure 4.15 and Table 4.14**).

Overall cytotoxicity was altered in certain samples. These changes came primarily from alterations to direct cytotoxicity. This setting would be best suited for examining changes which occurred in direct cytotoxicity elicited by the addition of ICIs.

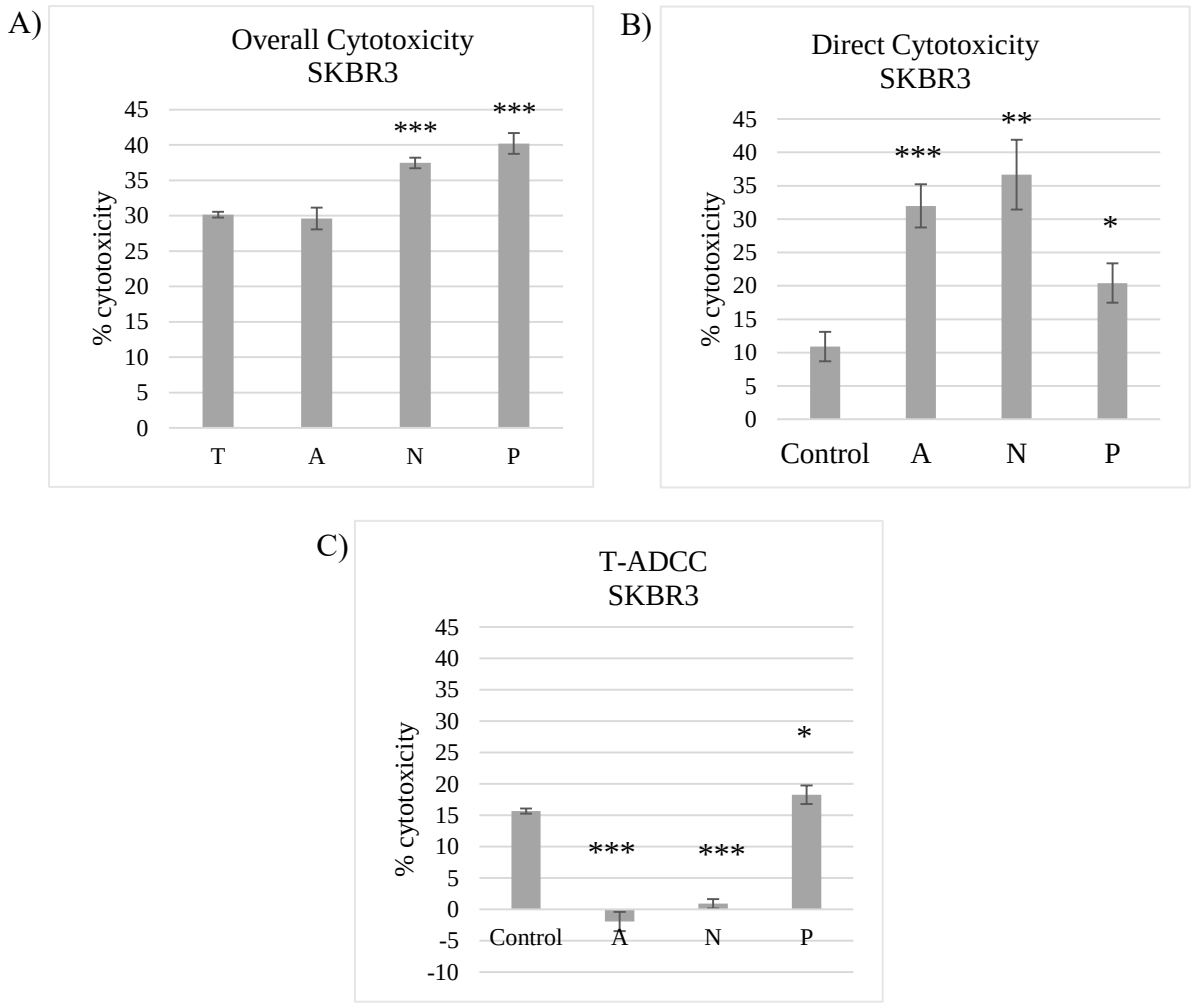

Figure 4.15: IL-2-stimulated NK cell-mediated cytotoxicity against the SKBR3 cell line from a representative volunteer sample (Volunteer 9). A) Overall cytotoxicity **B)** Direct cytotoxicity **C)** T-ADCC. Error bars represent standard deviation of technical triplicate experiments. The Student's t test was used to determine statistical significance. * $p < 0.05$, ** $p < 0.01$ and *** $p < 0.001$. All antibodies were used at a concentration of 10 µg/µL.

Table 4.14: IL-2-stimulated NK cell-mediated cytotoxicity against the SKBR3 cell line for all three volunteer samples A) Overall cytotoxicity **B)** Direct Cytotoxicity **C)** T-ADCC. Arrows denote statistically significant change in cytotoxicity levels. The Student's t test was used to determine statistical significance. NS=Not significant, - = No change. All antibodies were used at a concentration of 10 µg/µL.

A) Overall Cytotoxicity	Atezolizumab	Nivolumab	Pembrolizumab
Volunteer 8	↑	↑	NS↑
Volunteer 9	-	↑	↑
Volunteer 10	-	-	-

B) Direct Cytotoxicity	Atezolizumab	Nivolumab	Pembrolizumab
Volunteer 8	-	↑	-
Volunteer 9	↑	↑	↑
Volunteer 10	↑	↑	↑

C) T-ADCC	Atezolizumab	Nivolumab	Pembrolizumab
Volunteer 8	↑	↓	↑
Volunteer 9	↓	↓	↑
Volunteer 10	↓	-	↓

4.8.4.2 HCC1954

Overall cytotoxicity elicited by the NK cells was increased in the presence of atezolizumab for volunteer sample 8 by 7.70 % (p=0.005) and volunteer sample 10 by 6.83 % (p=0.004) (**Figure 4.16 and Table 4.15**). Overall cytotoxicity elicited by NK cells in the presence of nivolumab was increased with samples from volunteers 8, 9 and 10 by 5.57 (p=0.049), 5.57 (p=0.008) and 5.67 % (p=0.029) respectively (**Figure 4.16 and Table 4.15**). Overall levels of cytotoxicity elicited by the NK cells was increased in volunteer 8 by 8.85 % (p=0.005) and volunteer 9 by 6.07 % (p=0.012) in the presence of pembrolizumab (**Figure 4.16 and Table 4.15**).

Nivolumab treatment increased direct cytotoxicity for volunteer 9 by 5.93 % (p=0.018) and volunteer 10 by 4.70 % (p=0.027). (**Figure 4.16 and Table 4.15**). Pembrolizumab treatment increased in T-ADCC from volunteer 8 and 9 by 5.4 % (p=0.028) and 7.37 % (p=0.006) respectively (**Figure 4.16 and Table 4.15**). All other changes in overall cytotoxicity were accounted for by non-significant increases in either direct cytotoxicity, T-ADCC or both (**Table 4.15**).

There was an increase in overall cytotoxicity elicited by NK cells in most samples with the addition of the ICI. These increases were mediated by increases in direct cytotoxicity and T-ADCC depending on the ICI and the sample used. Using IL-2 stimulated NK cells against HCC1954 cells may be useful in examining the effects of ICIs *in vitro* on overall cytotoxicity in the presence of trastuzumab.

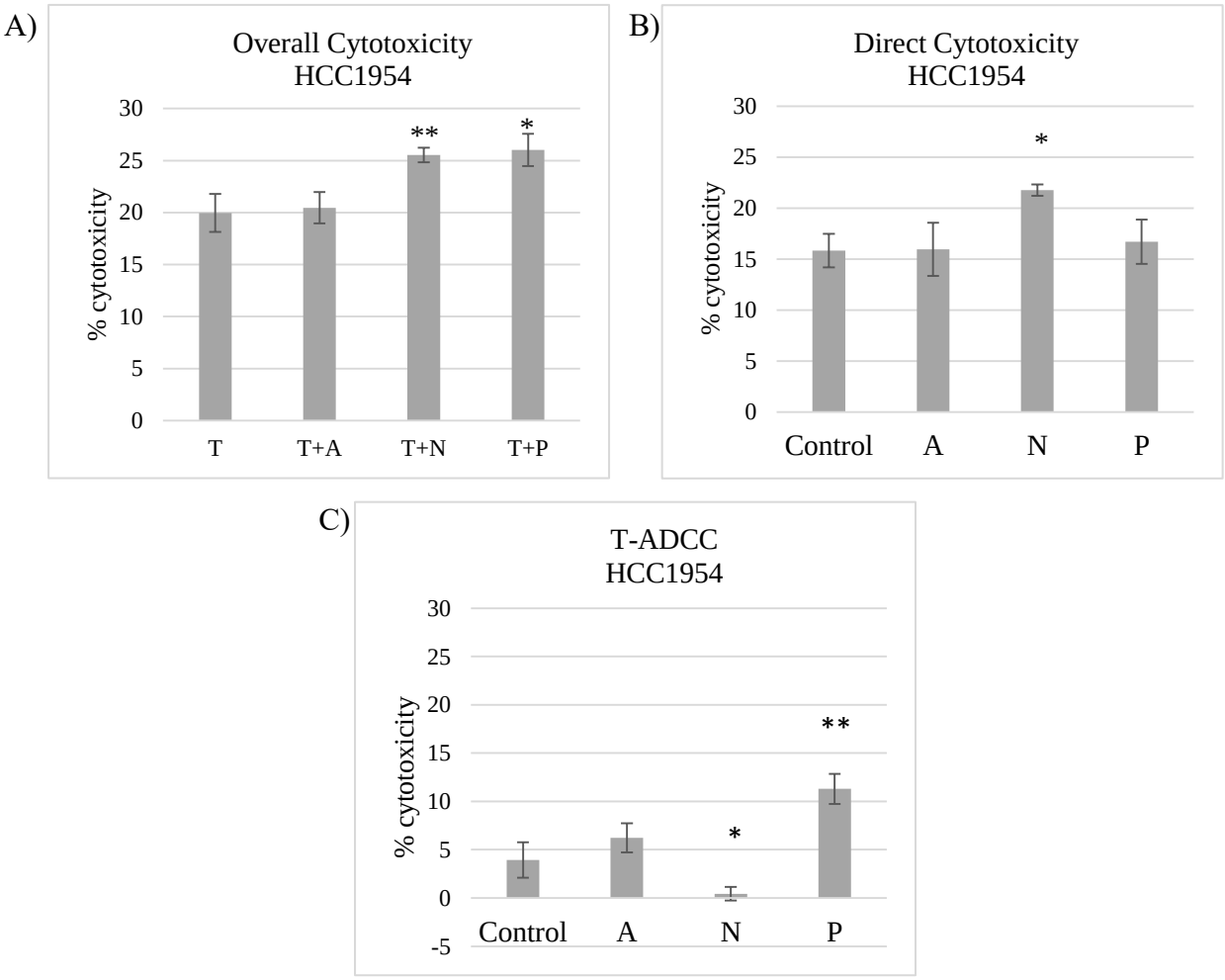

Figure 4.16: IL-2-stimulated NK cell-mediated cytotoxicity against the HCC1954 cell line from a representative volunteer sample (Volunteer 9) A) Overall cytotoxicity **B)** Direct cytotoxicity **C)** T-ADCC. Error bars represent standard deviation of technical triplicate experiments. The Student's t test was used to determine statistical significance. * $p < 0.05$, ** $p < 0.01$ and *** $p < 0.001$. All antibodies were used at a concentration of 10 µg/µL.

Table 4.15: IL-2-stimulated NK cell-mediated cytotoxicity against the HCC1954 cell line for all three volunteer samples A) Overall cytotoxicity **B)** Direct Cytotoxicity **C)** T-ADCC. Arrows denote statistically significant change in cytotoxicity levels. The Student's t test was used to determine statistical significance. NS= Not significant, - = No change. All antibodies were used at a concentration of 10 µg/µL.

A) Overall Cytotoxicity	Atezolizumab	Nivolumab	Pembrolizumab
Volunteer 8	↑	↑	↑
Volunteer 9	-	↑	↑
Volunteer 10	↑	↑	-

B) Direct Cytotoxicity	Atezolizumab	Nivolumab	Pembrolizumab
Volunteer 8	NS ↑	-	-
Volunteer 9	-	↑	-
Volunteer 10	NS ↑	↑	-

C) T-ADCC	Atezolizumab	Nivolumab	Pembrolizumab
Volunteer 8	NS ↑	NS↑	↑
Volunteer 9	NS ↑	↓	↑
Volunteer 10	-	-	↓

4.9 Expression of other immune-response relevant proteins in HCC1954 vs. SKBR3 cell lines

There is a difference in susceptibility of SKBR3 and HCC1954 to immune cell cytotoxicity. This is reflected in the SKBR3 cell line being more susceptible to direct immune cell mediated cytotoxicity (**Section 4.4.2.1 and 4.8.4.1**), while the HCC1954 cell line is more susceptible to T-ADCC than SKBR3 (**Section 4.8.4.2**). There is a clear difference in PD-L1 expression (**Section 4.2**) but there may be changes to other immune response–related proteins which contributes to these changes.

Expression of four additional proteins (MHC class-I, MICA, NKTR and E-cadherin) associated with immune response was determined in these two cell line models (**Section 6.6**). MHC class-I, MICA, PD-L1 and E-Cadherin expression were much higher in the HCC1954 cell line compared to the SKBR3 cell line (**Table 4.16**). NKTR expression however, was much higher in the SKBR3 cell line (**Table 4.16**). Western blots for these proteins are shown in Section 6.6. The differential expression of these proteins may impact the susceptibility of these cells to different mechanisms of cell killing, such as direct cytotoxicity and T-ADCC.

Table 4.16: Fold change in expression for immune relevant proteins in HCC1954 cell line versus SKBR3 cell lines. Fold difference is expression in HCC1954 relative to SKBR3. Values represent densitometry for triplicate blots run together and normalised to alpha tubulin.

Protein	Fold difference in expression between HCC1954 vs. SKBR3	P value
MHC class-I	4.29	0.011
MICA	4.14	0.002
NKTR	0.32	0.010
PD-L1	7.59	8.33×10^{-5}
E-Cadherin	SKBR3- HCC1954 +	0.023

4.10 Summary

Two cell lines were examined in the development of this assay. The HCC1954 cell line had much greater expression of PD-L1 compared to SKBR3 (**Section 4.2.1**). Neither atezolizumab, nivolumab nor pembrolizumab had an effect on the proliferation of either cell line and had no effect on the anti-proliferative effects of trastuzumab (**Section 4.2.2**).

The goal of this work was to establish if any of five different effector cell groups from healthy volunteers could provide consistent ICI-altered direct, T-ADCC or overall cytotoxicity against a PD-L1-low or PD-L1-high HER2+ breast cancer cell line model *in vitro*. Identifying a mechanism of immune-mediated tumour cell killing that can be altered by ICIs *in vitro* could then provide mechanistic understanding of ICI action and form the basis for assays examining novel ICI combinations pre-clinically.

Unstimulated PBMCs consistently elicited an increased level of direct cytotoxicity against the SKBR3 cell line in the presence of ICIs (**Section 4.4.2.1**). Unstimulated PBMCs could be used with SKBR3 cells in this assay to examine changes in direct cytotoxicity related to ICIs. Unstimulated PBMCs could also be used with HCC1954 cells to examine alterations to direct cytotoxicity related to atezolizumab treatment.

Un-activated T cells are not an appropriate model to examine ICI activity (**Section 4.5**). CD3/CD28 activated T cells showed increased PD-1 and PD-L1 expression on day 6 of stimulation (**Section 4.6.1**). Activated T cells could be used to examine the effect of ICIs on direct cytotoxicity but do not provide very consistent results (**Section 4.6.3 and 4.6.4**).

There was no consistent effect seen with ICI treatment on cytotoxicity elicited by unstimulated NK cells (**Section 4.7**). Stimulation of the NK cells with IL-2 increased activation of the NK cells and induced a small increase in PD-1 and PD-L1 expression (**Section 4.8.1**). IL-2 stimulated NK cells could be used as a relatively consistent method of examining changes in both direct cytotoxicity and T-ADCC associated with ICI depending on the cell line used (**Section 4.8.3 and 4.8.4**).

Within these models there were differences in the mechanism of cell death induced by immune cells. SKBR3 cells were more susceptible to increases in direct cytotoxicity mediated by the ICIs. HCC1954 cells were more susceptible to differences in T-ADCC and overall cytotoxicity. This may be due to differential expression of immune relevant proteins between the two cell lines (**Section 4.7**).

4.11 Discussion

4.11.1 Unstimulated healthy volunteer PBMCs can be used to examine the effects of ICIs against HER2+ breast cancer cell lines

Pembrolizumab altered cytotoxicity against the PD-L1-low SKBR3 cell line for some patient PBMC samples (**Section 3.5**). This shows the capacity of a population present in PBMCs to elicit an effect with ICI treatment *in vitro*. This provided the rationale to explore the effector capacity of healthy volunteer PBMCs and two PBMC immune cell subsets, NK cells and T cells in this setting. PBMCs are a mixed immune cell population made up of lymphocytes (70-90 %) (T cells (45-70 %), NK cells (5-20 %) and B cells (5-20 %)), monocytes (10-30 %) and dendritic cells (1-2 %) [29]. NK cells are the main cytotoxic effector population of T-ADCC, and can also be immunosuppressed by the PD-1 signalling axis [29,58]. T cells are classical mediators of ICI efficacy as they can also be suppressed by the PD-1 axis [55,105].

Overall cytotoxicity elicited by unstimulated PBMCs against the SKBR3 cell line was increased by the addition of ICIs (pembrolizumab, nivolumab and atezolizumab) in almost every incidence. This was primarily due to an increase in direct cytotoxicity (**Section 4.4.2.1**). This suggests that there is a low level of PD-1/PD-L1 inhibition in a healthy volunteer PBMC population capable of direct cytotoxicity. This effect may be mediated by NK cells due to their role in eliciting an immune response in the absence of MHC class-I expression, as is the case in the SKBR3 cell line [22]. The susceptibility of this cell line to direct cytotoxicity may be due to the expression of immune response-related proteins (eg HLA-E, PD-L1) that are a key gateway in the kill/don't kill response of innate immune cells like NK cells. This will be further discussed in Section 8.3.5.

Direct cytotoxicity elicited by unstimulated PBMCs was increased against the HCC1954 cell line with the addition of anti-PD-L1 ICI atezolizumab in all instances but there was no consistent alteration to direct cytotoxicity with the pembrolizumab or nivolumab treatment (**Section 4.4.2.2**). The HCC1954 cell line was defined as PD-L1 high due to a major level of PD-L1 over-expression (**Section 5.2.2.1**). By inhibiting the PD-L1 present on HCC1954, this may have removed the major checkpoint inhibiting direct cytotoxicity against this cell line. Nivolumab and pembrolizumab target PD-1 and would most likely not have overcome the level of PD-L1 over-expression on HCC1954 coupled with the fact PD-L1 also interacts with another signalling receptor on immune cells, CD80 [104,105].

Neither cell line showed an alteration to T-ADCC elicited by the healthy volunteer unstimulated PBMCs with the addition of ICI. This is different to the response seen in T-ADCC with the TCHL patient samples. This is most likely due to an alteration in phenotype of patient PBMCs.

Overall this suggests that the PD-L1-low SKBR3 cell line could be used to examine the effects of pembrolizumab, nivolumab and atezolizumab on the ability of PBMCs to elicit direct cytotoxicity. The HCC1954 cell line could be used in the unstimulated PBMC model to examine the effects of atezolizumab on direct cytotoxicity.

4.11.2 Healthy volunteer T cells provide an inconsistent method for examining the effects of ICIs *in vitro*

T cells are a major component of the tumour specific immune response and are of particular clinical interest in immune checkpoint inhibition [14]. Chiang *et al.* showed that cytotoxic T cells from healthy volunteers can be positive for cytotoxic granules and were capable of lytic granule exocytosis [320]. Rentzsch *et al.* demonstrated that healthy volunteers and patients with primary breast cancer had T cells capable of recognising the HER2 receptor [321]. This indicates healthy volunteer T cells have the capacity to be used as effector cells in *in vitro* assays to recognise and kill cancer cells.

Un-activated T cells showed very little direct cytotoxicity against any of the cell lines examined in the absence of ICIs (**Section 4.5**). This is expected when using healthy volunteer T cells as there should not be a presence of a large amount of T cells capable of mounting an immune response against cancer cell line specific antigens. The addition of the ICIs has very little impact. This is due to the aforementioned point and the fact that PD-1/PD-L1 expression levels are low on healthy volunteer T cells (**Section 4.6.1**).

T-ADCC increased against the SKBR3 cell line with the addition of atezolizumab for two volunteer samples and with pembrolizumab for one volunteer sample (**Section 4.5**). This was unexpected as only a minority of T cell subsets are capable of ADCC including γδ T cells [28]. It is possible that enriching for T cells concentrated the number of ADCC-capable T cells. As a negative selection method was used it is also possible that another ADCC-capable cell population was not fully removed from the PBMC fraction.

Interestingly, there were no increases in T-ADCC in the CD3/CD28/IL-2-activated T cell population with the addition of an ICI (**Section 4.6.4**). Activation occurred over six days and led to high levels of proliferating CD3+ T cells (**Section 4.6.1**). In this setting, it is unknown if any other ADCC-capable immune cell type other than T cells would be able to exist and be viable after six days.

T cells were activated with CD3/CD28 beads and IL-2 treatment, stimulating activation and proliferation leading to eventual exhaustion of the T cells which was characterised by an increase in PD-1 and PD-L1 expression (**Section 4.6.1**). This has been shown to be a robust method of activating CD4+ and CD8+ T cells, leading to T cell exhaustion upon continuous activation in other studies [315,316,322]. The addition of ICIs to these exhausted T cells resulted in an increased level of direct

cytotoxicity against the SKBR3 and HCC1954 cell lines with certain healthy volunteer samples (**Section 4.6.4**). This is most likely due to the expansion of cytotoxic T cells capable of recognising cancer cell antigens which can be present in healthy volunteer samples [321].

Activated healthy volunteer T cells are an inconsistent effector cell population to examine the effects of ICIs *in vitro*. Further work is required to characterise the T cell populations that do respond to ICIs in the immune cytotoxicity assay. Profiling of cancer-related antigen recognition, such as HER2, in healthy volunteer T cells may be a route to help improve the consistency of the assay through identification of T cells that will react before the assay commences.

4.11.3 IL-2 stimulated NK cells as a consistent effector cell population in *in vitro* ICI assays

NK cells are beginning to emerge as important effector cells of cytotoxicity in the presence of ICIs [323]. PD-1 expression has been found predominantly on $CD56^{dim}$ $CD16^{bright}$ NK cells [304,305,324]. These cells are known to be the main effectors of NK cell-mediated cytotoxicity and ADCC [29]. In Section 4.7.2, ICIs (atezolizumab, pembrolizumab and nivolumab) showed little effect on the ability of unstimulated NK cells to elicit overall cytotoxicity. Changes to direct cytotoxicity and T-ADCC were also inconsistent (**Section 4.7**). NK cells from healthy volunteers are not expected to innately have an exhausted phenotype [325].

IL-2 is well characterised as a stimulator of NK cells and T cells [326–328]. IL-2 treatment increases the ability of NK cells to elicit a cytotoxic response due to down regulation of inhibitory and quiescent cell pathways and the stimulation of activating receptors, death receptor ligand, chemokine receptors, interleukin receptors and members of secretory pathways, such as perforin and granzyme production [326,328] (**Section 1.2.2**). IL-2 stimulation of NK cells *in vitro* elicits a stronger and more consistent level of cytotoxicity [317,329,330].

The IL-2 stimulated NK cells examined in Section 4.8.3 were highly cytotoxic against the K562 cell line, which is particularly susceptible to NK cell-mediated cytotoxicity (**Section 4.8.1**). The cytotoxicity seen with IL-2 stimulated NK cells was much higher and more consistent between volunteers than unstimulated NK cells (**Section 4.7.1**). This indicates that IL-2 stimulated NK cells elicit a more consistent level of cytotoxicity, as has been previously reported in the literature [317,327]. NK cells showed an increase in PD-1 and PD-L1 expression following continued IL-2 stimulation, implying these cells started to develop an exhausted phenotype. IL-2 stimulated NK cells were capable of increasing overall cytotoxicity against the PD-L1-low SKBR3 cell line with the addition of atezolizumab, nivolumab and pembrolizumab (**Section 4.8.2**). This is similar to the effects seen with the PBMC population (**Section 4.4.2**).

IL-2 stimulated NK cells showed increased overall cytotoxicity against the PD-L1-high HCC1954 cell line in the presence of atezolizumab, nivolumab and pembrolizumab. Increases in both direct cytotoxicity and T-ADCC contributed to the increase (**Section 4.8**). This model allows the measurement of alterations to both direct cytotoxicity and T-ADCC in the presence of ICIs.

This shows that IL-2 stimulated NK cells could be used consistently to examine on the effects of ICIs on cytotoxicity. SKBR3 and HCC1954 cell lines were susceptible to different mechanisms of cell death, these cell lines could be used to concentrate on different aspects of the immune response.

Further optimisation of these assays requires phenotyping of volunteer samples to define specific effector cell subsets with relevant immune marker expression.

4.11.4 Alterations in immune response-related protein expression affect mechanisms of immune-mediated cytotoxicity against HER2+ breast cancer cell lines

The SKBR3 and HCC1954 cell lines appear to show altered susceptibility to PBMC-mediated and NK cell-mediated cytotoxicity (**Section 4.4 and 4.8**). This may be due to differences in expression of cell surface immune-related proteins seen between the two cell lines (**Section 4.9**).

As already stated, there is a sizable difference in PD-L1 expression between the two cell lines which may affect the capability of an immune cell to elicit cytotoxicity. Low MHC class-I expression and increased NKTR expression are known to predispose cells to direct NK cell-mediated destruction, while limiting T cell mediated cytotoxicity [313,331,24]. SKBR3 cells show lower MHC class-I and increased levels of NKTR which may play a role in the susceptibility of SKBR3 cells to direct cytotoxicity. This also indicates that the direct cytotoxicity seen against the SKBR3 cell line using a mixed PBMC population may be mediated by NK cells.

MICA acts as a stress-induced ligand to the NKG2D receptor on NK cells. MICA expression acts as a signal to elicit NK cell destruction [23]. MICA expression has been hypothesised to predispose cells to higher levels of ADCC [267–269]. Yamauchi *et al.* showed that HER2+ breast cancer patients had a more favourable response to trastuzumab if they were positive for E-cadherin expression [332]. Loss of E-cadherin expression can also be a marker of EMT, which has been shown to have a negative effect on NK cell-mediated direct cytotoxicity [333]. These proteins were increased in the HCC1954 cell line compared with the SKBR3 cell line and may be associated with the increased predisposition to T-ADCC in the HCC1954 cell line (**Section 4.9**).

Low MHC class-I and high NKTR expression may lead to increased susceptibility to direct cytotoxicity. Increased MICA and E-cadherin protein expression may lead to predisposition to T-ADCC. Differences in immune response-related proteins may be the cause of the alterations in the susceptibility of SKBR3 and HCC1954 cell lines to different mechanisms of immune cell-mediated cytotoxicity.

5. EGF signalling and PD-L1 expression in breast cancer cell line models

5.1 Introduction

Rational treatment combinations may increase response rates to ICIs. As shown in Sections 3 and 4, targeting HER2 with trastuzumab and an ICI may be beneficial in increasing immune cell mediated-cytotoxicity against HER2+ breast cancer cells. Inhibiting the HER family member EGFR may also have the potential to alter expression of PD-L1 on the tumour cell through intracellular signalling pathways [97,98,102,279]. This potential link between EGFR and PD-L1 has been investigated in lung cancer.

EGFR-related pathways can be over-activated and mutated in NSCLC, particularly adenocarcinomas [334]. EGFR targeted therapies (getfitinib and erlotinib) are approved for the treatment of EGFR-mutated NSCLCs [334,335]. Targeting EGFR has led to more favourable outcomes in EGFR over-expressing lung cancer [335]. It has been demonstrated that inhibition of EGFR signalling altered PD-L1 expression in lung cancer cell line models [97]. In patient samples, a number of studies found an association between PD-L1 and EGFR expression [97,279,280,336]. In two clinical studies, the co-expression of PD-L1 and EGFR was associated with poorer overall survival [98,279]. It was also shown that EGFR overexpression meant a greater likelihood of responding to PD-1 inhibition, as well as patients having a longer response rate and survival time to EGFR-targeted therapies if they were PD-L1+ [280].

This potential link suggests the use of EGFR inhibition may work well in combination with PD-1/PD-L1 inhibition in lung cancer but the underlying molecular association may also be present in other cancer types. In order to examine the link between EGFR and PD-L1, expression levels of both proteins were determined across a range of cancer cell line models (breast cancer, lung cancer and melanoma). Based on the results of this screen, selected breast cancer cell lines were then treated with EGF to determine if EGFR activation impacted on PD-L1 expression. Potential intracellular mediators of the link between EGFR and PD-L1 were examined. The impact of altered PD-L1 levels on the immune response against the cancer cells was also investigated.

5.2 PD-L1 expression in cancer cell line models

The PD-L1 antibody used (CST E1L3N) detected multiple bands when PD-L1 protein expression was examined by western blotting. The correct bands were determined by siRNA and deglycosylation assays. PD-L1 and EGFR expression was examined in cell line models of breast cancer (HER2 and TNBC subtypes), melanoma and lung cancer (NSCLC and SCLC). PD-L1 and EGFR expression was also determined in chemotherapy-resistant and targeted therapy-resistant cell line models. This study examined the range of PD-L1 expression in cancer cell line models, determined EGFR/PD-L1 co-expression, and also investigated any changes to PD-L1 and EGFR expression related to the development of resistance to treatment.

5.2.1 PD-L1 antibody validation

The unmodified weight of the PD-L1 protein is 33 kDa (Uniprot). The predicted molecular weight of PD-L1 using the CST E1L3N antibody was between 40 and 50 kDa. This alteration in protein weight was stated by CST to be due to post-translational glycosylation. In order to confirm this, protein lysates from 4 cell lines MDA-MB-231 (TNBC), HCC1954 (HER2+), SKBR3-Par (HER2+) and SKBR3-Lap (HER2+ and lapatinib-resistant) were treated with an enzyme deglycosylation mix. The deglycosylated proteins were then examined by western blot. The untreated MDA-MB-231 and HCC1954-Par cell line showed high expression of bands at 55 kDa and 43 kDa. Following deglycosylation, the bands resolved to one band at 33 kDa (**Figure 5.1**). SKBR3-Par and SKBR3-Lap had much lower expression of bands at 55 kDa and 43 kDa for PD-L1, but also showed a moderate shift in band expression to 33 kDa when treated with the deglycosylation mix (**Figure 5.1**).

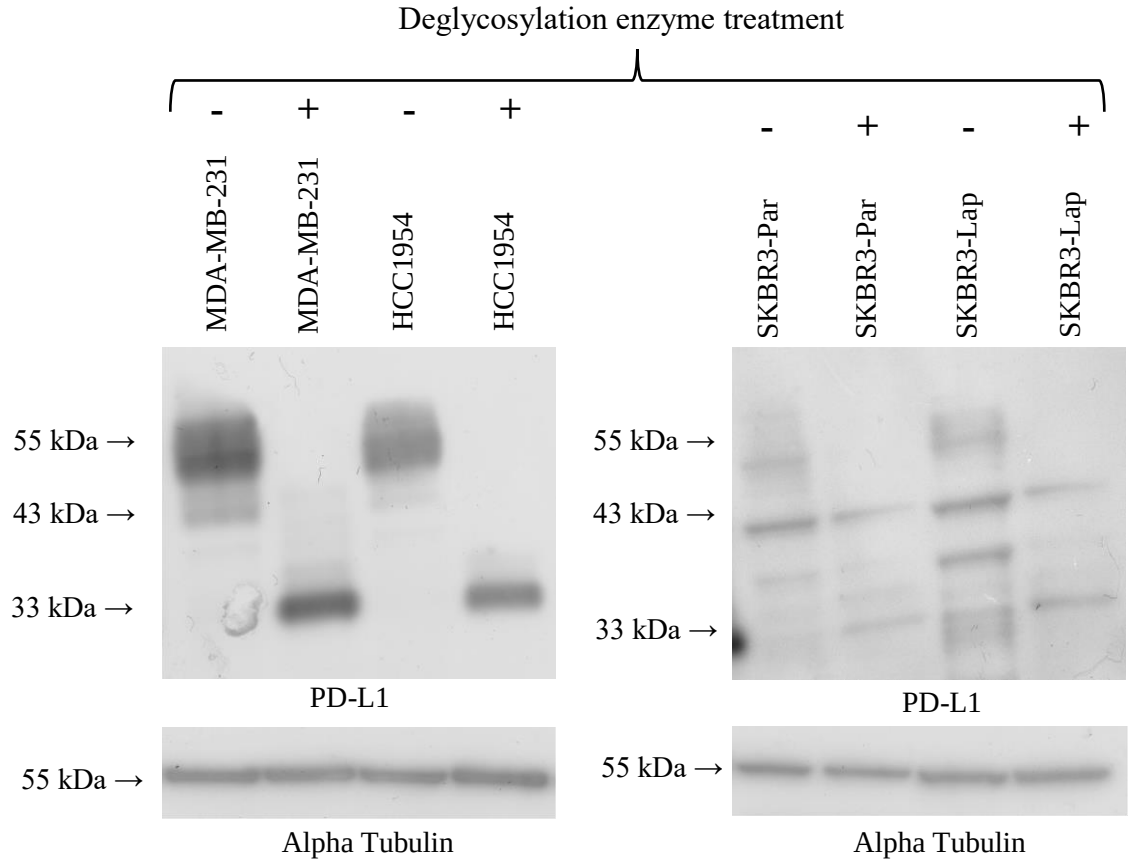

Figure 5.1: Western blotting for PD-L1 with and without deglycosylation enzyme treatment in MDA-MB-231, HCC1954, SKBR3-Par and SBR3-Lap cell lines. Glycosylated PD-L1 appears as a double band at 55kDa and a single band at 43kDa. Deglycosylated PD-L1 appears as a single band at 33kDa. Images shown are representative of triplicate blots. Alpha tubulin was used as a loading control.

To further validate the antibody, the MDA-MB-231, HCC1954 and SKBR3-Par cell lines were transfected with PD-L1 targeted siRNA. When transfection was successful, the bands at 55 kDa and 43 kDa were reduced. MDA-MB-231 cells were successfully transfected with PD-L1 siRNA in triplicate with a significant reduction (3.4-fold) in PD-L1 expression compared to the negative control of scrambled siRNA (p=0.017) (**Figure 5.2**). The HCC1954 cell line was also successfully transfected with PD-L1 siRNA in triplicate with a significant reduction (2.7-fold) in PD-L1 expression (p=0.009) compared to scrambled siRNA (**Figure 5.2**). Transfection of the SKBR3-Par cell line with PD-L1 targeted siRNA was only achieved once. For that experiment, PD-L1 expression at 55 kDa and 43 kDa was reduced compared to scrambled siRNA (**Figure 5.2**).

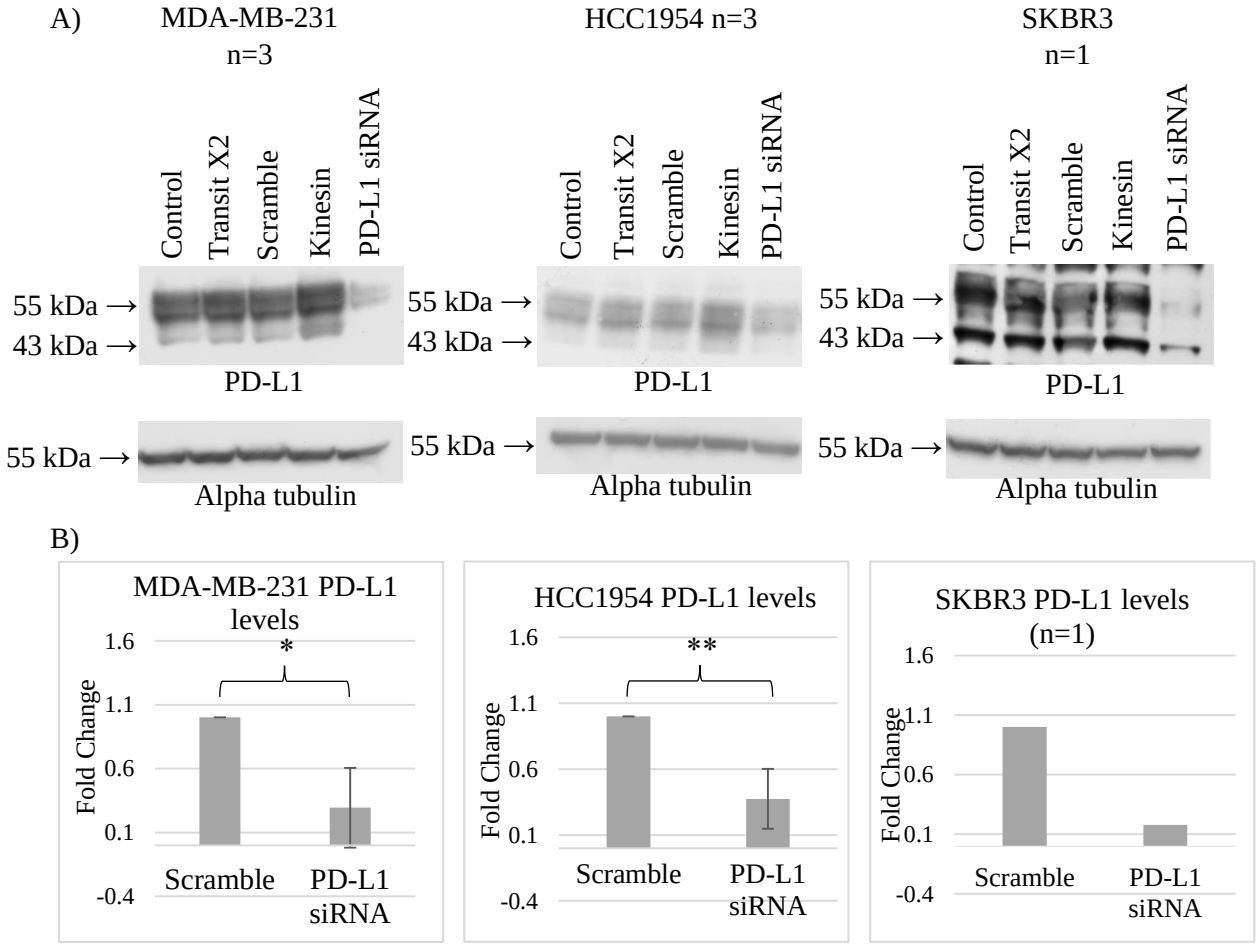

Figure 5.2: A) Western blotting for PD-L1 protein levels after PD-L1 protein siRNA knockdown in MDA-MB-231, HCC1954-Par and SKBR3-Par (n=1) cell lines. Blots shown are representative of triplicate blots unless otherwise stated. Alpha tubulin was used as a loading control. **B)** Densitometry analysis of immunoblots of MDA-MB-231, HCC1954 and SKBR3-Par (n=1) for PD-L1 protein levels after PD-L1 protein siRNA knockdown. PD-L1 expression is normalised to the scramble control. Error bars represent standard deviation of biological triplicate experiments. The Student's t test was used to determine statistical significance. * $p < 0.05$, ** $p < 0.01$ and *** $p < 0.001$.

Validation studies show that the CST E1L3N antibody detects PD-L1 protein expression as a double band at 55 kDa and a single band at 43 kDa. These proteins are post-translationally modified by glycosylation and expression of the protein can be silenced by PD-L1 targeted siRNA.

5.2.2 PD-L1 expression in treatment-naive cancer cell line models

PD-L1 and EGFR expression was examined in cell line models of HER2+ breast cancer (n=8), TNBC (n=13), melanoma (n=7) and lung cancer (n=7). Chemotherapy-resistant cell line models of lung cancer and breast cancer (n=5) and targeted therapy resistant breast cancer cell lines (n=7) were also examined. RAJI B cell lysate is listed as a positive control for PD-L1 expression [14]. In order to subjectively stratify PD-L1 expression, protein levels were compared to PD-L1 expression in 30 μg/ml RAJI B lysate. Cell lines were denoted as PD-L1 high if expression levels were significantly higher than PD-L1 expression in RAJI B. Certain cell lines had a clear presence of high PD-L1 expression, which did not qualify as significant due to high deviations in densitometry values at high expression levels. These cell lines were included as PD-L1 high due to obvious PD-L1 over-expression. Cell lines that were not statistically significantly greater than RAJI B were classified as PD-L1 medium and cell lines that had statistically significantly less PD-L1 expression than RAJI B were deemed PD-L1 low.

5.2.2.1 PD-L1 and EGFR expression in HER2+ breast cancer models

In the HER2+ panel (n=8), 2 cell lines JIMT1 and HCC1954 were designated PD-L1 high (p=0.025 and p=0.033 respectively). The 6 other cell lines were classified as PD-L1 medium (**Figure 5.3**). JIMT1 had a 3.57-fold increase in PD-L1 compared to RAJI B expression and HCC1954 had a 7.26-fold increase in PD-L1 compared to RAJI B expression. SKBR3, JIMT1 and HCC1954 cell lines were positive for EGFR expression and BT474 showed low levels of EGFR expression (**Figure 5.3**). All other cell lines were PD-L1 medium without expression of EGFR.

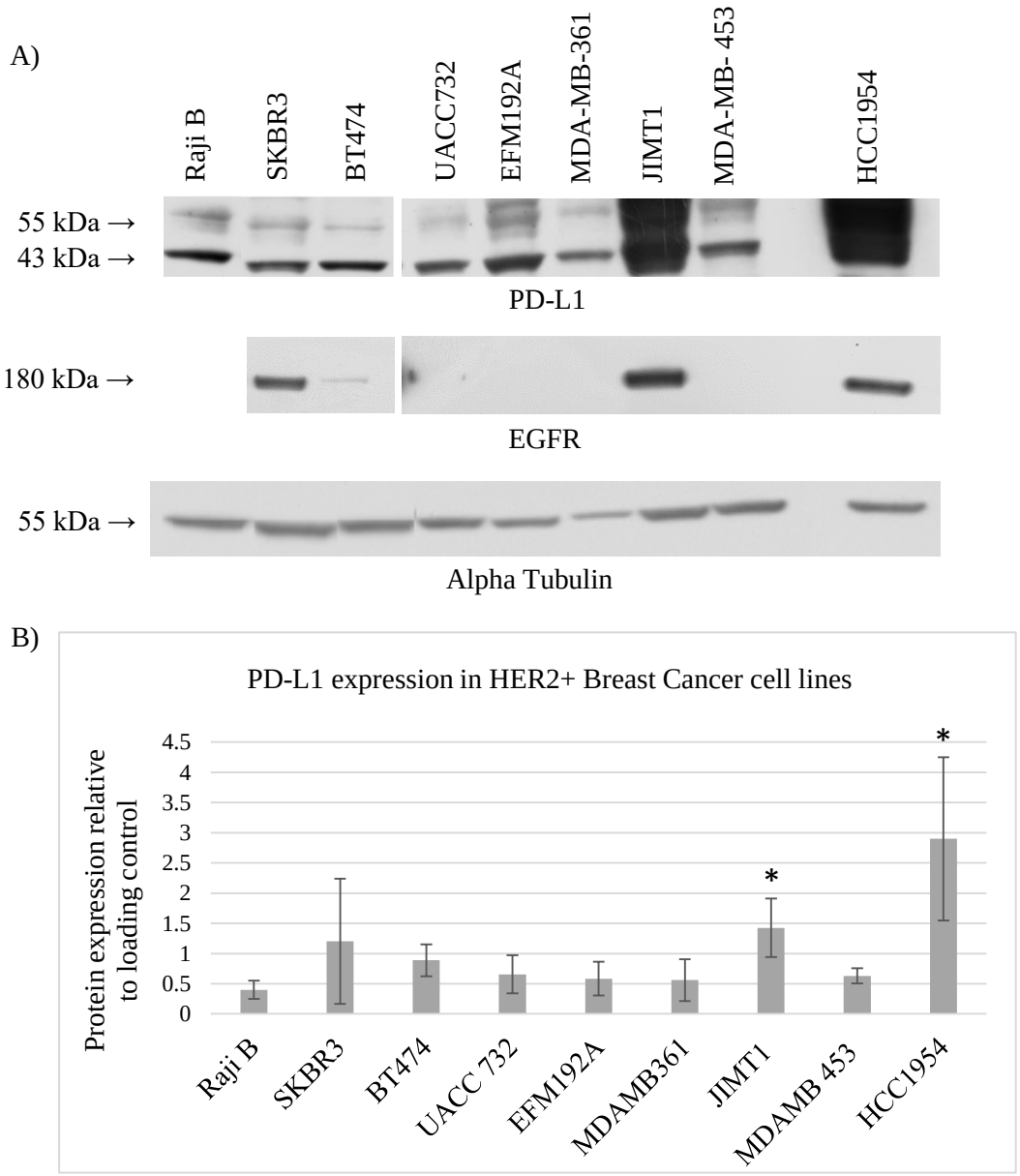

Figure 5.3: A) Western blotting for PD-L1 and EGFR protein expression in HER2+ breast cancer cell lines. Image is representative of triplicate blots. Alpha tubulin was used as a loading control. **B)** Densitometry analysis of immunoblots of HER2+ breast cancer cell lines for PD-L1 protein levels. Error bars represent standard deviation of biological triplicate experiments. The Student's t test was used to determine statistical significance. * $p < 0.05$, ** $p < 0.01$ and *** $p < 0.001$.

5.2.2.2 PD-L1 and EGFR expression in TNBC cell line models

There were 7/13 PD-L1 high TNBC cell lines when expression levels were compared to RAJI B. The other 6 TNBC cell lines were PD-L1 medium. MDA-MB-231 showed a 4.86-fold change in PD-L1 (p=0.031), CAL-85-1 showed a 5.22-fold change in PD-L1 (p=0.031), HDQP-1 showed a 4.56-fold change in PD-L1 (p=0.071), HCC70 showed a 4.63-fold change in PD-L1 (p=0.044), CAL120 showed a 4.63-fold change in PD-L1 (p=0.19), BT20 showed a 4.27-fold change in PD-L1 (p=0.034) and HS578T showed a 5.38-fold change in PD-L1 (p=0.045) (**Figure 5.4**). All other cell lines were PD-L1 medium. All TNBC cell lines examined expressed EGFR (**Figure 5.4**).

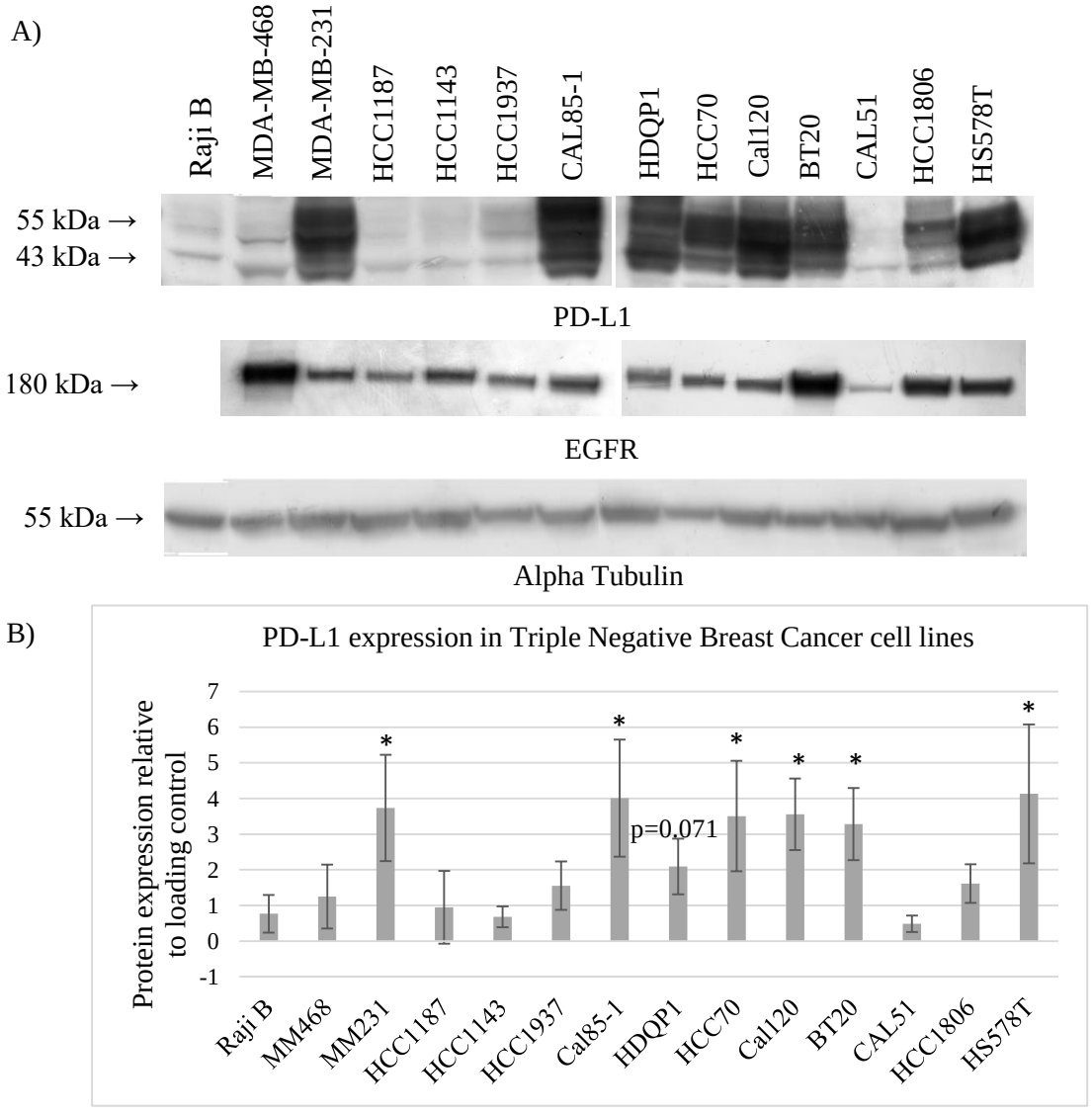

Figure 5.4: A) Western blotting for PD-L1 and EGFR protein expression in TNBC cell lines. Image is representative of triplicate blots. Alpha tubulin was used as a loading control. **B)** Densitometry analysis of immunoblots of TNBC cell lines for PD-L1 protein levels. Error bars represent standard deviation of biological triplicate experiments. The Student's t test was used to determine statistical significance. * $p < 0.05$, ** $p < 0.01$ and *** $p < 0.001$.

5.2.2.3 PD-L1 and EGFR expression in melanoma cell line models

In the melanoma panel, the LOX IMVI cell line was PD-L1 high when compared to RAJI B PD-L1 expression (p=0.079), with a fold change of 3.27 compared with RAJI B levels (**Figure 5.5**). All other cell lines were designated PD-L1 medium (n=6). MALME3M, WM-226-4 and LOX IMVI all showed detectable levels of EGFR expression (**Figure 5.5**).

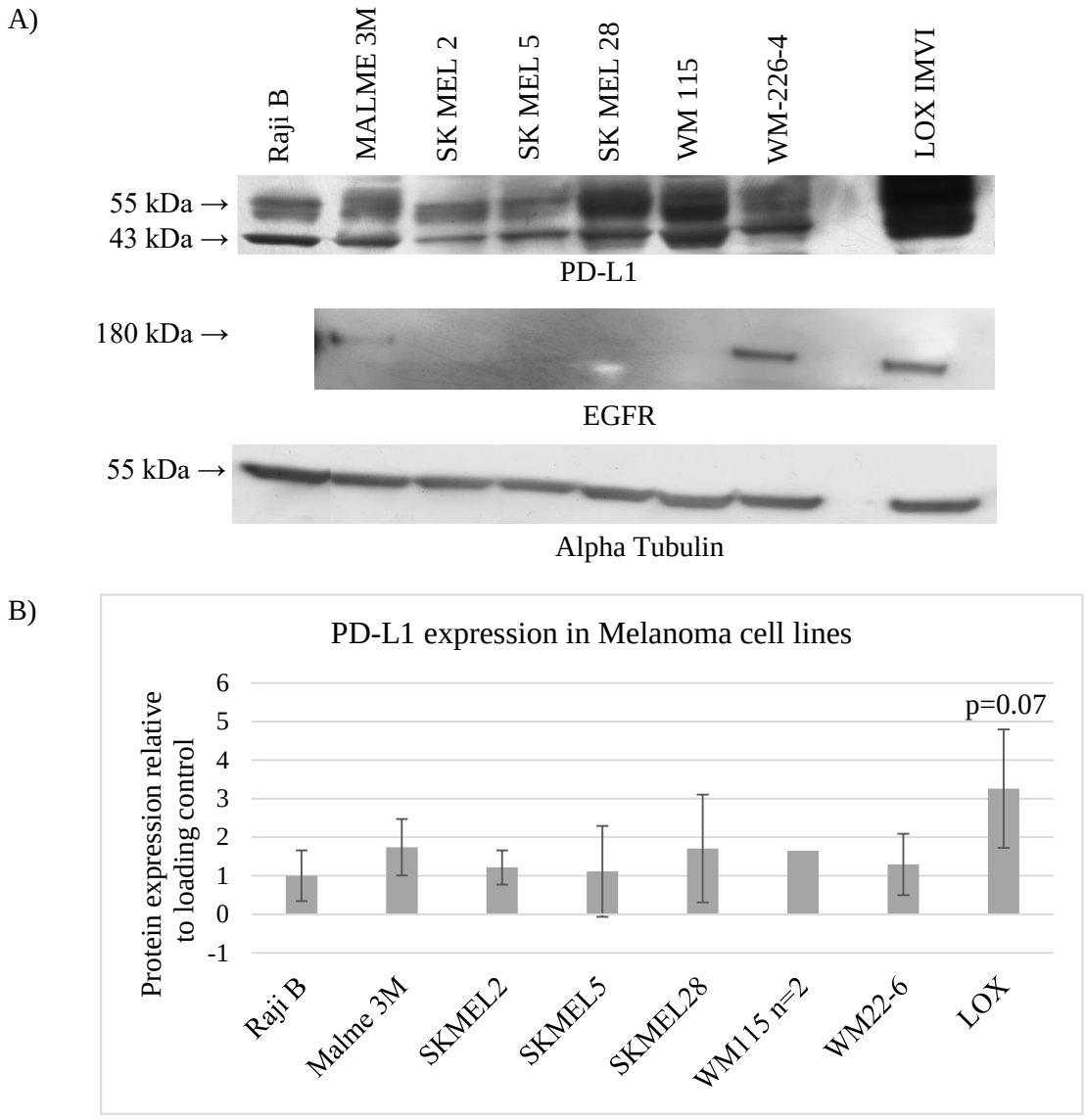

Figure 5.5: A) Western blotting for PD-L1 and EGFR protein expression in melanoma cell lines. Image is representative of triplicate blots. Alpha tubulin was used as a loading control. **B)** Densitometry analysis of immunoblots of melanoma cell lines for PD-L1 protein levels. Error bars represent standard deviation of biological triplicate experiments, with the exception of WM115 which shows mean of two biological experiments. The Student's t test was used to determine statistical significance. * $p < 0.05$, ** $p < 0.01$ and *** $p < 0.001$.

5.2.2.4 PD-L1 and EGFR expression in lung cancer cell line models

In the lung cancer panel, the NCI-H460 cell line was PD-L1 high when compared to RAJI B PD-L1 levels (p=0.049) (**Figure 5.6**). NCI-H460 showed a fold change increase of 1.79 in PD-L1 expression compared to RAJI B expression. All other cell lines were classified as PD-L1 medium (n=6). SK-LU-1, A549, NCI-H460 and NCI-H1229 cell lines were positive for EGFR expression (**Figure 5.6**).

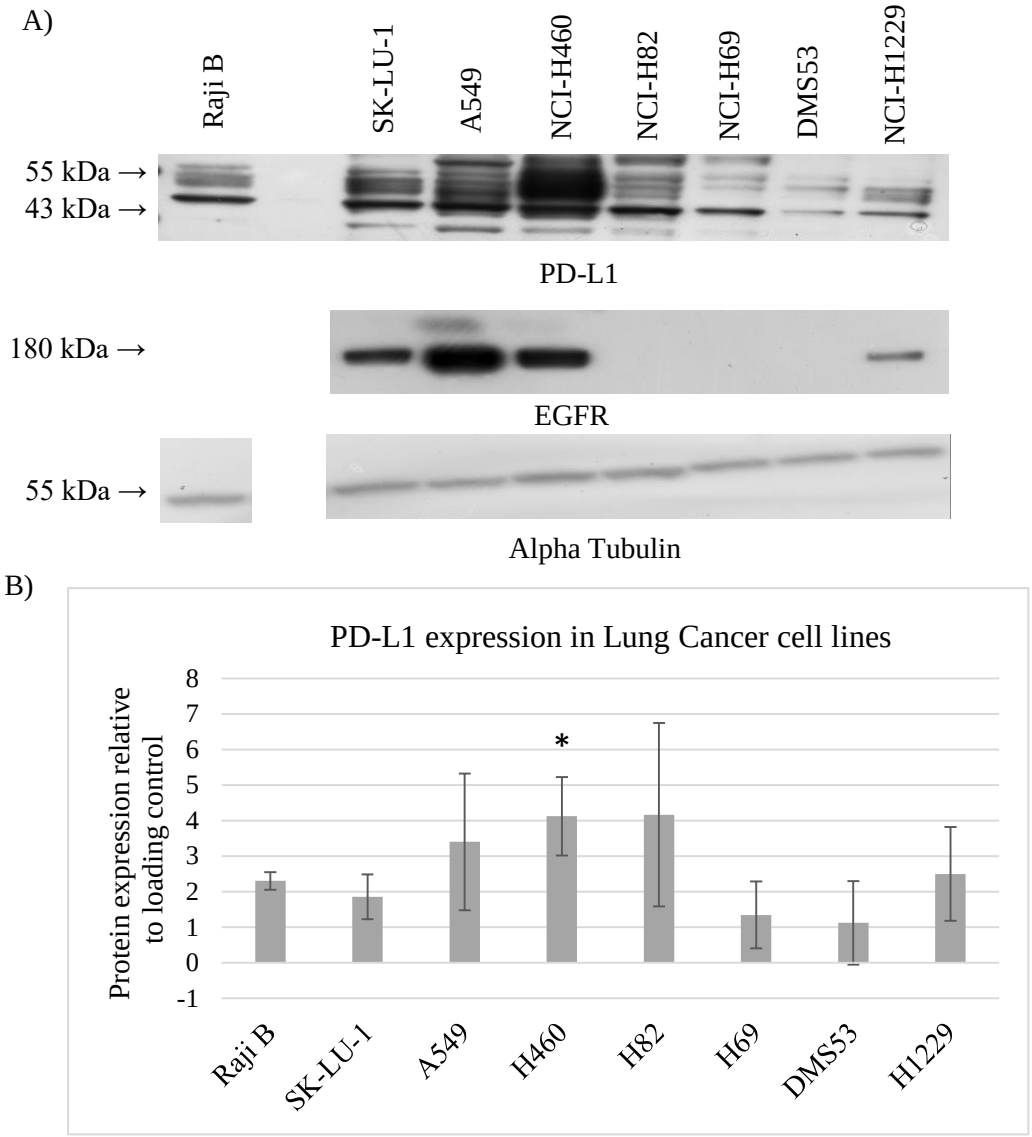

Figure 5.6: A) Western blotting for PD-L1 and EGFR protein expression in lung cancer cell lines. Image is representative of triplicate blots. Alpha tubulin was used as a loading control. **B)** Densitometry analysis of immunoblots of lung cancer cell lines for PD-L1 protein levels. Error bars represent standard deviation of biological triplicate experiments. The Student's t test was used to determine statistical significance. * $p < 0.05$, ** $p < 0.01$ and *** $p < 0.001$.

5.2.2.5 PD-L1 and EGFR co-expression in cell line models

There were 11 cell lines classified as PD-L1 high across all panels of the treatment naïve cell lines. In the HER2+ breast cancer panel 2/7 cell lines were PD-L1 high and 7/13 TNBC cancer cell lines were PD-L1 high. In the Lung cancer and melanoma cell line panels 1/7 were PD-L1 high in both cancer types (**Table 5.1**). All PD-L1 high cell lines expressed detectable levels of EGFR. Irrespective of expression level, co-expression of EGFR and PD-L1 was detected in 3/8 HER2+ cell lines, 13/13 TNBC cell lines, 3/7 melanoma cell lines and 4/7 lung cancer cell lines.

Table 5.1: PD-L1 high cell lines across HER2+ breast cancer, TNBC, lung cancer and melanoma. PD-L1 expression determined by western blot. Any cell line which had expression which was significantly greater than positive control (RAJI B) PD-L1 expression was classified as being PD-L1 high.

HER2+ breast cancer	TNBC	Lung	Melanoma
JIMT1	MDA-MB-231	NCI-H460	LOX IMVI
HCC1954	CAL-85-1		
	HCC70		
	CAL120		
	BT20		
	HS578T		
	HDQP-1		

5.2.3 PD-L1 levels in treatment-resistant cell line models

PD-L1 and EGFR levels were also determined in chemotherapy- and targeted therapy-resistant cell line models. Protein expression in treatment-resistant cell lines was normalised to protein expression in the parental cell lines to determine changes caused by resistance to treatment. It was ensured that all cell lines were resistant to the relevant drug by acid phosphatase-based IC_{50} assays (**Table 5.2 and Table 5.3**).

5.2.3.1 EGFR/PD-L1 expression in chemotherapy-resistant cell line models

IC_{50} values for parental and chemotherapy-resistant cell lines and fold change resistance to the relevant drugs are in Table 5.2. PD-L1 levels were not significantly changed in any of the chemotherapy-resistant cell lines examined (**Figure 5.7**). EGFR expression was detected in parental and resistant A549 and SK-LU-1 cell lines and was unchanged between parental and resistant cell lines (**Figure 5.7**). There were no alterations to PD-L1 or EGFR expression due to chemotherapy resistance in the cell lines examined.

Table 5.2: IC_{50} values and fold change resistance for parental and chemotherapy-resistant cell lines.

Cell line	Drug	Parental IC50	Resistant IC50	Fold Change
MCF7	Adriamycin	27.31 ± 0.56 nM	80.48 ± 0.7 nM	2.95
MCF7	Taxotere	0.003 ± 0.00 nM	0.007 ± 0.00 nM	2.74
MCF7	Cisplatin	1235 ± 60 nM	2140 ± 90 nM	1.73
A549	Carboplatin	7319 ± 90 nM	10776 ± 94 nM	1.47
SK-LU-1	Taxol	2.34 ± 0.62 nM	10.59 ± 0.61 nM	4.52

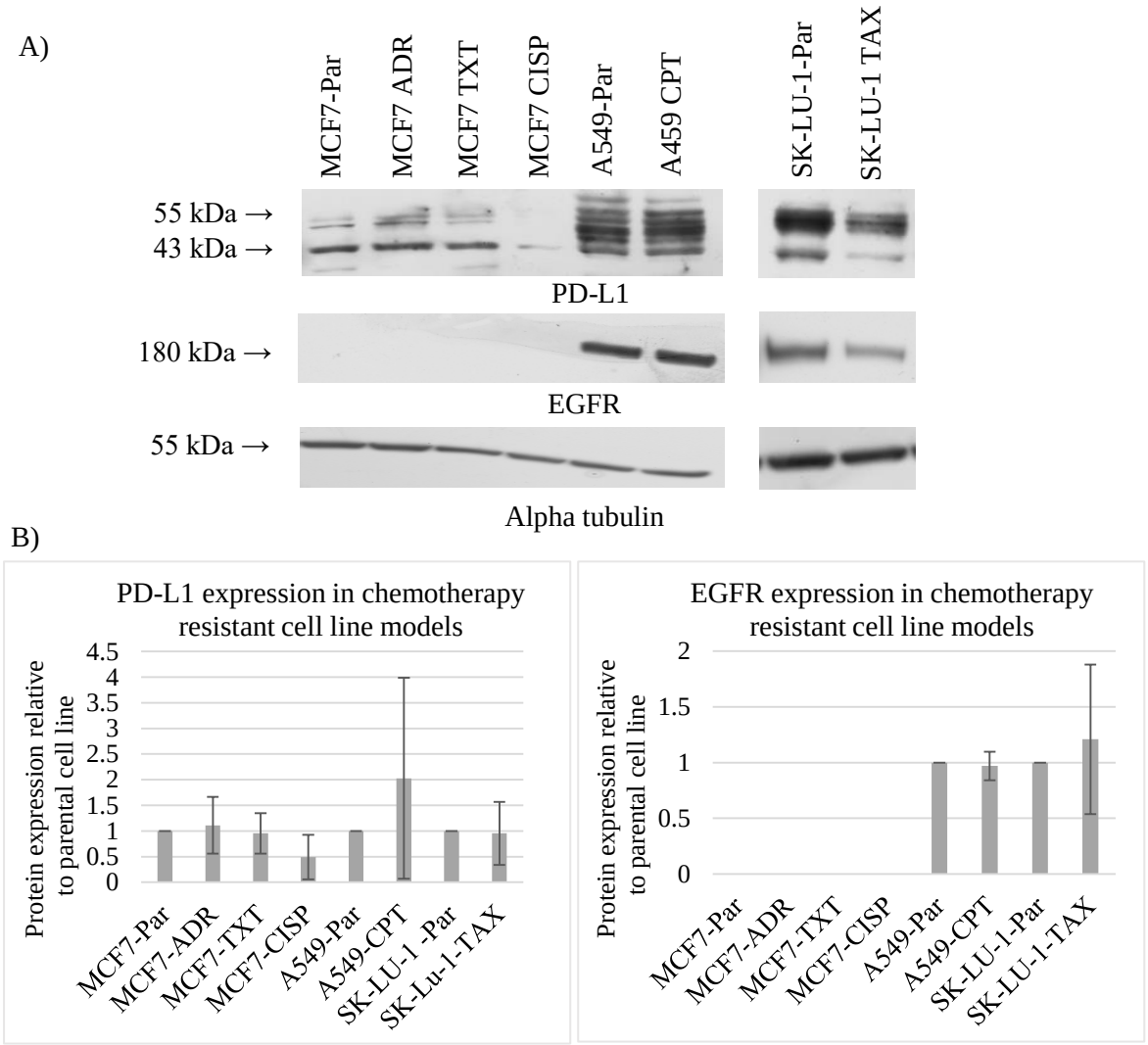

Figure 5.7: A) Western blotting for PD-L1 and EGFR protein expression in chemotherapy resistant cell lines. Image is representative of triplicate blots. Alpha tubulin was used as a loading control. **B)** Densitometry analysis of PD-L1 and EGFR protein levels. Protein levels are normalised to parental cell line. Error bars represent standard deviation of biological triplicate experiments. The Student's t test was used to determine statistical significance. * $p < 0.05$, ** $p < 0.01$ and *** $p < 0.001$.

5.2.3.2 EGFR/PD-L1 expression in targeted therapy-resistant cell line models

Seven targeted therapy resistant breast cancer cell lines were examined for PD-L1 and EGFR expression. IC_{50} values for parental and resistant cell lines as well as fold change resistance are shown in Table 5.3. PD-L1 and EGFR levels were significantly different to parental cell line expression in a number of the targeted therapy resistant cell line models examined. HCC1954-Lap showed decreased expression of PD-L1 (p=0.017) and EGFR (p=0.001) when compared to the HCC1954-Par cell line (**Figure 5.8**). BT474-Tr cells showed an increased level of PD-L1 (p=0.004) and EGFR (p=0.010) when compared to the parental BT474 cell line (**Figure 5.8**). SKBR3-Lap showed an increase in PD-L1 (p=0.047) and EGFR (p=0.034) expression when compared to SKBR3-Par (**Figure 5.8**). SKBR3-Afa also showed an increase in PD-L1 (p=0.0001) and EGFR (p=0.003) expression compared to parental cell line levels (**Figure 5.8**). HCC1954-Ner and SKBR3-T/L showed an increase in EGFR expression (p=0.001 and p=0.039 respectively) but the associated increase in PD-L1 expression did not reach significance (**Figure 5.8**).

In the targeted therapy resistant cell lines there were a number of significant alterations to PD-L1 and EGFR levels. Any change seen in PD-L1 expression in these cell lines was accompanied by a corresponding change in EGFR. This suggests that acquired resistance to HER-family targeted therapies that alter EGFR levels could also alter PD-L1 expression in a similar manner with the potential to affect the immune response against targeted therapy resistant cell lines.

Table 5.3: IC_{50} values and fold change for parental and targeted therapy resistant cell lines. Values listed in bold were provided by Dr. Neil Conlon. T= Trastuzumab, L=Lapatinib.

Cell line	Drug	Parental IC_{50}	Resistant IC_{50}	Fold Change
HCC1954-Lap	Lapatinib	0.31 ± 0.15 µM	1.65 ± 0.22 µM	5.3
HCC1954-Ner	**Neratinib**	**0.03 ± 0.00 µM**	**0.78 ± 0.14 µM**	**30**
SKBR3-Lap	**Lapatinib**	**0.05 ± 0.02 µM**	**2.37 ± 0.53 µM**	**47.4**
SKBR3-Afat	Afatinib	0.01 ± 0.01 µM	0.28 ± 0.01 µM	33
Cell line	**Drug** 10 µg/mL T 100 nM L	**% Growth Parental cell line**	**% Growth Resistant cell line**	**Fold Change**
BT474-Tr	**Trastuzumab**	**44.7 ± 1.8 %**	**97.0 ± 5.2 %**	**2.17**
SKBR3-Tr	**Trastuzumab**	**66.1 ± 4 %**	**94.3 ± 7.8 %**	**1.43**
SKBR3-T/L	**Trastuzumab and Lapatinib**	**29.6 ± 2.8 %**	**66.6 ± 10.3 %**	**2.25**

A)

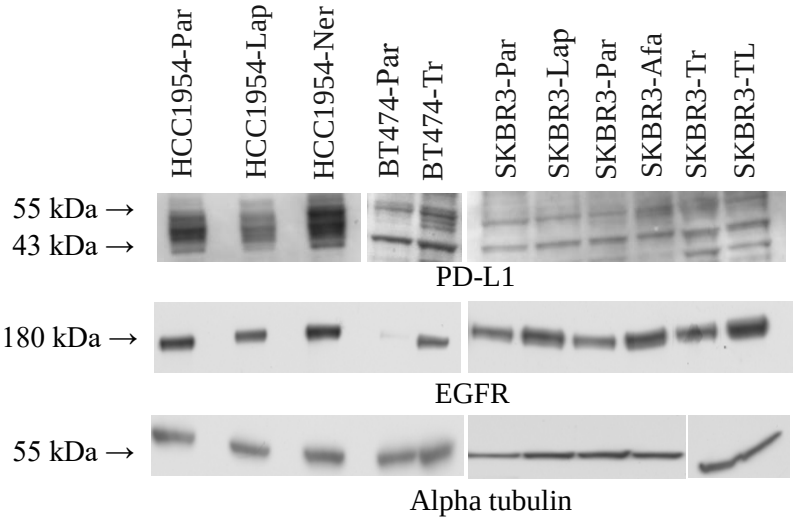

B)

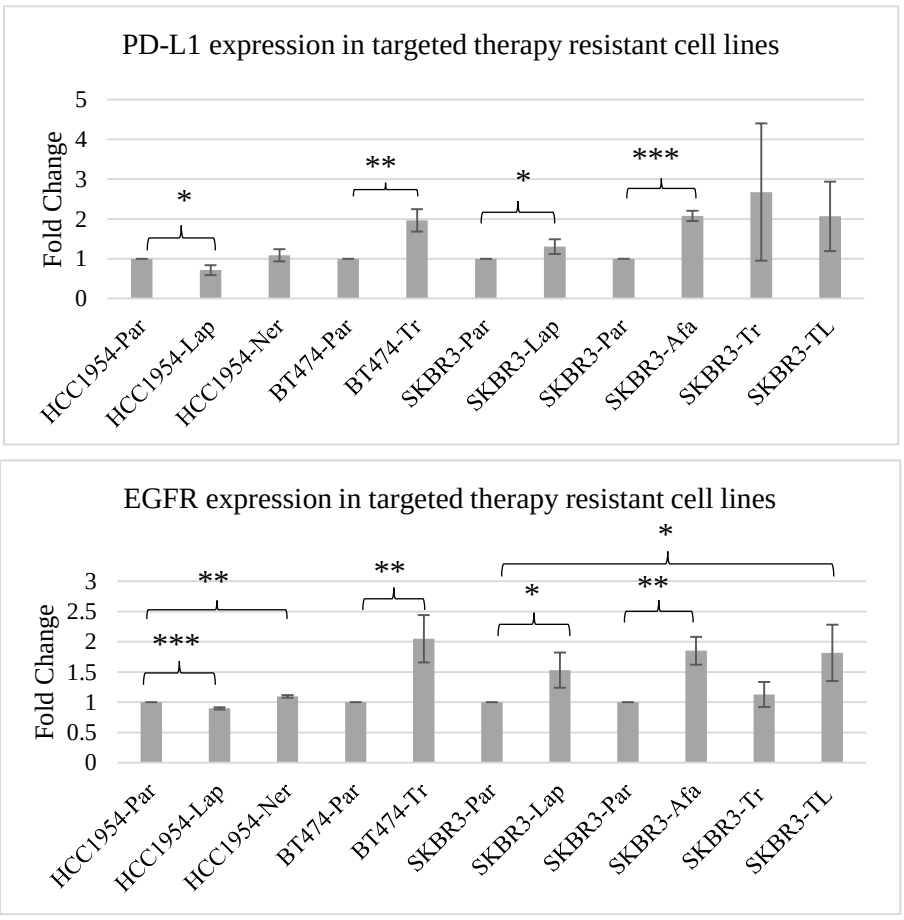

Figure 5.8: A) Western blotting for PD-L1 and EGFR protein expression in targeted therapy resistant cell lines. Image is representative of triplicate blots using dark room development. Alpha tubulin was used as a loading control. **B)** Densitometry analysis of immunoblots of targeted therapy resistant cell lines for PD-L1 and EGFR protein levels. Protein levels are normalised to parental cell line. Error bars represent standard deviation of biological triplicate experiments. The Student's t test was used to determine statistical significance. * $p < 0.05$, ** $p < 0.01$ and *** $p < 0.001$.

5.3 The effect of EGFR stimulation on PD-L1 expression

The effect of EGFR activation on PD-L1 expression was examined due to the link between EGFR activation and PD-L1 expression seen in NSCLC [97,98,280] and the induction of PD-L1 expression due to EGF treatment seen in TNBC cell lines [102]. From this we hypothesise that EGF treatment may cause PD-L1 upregulation in HER2+ breast cancer cell lines via activation of EGFR. In order to examine if EGFR activation could directly alter PD-L1 expression, parental and targeted therapy resistant breast cancer cell lines were treated with 10 ng/mL of EGF ligand. PD-L1 expression was then examined. The HCC1954-Par, HCC1954-Lap, SKBR3-Par and SKBR3-Afa cell lines were selected for treatment with EGF, as the parental lines show different levels of PD-L1 expression and the resistant cell lines chosen had inverse alterations to PD-L1/EGFR expression for comparison purposes (HCC1954-Lap: expression of both proteins decreased relative to parental, SKBR3-Afa: expression of both proteins increase relative to parental) (**Section 5.2**).

5.3.1 Time course treatment with EGF

To determine the correct time-point to examine the association between EGFR and PD-L1, cells were exposed to EGF for 2, 6, 12 and 24 hours. Lysates were taken at these time points and PD-L1 expression was examined.

In the HCC1954-Par cell line, PD-L1 levels were increased upon EGF treatment. This difference is significant at the 24-hour time point with a 1.55-fold change in PD-L1 expression (p=0.039) (**Figure 5.9**). When treated with EGF, SKBR3-Par cells showed an increase in PD-L1 expression after 2 hours, at 6 hours this increase was significant (2.56-fold change increase, p=0.028). At 12 hours and 24 hours there was also an increase in PD-L1 expression in SKBR3-Par which was approaching significance (p=0.08 and p=0.09 respectively) (**Figure 5.9**).

No time point examined produced a significant increase in PD-L1 expression in both cell lines. The 24-hour time point was chosen to further examine the effects of EGF treatment on PD-L1 expression in more detail, as both cell lines showed alterations to PD-L1 expression at this time point which were significant in HCC1954-Par and approaching significance in SKBR3.

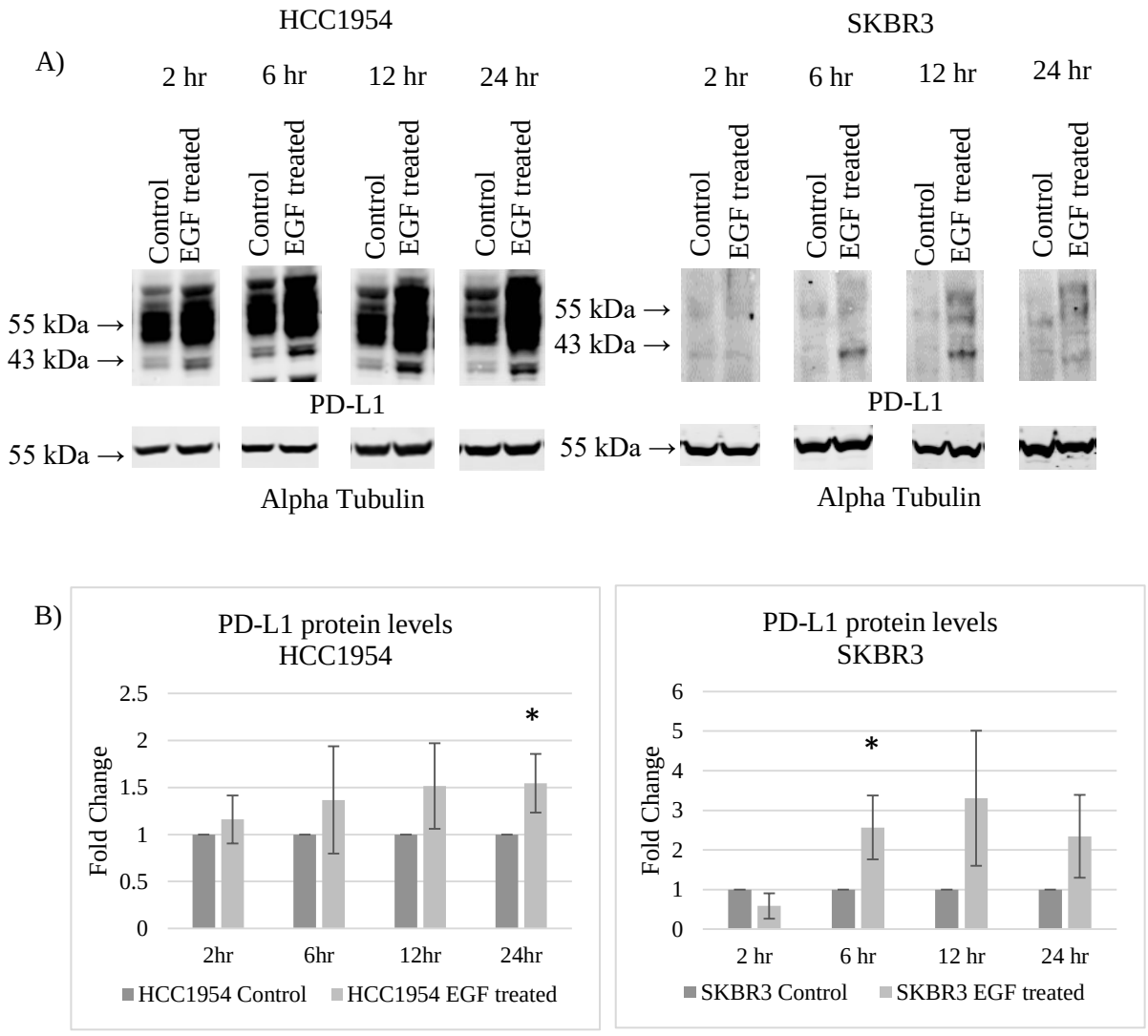

Figure 5.9: A) Western blotting for PD-L1 protein expression over the course of 2, 6, 12 and 24 hours +/- EGF treatment in HCC1954-Par and SKBR3-Par cell lines. Image is representative of triplicate blots. Alpha tubulin was used as a loading control. **B)** Densitometry analysis of immunoblots of HCC1954-Par and SKBR3-Par cell lines for PD-L1 protein levels over the course of 2, 6, 12 and 24 hours with and without EGF treatment. Protein levels are normalised to control protein levels. Error bars represent standard deviation of biological triplicate experiments. The Student's t test was used to determine statistical significance. * $p < 0.05$, ** $p < 0.01$ and *** $p < 0.001$.

5.3.2 The effect of EGF treatment on parental and targeted therapy resistant HER2+ breast cancer cell lines

Using the 24-hour time-point (**Section 5.3.1**), the impact of EGF, the EGFR/HER2 targeting TKI lapatinib and the combination of both on PD-L1 was examined in the two parental and two resistant cell lines. Lapatinib was employed to inhibit EGFR activity and potentially block the effects of EGF. Cells were treated in serum free and in HI FBS conditions to discount the impact of HI FCS ligand content when examining the effects of EGF treatment. Media and DMSO controls were included, as lapatinib is dissolved in DMSO.

5.3.2.1 The effect of EGF treatment on protein expression in HCC1954-Par cells

5.3.2.1.1 EGF treatment and PD-L1 expression in HCC1954-Par cells

When treated with 10 ng/mL EGF for 24 hours, HCC1954-Par cells showed a 2.76-fold increase in PD-L1 in serum free conditions (p=0.007) and a 2.95-fold increase in PD-L1 in the presence of HI FBS (p=0.024) (**Figure 5.10**). In HI FBS, lapatinib caused a small but significant decrease in PD-L1 expression (p=0.033) (**Figure 5.10**). In both serum free and serum conditions, PD-L1 levels were 2.26 (p=0.034) and 2.24 (p=0.043) times lower respectively when treated with EGF and lapatinib compared to EGF alone (**Figure 5.10**). Showing lapatinib was capable of blocking EGF-mediated PD-L1 upregulation in the HCC1954-Par cell line. As the effect of EGF on PD-L1 was similar in both serum free and serum conditions, cell lysates for further studies were prepared in HI FCS only.

5.3.2.1.2 EGF treatment and EGFR expression in HCC1954-Par cells

In the presence of EGF and/or lapatinib, total EGFR protein levels remain unchanged. pEGFR showed a 1.48-fold upregulation with EGF treatment (p=0.046) (**Figure 5.11**). Following treatment with lapatinib, pEGFR levels were 3.45 times lower in the presence of lapatinib ($p=1 \times 10^{-4}$) and 1.67 times lower in the presence of EGF plus lapatinib versus EGF alone (p=0.005) (**Figure 5.11**). This demonstrated that lapatinib was capable of blocking EGF mediated pEGFR upregulation in the HCC1954-Par cell line. In the presence of lapatinib and EGF treatment, pEGFR levels followed a similar trend as PD-L1 levels

5.3.2.1.3 EGF treatment and ERK and AKT activity in HCC1954-Par cells

Total AKT protein levels were unchanged with EGF or lapatinib treatments (**Figure 5.11**). EGF also had no effect on pAKT protein levels, but pAKT protein levels were 1.69 times lower in the presence of lapatinib (p=0.054) (**Figure 5.11**). The HCC1954 cell line harbours a PI3K mutation leading to

constitutive activation of AKT without a ligand present. The HCC1954-Par cell line is innately resistant to trastuzumab but remains sensitive to lapatinib treatment, characterised by dephosphorylation of AKT [337]. This indicates the effects of lapatinib, on pAKT, in this model may be related to HER2 inhibition. Total ERK protein levels were unchanged in the HCC1954-Par cell line with either EGF or lapatinib treatment (**Figure 5.11**). EGF did not affect pERK expression. Lapatinib significantly decreased pERK protein expression for both ERK1 ($p=2.14 \times 10^{-5}$) and ERK2 ($p=0.012$). In the presence of EGF and lapatinib, pERK levels were increased (ERK1 $p=0.068$ and ERK2 $p=0.005$) (**Figure 5.11**). Because of constitute activation of PI3K signalling in this cell line it is not dependent on MAPK activity for growth signals [318].

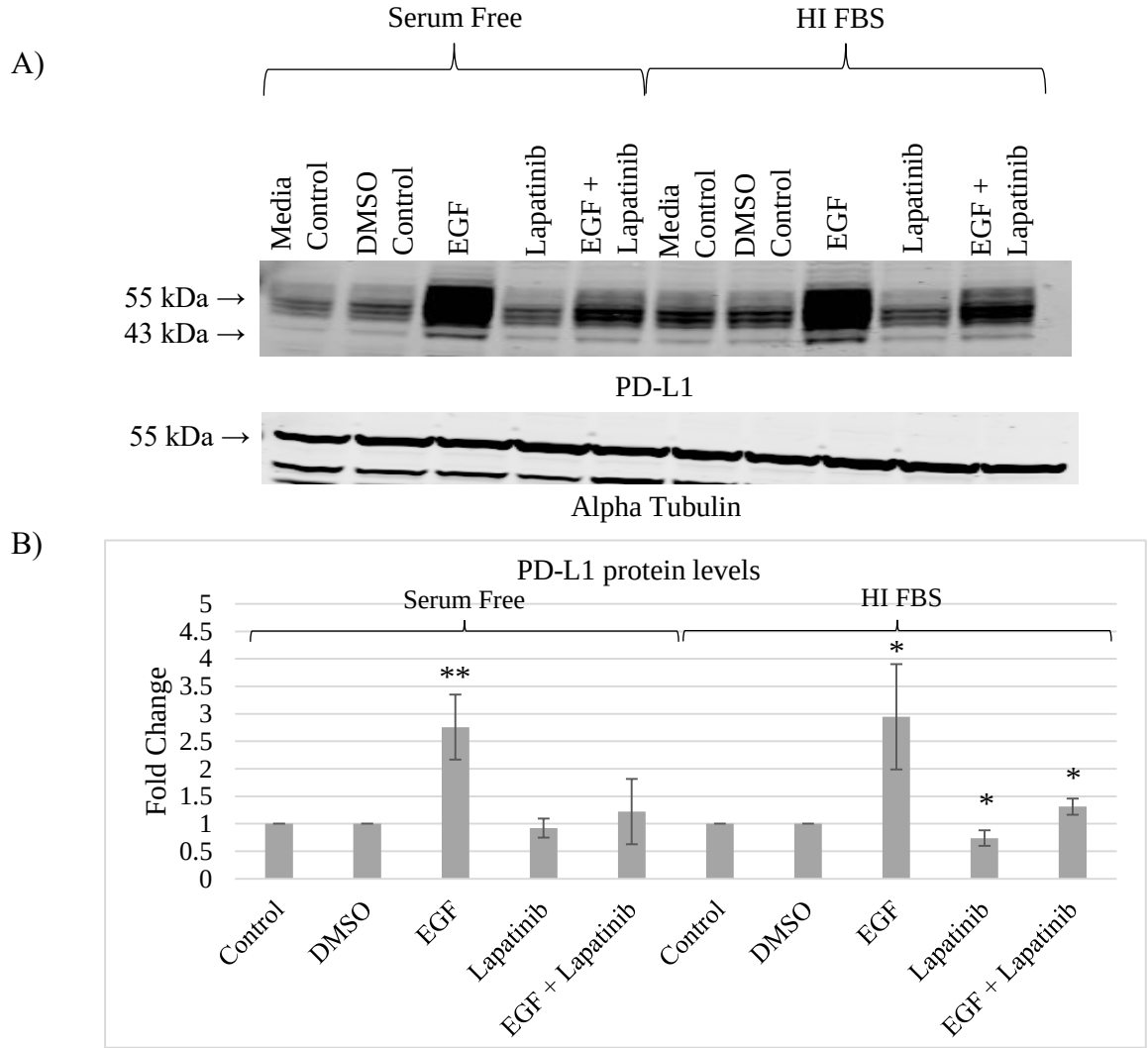

Figure 5.10: A) Western blotting for PD-L1 protein expression in serum- free and HI serum conditions in the HCC1954-Par cell line. Image is representative of triplicate blots. Alpha tubulin was used as a loading control. **B)** Densitometry analysis of immunoblots of the HCC1954-Par cell line for PD-L1 protein levels in serum-free and HI serum conditions. Protein levels are normalised to control protein levels. Error bars represent standard deviation of biological triplicate experiments. The Student's t test was used to determine statistical significance. * $p < 0.05$, ** $p < 0.01$ and *** $p < 0.001$.

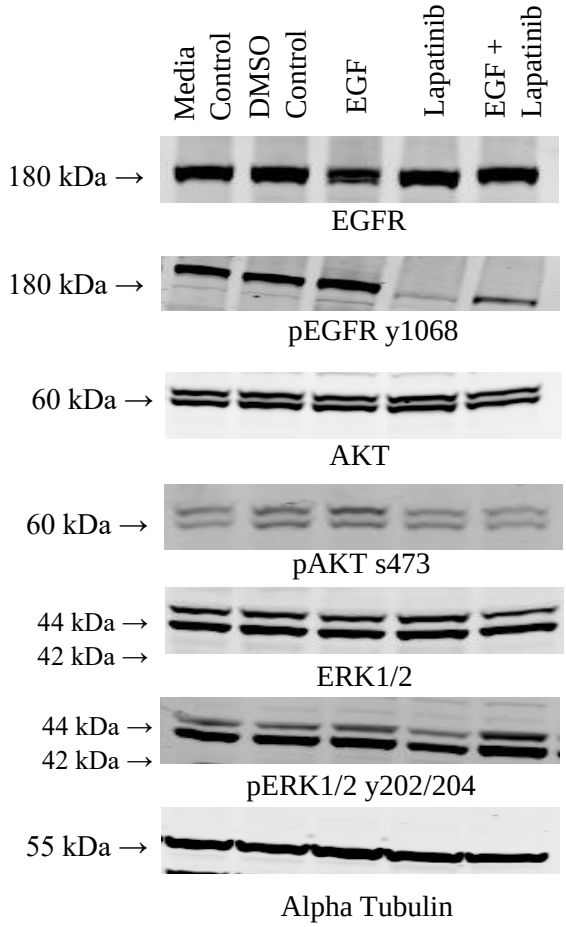

Figure 5.11: Western blotting for EGFR, pEGFR y1068, AKT, pAKT s473, ERK1/2 and pERK1/2 y202/204 protein expression in HI serum conditions in the HCC1954-Par cell line. Image is representative of triplicate blots. Alpha tubulin was used as a loading control. Densitometry analysis of immunoblots of the HCC1954-Par cell line are available in Appendix 2. The Student's t test was used to determine statistical significance. * $p < 0.05$, ** $p < 0.01$ and *** $p < 0.001$.

5.3.2.1.4 Summary- HCC1954-Par

In the HCC1954-Par cell line, EGF causes an increase in PD-L1 protein expression that is associated with pEGFR activity (**Section 5.3.2.11 and 5.3.2.1.2**). Neither AKT nor ERK levels mirrored the expression trend of PD-L1 in this cell line (**Section 5.3.2.3**). EGF treatment did not cause an increase in AKT or ERK activity in this cell line. Lapatinib treatment alone caused a decrease in AKT and ERK pathway activation in HCC1954-Par, which was likely due to the effect of lapatinib on HER2 signalling (**Section 5.3.2.3**).

5.3.2.2 The effect of EGF treatment on protein expression in HCC1954-Lap cells

5.3.2.2.1 EGF treatment and PD-L1 expression in HCC1954-Lap cells

When treated with 10 ng/mL EGF for 24 hours, HCC1954-Lap cells showed a 2.35-fold increase in PD-L1 in serum free conditions ($p=1 \times 10^{-4}$) and a 2.46-fold increase in PD-L1 in the presence of HI FBS (p=0.034) (**Figure 5.12**). Lapatinib treatment alone did not alter PD-L1 expression in serum free or serum conditions (**Figure 5.12**). In serum free conditions, lapatinib blocked EGF-mediated PD-L1 upregulation (p=0.003), this effect was seen in serum conditions but was not significant (**Figure 5.12**). As the effect of EGF on PD-L1 was similar in both serum free and serum conditions, cell lysates prepared in serum were utilised for further investigation.

5.3.2.2.2 EGF treatment and EGFR expression in HCC1954-Lap cells

EGFR expression was decreased upon EGF treatment in the HCC1954-Lap cell line, this decrease was approaching significance (p=0.053), lapatinib blocked this effect and EGFR levels were not significantly altered compared to control (**Figure 5.13**). There was a 2.11-fold increase in pEGFR levels with EGF treatment (p=0.078), lapatinib partially blocked this effect (p=0.079) (**Figure 5.13**). pEGFR levels follow a similar trend as PD-L1 levels in the presence of lapatinib and EGF treatment.

5.3.2.2.3 EGF treatment and ERK and AKT activity in HCC1954-Lap cells

Total AKT protein levels were unchanged in the HCC1954-Lap cell line with EGF or lapatinib treatments (**Figure 5.13**). However, EGF caused an upregulation of pAKT levels (p=0.021) which again was only partially blocked by lapatinib treatment (**Figure 5.13**). Total ERKprotein levels were unchanged in the HCC1954-Lap cell line with either EGF or lapatinib treatment (**Figure 5.13**). EGF treatment caused a 2.92-fold increase in pERK2 (p=0.049) and in the presence of lapatinib alone pERK1 levels were decreased compared to control (p=0.017). Again, lapatinib was not capable of blocking EGF-mediated increases in pERK1 and pERK2 which were both significantly increased compared to control levels (p=0.012 and p=0.062 respectively).

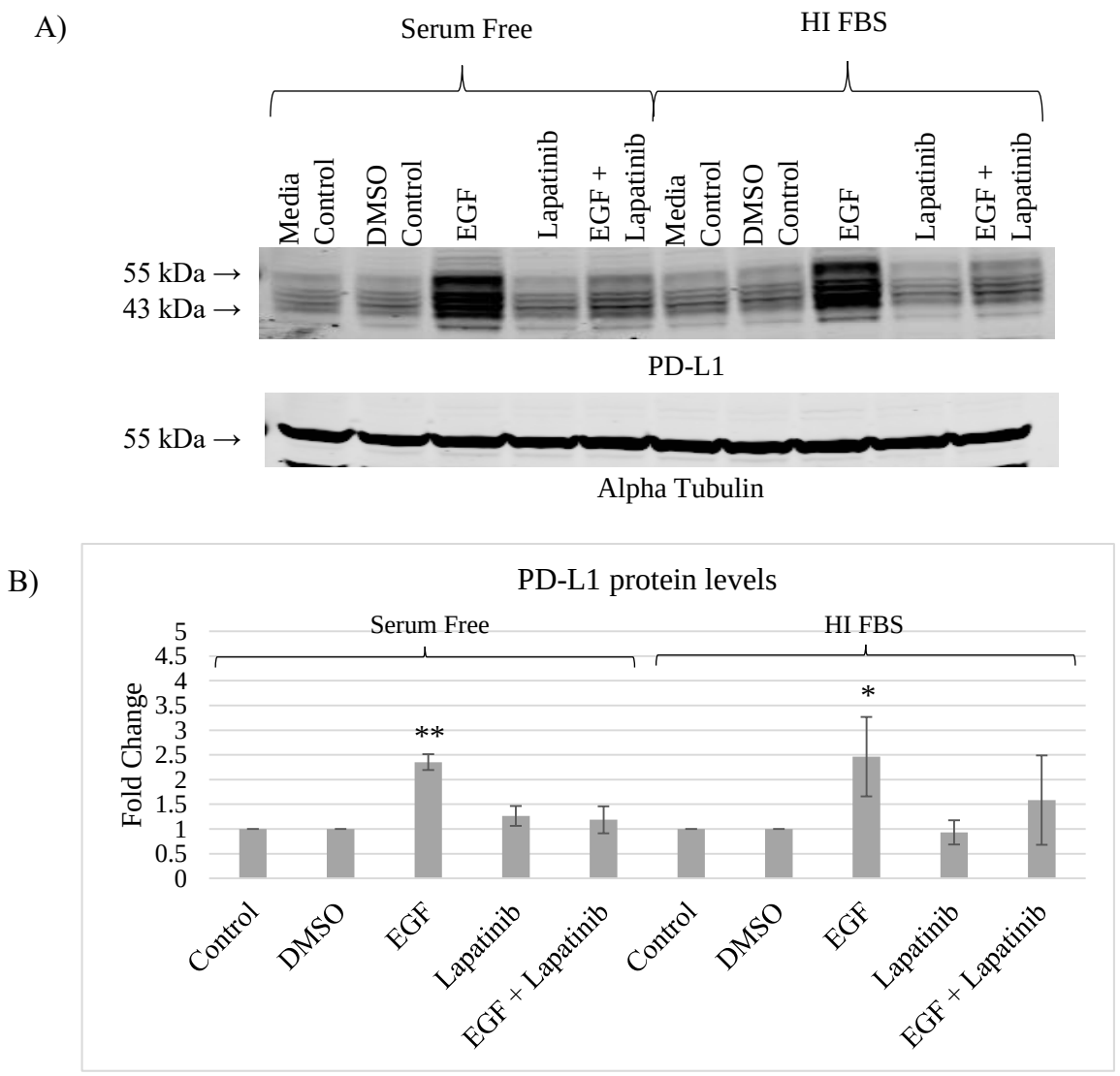

Figure 5.12: A) Western blotting for PD-L1 protein expression in serum free and HI serum conditions in the HCC1954-Lap cell line. Image is representative of triplicate blots. Alpha tubulin was used as a loading control. **B)** Densitometry analysis of immunoblots of the HCC1954-Lap cell line for PD-L1 protein levels in serum free and HI serum conditions. Protein levels are normalised to control protein levels. Error bars represent standard deviation of biological triplicate experiments. The Student's t test was used to determine statistical significance. * $p < 0.05$, ** $p < 0.01$ and *** $p < 0.001$.

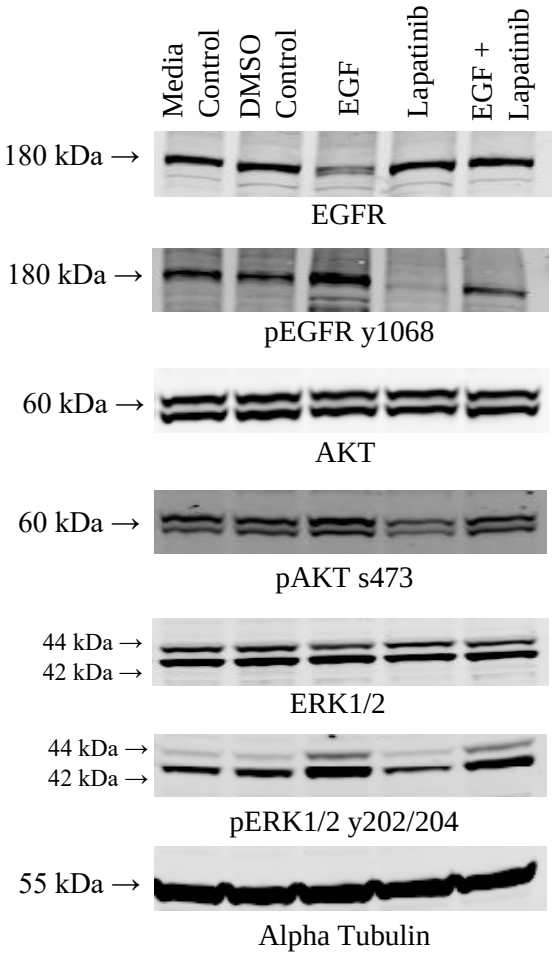

Figure 5.13: Western blotting for EGFR, pEGFR y1068, AKT, pAKT s473, ERK1/2 and pERK1/2 y202/204 protein expression in HI serum conditions in the HCC1954-Lap cell line. Image is representative of triplicate blots. Alpha tubulin was used as a loading control. Densitometry analysis of immunoblots of the HCC1954-Lap cell line are available in Appendix 2. The Student's t test was used to determine statistical significance. * $p < 0.05$, ** $p < 0.01$ and *** $p < 0.001$.

5.3.2.2.4 Summary- HCC1954-Lap

As seen in the parental HCC1954-Par cell line, EGF also mediated an increase in PD-L1 and pEGFR expression in the HCC1954-Lap cells (**Section 5.3.2.2.1 and 5.3.2.2.2**). Activation of the intracellular EGFR-related signalling through ERK and AKT was seen upon EGF treatment in the HCC1954-Lap cell line (**Section 5.3.2.2.3)**. This effect was not seen in the parental cell line, alteration to EGF related signalling pathways ERK, and AKT may be associated with the development of lapatinib resistance in this model. Lapatinib was not effective at blocking the EGF-associated intracellular signalling proteins ERK and AKT in the resistant cell line, showing alterations in EGF-mediated signalling associated with the development of lapatinib resistance (**Section 5.3.2.2.3**).

5.3.2.3 The effect of EGF treatment on protein expression in SKBR3-Par cells

5.3.2.3.1 EGF treatment and PD-L1 expression in SKBR3-Par cells

When treated with 10 ng/mL EGF for 24 hours, SKBR3-Par cells showed a 6.52-fold increase in PD-L1 in serum free conditions (p=0.0008) and a 4.38-fold increase in PD-L1 in the presence of HI FBS (p=0.032) (**Figure 5.14**). Lapatinib treatment alone caused a small decrease in PD-L1 expression in serum free conditions (p=0.001) and in HI FBS (p=0.094) (**Figure 5.14**). In serum-free and serum conditions, lapatinib blocked EGF-induced PD-L1 upregulation. Significantly lower PD-L1 expression was observed in the presence of EGF/lapatinib compared to EGF alone (p=0.002 and p=0.041, respectively) (**Figure 5.14**). As the effect of EGF on PD-L1 was similar in both serum free and serum conditions, cell lysates prepared in serum were utilised for further studies.

5.3.2.3.2 EGF treatment and EGFR expression in SKBR3-Par cells

EGFR expression was increased upon EGF treatment in the SKBR3-Par cell line (p=0.055), lapatinib blocked this effect, as EGFR levels were not significantly altered compared to control levels (**Figure 5.15**). There was an increase in pEGFR levels with EGF treatment (p=0.058) (**Figure 5.15**). Lapatinib caused a decrease in pEGFR expression alone and in the presence of EGF ($p=2.66x10^{-6}$ and $4.3x10^{-5}$ respectively) (**Figure 5.15**).

5.3.2.3.3 EGF treatment and ERK and AKT activity in SKBR3-Par cells

Total AKT protein levels were unchanged in the SKBR3-Par cell line following EGF or lapatinib treatment (**Figure 5.15**). EGF caused an upregulation of pAKT levels (p=0.054). Lapatinib treatment inhibited EGF-induced pAKT increases (p=0.049) (**Figure 5.15**). Total ERK protein levels were significantly decreased in the SKBR3-Par cell line in the presence of lapatinib treatment (p=0.001 for ERK1 and p=0.002 for ERK2) (**Figure 5.15**). EGF treatment caused an increase in pERK2 (p=0.049), lapatinib treatment caused a decrease in pERK1 and ERK2 ($p=3.34x10^{-5}$ and p=0.003 respectively). In the presence of EGF and lapatinib, pERK levels were unaltered compared to control (**Figure 5.15**).

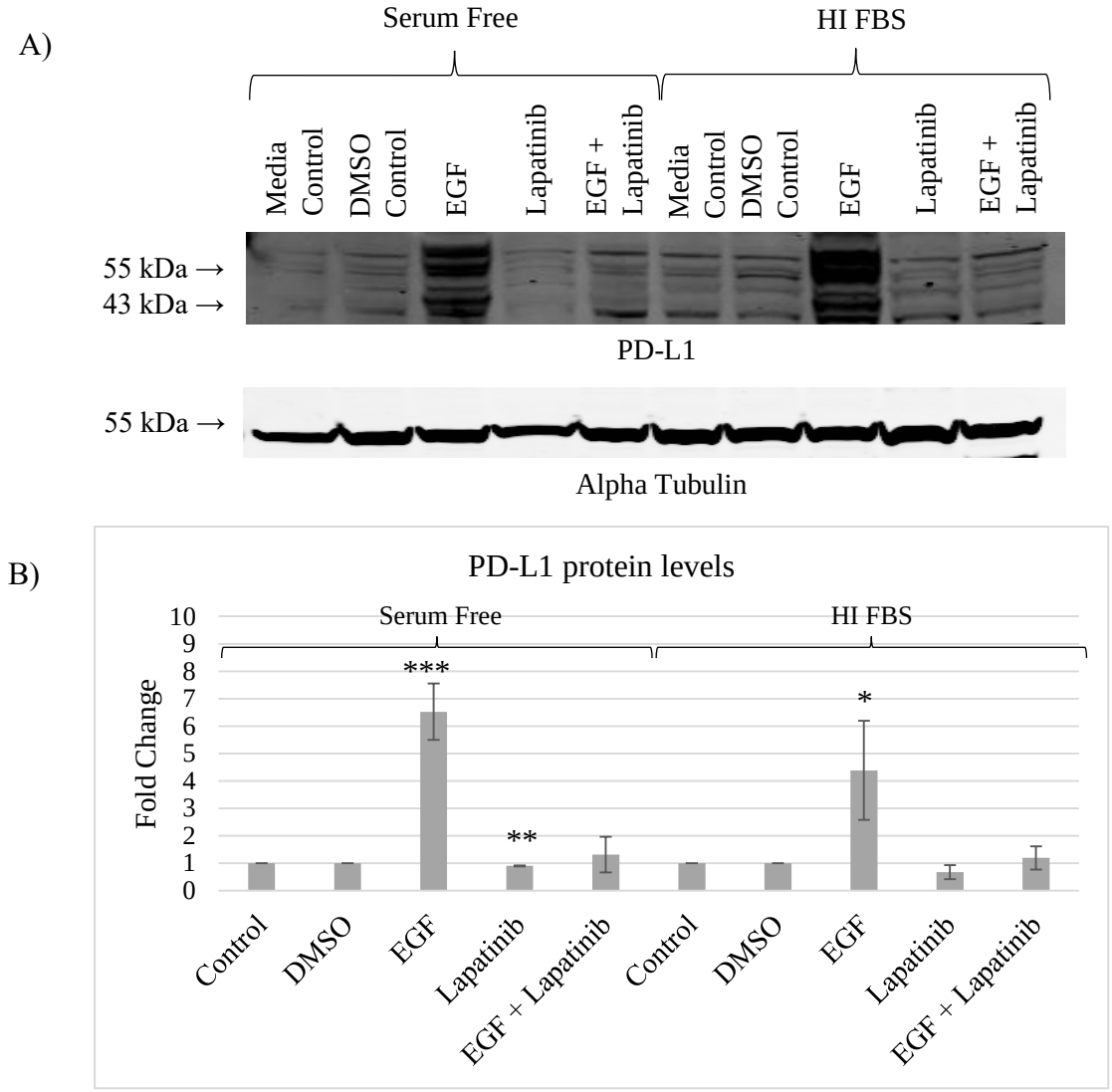

Figure 5.13: A) Western blotting for PD-L1 protein expression in serum free and HI serum conditions in the SKBR3-Par cell line. Image is representative of triplicate blots. Alpha tubulin was used as a loading control. **B)** Densitometry analysis of immunoblots of the SKBR3-Par cell line for PD-L1 protein levels in serum free and HI serum conditions. Protein levels are normalised to control protein levels. Error bars represent standard deviation of biological triplicate experiments. The Student's t test was used to determine statistical significance. * $p < 0.05$, ** $p < 0.01$ and *** $p < 0.001$.

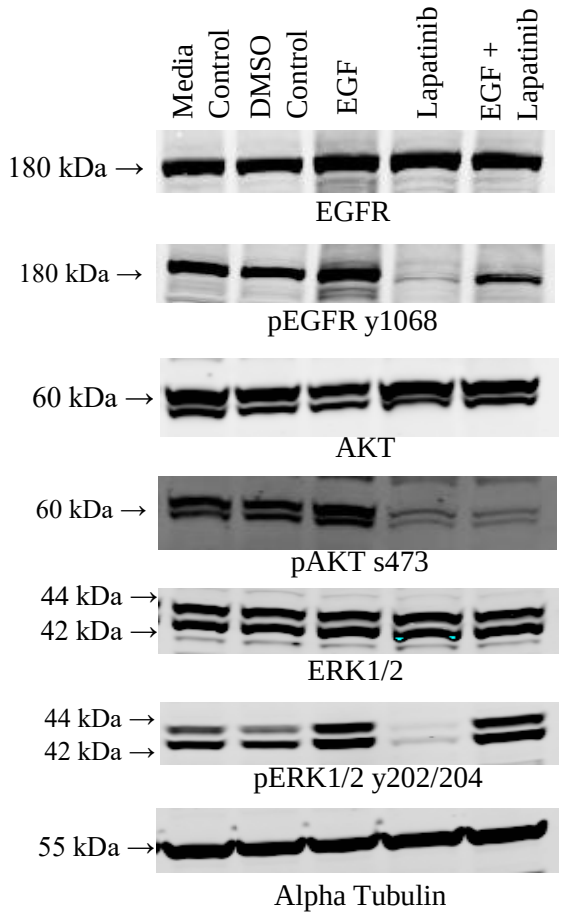

Figure 5.15: Western blotting for EGFR, pEGFR y1068, AKT, pAKT s473, ERK1/2 and pERK1/2 y202/204 protein expression in HI serum conditions in the SKBR3-Par cell line. Image is representative of triplicate blots. Alpha tubulin was used as a loading control. Densitometry analysis of immunoblots of the SKBR3-PAR cell line are available in Appendix 2. The Student's t test was used to determine statistical significance. * $p < 0.05$, ** $p < 0.01$ and *** $p < 0.001$.

5.3.2.3.4 Summary- SKBR3-Par

EGF is capable of upregulating PD-L1 in the SKBR3-Par cell line and lapatinib blocked this effect (**Section 5.3.2.3.1**). Lapatinib was capable of completely blocking the effects of EGF on pEGFR in the SKBR3-Par cell line (**Section 5.3.2.3.2**). pEGFR levels follow a similar trend as PD-L1 levels in the presence of lapatinib and EGF. EGF activated intracellular ERK and AKT phosphorylation which was blocked by lapatinib treatment (**Section 5.3.2.3.3**).

5.3.2.4 The effect of EGF treatment on protein expression in SKBR3-Afa cells

5.3.2.4.1 EGF treatment and PD-L1 expression in SKBR3-Afa cells

When treated with 10 ng/mL EGF for 24 hours, SKBR3-Afa cells showed a 3.09-fold increase in PD-L1 expression in serum free conditions (p=0.051) and a 1.89-fold increase in PD-L1 in the presence of HI FBS (p=0.001) (**Figure 5.16**). This increase was not as great as that observed in the SKBR3-Par cell line (**Section 5.3.2.3.1**). Lapatinib treatment alone did not alter PD-L1 levels (**Figure 5.16**). In serum free and serum conditions, lapatinib blocked EGF-mediated PD-L1 upregulation, compared to EGF treatment alone (p=0.051 and p=0.008 respectively) (**Figure 5.16**). This indicates that EGF is also capable of upregulating PD-L1 in the SKBR3-Afa cell line and that lapatinib blocked this effect (**Figure 5.16**). As EGF increased PD-L1 expression in both serum-free and serum-containing conditions, cell lysates were prepared in serum for further studies.

5.3.2.4.2 EGF treatment and EGFR expression in SKBR3-Afa cells

EGFR expression was significantly decreased upon EGF treatment in the SKBR3-Afa cell line (p=0.048) but lapatinib blocked this effect (**Figure 5.17**). There was no change in pEGFR levels with EGF treatment, showing EGFR activation is ligand independent in this afatinib-resistant cell line (**Figure 5.17**). Lapatinib caused a decrease in pEGFR expression alone ($p=3.6x10^{-5}$). There was no significant reduction in pEGFR in the presence of EGF and lapatinib (**Figure 5.17**).

5.3.2.4.3 EGF treatment and ERK and AKT activity in SKBR3-Afa cells

Total AKT protein levels were unchanged in the SKBR3-Afa cell line with EGF or lapatinib treatments (**Figure 5.17**). EGF treatment did not alter pAKT levels, although lapatinib alone and lapatinib/EGF decreased pAKT expression (p=0.0006 and p=0.0002 respectively) (**Figure 5.17**). EGF treatment upregulated total ERK1 (p=0.001), pERK1 (p=0.001) and pERK2 (p=0.035) (**Figure 5.17**). Lapatinib treatment caused a decrease in pERK1 and ERK2 (p=0.004 and $p=1.65x10^{-5}$ respectively). Lapatinib was not capable of blocking EGF-mediated increases in pERK with the combination (**Figure 5.17**).

A)

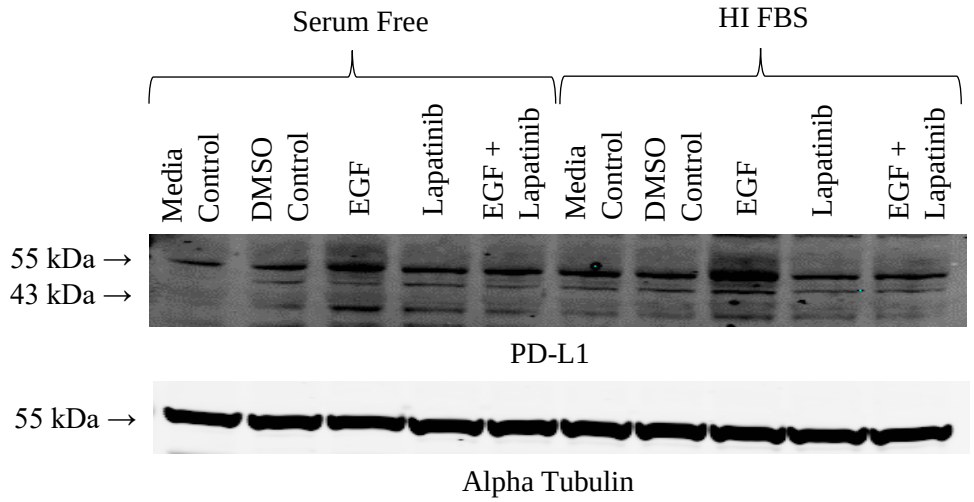

B)

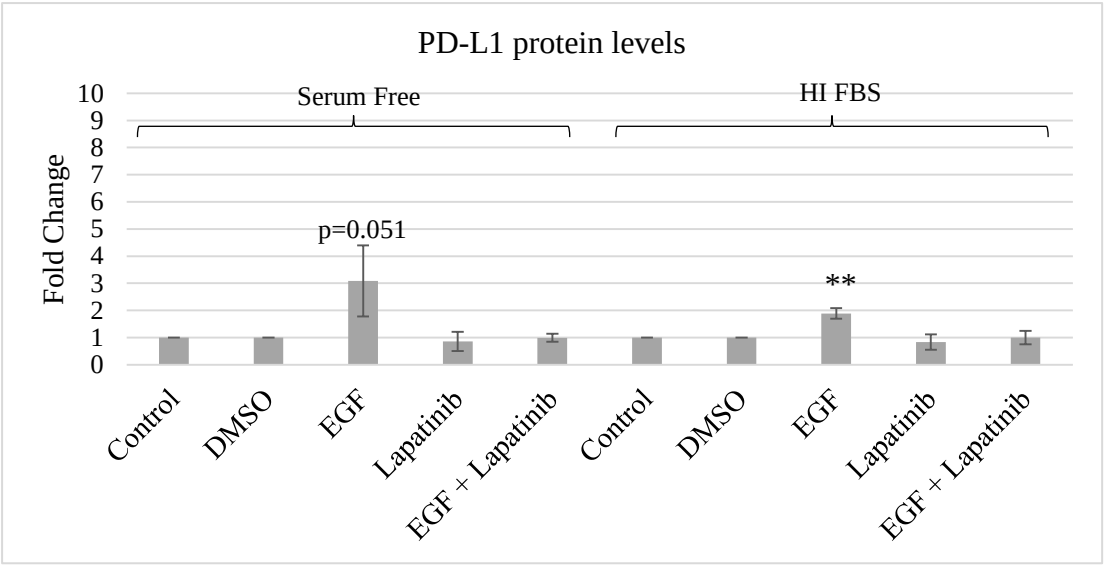

Figure 5.16: A) Western blotting for PD-L1 protein expression in serum free and HI serum conditions in the SKBR3-Afa cell line. Image is representative of triplicate blots. Alpha tubulin was used as a loading control. **B)** Densitometry analysis of immunoblots of the SKBR3-Afa cell line for PD-L1 protein levels in serum free and HI serum conditions. Protein levels are normalised to control protein levels. Error bars represent standard deviation of biological triplicate experiments. The Student's t test was used to determine statistical significance. * $p < 0.05$, ** $p < 0.01$ and *** $p < 0.001$.

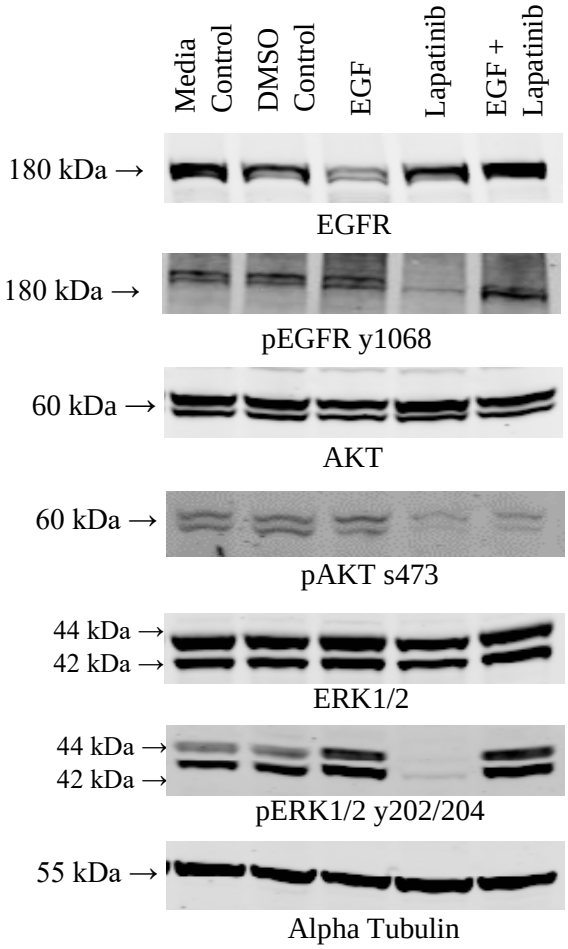

Figure 5.17: Western blotting for EGFR, pEGFR y1068, AKT, pAKT s473, ERK1/2 and pERK1/2 y202/204 protein expression in HI serum conditions in the SKBR3-Afa cell line. Image is representative of triplicate blots. Alpha tubulin was used as a loading control. Densitometry analysis of immunoblots of the SKBR3-Afa cell line are available in Appendix 2. The Student's t test was used to determine statistical significance. * $p < 0.05$, ** $p < 0.01$ and *** $p < 0.001$.

5.3.2.4.4 Summary- SKBR3-Afa

EGF was again capable of mediating an increase in PD-L1 expression in the SKBR3-Afa cell line (**Section 5.3.2.4.1**), the magnitude of increase in the afatinib resistant SKBR3-Par cells with EGF treatment was much lower than the parental cell line (**Section 5.3.2.3.1**). pEGFR and pAKT levels were not influenced by EGF treatment in the SKBR3-Afa cell line (**Section 5.3.2.4.2**) as is consistent with a targeted therapy resistance phenotype. This suggests that pEGFR needs to be increased by EGF treatment to elicit the effects seen in the parental cell line. ERK signalling was activated with EGF treatment (**Section 5.3.2.4.3**).

5.3.3 Overall summary

EGF caused an increase in PD-L1 in all cell lines examined. Lapatinib blocked this increase indicating that the effect is mediated through EGFR (**Section 5.3.2.1.1, 5.3.2.2.1, 5.3.2.3.1 and 5.3.2.4.1**). pEGFR levels showed a similar expression trend as PD-L1 in the presence of EGF and lapatinib treatments indicating activation of EGFR is associated with EGF-mediated upregulation of PD-L1 expression (**Section 5.3.2.1.2, 5.3.2.2.2, 5.3.2.3.2 and 5.3.2.4.2**). While EGFR activity and PD-L1 expression were shown to be linked in this study, the changes in ERK and AKT activity were not fully consistent across all cell lines which suggests it is unlikely that ERK and AKT are the sole mediators of the link between EGFR and PD-L1 (**Section 5.3.2.1.3, 5.3.2.2.3, 5.3.2.3.3 and 5.3.2.4.3**).

The phenotype of the lapatinib and afatinib resistant cell lines examined showed altered EGF-mediated signalling compared with their respective parental cell line. The HCC1954-Lap cell line showed activation of AKT and ERK pathways upon EGF treatment which was not present in the parental cell line (**Section 5.3.2.1.3 and 5.3.2.2.3**). In the afatinib resistant SKBR3 model, there were alterations to EGFR and AKT activity upon EGF treatment which were not present in the parental cell line (**Section 5.3.2.4.2 and 5.3.2.4.3**).

5.4 Potential mediators of a link between EGFR and PD-L1

A link between EGFR and PD-L1 expression in breast cancer cell lines was identified through the observation of co-expression/alteration in targeted therapy-resistant cell lines and EGF/lapatinib studies. The mediators of the EGFR/PD-L1 effect have not yet been fully characterised. To determine potential candidates, protein: protein interaction databases were employed. Once candidate proteins were identified, inhibitors of these targets were used to determine whether they blocked an EGFR - mediated increase in PD-L1 expression. A limitation of this approach is that only previously described interactions can be investigated, and only targets with available inhibitors can be interrogated.

5.4.1 STRING database interrogation

The STRING protein database was used to determine proteins that interacted with EGFR and PD-L1 directly (https://string-db.org). The crossover of proteins that interacted directly with both EGFR and PD-L1 yielded two targets - LCK and PTPN11 (**Figure 5.18**). LCK, or Tyrosine-protein kinase LCK, is a non-receptor tyrosine kinase which is part of the SRC kinase family that plays a vital role in T cell proliferation and maturation, the role of LCK in breast cancer is not well defined. PTPN11 (Tyrosine-protein phosphatase non-receptor type 11) is a protein phosphatase involved in the MAPK signalling pathway.

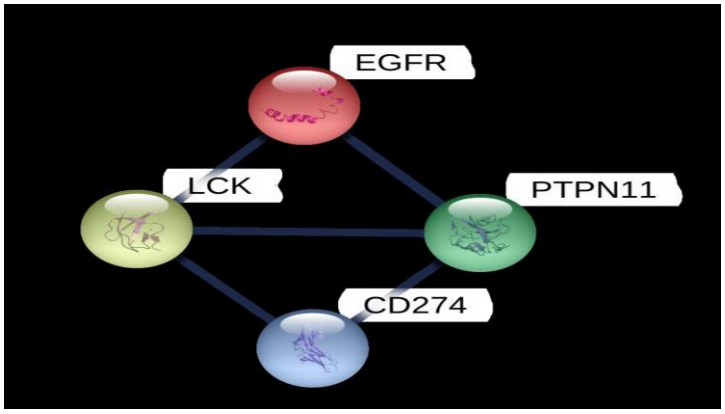

Figure 5.18: Protein interaction model build from STRING database showing high confidence links (blue line) (>0.7 on a scale of 0-1) between EGFR, LCK, CD274 and PTPN11.

5.4.2 UCSC Xena browser database interrogation

UCSC Xena browser (https://xenabrowser.net/) is an online database used "to explore functional genomic data sets for correlations between genomic and/or phenotypic variables". The heatmap allows for the examination of the range of gene expression within a patient cohort. Gene expression levels for each target range from high (red) to low (blue). This allows for the assessment of gene co-expression within patient cohorts. Gene co-expression of PD-L1, EGFR. LCK and PTPN11 was examined in the TCGA breast cancer patient sample dataset (n=1247). Using PD-L1 as the reference variable, EGFR had a similar trend in gene expression in the dataset (**Figure 5.19 A**). LCK showed a relatively strong trend for co-expression with PD-L1. PTPN11 expression was low across the data set. When EGFR was used as the reference variable, gene expression a subset of patients with high EGFR also had high PTPN11 expression. However, LCK was not as strongly associated with EGFR expression (**Figure 5.19 B**).

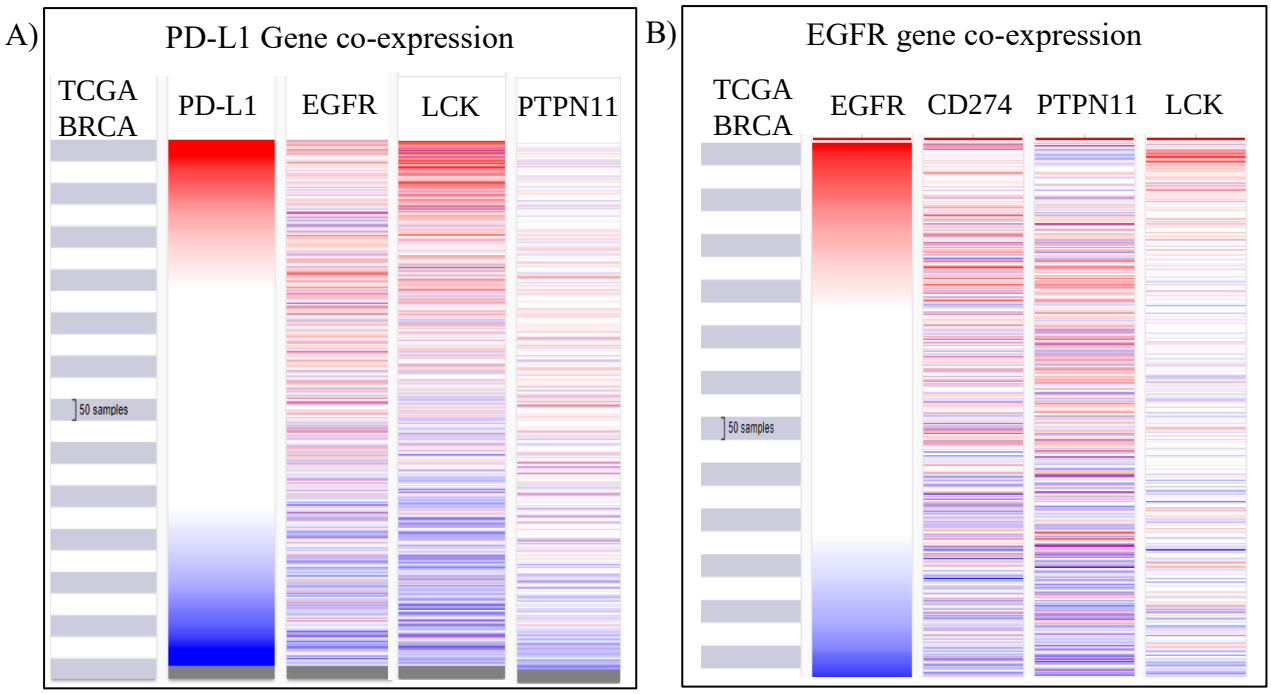

Figure 5.19: A) PD-L1 gene co-expression with EGFR, LCK and PTPN11 in the TCGA breast cancer dataset. **B)** EGFR gene co-expression with PTPN11 and LCK in TCGA breast cancer dataset. Red = high expression, blue = low expression (the cut-off is 50% expression).

5.4.3 PTPN11 and LCK expression in targeted therapy-resistant cell line models

Protein expression of PTPN11, pPTPN11 and LCK was determined using western blotting in a selection of parental and resistant breast cancer cell lines which previously showed alterations to PD-L1 expression (**Section 5.2.3**). Total PTPN11 expression was detectable across the cell lines examined but no changes in expression levels were observed between cell lines (**Figure 5.20**). pPTPN11 expression was also detectable and showed a similar expression profile to PD-L1 (**Section 5.2.3.2**) (**Figure 5.20**). LCK protein expression or pLCK protein expression was not detectable in the cell lines examined using CST ab # 2752 and 2753 respectively (**Figure 5.20**).

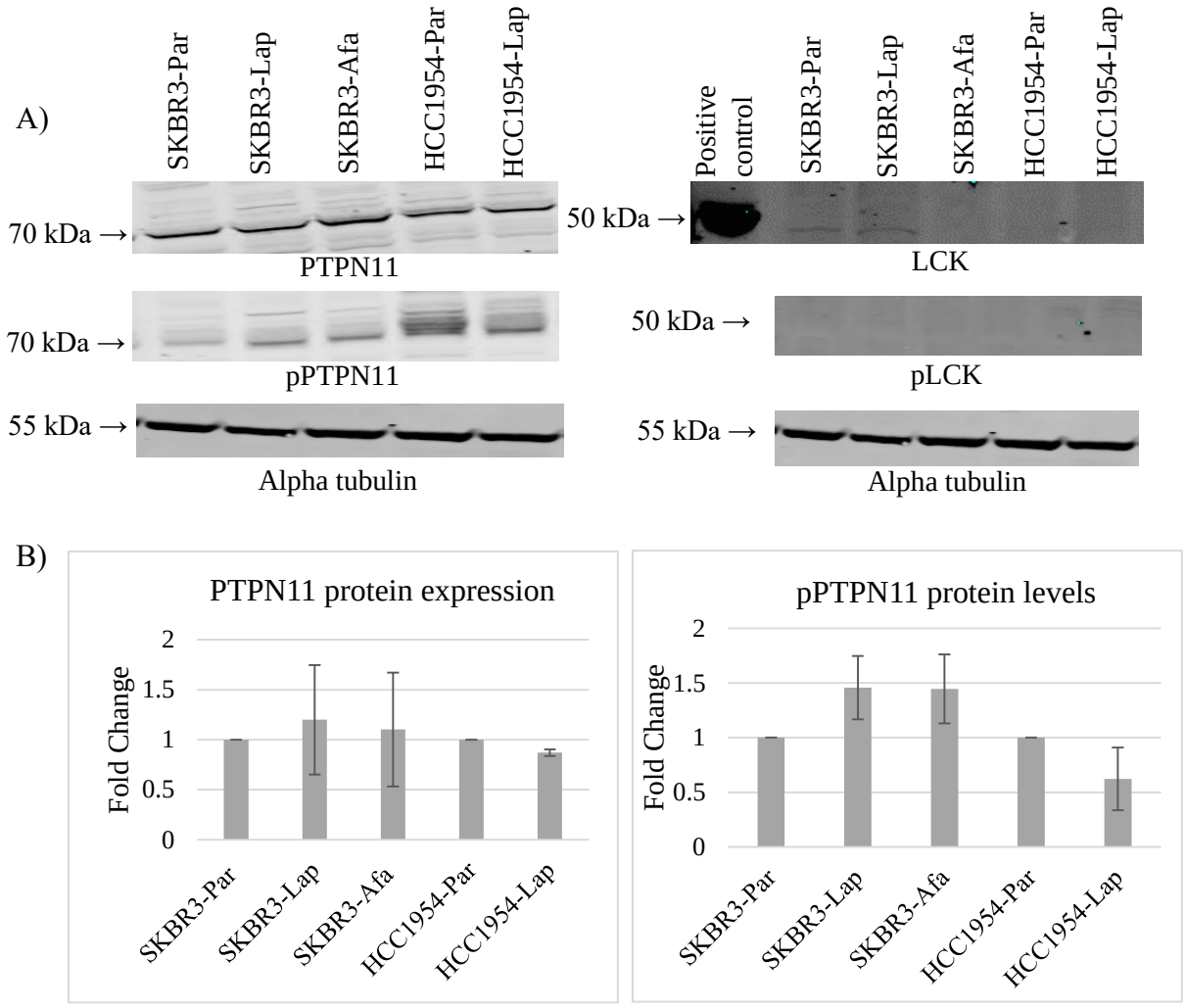

Figure 5.20: A) Western blotting for PTPN11, pPTPN11 and LCK protein in HER2+ breast cancer cell lines. Image is representative of triplicate blots. Alpha tubulin was used as a loading control. Activated T cells were used as a positive control for LCK **B)** Densitometry analysis of immunoblots of HER2+ breast cancer cell lines for PTPN11 and pPTPN11. Protein levels are normalised to parental cell line protein levels. Error bars represent standard deviation of biological triplicate experiments. The Student's t test was used to determine statistical significance. * $p < 0.05$, ** $p < 0.01$ and *** $p < 0.001$.

5.4.4 Impact of PTPN11 and LCK inhibition on PD-L1 and EGFR expression in HCC1954

Inhibitors of PTPN11 and LCK were selected to determine if they had any effect on EGF-associated PD-L1 upregulation. SHP099 is a small molecule PTPN11 inhibitor [338]. Saracatinib is a SRC family kinase inhibitor which targets LCK along with other SRC family members c-Yes, Fyn, Lyn, Blk and Fgr [339]. A concentration of 300 nM SHP099 or saracatinib, or 1 µM lapatinib were added to HCC1954-Par cells for 12 hours with and without EGF stimulation. 12 hours was selected in this instance due to the potential use of these treatments in an immune cytotoxicity assay which would use a 12-hour time point. Concentrations were derived from company supplied protocols and previous experiments within the lab group. This was to determine whether the inhibitors were successful at inhibiting EGF-mediated PD-L1 upregulation.

5.4.4.1 Impact of inhibitors +/- EGF on PD-L1 expression

EGF treatment resulted in a 2.93-fold increase in PD-L1 expression in HCC1954 (p=0.014) (**Figure 5.21**). In the presence of lapatinib and EGF, PD-L1 levels remained at control levels, these results supported previous findings at a 24-hour time point (**Figure 5.21, Section 5.3.2.1.1**). Neither SHP099 nor saracatinib had any effect on PD-L1 expression alone (p=0.083 and p=0.15 respectively) (**Figure 5.21**). Neither drug affected the increase in PD-L1 expression arising from EGF exposure. In the presence of EGF and SHP099, PD-L1 levels were 2.82-fold higher (p=0.003) (**Figure 5.21**) and in the presence of EGF and saracatinib, PD-L1 levels were 2.71-fold higher than control levels (p=0.002) (**Figure 5.21**).

5.4.4.2 Impact of inhibitor +/- EGF on EGFR expression/activity

EGFR expression was significantly decreased after 12 hours of EGF treatment (p=0.035) and lapatinib blocked this effect (**Figure 5.22**). EGFR levels were increased but not significantly so in the presence of saracatinib (p=0.066). Co-treatment with saracatinib and EGF resulted in a significantly higher level of EGFR expression than seen with EGF alone (p=0.024) (**Figure 5.22**). This indicated that saracatinib may have an inhibitory effect on EGF-mediated, EGFR downregulation. SHP099 treatment alone or in the presence of EGF did not alter EGFR expression (**Figure 5.22**). EGF treatment increased pEGFR Y1068 levels (p=0.036) and lapatinib treatment blocked this effect (p=0.015) (**Figure 5.22**). Neither SHP099 nor saracatinib had a significant effect on pEGFR expression at Y1068 (**Figure 5.22**).

5.4.4.3 Impact of inhibitors +/- EGF on LCK and PTPN11 expression/activity

LCK or pLCK expression was still not detectable under any treatment condition (**Figure 5.23**). Total PTPN11 levels were unchanged with any of the added treatments (**Figure 5.24**). pPTPN11 levels were unchanged on the addition of EGF (**Figure 5.24**). In the presence of lapatinib, pPTPN11 levels were decreased compared to control (p=0.001) (**Figure 5.24**). pPTPN11 levels were unchanged in the presence of saracatinib and SHP099 alone, however in combination with EGF, both inhibitors produced an increased level of pPTPN11 (p=0.013 and p=0.001 respectively) (**Figure 5.24**).

5.4.4.4 Summary

Inhibition of PTPN11 or LCK did not modulate EGF-mediated PD-L1 expression (**Section 5.4.3.1**). Both proteins appear to be relevant to EGFR signalling pathways and are affected by EGF treatment in a similar way (**Section 5.4.3.2**). PTPN11 and LCK may be relevant in the link between EGFR and PD-L1 but are not key mediators of the effect.

A)

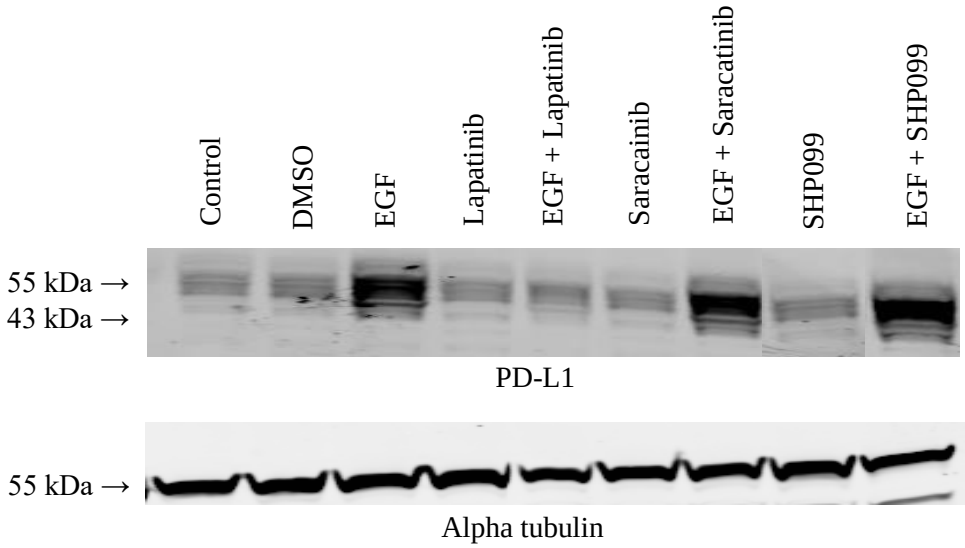

B)

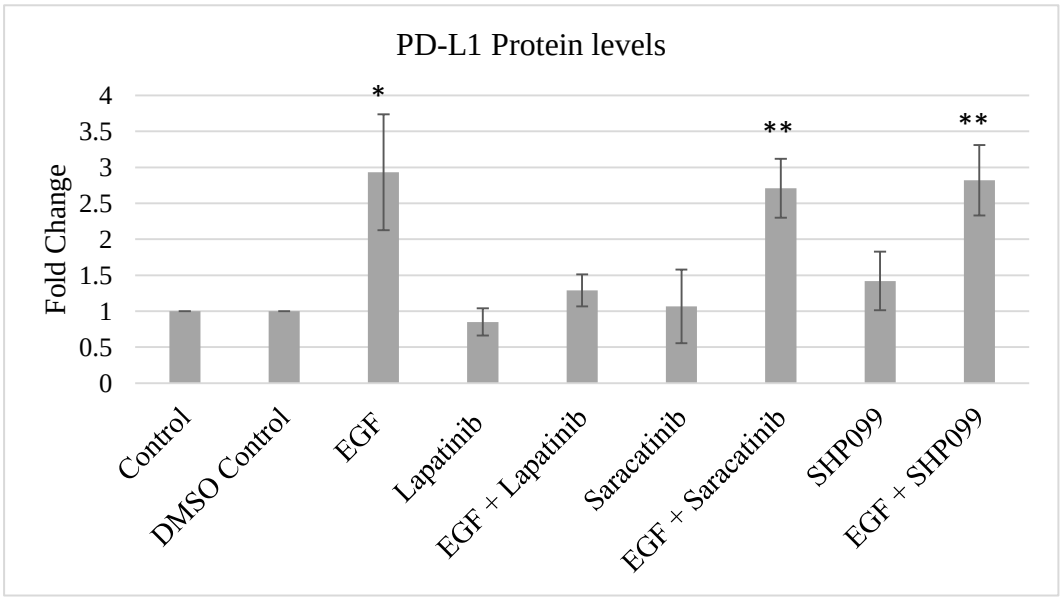

Figure 5.21: A) Western blotting for PD-L1 protein expression after 12 hours of treatment in the HCC1954-Par cell line. Image is representative of triplicate blots. Alpha tubulin was used as a loading control. **B)** Densitometry analysis of immunoblots of the HCC1954-Par cell line for PD-L1 protein expression. Protein levels were normalised to the relevant control treatment protein levels. Error bars represent standard deviation of biological triplicate experiments. The Student's t test was used to determine statistical significance. * $p < 0.05$, ** $p < 0.01$ and *** $p < 0.001$.

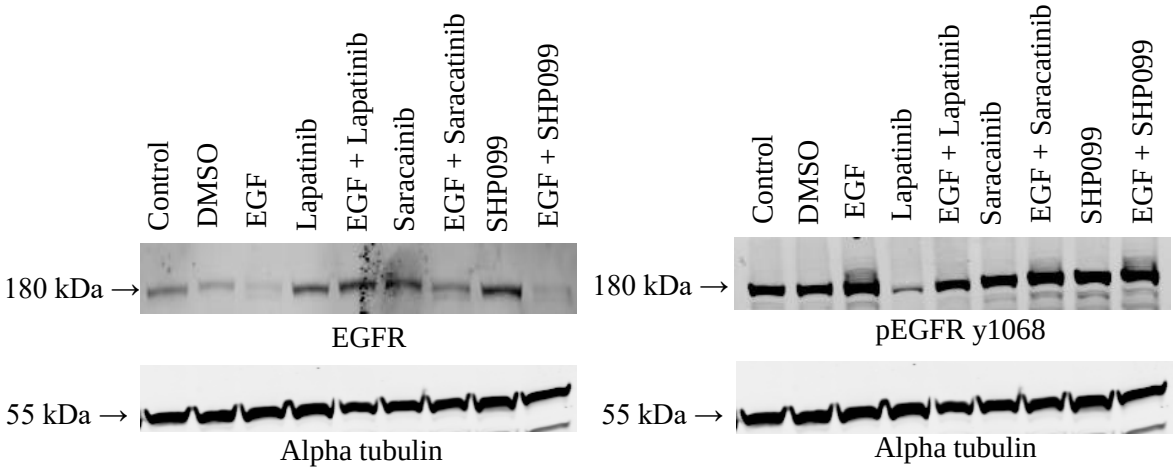

Figure 5.22: Western blotting for EGFR and pEGFR y1068 protein expression after 12 hours of treatment in the HCC1954-Par cell line. Image is representative of triplicate blots. Alpha tubulin was used as a loading control. The Student's t test was used to determine statistical significance. * $p < 0.05$, ** $p < 0.01$ and *** $p < 0.001$. Densitometry analysis of these blots are included in Appendix 2.

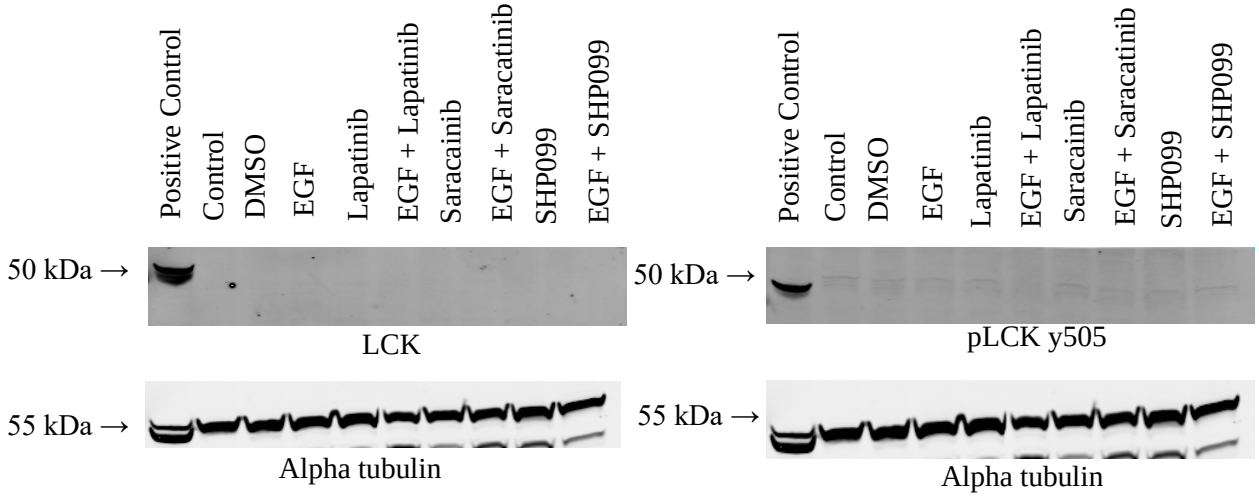

Figure 5.23: Western blotting for LCK and pLCK y505 protein expression after 12 hours of treatment in the HCC1954-Par cell line. Image is representative of triplicate blots. Alpha tubulin was used as a loading control.

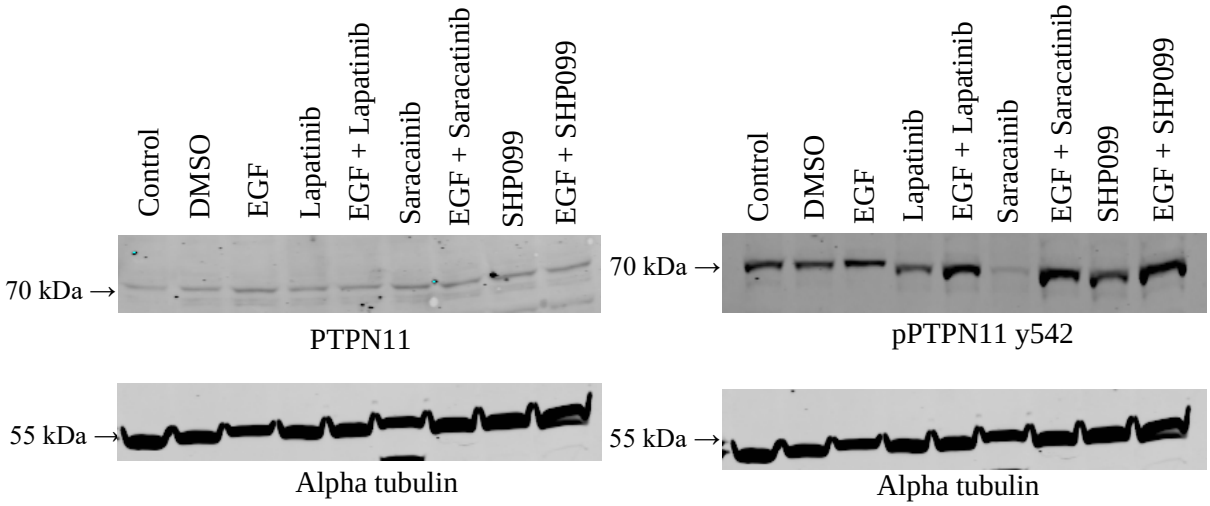

Figure 5.24: Western blotting for PTPN11 and pPTPN11 y542 protein expression after 12 hours of treatment in the HCC1954-Par cell line for. Image is representative of triplicate blots. Alpha tubulin was used as a loading control. The Student's t test was used to determine statistical significance. * $p < 0.05$, ** $p < 0.01$ and *** $p < 0.001$. Densitometry values are found in Appendix 2.

5.5 The effect of EGF treatment on the susceptibility of breast cancer cell lines to immune cell mediated killing

As EGF-treatment increased PD-L1 expression through activation of EGFR in the HCC1954-Par, HCC1954-Lap, SKBR3-Par and SKBR3-Afa cell lines, it was necessary to determine if this increase in PD-L1 affected the susceptibility of these cells to immune cell-mediated killing. PBMCs were isolated from healthy volunteers 11, 12 and 13 and utilised as effector cells (**Table 5.4**). Target cells were pre-treated with EGF for 24 hours based on results from Section 5.3.2 then run in the assay. Trastuzumab was assessed to determine the effect on T-ADCC, and atezolizumab was added to determine the impact of PD-L1 blockade on target tumour cell line death. Plate layout as described in Section 2, Figure 12.

Table 5.4: Healthy volunteer blood samples used in this section.

Healthy Volunteer	Sex	Age range	Assay
Volunteer 11	Female	45-54	EGF pre-treatment ADCC assay
Volunteer 12	Female	25-34	EGF pre-treatment ADCC assay
Volunteer 13	Female	35-45	EGF pre-treatment ADCC assay

5.5.1 Direct cytotoxicity against K562 cells

The unstimulated PBMCs elicited a range of cytotoxicity against the K562 cell line (**Table 5.5**). Volunteer 11's sample elicited 13.27 +/- 0.50% cytotoxicity, volunteer 12's sample elicited 5.23 +/- 1.65% cytotoxicity and volunteer 13's sample elicited 22.23 +/- 2.41% cytotoxicity against K562 cells. The Volunteer 13's sample had a significant increase in cytotoxicity (6.93%) against the K562 cell line in the presence of atezolizumab. Atezolizumab had no consistent effect on cytotoxicity elicited against the K562 cells (**Table 5.5**).

Table 5.5: % cytotoxicity elicited by PBMCs against the K562 cell line for samples from volunteers 11, 12 and 13 at a ratio of 5:1 EC:TC and significant changes in cytotoxicity against the K562 cell line in the presence of atezolizumab (10 µg/mL).

Direct Cytotoxicity	% Direct Cytotoxicity at 5:1	Effect of Atezolizumab
Volunteer 11	13.27 +/- 0.50%	-
Volunteer 12	5.23 +/- 1.65%	-
Volunteer 13	22.23 +/- 2.41%	↑

5.5.2 Immune-mediated cytotoxicity against EGF-treated HCC1954-Par cells

In section 5.3.2.1.1 an increase in PD-L1 levels was seen with EGF treatment in HCC1954-Par cells, this effect was associated with increased EGFR activity.

Overall cytotoxicity levels were significantly increased with EGF pre-treatment with PBMCs isolated from volunteer 12 only (4.8 %, p=0.042). Direct cytotoxicity levels were increased with EGF pre-treatment for PBMCs isolated from volunteer 11 (6.23 %, p=0.045). T-ADCC levels were significantly decreased with PBMCs from volunteer 12 by 6.30 % (p=0.015). There was also a decrease in T-ADCC in the presence of atezolizumab in the EGF pre-treated cells by 6.07 % (p=0.028) elicited by PBMCs from volunteer 11 (**Table 5.6**).

Pre-treatment of the HER2+/PD-L1 high HCC1954-Par cell line with EGF did not lead to any consistent alterations in overall cytotoxicity, direct cytotoxicity or T-ADCC levels (**Table 5.6**). The inconsistent effects of EGF treatment on cytotoxicity against the HCC1954 cell lines may be due to the pre-existing high levels of PD-L1 expression seen in this cell line prior to EGF treatment.

Table 5.6: PBMC-mediated cytotoxicity at a 5:1 EC: TC ratio against the HCC1954-Par cell line for all three volunteer samples. A) Overall cytotoxicity **B)** Direct Cytotoxicity **C)** T-ADCC. Arrows denote statistically significant change in cytotoxicity levels caused by EGF pre-treatment with and without atezolizumab present in the assay. The Student's t test was used to determine statistical significance. * $p < 0.05$, ** $p < 0.01$ and *** $p < 0.001$. All antibodies were used at a concentration of 10 µg/µL.

A) Overall Cytotoxicity	EGF pre-treatment	EGF pre-treatment atezolizumab
Volunteer 11	-	-
Volunteer 12	-	↑
Volunteer 13	-	-

B) Direct Cytotoxicity	EGF pre-treatment	EGF pre-treatment atezolizumab
Volunteer 11	↑	-
Volunteer 12	-	-
Volunteer 13	-	-

C) T-ADCC	EGF pre-treatment	EGF pre-treatment atezolizumab
Volunteer 11	-	↓
Volunteer 12	↓	-
Volunteer 13	-	-

5.5.3 Immune-mediated cytotoxicity against EGF-treated HCC1954-Lap cells

As shown in Section 5.3.2.2.1 PD-L1 expression was increased with EGF treatment in the HCC1954-Lap cell line, this effect was associated with increased EGFR activity.

When the lapatinib-resistant, HCC1954-Lap cell line was pre-treated with EGF there were no consistent alterations to overall cytotoxicity or T-ADCC with or without atezolizumab *versus* control (**Table 5.7**).

There was a decrease in direct cytotoxicity in all three volunteer samples when the cells were pre-treated with EGF by 8.60 % (p=0.08), 4.13 % (p=0.008) and 8.25 % (p=0.004). There was a significant increase in direct cytotoxicity in the presence of atezolizumab (6.22 %, p=0.008) when cells were EGF pre-treated using the volunteer 12 sample. PBMCs from volunteer 13 elicited 7.77 % less direct cytotoxicity in the presence of atezolizumab against EGF pre-treated cells than non-EGF pre-treated cells (p=0.001) (**Table 5.7**).

EGF pre-treatment caused a decrease in direct cytotoxicity levels against the HCC1954-Lap cells. This effect was blocked in one volunteer sample by atezolizumab (Volunteer 12) but enhanced with PBMCs from volunteer 13. Further work is needed to determine if the effects of EGF pre-treatment on direct cytotoxicity are mediated by PD-L1 upregulation.

Table 5.7: PBMC-mediated cytotoxicity at a 5:1 EC: TC ratio against the HCC1954-Lap cell line for all three volunteer samples. A) Overall cytotoxicity **B)** Direct Cytotoxicity **C)** T-ADCC. Arrows denote statistically significant change in cytotoxicity levels caused by EGF pre-treatment with and without atezolizumab present in the assay. The Student's t test was used to determine statistical significance. * $p < 0.05$, ** $p < 0.01$ and *** $p < 0.001$. All antibodies were used at a concentration of 10 µg/µL.

A) Overall Cytotoxicity	EGF pre-treatment	EGF pre-treatment atezolizumab
Volunteer 11	-	↓
Volunteer 12	-	↑
Volunteer 13	↓	↓

B) Direct Cytotoxicity	EGF pre-treatment	EGF pre-treatment atezolizumab
Volunteer 11	NS↓	-
Volunteer 12	↓	↑
Volunteer 13	↓	↓

C) T-ADCC	EGF pre-treatment	EGF pre-treatment atezolizumab
Volunteer 11	-	
Volunteer 12	↑	↑
Volunteer 13	-	↓

5.5.4 Immune-mediated cytotoxicity against EGF-treated SKBR3-Par cells

In Section 5.3.2.3.1 PD-L1 expression was increased with EGF treatment in the SKBR3-Par cell line, which was again associated with activation of the EGFR signalling pathway.

When the HER2+/PD-L1 medium SKBR3-Par cell line was pre-treated with EGF there was a general increase in overall cytotoxicity levels, this was related to increases in direct cytotoxicity and T-ADCC (**Table 5.8**). Atezolizumab did not block this effect in any of the volunteer samples (**Table 5.8**).

Overall cytotoxicity was increased in the EGF pre-treated cells by 3.8 % (p=0.003) without atezolizumab and 4.2 % (p=0.10) in the presence of atezolizumab for volunteer 11 due to cumulative increases in both direct cytotoxicity and T-ADCC (**Table 5.8**). PBMCs from volunteer 12 showed an increase in overall cytotoxicity in the EGF pre-treated cells by 15.1 % (p=0.001) without atezolizumab and 14.03 % (p=0.018) in the presence of atezolizumab. These changes were primarily related to increases in direct cytotoxicity (**Table 5.8**). EGF pre-treatment led to an increase in overall cytotoxicity by 12.33 % (p=0.023) without atezolizumab and 15.40% (p=0.0025) in the presence of atezolizumab for volunteer 13. These changes were due to significant increases in both direct cytotoxicity and T-ADCC (**Table 5.8**).

In summary, there was an increase in susceptibility to immune cell-mediated cytotoxicity in the PD-L1-low SKBR3-Par cell line with EGF pre-treatment, which may be of relevance when examining immune-relevant treatments in EGF driven cancers. This effect was not blocked by atezolizumab indicating that this effect was not due to alteration to PD-L1 expression caused by EGF pre-treatment. Further work using a PD-1 expressing “exhausted” immune cell effector population may be necessary to examine the effect of upregulated PD-L1 expression in this cell line model.

Table 5.8: PBMC-mediated cytotoxicity at a 5:1 EC: TC ratio against the SKBR3-Par cell line for all three volunteer samples. A) Overall cytotoxicity **B)** Direct Cytotoxicity **C)** T-ADCC. Arrows denote statistically significant change in cytotoxicity levels caused by EGF pre-treatment with and without atezolizumab present in the assay. The Student's t test was used to determine statistical significance. * $p < 0.05$, ** $p < 0.01$ and *** $p < 0.001$. All antibodies were used at a concentration of 10 µg/µL.

A) Overall Cytotoxicity	EGF pre-treatment	EGF pre-treatment atezolizumab
Volunteer 11	↑	-
Volunteer 12	↑	↑
Volunteer 13	↑	↑

B) Direct Cytotoxicity	EGF pre-treatment	EGF pre-treatment atezolizumab
Volunteer 11	-	-
Volunteer 12	NS ↑	↑
Volunteer 13	↑	↑

C) T-ADCC	EGF pre-treatment	EGF pre-treatment atezolizumab
Volunteer 11		-
Volunteer 12	-	-
Volunteer 13	↑	↑

5.5.5 Immune-mediated cytotoxicity against EGF-treated SKBR3-Afa cells

In Section 5.3.2.4.1 PD-L1 expression was upregulated with EGF treatment in the SKBR3-Afa cell line but not to the same extent as the parental cell line, also there was no increase in EGFR activity with EGF treatment in this cell line (**Section 5.3.2.4.2**).

There was a decrease in overall cytotoxicity levels of 8.92 % (p=0.003) in the absence of atezolizumab and 12.69 % (p=0.003) in the presence of atezolizumab elicited by PBMCs from volunteer 11 against EGF pre-treated cells. These changes were attributable to changes in direct cytotoxicity and T-ADCC (**Table 5.9**). Overall cytotoxicity levels elicited by PBMCs isolated from volunteer 13 were decreased when cells were pre-treated with EGF by 10.63 % (p=0.001) in the absence of atezolizumab and by 9.43 % (p=0.001) when atezolizumab was present. This was related to decreases in direct cytotoxicity and T-ADCC (**Table 5.9**). PBMCs from volunteer 12 elicited less direct cytotoxicity against the SKBR3-Afa cells when they were pre-treated with EGF in the presence of atezolizumab (4.7 % p=0.031) (**Table 5.9**).

There was a general decrease in cytotoxicity levels against the SKBR3-Afa cell line when pre-treated with EGF, which again may be relevant to immune-relevant treatments given in EGF-driven tumours. The difference between parental and resistant cell lines in EGF-mediated changes to susceptibility to immune cell-mediated cytotoxicity also merits further investigation in this setting. Atezolizumab was not capable of blocking these effects, which indicates that these effects are unlikely to be mediated by the effect of EGF on PD-L1 expression. It may be more appropriate to examine the effects of altered PD-L1 levels in the cell line using a PD-1 expressing “exhausted” immune cell population as the effector cells.

Table 5.9: PBMC-mediated cytotoxicity at a 5:1 EC: TC ratio against the SKBR3-Afa cell line for all three volunteer samples. A) Overall cytotoxicity **B)** Direct Cytotoxicity **C)** T-ADCC. Arrows denote statistically significant change in cytotoxicity levels caused by EGF pre-treatment with and without atezolizumab present in the assay. The Student's t test was used to determine statistical significance. * $p < 0.05$, ** $p < 0.01$ and *** $p < 0.001$. All antibodies were used at a concentration of 10 µg/µL.

A) Overall Cytotoxicity	EGF pre-treatment	EGF pre-treatment atezolizumab
Volunteer 11	↓	↓
Volunteer 12	-	-
Volunteer 13	↓	↓

B) Direct Cytotoxicity	EGF pre-treatment	EGF pre-treatment atezolizumab
Volunteer 11	↓	↓
Volunteer 12		↓
Volunteer 13	↓	-

C) T-ADCC	EGF pre-treatment	EGF pre-treatment atezolizumab
Volunteer 11	-	↑
Volunteer 12	-	-
Volunteer 13	↓	↓

5.6 Summary

PD-L1 and EGFR expression was characterised in a range of cell line models, with all PD-L1 high cell lines expressing EGFR (**Section 5.2.2.1-5.2.2.5**). There were alterations in PD-L1 expression in most of the targeted therapy resistant cell lines and any change in PD-L1 expression in these cell lines was mirrored by a concomitant change in EGFR expression (**Section 5.2.3.2**). Supporting evidence of a link between PD-L1 and EGFR in breast cancer.

In order to examine PD-L1/EGFR further, a selection of parental (HCC1954, SKBR3) and resistant cell lines (HCC1954-Lap, SKBR3-Afa) were treated with EGF, which increased PD-L1 expression in all cell lines examined (**Section 5.3.2**). Lapatinib blocked this effect, and pEGFR levels corresponded with PD-L1 response to EGF treatment (**Section 5.3.2**). Alterations to AKT and ERK activity did not always concur with PD-L1 expression. This would suggest that there are other key mediators in the link between PD-L1 and EGFR (**Section 5.3.2**). There were differences in EGFR, AKT and ERK signalling in response to EGF treatment between parental and resistant cell lines, these changes may be associated with the development of resistance to HER family targeted TKIs.

PTPN11 and LCK were identified as potential mediators in the link between PD-L1 and EGFR but did not interfere with EGFR-mediated PD-L1 expression when inhibited (**Section 5.4.3**).

Targeted therapy resistant cell lines (HCC1954-Lap and SKBR3-Afa) showed a decrease in susceptibility to PBMC-mediated cytotoxicity with EGF pre-treatment. EGF pre-treatment showed no effect on PBMC-mediated cytotoxicity against the HCC1954-Par cell line and showed an increase in susceptibility to PBMC-mediated cytotoxicity in the SKBR3-Par cell line. These changes in PBMC-mediated cytotoxicity upon EGF pre-treatment between cell lines may be associated with the development of resistance to a HER family targeted agent (**Section 5.4**).

The effects of EGF pre-treatment on PBMC-mediated cytotoxicity against the HCC1954-Par, SKBR3-Par and SKBR3-Afa cell lines were not altered by blocking PD-L1 with atezolizumab and therefore are unlikely to be due to the alteration of PD-L1 expression by EGF pre-treatment (**Section 5.4.2, 5.4.4 and 5.4.5**). In the HCC1954-Lap cell line there was a decrease in direct cytotoxicity with EGF pre-treatment, this was blocked in one instance with atezolizumab treatment (**Section 5.4.3**). Further work would be needed to examine, whether this effect was due to alterations in PD-L1 expression.

Taken together these results support evidence of a link between PD-L1 and EGFR in breast cancer and indicate blocking EGFR in an EGF driven tumour would reduce PD-L1 expression. Results also suggest that the development of targeted therapy resistance should be seen as a factor when considering targeting the immune response in HER2+ breast cancer.

5.7 Discussion

5.7.1 High PD-L1 cell lines are EGFR+ across all cancer cell line models

HER2+ breast cancer and TNBC are classed as immunogenic cancers [216,238]. Wang *et al.* [340] demonstrated 25.8 % of all breast cancers were PD-L1+ using data from 9 studies and 8583 patients. EGFR was shown to be expressed in almost 20 % of 2567 breast cancer tumours [275].

Multiple studies have shown an increased rate of PD-L1 expression in basal-like tumours [341,342]. It has also been shown that basal-like tumours are more likely to express EGFR [276,343]. PD-L1 expression has been shown in basal-like HER2+ cell lines using IHC and FACS analysis [236,344]. Within this analysis, the basal-like HER2+ breast cancer cell lines HCC1954 and JIMT1 were classified as PD-L1 high, these cell lines also expressed EGFR (**Section 5.2.2.1**).

Approximately 70 % of TNBC has been classified as basal-like [246]. TNBC cell lines have also been shown to have a relatively high level of PD-L1 and EGFR expression by IHC, western blotting and at an mRNA level compared with other cancer cell lines [216,345]. Results from this thesis show a higher level of PD-L1 expression compared with the other cancer cell line models examined, 6/13 cell lines were PD-L1 high, with EGFR and PD-L1 co-expression seen in all cell lines (**Section 5.2.2.2**).

This may suggest a that subset of patients with basal-like HER2+ or TNBC tumours are more likely to highly express PD-L1 while also co-expressing EGFR.

Melanoma and lung cancer are the cancer types in which immune checkpoint inhibition has been most thoroughly investigated clinically to date (**Table 1.1, 1.2 and 1.3 Section 1.2**). The success of immune checkpoint inhibition in these cancers is thought to be due in part to their high tumour mutational burden and neo-antigen load [14,109]. In clinical trials, melanomas have been reported to have >5 % tumour cells that are PD-L1+ in 23.6-80 % of tumours [69,82,85]. In this study (1/7) melanoma cell line was classified as PD-L1 high (LOX IMVI) and this cell line also expressed EGFR. All other melanoma cell lines examined expressed PD-L1 but were not PD-L1 high and two of these cell lines co-expressed EGFR (**Section 5.2.2.3**).

Lung cancers have also shown high levels of tumour and immune cell PD-L1 expression in clinical samples. Yu *et al.* [346] reports PD-L1 expression of greater than 5 % on tumour cells in 24-60 % of NSCLC tumours across 17 different studies. PD-L1 expression has been shown in lung cancer cell line models and the link between EGFR and PD-L1 has been best investigated in this setting [97,98,280]. In this study, only 1 from 7 lung cancer cell line was subjectively classified as PD-L1 high (NCI-H460). This cell line was also EGFR+. The remaining cell lines expressed medium levels of PD-L1 and three of these cell lines expressed EGFR (**Section 5.2.2.4**).

PD-L1-high cell lines were not as plentiful in lung and melanoma panels as expected when compared to PD-L1 expression in patient tumour samples. All PD-L1 high cell lines did however co-express EGFR which was consistent within the breast cancer models. It is also important to note however that cell lines can come from founder tumours that were initially a heterogeneous group but become more homogenous through the initial culturing process and that the PD-L1 high/medium classification used in this thesis is subjective. PD-L1 medium cell lines could be the equivalent of the PD-L1+ tumour cells by IHC for instance but this comparison was not examined in this thesis.

PD-L1 expression in multiple cancer types is consistent with the use of PD-1/PD-L1 axis targeted ICIs across a range of cancer types. All cell lines classified as PD-L1-high also expressed EGFR, this supports the link between EGFR and PD-L1 expression which has been put forward in pre-clinical lung cancer models.

5.7.2 PD-L1 and EGFR expression is altered in tandem in targeted therapy resistant cell lines

As previously stated, alterations to EGFR can be used as an escape mechanism for HER2-targeted therapy resistance [347,348]. Dr Martina Mc Dermott, NICB, developed the SKBR3-Lap cell line and she showed an increased level of pEGFR signalling in this model [347]. Ritter *et al.* [348] also demonstrated EGFR upregulation in the BT474 cell line which were resistant to trastuzumab-mediated destruction in xenograft mouse models.

PD-L1 expression accompanied by a mirrored alteration in EGFR expression was observed in HER2 targeted therapy resistant HER2+ breast cancer cell line models. (**Section 5.2.3.2**). This paired alteration in EGFR and PD-L1 expression reinforces the link between the two proteins and has not been reported in the literature previously. These results implicate PD-L1 in acquired resistance to HER2-targeted agents. Alterations to both EGFR and PD-L1 in tandem may make a case for dual inhibition in resistant models/cancers. Also, as upregulation of PD-L1 protects cells from immune mediated destruction [14], increased PD-L1 expression may be a mechanism employed by stressed cells to protect against immune destruction that is then maintained in those cells that go on to become resistant.

5.7.3 EGFR activation upregulated PD-L1 expression in HER2+ breast cancer cell lines

PD-L1 expression can be constitutive or induced. The most well documented method of inducing PD-L1 expression is IFN-γ treatment [99] but other pathways may be relevant in inducing PD-L1 expression. Increased PD-L1 expression has been shown to be due to a decrease in the cells capability of breaking down stabilised PD-L1 through GSK3β [102]. There is no evidence of the effect of EGF on PD-L1 expression in HER2+ breast cancer or treatment-resistant breast cancer.

In this analysis, PD-L1 was upregulated upon EGF treatment which was associated with an increase in pEGFR activity (**Section 5.3.2**). This shows that EGF treatment has the same effect on PD-L1 in HER2+ breast cancer cell lines as in the two TNBC cell lines examined by Chia-Wei Li *et al.* [102] . As this effect relies upon activation of EGFR, it was expected that co-treatment with lapatinib and EGF would inhibit the impact on PD-L1 (**Section 5.3.2**).

MAPK and AKT have also been pre-clinically linked with PD-L1 expression in lung cancer and melanoma [349–351]. MAPK and AKT activity was not consistent PD-L1 expression in this study. This shows that in HER2+ breast cancer MAPK and AKT are not the key mediators for the link between PD-L1 and EGFR.

5.7.4 PTPN11 and LCK are not sole mediators of a link between PD-L1 and EGFR

There is no conclusive evidence regarding the mediators of PD-L1 and EGFR interactions in the literature, although a number of targets that may be involved in some capacity have been identified. Monypenny *et al.* [352] showed ALIX, a transport regulating protein, controlled PD-L1 and EGFR expression on the cell surface in breast cancer. Chia-Wei Li *et al.* [102] provided evidence of EGF mediated GSK3ß inhibition regulating PD-L1 expression on the cell surface in breast cancer. Tung *et al.* [353] demonstrated the link between PD-L1 and EGFR was associated with YAP-1 and HIF-1α in NSCLC. There is no consensus on the link between EGFR and PD-L1 in breast cancer and the definitive signalling network between these two proteins has not been fully characterised.

PTPN11 is a protein-tyrosine phosphatase that is important in the phosphorylation cascade of PD-1 in T cells, PTPN11 signalling inhibits TCR and MAPK signalling pathways which lead to T cell inactivation [123]. Liu *et al.* [354] have shown that PTPN11 knockdown increased PD-L1 expression through increased pSTAT1 in prostate cancer cell line models. In this model PTPN11 knockdown also lead to an increased level of HLA-ABC protein expression [354]. PTPN11 can also contribute to the activation of MAPK and AKT related pathways in cancer cells, Han *et al.* showed increased cell growth and invasion driven by PTPN11-mediated PI3K and MAPK signalling activation in hepatocellular carcinoma models [355]. PTPN11 is linked with control of immune checkpoint signalling through PD-L1 expression and EGFR signalling pathways through its phosphatase activity, putting it forward as a potential mediator of the link between EGFR and PD-L1.

LCK is a Src family kinase which phosphorylates CD3 and CD28 cytosolic domains leading to propagation of the TCR signalling pathways, LCK also phosphorylates ZAP70 which is vital in the TCR activation cascade. Activation of LCK is inhibited by PD-1 signalling in order to prevent T cell activation [53,54]. LCK expression is present in many different malignancies, Shi *et al.* [356] demonstrated it played a role in promoting cell proliferation and resistance to apoptosis but the role of LCK in cancer

cell signalling pathways remains largely unknown. Due to the role of LCK in immune checkpoint signalling in immune cells it may potentially play a role in controlling PD-L1 expression in cancer cells.

PTPN11 and LCK were examined as mediators of a link between EGFR and PD-L1 due to potential interacting signalling networks with EGFR and PD-L1 and co-expression with EGFR and PD-L1 in TCGA breast cancer patient samples (**Section 5.4**). LCK protein levels were undetectable in the HER2+ parental and targeted therapy resistant cell lines examined. LCK inhibition was still examined in the event that EGF treatment stimulated expression of the protein. pPTPN11 expression loosely correlated with the trend of PD-L1 and EGFR expression seen in the parental and resistant HER2+ breast cancer cell lines examined (**Section 5.4.3**). This indicated that this protein may be related to PD-L1 and/or EGFR signalling. The HCC1954-Par cell line was selected to examine the effects of PTPN11 and LCK inhibition due to high PD-L1 expression which could show demonstrable increase or decrease to PD-L1 levels. When pPTPN11 and LCK were inhibited in the presence of EGF treatment in the parental HER2+ PD-L1 high HCC1954 cell line they did not alter PD-L1 or EGFR expression (**Section 5.4.3**). Both proteins may still play a role in the EGFR:PD-L1 link but they do not appear to be its key mediators. PTPN11 proteins may regulate PD-L1 expression, Liu *et al.* [354] showed that PTPN11 knockdown led to increased PD-L1 protein expression which was mediated through increased STAT1 activity in prostate cancer cell line models. If this is also a relevant mechanism in breast cancer models the case inhibition of PTPN11 may not be additive to EGF-mediated PD-L1 expression, which would not allow for an increase to be seen. Further investigation is required to fully characterise the regulatory mechanisms and interactions common to EGFR and PD-L1 to provide information to inform novel ways of targeting this system in the clinic.

5.7.5 EGF pre-treatment alters the susceptibility of cancer cell lines to PBMC-mediated cytotoxicity

EGF treatment caused an increase in PD-L1 expression in HCC1954-Par, HCC1954-Lap, SKBR3-Par and SKBR3-Afa cell lines. The link between EGFR and PD-L1 in an EGF rich environment may hinder the immune response against the tumour due to an increase in PD-L1 mediated immunosuppression. Immune cytotoxicity assays with EGF pre-treated cell lines were used to examine whether EGF mediated PD-L1 upregulation would alter PBMC-mediated cytotoxicity against the cell lines.

As well as its effect on PD-L1 expression EGF has been shown to alter the immune response against the tumour. Im *et al.*[357] showed upregulated MHC class-I and MHC class-II expression when lung cancer cell lines were treated with the EGFR inhibitor erlotinib. Dominguez *et al.*[333] demonstrated an increased level of NK cell-mediated lysis of lung cancer cells with erlotinib treatment due to inhibition of epithelial to mesenchymal transition (EMT).

In this analysis the effects of EGF pre-treatment of the tumour cell lines on PBMC-mediated cytotoxicity were inconsistent against the PD-L1 high HCC1954-Par cell line (**Section 5.4.2**). EGF pre-

treatment of the HCC1954-Lap cell line caused a decrease in the cell lines susceptibility to direct PBMC-mediated cytotoxicity (**Section 5.4.3**). PD-L1 expression is lower in the lapatinib-resistant HCC1954 cell line than the parental which allowed more scope for the effects of increased PD-L1 expression to be observed. Further investigation is warranted to examine whether the changes in direct cytotoxicity in this cell line are mediated by EGF-mediated PD-L1 upregulation.

The SKBR3-Par cell line showed an increase in susceptibility to overall cytotoxicity when pre-treated with EGF (**Section 5.4.4**). The SKBR3-Afa cell line showed a decrease in susceptibility to overall cytotoxicity when pre-treated with EGF (**Section 5.4.5**). Atezolizumab did not block these effects in either cell line, therefore these effects are unlikely to be mediated through PD-L1 and are more likely a consequence of other EGF-mediated effects on the immune response, such as those demonstrated by Im *et al.* [357] and Dominguez *et al.* [333].

EGF pre-treatment caused alterations to PBMC-mediated cytotoxicity. These effects were not always mediated through the effects of EGF on PD-L1 expression. The development of resistance to afatinib altered response to EGF which produced a different result to the parental cell line with regards susceptibility to PBMC-mediated cell kill. pEGFR levels do not increase upon EGF treatment in the SKBR3-Afa model as they do in the parental, showing that EGFR activation is independent of extracellular EGF ligand levels in this model (**Section 5.3.2**). Alterations in EGF-stimulated signalling pathways in tumour cells may be important in the recognition and destruction of cancer cells by the immune response. Further investigation is required to determine the mechanisms involved in the effect.

6. The effect of adenosine receptor activation on immune cell-mediated cytotoxicity against breast cancer cell line models

6.1 Introduction

Immunosuppression can also be mediated by the tumour microenvironment. Adenosine is a purine nucleoside formed in the breakdown of adenosine mono-phosphate (AMP). It has been termed a metabolic immune checkpoint due to its role in immunosuppression of immune cells in the tumour microenvironment [202,358,359].

In hypoxic and inflammatory conditions, high concentrations of adenosine are formed via CD39-mediated conversion of ATP to ADP [184]. Followed by CD73-mediated conversion of ADP to adenosine [186]. Adenosine kinase, which is responsible for adenosine breakdown, is also decreased in hypoxic conditions [191]. This leads to the accumulation of high concentrations of adenosine in the tumour microenvironment. Adenosine can form a negative feedback immunosuppressive system through the adenosine receptor family, the A2A receptor (A2AR) in particular [202,358,359]. A2AR is expressed on normal tissues, tumours and immune cells. Ligation of A2AR by adenosine leads to increased cAMP through adenylate cyclase activity. This increase in cAMP leads to the transcription of immunosuppressive proteins such as PD-1, CTLA4, TGF-ß and IL-10 [191]. A2AR activation can also inhibit T cell stimulation through dampening CD28 and IL-2 [192–194]. This adenosine-mediated immunosuppressive system may hinder the immune response against the tumour. Therefore, by inhibiting the receptor for adenosine it may be possible to increase the immune response against the tumour.

Previous work within the lab group examined the effect of trastuzumab in eliciting ADCC against HER2-low, luminal breast cancer cell lines. To further examine the immune response in this setting, ER+ HER2-low breast cancer cell lines (MCF7 and CAMA-1) were treated with adenosine to determine its effect on PBMC-mediated direct cytotoxicity and T-ADCC. Adenosine can elicit different effects through the four adenosine receptors (A1, A2A, A2B and A3) [184]. The immunosuppressive effects of adenosine appear to be mediated primarily through A2AR. These cell lines were also pre-treated with lapatinib. Lapatinib treatment has been shown to stabilise HER2 expression on the cell membrane, this is of particular importance in HER2-low cell lines as it provides the antigen for trastuzumab to bind to in order to elicit ADCC [360]. Therefore, lapatinib pre-treatment could produce further alterations to T-ADCC in the presence of adenosine in these cell lines.

As the work in other chapters has been focused on HER2+ breast cancer, the effect of A2AR on immunosuppression was also examined in this setting. CGS21680, a synthetic A2AR agonist, and preladenant, an A2AR inhibitor, were used in combination with trastuzumab in HER2+ breast cancer cell lines. The effects of these agents on direct cytotoxicity and T-ADCC elicited by NK cells were examined. NK cells were used in this model as they are known to be the main mediators of T-ADCC

[29]. Potential indicators of response to adenosine inhibition were also examined in relevant cell line models with the aim of understanding adenosine relevant signalling mechanisms.

6.2 Healthy volunteer samples used in this analysis

Table 6.1 details the healthy volunteer samples used in this analysis. Samples taken from healthy volunteers 14-19 were taken under ethical approval obtained by Dr. Denis Collins (**DCUREC/2009/063 Appendix 1**). The remaining samples were taken under the ethical approval procedure outlined in Section 2.7 with age range given for these volunteers. The assay used is also briefly detailed in Table 6.1.

Table 6.1 Healthy volunteer samples taken for this analysis

Healthy Volunteer	Sex	Age range	Assay
Volunteer 14	Female	-	PBMC-mediated cytotoxicity- CAMA-1
Volunteer 15	Female	-	Cytotoxicity lower than 3%
Volunteer 16	Female	-	Cytotoxicity lower than 3%
Volunteer 17	Female	-	PBMC-mediated cytotoxicity- ER+ cell line
Volunteer 18	Female	-	PBMC-mediated cytotoxicity- ER+ cell line
Volunteer 19	Female	-	PBMC-mediated cytotoxicity- MCF7
Volunteer 20	Female	25-34	NK cell-mediated cytotoxicity- HER2+ cell line
Volunteer 21	Female	25-34	NK cell-mediated cytotoxicity- HER2+ cell line
Volunteer 22	Female	25-34	NK cell-mediated cytotoxicity- HER2+ cell line
Volunteer 23	Female	25-34	NK cell-mediated cytotoxicity- HER2+ cell line

6.3 The effect of adenosine on PBMC-mediated cytotoxicity elicited against ER+/HER2-low breast cancer cell lines

CAMA-1 and MCF7 are ER+ HER2-low breast cancer cell lines [282]. These cell lines along with the K562 cell line were used to examine the effect of adenosine on direct PBMC-mediated cytotoxicity and T-ADCC. As the assays with ER+ HER2-low cell lines were performed in duplicate wells, the data presented for direct cytotoxicity, T-ADCC and overall cytotoxicity values are presented as an average of three experiments using three individual volunteer samples to allow for the determination of statistical significance.

6.3.1 HER2 and A2AR protein expression

Cell lines were treated with 100 μM adenosine for 12 hours (assay duration) with and without trastuzumab to assess if adenosine would change HER2 expression in the course of the assay and alter T-ADCC in this manner. Western blotting was used to determine whether adenosine affected HER2 expression as this may affect T-ADCC levels. In the presence of trastuzumab, HER2 levels were significantly decreased in the CAMA-1 cell line ($p=0.016$). Adenosine alone did not alter HER2 expression and did not affect the decrease in HER2 expression seen with trastuzumab treatment ($p=0.012$) (**Figure 6.1**). In the MCF7 cell line, neither trastuzumab or adenosine treatment altered HER2 expression (**Figure 6.1**). A2AR expression was also detectable in both cell lines with no significant difference in expression between the two cell lines (**Figure 6.1**).

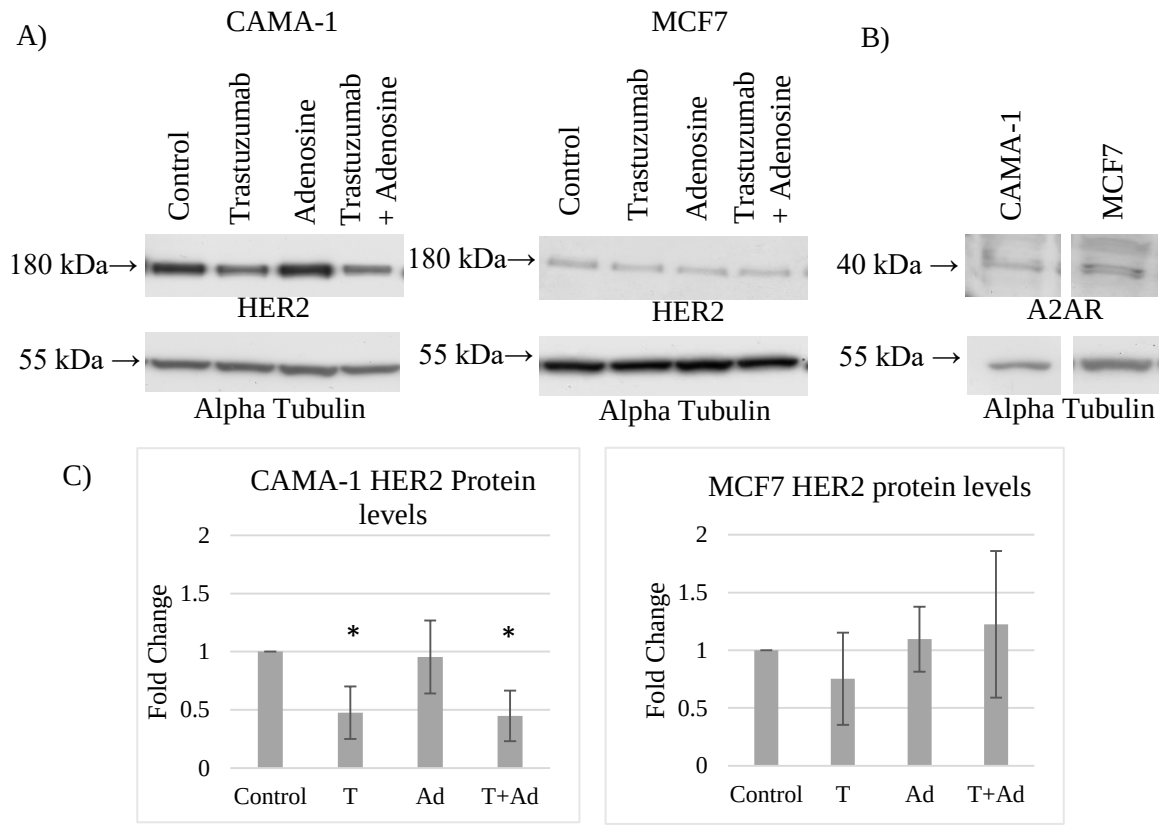

Figure 6.1: A) Western blotting for HER2 protein levels in CAMA-1 and MCF7 cell lines. Blots shown are representative of triplicate blots. Alpha tubulin was used as a loading control. B) Western blotting for A2AR protein expression levels in CAMA-1 and MCF7 cell lines. C) Densitometry analysis of immunoblots of CAMA-1 and MCF7 for HER2 protein levels. Error bars represent standard deviation of biological triplicate experiments.

6.3.2 Immune-mediated cytotoxicity against the K562 cell line +/- adenosine

When assessed, volunteer samples 15 and 16 had a cytotoxicity level of less than 3 % against the K562 cell line, and therefore were not suitable for use in this analysis. This very low cytotoxicity level did not provide a high enough level of cytotoxicity to measure changes, particularly decreases, in immune-mediated cytotoxicity consistently (**Table 6.1**). There was a range of cytotoxicity levels elicited by the remaining PBMC samples from volunteers 14, 17, 18 and 19 (**Table 6.2**). The amount of cytotoxicity increased with the ratio of EC:TC (**Table 6.2**). When adenosine was present there was no consistent effect on cytotoxicity levels against the K562 cell line by the healthy volunteer PBMCs. There was an increase in cytotoxicity levels with healthy volunteer 17 by 7.69 % and volunteer 19 by 7.48 % but only at the 10:1 ratio (**Table 6.3**).

Table 2: Levels of direct cytotoxicity elicited against the K562 cell line for volunteers 14, 17, 18 and 19 seeded at a ratio of 1:1, 5:1 and 10:1 EC:TC.

% Direct Cytotoxicity	1:1	5:1	10:1
Volunteer 14	2.57 +/- 0.62 %	12.51 +/- 1.32 %	28.98 +/- 1.44 %
Volunteer 17	9.74 +/- 8.74 %	10.97 +/- 0.22 %	13.27 +/- 0.00 %
Volunteer 18	1.25 +/- 0.14 %	3.75 +/- 1.61 %	6.55 +/- 1.34 %
Volunteer 19	7.82 +/- 0.39 %	39.46 +/- 1.46 %	51.2 +/- 5.5 %

Table 3: Percentage change in direct cytotoxicity mediated against K562 cells by PBMCs with the addition of adenosine (100 µM) for volunteers 14, 17, 18 and 19 seeded at a ratio of 1:1, 5:1 and 10:1 EC:TC.

Direct Cytotoxicity	1:1	5:1	10:1
Volunteer 14	+1.56 %	+0.83 %	-0.80 %
Volunteer 17	-4.91 %	-0.08 %	+ 7.69 %
Volunteer 18	-0.31 %	0.16 %	-0.17 %
Volunteer 19	-1.84 %	+0.45 %	+ 7.48 %

6.3.3 Immune-mediated cytotoxicity against the CAMA-1 cell line +/- adenosine

In the CAMA-1 cell line there was a 12.70 ± 5.47 % increase in overall cytotoxicity with the addition of adenosine at the 10:1 ratio (p=0.056) (**Figure 6.2**). This effect did not occur at the lower ratios. This increase in overall cytotoxicity was primarily due to an increase in direct cytotoxicity (11.08 ± 3.50 %) in the presence of adenosine at 10:1 (p=0.032) (**Figure 6.2**). There was no significant change in T-ADCC levels elicited against the CAMA-1 cell line in the presence of adenosine (**Figure 6.2**).

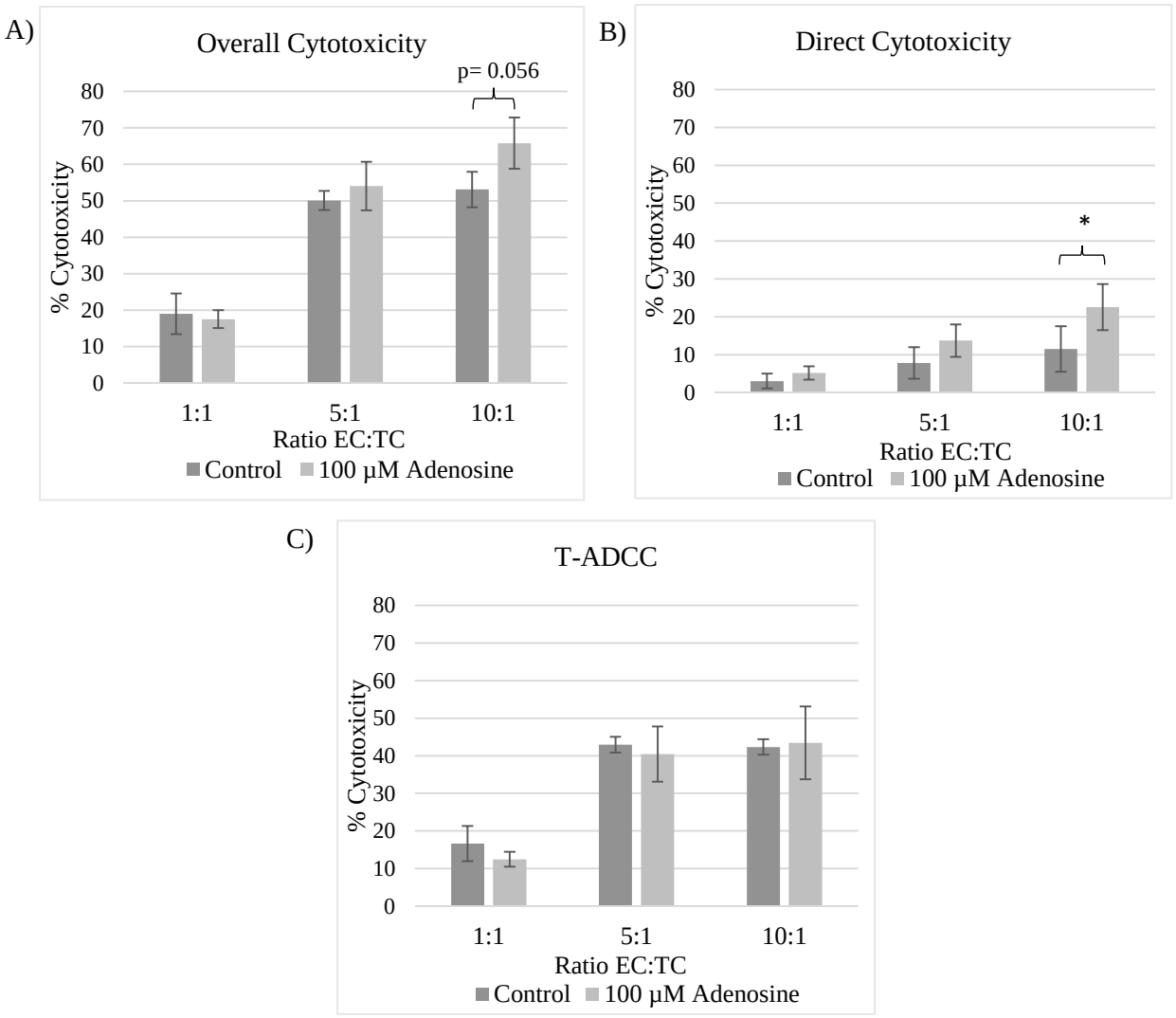

Figure 6.2: PBMC-mediated cytotoxicity against the CAMA-1 cell line using samples from three healthy volunteers A) Overall cytotoxicity. **B)** Direct cytotoxicity **C)** T-ADCC. Effector cells were seeded at a ratio of 1:1, 5:1 and 10:1 to target cells. Error bars represent biological triplicate experiments from healthy volunteers 14, 17 and 18. A paired Student's t test was used to determine statistical significance. * $p < 0.05$, ** $p < 0.01$ and *** $p < 0.001$.

6.3.4 Immune-mediated cytotoxicity against the CAMA-1 cell line +/- adenosine +/- lapatinib

There was an increase in overall cytotoxicity levels with the addition of adenosine when CAMA-1 cells were pre-treated with DMSO or lapatinib for 48 hours. This was a significant increase in cytotoxicity levels for DMSO pre-treated cells at a ratio of 5:1 EC:TC (6.48 ± 2.36 %, p=0.041) and a for lapatinib pre-treated cells at a ratio of 10:1 EC:TC (16.72 ± 0.93 %, p=0.001) (**Figure 6.3**). This was again due to the effect of adenosine on direct cytotoxicity levels, as T-ADCC levels remained unchanged in both instances (**Figure 6.3**). Adenosine increased direct cytotoxicity in DMSO pre-treated cells (5:1, p=0.07) and lapatinib pre-treated cells (1:1, p=0.013 and 5:1, p=0.036) There was also a non-significant increase in direct cytotoxicity in lapatinib pre-treated cells in the presence of adenosine at a ratio of 10:1 (**Figure 6.3**). Adenosine elicits a similar effect on overall cytotoxicity and direct cytotoxicity in control CAMA-1 cells and lapatinib pre-treated cells. This indicates the effect of adenosine on PBMC-mediated cytotoxicity was primarily through direct cytotoxicity.

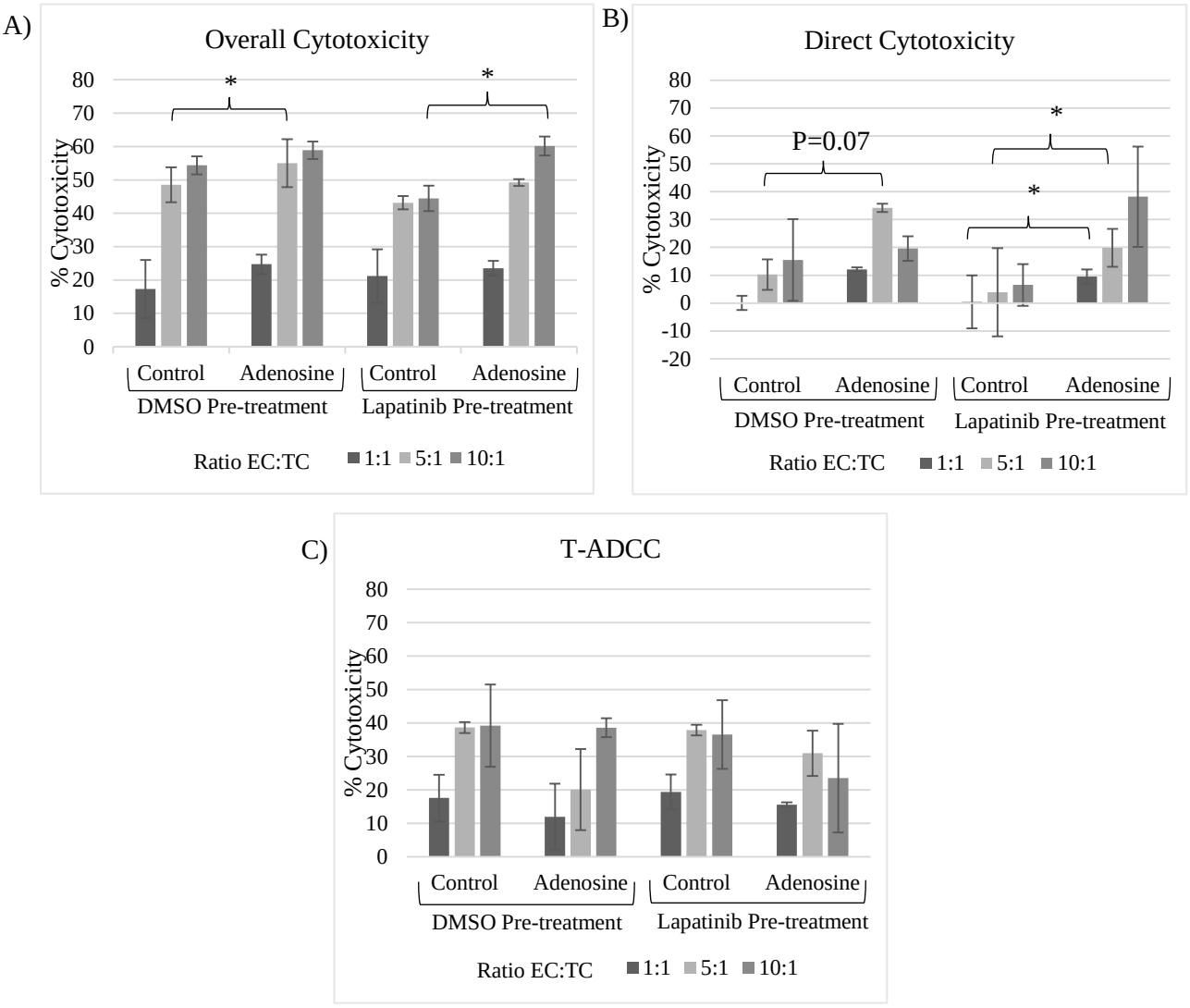

Figure 6.3: PBMC-mediated cytotoxicity against lapatinib pre-treated CAMA-1 cells using samples from three healthy volunteers A) Overall cytotoxicity. **B)** Direct cytotoxicity **C)** T-ADCC. Effector cells were seeded at a ratio of 1:1, 5:1 and 10:1 to target cells. Error bars represent biological triplicate experiments from healthy volunteers 14, 17 and 18. A paired Student's t test was used to determine statistical significance. * $p < 0.05$, ** $p < 0.01$ and *** $p < 0.001$.

Adenosine treatment increased the susceptibility of CAMA-1 cells to direct cytotoxicity elicited by healthy volunteer PBMCs. This led to an increase in overall immune-mediated cytotoxicity levels in the presence of trastuzumab. This occurred with or without lapatinib treatment and occurred across a range of effector to target cell ratios (**Section 6.3.3 and 6.3.4**).

6.3.5 Immune-mediated cytotoxicity against the MCF-7 cell line +/- adenosine

There was no significant alteration to overall cytotoxicity elicited by healthy volunteer PBMCs against MCF7 cells in the presence of adenosine. Nor were there alterations to direct cytotoxicity or T-ADCC levels in the presence of adenosine (**Figure 6.4**).

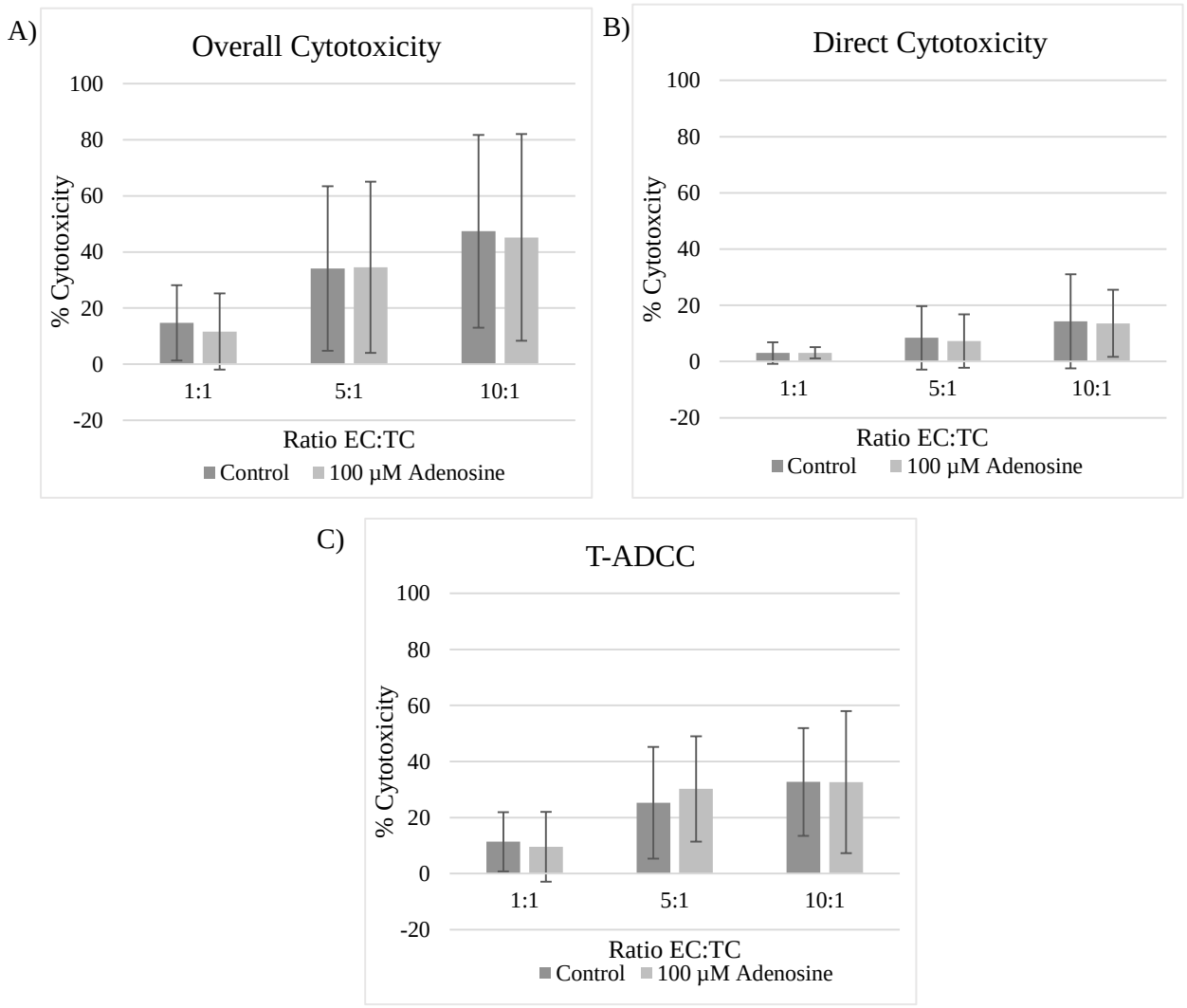

Figure 6.4: PBMC-mediated cytotoxicity against MCF7 cells using samples from three healthy volunteers A) Overall cytotoxicity. **B)** Direct cytotoxicity **C)** T-ADCC. Effector cells were seeded at a ratio of 1:1, 5:1 and 10:1 to target cells. Error bars represent biological triplicate experiments from healthy volunteers 17, 18 and 19. A paired Student's t test was used to determine statistical significance. * $p < 0.05$, ** $p < 0.01$ and *** $p < 0.001$.

6.3.6 Immune-mediated cytotoxicity against the MCF-7 cell line +/- adenosine +/- lapatinib

There were no consistent changes to overall cytotoxicity, direct cytotoxicity or T-ADCC in the MCF7 cell line with the addition of adenosine to DMSO and lapatinib pre-treated cells (**Figure 6.5**). There was an 11.39 ± 3.29 % increase in direct cytotoxicity at a ratio of 10:1 in the DMSO treated cells (p=0.027) (**Figure 6.5**). This effect was not seen in the media-treated control or in the lapatinib-treated cells or at the other ratio for DMSO pre-treatment (**Figure 6.5**).

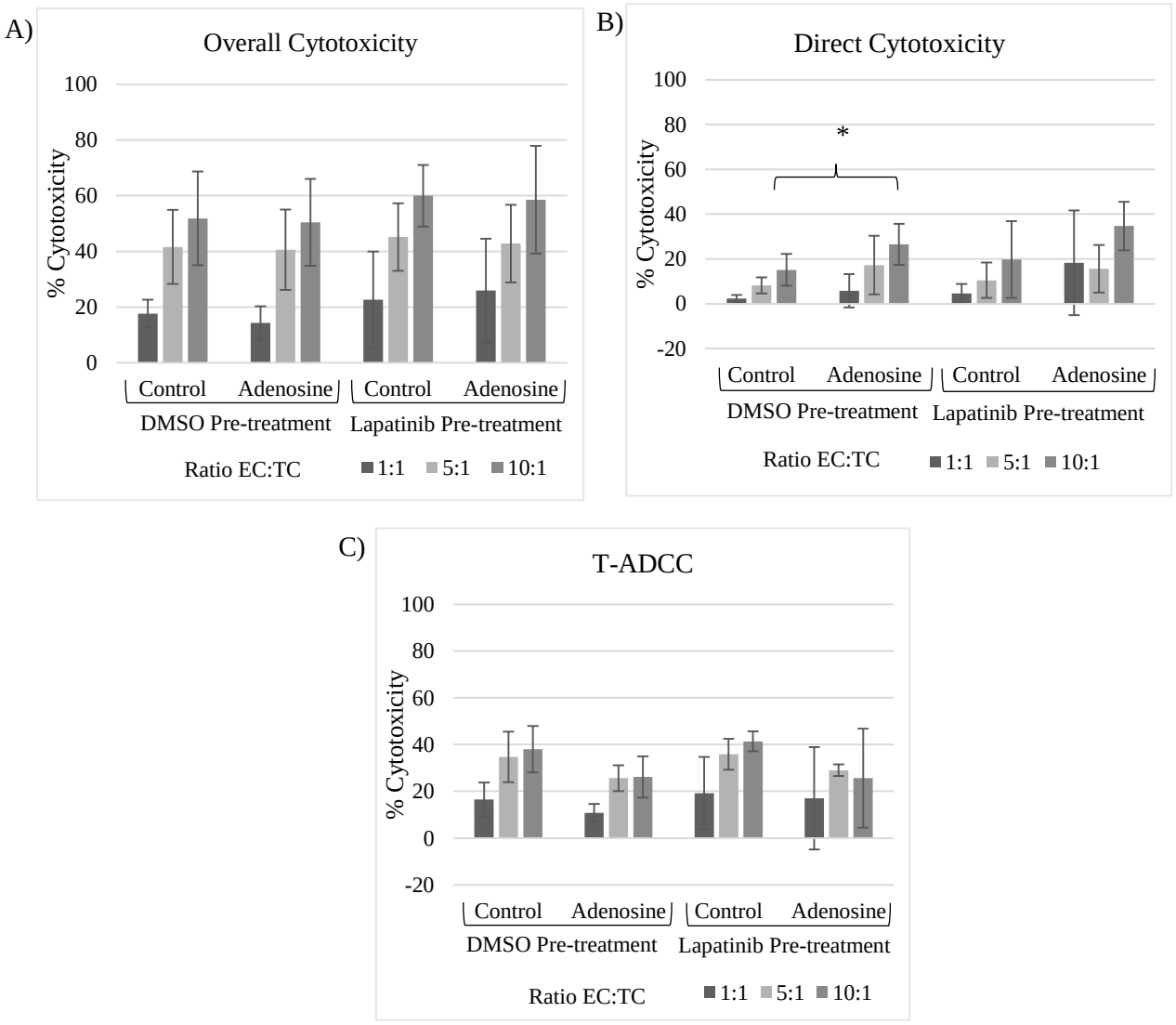

Figure 6.5: PBMC-mediated cytotoxicity against lapatinib pre-treated MCF7 cells using samples from three healthy volunteers A) Overall cytotoxicity. **B)** Direct cytotoxicity **C)** T-ADCC. Effector cells were seeded at a ratio of 1:1, 5:1 and 10:1 to target cells. Error bars represent biological triplicate experiments from healthy volunteers 17, 18 and 19. A paired Student's t test was used to determine statistical significance. * $p < 0.05$, ** $p < 0.01$ and *** $p < 0.001$.

6.3.7 Summary

Adenosine treatment did not alter CAMA-1 or MCF7 HER2 expression, nor did it interfere with the effect of trastuzumab on HER2 expression in either cell line (**Section 6.3.1**). Both cell lines showed similar expression of adenosine receptor A2AR (**Section 6.3.1**). Adenosine did not alter cytotoxicity levels against the K562 cell line, or the MCF7 cell line (**Section 6.3.2, 6.3.5 and 6.3.6**). There was no effect seen on T-ADCC in either CAMA-1 or MCF7 cell lines with the addition of adenosine treatment (**Section 6.3.3-6.3.6**). However, adenosine treatment was capable of increasing direct cytotoxicity against the CAMA-1 cell line, leading to an increase in overall cytotoxicity levels (**Section 6.3.3 and 6.3.4**). Lapatinib pre-treatment did not have any effect on PBMC-mediated cytotoxicity elicited against either cell line in the presence of adenosine (**Section 6.3.4 and 6.3.6**). There is no evidence in the literature regarding the effects of adenosine on immune cell-mediated cytotoxicity against HER2 low/ER+ breast cancer cells. The effect of adenosine on immune cell-mediated cytotoxicity against the CAMA-1 cell line is a novel finding which merits further investigation.

6.4 The effect of A2AR activation and inhibition on PBMC-mediated cytotoxicity and T-ADCC against HER2+ breast cancer cell lines

Using an A2AR antagonist to boost the ADCC response to an antibody therapy like trastuzumab has most clinical relevance in HER2+ breast cancer. Section 6.3 utilised adenosine in assays but adenosine can interact with all four adenosine receptors [188]. In order to examine A2AR-mediated effects specifically, an A2AR agonist (CGS21680) and an A2AR antagonist (preladenant) were employed in this study. The compounds were included in the assay so both effector cells and target cells were exposed. Blood samples were taken from healthy volunteers 20, 21, 22 and 23 to measure cytotoxicity against the HER2+ cell lines SKBR3 and HCC1954. HCC1954-Lap and SKBR3-Afa were also included in this analysis as models of targeted therapy resistance and there were differences in PD-L1 expression levels between these cell lines and the parental cell lines (**Section 5.2**). In order to determine the specific effect of A2AR-mediated immunosuppression on T-ADCC against parental and targeted therapy resistant HER2+ breast cancer cell lines, NK cells were used as the effector cells to enrich for the PBMC subset most responsible for mediating ADCC [29].

6.4.1 Immune-mediated cytotoxicity against K562 cells +/- A2AR modulation

The cytotoxicity elicited against the K562 cell line by volunteers 20-23 ranged from 11.4 -39.2 % (**Table 6.4**). There were no consistent significant alterations to cytotoxicity levels against the K562 cell line in the presence of CGS21680 and/or preladenant treatment (**Table 6.4**). Volunteer sample 23 did show a small but statistically significant increase in cytotoxicity against K562 with the addition of CGS21680 (3.92 %, p=0.009) and preladenant (2.87 %, p=0.026) alone. This effect was not seen in any of the other samples (**Table 6.4**).

Table 6.4: Levels of direct cytotoxicity elicited against the K562 cell line at a 10:1 EC:TC ratio for volunteers 20, 21, 22 and 23. Significant changes in direct cytotoxicity mediated against K562 cells by PBMCs with the addition of CGS21680 and/or preladenant. ↑ denotes a significant increase in cytotoxicity, ↓ denotes a significant decrease in cytotoxicity in the presence of A2AR modulator.

Direct Cytotoxicity	% Direct Cytotoxicity at 10:1	CGS21680	Preladenant	CGS21680 + Preladenant
Volunteer 20	39.2 +/- 3.7%	-	-	-
Volunteer 21	29.9 +/- 9%	-	-	-
Volunteer 22	16.7 +/- 6%	-	-	-
Volunteer 23	11.4 +/- 1.3%	↑	↑	-

6.4.2 Immune-mediated cytotoxicity against HCC1954-Par cells +/- A2AR modulation

Overall cytotoxicity levels elicited by NK cells from volunteers 20, 22 and 23 against HCC1954-Par cells in the presence of trastuzumab were not affected by CGS21680 or preladenant alone. However, there was a 3.89 % increase in overall cytotoxicity in the presence of CGS21680, preladenant and trastuzumab combined (p=0.022) (**Figure 6.6**). This increase was primarily due to an increase of 8.05 % in T-ADCC in the presence of the triple combination (p=0.074). There was no effect of either CGS21680 or preladenant alone on T-ADCC levels (**Figure 6.6**). Neither CGS21680 nor preladenant alone, or in combination, had an effect on direct cytotoxicity against HCC1954 cells (**Figure 6.6**).

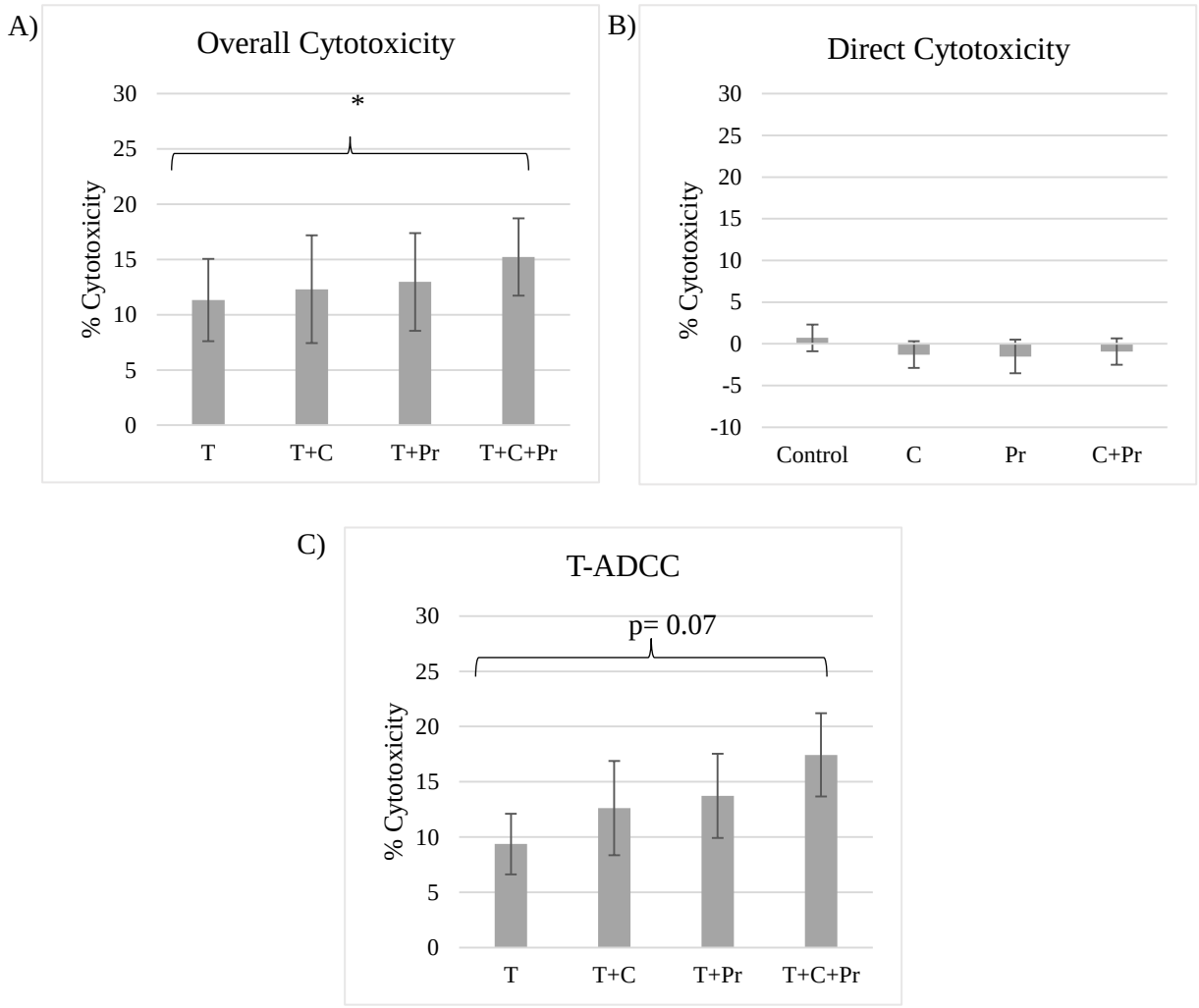

Figure 6.6: NK cell-mediated cytotoxicity against HCC1954-Par cells from three healthy volunteers in the presence of CGS21680 (C) (1 µM) and/or preladenant (Pr) (100 nM) A) Overall cytotoxicity. **B)** Direct cytotoxicity **C)** T-ADCC. Effector cells were seeded at a ratio of 1:1 to target cells. Error bars represent biological triplicate experiments from healthy volunteers 20, 22 and 23. A paired Student's t test was used to determine statistical significance. * $p < 0.05$, ** $p < 0.01$ and *** $p < 0.001$.

6.4.3 Immune-mediated cytotoxicity against HCC1954-Lap cells +/- A2AR modulation

There was no change in overall cytotoxicity elicited against the HCC1954-Lap cells by the NK cells isolated from volunteers 20, 22 and 23 with the addition of CGS21680, preladenant or a combination of both agents (**Figure 6.7**). There were also no alterations to direct cytotoxicity or T-ADCC with either agent alone or both in combination (**Figure 6.7**).

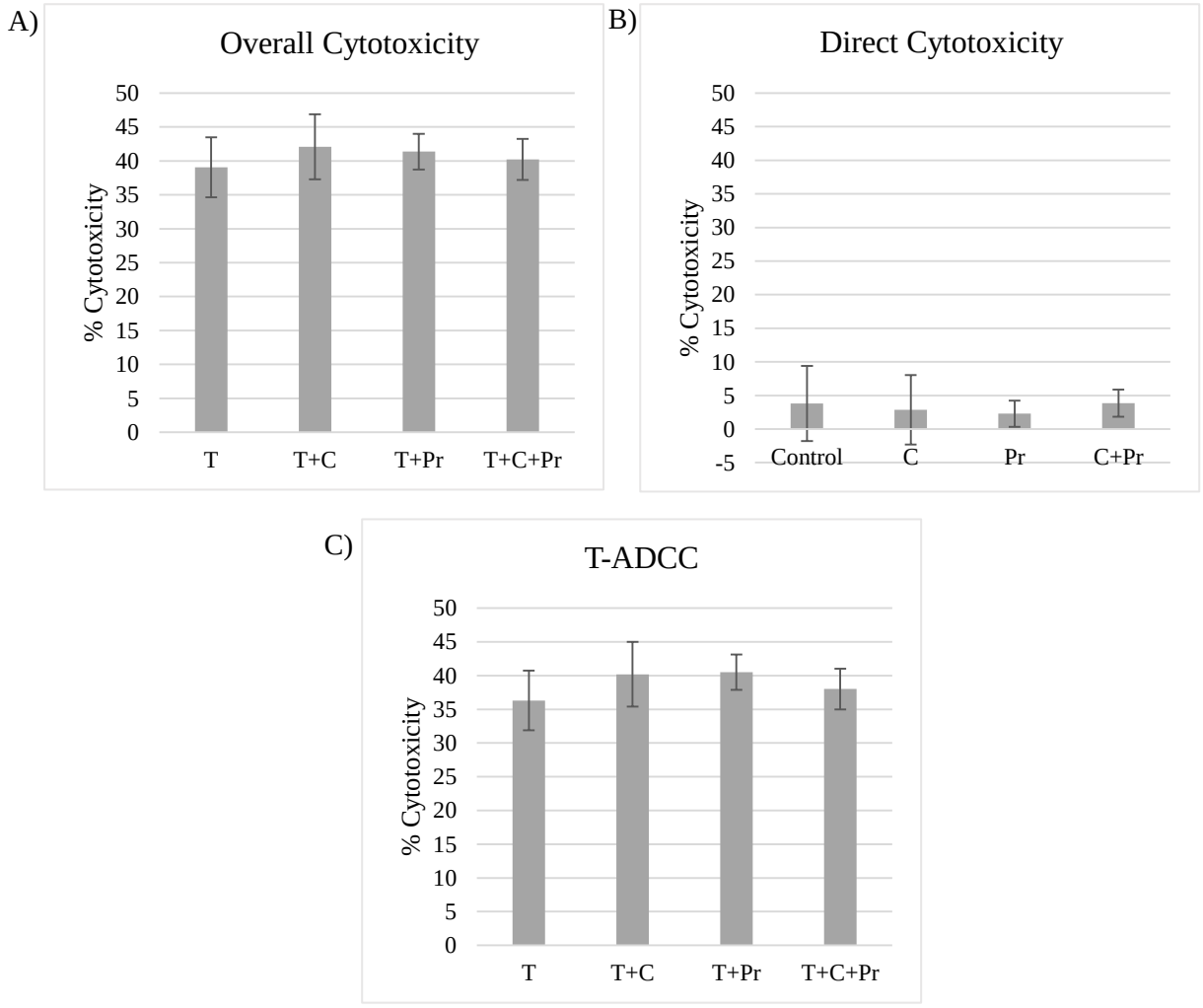

Figure 6.7: NK cell-mediated cytotoxicity against HCC1954-Lap cells from three healthy volunteers in the presence of CGS21680 (C) (1 µM) and/or preladenant (Pr) (100 nM) A) Overall cytotoxicity. **B)** Direct cytotoxicity **C)** T-ADCC. Effector cells were seeded at a ratio of 1:1 to target cells. Error bars represent biological triplicate experiments from healthy volunteers 20, 22 and 23. A paired Student's t test was used to determine statistical significance. * $p < 0.05$, ** $p < 0.01$ and *** $p < 0.001$.

6.4.4 NK cell-mediated cytotoxicity against SKBR3-Par cells +/- A2AR modulation

Overall cytotoxicity levels elicited by NK cells from healthy volunteer 20, 22 and 23 against SKBR3-Par cells in the presence of trastuzumab were not affected by CGS21680 or preladenant alone. However, there was a 3.78 % increase in overall cytotoxicity in the presence of CGS21680, preladenant and trastuzumab (p=0.034) (**Figure 6.8**). A small increase of 4.63 % in T-ADCC in the presence of the triple combination seemed to be the main contributor to the significant increase in overall cytotoxicity. CGS21680 or preladenant alone had no effect on T-ADCC (**Figure 6.8**). Neither CGS21680, preladenant alone nor the combination of both had any effect on direct cytotoxicity against the SKBR3-Par cell line (**Figure 6.8**).

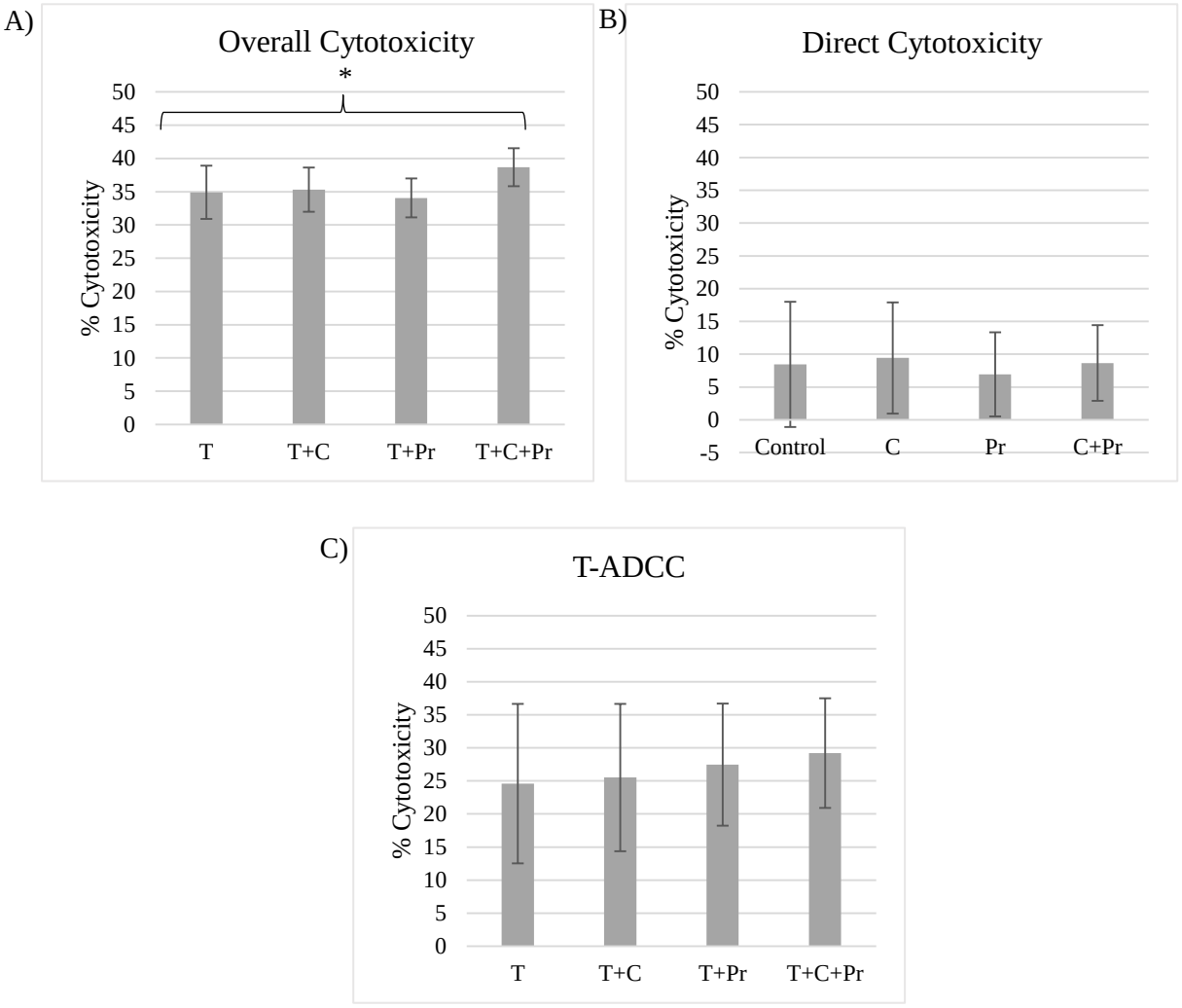

Figure 6.8: NK cell-mediated cytotoxicity against SKBR3-Par cells from three healthy volunteers in the presence of CGS21680 (C) (1 µM) and/or preladenant (Pr) (100 nM) A) Overall cytotoxicity. **B)** Direct cytotoxicity **C)** T-ADCC. Effector cells were seeded at a ratio of 1:1 to target cells. Error bars represent biological triplicate experiments from healthy volunteers 20, 22 and 23. A paired Student's t test was used to determine statistical significance. * $p < 0.05$, ** $p < 0.01$ and *** $p < 0.001$.

6.4.5 NK cell-mediated cytotoxicity against SKBR3-Afa cells +/- A2AR modulation

There was no change in overall cytotoxicity elicited against the SKBR3-Afa cells by the NK cells isolated from volunteers 20, 21 and 23 with the addition of CGS21680, preladenant or a combination of both agents (**Figure 6.9**). There were also no alterations to direct cytotoxicity or T-ADCC with either agent alone or in combination (**Figure 6.9**).

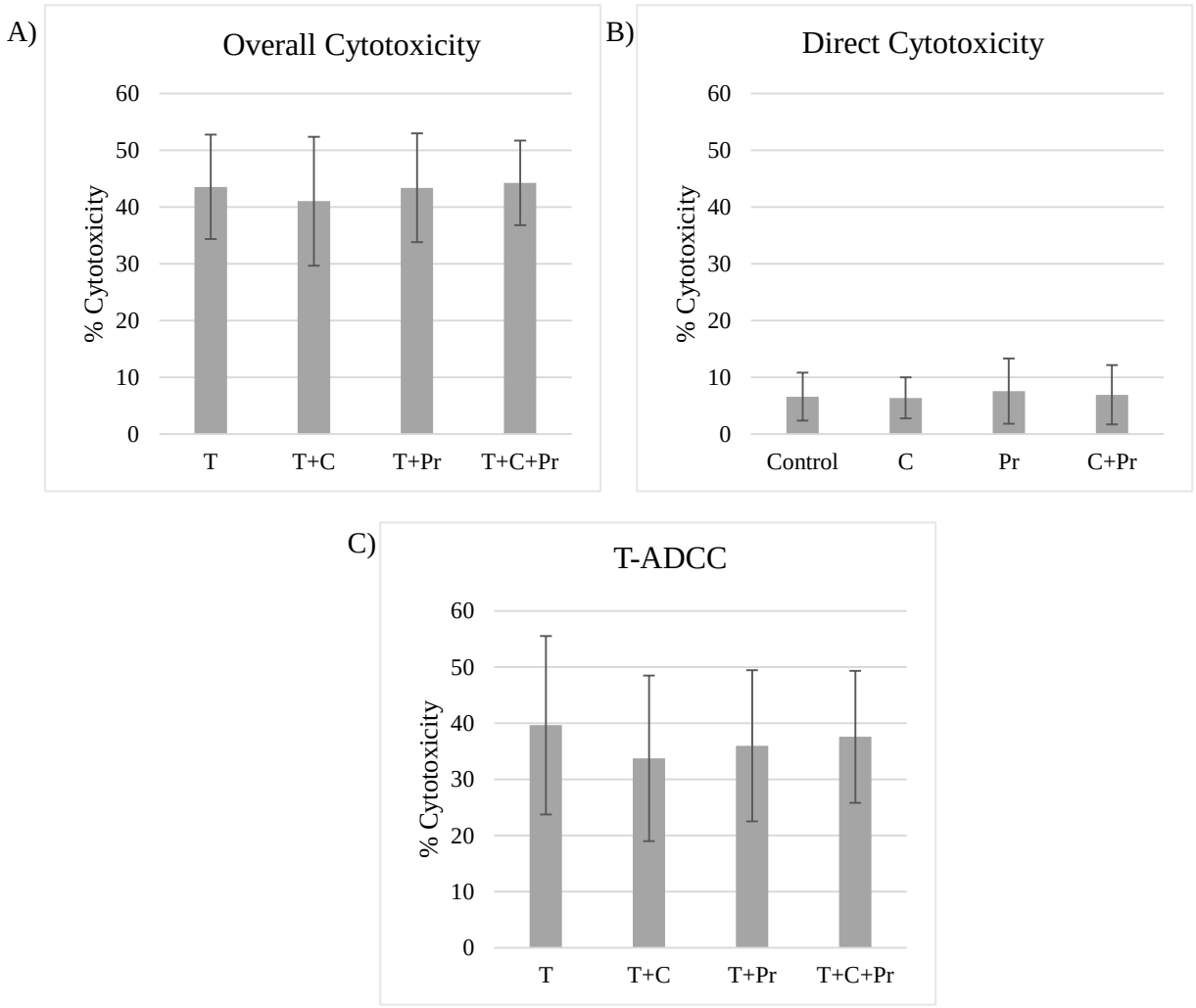

Figure 6.9: NK cell-mediated cytotoxicity against SKBR3-Afa cells from three healthy volunteers in the presence of CGS21680 (C) (1 µM) and/or preladenant (Pr) (100 nM) A) Overall cytotoxicity. **B)** Direct cytotoxicity **C)** T-ADCC. Effector cells were seeded at a ratio of 1:1 to target cells. Error bars represent biological triplicate experiments from healthy volunteers 20, 21 and 23. A paired Student's t test was used to determine statistical significance. * $p < 0.05$, ** $p < 0.01$ and *** $p < 0.001$.

6.4.6 Summary

In our assay model, single agent modulation of A2AR alone, or in the presence of trastuzumab had no effect on NK cell-mediated cytotoxicity. However, the combination of A2AR agonist (CGS21680) and antagonist (preladenant) in the presence of trastuzumab resulted in an increase in overall cytotoxicity in both parental cell lines examined. This was principally due to increases in T-ADCC in the presence of CGS21680 and preladenant (**Section 6.4.2 and 6.4.4**). This effect was not seen in the targeted therapy resistant cell lines HCC1954-Lap or SKBR3-Afa (**Section 6.4.3 and 6.4.5**).

6.5 A comparison of immune cell-mediated cytotoxicity levels between parental and targeted therapy-resistant cell lines

The impact of A2AR modulation on NK cell-mediated cytotoxicity is described in Section 6.4. Overall cytotoxicity, direct cytotoxicity and T-ADCC elicited by NK cells was compared within the resistance models used in Section 6.4. PBMC-mediated cytotoxicity was also investigated in these cell lines in Section 5.4. To this point, the impact of EGF on PBMC-mediated cytotoxicity and A2AR receptor modulators on NK cell-mediated cytotoxicity has been examined in HCC1954, HCC1954-Lap, SKBR3 and SKBR3-Afa.

Results have been reported for treatment-related differences that occurred within each cell line. No direct comparison of the absolute cytotoxicity levels between cell lines was made. This section compares the direct cytotoxicity and T-ADCC levels between the parental and the resistant cell line models, as elicited by PBMCs or NK cells, in order to assess the impact of a targeted therapy resistant phenotype on immune cell-mediated cytotoxicity.

6.5.1 The impact of targeted therapy resistance on PBMC-mediated cytotoxicity

Direct PBMC-mediated cytotoxicity was 8.12 % higher ($p=0.012$) in the SKBR3-Afa than the SKBR3-Par cell line. Direct PBMC-mediated cytotoxicity was 8.02 % higher ($p=0.017$) in the lapatinib-resistant HCC1954-Lap cells compared with the parental HCC1954 (**Figure 6.10**).

T-ADCC was 19.78 % higher ($p=0.038$) in the lapatinib-resistant HCC1954-Lap cells compared to the parental cell line. The increase in T-ADCC between SKBR3-Par and SKBR3-Afa was not significant (**Figure 6.10**).

These changes led to an increase in overall cytotoxicity of 12.98 % ($p=0.095$) in the HCC1954-Lap compared with parental. The increase seen between the SKBR3-Par/SKBR3-Afa cell lines did not reach significance (**Figure 6.10**).

Direct cytotoxicity was increased by 8.68 % in the SKBR3-Par cell line *versus* the HCC1954-Par cell line (p=0.044). Leading to overall cytotoxicity being significantly higher in the SKBR3-Par cell line compared to the HCC1954-Par cell line with an increase of 8.99 % (p=0.041) (**Figure 6.10**).

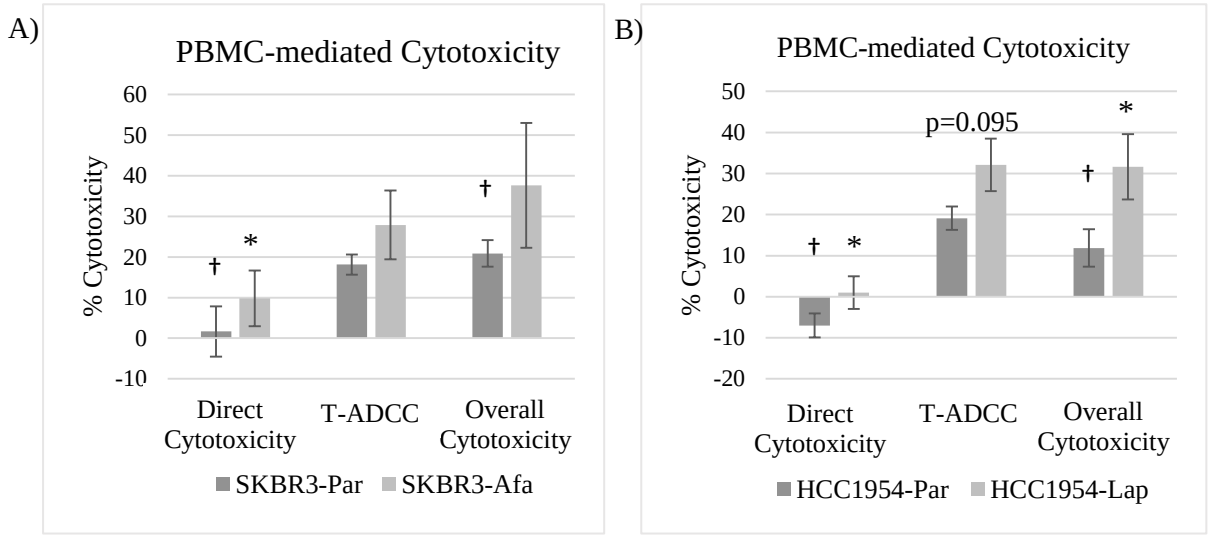

Figure 6.10: A) Direct PBMC-mediated cytotoxicity, T-ADCC and overall cytotoxicity levels for SKBR3-Par and SKBR3-Afa cell lines. **B)** Direct PBMC-mediated cytotoxicity, T-ADCC and overall cytotoxicity levels for HCC1954-Par and HCC1954-Lap cell lines. Effector cells were seeded at a ratio of 5:1 EC:TC. Error bars represent biological triplicate experiments from healthy volunteers 11, 12 and 13. The paired Student's t test was used to determine statistical significance. * $p < 0.05$, ** $p < 0.01$ and *** $p < 0.001$. † denotes statistical significance between SKBR3-Par and HCC1954-Par cell lines.

6.5.2 <u>The impact of targeted therapy resistance on NK cell-mediated cytotoxicity</u>

There was no change in direct NK cell-mediated cytotoxicity between SKBR3-Par and SKBR3-Afa or the HCC1954-Par or HCC1954-Lap cell lines (**Figure 6.11**).

T-ADCC was 18.46 % (p=0.87) higher in the afatinib-resistant SKBR3-Afa cells compared with parental SKBR3. T-ADCC was 26.93 % (p=0.022) higher in the lapatinib-resistant HCC1954-Lap cells compared with parental HCC1954 (**Figure 6.11**).

Overall NK cell-mediated cytotoxicity was higher in the SKBR3-Afa than the SKBR3-Par by 13.62 % (p=0.010). Overall cytotoxicity was 27.72 % higher (p=0.032) in the lapatinib-resistant HCC1954 cells compared with parental (**Figure 6.11**).

Overall cytotoxicity was 18.59 % higher in the SKBR3-Par cell line compared to the HCC1954-Par cell line (p=0.044). This was due to non-significant increases in direct cytotoxicity and T-ADCC (**Figure 6.11**).

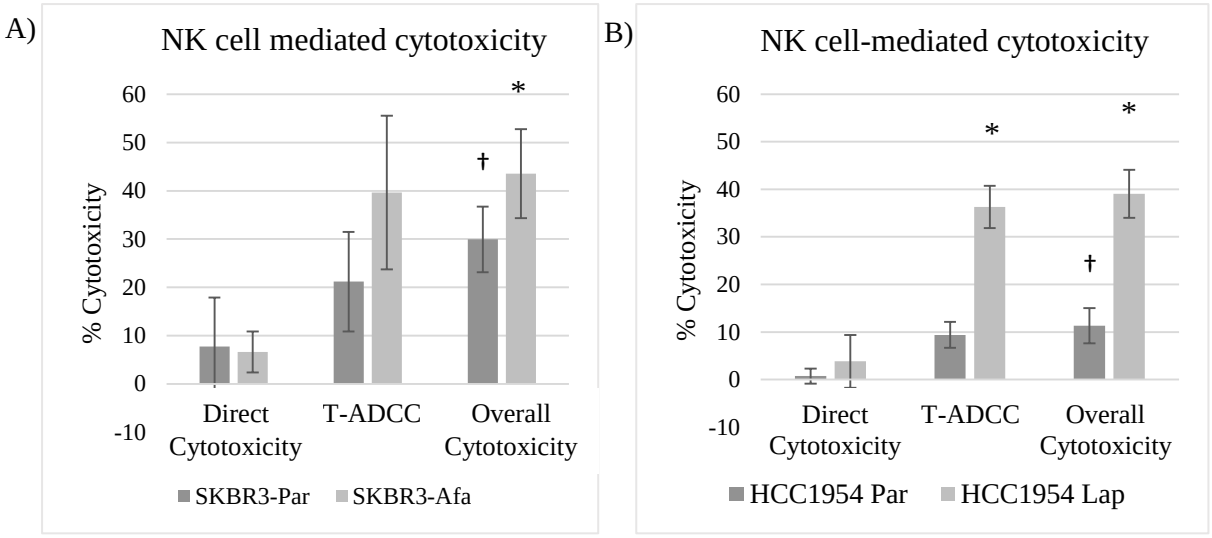

Figure 6.11: A) Levels of direct cytotoxicity, T-ADCC and all cytotoxicity elicited by NK cells against SKBR3-Par and SKBR3-Afa cell lines. B) Levels of direct cytotoxicity, T-ADCC and overall cytotoxicity elicited by NK cells against HCC1954-Par and HCC1954-Lap cell lines. Effector cells were seeded at a ratio 1:1 to target cells. Error bars represent biological triplicate experiments from healthy volunteers 20, 22 and 23. The Student's t test was used to determine statistical significance. * $p < 0.05$, ** $p < 0.01$ and *** $p < 0.001$. † denotes statistical significance between SKBR3-Par and HCC1954-Par cell lines.

6.5.3 Summary

Afatinib resistant and lapatinib resistant HER2+ breast cancer cell lines SKBR3-Afa and HCC1954-Lap were more susceptible to PBMC and NK cell mediated cytotoxicity than their respective parental cell lines (**Section 6.5.1 and 6.5.2**). This indicates the development of resistance to HER2 targeted TKIs affects the immunogenicity of the cell lines. This may affect immune-relevant treatments against resistant cells, such as the alterations seen with response to A2AR inhibition.

Also, the SKBR3-Par cell line showed a greater susceptibility to PBMC and NK cell mediated cytotoxicity than the HCC1954-Par cell line (**Section 6.5.1 and 6.5.2**), which indicates different immunogenicity patterns between these two cell lines.

6.6 HER family and immune-related protein expression in parental and resistant cell lines

Expression of HER family proteins and immune-response associated proteins were assessed in the SKBR3-Afa and HCC1954-Lap cell lines in order to investigate the resistance phenotype and potential mediators of the difference in susceptibility to the immune response (**Section 5, Section 6**).

6.6.1 HER family expression

There was no significant difference in HER2 expression between any of the cell lines examined which could be associated with changes in T-ADCC (**Figure 6.12**). There were significant alterations in EGFR between cell lines as previously described in Section 5.2. SKBR3-Afa showed an increase in total EGFR expression (p=0.006) compared to parental cell line expression. HCC1954-Lap show decreased total EGFR expression (p=0.009) compared to parental cell line (**Figure 6.12**). pEGFR levels at y1068 were decreased in the SKBR3-Afa cell line compared with the parental cell line (p=0.016) (**Figure 6.12**).

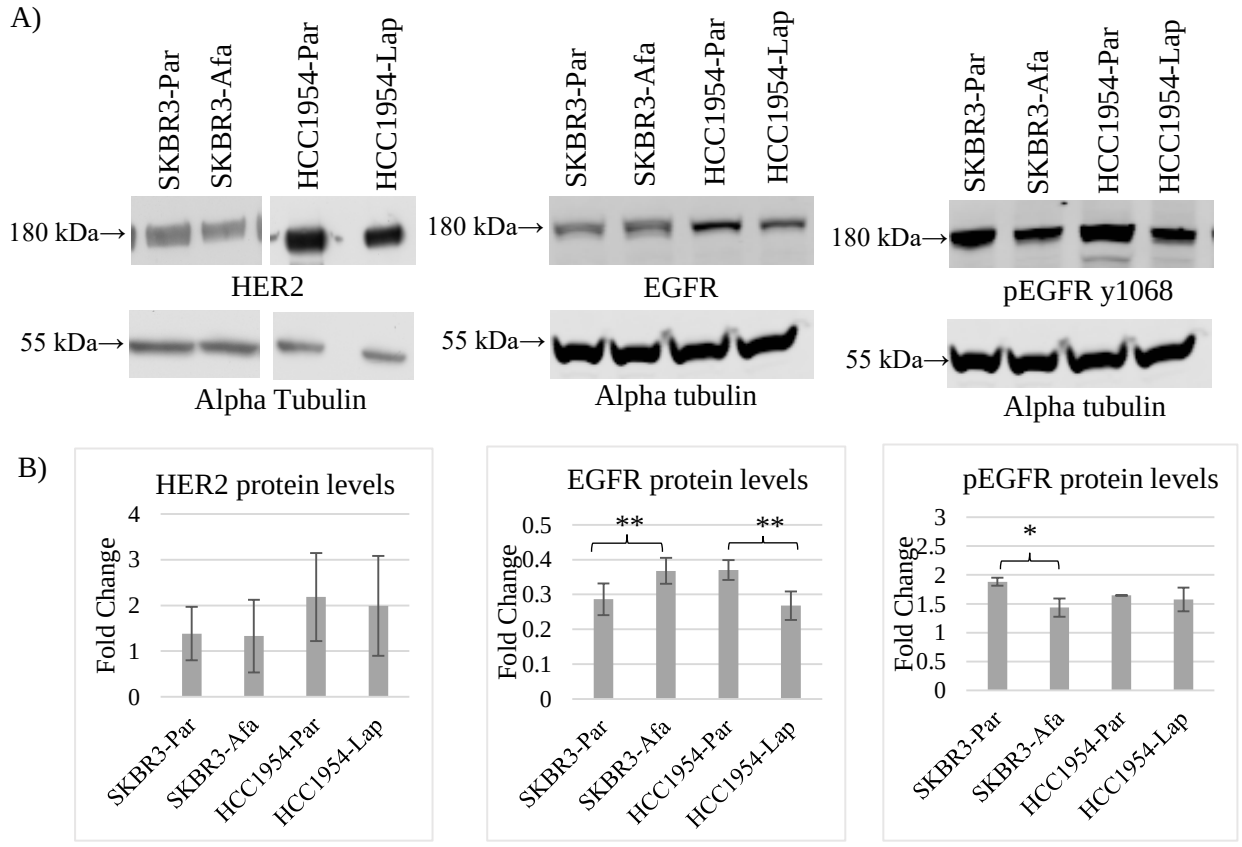

Figure 6.12: A) Western blotting for HER2, EGFR and pEGFR y1068 protein levels in SKBR3-Par, SKBR3-Afa, HCC1954-Par and HCC1954-Lap cell lines. Blots shown are representative of triplicate blots. Alpha tubulin was used as a loading control. **B)** Densitometry analysis of SKBR3-Par, SKBR3-Afa, HCC1954-Par and HCC1954-Lap cell lines for HER2, EGFR and pEGFR protein levels. Error bars represent standard deviation of biological triplicate experiments.

6.6.2 Immune checkpoint inhibitor expression

There was no significant change in A2AR expression between any of the cell lines examined (**Figure 6.13**). There was a significant alteration in PD-L1 expression between the cell lines as shown in Section 5. SKBR3-Afa displayed a small but significant increase in PD-L1 expression (p=0.036) compared to SKBR3-Par. PD-L1 expression was significantly decreased in the HCC1954-Lap cells compared to the parental cell line (p=0.006) (**Figure 6.13**). There was no significant difference in PD-1 expression between any of the cell lines examined (**Figure 6.13**).

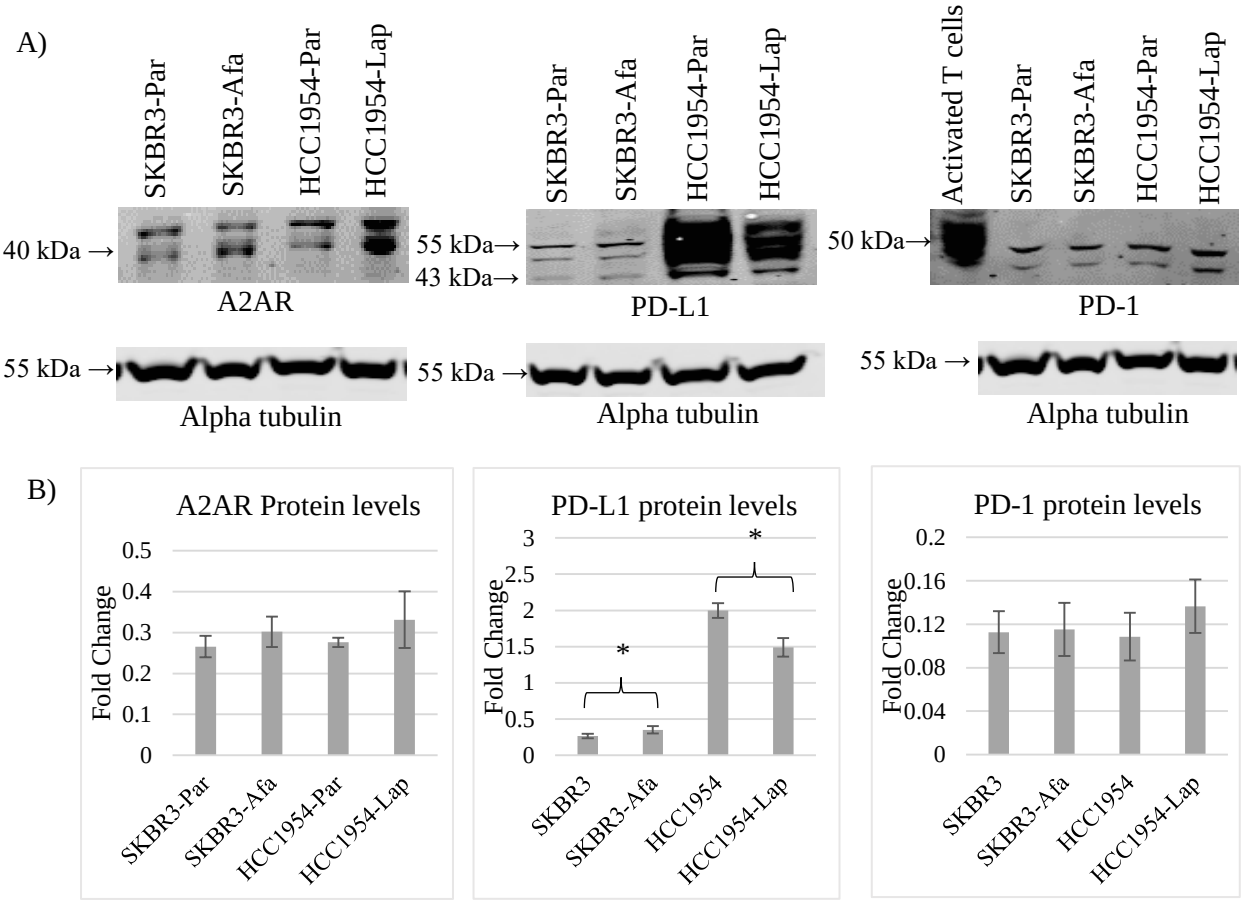

Figure 6.13: A) Western blotting for A2AR, PD-L1 and PD-1 protein levels in SKBR3-Par, SKBR3-Afa, HCC1954-Par and HCC1954-Lap cell lines. Blots shown are representative of triplicate blots. Alpha tubulin was used as a loading control. **B)** Densitometry analysis of A2AR, PD-L1 and PD-1 protein levels in SKBR3-Par, SKBR3-Afa, HCC1954-Par and HCC1954-Lap cell lines. Error bars represent standard deviation of biological triplicate experiments.

6.6.3 Immune response-related proteins

Protein expression of immune response-related proteins MICA, MHC class-I, HLA-E, NKTR and E-Cadherin was examined in the SKBR3-Par, SKBR3-Afa, HCC1954-Par and HCC1954-Lap cell lines **(Figure 6.14)**. While there were differences in the expression of immune-related proteins between SKBR3 and HCC1954 parental cell lines (**Section 4**), there was no significant alterations in the proteins examined between both parental and resistant cell lines **(Figure 6.14)**.

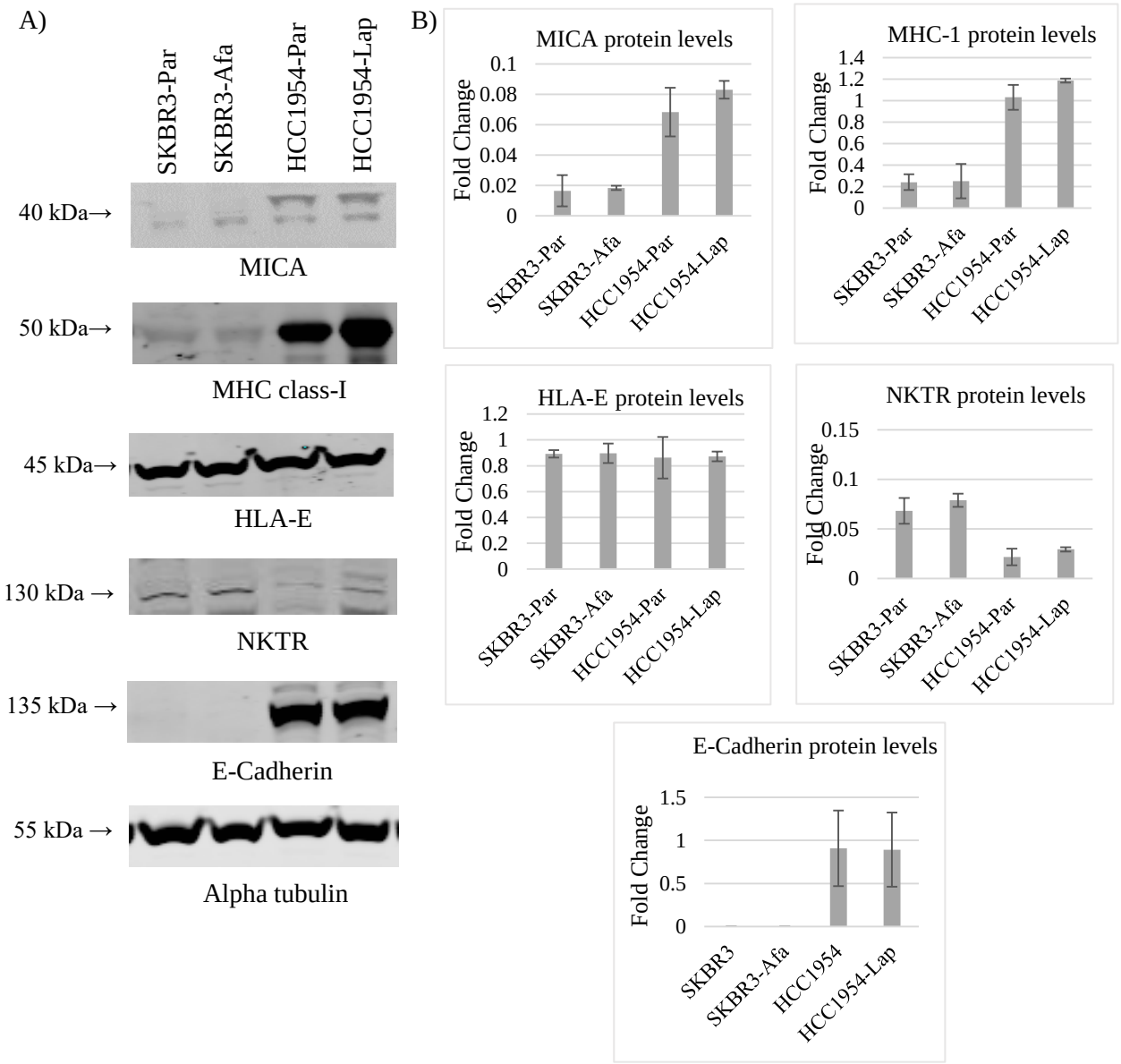

Figure 6.14:A) Western blotting for MICA, MHC-I, HLA-E, NKTR and E-Cadherin protein levels in SKBR3-Par, SKBR3-Afa, HCC1954-Par and HCC1954-Lap cell lines. Blots shown are representative of triplicate blots. Alpha tubulin was used as a loading control. **B)** Densitometry analysis of MICA, MHC-1, HLA-E, NKTR and E-Cadherin protein levels in SKBR3-Par, SKBR3-Afa, HCC1954-Par and HCC1954-Lap cell lines. Error bars represent standard deviation of biological triplicate experiments.

6.6.4 Summary

Alterations in EGFR and PD-L1 expression between parental and resistant cell lines as previously reported were confirmed (**Section 5.2**). There was no alteration in A2AR expression between any of the cell lines examined, which eliminates differences in A2AR expression contributing to the differences in response to A2AR inhibition observed between the cell lines (**Section 6.6.2**). None of the immune-related proteins examined, were associated with the increased susceptibility to immune-mediated killing of resistant cell line models (**Section 6.6.3**). There were alterations in immune-related protein expression between the HCC1954 and SKBR3 parental cell lines (**Section 6.6.3**). The expression profile of immune-related proteins in these cancer cell line models could contribute to the significantly reduced immune cell-mediated cytotoxicity against the HCC1954 compared to SKBR3 (**Section 6.5**). Reduced MHC class-I levels, as observed in SKBR3, are associated with higher immune cell-mediated cytotoxicity [331]. The immune response to tumour cells is dependent on the balance of expression of a myriad of proteins on the tumour cells and the immune cells, a broader proteomics-based approach may be required to identify the proteins involved (**Section 2**).

6.7 SKBR3-Lap cells as a model to examine adenosine-mediated immunosuppression

There was a difference detected between HCC1954-Par and -Lap cell lines and SKBR3-Par and -Afa cell lines in their response to inhibition of the A2AR pathway (**Section 6.4**). The mediators of this effect are not yet determined as there was no significant change in the immune-related proteins examined. However, the lapatinib resistant SKBR3 cells may be better model to study these effects.

Previous work done by the group show that SKBR3-Lap cells show a decreased level of T-ADCC versus the SKBR3-Par cell line [361]. T-ADCC was 45-50% lower in SKBR3-Lap compared to the SKBR3-Par cell line at the three effector:target cell ratios examined, 1:1 (p=0.01), 5:1 (p=0.001) and 10:1 (p=0.024) (**Figure 6.15**). There was no significant alteration in direct cytotoxicity between parental and resistant cell lines in the SKBR3-Par/SKBR3-Lap model (**Figure 6.15**).

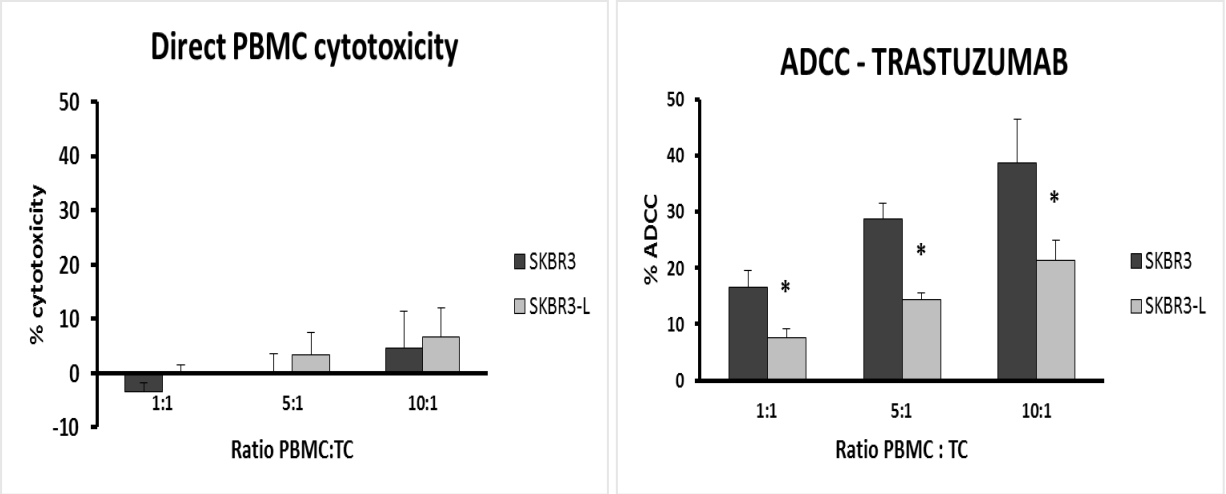

Figure 6.15: Direct PBMC-mediated cytotoxicity against SKBR3-Par and SKBR3-Lap cell lines. Trastuzumab-mediated ADCC levels in SKBR3-Par *vs.* SKBR3-Lap. EC:TC ratios of 1:1, 5:1 and 10:1. * denotes p value <0.05 using unpaired Student's T test. Graphs taken from unpublished data from Dr. Denis Collins

6.7.1 SKBR3-Par versus SKBR3-Lap comparison by DNA microarray

DNA microarray studies were carried out as part of Dr. Martina McDermott's thesis project in order to examine changes in mRNA associated with the development of lapatinib resistance in the SKBR3-Par and SKBR3-Lap cell line models. For this analysis this data was retrospectively analysed to examine SKBR3-Lap and SKBR3-Par at the mRNA level. EGFR was found to be 1.63-fold upregulated ($p=2 \times 10^{-5}$) in SKBR3-Lap compared to SKBR3-Par levels. A2AR showed a 4.34-fold upregulation of expression in the SKBR3-Lap cell line ($p=6.5 \times 10^{-14}$) in comparison to the parental cell line. HLA-E showed a 1.53-fold increase in the SKBR3-Lap cell line versus SKBR3-Par (p=0.004) (**Table 6.5**).

Expression of other immune-relevant proteins, MHC class-I and NKTR, were decreased in the lapatinib-resistant cell line (-1.55 p=0.003 and -1.53 p=0.004 respectively) (**Table 6.5**).

6.7.2 Validation of DNA microarray results by western blot

Western blotting was used to examine the expression of the targets identified in the mRNA microarray analysis. EGFR was again found to be upregulated in the SKBR3-Lap cell line (p=0.034), HER2 expression was not significantly different between the two cell lines (**Figure 6.16**). A2AR expression was increased (not significant, p=0.187) and as previously mentioned PD-L1 levels were increased (p=0.047) (**Figure 6.16**). As in the microarray data, MHC class-I expression was decreased in the SKBR3-Lap cell line (p=0.007), and HLA-E expression was increased (p=0.001) (**Figure 6.17**). MICA protein expression was also 1.52-fold greater in the SKBR3-Lap cells (p=0.004). NKTR levels were not significantly changed when examined by western blot (**Figure 6.17**).

Table 6.5: Genes differentially expressed between SKBR3-Par and SKBR3-Lap based on DNA microarray analysis carried out as part of Dr. Martina McDermott's thesis.

Gene	Fold Change in SKBR3-Lap	P value
EGFR	1.63	2×10^{-5}
A2AR	4.34	6.5×10^{-14}
MHC class-I	-1.55	0.003
HLA-E	1.53	0.004
NKTR	-1.53	0.004

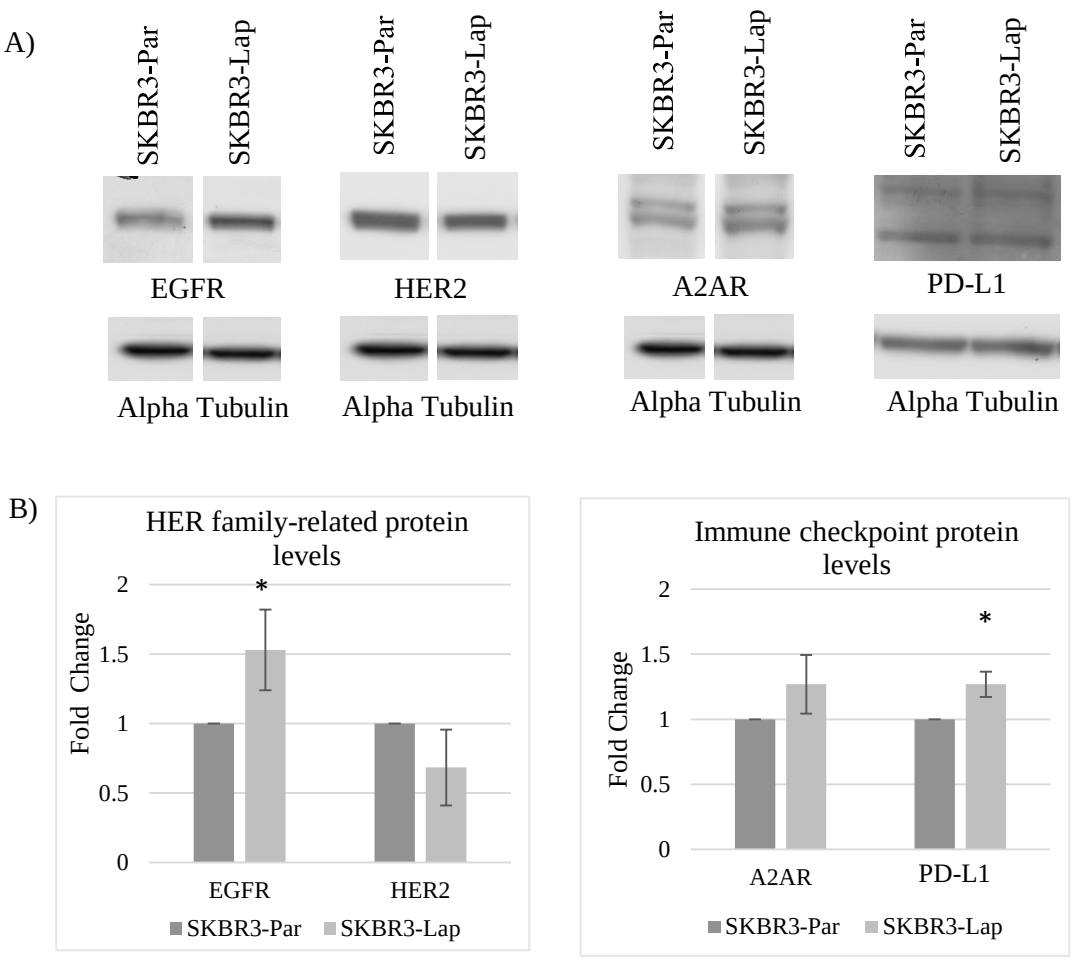

Figure 6.16: Protein expression levels for SKBR3-Par vs. SKBR3-Lap for validation of DNA microarray identified proteins. **A)** Representative Western blot images for HER family related proteins EGFR and HER2 and Immune checkpoint proteinsA2AR and PD-L1. **B)** Densitometry for triplicate HER family related proteins EGFR and HER2 and Immune checkpoint proteins A2AR and PD-L1. Blots normalised to SKBR3-Par expression. * $p<0.05$, ** $p<0.01$, *** $p<0.001$, significance values determined by Student's T test.

A)

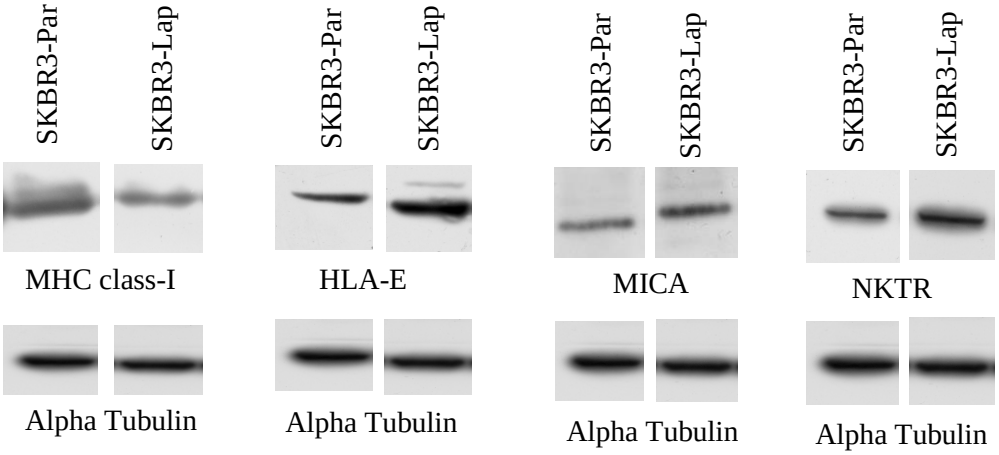

B)

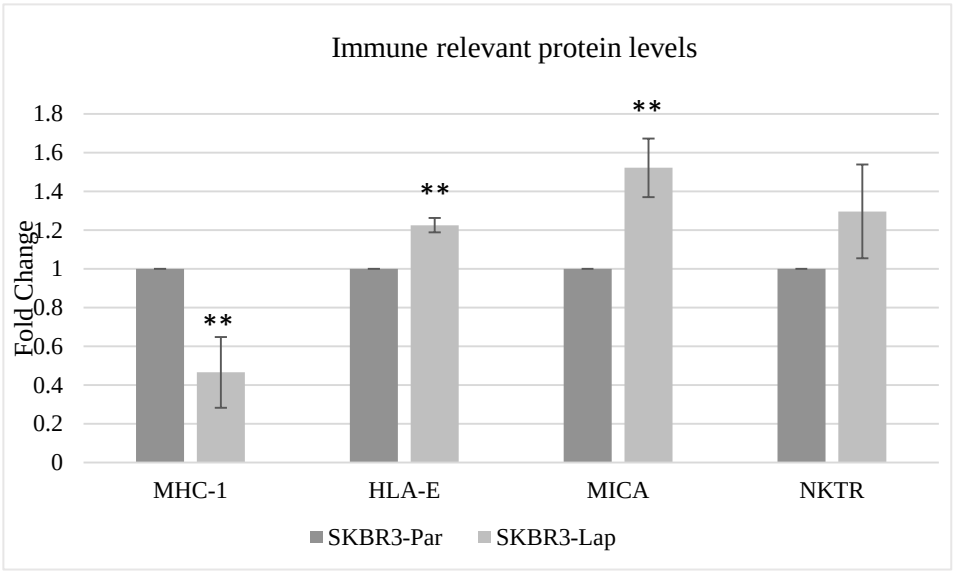

Figure 6.17: A) Representative Western blot image showing MHC class-I, HLA-E, MICA and NKTR expression levels in SKBR3-Par and SKBR3-Lap. B) Densitometry for triplicate MHC Class I, HLA-E, MICA and NKTR blots normalised to SKBR3-Par expression. * $p<0.05$, ** $p<0.01$, *** $p<0.001$, significance values determined by Student's T test.

6.7.3 Summary

Unlike the previous models HCC1954-Lap and SKBR3-Afa, a significant decrease in T-ADCC elicited by PBMCs against the SKBR3-Lap cell line was associated with a change in immune-related proteins (**Section 6.7**). HLA-E, MICA, MHC class-I and PD-L1 were altered in SKBR3-Lap *versus* SKBR3-Par on a protein level (**Section 6.7.2**). There were also changes in A2AR and NKTR mRNA expression between SKBR3-Par and SKBR3-Lap (**Section 6.7.1**). The SKBR3-Lap model should be examined in greater detail to investigate response to A2AR inhibition and to further dissect the impact of the altered immune expression profile on immune cell-mediated cytotoxicity.

6.8 Summary

Adenosine is a metabolic immune checkpoint capable of eliciting immunosuppression through A2AR. Adenosine treatment caused an increase in cytotoxicity in the ER+ HER2-low CAMA-1 cell line, this also occurred in lapatinib pre-treated CAMA-1 cells (**Section 6.3.3 and 6.3.4**). There was no change in cytotoxicity with the addition of adenosine in the MCF7 cell line, with or without lapatinib pre-treatment (**Section 6.3.5 and 6.3.6**).

Adenosine is capable of interacting with all four members of the adenosine receptor family. A2AR is the member reported to be the primary mediator of the immunosuppressive effects of adenosine. A more specific model was employed to examine A2AR-mediated immunosuppression in HER2+ breast cancer. CGS21680, an A2AR agonist, and preladenant, an A2AR antagonist, were used in combination with trastuzumab and NK cells in HER2+ breast cancer cell lines. In this model, the combination of CGS21680/preladenant and trastuzumab increased overall NK-cell-mediated cytotoxicity against both parental HER2+ breast cancer cell lines HCC1954 and SKBR3 (**Section 6.4.2 and 6.4.4**). This effect did not occur in the resistant cell line models HCC1954-Lap and SKBR3-Afa (**Section 6.4.3 and 6.4.5**).

It was also shown that there was an increase in both PBMC-mediated cytotoxicity and NK cell mediated cytotoxicity against the resistant cell lines compared to the parental cell lines (**Section 6.5**). This suggests an increase in susceptibility to immune cell-mediated destruction with the development of targeted therapy resistance. The SKBR3-Afa and HCC1954-Lap cell lines revealed that the development of targeted therapy resistance can sensitise cancer cells to immune cell-mediated destruction but provides protection against A2AR inhibition-associated increases in T-ADCC.

Protein expression of relevant HER family members (EGFR and HER2) and immune-related proteins (A2AR, PD-L1, MHC class-I, HLA-E, MICA and NKTR) were examined in the parental and resistant cell lines to determine possible mechanisms responsible for the difference in response to A2AR inhibition as well as altered susceptibility to immune cell-mediated destruction. There were no significant alterations in immune-related protein expression between parental and resistant cell lines (**Section 6.6**). The mediators of the changes in immune-mediated cytotoxicity and response to A2AR inhibition are as of yet undetermined. Further work is warranted to examine these trends and determine the mediators of these effects.

Although candidate proteins for the mediation of increased sensitivity to immune-cell mediated cytotoxicity were not identified in SKBR3-Afa and HCC1954-Lap, another model of HER2-targeted therapy resistance, SKBR3-Lap was profiled. The SKBR3-Lap cell line displayed altered levels of T-ADCC versus the parental cell line in conjunction with altered immune-related proteins. SKBR3-Lap cells also exhibited an increase in expression of A2AR and PD-L1 (**Section 6.7**). SKBR3-Lap may be an ideal model to examine the effect of A2AR inhibition in the future.

6.9 Discussion

6.9.1 Adenosine increases the susceptibility of an ER+ breast cancer cell line to PBMC-mediated cytotoxicity

Adenosine interacts with the four adenosine receptors. Adenosine receptors A1 and A3 have counteractive effects to the immunosuppressive effects of the A2A and A2B receptors [202]. There is no published data showing the effects of adenosine on ER+ breast cancer cell line models.

Adenosine treatment of tumour cells and PBMCs increased direct PBMC-mediated cytotoxicity in the CAMA-1 cell line but did not affect direct cytotoxicity against the MCF7 cell line (**Section 6.3**). Pre-treatment with the EGFR/HER2 targeting lapatinib did not affect adenosine-mediated effects in either cell line (**Section 6.3**). Lapatinib stabilises and HER2 expression on the cell surface which could alter T-ADCC response [282]. The similarities of T-ADCC response to adenosine with and without lapatinib treatment indicate the results are independent of HER2 signalling mechanisms.

There is no difference in A2AR expression between the two cell lines (**Section 6.3.1**), although there was a difference in response to adenosine treatment. This implies that A2AR expression levels on tumour cells do not mediate the changes in response to adenosine treatment in the models examined. Adenosine treatment did not lead to an immunosuppressive effect on PBMC-mediated cytotoxicity in the MCF-7 or CAMA-1 cell lines. These effects may be mediated through other members of the adenosine receptor family (A1R, A2BR or A3R) or may be due to A2AR signalling being redundant in respect to the immune response in these cell lines. Further examination of the other adenosine receptors and inhibitors of these receptors would be required to determine the mediators of this effect.

6.9.2 Inhibition of A2AR activation increases T-ADCC in parental but not targeted therapy resistant HER2+ breast cancer cell lines

The immunosuppressive effects of adenosine are mediated through A2AR. This may impact the immune response elicited against HER2+ tumours by trastuzumab. There are studies in the literature which show the potential benefit in suppressing A2AR signalling in the promotion of immune cells capable of eliciting T-ADCC. Cekic *et al.* demonstrated that NK cells can be inhibited through A2AR using A2AR knockout mouse models of melanoma and lung cancer [362]. Young *et al.* [363] showed inhibition of A2AR and CD73, an adenosine precursor, increased immune cell infiltration and decreased tumour growth in mouse models of mammary carcinoma, melanoma and lung cancer. Turcotte *et al.* [364] demonstrated that high gene expression of CD73 was associated with worse clinical outcome in trastuzumab treated breast cancer patients using data from the FinHER and METABRIC patient cohorts [364]. They also showed that CD73 inhibition in mouse models led to an increase in the ADCC response

elicited by a HER2-targeted trastuzumab-like monoclonal antibody. This was associated with an increased immune response against the tumour [364]. This is in addition to studies which have shown as association between hypoxia and resistance to trastuzumab in pre-clinical and clinical models [365,366].

A2AR agonist CGS21680 and A2AR antagonist preladenant, which is currently being evaluated in the clinic (NCT03099161), were used to examine A2AR immunosuppression. Inhibition of CGS21680-activated A2AR by preladenant caused an increase in NK cell-mediated T-ADCC and therefore overall cytotoxicity against the parental HER2+ breast cancer cell lines HCC1954 and SKBR3 (**Section 6.4.2 and 6.4.4**). This is in agreement with the increase in ADCC elicited when CD73 was inhibited by Turcotte *et al.* [364]. This finding indicates that NK cells capable of ADCC can be suppressed by A2AR signalling, by demonstrating that interfering with A2AR signalling has the potential to increase the immune response elicited by trastuzumab.

In the resistant cell line models there was no effect on T-ADCC or overall cytotoxicity with the inhibition of CGS21680-activated A2AR with preladenant (**Section 6.4.3 and 6.4.5**). As the difference in these assays is down to target cell targeted therapy resistance, this indicates that the A2AR-associated enhancement of NK cell toxicity is dependent on the resistance phenotype of the target cell. This is a novel observation. Other models have shown hypoxia as well as increased CD73 as mediating resistance to trastuzumab [364–366]. This supports an association between adenosine, the hypoxic tumour microenvironment and resistance to HER2 targeted therapy. As trials are currently being conducted in advanced cancers the lack of effect in therapy resistant models may impact response to A2AR inhibition. Further examination of A2AR inhibition is required particularly in targeted therapy resistant cell lines. Also, combination of an immune checkpoint inhibitor within this model is needed to more accurately model the clinical landscape.

The magnitude of the responses seen using the immune cytotoxicity assay were small but remained significant. This establishes these effects as being consistent between the three healthy volunteer samples examined. However, to maximise the volume of these changes and due to the lack of effect of the A2AR agonist on its own, it is necessary to develop a method which shows the effects of hypoxia and/or adenosine on the cell line and the immune response against the cell line.

Adenosine and A2AR antagonists, hypoxia mimetics and hypoxia chambers could be employed to mimic a hypoxia-induced immunosuppressive microenvironment. These models need to be investigated for their effects on A2AR, cAMP, PD-L1 and expression of other immune-relevant proteins. A model showing A2AR or hypoxia-induced immunosuppression could then be used in an immune cytotoxicity assay with inhibition of these pathways focusing on preladenant and pembrolizumab as they are the most clinically relevant. Incorporating the models developed in Chapter 2 using exhausted effector cells may also be of benefit.

The SKBR3-Lap cell line is another resistant cell line model which should be investigated in this setting. SKBR3-Lap cell line may have potential for further investigation of A2AR activation and inhibition (**Section 6.7**) as it shows attenuated T-ADCC accompanied by changes in A2AR, MHC class-I, HLA-E, NKTR and MICA (**Section 6.7.1 and 6.7.2**). These changes may allow for a contextualised examination of changes to the immune response against the cell line with regards A2AR inhibition.

6.9.3 Increase in susceptibility to PBMC- and NK cell-mediated cytotoxicity of targeted therapy resistant cell lines

The development of targeted therapy resistance results in alterations to key signalling pathways within the cancer cell to allow continued growth [337,347]. The development of afatinib and lapatinib resistance in the SKBR3-Afa and HCC1954-Lap cell lines was associated with increased susceptibility to immune cell-mediated destruction, using both PBMCs and NK cells as effector cells (**Section 6.5.1 and 6.5.2**).

HER2 expression was not altered between the parental and resistant cell lines. This shows that the change in T-ADCC was not due to different levels of HER2 antigen expression. MHC class-I, NKTR, HLA-E, E-cadherin are different between the parental SKBR3 and HCC1954 cell lines. The expression level of these proteins was not altered between either of the parental and resistant models examined, showing that in this case, they are not the mediators of the susceptibility of the resistant SKBR3-Afa and HCC1954-Lap cell lines. Other mediators may be playing a role in the susceptibility of these cell lines to immune-mediated destruction.

Retained HER2 expression and a high susceptibility to T-ADCC may indicate potential benefit of restarting trastuzumab treatment in patients who have become refractory to HER2-targeted TKI therapies. An altered immune response against treatment refractory breast cancer tumours would also have a huge impact on the use of immunotherapies in this setting. This may be associated with the high response rate in heavily pre-treated cancers and cancers with a high mutational burden. Further work is needed to understand the mechanisms behind this response.

7. Chromosomal instability in cancer-related and immune-related gene-sets

7.1 Introduction

Immunotherapies have exhibited relatively high response rates in previously treated and treatment-resistant cancers (**Table 1.1, 1.2, 1.3, Section 1.2**). It has also been demonstrated that immunotherapies have had a positive response against cancers which have a high mutational burden, such as melanoma and lung cancer (**Table 1.1, 1.2, 1.3, Section 1.2**). The responses that occur with immunotherapy appear to be relatively durable. Ribas *et al.* [367] has shown a continued response of greater than 3 years in 70-80 % of advanced melanoma patients who showed an initial response to pembrolizumab, whereas resistance to targeted therapy often occurs in patients who initially respond [368].

The hypothesis explored in this section is that immunotherapies have been able to elicit a response in these cases due to a lower rate of mutation in immune-related genes than in the more commonly targeted tumour cell signalling pathways. This would infer that the targets for immunotherapies are inherently more stable with a reduced likelihood of mutation, therefore allowing for an initial response to treatment and a potentially greater likelihood of a durable response.

There is no evidence in the literature regarding differences in genomic alteration rate between immune-related genes and cancer-related genes. To test this novel hypothesis, lists of immune-related genes and genes involved in commonly targeted cancer pathways were assembled. The cancer-related gene lists included oncogenes and tumour suppressors constructed from TCGA datasets and genes involved in the PI3K and MAPK signalling pathways, taken from KEGG pathway. The immune-related genes included lists of genes associated with the immune system and compiled from a literature search (Immunity), genes expressed in immune cells (IRIS), innate immune genes (Innate GO) and genes relevant to current immunotherapies (CIT).

The promoter conservation rate of the lists was determined, followed by the amplification and deletion (AMP/DEL) rate and the point mutation rate of all lists across a range of cancer types. Point mutation was determined by the number of single nucleotide variations (SNV) per kilobase (Kb) for each gene on a gene list. This allowed for examination of mutations occurring throughout the gene. The total SNV rate in a gene was also measured, this determined the number of mutations recurring in the same location i.e. hotspots. The frequencies of AMP/DEL and point mutations in each list was compared to background levels to ascertain any changes in frequency of mutation. It also allowed for comparison between immune-related gene lists and cancer-related gene lists.

These results supported evidence of a lower AMP/DEL rate in immune-related gene-sets *vs.* cancer-related gene-sets, as well as a lower rate of hotspot mutation in genes being currently targeted with immunotherapy.

Trends between cancer types could also be analysed to determine mutational patterns. Which allowed for an interesting observation regarding mutation of the innate immune system and viral infection in ovarian and cervical cancers.

7.2 Gene list assembly

Cancer- and immune-related genes were assembled from literature and database searches (**Table 7.1 and Section 2.11**).

7.2.1 Cancer-related gene list assembly

Oncogenes and tumour suppressors were chosen due to an expected high rate of mutation in tumour samples. A list of tumour suppressor genes was obtained from the COSMIC database. A gene was listed as a tumour suppressor based on the ratio of inactivating mutations in relation to other mutations, this provided a list of 286 genes [283]. Oncogenes were also obtained from the COSMIC database. Genes were included if they; i) had the same amino acid mutated in at least two tumours, ii) if there were more than 4 different mutations present in the gene or iii) if they were not listed as a tumour suppressor. This gave a list of 561 oncogenes [283,284]. A list of genes involved in the MAPK and PI3K signalling pathways were taken from KEGG pathway searches. The MAPK list was 256 genes long and the PI3K list was 238 genes long [285]. These pathways were chosen as they are often deregulated in cancer and they are often targeted with anti-cancer therapies (Ras/Raf inhibitors, PI3K inhibitors [318,369,370]). Dr. Moran also assembled a list of 239 genes involved in cancer hotspot mutations from the TCGA database for point mutation analysis. These lists formed the basis of the cancer-related gene lists.

7.2.2 Immune-related gene list assembly

Immune-related genes were assembled from Kelley *et al.* and comprised of 1532 genes which were gathered from literature searches for common immunological terms, including genes from the innate and adaptive immune system [286]. This broad spectrum immune-related gene list was named "Immunity" in this analysis [286]. Work from Abbas *et al.*[288] formed the Immune Response *In Silico* (IRIS) gene list of 1528 genes. These genes were compiled based on the proteins of these genes being expressed in immune cells, obtained from microarray profiling of immune cells. This list was chosen as it contained immune genes that are expressed in immune cells and not cancer cells to investigate whether they would be subject to the same mutational pressures.

To examine different aspects of the immune system, a list of innate immune genes was assembled (Innate GO). 780 genes were assembled based on their "innate immune system" gene ontology from

the Amigo gene ontology database [287]. The Current Immune Targets (CIT) list is 28 genes in size and was assembled in order to examine genes of therapeutic relevance to the current immunotherapy targets including the immune checkpoints PD-1 and PD-L1 [14]. These lists; Immunity, IRIS, Innate GO and CIT formed the basis of the immune- related gene lists.

As a positive control for immunity-related mutations, a list of TCR, HLA and IgG genes were collated. These gene-sets contain variable domain regions which undergo gene re-arrangement and somatic mutation to allow for the recognition of a wide variety of antigens [371–373]. The TCR gene list was 248 genes in length, the HLA gene list was 45 genes in length and the IgG list was 432 genes in length. These three gene lists were taken from the Hugo Gene Nomenclature Committee [289].

7.2.3 Promoter conservation gene lists

For promoter conservation studies, transcription factor and housekeeping gene lists were assembled. As transcription factors have a high rate of promoter conservation and housekeeping genes have a lower rate of promoter conservation [290,293], these lists were included to ensure a spectrum of promoter conservation within the lists of interest. A list of 407 housekeeping genes was assembled from Zhu *et al.* based on gene expression across different tissue types [290]. A list of 812 transcription factors was composed from published databases [291–294].

Table 7.1: Cancer- and immune-related gene lists assembled from literature and database searches.

Gene list	No. of genes	Rationale for using list	List curation
Tumour Suppressors [283]	286	Commonly targeted cancer pathways associated with cancer development and progression	Genes from COSMIC database
Oncogenes [283,284]	561		
PI3K [285]	238	Commonly mutated cancer pathways	KEGG pathway search for relevant pathway
MAPK [285]	256		
Cancer Hotspots	239	Mutations involved in hotspot cancer mutations	Assembled from the TCGA dataset by Dr. Bruce Moran
Immunity genes [286]	1532	Included were complete genes with a functional transcript that demonstrates a defence characteristic	The gene list was curated from literature searches for immunologically relevant genes
Innate GO [287]	780	Specifically innate immune genes as classified by their gene ontology	Genes involved in the innate immune system only by Amigo Gene Ontology
IRIS [288]	1528	Immune genes expressed in immune cell populations. Immune cell specific expression is an indicator of importance in the function of the immune system	List was assembled from genome wide microarray expression profiling of immune cells
Current immune targets [14]	28	Genes are of relevance to clinical situation	Genes list assembled from currently used or prospective immune checkpoint targets

TCR [289]	248	T cell receptor genes included as a control of individual mutation rate	List compiled using Hugo Gene Nomenclature Committee (HGNC)
IgG [289]	432	Immunoglobulin genes included as a control of individual mutation rate	List compiled using HGNC
HLA [289]	45	HLA genes included as a control of individual mutation rate	List compiled using HGNC
House Keeping [290]	407	Housekeeping genes included as a control for low promoter conservation levels	Used microarray and EST data to determine housekeeping genes across 18 human tissue types.
Transcription Factors [291–294]	812	Transcription factor genes included as a control for high promoter conservation levels	Literature search for lists of transcription factor and curation of transcription factor databases

7.3 Promoter conservation levels

Dr. Madden performed analysis on the tumour suppressor, oncogene, Immunity, Innate GO, transcription factor and housekeeping gene lists to determine the average promoter conservation of these lists (**Figure 7.1**). This was a preliminary test to determine how likely the genes were to be conserved. The transcription factor gene lists were used as a measure of higher conservation and the housekeeping genes as a lower rate of conservation. The average number of nucleotides conserved in the transcription factor list was 2966, whereas the average number of nucleotides conserved in the housekeeping gene list was 2048 (**Figure 7.1**). The overall average of all the lists was 2328 nucleotides (**Figure 7.1**). The immunity and innate gene lists were similar to the overall average level of promoter conservation with 2294 and 2331 nucleotides conserved, respectively (**Figure 7.1**). Oncogene and tumour suppressor genes had an average promoter conservation of 2728 and 2554 nucleotides respectively (**Figure 7.1**). As all lists of interest fell between the transcription factors and housekeeping genes, these lists were used for further analysis.

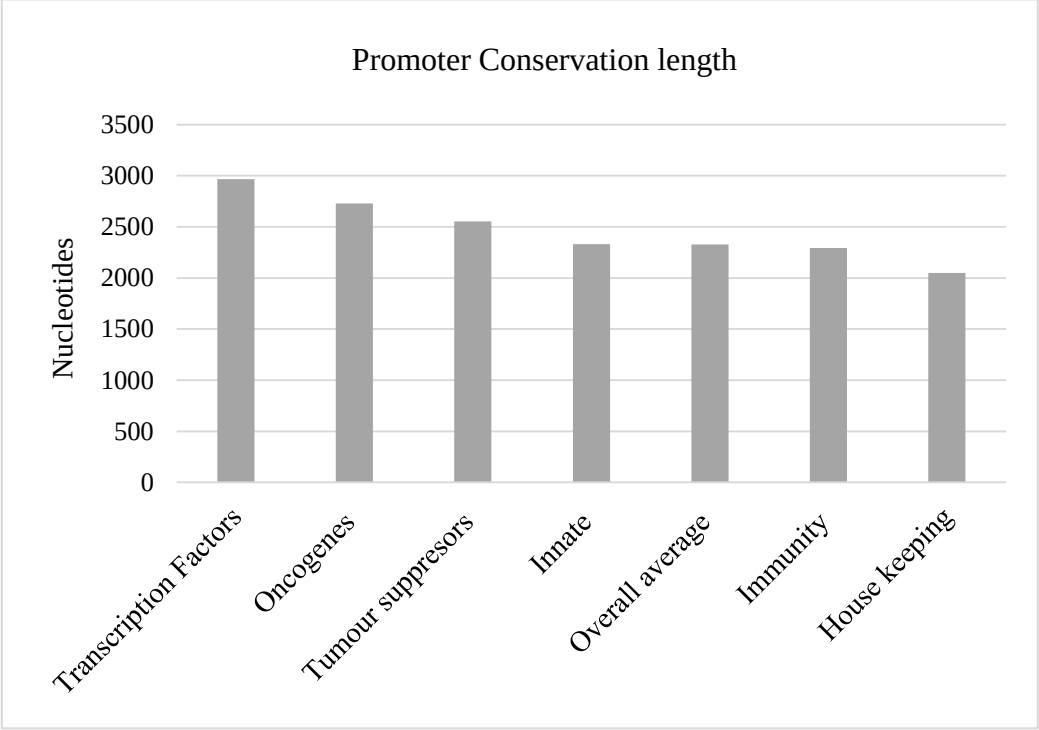

Figure 7.1: Average promoter nucleotide conservation length for genes included on the transcription factor, housekeeping, oncogene, tumour suppressor, innate and immunity gene lists. Also included is an overall average promoter conservation level for all lists.

7.4 Amplification and Deletion rate of cancer-related and immune-related gene lists

Determination of the AMP/DEL rate of the gene lists was performed by Dr. Madden. The aCGH data for 10 cancer types (n=602 patients) was downloaded from Geo (**Table 7.2**). The genomic breakpoints of AMP/DEL were determined across this dataset using GLAD/DNAcopy. The gene lists; oncogenes, tumour suppressors, PI3K, MAPK, Immunity, IRIS, Innate GO and CIT, were overlapped with the genomic breakpoints. The AMP/DEL points within each list were determined and compared to background levels of AMP/DEL within the aCGH dataset. This allowed for comparison of the AMP/DEL rate in cancer-related genes *versus* immune-related genes across a number of cancer types.

Table 7.2: Cancer types and sample size of dataset downloaded from Geo for AMP/DEL analysis. Hormone receptor + (HR+), Triple negative (TN), Cervical squamous cell carcinoma (CSCC) and Chronic lymphocytic leukaemia (CLL).

Cancer type	Number of samples	GSE
Breast cancer HER2+	50	GSE20393
Breast cancer HR+	54	GSE20393
Breast cancer TN	53	GSE20393
Prostate cancer	57	GSE20393
Melanoma	51	GSE20393
Ovarian cancer	51	GSE20393
Lung cancer	52	GSE20393
Colon cancer	95	GSE18638
Mesothelioma	53	GSE29902
CSCC	37	GSE27333
Glioblastoma	9	GSE19612
CLL	40	GSE24823

7.4.1 Cancer-related gene lists

7.4.1.1 Oncogene gene list

Within the Oncogene list, the AMP/DEL rate was significantly lower than background for prostate cancer ($p=3.1x10^{-4}$) and ovarian cancer ($p=0.002$) (**Figure 7.2 and Table 7.3**). The AMP/DEL rate was not significantly lower than background levels for breast cancer (HER2, TNBC, HR+), melanoma, lung, colon, glioblastoma, CLL, cervical or mesothelioma. The AMP/DEL rate within the oncogene list was not significantly lower than background levels across all patients examined (n=602) (**Figure 7.2 and Table 7.3**).

For 8/10 cancer types examined and across the average of all cancers combined AMP/DEL rate was not significantly lower than background for the oncogenes gene list.

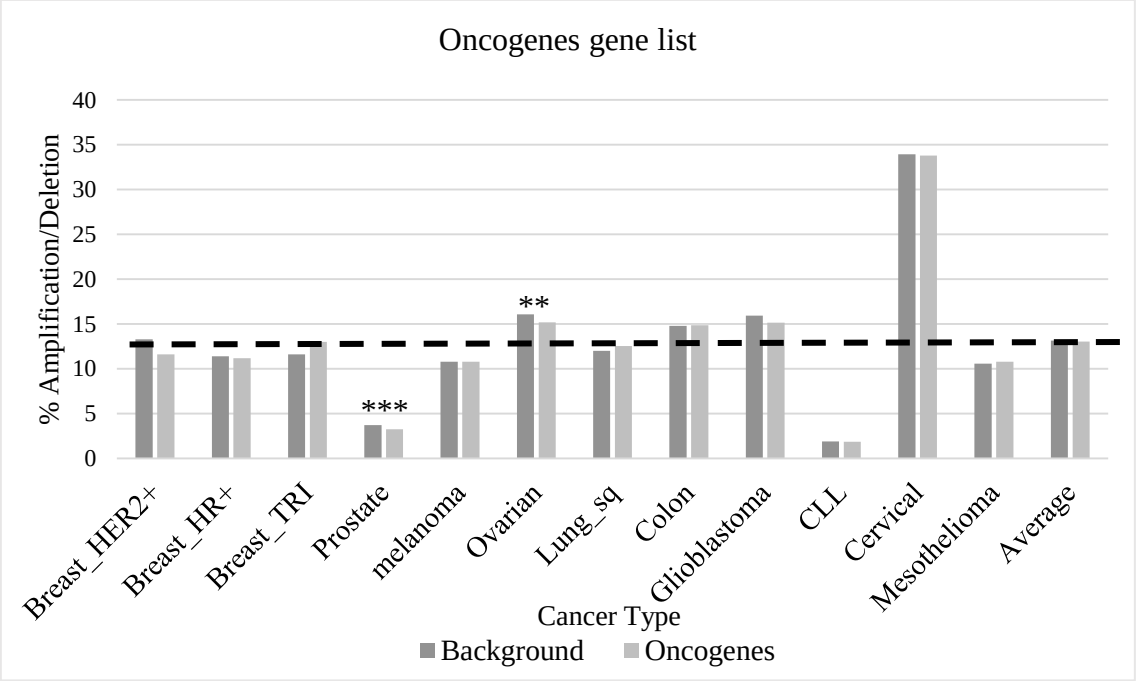

Figure 7.2: The Oncogenes gene list which was mapped to aCGH array to determine AMP/DEL rate of the list across a range of cancer types and on average across all cancer types combined. * $p<0.05$, ** $p<0.01$, ***$p<0.001$ for background *versus* gene list within each cancer type. Dotted line represents average AMP/DEL rate across all cancers combined.

7.4.1.2 Tumour suppressor gene list

The AMP/DEL rate was significantly lower than background within the tumour suppressor list for prostate cancer, colon cancer and mesothelioma (p=0.013, 0.002 and p=0.001 respectively) (**Figure 7.3 and Table 7.3**). The AMP/DEL rate was not significantly lower than background levels for breast cancer (HER2, TNBC, HR+), melanoma, ovarian, lung, glioblastoma, CLL or cervical or across all patients examined (n=602) (**Figure 7.3 and Table 7.3**).

The AMP/DEL rate was not significantly lower than background level for the tumour suppressor list in 7/10 of the cancer types examined and across the average of all cancers combined.

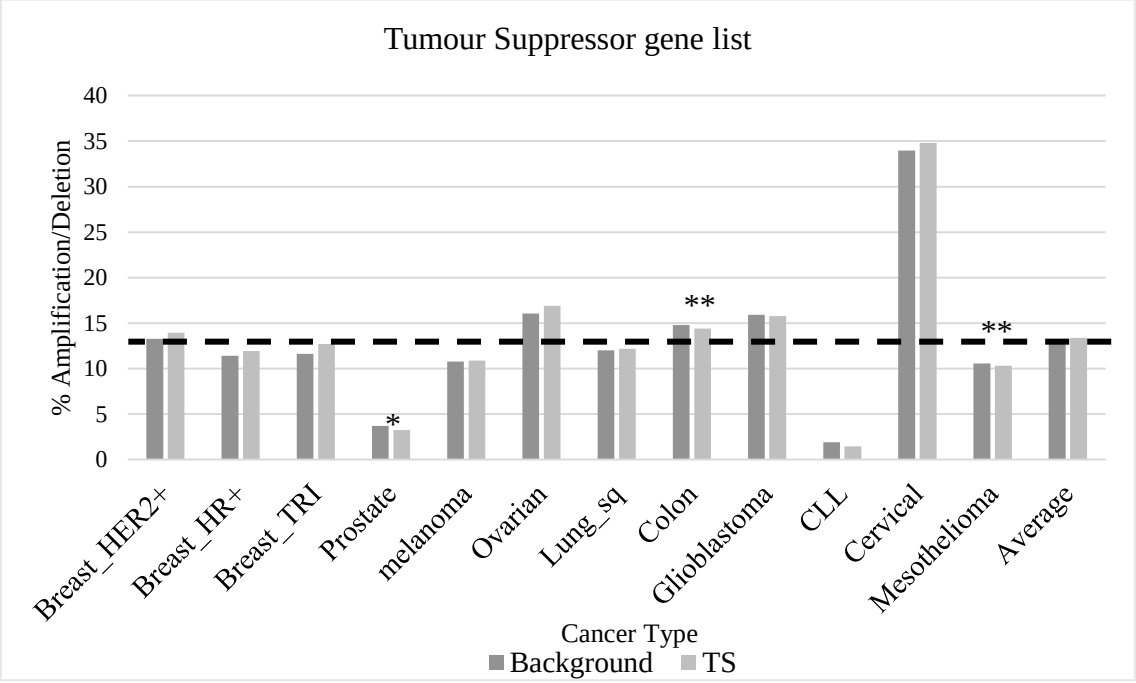

Figure 7.3: The Tumour suppressor gene list which was mapped to aCGH array to determine AMP/DEL rate of the list across a range of cancer types and on average across all cancer types combined. * p<0.05, ** p<0.01, ***p<0.001 for background *versus* gene list within each cancer type. Dotted line represents average AMP/DEL rate across all cancers combined.

7.4.1.3 PI3K gene list

Within the PI3K list, the AMP/DEL rate was significantly lower than background for prostate cancer (p=0.013) (**Figure 7.4 and Table 7.3**). The AMP/DEL rate was not significantly lower than background levels for any of the other cancer types or across all patients examined (n=602) (**Figure 7.4 and Table 7.3**).

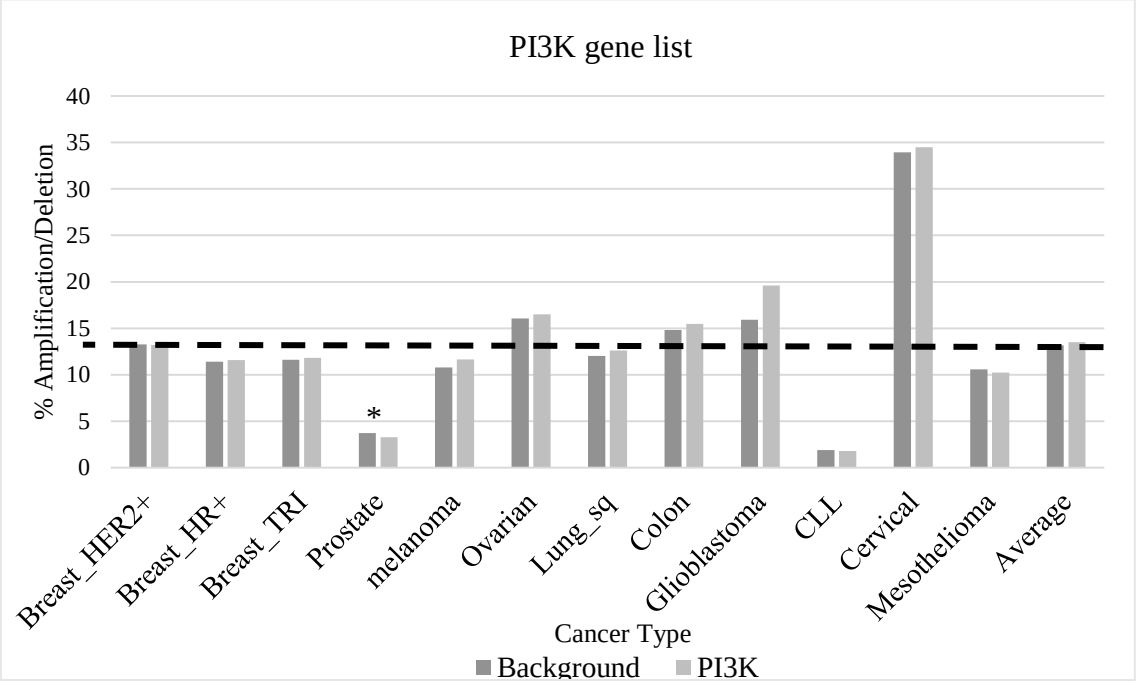

Figure 7.4: The PI3K gene list which was mapped to aCGH array to determine AMP/DEL rate of the list across a range of cancer types and on average across all cancer types combined. * p<0.05, ** p<0.01, ***p<0.001 for background *versus* gene list within each cancer type. Dotted line represents average AMP/DEL rate across all cancers combined.

7.4.1.4 MAPK gene list

The MAPK gene list showed a lower rate of AMP/DEL when compared across all cancers examined (n=602) (p=0.001) (**Figure 7.5 and Table 7.3**). The AMP/DEL rate was significantly lower than background for HER2+ breast cancer (p=0.044), prostate ($p=3.4 \times 10^{-8}$), melanoma (p=0.001), colon ($p=8.7 \times 10^{-9}$) and glioblastoma (p=0.044) (**Figure 7.5 and Table 7.2**). The AMP/DEL rate was not significantly lower than background for breast cancer (HR+ and TNBC), ovarian, lung, CLL, cervical or mesothelioma (**Figure 7.5 and Table 7.3**).

Across the average of all cancers combined and within a number of cancer subtypes the AMP/DEL rate was lower than background level for the MAPK gene list.

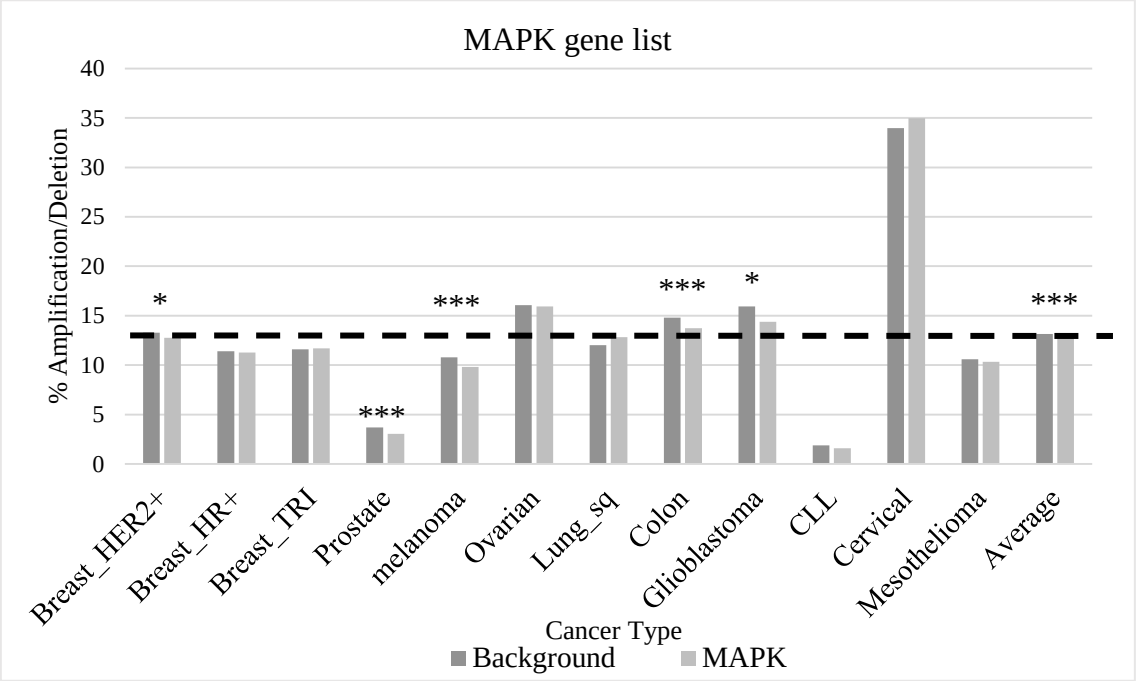

Figure 7.5: The MAPK gene list which was mapped to aCGH array to determine AMP/DEL rate of the list across a range of cancer types and on average across all cancer types combined. * p<0.05, ** p<0.01, ***p<0.001 for background *versus* gene list within each cancer type. Dotted line represents average AMP/DEL rate across all cancers combined.

Table 7.3: p values associated with lower AMP/DEL rate in cancer-related gene lists compared with background level using aCGH data.

Cancer Type (n= 602)	Oncogenes	Tumour Suppressors	PI3K	MAPK
Overall (n=602)	-	-	-	0.001
Breast HER2+ (n=50)	-	-	-	0.044
Breast HR+ (n=54)	-	-	-	-
Breast TNBC (n=53)	-	-	-	-
Prostate(n=57)	$3.1x10^{-4}$	0.013	0.013	3.4×10^{-8}
Melanoma (n=51)	-	-	-	0.001
Ovarian (n=51)	0.002	-	-	-
Lung (n=52)	-	-	-	-
Colon (n=95)	-	0.002	-	8.7×10^{-9}
Glioblastoma (n=9)	-	-	-	0.044
CLL (n=40)	-	-	-	-
CSCC (n=37)	-	-	-	-
Mesothelioma (n=53)	-	0.001	-	-

7.4.2 Immune-related gene lists

7.4.2.1 Immunity gene list

When genes from the Immunity gene list were analysed, they had a lower AMP/DEL rate than background across all cancers combined ($p=2x10^{-4}$) (**Figure 7.6 and Table 7.4**). Within the cancer subtypes, there was a lower AMP/DEL rate than background for HER2+ breast cancer (p=0.013), HR+ breast cancer (p=0.008), prostate (p=0.007), ovarian ($p=1x10^{-4}$) and lung (p=0.019) (**Figure 7.6 and Table 7.4**). AMP/DEL rate was not significantly lower than background in TNBC, melanoma, colon, glioblastoma, CLL, cervical or mesothelioma (**Figure 7.6 and Table 7.4**).

The AMP/DEL rate was significantly lower within the genes of the Immunity list on average across all cancers combined as well as within a number of cancer subtypes specifically.

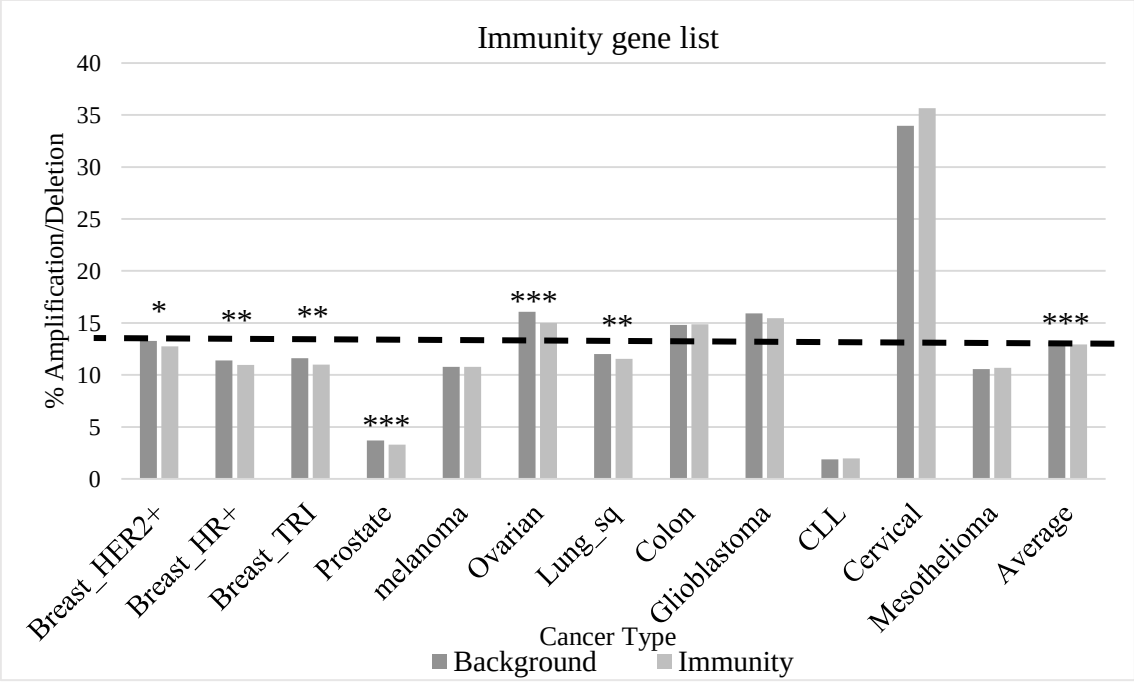

Figure 7.6: Immunity gene list which was mapped to aCGH array to determine AMP/DEL rate of the list across a range of cancer types and on average across all cancer types combined. * p<0.05, ** p<0.01, ***p<0.001 for background *versus* gene list within each cancer type. Dotted line represents average AMP/DEL rate across all cancers combined.

7.4.2.2 IRIS gene list

Genes from the IRIS gene list there showed a lower rate of AMP/DEL than background levels across all cancers combined ($p=2.0 \times 10^{-20}$) (**Figure 7.7 and Table 7.4**). As well as a lower rate of AMP/DEL than background for most cancer subtypes examined; HER2+ breast cancer (p=0.005), HR+ breast cancer (p=0.005), TNBC ($p=6.1 \times 10^{-8}$), prostate (p=0.01), ovarian ($p=3.3 \times 10^{-5}$), lung (p=0.002), colon ($p=4.4 \times 10^{-4}$), CLL (p=0.01) and mesothelioma ($p=1.8 \times 10^{-4}$) (**Figure 7.7 and Table 7.4**). The only cancer types where the AMP/DEL was not lower than background were melanoma, glioblastoma and cervical (**Figure 7.7 and Table 7.4**).

The IRIS gene list had a lower AMP/DEL rate than background for 7/10 of the cancer subtypes examined, as well as across the average of all cancers examined combined.

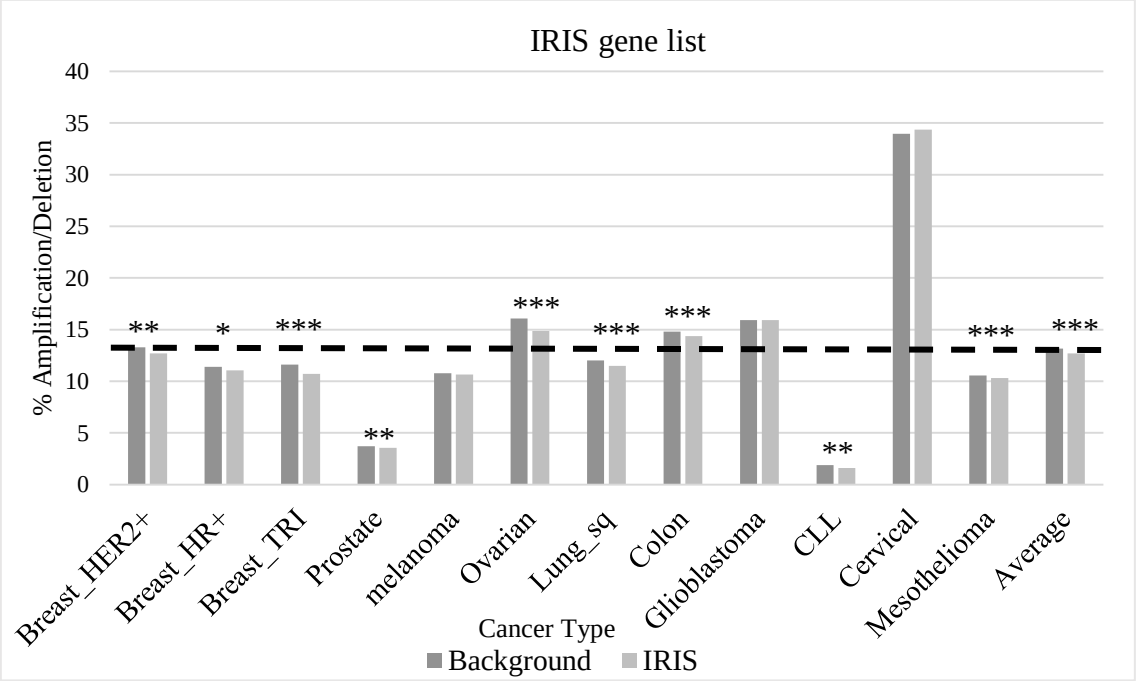

Figure 7.7: IRIS gene list which was mapped to aCGH array to determine AMP/DEL rate of the list across a range of cancer types and on average across all cancer types combined. * p<0.05, ** p<0.01, ***p<0.001 for background *versus* gene list within each cancer type. Dotted line represents average AMP/DEL rate across all cancers combined.

7.4.2.3 Innate GO gene list

From the Innate GO list only glioblastoma and mesothelioma had a lower AMP/DEL rate than background (p=0.005 and p=0.012 respectively) (**Figure 7.8 and Table 7.4**). This was not the case across all cancers combined and within breast cancer, prostate, melanoma, ovarian, lung, colon, CLL and cervical cancers where the Innate GO gene list did not have a significantly lower AMP/DEL rate than background. **(Figure 7.8 and Table 7.4)**.

Within 8/10 cancer subtypes and across all cancers combined the Innate GO list did not show a lower AMP/DEL rate than background.

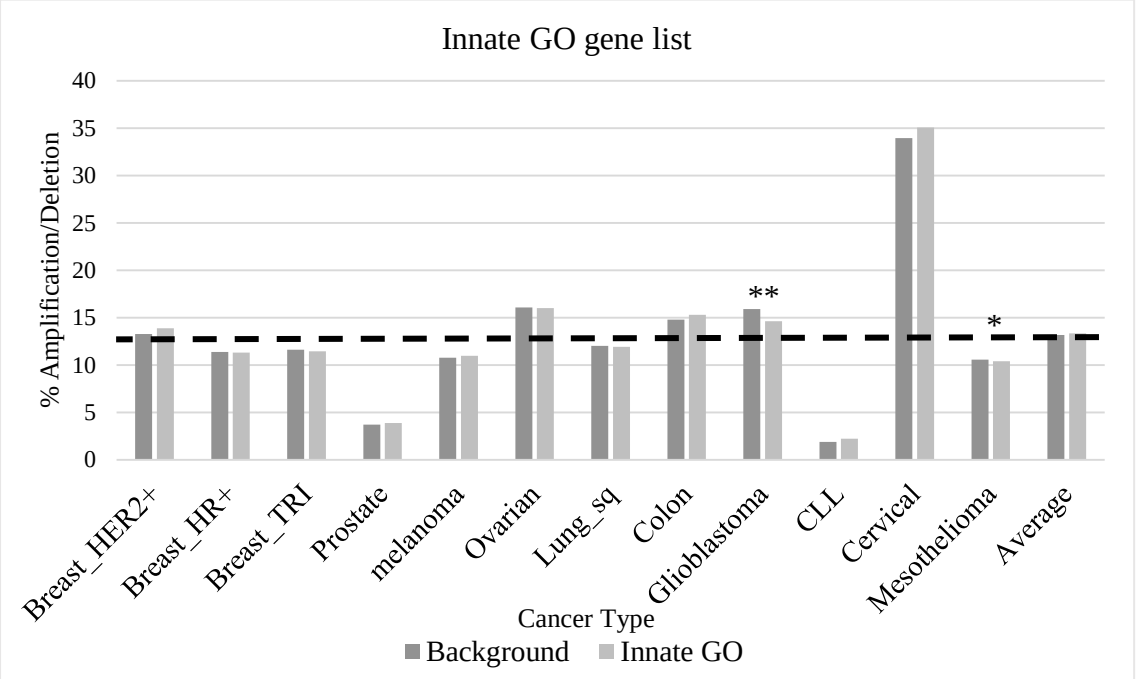

Figure 7.8: Innate GO gene list which was mapped to aCGH array to determine AMP/DEL rate of the list across a range of cancer types and on average across all cancer types combined. * p<0.05, ** p<0.01, ***p<0.001 for background *versus* gene list within each cancer type. Dotted line represents average AMP/DEL rate across all cancers combined.

7.4.2.4 CIT gene list

Across all cancers combined, the genes in the CIT list had a lower AMP/DEL rate than background ($p=2.8 \times 10^{-7}$) (**Figure 7.9 and Table 7.4**). Within cancer subtypes, the CIT list had a lower AMP/DEL rate than background for HER2+ breast cancer (p=0.02), TNBC (p=0.04), ovarian (p=0.03), colon ($p=4.1 \times 10^{-6}$) and glioblastoma (p=0.02) (**Figure 7.9 and Table 7.4**). HR+ breast cancer, prostate, melanoma, lung, CLL, cervical and mesothelioma did not have a significantly lower AMP/DEL rate when compared to background levels (**Figure 7.9 and Table 7.4**).

The AMP/DEL rate for genes in the CIT list was lower than background across all cancers combined and in a number of cancer subtypes.

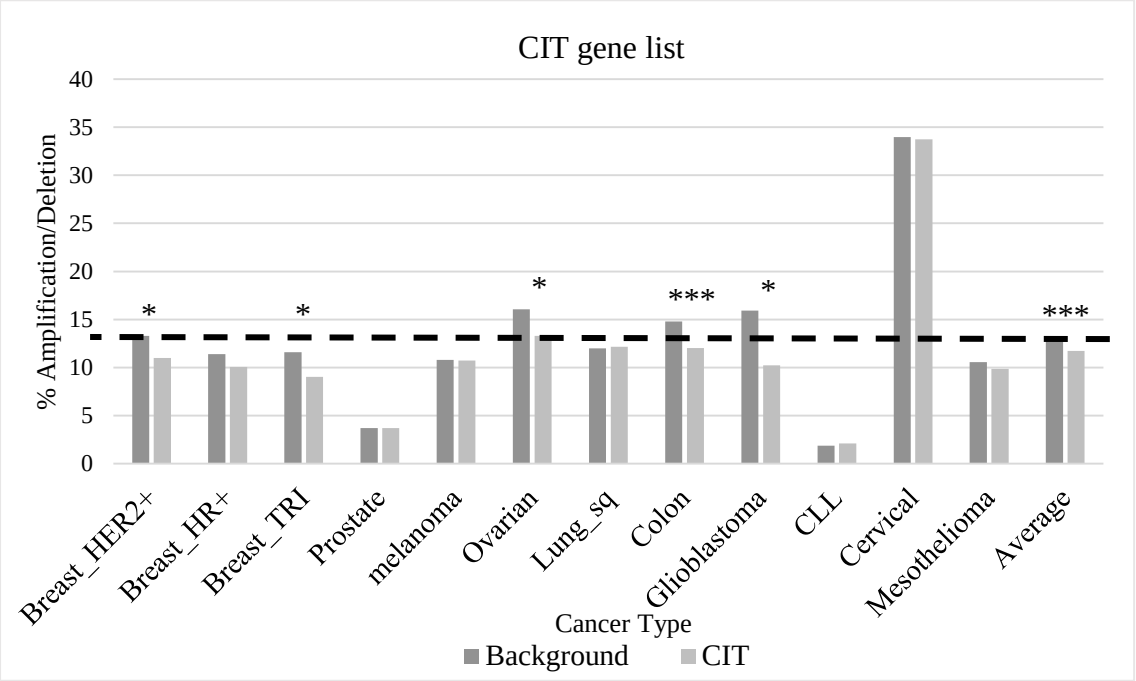

Figure 7.9: CIT gene list which was mapped to aCGH array to determine AMP/DEL rate of the list across a range of cancer types and on average across all cancer types combined. * p<0.05, ** p<0.01, ***p<0.001 for background *versus* gene list within each cancer type. Dotted line represents average AMP/DEL rate across all cancers combined.

Table 7.4: p values associated with lower AMP/DEL rate in cancer related gene lists compared with background level using aCGH data.

Cancer Type	Immunity	IRIS	Innate GO	CIT
Overall (n=602)	$2x10^{-4}$	2.0×10^{-20}	-	2.8×10^{-7}
Breast HER2+ (n=50)	0.013	0.005	-	0.02
Breast HR+ (n=54)	0.008	0.01	-	-
Breast TNBC (n=53)	-	6.1×10^{-8}	-	0.04
Prostate (n=57)	0.007	0.01	-	-
Melanoma (n=51)	-	-	-	-
Ovarian (n=51)	$1x10^{-4}$	3.3×10^{-5}	-	0.03
Lung (n=52)	0.002	0.002	-	-
Colon (n=95)	-	4.4×10^{-4}	-	4.1×10^{-6}
Glioblastoma (n=9)	-	-	0.005	0.02
CLL (n=40)	-	0.01	-	-
CSCC (n=37)	-	-	-	-
Mesothelioma (n=53)	-	1.8×10^{-4}	0.012	-

7.4.3 Summary

For the oncogene, tumour suppressor and PI3K gene lists, the rate of AMP/DEL was not lower than background levels when examining all cancer types combined (**Section 7.4.1.1, 7.4.1.2 and 7.4.1.3**). The MAPK list did not follow this trend, it showed lower AMP/DEL than background across cancer types combined (**Section 7.4.1.4**).

Immunity, IRIS and CIT had a lower AMP/DEL rate than background for all cancers combined (**Section 7.4.2.1, 7.4.2.2 and 7.4.2.4**). Innate GO did not follow this trend, genes on this list were not significantly lower than background levels across all cancers combined (**Section 7.4.2.3**).

The overall trend showed significantly lower AMP/DEL in the immune-related gene sets; IRIS, Immunity and CIT *versus* the PI3K pathway, oncogenes and tumour suppressors across a range of cancer types. The analysis of the AMP/DEL rate of the cancer-related and immune-related gene lists supported the original hypothesis, as immune genes are less prone to AMP/DEL than cancer-related genes.

7.5 Point mutation rate in cancer-related and immune-related gene lists

To further investigate the hypothesis, the point mutation rate of these gene lists was determined by Dr. Moran using the TCGA dataset for 33 cancer types (**Table 7.5**). MuTect was used to detect point mutations in the dataset. The point mutation rate of the genes in each gene list were analysed per gene and per kilobase of each gene.

Mutation per kilobase (SNV/Kb) was used in order to examine point mutation rate regardless of the discrepancies in the length of different genes and to examine the rate of continuous mutation throughout the gene. Accounting for the number of amino acid positions with mutations but ignoring the number of mutations at those positions.

The total SNV level was also determined across each gene in the gene lists. This gave a value for total number of mutations within that gene which allowed mutation hotspots to register e.g. more than one occurrence of a mutation at the same amino acid position.

Bootstrap gene lists were randomly selected from the dataset. The number of genes per bootstrap list was determined from the amount of mutations in the relevant gene list it was being compared to. The rate of mutation per kilobase was compared to 100 bootstrap gene lists to obtain 100 p values for SNV/Kb, the average of the 100 p values could then be used to provide a p score for each gene list.

The median number of SNV/Kb and median number of total SNV per gene list were also compared to the median number of SNV/Kb and median number of total SNV for 3 bootstrap lists which allowed the fold change in median values compared to background to be calculated.

The lists examined in this analysis were; oncogenes, tumour suppressors, PI3K, MAPK, Cancer Hotspots, Immunity, IRIS, Innate GO, CIT, TCR, HLA and IgG. The Cancer Hotspots list was an additional gene list made by Dr. Moran. This list comprised of 239 genes which are implicated in hotspot mutations in cancer, this list was developed from the TCGA dataset.

Table 7.5: 33 TCGA abbreviations, cancer types and sample size used in this analysis

Cancer type Abbreviation	Cancer type	Sample size (n=11,315)
ACC	Adrenocortical carcinoma	92
BLCA	Bladder Urothelial Carcinoma	412
BRCA	Breast Invasive Carcinoma	1098
CESC	Cervical Squamous Cell Carcinoma and Endocervical Adenocarcinoma	307
CHOL	Cholangiocarcinoma	51
COAD	Colon Adenocarcinoma	461
DLBC	Lymphoid Neoplasm Diffuse Large B-cell Lymphoma	58
ESCA	Oesophageal Carcinoma	185
GBM	Glioblastoma Multiforme	617
HNSC	Head and Neck Squamous Cell Carcinoma	528
KICH	Kidney Chromophobe	113
KIRC	Kidney Renal Clear Cell Carcinoma	537
KIRP	Kidney Renal Papillary Cell Carcinoma	291
LAML	Acute Myeloid Leukaemia	200
LGG	Brain Lower Grade Glioma	516
LIHC	Liver Hepatocellular Carcinoma	377
LUAD	Lung Adenocarcinoma	585
LUSC	Lung Squamous Cell Carcinoma	504
MESO	Mesothelioma	87
OV	Ovarian Serous Cystadenocarcinoma	608
PAAD	Pancreatic Adenocarcinoma	185
PCPG	Pheochromocytoma and Paraganglioma	179
PRAD	Prostate Adenocarcinoma	500
READ	Rectum Adenocarcinoma	172
SARC	Sarcoma	261
SKCM	Skin Cutaneous Melanoma	470
STAD	Stomach Adenocarcinoma	443
TGCT	Testicular Germ Cell Tumours	150
THCA	Thyroid Carcinoma	507
THYM	Thymoma	124
UCEC	Uterine Corpus Endometrial Carcinoma	560
UCS	Uterine Carcinosarcoma	57
UVM	Uveal Melanoma	80

7.5.1 Examining SNV/Kb in gene lists across all cancer types

To analyse the mutations occurring throughout each gene for the cancer-related and immune-related gene lists the SNV/Kb rate was determined. This was compared to 100 bootstrap lists to obtain significance values, the median of which was taken as a p score. Fold change of SNV/Kb was also determined by comparing median SNV/Kb with the median SNV/Kb of 3 bootstrap lists.

7.5.1.1 Cancer-related gene lists across all cancer types

The median p score for tumour suppressors and oncogenes showed a significantly lower SNV/Kb than background levels (p=0.002 and p=0.004, respectively). The fold change of median SNV/Kb compared to background levels for cancer-related genes was less than 1 for all lists across all cancer types examined (**Table 7.6**).

7.5.1.2 Immune-related gene lists across all cancer types

The immune-related gene lists; IRIS, Innate Go and CIT showed a fold change in median SNV/Kb compared to background levels of approximately 1 across all 33 cancer types. The immunity gene list showed a fold change in median SNV/Kb which was significantly higher than background levels 1.38 ($p=2.96x10^{-5}$) across all cancer types (**Table 7.6**).

The median SNV/Kb for the variable immune gene lists was higher than the other lists examined across all 33 cancer types. The TCR list had a median SNV/Kb of 2.99 with a fold change of 27.35 ($p=1.92x10^{-7}$) compared to background. The IgG list had a median SNV/Kb of 3.17 with a fold change of 39.62 ($p=5.72x10^{-18}$) compared to background. The HLA gene list had a median SNV/Kb of 0.32 with a fold change of 3.24 (p=0.064) compared to background (**Table 7.6**).

Housekeeping genes had a median SNV/Kb of 0.16 with a fold change compared to background of 1.31 (p=0.07) (**Table 7.6**).

Table 7.6: The median SNV/Kb for each of the gene lists examined along with fold change in median SNV/Kb when compared to background levels and p score values for all SNV/Kb bootstrap tests. p score <0.05 denoted as significant. Significant p scores listed in bold.

Gene list	Median SNV/KB	Fold change SNV/Kb	p Score
Cancer-related gene lists			
Tumour Suppressors	0.101	0.642	**0.002**
Oncogenes	0.107	0.751	**0.003**
MAPK	0.102	0.726	0.076
PI3K	0.123	0.927	0.562
Cancer Hotspots	0.117	0.804	0.223
Immune-related gene lists			
Immunity	0.181	1.379	**2.96E-05**
IRIS	0.119	0.945	0.056
Innate GO	0.149	1.090	0.32
CIT	0.154	1.371	0.564
Control Gene lists			
TCR	2.991	27.349	**1.92E-07**
IgG	3.168	39.625	**5.72E-18**
HLA	0.322	3.241	0.064
House Keeping genes	0.159	1.311	0.071

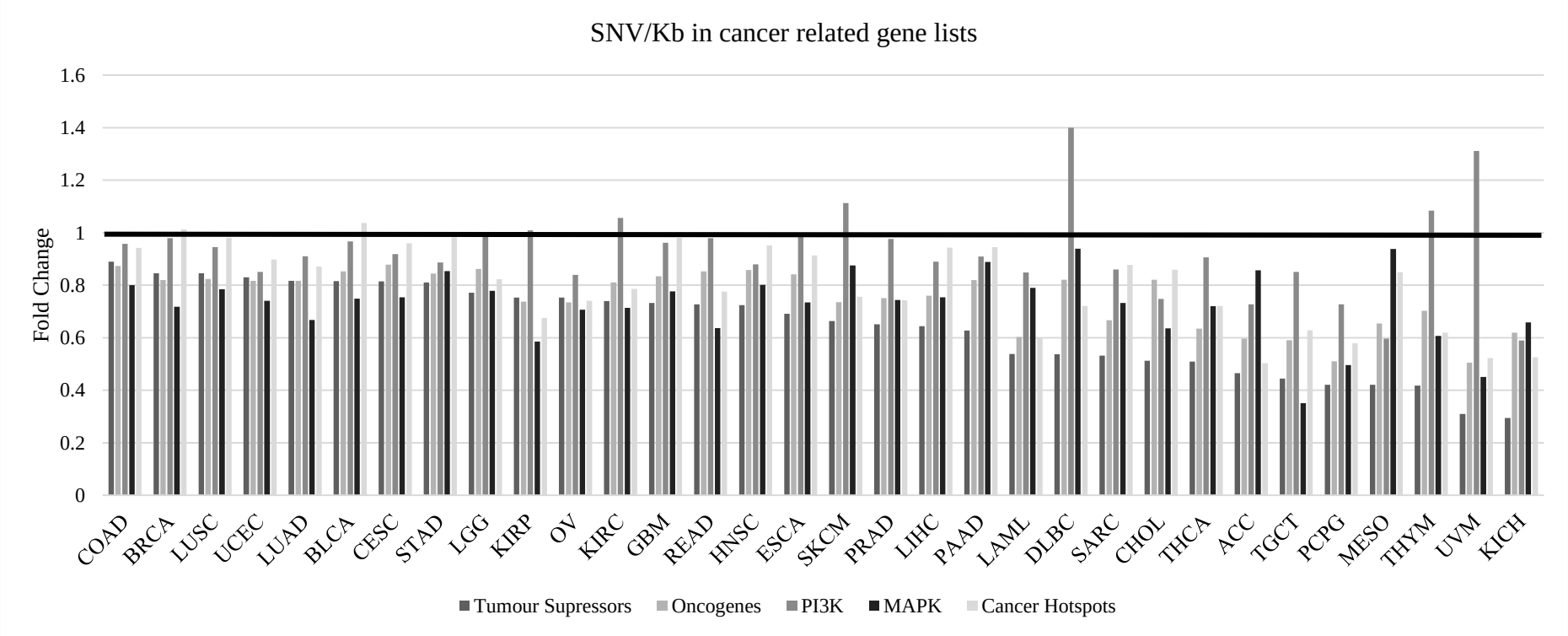

Figure 7.10: Fold change of SNV/Kb of cancer-related gene lists compared with background levels for 33 cancer types from TCGA dataset. Fold change of 1 denoted by black line. Significant p scores came from overall values of greater than 1.2- and less than 0.8-fold change.

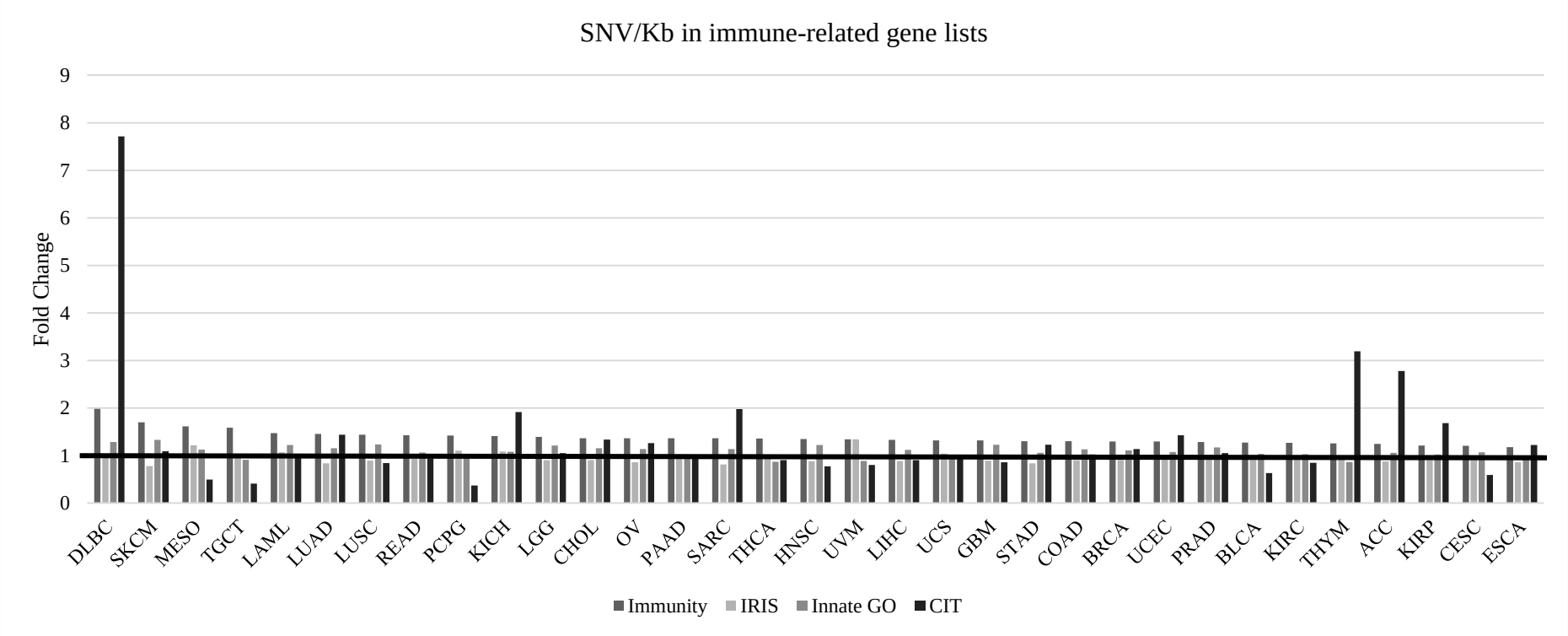

Figure 7.10: Fold change of SNV/Kb of immune-related gene lists compared with background levels for 33 cancer types from TCGA dataset. Fold change of 1 denoted by black line. Significant p scores came from overall values of greater than 1.2- and less than 0.8-fold change.

7.5.3 Summary

Overall this showed that cancer-related genes have a point mutation rate similar or less than background level if the mutation rate is examined by SNV/Kb in the gene (**Section 7.5.1.1**). As expected, there was a high mutation rate throughout the genes in highly variable gene sets such as TCR, IgG and HLA genes (**Section 7.5.1.2**).

The Immunity gene list showed a relatively high fold change in SNV/Kb compared to background levels across all cancer types (**Section 7.5.1.2**). Indicating the genes on this list have a relatively high rate of mutation occurring through the gene. IRIS and Innate GO gene lists had a SNV/Kb rate comparable to background for all cancers examined (**Section 7.5.1.2**). Indicating that throughout each of the genes on these lists the rate of mutation along the gene was stable and similar to background levels.

There were a number of cancer types that had a high rate of SNV/Kb in the CIT list (**Section 7.5.1.2**). This was particularly evident in DLBC, which also showed high fold change SNV/Kb in PI3K and Immunity gene lists. As DLBC is a lymphoma, it is not surprising that the rate of SNV/Kb is high in immune-related genes. The majority of other cancers in which the SNV/Kb rate was determined for the CIT list were approximately 1. The CIT list showed a similar level of continuous mutation as background levels for most cancers examined.

Together this data shows that the rate of SNV/Kb in cancer-related genes is similar or less than background levels. This indicates that mutations occurring throughout the gene are less frequent in these genes than background level. In most cancer types the immune-related gene lists show a SNV/Kb similar to background levels. This shows these genes are no different to other genes within cancer in terms of the acquisition of mutations throughout the gene. As expected, this is the opposite for highly variable immune genes, TCR, IgG and HLA, which show a high level of SNV/Kb.

7.5.4 Examining mutational hotspots in gene lists through median total SNV number

To analyse recurrent mutations/mutation hotspots in the gene lists, the median total SNV was assessed. Median total SNV levels were also compared to 3 bootstrap median total SNV values to obtain a fold change value for comparison with background levels.

7.5.5 Total SNV number in cancer-related gene lists across all cancer types

Tumour suppressor genes had a median SNV of 8.41 and a 1.67-fold increase in SNV compared to background over all cancers examined. The median SNV for the Cancer Hotspots list was of 6.59 with a 1.42-fold increase in SNV across all cancers combined. Oncogenes had a value of 5.91 for median SNV and a 1.25-fold increase in SNV for all cancers examined. PI3K genes had a median SNV of 5.03 and a 1.19-fold increase in SNV over all cancers examined. The median SNV for the MAPK gene list was 4.67 with a 1.06-fold increase in SNV across all cancers examined (**Table 7.7**). All cancer-related gene lists showed a higher fold change in total SNV compared with SNV/Kb. As well as showing a higher level of recurrent mutation than background level across all cancer types in tumour suppressor, oncogene, Cancer Hotspots and PI3K gene lists.

7.5.6 Total SNV number in immune-related gene lists across all cancer types

The median SNV for the IRIS gene list was 4.12 with a 0.98-fold change in SNV compared to background over all cancers examined. The Innate GO gene list had a value of 4.11 for median SNV and a 0.99-fold change in SNV for all cancers examined (**Table 7.7**). Both IRIS and Innate GO gene lists showed a total SNV and SNV/Kb rate close to background levels.

Immunity had a 3.91 median SNV and a 0.94-fold change in SNV over all cancers examined. CIT genes had a median SNV of 3.09 and a 0.79-fold change in SNV over all cancers examined (**Table 7.7**). Both Immunity and CIT lists showed a lower fold-change in total SNV when compared to SNV/Kb. The CIT list showed a lower level of recurrent mutation than background level across all cancer types combined.

Highly variable immune gene lists, TCR, IgG and HLA, showed a lower rate of total SNV and a lower fold change in total SNV compared to SNV/Kb (**Table 7.7**). This is as expected as alterations in these genes are variable to provide a diverse immune response, therefore it is unlikely that recurrent mutations in these genes should form.

Table 7.7 The median SNV for each of the gene lists examined along with fold change compared with background SNV level.

Gene list	Median SNV	Fold change SNV
Cancer related gene lists		
Tumour Suppressors	8.409	1.669
Oncogenes	5.909	1.248
MAPK	4.667	1.061
PI3K	5.030	1.188
Cancer Hotspots	6.590	1.421
Immune-related gene lists		
Immunity	3.909	0.943
IRIS	4.121	0.985
Innate GO	4.106	0.985
CIT	3.090	0.788
Control Gene lists		
TCR	1.652	0.570
IgG	1.667	0.612
HLA	2.697	0.772

7.5.7 Median SNV number in gene lists in individual cancer types

When broken down into specific cancer types, the tumour suppressor, oncogene, Cancer Hotspot and PI3K gene lists had a greater than 1-fold change in median SNVs in the majority of the cancers examined (**Figure 7.11**). This indicates the presence of a greater number of recurrent mutations in these genes compared to background levels. The cancer types that showed a SNV rate of close to background levels in the cancer-related genes were all cancers that had a lower sample size. The MAPK gene list showed a SNV rate close to background levels for most cancer types examined (**Figure 7.11**).

When the immune-related genes were broken down into cancer subtypes there were very few cancer types that had a SNV fold change of greater than 1 when compared to background (**Figure 7.11**). Indicating that the presence of recurrent mutations or hotspot mutations were the same as background genes within cancer. In the Immunity and IRIS gene lists all cancer types had a fold change in median SNV of approximately 1 when compared to background (**Figure 7.11**). In the Innate GO list the majority of cancer subtypes had a fold change of approximately 1. However, OV and CESC both had a

fold change greater than 1. (1.33 and 1.15 respectively), this indicates a greater presence of recurrent in the innate immune system in these cancers (**Figure 7.11**). In the CIT list, DLBC and KICH had a fold change in median SNV of greater than 1 (2 and 1.5 respectively). For all other cancers, the fold change in median SNV was 1 or less. Indicating that the level of cumulative SNVs in this gene list is generally lower than background levels of mutation, suggesting there is less likely to be recurrent or hotspot mutations present in these genes than in cancer-related genes (**Figure 7.11**).

This suggests that the overall mutation rate for cancer-related genes is higher than background levels. The general immune-related genes have a total mutation rate similar to background levels for most cancer types. Within the CIT list, which is composed of clinically relevant immunotherapy targets, there appears to be a lower rate of overall mutation in most cancer types examined.

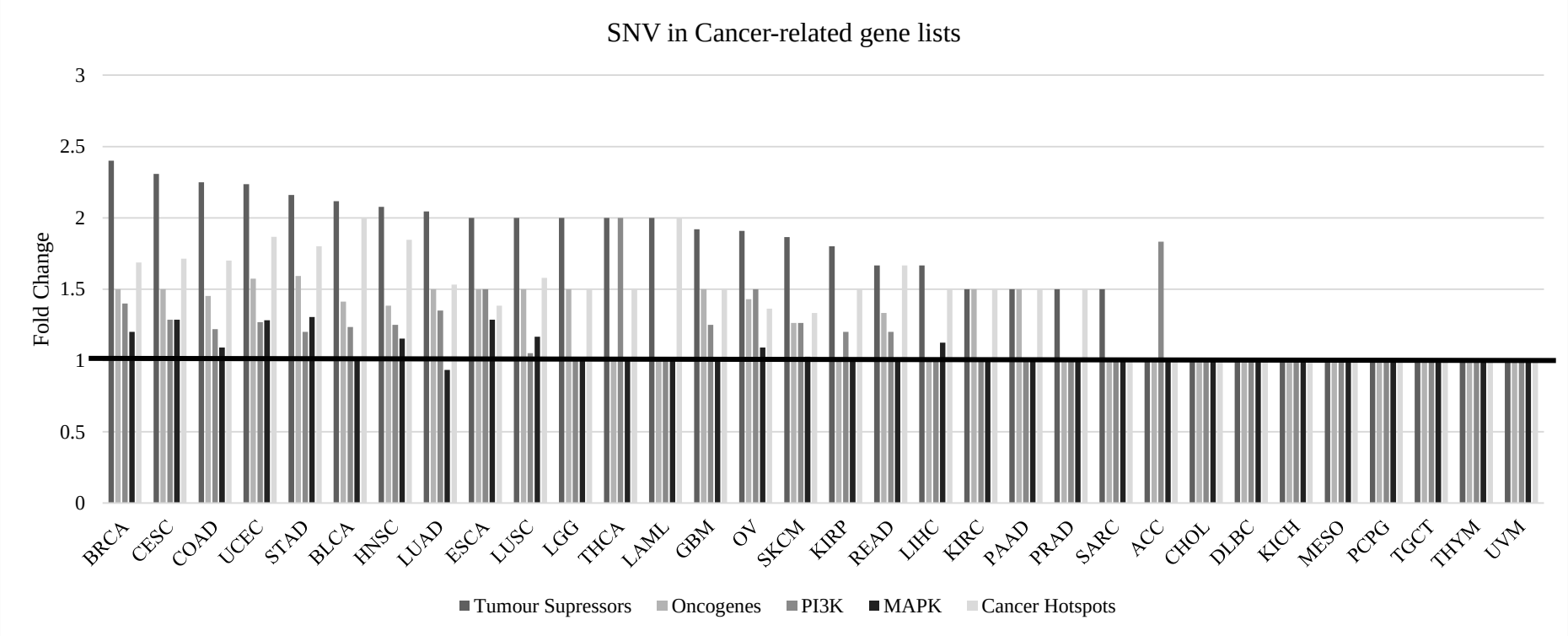

Figure 7.11: Fold change of median number of SNV in cancer-related gene lists compared with background levels for 33 cancer types from TCGA dataset. Fold change of 1 denoted by black line. Fold changes of greater than 1 show an increased level of total SNV compared with background, indicating the presence of recurrent mutation.

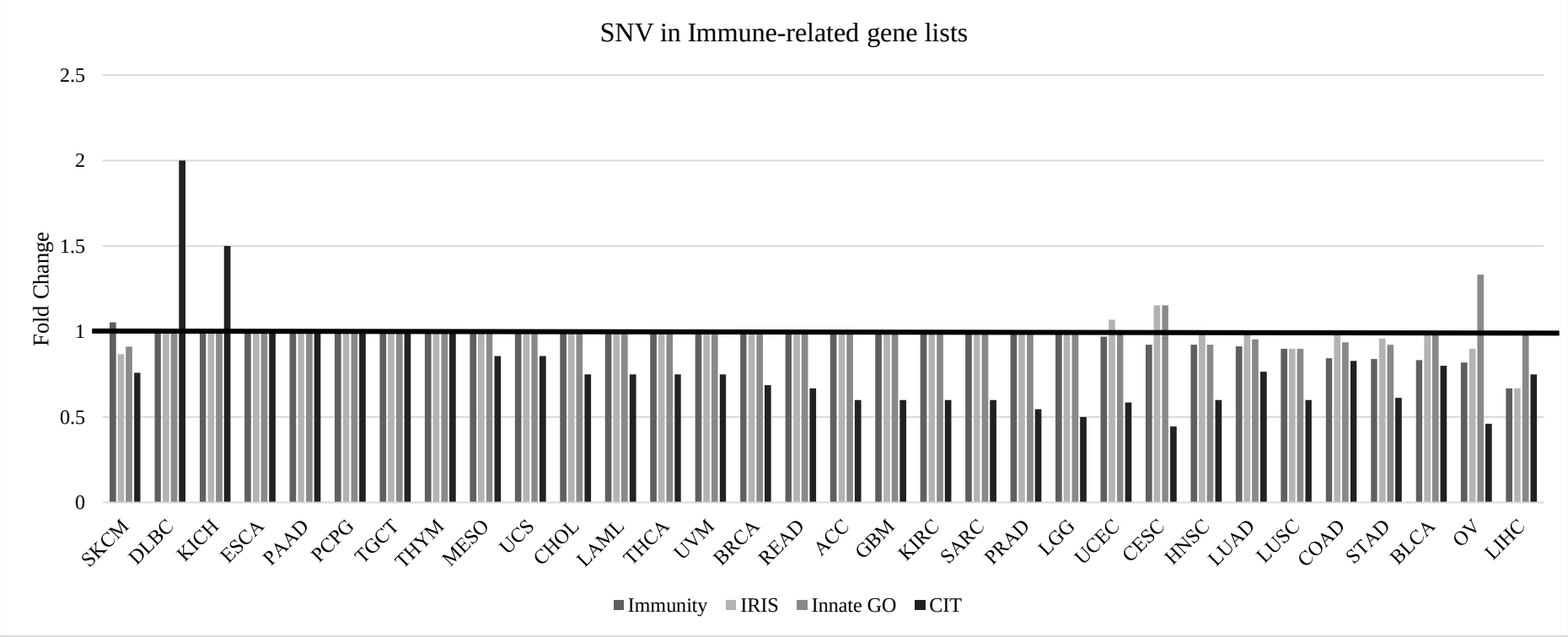

Figure 7.12: Fold change of median number of SNV in immune-related gene lists compared with background levels for 33 cancer types from TCGA dataset. Fold change of 1 denoted by black line. Fold changes of greater than 1 show an increased level of total SNV compared with background, indicating the presence of recurrent mutation.

7.5.8 Summary

Overall this showed that cancer-related genes have a higher level of recurrent or hotspot mutations present than other genes present in cancer cells (**Section 7.5.5**).

All immune-related gene lists examined had a total SNV fold change of less than 1. This indicates that immune-related genes contain similar or lesser amount of recurrent and hotspot mutations than background (**Section 7.5.6**). This was particularly seen in the CIT list which had the low fold change across the majority of cancers examined (**Section 7.5.6**).

This data shows that immune-related genes, particularly those being targeted clinically with immunotherapies, harbour less recurrent or hotspot mutations than cancer-related genes. This evidence supports the original hypothesis that immune-related genes are less susceptible to mutation.

7.6 Mutations in the Innate GO gene list

The fold change in median SNV was higher than background for the Innate GO gene list for cervical (CESC) and ovarian (OV) cancer (**Figure 7.12**). This would suggest the innate immune system has a higher rate of mutation than background in these cancers. This did not occur for other cancer types.

To further investigate, the top 25 genes with the highest number of SNVs in the Innate GO list that occurred in ovarian cancer were identified. This had to be expanded to the top 27 genes as some genes had the same number of SNVs occurring (**Table 7.8**). These genes were put through gene ontology analysis in order to examine what relevance the higher mutation rate was [287]. One of the significant gene ontology functions that came from this was the defence response to viral infection (**Table 7.9**). This was also the case when the gene ontology for cervical cancer was assessed. Cervical cancer has a proven clinical link with viral infection [374], ovarian cancer does not.

As a preliminary test, the top 27 mutated genes in ovarian cancer were compared with the top mutated genes in Innate GO gene list for other cancer types. The percentage crossover in top mutated genes was determined and the link to viral infection in these cancers was investigated in the literature. Out of the 7 cancer types that shared greater than 40% of the top mutated genes with ovarian cancer (including cervical cancer), 4 had a clinically proven viral association (**Table 7.10**). As the percentage crossover with the top 27 ovarian gene lists decreased, the proven clinical association with viral infection reduced (**Table 7.10**).

Table 7.8: Top 27 genes with most mutations in the Innate GO gene list in ovarian cancer

Gene	SNV in OV
MTOR	27
ITPR3	24
TRIM5	24
NLRP3	22
CREBBP	21
NLRC5	21
EGFR	20
PRKDC	20
DOCK1	19
ADCY9	17
ADCY3	16
ERBB3	16
LYST	16
PDE1C	16
ADCY2	15
C2	15
C5	15
MASP1	15
MYH2	15
TLR1	15
TNRC6A	15
EP300	14
IRS1	14
ITK	14
ITPR1	14
MALT1	14
NCAM1	14

Table 7.9: Viral gene ontology associated with genes from Table 2.8. Shown are the relevant ontologies with the number of genes involved in the process in total and on the list submitted. Also shown are the expected number of genes from the list to be included in the process based on the size of the list submitted and the number of genes involved in the process, as well as the fold enrichment based on how many genes are actually involved, a + or – sign is then used to denote whether this is a positive enrichment. The p value is the significance attached to the likelihood of these genes being involved based on the fold enrichment determined by Fisher's exact test, with the false discovery rate (FDR) to minimise non-significant findings.

Gene Ontology	Genes involved in process	Genes involved from Table 2.8	Expected	Fold enrichment	+/-	raw P value	FDR
Defence response to virus	186	4	0.24	16.76	+	9.56E-05	1.25E-02
Defence response	1261	12	1.62	7.42	+	1.67E-08	1.31E-05
Response to stress	3367	22	4.32	5.09	+	1.16E-13	9.06E-10
Response to external stimulus	1975	12	2.53	4.74	+	2.16E-06	7.35E-04
Multi-organism process	2336	12	3	4	+	1.24E-05	2.82E-03
Response to virus	275	4	0.35	11.34	+	4.15E-04	3.44E-02
Immune effector process	1059	10	1.36	7.36	+	4.15E-07	2.24E-04

Table 7.10: % list homology of top 27 mutated genes in Innate GO for ovarian cancer other TCGA cancer subtypes. Proven clinical and published viral association with TCGA cancer subtypes.

Cancer type	% genes in top 27 of OV Innate GO list	Proven clinical association	Evidence of association of virus and cancer in literature	Reference
OV	100	-	(queried Human papillomavirus (HPV), cytomegalovirus (CMV))	[375]
UCEC	51.85	-	-	-
STAD	48.39	EBV	Epstein-Barr virus (EBV)	[376]
BRCA	48.15	-	mouse mammary tumour virus (MMTV), HPV, EBV.	[377]
CESC	48.15	HPV	HPV	[374]
GBM	48.15	-	human cytomegalovirus (HCMV)	[378]
HNSC	44.44	HPV	HPV	[379]
READ	41.38	HPV	HPV	[380]
LUAD	40.74	-	(queried link with HPV, EBV)	[381]
PAAD	40.74	-	(queried link with chronic hepatitis)	[382]
BLCA	40.00	-	HPV	[383]
LUSC	39.29	-	(queried link with HPV, EBV)	[380]
LGG	38.71	-	(queried link with EBV, SV40, WMSV)	[384,385]
PRAD	37.50	-	(queried link with HPV)	[386]
LIHC	36.11	HCV, CHBV	Hepatitis C (HCV), chronic hepatitis B (CHBV)	[387]
ESCA	34.48	-	(queried HPV)	[388]
KIRP	33.33	-	-	-
SKCM	32.14	-	-	-
UCS	29.63	-	-	-
COAD	28.57	-	EBV	[389]
LAML	25.81	-	-	-
ACC	24.14	-	-	-
SARC	21.43	Kaposi Sarcoma HHV-8, HIV	Kaposi Sarcoma- HHV-8 and HIV	[380]
KIRC	20.93	-	-	-
CHOL	19.15	-	HCV, CHBV	[390]

THCA	18.75	-	(queried EBV)	[391]
UVM	16.67	-	-	-
TGCT	11.11	-	HIV	[392]
PCPG	8.91	-	-	-
KICH	8.49	-	-	-
DLBC	8.33	-	HHV-8, EBV	[393]
THYM	7.74	-	-	-
MESO	4.80	-	(queried SV40)	[394]

7.7 Summary

The aim of this analysis was to investigate the hypothesis that the immune system is a more stable target for anti-cancer treatment as it is less susceptible to mutation than commonly targeted cancer-related genes. A lower rate of genomic alteration of immune-related genes may allow for the relatively high and durable response rate in previously difficult to treat, highly mutated, treatment refractory cancer types.

A range of cancer-related and immune-related gene lists were assembled from literature and database searches (**Section 7.2**). The promoter conservation rate of certain gene lists was determined as a preliminary investigation, the gene lists used in the analysis were present in the range between high conservation and low conservation as categorised by the transcription factor and housekeeping gene lists (**Section 7.3**).

The AMP/DEL rate was generally lower than background for the immune-related gene lists (Immunity, IRIS and CIT), whereas the cancer-related gene lists - oncogenes, tumour suppressors, and PI3K, did not have a lower than background rate of AMP/DEL. This suggests that immune genes, bar those associated with the innate immune response (Innate GO), are less susceptible to AMP/DEL than cancer-related genes, supporting the original hypothesis (**Section 7.4**). The relative increase in AMP/DEL in the innate immune system is an interesting observation which may indicate these genes are less conserved than other immune-related gene sets.

Point mutation rates for the gene lists were reported as SNV (overall numbers of mutations including multiple mutations at the same site) or SNV/Kb (the number of mutation sites per kilobase of gene). A median value and a fold-change versus background was generated for each. The general frequency of mutation per kilobase among cancer-related genes is similar to or lower than background level of mutation, but the overall rate of mutation taking into account recurrent mutations in the same location, is higher than background levels. This would be expected in the context of driver mutations in cancer-related genes (**Section 7.5.1.1 and 7.5.5**).

When the point mutation rate was examined in the immune-related genes, the fold change in median SNV/Kb was approximately 1 for most cancers, indicating the frequency of mutation per kilobase occurring throughout the gene similar to background levels (**Section 7.5.1.2**). When the total SNV was examined, it was 1 or less for the majority of the cancer types examined, particularly in the CIT list where many cancer subtypes had a fold change of less than 1, with an average fold change of 0.788 in SNV across all cancers examined compared to background (**Section 7.5.6**).

For immune-related genes, the fold change of SNV/Kb and total SNV were either similar to background or lower than background for most cancers. Which is as expected as immune-related genes should not contain oncogenic driver mutations.

The immune gene lists studied displayed decreased AMP/DEL levels and do not have point mutations that exceed background mutational levels in cancer for the majority of cancer types examined, with the immune checkpoint gene list (CIT) displaying reduced frequency of recurrent or hotspot mutation (total SNV) *versus* background in 25/32 cancer types examined. These results support the hypothesis that the genes of the immune system are less susceptible to mutation in cancer providing a stable target

Within the Innate GO list, 2/32 cancers, ovarian cancer and cervical cancer, had a higher fold change in total SNV compared to background. This suggests that the innate immune system is more mutated than average in these cancers. Cervical cancer is known to be associated with viral infection (HPV). Examining the ontology of the most mutated innate GO genes in ovarian cancer suggests these genes play a role in viral defence. An investigation of mutated viral-defence associated genes in ovarian cancer and cervical cancer is warranted.

7.8 Discussion

7.8.1 AMP/DEL rate is lower in immune-related gene lists

Amplification and deletion are specific types of genetic alterations that contribute to oncogenesis and therapy resistance [395]. Beroukhim *et al.* found that across the 3,131 cancers examined that per sample, 17 % of the genome was amplified and 16 % deleted [395]. Within this they showed that the most oncogenic amplifications or deletions occurred across multiple cancer types implicating it as a common genomic alteration across cancer [395]. Amplified genes can be targeted with anti-cancer therapies because they can result in oncogenic pathway activation, or oncogene addiction, as is the case with trastuzumab and HER2 amplification [295,396]. However, the genomic instability within tumours means amplification and deletion events can continue to occur throughout treatment, allowing cancer cells to develop resistance to therapy [397–401].

Microarray-based comparative genomic hybridisation (aCGH) data is a method for analysing copy number variations (CNVs), or AMP/DEL levels, relative to ploidy level in tumour samples DNA [402]. Using an aCGH dataset (244A), Dr. Stephen Madden examined the AMP/DEL rate in 4 immune gene lists in 10 cancer subtypes (**Section 7.4**). In this analysis, the AMP/DEL rate was lower than background sample CNV levels for three sets of the immune gene lists (Immunity, IRIS and CIT) over all cancer types combined (**Section 7.4.2**). The AMP/DEL rate was not lower than the background level of CNV for the tumour suppressor, oncogene or PI3K related genes in the cancers examined (**Section 7.4.1**). This implies that genes of the immune system are less susceptible to AMP/DEL than cancer-related genes in the dataset examined and, more interestingly, may be less susceptible to AMP/DEL in general. The fact that the CIT list followed this trend is of particular importance as that list contains the genes currently being targeted by ICIs. These genes are therefore less likely to be susceptible to *de novo* resistance through AMP/DEL events.

The Innate GO gene list did not follow the same trend as the other immune-related gene lists (**Section 7.4.2**). This shows that the genes associated with the innate immune system in tumours are not as protected from AMP/DEL as other components of the immune system. This may affect targeting aspects of the innate immune system therapeutically. The MAPK gene list also had a lower rate of AMP/DEL than background across all cancers combined (**Section 7.4.1**). This indicates the MAPK pathway may be more conserved than other cancer-related signalling pathways when it comes to AMP/DEL. However, the MAPK pathway is a hotbed for oncogenic driver point mutations [350,403,404]. This highlights the importance of examining both AMP/DEL and point mutations in this study.

It is worth investigating the mechanisms that could underlie the lower than background levels of CNVs in particular datasets. The genetic instability which occurs in malignant cells allows for multiple

genomic alterations which can lead to amplification [405]. These events are caused by aberrant homologous recombination and DNA annealing [405]. This can lead to tandem arrays of copies in alternating direction (TID) which progressively adds copies of the gene to the genome. Amplification can also be stimulated by double strand breaks in DNA, this often occurs in A/T rich, G/C skewed "fragile" DNA regions [406]. Palindromic sequences can also lead to genomic amplification, these sequences can generate breaks and form a dicentric chromosome [407]. Deletions also occur through multiple mechanisms, primarily through the loss of DNA sequences. One example of deletion is through the loss of the sequence which spans the centromere leading to the gene being lost during cell division [408]. Immune-related genes may be less likely to undergo these kinds of events which leads to lower rates of AMP/DEL than background. It has also been shown that mismatch repair, which is often absent in malignant cells, can conserve genomic integrity by protecting epigenetic systems [409]. Mechanisms such as this may be present in immune-related genes and protect from amplification and deletion occurring.

Overall, the results suggest that the AMP/DEL rate is lower in three of the immune-related gene lists (innate genes excluded) than cancer-related genes (MAPK genes excluded). This provisionally supports the initial hypothesis surrounding the conservation of immune system-related genes.

7.8.2 Hotspot mutations are reduced in immune-related genes

The point mutation rate of the gene lists was also determined (**Section 7.5**). Bozic *et al.* state that cancer driving mutations form until a threshold for cancer development is reached [283]. Therefore, the genes which are key to cancer developing are more likely to be mutated and selected for, to be mutated in a crucial location i.e. a hotspot. Miller *et al.* and Chang *et al.* confirmed the presence of recurrent hotspot mutations, in genes such as TP53, Ras, EGFR and RAF [410,411]. This occurred across different cancer types, showing singular mutations throughout the gene to be rarer events in cancer driving genes [410,411]. The recurrence of these mutations and the key role they play in cancer growth marks them targets for therapeutic intervention. Examples include the EGFR inhibitor getfitinib and BRAF inhibitor vemurafanib. The major clinical issue is that the genomic instability within cancer genomes allows resistance to these therapies to develop more often than not [412–414].

In this analysis the point mutation rate of the gene lists was determined across 33 different cancer types by Dr. Bruce Moran. Dr. Moran used the MuTect method developed by the Broad Institute to determine the somatic point mutation rate in next generation sequenced cancer e.g. TCGA data set. The SNV occurring per kilobase and the total number of SNVs were determined to examine continuous and hotspot mutation (**Section 7.5**). The background level of mutation in this study is the mutation rate in sequenced genes from tumours. This means a mutation rate similar to background level with the general mutation rate within cancer.

Cancer-related genes (tumour suppressors, oncogenes, PI3K, MAPK and cancer hotspot lists) showed a lower rate of mutation throughout the gene than background over all cancer types combined but more commonly possessed recurrent hotspot mutations across all cancer types combined (**Section 7.5.1 and 7.5.5**). This shows that in cancer-related genes there is a predisposition to hotspot mutation compared with all genes in the tumour, and that mutations throughout the gene in the cancer-related gene lists are occurring at a less common rate than in other genes present in cancer. This is supported by general consensus of the presence of hotspot mutations in cancer driving genes as stated earlier [410,411].

Immune-related genes (Immunity, Immune Response *In Silico* (IRIS), Innate GO and Current Immune Targets (CIT) lists) had a mutation rate close to background level for mutations occurring throughout the gene (**Section 7.5.1**). This suggests that immune-related genes undergo a "normal" amount of point mutation within cancer. Across all immune gene lists there was a recurrent point mutation rate equivalent to background, or lower, for most cancer types examined (27/33 caner types) (**Section 7.5.6**). These results demonstrate that for the majority of cancer types examined, immune-related genes are not as susceptible to hotspot mutations as cancer-related genes. This makes sense as the process of immune escape and immunoediting e.g. reduction of MHC class-I expression, can occur at the transcriptional and post-translational level while selection for characteristics such as oncogenic proliferation is more successfully driven through persistent genomic mutations.

In 26/33 cancer types the CIT list had a lower point mutation rate than background levels. This shows that the genes being targeted by current immunotherapies do in fact have a lower rate of hotspot mutation (total SNV) and are a more genetically stable target than cancer pathways in the majority of cancers. The CIT list showed some exceptions to this with a particularly high rate of mutation in DLBC. This did not occur in Acute Myeloid Leukaemia which was the other immune cell cancer examined (**Section 7.5.1**). DLBC may be an exceptional case and requires further investigation to determine the reasons underlying the results found.

Immune-related genes may not be under the same mutational pressure as cancer-associated genes. The level of recurrent mutation is higher than background in all cancer-related gene lists examined across the majority of cancer types investigated. Immune-related gene lists possessed an average amount of continuous mutations occurring throughout the gene but these genes do not contain as many recurrent or hotspot mutations as the cancer-related gene lists. The rate of recurrent mutations was particularly low in genes in the CIT list. This indicates that the targets of clinically relevant treatments are less likely to be altered by commonly occurring mutation. Overall the data generated supports the hypothesis that immune-related genes, including those currently targeted by ICIs, are generally more conserved (AMP/DEL, point mutation) and a more stable target for ICIs in the majority of cancer types.

7.8.3 Mutation of the innate immune system in ovarian and cervical cancer

From the point mutation analysis in this thesis, ovarian cancer and cervical cancer were the only cancer types of 33 which showed a total SNV rate higher than background level for the Innate GO gene list (**Section 7.6**). This suggests a higher level of dysfunction in innate immune-related genes in these cancer types.

The innate immune system provides rapid defence via pattern-recognition receptors and Toll-like receptors which recognise and destroy pathogens [415]. This is also how the body defends against viral infection. The link between cervical cancer development and HPV infection has been proven beyond reasonable doubt. Integration of HPV, particularly HPV 16 and 18, into cervical cells causes deregulation of the cell cycle in order to allow for viral replication [416]. This can lead to cancer developing in these cells. This can be the result of ineffective innate immune response or by damage to the immune response caused by the virus [417].

Ovarian cancer arises from the ovary, the fallopian tube, or the mesothelium-lined peritoneal cavity [418]. There are two types of ovarian cancer. Type I is a slow growing tumour which progresses into a well-differentiated carcinoma [418]. Type II involves a high rate of mutation and the development of a high-grade serous carcinoma which is more aggressive [418]. High-grade serous carcinoma accounts for 70 % of death resulting from ovarian cancer [419]. This cancer type possesses a high rate of genetic instability. Chronic infection leads to immune dysregulation and is shown to cause 15 % of malignancies [375]. Trabert *et al.* [420] found that the risk of ovarian cancer was lessened in people treated with anti-inflammatory agents (n=7776). Protection from continuous inflammation caused by chronic infection, which leads to potential damage of the innate immune system, may decrease the risk of ovarian cancer. Therefore, it is relevant to investigate causes of inflammation, infection and innate immune response damage in ovarian cancer.

Some studies have shown a provisional link between HPV and HCMV in ovarian cancer [421–423]. Although a clinical association between viral infection and ovarian cancer has not been proven. Studies have shown that inflammatory mediators and defective immune responses can be important in ovarian cancer development and progression [420]. However, there remains no conclusive evidence of a link between ovarian cancer, a dysfunctional innate immune response and viral infection.

The most mutated genes in the Innate GO list for ovarian and cervical cancers were associated with viral defence based on their gene ontology. This is expected for cervical cancer due to the nature of its viral aetiology. There is already a clinically proven link between HPV and cervical cancer. The most mutated genes in the Innate GO list in ovarian cancer had a high homology with the top mutated genes in cervical cancer. The overlap of these genes in other cancers was highest in cancers clinically

associated with viral infection. The nature of these genes and their involvement in cancer as well as viral infection should be investigated further.

Due to the ontology of the most mutated innate immune genes in ovarian cancer and the overlap with other classically virally associated cancers, this thesis proposes a speculative hypothesis that there may be a link between viral infection and ovarian cancer based on the data analysis carried out. HPV and CMV viruses have been linked to ovarian cancer [375]. These links have not led to a proven clinical association between ovarian cancer and viral infection. A comprehensive investigation of HPV and CMV alongside other known cancer-causing viruses EBV, HPV, CHBV, Kaposi and HHV-8 in patient material is needed.

8. Overall discussion and conclusions

8.1 Introduction

Immune checkpoint inhibition has revolutionised the treatment of certain cancer types. PD-1/PD-L1 ICIs nivolumab, pembrolizumab and atezolizumab have been approved as first line treatment options as well as across a range of heavily pre-treated, metastatic and advanced cancers (**Table 1.1, 1.2 and 1.3 Section 1.2**). More needs to be done to understand how these drugs and their targets work with the aim of increasing response rates and developing rational treatment combinations.

There are no ICIs currently approved for the treatment of breast cancer. The HER2+ and TNBC subtypes are classed as immunogenic, due to infiltration of TILs and a primed immune response [214,215,217,239]. This indicates that certain types of breast cancer may benefit from immune checkpoint inhibition. Trastuzumab is a gold standard treatment for HER2+ breast cancer [295]. An active immune response is crucial in responding well to trastuzumab treatment [264,424]. Understanding factors that affect the immune response may benefit those who do not respond to trastuzumab or relapse on trastuzumab treatment. This is investigated in Chapter 3 using patient PBMC samples from the TCHL (ICORG10-05) trial.

Due to an active immune response being beneficial in clinical response to trastuzumab, there may be a potential benefit of combining ICIs with trastuzumab therapy. This is currently being investigated in clinical trials in breast cancer [258,260]. The interaction of these drugs needs to be examined further pre-clinically to examine mechanisms of action, rationale for novel combinations and potential for predicting response to treatment. An *in vitro* model of examining the combination of trastuzumab and ICIs was developed in Chapter 4.

Targeting tumour signalling pathways may also affect immune checkpoint-mediated immunosuppression. In lung cancer, there is pre-clinical evidence of a link between EGFR activity and PD-L1 expression [97,98,279,280]. Within breast cancer this could indicate potential for targeting EGFR in combination with immune checkpoint inhibition. A link between EGFR activity and PD-L1 expression in breast cancer was examined in Chapter 5.

There are also emerging immune checkpoints in the tumour microenvironment, such as the adenosine receptor A2AR [358]. An immunosuppressive tumour microenvironment allows tumours to grow unchecked, it also lessens likelihood of response to trastuzumab treatment [264]. The effect of adenosine and the inhibition of A2AR was examined in Chapter 6 to examine the factors underlying immunosuppression in the tumour microenvironment. This approach is currently under clinical investigation [202].

Targeting the immune system appears to be eliciting durable responses in patients who have relapsed on multiple treatment regimens [109,311]. A lower susceptibility to genomic alteration may provide

rationale for the immune system as a more robust, stable target for anti-cancer treatment than the frequently targeted oncogenic drivers within the tumour to which resistance often arises. The mutation rate of the immune system in cancer was investigated in Chapter 7.

8.2 Cytotoxicity profile of PBMCs isolated from HER2+ breast cancer patients on the TCHL clinical trial (ICORG10-05)

Trastuzumab binds to HER2 and acts by inhibiting intracellular signalling and by generating an ADCC response against the tumour cell. ADCC is a normal effector cell-mediated process of immune response within the body, relying on antibodies generated against specific antigens which are part of the humoral immune response. These antibodies bind to antigens on the surface of cells that are recognised as foreign, such as tumour cells. Effector cells of the immune system, such as NK cells, interact with the antibodies through Fc receptors causing the effector cell to release cytotoxic factors and lyse the target cell. The ADCC response is an important part of the mechanism of action of trastuzumab. Clynes *et al.* demonstrated that CD16 knockout mice show a severely attenuated response to trastuzumab, and that if the Fc region of trastuzumab is mutated the anti-tumour effects of the antibody are greatly reduced [26]. It has also been demonstrated in multiple *in vitro* studies using patient immune cells that T-ADCC correlated with response to trastuzumab treatment [263–265]. Beano *et al.* [265] measured NK cell mediated-ADCC using NK cells isolated from patients with metastatic HER2+ breast cancer following one round of neo-adjuvant trastuzumab and chemotherapy treatment. They showed that increased NK cell activity and ADCC levels correlated with a long-term clinical response to trastuzumab treatment [265]. Varchetta *et al.* demonstrated a partial correlation between ADCC levels and response to treatment, they used primary HER2+ breast cancer patient PBMC samples which were taken after the commencement of neo-adjuvant trastuzumab monotherapy [263]. They also showed the importance of CD16+ NK cells in eliciting a positive response to trastuzumab [263]. Gennari *et al.* [264] found that a higher level of ADCC and TILs correlated with a positive clinical response to trastuzumab in HER2+ breast cancer patients treated with neo-adjuvant trastuzumab. These studies provide evidence for the importance of ADCC in eliciting a positive response to trastuzumab and therefore the importance of having an immune response capable of engaging in ADCC when receiving trastuzumab treatment. All of these studies showed a correlation between T-ADCC and response to trastuzumab after patients had received treatment, none were capable of using pre-treatment T-ADCC levels as an indicator of response to neo-adjuvant therapy.

The phase II TCHL (ICORG10-05) neoadjuvant clinical trial compared chemotherapy (TC) in combination with either trastuzumab alone (TCH), lapatinib alone (TCL) or lapatinib with trastuzumab (TCHL) in 88 HER2+ breast cancer patients. There was no significant difference in response to neo-adjuvant therapy between the TCH and TCHL arms (pCR rates were 48% (16/33) for the TCH arm and 44% (7/16) for the TCHL arm) [425]. The Neo-ALTTO study did show an advantage for the addition of

lapatinib to trastuzumab plus chemotherapy but a different chemotherapy backbone was used and it also had a larger number of patients (n=455) [426]. The final overall survival data from the TCHL study will be available in 2019. Blood samples were taken from patients before (pre-treatment) and after they received treatment, pre-surgery (post-treatment). This time period covered 6 cycles of chemotherapy over approximately three months. PBMCs were isolated from whole blood and frozen until needed for use in the assay. Immune cytotoxicity assays and SNP analysis were performed using the PBMCs from the trial to examine the immune activity of PBMCs isolated from these patients and to phenotype a number of immune response-related and drug response-related genes for variations that could be associated with patient response to therapy.

The status of tumour-associated immune cells is generally accepted as the most important factor when assessing the anti-cancer immune response but results from this thesis, and from others, suggest that circulating immune cells may also have tumour and patient outcome relevant information. The complex interaction between patient PBMCs and tumour cells was explored. Samples from patients who progressed through chemotherapy-containing treatment elicited a lower level of T-ADCC than pre-treatment levels. This decrease in post-treatment T-ADCC is associated with patients who had a CR to treatment. Indicating that completion of this neo-adjuvant treatment regimen leads to a downregulating of the cytotoxic capacity of circulating immune cells which can be affected by response to treatment.

It has also been shown that 50 % of patients with a Non-CR have PBMCs who's T-ADCC functions are enhanced through exposure to an anti- PD-1 inhibitor. This *in vitro* response to PD-1 inhibition does not occur in the CR cohort examined. This may allow for the immune cytotoxicity test to be used to predict response to neo-adjuvant chemotherapy in HER2+ breast cancer and potentially indicate patients that have immune cells that can respond to PD-1 inhibition. More work is needed to expand the number of HER2+ BC patients to further validate these findings. Blood samples from patients currently receiving ICIs are also required to examine the potential ability of the test to predict response to ICIs. The current results form the basis of a patent application. If successful, this test could be used commercially to assess the likely outcome of a patients' treatment regimen or potentially indicate a treatment of benefit (i.e. an immune checkpoint inhibitor).

This study has also shown that SNPs present in the patients' genome can affect cytotoxicity. SNPs in the ABCB1 gene affect direct cytotoxicity while SNPs in the KLKR1 gene showed differences in pre-treatment T-ADCC, which may be important in the success of neo-adjuvant trastuzumab. SNPs in FCG3A showed alterations to direct cytotoxicity after receiving neo-adjuvant chemotherapy and trastuzumab. Further investigation of the impact of these SNPs on response to treatment and PBMC-mediated cytotoxicity is needed in a larger patient cohort.

8.3 The development of an assay to examine the effect of immune checkpoint inhibitors *in vitro* using immune cells isolated from healthy volunteers

A minority of patients respond to ICI monotherapy and there are severe adverse effects associated with treatment. ICIs are expensive, putting additional emphasis on those patients that will receive therapy but will not respond to it. Robust and reliable pre-clinical systems would allow for exploration of the mechanisms of action of ICIs to inform disease types, biomarkers of response and rational treatment combinations.

It is difficult to examine the functions of ICIs *in vitro* due to the complex interplay between the immune system and the tumour. Most pre-clinical evidence for the efficacy of ICIs are seen in syngeneic and humanised mouse models.

Syngeneic mouse models are allograft tumour systems which use immortalised mouse cancer cell lines [146]. These cells are then engrafted into a mouse model with the same genetic background. Syngeneic mice possess a functional murine immune response. The identical host and cell line genetic background means the tumour is not rejected [146]. The intact immune response allows it to be used for pre-clinical investigation of immunotherapies. This model is limited as it is examining the murine system rather than human system. There is also a limit on the flexibility of the system as only certain cell lines and strains can be examined [146]. These models are also costly and time consuming.

Humanised mouse models are also available, these models are complex due to the need for implantation of a functional humanised immune response. Human cell lines or patient-derived xenografts can be implanted into immunocompromised mice, as is routine for examination of cytotoxic agents [147,427]. In order to provide a competent human immune response against the tumour, human PBMCs or hematopoietic stem cells are co-implanted with the tumour [147,427]. These models are complex and expensive. There are also limitations on the mouse models that can be used. Severe combined immune deficiency (SCID) mice are most commonly used but these mice develop host vs. graft disease at approximately 4 weeks which limits duration of the experiment [147].

In vitro tests often examine the effect of ICIs on specific immune cell functions in isolation, e.g. T cell activation, proliferation, exhaustion, chemotaxis, cytokine response and ICI binding [148–150]. The impact of ICIs on tumour cell death is rarely looked at *in vitro* as the standard immunological model for the efficacy of ICIs depends on the presence of checkpoint-inhibited antigen –specific T cells only [146]. Immortalised T cell effector cell populations against existing cell line models are not readily available. Studies are now emerging that other immune cell types express immune checkpoints (e.g. NK cells [58,304,323]) and the impact of ICIs on these immune subsets could be evaluable *in vitro* as anti-cancer cytotoxicity effects are not antigen-dependent [22]. Some models have shown T cells/tumour cell co-

culture results but rely on surrogate markers for T cell-induced cell death such as activation of the PD-1/PD-L1 signalling axis quantified using luminescent luciferase reporter assays [151,152].

Flow cytometry-based models which co-incubate immune cells and cancer cells and use viability dyes to determine cell death have emerged as mechanisms of examining immune relevant treatments *in vitro* [105,153]. This allows for single cell analysis of the cancer cells and measurement of cancer cell death due to specific a treatment condition. These models are still under development and there is no current consensus on immune effector cells and conditions for consistent assay success.

In Chapter 3 the model developed to measure cell death caused by ICI treatment used patient immune cells. The aim of this chapter was to develop a method of examining the mechanisms of ICIs using more readily accessible healthy volunteer immune cells. The development of the assay was based on functional assessment of effector cells against breast cancer cell lines and did not include detailed volunteer-specific phenotyping of PBMC, T cell or NK cell subsets. The goal was the identification of a cytotoxic anti-tumour, healthy volunteer immune response to breast cancer cell line models that could be consistently measured and used to assess the impact of ICIs *in vitro*.

This thesis shows that the effects of ICIs on immune cell-mediated cytotoxicity can be examined *in vitro* using the flow-cytometry-based immune cytotoxicity assay utilised in this thesis. Healthy volunteer PBMCs and IL-2 stimulated NK cells were found to be consistently capable of examining the effects of ICIs *in vitro*. This shows that this method can be used to assess the effects of ICIs *in vitro* allowing for relatively inexpensive and high throughput pre-clinical analysis of these drugs against a range of cancer cell line models with a variety of treatment conditions. Healthy volunteer activated T cells can also be used to examine changes to direct cytotoxicity caused by ICI but this is not as consistent an approach as it is most likely dependent on the chance presence of T cells that have specificity for antigens present on the cancer cell lines used.

The SKBR3 and HCC1954 cell lines examined showed different susceptibilities to direct cytotoxicity and T-ADCC which may be due to differential expression of immune-related proteins. These differences could be exploited in assays to examine different aspects of the immune response *in vitro* or to model low vs. high tumour PD-L1 expression.

Further investigation of the effects of ICIs on cancer cell line models should be carried out with PBMCs and IL-2-stimulated NK cells. Additionally, different ratios of effector:target cell ratios and a more comprehensive FACS analysis of immune cells should allow for a more robust analysis of these provisional effects. The completely optimised method could be used to assess the ICI and trastuzumab response against other HER2+ breast cancer cell lines, including models of resistance to trastuzumab. In theory, the immune cytotoxicity assay could be used to examine the effects of ICIs with or without other immune relevant treatments against any cancer cell line model. An example of this would be to

examine cetuximab, an EGFR-targeted ADCC-capable monoclonal antibody, in combination with ICIs against TNBC.

8.4 EGF signalling and PD-L1 expression in breast cancer cell line models

Rational treatment combinations may improve response rates to inhibition of the PD-1 axis. Combination of immune checkpoint inhibitors and targeted therapy may be beneficial, particularly if there is mechanistic evidence for potential synergy. Numerous studies in lung cancer, particularly NSCLC, have shown correlation between PD-L1 and EGFR expression [97,98,279,280,428]. D'incecco *et al.* found a significant correlation between PD-L1 expression and EGFR mutation in NCSLC patients [280]. They also showed that patients who were PD-L1+ showed a significant increase in response rate, longer progression free survival and overall survival to EGFR inhibition than PD-L1 negative patients [280].

Clinical trials examining immune checkpoint monotherapy in EGFR+ lung cancer were unsuccessful in improving overall survival [429]. Clinical investigation of dual EGFR and PD-L1 inhibition has begun in lung cancer (NCT02143466, NCT02013219 and NCT01998126). NCT02143466 evaluated durvalumab and osimertinib (a 3rd generation EGFR TKI), the trial was discontinued early due to lung-based toxicity issues [430]. NCT01998126 has enrolled 14 patients to receive either ipilimumab or nivolumab in combination with erlotinib if patients are EGFR+ [431]. Results of this trial have not yet been reported. NCT02013219 is a phase Ib trial investigating atezolizumab in combination with erlotinib [432]. Adverse effects were more tolerable in this combination, although there was still a high level of toxicity, serious irAEs occurred in 50 % of patients but there were no grade 5 events or incidences of pneumonitis [432]. A 75 % response rate and progression free survival of 11.3 months was reported out of the 20 patients treated [432]. The benefit of EGFR and PD-L1 inhibition requires further investigation in lung cancer, although treatment related lung toxicity may be an issue. The underlying signalling pathways mediating the link between EGFR and PD-L1 are unknown. Further understanding of the interaction between both proteins may help provide a clearer mechanism to target clinically. This combination may also be of benefit in other cancer types. Investigation of the different methods of blocking EGFR may also help reduce toxicity. For example, EGFR-targeted monoclonal antibodies, such as cetuximab, have not yet been examined in combination with ICIs and may be less toxic than the small molecules tested to date.

The link between EGFR and PD-L1 has been provisionally examined in breast cancer, Chia-Wei Li *et al.* [102] showed EGF treatment stabilised PD-L1 expression in two TNBC cell lines (MDA-MB-231 and BT549). They also showed a decrease in T cell exhaustion in a syngeneic mouse model following EGFR inhibition with gefitinib [102]. EGFR is expressed in 18 % of all breast cancers [275]. Dual EGFR/HER2 TKI lapatinib and pan-EGFR, -HER2 and -HER4 TKI neratinib are approved for the treatment of HER2+ breast cancer [234,235]. EGFR signalling has also been implicated in HER2-targeted therapy resistance to

trastuzumab and lapatinib [347,348]. A link between EGFR signalling and PD-L1 could be targeted with already approved breast cancer treatments which could decrease PD-L1 expression in an EGF-driven tumour. This approach may be beneficial in combination with anti-PD-1/PD-L1 therapies.

This thesis has shown the link between EGFR and PD-L1 shown in lung cancer in the literature is also present in HER2+ breast cancer. All PD-L1 high cell lines examined exhibited EGFR co-expression. There is a novel association between EGFR and PD-L1 co-alteration in HER2+ targeted therapy resistant cell lines. The link between EGFR and PD-L1 was further characterised by evidence that EGF stimulates PD-L1 upregulation through EGFR activity in both parental and resistant cell lines. Lapatinib was capable of blocking this effect. This indicates that combination of an EGFR inhibitor with anti-PD-1/PD-L1 treatment may be beneficial in controlling PD-L1 expression, particularly in an EGF driven tumour.

EGF pre-treatment of tumour cells altered the susceptibility of tumour cells to PBMC-mediated cytotoxicity. This effect was altered between parental and targeted therapy resistant cell lines showing differential EGF-mediated pathway activation between the models. The link between EGF-mediated signalling and susceptibility to the immune response requires further investigation.

The mediators of the link between EGFR and PD-L1 have not yet been fully elucidated. Future work for this study would be to investigate the potential mediators of a link between EGFR and PD-L1 other than PTPN11 and LCK in the cell line models examined. This could be done by examining the EGFR signalling network systematically with siRNA or target-specific inhibitors in combination with EGF treatment and examination of PD-L1 levels. Further work could also examine the effects of EGF treatment on immune response -related protein expression in parental and resistant HER2+ breast cancer cell lines as it appears this affects the susceptibility to the immune response.

8.5 The effect of adenosine receptor activation on immune cell-mediated cytotoxicity against breast cancer cell line models

As well as the classical immunosuppressive interaction of cancer cell:immune cell and immune cell:immune cell immune checkpoints, immunosuppression mediated by factors in the tumour microenvironment are now being considered as immune checkpoints [358]. One of these novel checkpoints is the adenosine receptor A2AR, which has been termed a metabolic checkpoint [183]. Adenosine elicits immunosuppressive effects in the hypoxic tumour microenvironment which may be detrimental to the immune response against trastuzumab [358]. Koukourakis *et al.* [365] demonstrated that increased hypoxia characterised by HIF-1α expression was associated with resistance to neo-adjuvant chemotherapy and trastuzumab treatment in 28 HER2+ breast cancer patients. Aghazadeh *et al.* [366] have also shown increased HIF-1α in trastuzumab-resistant SKBR3 cell which was associated with STAT3 and HES1 pathway activation. Inhibition of these pathways restored sensitivity to trastuzumab in this model [366].

This links resistance to trastuzumab and an immunosuppressive hypoxic microenvironment. A2AR is known to mediate the immunosuppressive functions of adenosine which is associated within a hypoxic tumour microenvironment [190].

Inhibition of A2AR as a strategy of relieving immunosuppression has recently begun to progress into the clinic. A2AR inhibition is currently being investigated in 4 early stage clinical trials (NCT02655822, NCT02403193, NCT03099161, NCT02740985). These trials are all using an A2AR antagonist in combination with either PD-1 or PD-L1 inhibition [202]. NCT02403193(PBF-509) NCT03099161(MK-3814 (preladenant)) and NCT02740985(AZD4635) have not yet reported their results [202]. In the phase Ia/Ib NCT02655822 trial, anti-A2AR agent CPI-444 is being trialled in combination with atezolizumab in advanced melanoma, NSCLC, TNBC and RCC. 48 patients were treated and the disease control rate (CR/PR or stable disease) was seen in 45 % of patients across all tumour types, particularly in NSCLC and RCC [203]. The relief of immunosuppression by combining A2AR inhibition with PD-1/PD-L1 axis inhibition appears to be a clinically attractive model. Trastuzumab is standard of care treatment in HER2+ breast cancer. The immunosuppressive effects of A2AR on the efficacy of trastuzumab needs to be established. A fully characterised approach could then proceed examining the combination of ICIs and A2AR inhibition with trastuzumab pre-clinically in HER2+ breast cancer cell lines.

Results from this thesis showed that inhibition of A2AR activation (combination of CGS21680 /preladenant) increased the immune response to trastuzumab in treatment naïve HER2+ breast cancer cell lines, but not in targeted therapy resistant models. Indicating a benefit to the combination of A2AR inhibition and trastuzumab in HER2+ breast cancer. The SKBR3-Lap cell line showed alterations in A2AR expression compared to the parental cell line. Further examination of the effects of A2AR inhibition in the SKBR3-Lap cell line in this setting may provide more information regarding A2AR inhibition in targeted therapy resistant models.

Also shown was an increase in susceptibility to immune-mediated cell killing in targeted therapy resistant cell line models, which may have implications for the use of ICIs in tumours that have become resistant to targeted therapies.

8.6 Chromosomal instability in cancer-related and immune-related gene sets

Therapies targeted at the oncogenic drivers of cell survival and growth have shown benefit in a wide range of cancers. Examples include trastuzumab targeting HER2, gefitinib which targets EGFR and vemurafanib which targets at BRAF [396,413,414]. However, *de novo* or acquired resistance is a major issue for these therapies [433–435]. In many instances, monotherapy with targeted agents can only produce an increase in progression free survival and overall survival for a limited time, with the development of resistance occurring in a significant proportion of patients [368]. There are many mechanisms of targeted therapy resistance, such as amplification of the target, mutation in the target binding site, down

regulation of the target, alternative signalling pathway co-option or alterations to upstream and downstream signalling pathways [433–435]. These mechanisms of resistance all centre on the inherent genomic instability of cancer which selects for tumour cells capable of survival and growth in the presence of anti-cancer therapies. Targeted therapies are particularly susceptible to this as they generally have one primary target.

Immune checkpoint inhibitors are a targeted therapy but they target the immune system, not the cancer [14]. The exception among current immune checkpoint inhibitors are anti-PD-L1 therapies, as PD-L1 can be expressed on tumour cells as well as immune cells [46]. Studies have shown that mutation of immune-related genes can occur within the tumour as part of the immune escape mechanism [436]. CASP8 mutations have been shown to confer resistance to FASL and TRAIL-induced apoptosis. MHC class-I mutation have been shown to occur to avoid effective antigen presentation to immune cells. As well as amplification of immune checkpoints such as PD-L1 and IDO signalling which have been shown to promote immunosuppression [436].

Resistance to ICIs is emerging clinically. Mechanisms of resistance to immune checkpoint inhibition appear to be largely tumour-intrinsic with a similar phenotype to immune escape. Alterations in neo-antigen formation, presentation by MHC class-I proteins, downregulation of targeted immune checkpoints or upregulation of alternative immune checkpoints have been reported [204,437]. The incidence of resistance to ICIs appears to be developing in a minority of patients who initially respond. Ribas *et al.* showed an initial response rate to pembrolizumab of 33 % in advanced melanoma, with 70-80 % of these patients maintaining a clinical response at three years post-treatment [367].

Durable responses to ICIs are occurring in patients with heavily pre-treated cancers, even after relapses on multiple therapies (**Table 1.1, 1.2 and 1.3 section 1.2**). For these initial and durable responses to occur, the immune system, once reactivated, must be able to engage with tumour cells to eliminate them. This suggests the tumour proteins that engage with the immune system are more likely to remain functional and were not subject to the random mutations that occur within tumour cells in mutation-heavy, therapy refractory tumours.

Our hypothesis states that the immune system is a more stable target for anti-cancer treatment than commonly targeted cancer pathways due to a lower mutation rate in immune-related genes within the tumour. A lower rate of genomic alteration in the targets of immunotherapies indicates a greater likelihood for an initial response and a lower susceptibility to alteration would allow for a sustained durable response to immunotherapies.

Overall this data supports this hypothesis and shows that genes associated with the immune response, in particular current targets of immunotherapy, do have a lower rate of AMP/DEL and hotspot mutations than commonly targeted cancer related pathways such as tumour suppressors and oncogenes. This

provides a potential reason for the durable responses seen with immunotherapy in patients who have heavily mutated tumours. The lower rate of mutation in the immunotherapy targets make them a more stable target within the tumour genome.

Particularly of interest is an observation that the mutation rate of innate immune genes is increased in ovarian cancer and cervical cancer compared to background level. This finding implicates mutation of the viral defence in ovarian and cervical cancer. To further investigate this novel finding, ovarian and cervical cancer tumour samples will be obtained from patients. DNA and RNA will be extracted and sequenced for identified genomic mutations and the concurrent presence of viral sequences. The viruses which will be examined are CMV, EBV, HPV, HCV, CHBV, Kaposi and HHV-8. The expected prevalence of these viruses will be explored and compared to the frequency of occurrence in tissue. HPV and CMV are potentially linked with ovarian cancer [375], while EBV, HPV, CHBV, Kaposi and HHV-8 are clinically established cancer-related viruses [380]. This would provide a pilot dataset for a larger study should viral sequences be found in the ovarian tissue.

8.7 Conclusions

This thesis investigated potential mechanisms of increasing the immune response against breast cancer. Given the success of immunotherapies in multiple cancer types it is beneficial to examine mechanisms for improving the immune response further within breast cancer.

Six rounds of neo-adjuvant chemotherapy/HER2-targeted therapy reduces the cytotoxic capacity of circulating immune cells. The down regulation of this cytotoxicity post-treatment was primarily associated with patients who had a CR to treatment. The HER2-targeted therapies, trastuzumab or lapatinib, received by the patient had an impact on the cytotoxicity of the circulating PBMCs. This will need to be investigated further in a larger cohort.

Pre-clinical results suggest that targeting immune checkpoints in HER2+ breast cancer in combination with trastuzumab is a viable option. Inhibition of the PD-1 signalling axis with pembrolizumab has been shown to be effective in increasing the efficacy of trastuzumab in a subset of HER2+ breast cancer patients. A biomarker assay (Patent application GB 1811892.2) was developed that can predict response to neo-adjuvant chemotherapy, and potentially ICIs, which could be used to stratify HER2+ breast cancer patients to receive these treatments.

SNPs in ABCB1, KLRK1 and FCG3A were found to be associated with alterations in PBMC cytotoxicity levels pre- and post- neo-adjuvant chemotherapy in HER2+ breast cancer.

This work developed a novel method for examining ICIs *in vitro* using healthy volunteer PBMCs and healthy volunteer IL-2 stimulated NK cells.

Immune-related protein expression alterations which may predispose cancer cells to different mechanisms of immune cell-mediated cell death with and without the addition of ICIs.

Targeted therapy resistance results in an increased susceptibility to PBMC- and NK cell-mediated cytotoxicity. This effect may be important in the context of immune-related therapies given in advanced targeted therapy resistant/treatment refractory cancers.

EGFR activation alters PD-L1 expression in HER2+ breast cancer cell line models and targeted therapy-resistant models. This effect can be blocked with EGFR inhibition in lapatinib sensitive cell lines which may indicate a potential benefit in combining EGFR inhibition with ICI treatment.

EGF treatment can also alter the susceptibility of cancer cell lines to immune cell-mediated cytotoxicity. The effects of EGF on the immune response were different between the parental and targeted therapy resistant cell lines examined, further indicating alternative EGF-mediated signalling between the cell lines.

Inhibition of activated A2AR was shown to increase T-ADCC. This suggests potential benefit for A2AR inhibition in combination with trastuzumab in HER2+ breast cancer with high levels of adenosine. This beneficial effect was absent in HER2-targeted therapy resistant cell lines suggesting the development of resistance may be associated with an alteration in response to A2AR inhibitors.

Immune genes are a more stable target within the tumour due to lower levels of AMP/DEL and point mutations. The stability of the targets of immunotherapies are therefore hypothesised to aid the response rates to immunotherapies in heavily pre-treated treatment refractory cancers.

A set of viral defence associated genes that are heavily mutated in ovarian and cervical cancer have been identified which require further investigation.

8.8 Future work

8.8.1 Cytotoxicity profile of PBMCs isolated from HER2+ breast cancer patients on the TCHL clinical trial (ICORG10-05)

The remaining PBMC samples from the TCHL clinical trial have been immunophenotyped using a 21-colour flow cytometry-based experiment. This data has yet to be assessed and will be analysed in the context of the results presented in chapter 3. The goal is to identify the cell types that are associated with the *in vitro* ICI response of the patient PBMC samples.

Ethical approval has been obtained from SVUH for pre-treatment blood samples from patients treated with monoclonal antibodies or ICIs. Plasma and PBMC samples will be isolated from these samples. PBMCs will be used in immune cytotoxicity assays with trastuzumab and ICIs pembrolizumab and

nivolumab to expand the dataset for GB 1811291.2 (number of samples and relevance to other cancer types). A range of cancer cell line models (lung, breast, melanoma) will be used as target cells in these experiments. Follow-up response data for each patient sample will be obtained (post-treatment for neo-adjuvant therapy, on progression for patients treated in the metastatic or adjuvant setting). These experiments will also act as a comparison of the effects of pembrolizumab and nivolumab *in vitro*. The TCHL dataset will be published once the patent application is assessed in July 2019.

Analysis of SNPs in ABCB1, KLRK1 and FCG3A will be further examined with regards response to chemotherapy and trastuzumab treatment in a larger patient cohort available from collaborators in Beaumont Hospital. This larger dataset will provide a publishable unit.

8.8.2 The development of an assay to examine the effect of immune checkpoint inhibitors in vitro using immune cells isolated from healthy volunteers

Further examination of the effects of ICIs (atezolizumab, nivolumab and pembrolizumab) using unstimulated PBMCs and IL-2 stimulated NK cells as effector cells is warranted. Different effector to target cell ratios will be investigated to further strengthen the model system. Concurrent FACS analysis of effector cells used in the assays will provide mechanistic evidence of the effects occurring.

This model will be used to examine the effects of ICIs in combination with trastuzumab against other HER2+ breast cancer cell lines. The SKBR3 cell line, will be used to examine the effects of ICIs on direct cytotoxicity. Also, there is potential to investigate other novel and therapeutically relevant monoclonal antibodies/ICI combinations. Cetuximab is an EGFR-targeted ADCC-capable monoclonal antibody used to treat colon cancer. Cetuximab will be used in EGFR+/HER2- TNBC and lung cancer cell line models to examine the potential rational of cetuximab/ICI combinations in these disease settings.

8.8.3 EGF signalling and PD-L1 expression in breast cancer cell line models

The main aim of future work associated with this chapter will be to find the mediator of the link between PD-L1 and EGFR. A systematic approach may be effective. Cell lines will be examined with EGF alone and in combination with an inhibitor/siRNA of each signalling node of the EGF pathway. This will allow for systematic analysis through the relevant signalling pathways to determine the key mediators of the link. Characterising the signalling nodes linking EGFR and PD-L1 may allow for the development of pre-clinical rationale for therapies to be used in combination with PD-1 signalling axis inhibition. Identification of the mediator would also provide a conclusive end to this publishable unit.

8.8.4 The effect of adenosine receptor activation on immune cell-mediated cytotoxicity against breast cancer cell line models

Future work will be to develop a more accurate model to show the effects of adenosine or hypoxia on the tumour cells and the immune response against said tumour cells. A range of cell lines will be treated with adenosine agonists, hypoxia mimics or placed in a hypoxia chamber for a range of time points. A2AR, PD-L1 and other immune relevant protein expression will be examined. The appropriate time-point and treatment will be selected. This experimental set-up will then be used in immune cytotoxicity assays to examine the effects of relevant treatments in this immunosuppressive system. Further experiments will expose the immune cell populations to the adenosine relevant treatments either in a pre-treatment setting or within the immune cytotoxicity assay.

With the establishment of the new model it will be of interest to introduce ICIs. This will allow for the examination of the combination of A2AR and PD-1 axis inhibition which is currently being trialled in the clinic.

8.8.5 Chromosomal instability in cancer-related and immune-related gene-sets

The data to date will be prepared as a publishable unit. Further work will be done to follow-up the cancers that stood out as different in this study: ovarian cancer, cervical cancer, diffuse large cell B cell lymphoma and kidney chromophobe. Of particular interest, the innate immune genes altered in ovarian cancer and cervical cancer will be further developed. Provisional analysis has linked the mutated genes in the innate immune system with viral defence. Ovarian and cervical cancer tumour samples will be requested from collaborators in the Mater Hospital. DNA and RNA will be extracted and sequenced for genomic alterations to innate immune response-related genes and the presence of viral sequences. The viruses which will be examined are CMV, EBV, HPV, HCV, CHBV, Kaposi and HHV-8. A literature review on the prevalence of viruses in the Irish population will be carried out as well. These results may lead to the development of a wider research project on innate immune gene dysregulation and viral infection in ovarian and cervical cancer.

9. References

1. Burnet, F. M. IMMUNOLOGICAL ASPECTS OF MALIGNANT DISEASE. *Lancet* **289,** 1171–1174 (1967).

2. Mittal, D., Gubin, M. M., Schreiber, R. D. & Smyth, M. J. New insights into cancer immunoediting and its three component phases—elimination, equilibrium and escape. *Curr. Opin. Immunol.* **27,** 16–25 (2014).

3. Chen, D. S. & Mellman, I. Elements of cancer immunity and the cancer–immune set point. *Nature* **541,** 321–330 (2017).

4. Hanahan, D., Weinberg, R. A., Allison, J. P., Frey, A. B. & Coyle, A. J. Hallmarks of cancer: the next generation. *Cell* **144,** 646–74 (2011).

5. Vajdic, C. M. & van Leeuwen, M. T. Cancer incidence and risk factors after solid organ transplantation. *Int. J. Cancer* **125,** 1747–1754 (2009).

6. Shankaran, V. *et al.* IFNgamma and lymphocytes prevent primary tumour development and shape tumour immunogenicity. *Nature* **410,** 1107–11 (2001).

7. Diamond, M. S. *et al.* Type I interferon is selectively required by dendritic cells for immune rejection of tumors. *J. Exp. Med.* **208,** 1989–2003 (2011).

8. Street, S. E., Cretney, E. & Smyth, M. J. Perforin and interferon-gamma activities independently control tumor initiation, growth, and metastasis. *Blood* **97,** 192–7 (2001).

9. Street, S. E. A., Trapani, J. A., MacGregor, D. & Smyth, M. J. Suppression of lymphoma and epithelial malignancies effected by interferon gamma. *J. Exp. Med.* **196,** 129–34 (2002).

10. Ribas, A., Hodi, F. S., Callahan, M., Konto, C. & Wolchok, J. Hepatotoxicity with combination of vemurafenib and ipilimumab. *N. Engl. J. Med.* **368,** 1365–6 (2013).

11. Wu, X. *et al.* Immune microenvironment profiles of tumor immune equilibrium and immune escape states of mouse sarcoma. *Cancer Lett.* **340,** 124–133 (2013).

12. Beatty, G. L. & Gladney, W. L. Immune escape mechanisms as a guide for cancer immunotherapy. *Clin. Cancer Res.* **21,** 687–92 (2015).

13. Shankaran, V. *et al.* IFNgamma and lymphocytes prevent primary tumour development and shape tumour immunogenicity. *Nature* **410,** 1107–1111 (2001).

14. Pardoll, D. M. The blockade of immune checkpoints in cancer immunotherapy. *Nat. Rev. Cancer* **12,** 252–64 (2012).

15. Mumm, J. B. *et al.* IL-10 Elicits IFNγ-Dependent Tumor Immune Surveillance. *Cancer Cell* **20,** 781–796 (2011).

16. David, C. J. & Massagué, J. Contextual determinants of TGFβ action in development, immunity and cancer. *Nat. Rev. Mol. Cell Biol.* **19,** 419–435 (2018).

17. Zúñiga-Pflücker, J. C. T-cell development made simple. *Nat. Rev. Immunol.* **4,** 67–72 (2004).

18. Zhu, J. & Paul, W. E. CD4 T cells: fates, functions, and faults. *Blood* **112,** 1557–69 (2008).

19. Zhang, N. & Bevan, M. J. CD8+ T Cells: Foot Soldiers of the Immune System. *Immunity* **35,** 161–168 (2011).

20. Halle, S., Halle, O. & Förster, R. Mechanisms and Dynamics of T Cell-Mediated Cytotoxicity In Vivo. *Trends Immunol.* **38,** 432–443 (2017).

21. Trapani, J. A. & Smyth, M. J. Functional significance of the perforin/granzyme cell death pathway. *Nat. Rev. Immunol.* **2,** 735–747 (2002).

22. Smyth, M. J. *et al.* Activation of NK cell cytotoxicity. *Mol. Immunol.* **42,** 501–510 (2005).

23. Ghadially, H. *et al.* MHC class I chain-related protein A and B (MICA and MICB) are predominantly expressed intracellularly in tumour and normal tissue. *Br. J. Cancer* **116,** 1208–1217 (2017).

24. Vujanovic, N. L., Nagashima, S., Herberman, R. B. & Whiteside, T. L. *Nonsecretory Apoptotic Killing by Human N K Cells'. The lournal of Immunology* **157,** (1996).

25. Botticelli, A. *et al.* FCGRs Polymorphisms and Response to Trastuzumab in Patients With HER2-Positive Breast Cancer: Far From Predictive Value? *World J. Oncol.* **6,** 437–440 (2015).

26. Clynes, R. A., Towers, T. L., Presta, L. G. & Ravetch, J. V. Inhibitory Fc receptors modulate in vivo cytotoxicity against tumor targets. *Nat. Med.* **6,** 443–6 (2000).

27. Kinder, M., Greenplate, A. R., Strohl, W. R., Jordan, R. E. & Brezski, R. J. An Fc engineering approach that modulates antibody-dependent cytokine release without altering cell-killing functions. *MAbs* **7,** 494–504 (2015).

28. Seidel, U. J. E. *et al.* γδ T Cell-Mediated Antibody-Dependent Cellular Cytotoxicity with CD19 Antibodies Assessed by an Impedance-Based Label-Free Real-Time Cytotoxicity Assay. *Front. Immunol.* **5,** 618 (2014).

29. Kute, T. *et al.* Understanding key assay parameters that affect measurements of trastuzumab-mediated ADCC against Her2 positive breast cancer cells. *Oncoimmunology* **1,** 810–821 (2012).

30. Varchetta, S. *et al.* Elements Related to Heterogeneity of Antibody-Dependent Cell

Cytotoxicity in Patients Under Trastuzumab Therapy for Primary Operable Breast Cancer Overexpressing Her2. *Cancer Res.* **67,** 11991–11999 (2007).

31. Murphy, K. (Kenneth M. ., Travers, P., Walport, M. & Janeway, C. *Janeway's immunobiology.* (Garland Science, 2008). at <http://vufind.proxy.midlandstech.edu/Record/144483>

32. Gómez Román, V. R., Murray, J. C. & Weiner, L. M. Antibody-Dependent Cellular Cytotoxicity (ADCC). *Antib. Fc* 1–27 (2014). doi:10.1016/B978-0-12-394802-1.00001-7

33. Oshimi, Y., Oda, S., Honda, Y., Nagata, S. & Miyazaki, S. Involvement of Fas ligand and Fas-mediated pathway in the cytotoxicity of human natural killer cells. *J. Immunol.* **157,** 2909–15 (1996).

34. Kawaguchi, Y., Kono, K., Mizukami, Y., Mimura, K. & Fujii, H. Mechanisms of escape from trastuzumab-mediated ADCC in esophageal squamous cell carcinoma: relation to susceptibility to perforin-granzyme. *Anticancer Res.* **29,** 2137–46 (2009).

35. Lehmann C, Zeis M, SchmitzN, U. L. Impaired binding of perforin on the surface of tumor cells is a cause of target cell resistance against cytotoxic effector cells. - PubMed - NCBI. *Blood* **96,** 594–600 (2000).

36. Kim, T. *et al.* Combining targeted therapy and immune checkpoint inhibitors in the treatment of metastatic melanoma. *Cancer Biol. Med.* **11,** 237–46 (2014).

37. Brahmer, J. R. & Pardoll, D. M. Immune checkpoint inhibitors: making immunotherapy a reality for the treatment of lung cancer. *Cancer Immunol. Res.* **1,** 85–91 (2013).

38. Keir, M. E. *et al.* Tissue expression of PD-L1 mediates peripheral T cell tolerance. *J. Exp. Med.* **203,** 883–895 (2006).

39. Freeman, G. J. *et al.* Engagement of the PD-1 immunoinhibitory receptor by a novel B7 family member leads to negative regulation of lymphocyte activation. *J. Exp. Med.* **192,** 1027–34 (2000).

40. Chen, L. Co-inhibitory molecules of the B7–CD28 family in the control of T-cell immunity. *Nat. Rev. Immunol.* **4,** 336–347 (2004).

41. Yang, Y. F. *et al.* Enhanced induction of antitumor T-cell responses by cytotoxic T lymphocyte-associated molecule-4 blockade: the effect is manifested only at the restricted tumor-bearing stages. *Cancer Res.* **57,** 4036–41 (1997).

42. Egen, J. G. & Allison, J. P. Cytotoxic T lymphocyte antigen-4 accumulation in the immunological synapse is regulated by TCR signal strength. *Immunity* **16,** 23–35 (2002).

43. Rudd, C. E., Taylor, A. & Schneider, H. CD28 and CTLA-4 coreceptor expression and signal transduction. *Immunol. Rev.* **229,** 12–26 (2009).

44. Brunet, J.-F. *et al.* A new member of the immunoglobulin superfamily—CTLA-4. *Nature* **328,** 267–270 (1987).

45. Oosterwegel, M. A. *et al.* The role of CTLA-4 in regulating Th2 differentiation. *J. Immunol.* **163,** 2634–9 (1999).

46. Quezada, S. a & Peggs, K. S. Exploiting CTLA-4, PD-1 and PD-L1 to reactivate the host immune response against cancer. *Br. J. Cancer* **108,** 1560–5 (2013).

47. Hodi, F. S. *et al.* Improved survival with ipilimumab in patients with metastatic melanoma. *N. Engl. J. Med.* **363,** 711–23 (2010).

48. Eggermont, A. M. M. *et al.* Adjuvant ipilimumab versus placebo after complete resection of high-risk stage III melanoma (EORTC 18071): a randomised, double-blind, phase 3 trial. *Lancet Oncol.* **16,** 522–530 (2015).

49. Comprehensive Cancer Information - National Cancer Institute. at <https://www.cancer.gov/>

50. Calabrò, L. *et al.* Tremelimumab for patients with chemotherapy-resistant advanced malignant mesothelioma: an open-label, single-arm, phase 2 trial. *Lancet Oncol.* **14,** 1104–1111 (2013).

51. Maio, M. *et al.* Tremelimumab as second-line or third-line treatment in relapsed malignant mesothelioma (DETERMINE): a multicentre, international, randomised, double-blind, placebo-controlled phase 2b trial. *Lancet Oncol.* **18,** 1261–1273 (2017).

52. Shlapatska, L. M. *et al.* CD150 Association with Either the SH2-Containing Inositol Phosphatase or the SH2-Containing Protein Tyrosine Phosphatase Is Regulated by the Adaptor Protein SH2D1A. *J. Immunol.* **166,** 5480–5487 (2001).

53. Okazaki, T., Maeda, A., Nishimura, H., Kurosaki, T. & Honjo, T. PD-1 immunoreceptor inhibits B cell receptor-mediated signaling by recruiting src homology 2-domain-containing tyrosine phosphatase 2 to phosphotyrosine. *Proc. Natl. Acad. Sci. U. S. A.* **98,** 13866–71 (2001).

54. Chemnitz, J. M., Parry, R. V., Nichols, K. E., June, C. H. & Riley, J. L. SHP-1 and SHP-2 Associate with Immunoreceptor Tyrosine-Based Switch Motif of Programmed Death 1 upon Primary Human T Cell Stimulation, but Only Receptor Ligation Prevents T Cell Activation. *J. Immunol.* **173,** 945–954 (2004).

55. Sheppard, K.-A. *et al.* PD-1 inhibits T-cell receptor induced phosphorylation of the ZAP70/CD3zeta signalosome and downstream signaling to PKCtheta. *FEBS Lett.* **574,** 37–41

(2004).

56. Brown, J. A. *et al.* Blockade of programmed death-1 ligands on dendritic cells enhances T cell activation and cytokine production. *J. Immunol.* **170,** 1257–66 (2003).

57. Barber, D. L. *et al.* Restoring function in exhausted CD8 T cells during chronic viral infection. *Nature* **439,** 682–7 (2006).

58. Beldi-Ferchiou, A. & Caillat-Zucman, S. Control of NK Cell Activation by Immune Checkpoint Molecules. *Int. J. Mol. Sci.* **18,** (2017).

59. Asai, A. *et al.* PD-L1 expression of monocytes may be used a new marker of the classification for the cancer progression in hepatocellular carcinoma. *J. Immunol.* **200,** (2018).

60. Gordon, S. R. *et al.* PD-1 expression by tumour-associated macrophages inhibits phagocytosis and tumour immunity. *Nature* **545,** 495–499 (2017).

61. Liu, X. *et al.* B7DC/PDL2 promotes tumor immunity by a PD-1-independent mechanism. *J. Exp. Med.* **197,** 1721–30 (2003).

62. Ghiotto, M. *et al.* PD-L1 and PD-L2 differ in their molecular mechanisms of interaction with PD-1. *Int. Immunol.* **22,** 651–60 (2010).

63. Yearley, J. H. *et al.* PD-L2 Expression in Human Tumors: Relevance to Anti-PD-1 Therapy in Cancer. *Clin. Cancer Res.* **23,** 3158–3167 (2017).

64. Latchman, Y. *et al.* PD-L2 is a second ligand for PD-1 and inhibits T cell activation. *Nat. Immunol.* **2,** 261–8 (2001).

65. Fessas, P., Lee, H., Ikemizu, S. & Janowitz, T. A molecular and preclinical comparison of the PD-1-targeted T-cell checkpoint inhibitors nivolumab and pembrolizumab. *Semin. Oncol.* **44,** 136–140 (2017).

66. Scapin, G. *et al.* Structure of full-length human anti-PD1 therapeutic IgG4 antibody pembrolizumab. *Nat. Struct. Mol. Biol.* **22,** 953–958 (2015).

67. Lee, J. Y. *et al.* Structural basis of checkpoint blockade by monoclonal antibodies in cancer immunotherapy. *Nat. Commun.* **7,** 13354 (2016).

68. Robert, C. *et al.* Anti-programmed-death-receptor-1 treatment with pembrolizumab in ipilimumab-refractory advanced melanoma: a randomised dose-comparison cohort of a phase 1 trial. *Lancet* **384,** 1109–1117 (2014).

69. Robert, C. *et al.* Pembrolizumab versus Ipilimumab in Advanced Melanoma. *N. Engl. J. Med.* **372,** 2521–2532 (2015).

70. Boyiadzis, M. M. *et al.* Significance and implications of FDA approval of pembrolizumab for biomarker-defined disease. *J. Immunother. cancer* **6,** 35 (2018).

71. Sul, J. *et al.* FDA Approval Summary: Pembrolizumab for the Treatment of Patients With Metastatic Non-Small Cell Lung Cancer Whose Tumors Express Programmed Death-Ligand 1. *Oncologist* **21,** 643–50 (2016).

72. Reck, M. *et al.* Pembrolizumab versus Chemotherapy for PD-L1–Positive Non–Small-Cell Lung Cancer. *N. Engl. J. Med.* **375,** 1823–1833 (2016).

73. Fuchs, C. S. *et al.* Safety and Efficacy of Pembrolizumab Monotherapy in Patients With Previously Treated Advanced Gastric and Gastroesophageal Junction Cancer. *JAMA Oncol.* **4,** e180013 (2018).

74. Schellens, J. H. M. *et al.* Pembrolizumab for previously treated advanced cervical squamous cell cancer: Preliminary results from the phase 2 KEYNOTE-158 study. *J. Clin. Oncol.* **35,** 5514–5514 (2017).

75. ASCO 2017: KEYNOTE-045, -052 Support Pembrolizumab For Advanced Urothelial Cancer Populations | OncologyPRO. at <https://oncologypro.esmo.org/Oncology-News/Daily-News/ASCO-2017-KEYNOTE-045-052-Support-Pembrolizumab-For-Advanced-Urothelial-Cancer-Populations>

76. Gandhi, L. *et al.* Pembrolizumab plus Chemotherapy in Metastatic Non–Small-Cell Lung Cancer. *N. Engl. J. Med.* **378,** 2078–2092 (2018).

77. Efficacy and safety of pembrolizumab in recurrent/metastatic head and neck squamous cell carcinoma (R/M HNSCC): Pooled analyses after long-term follow-up in KEYNOTE-012. | 2016 ASCO Annual Meeting | Abstracts | Meeting Library. at <http://meetinglibrary.asco.org/content/168015-176>

78. Chen, R. *et al.* Phase II Study of the Efficacy and Safety of Pembrolizumab for Relapsed/Refractory Classic Hodgkin Lymphoma. *J. Clin. Oncol.* **35,** 2125–2132 (2017).

79. Langer, C. J. *et al.* Carboplatin and pemetrexed with or without pembrolizumab for advanced, non-squamous non-small-cell lung cancer: a randomised, phase 2 cohort of the open-label KEYNOTE-021 study. *Lancet. Oncol.* **17,** 1497–1508 (2016).

80. Zinzani, P. L. *et al.* Efficacy and Safety of Pembrolizumab in Relapsed/Refractory Primary Mediastinal Large B-Cell Lymphoma (rrPMBCL): Updated Analysis of the Keynote-170 Phase 2 Trial. *Blood* **130,** (2017).

81. Nivolumab in Previously Untreated Melanoma without BRAF Mutation — NEJM. at

<http://www.nejm.org/doi/full/10.1056/NEJMoa1412082>

82. Robert, C. *et al.* Nivolumab in Previously Untreated Melanoma without *BRAF* Mutation. *N. Engl. J. Med.* **372,** 320–330 (2015).

83. Weber, J. S. *et al.* Nivolumab versus chemotherapy in patients with advanced melanoma who progressed after anti-CTLA-4 treatment (CheckMate 037): a randomised, controlled, open-label, phase 3 trial. *Lancet Oncol.* **16,** 375–384 (2015).

84. Weber, J. S. *et al.* Adjuvant therapy with nivolumab (NIVO) versus ipilimumab (IPI) after complete resection of stage III/IV melanoma: Updated results from a phase III trial (CheckMate 238). *J. Clin. Oncol.* **36,** 9502–9502 (2018).

85. Larkin, J. *et al.* Combined Nivolumab and Ipilimumab or Monotherapy in Untreated Melanoma. *N. Engl. J. Med.* **373,** 23–34 (2015).

86. Brahmer, J. *et al.* Nivolumab versus Docetaxel in Advanced Squamous-Cell Non-Small-Cell Lung Cancer. *N. Engl. J. Med.* **373,** 123–35 (2015).

87. Borghaei, H. *et al.* Nivolumab versus Docetaxel in Advanced Nonsquamous Non–Small-Cell Lung Cancer. *N. Engl. J. Med.* **373,** 1627–1639 (2015).

88. Motzer, R. J. *et al.* Nivolumab plus Ipilimumab versus Sunitinib in Advanced Renal-Cell Carcinoma. *N. Engl. J. Med.* **378,** 1277–1290 (2018).

89. Motzer, R. J. *et al.* Nivolumab versus Everolimus in Advanced Renal-Cell Carcinoma. *N. Engl. J. Med.* 150925150201006 (2015). doi:10.1056/NEJMoa1510665

90. Sharma, P. *et al.* Nivolumab in metastatic urothelial carcinoma after platinum therapy (CheckMate 275): a multicentre, single-arm, phase 2 trial. *Lancet Oncol.* **18,** 312–322 (2017).

91. El-Khoueiry, A. B. *et al.* Nivolumab in patients with advanced hepatocellular carcinoma (CheckMate 040): an open-label, non-comparative, phase 1/2 dose escalation and expansion trial. *Lancet (London, England)* **389,** 2492–2502 (2017).

92. Ferris, R. L. *et al.* Nivolumab for Recurrent Squamous-Cell Carcinoma of the Head and Neck. *N. Engl. J. Med.* **375,** 1856–1867 (2016).

93. Kambhampati Swetha, Bauer Kelly, Hwang Jimmy, Bocobo Andrea Grace, Dozier Gordon John, K. R. K. Nivolumab in advanced hepatocellular carcinoma (HCC) and Child Pugh B (CPB) cirrhosis: Safety and clinical outcomes in a retrospective case series. *J. Clin. Oncol.* (2018). doi:10.1200/JCO.2018.36.4_SUPPL.496

94. Antonia, S. J. *et al.* Checkmate 032: Nivolumab (N) alone or in combination with ipilimumab

(I) for the treatment of recurrent small cell lung cancer (SCLC). *J. Clin. Oncol.* **34,** 100–100 (2016).

95. Younes, A. *et al.* Nivolumab for classical Hodgkin's lymphoma after failure of both autologous stem-cell transplantation and brentuximab vedotin: a multicentre, multicohort, single-arm phase 2 trial. *Lancet Oncol.* **17,** 1283–1294 (2016).

96. Overman, M. J. *et al.* Nivolumab in patients with metastatic DNA mismatch repair-deficient or microsatellite instability-high colorectal cancer (CheckMate 142): an open-label, multicentre, phase 2 study. *Lancet Oncol.* **18,** 1182–1191 (2017).

97. Akbay, E. A. *et al.* Activation of the PD-1 pathway contributes to immune escape in EGFR-driven lung tumors. *Cancer Discov.* **3,** 1355–63 (2013).

98. Azuma, K. *et al.* Association of PD-L1 overexpression with activating EGFR mutations in surgically resected nonsmall-cell lung cancer. *Ann. Oncol.* **25,** 1935–40 (2014).

99. Liang, M. *et al.* Nimesulide inhibits IFN-gamma-induced programmed death-1-ligand 1 surface expression in breast cancer cells by COX-2 and PGE2 independent mechanisms. *Cancer Lett.* **276,** 47–52 (2009).

100. Taube, J. M. *et al.* Colocalization of inflammatory response with B7-h1 expression in human melanocytic lesions supports an adaptive resistance mechanism of immune escape. *Sci. Transl. Med.* **4,** 127ra37 (2012).

101. Parsa, A. T. *et al.* Loss of tumor suppressor PTEN function increases B7-H1 expression and immunoresistance in glioma. *Nat. Med.* **13,** 84–8 (2007).

102. Li, C.-W. *et al.* Glycosylation and stabilization of programmed death ligand-1 suppresses T-cell activity. *Nat. Commun.* **7,** 12632 (2016).

103. Dong, H. *et al.* B7-H1 Determines Accumulation and Deletion of Intrahepatic CD8+ T Lymphocytes. *Immunity* **20,** 327–336 (2004).

104. Park, J.-J. *et al.* B7-H1/CD80 interaction is required for the induction and maintenance of peripheral T-cell tolerance. *Blood* **116,** 1291–8 (2010).

105. Butte, M. J., Keir, M. E., Phamduy, T. B., Sharpe, A. H. & Freeman, G. J. Programmed death-1 ligand 1 interacts specifically with the B7-1 costimulatory molecule to inhibit T cell responses. *Immunity* **27,** 111–22 (2007).

106. Rossille, D. *et al.* High level of soluble programmed cell death ligand 1 in blood impacts overall survival in aggressive diffuse large B-Cell lymphoma: results from a French multicenter clinical trial. *Leukemia* **28,** 2367–2375 (2014).

107. Chen, Y. *et al.* Development of a sandwich ELISA for evaluating soluble PD-L1 (CD274) in human sera of different ages as well as supernatants of PD-L1+ cell lines. *Cytokine* **56,** 231–238 (2011).

108. Current Issue | Archive | Adv Search |, Detection of Soluble B7-H4 Molecules in Serum of Patients with Breast Cancer and its Clinical Significance & Chen Junjun, Shi Hongbing, Zheng Xiao, Cheng Gui, Xie Jun, Chen Lujun, Jiang Jingting, W. C. Detection of soluble B7-H4 molecules in serum of patients with breast cancer and its clinical significance. *J. Int. Transl. Med.* **1,** 215–218

109. Herbst, R. S. *et al.* Predictive correlates of response to the anti-PD-L1 antibody MPDL3280A in cancer patients. *Nature* **515,** 563–567 (2014).

110. Powles, T. *et al.* MPDL3280A (anti-PD-L1) treatment leads to clinical activity in metastatic bladder cancer. *Nature* **515,** 558–562 (2014).

111. Hamilton, G. & Rath, B. Avelumab: combining immune checkpoint inhibition and antibody-dependent cytotoxicity. *Expert Opin. Biol. Ther.* **17,** 515–523 (2017).

112. Kaufman, H. L. *et al.* Updated efficacy of avelumab in patients with previously treated metastatic Merkel cell carcinoma after ≥1 year of follow-up: JAVELIN Merkel 200, a phase 2 clinical trial. *J. Immunother. Cancer* **6,** 7 (2018).

113. Patel, M. R. *et al.* Avelumab in metastatic urothelial carcinoma after platinum failure (JAVELIN Solid Tumor): pooled results from two expansion cohorts of an open-label, phase 1 trial. *Lancet. Oncol.* **19,** 51–64 (2018).

114. Powles, T. *et al.* Efficacy and Safety of Durvalumab in Locally Advanced or Metastatic Urothelial Carcinoma. *JAMA Oncol.* **3,** e172411 (2017).

115. Antonia, S. J. *et al.* Durvalumab after Chemoradiotherapy in Stage III Non–Small-Cell Lung Cancer. *N. Engl. J. Med.* **377,** 1919–1929 (2017).

116. Rosenberg, J. E. *et al.* Atezolizumab in patients with locally advanced and metastatic urothelial carcinoma who have progressed following treatment with platinum-based chemotherapy: a single-arm, multicentre, phase 2 trial. *Lancet (London, England)* **387,** 1909–1920 (2016).

117. Balar, A. V *et al.* Atezolizumab as first-line treatment in cisplatin-ineligible patients with locally advanced and metastatic urothelial carcinoma: a single-arm, multicentre, phase 2 trial. *Lancet (London, England)* **389,** 67–76 (2017).

118. Rittmeyer, A. *et al.* Atezolizumab versus docetaxel in patients with previously treated non-

small-cell lung cancer (OAK): a phase 3, open-label, multicentre randomised controlled trial. *Lancet* **389,** 255–265 (2017).

119. Fehrenbacher, L. *et al.* Atezolizumab versus docetaxel for patients with previously treated non-small-cell lung cancer (POPLAR): a multicentre, open-label, phase 2 randomised controlled trial. *Lancet (London, England)* **387,** 1837–46 (2016).

120. ESMO | Press Release | IMpassion130 atezolizumab triple negative | ESMO. at <https://www.esmo.org/Press-Office/Press-Releases/IMpassion130-atezolizumab-nab-pac-triple-negative-breast-cancer-Schmid>

121. Cancer Institute, N. *Common Terminology Criteria for Adverse Events (CTCAE) Version 4.0*. (2009). at <http://www.meddramsso.com>

122. O'Day, S. J. *et al.* Efficacy and safety of ipilimumab monotherapy in patients with pretreated advanced melanoma: a multicenter single-arm phase II study. *Ann. Oncol.* **21,** 1712–1717 (2010).

123. Wolchok, J. D. *et al.* Ipilimumab monotherapy in patients with pretreated advanced melanoma: a randomised, double-blind, multicentre, phase 2, dose-ranging study. *Lancet Oncol.* **11,** 155–164 (2010).

124. Fecher, L. A., Agarwala, S. S., Hodi, F. S. & Weber, J. S. Ipilimumab and its toxicities: a multidisciplinary approach. *Oncologist* **18,** 733–43 (2013).

125. Tai, X., Van Laethem, F., Sharpe, A. H. & Singer, A. Induction of autoimmune disease in CTLA-4-/- mice depends on a specific CD28 motif that is required for in vivo costimulation. *Proc. Natl. Acad. Sci. U. S. A.* **104,** 13756–61 (2007).

126. Haanen, J. B. A. G. *et al.* Management of toxicities from immunotherapy: ESMO Clinical Practice Guidelines for diagnosis, treatment and follow-up†. *Ann. Oncol.* **28,** iv119-iv142 (2017).

127. Topalian, S. L. *et al.* Safety, Activity, and Immune Correlates of Anti–PD-1 Antibody in Cancer. *N. Engl. J. Med.* **366,** 2443–2454 (2012).

128. Moslehi, J. J., Salem, J.-E., Sosman, J. A., Lebrun-Vignes, B. & Johnson, D. B. *Increased reporting of fatal immune checkpoint inhibitor-associated myocarditis*. *The Lancet* **391,** (2018).

129. Chen, Y. *et al.* Programmed Death (PD)-1-Deficient Mice Are Extremely Sensitive to Murine Hepatitis Virus Strain-3 (MHV-3) Infection. *PLoS Pathog.* **7,** e1001347 (2011).

130. Michot, J. M. *et al.* Immune-related adverse events with immune checkpoint blockade: a

comprehensive review. *Eur. J. Cancer* **54,** 139–148 (2016).

131. Buchbinder, E. I. & Desai, A. CTLA-4 and PD-1 Pathways. *Am. J. Clin. Oncol.* **39,** 98–106 (2016).

132. *Cost-effectiveness of pembrolizumab (Keytruda®) for previously untreated PD-L1 positive metastatic non-small cell lung cancer*. at <http://www.ncpe.ie/wp-content/uploads/2017/01/Summary-v1.2-pembro-1L.pdf>

133. *Cost-effectiveness of nivolumab (Opdivo®) for the treatment of locally advanced or metastatic non-squamous NSCLC after prior chemotherapy in adults*. at <http://www.ncpe.ie/wp-content/uploads/2016/04/Summary-Nivolumab-in-non-sq-NSCLC.pdf>

134. Oyan, B., Sonmez, O., Yazar, A. & Teomete, M. Comparison of SP142 (Ventana) and SP263 (Ventana) assays to test PD-L1 expression in metastatic cancer patients to be treated with immune checkpoint inhibitors. *J. Clin. Oncol.* **36,** e24306–e24306 (2018).

135. Rizvi, H. *et al.* Molecular Determinants of Response to Anti-Programmed Cell Death (PD)-1 and Anti-Programmed Death-Ligand 1 (PD-L1) Blockade in Patients With Non-Small-Cell Lung Cancer Profiled With Targeted Next-Generation Sequencing. *J. Clin. Oncol.* **36,** 633–641 (2018).

136. Goodman, A. M. *et al.* Tumor Mutational Burden as an Independent Predictor of Response to Immunotherapy in Diverse Cancers. *Mol. Cancer Ther.* **16,** 2598–2608 (2017).

137. Kowanetz, M. *et al.* Tumor mutation load assessed by FoundationOne (FM1) is associated with improved efficacy of atezolizumab (atezo) in patients with advanced NSCLC. *Ann. Oncol.* **27,** (2016).

138. Le, D. T. *et al.* PD-1 Blockade in Tumors with Mismatch-Repair Deficiency. *N. Engl. J. Med.* **372,** 2509–20 (2015).

139. Jochems, C. & Schlom, J. Tumor-infiltrating immune cells and prognosis: the potential link between conventional cancer therapy and immunity. *Exp. Biol. Med. (Maywood).* **236,** 567–79 (2011).

140. Galon, J. *et al.* Type, density, and location of immune cells within human colorectal tumors predict clinical outcome. *Science* **313,** 1960–4 (2006).

141. Pagès, F. *et al.* International validation of the consensus Immunoscore for the classification of colon cancer: a prognostic and accuracy study. *Lancet* **391,** 2128–2139 (2018).

142. Fridman, W. H., Pagès, F., Sautès-Fridman, C. & Galon, J. The immune contexture in human tumours: impact on clinical outcome. *Nat. Rev. Cancer* **12,** 298–306 (2012).

143. Mlecnik, B. *et al.* Biomolecular Network Reconstruction Identifies T-Cell Homing Factors Associated With Survival in Colorectal Cancer. *Gastroenterology* **138,** 1429–1440 (2010).

144. Bronger, H. *et al.* CXCL9 and CXCL10 predict survival and are regulated by cyclooxygenase inhibition in advanced serous ovarian cancer. *Br. J. Cancer* **115,** 553–63 (2016).

145. Mantovani, A., Allavena, P., Sica, A. & Balkwill, F. Cancer-related inflammation. doi:10.1038/nature07205

146. Allard, B., Allard, D. & Stagg, J. in *Methods in molecular biology (Clifton, N.J.)* **1458,** 159–177 (Humana Press, New York, NY, 2016).

147. Wege, A. K. Humanized Mouse Models for the Preclinical Assessment of Cancer Immunotherapy. *BioDrugs* **32,** 245–266 (2018).

148. Wang, X. *et al.* B7-H4 overexpression impairs the immune response of T cells in human cervical carcinomas. *Hum. Immunol.* **75,** 1203–1209 (2014).

149. Deppisch, N., Ruf, P., Eißler, N., Lindhofer, H. & Mocikat, R. Potent CD4⁺ T cell-associated antitumor memory responses induced by trifunctional bispecific antibodies in combination with immune checkpoint inhibition. *Oncotarget* **8,** 4520–4529 (2017).

150. Langdon, S. *et al.* Combination of dual mTORC1/2 inhibition and immune-checkpoint blockade potentiates anti-tumour immunity. *Oncoimmunology* **7,** e1458810 (2018).

151. Skalniak, L. *et al.* Small-molecule inhibitors of PD-1/PD-L1 immune checkpoint alleviate the PD-L1-induced exhaustion of T-cells. *Oncotarget* **8,** 72167–72181 (2017).

152. Jutz, S. *et al.* A cellular platform for the evaluation of immune checkpoint molecules. *Oncotarget* **8,** 64892–64906 (2017).

153. Stecher, C. *et al.* PD-1 Blockade Promotes Emerging Checkpoint Inhibitors in Enhancing T Cell Responses to Allogeneic Dendritic Cells. *Front. Immunol.* **8,** 572 (2017).

154. Workman, C. J., Dugger, K. J. & Vignali, D. A. A. Cutting Edge: Molecular Analysis of the Negative Regulatory Function of Lymphocyte Activation Gene-3. *J. Immunol.* **169,** 5392–5395 (2002).

155. Andreae, S., Piras, F., Burdin, N. & Triebel, F. Maturation and activation of dendritic cells induced by lymphocyte activation gene-3 (CD223). *J. Immunol.* **168,** 3874–80 (2002).

156. Goldberg, M. V & Drake, C. G. LAG-3 in Cancer Immunotherapy. *Curr. Top. Microbiol. Immunol.* **344,** 269–78 (2011).

157. Duhoux, F. P. *et al.* Combination of paclitaxel and LAG3-Ig (IMP321), a novel MHC class II agonist, as a first-line chemoimmunotherapy in patients with metastatic breast carcinoma (MBC): Interim results from the run-in phase of a placebo controlled randomized phase II. *J. Clin. Oncol.* **35,** 1062–1062 (2017).

158. Hong, D. S. *et al.* Phase I/II study of LAG525 ± spartalizumab (PDR001) in patients (pts) with advanced malignancies. *J. Clin. Oncol.* **36,** 3012–3012 (2018).

159. Ascierto, P. A. *et al.* Initial efficacy of anti-lymphocyte activation gene-3 (anti–LAG-3; BMS-986016) in combination with nivolumab (nivo) in pts with melanoma (MEL) previously treated with anti–PD-1/PD-L1 therapy. *J. Clin. Oncol.* **35,** 9520–9520 (2017).

160. Marin-Acevedo, J. A. *et al.* Next generation of immune checkpoint therapy in cancer: new developments and challenges. *J. Hematol. Oncol.* **11,** 39 (2018).

161. Du, W. *et al.* TIM-3 as a Target for Cancer Immunotherapy and Mechanisms of Action. *Int. J. Mol. Sci.* **18,** (2017).

162. Sakuishi, K. *et al.* TIM3 $^{+}$ FOXP3 $^{+}$ regulatory T cells are tissue-specific promoters of T-cell dysfunction in cancer. *Oncoimmunology* **2,** e23849 (2013).

163. Dempke, W. C. M., Fenchel, K., Uciechowski, P. & Dale, S. P. Second- and third-generation drugs for immuno-oncology treatment—The more the better? *Eur. J. Cancer* **74,** 55–72 (2017).

164. Chauvin, J.-M. *et al.* TIGIT and PD-1 impair tumor antigen-specific CD8^{+} T cells in melanoma patients. *J. Clin. Invest.* **125,** 2046–58 (2015).

165. Yu, X. *et al.* The surface protein TIGIT suppresses T cell activation by promoting the generation of mature immunoregulatory dendritic cells. *Nat. Immunol.* **10,** 48–57 (2009).

166. Stanietsky, N. *et al.* The interaction of TIGIT with PVR and PVRL2 inhibits human NK cell cytotoxicity. *Proc. Natl. Acad. Sci.* **106,** 17858–17863 (2009).

167. Prodeus, A. *et al.* VISTA.COMP - an engineered checkpoint receptor agonist that potently suppresses T cell-mediated immune responses. *JCI insight* **2,** (2017).

168. Lee, J. J. *et al.* Phase 1 trial of CA-170, a novel oral small molecule dual inhibitor of immune checkpoints PD-1 and VISTA, in patients (pts) with advanced solid tumor or lymphomas. *J. Clin. Oncol.* **35,** TPS3099-TPS3099 (2017).

169. Picarda, E., Ohaegbulam, K. C. & Zang, X. Molecular Pathways: Targeting B7-H3 (CD276) for Human Cancer Immunotherapy. *Clin. Cancer Res.* **22,** 3425–3431 (2016).

170. Powderly, J. *et al.* Interim results of an ongoing Phase I, dose escalation study of MGA271 (Fc-optimized humanized anti-B7-H3 monoclonal antibody) in patients with refractory B7-H3-expressing neoplasms or neoplasms whose vasculature expresses B7-H3. *J. Immunother. Cancer* **3,** O8 (2015).

171. Tolcher, A. W. *et al.* Phase 1, first-in-human, open label, dose escalation ctudy of MGD009, a humanized B7-H3 x CD3 dual-affinity re-targeting (DART) protein in patients with B7-H3-expressing neoplasms or B7-H3 expressing tumor vasculature. *J. Clin. Oncol.* **34,** TPS3105-TPS3105 (2016).

172. Kramer, K. *et al.* Compartmental intrathecal radioimmunotherapy: results for treatment for metastatic CNS neuroblastoma. *J. Neurooncol.* **97,** 409–418 (2010).

173. Burris, H. A. *et al.* Phase 1 safety of ICOS agonist antibody JTX-2011 alone and with nivolumab (nivo) in advanced solid tumors; predicted vs observed pharmacokinetics (PK) in ICONIC. *J. Clin. Oncol.* **35,** 3033–3033 (2017).

174. Angevin, E. *et al.* INDUCE-1: A phase I open-label study of GSK3359609, an ICOS agonist antibody, administered alone and in combination with pembrolizumab in patients with advanced solid tumors. *J. Clin. Oncol.* **35,** TPS3113-TPS3113 (2017).

175. Koon, H. B. *et al.* First-in-human phase 1 single-dose study of TRX-518, an anti-human glucocorticoid-induced tumor necrosis factor receptor (GITR) monoclonal antibody in adults with advanced solid tumors. *J. Clin. Oncol.* **34,** 3017–3017 (2016).

176. Siu, L. L. *et al.* Preliminary results of a phase I/IIa study of BMS-986156 (glucocorticoid-induced tumor necrosis factor receptor–related gene [GITR] agonist), alone and in combination with nivolumab in pts with advanced solid tumors. *J. Clin. Oncol.* **35,** 104–104 (2017).

177. Tran, B. *et al.* Dose escalation results from a first-in-human, phase 1 study of the glucocorticoid-induced TNF receptor-related protein (GITR) agonist AMG 228 in patients (Pts) with advanced solid tumors. *J. Clin. Oncol.* **35,** 2521–2521 (2017).

178. Chester, C., Ambulkar, S. & Kohrt, H. E. 4-1BB agonism: adding the accelerator to cancer immunotherapy. *Cancer Immunol. Immunother.* **65,** 1243–8 (2016).

179. Segal, N. H. *et al.* Cancer Therapy: Clinical Results from an Integrated Safety Analysis of Urelumab, an Agonist Anti-CD137 Monoclonal Antibody. (2016). doi:10.1158/1078-0432.CCR-16-1272

180. Tolcher, A. W. *et al.* Phase Ib study of PF-05082566 in combination with pembrolizumab in

patients with advanced solid tumors. *J. Clin. Oncol.* **34,** 3002–3002 (2016).

181. Vonderheide, R. H. Prospect of Targeting the CD40 Pathway for Cancer Therapy. *Clin. Cancer Res.* **13,** 1083–1088 (2007).

182. Naidoo, J., Page, D. B. & Wolchok, J. D. Immune modulation for cancer therapy. *Br. J. Cancer* **111,** 2214–9 (2014).

183. Ohta, A. A Metabolic Immune Checkpoint: Adenosine in Tumor Microenvironment. *Front. Immunol.* **7,** 109 (2016).

184. Blay, J. in *Encyclopedia of Cancer* 49–52 (Springer Berlin Heidelberg, 2011). doi:10.1007/978-3-642-16483-5_89

185. Muz, B., de la Puente, P., Azab, F. & Azab, A. K. The role of hypoxia in cancer progression, angiogenesis, metastasis, and resistance to therapy. *Hypoxia (Auckland, N.Z.)* **3,** 83–92 (2015).

186. Allard, B., Longhi, M. S., Robson, S. C. & Stagg, J. The ectonucleotidases CD39 and CD73: Novel checkpoint inhibitor targets. *Immunol. Rev.* **276,** 121–144 (2017).

187. Ohta, A. & Sitkovsky, M. Extracellular adenosine-mediated modulation of regulatory T cells. *Front. Immunol.* **5,** 304 (2014).

188. Safarzadeh, E., Jadidi-Niaragh, F., Motallebnezhad, M. & Yousefi, M. The role of adenosine and adenosine receptors in the immunopathogenesis of multiple sclerosis. *Inflamm. Res.* **65,** 511–20 (2016).

189. Jacobson, K. A. & Gao, Z.-G. Adenosine receptors as therapeutic targets. *Nat. Rev. Drug Discov.* **5,** 247–64 (2006).

190. Sitkovsky, M. V. & Ohta, A. The 'danger' sensors that STOP the immune response: the A2 adenosine receptors? *Trends Immunol.* **26,** 299–304 (2005).

191. Ohta, A. & Sitkovsky, M. Role of G-protein-coupled adenosine receptors in downregulation of inflammation and protection from tissue damage. *Nature* **414,** 916–920 (2001).

192. Linnemann, C. *et al.* Adenosine regulates CD8 T-cell priming by inhibition of membrane-proximal T-cell receptor signalling. *Immunology* **128,** e728-37 (2009).

193. Jimenez, J. L., Punzón, C., Navarro, J., Muñoz-Fernández, M. A. & Fresno, M. Phosphodiesterase 4 inhibitors prevent cytokine secretion by T lymphocytes by inhibiting nuclear factor-kappaB and nuclear factor of activated T cells activation. *J. Pharmacol. Exp. Ther.* **299,** 753–9 (2001).

194. Butler, J. J. *et al.* Adenosine inhibits activation-induced T cell expression of CD2 and CD28

co-stimulatory molecules: Role of interleukin-2 and cyclic AMP signaling pathways. *J. Cell. Biochem.* **89,** 975–991 (2003).

195. Cekic, C. & Linden, J. Adenosine A2A Receptors Intrinsically Regulate CD8+ T Cells in the Tumor Microenvironment. *Cancer Res.* **74,** 7239–7249 (2014).

196. Bao, R. *et al.* Adenosine promotes Foxp3 expression in Treg cells in sepsis model by activating JNK/AP-1 pathway. *Am. J. Transl. Res.* **8,** 2284–92 (2016).

197. Sevigny, C. P. *et al.* Activation of adenosine 2A receptors attenuates allograft rejection and alloantigen recognition. *J. Immunol.* **178,** 4240–9 (2007).

198. Huang, C.-T. *et al.* Role of LAG-3 in regulatory T cells. *Immunity* **21,** 503–13 (2004).

199. Ohta, A. *et al.* A2A adenosine receptor protects tumors from antitumor T cells. *Proc. Natl. Acad. Sci. U. S. A.* **103,** 13132–7 (2006).

200. Stagg, J. *et al.* CD73-Deficient Mice Have Increased Antitumor Immunity and Are Resistant to Experimental Metastasis. *Cancer Res.* **71,** 2892–2900 (2011).

201. Sun, X. *et al.* CD39/ENTPD1 Expression by CD4+Foxp3+ Regulatory T Cells Promotes Hepatic Metastatic Tumor Growth in Mice. *Gastroenterology* **139,** 1030–1040 (2010).

202. Leone, R. D. & Emens, L. A. Targeting adenosine for cancer immunotherapy. *J. Immunother. Cancer* **6,** 57 (2018).

203. Fong, L. *et al.* Safety and clinical activity of adenosine A2a receptor (A2aR) antagonist, CPI-444, in anti-PD1/PDL1 treatment-refractory renal cell (RCC) and non-small cell lung cancer (NSCLC) patients. *J. Clin. Oncol.* **35,** 3004–3004 (2017).

204. Pitt, J. M. *et al.* Resistance Mechanisms to Immune-Checkpoint Blockade in Cancer: Tumor-Intrinsic and -Extrinsic Factors. *Immunity* **44,** 1255–1269 (2016).

205. Fleming, V. *et al.* Targeting Myeloid-Derived Suppressor Cells to Bypass Tumor-Induced Immunosuppression. *Front. Immunol.* **9,** 398 (2018).

206. Joyce, J. A. & Fearon, D. T. T cell exclusion, immune privilege, and the tumor microenvironment. *Science (80-.).* **348,** 74–80 (2015).

207. National Cancer Registry Ireland | Essential information on cancer in Ireland. at <https://www.ncri.ie/>

208. Cancer Genome Atlas Network, T. C. G. A. Comprehensive molecular portraits of human breast tumours. *Nature* **490,** 61–70 (2012).

209. Perou, C. M. *et al.* Molecular portraits of human breast tumours. *Nature* **406,** 747–52 (2000).

210. Cleator, S., Heller, W. & Coombes, R. C. Triple-negative breast cancer: therapeutic options. *Lancet. Oncol.* **8,** 235–44 (2007).

211. Carey, L. A. *et al.* Race, breast cancer subtypes, and survival in the Carolina Breast Cancer Study. *JAMA* **295,** 2492–502 (2006).

212. Choi, J., Jung, W.-H. & Koo, J. S. Clinicopathologic features of molecular subtypes of triple negative breast cancer based on immunohistochemical markers. *Histol. Histopathol.* **27,** 1481–93 (2012).

213. Costa, R. L. B. & Gradishar, W. J. Triple-Negative Breast Cancer: Current Practice and Future Directions. *J. Oncol. Pract.* **13,** 301–303 (2017).

214. Adams, S. *et al.* Prognostic value of tumor-infiltrating lymphocytes in triple-negative breast cancers from two phase III randomized adjuvant breast cancer trials: ECOG 2197 and ECOG 1199. *J. Clin. Oncol.* **32,** 2959–66 (2014).

215. Loi, S. *et al.* Tumor infiltrating lymphocytes are prognostic in triple negative breast cancer and predictive for trastuzumab benefit in early breast cancer: results from the FinHER trial. *Ann. Oncol.* **25,** 1544–1550 (2014).

216. Mittendorf, E. A. *et al.* PD-L1 expression in triple-negative breast cancer. *Cancer Immunol. Res.* **2,** 361–70 (2014).

217. Solinas, C. *et al.* Tumor-infiltrating lymphocytes in patients with HER2-positive breast cancer treated with neoadjuvant chemotherapy plus trastuzumab, lapatinib or their combination: A meta-analysis of randomized controlled trials. *Cancer Treat. Rev.* **57,** 8–15 (2017).

218. Udall, M. *et al.* PD-L1 diagnostic tests: a systematic literature review of scoring algorithms and test-validation metrics. *Diagn. Pathol.* **13,** 12 (2018).

219. Shah, S. P. *et al.* The clonal and mutational evolution spectrum of primary triple-negative breast cancers. *Nature* **486,** 395–9 (2012).

220. Bianchini, G., Balko, J. M., Mayer, I. A., Sanders, M. E. & Gianni, L. Triple-negative breast cancer: challenges and opportunities of a heterogeneous disease. *Nat. Rev. Clin. Oncol.* **13,** 674–690 (2016).

221. Roskoski, R. ErbB/HER protein-tyrosine kinases: Structures and small molecule inhibitors. *Pharmacol. Res.* **87,** 42–59 (2014).

222. Cho, H.-S. *et al.* Structure of the extracellular region of HER2 alone and in complex with the

Herceptin Fab. *Nature* **421,** 756–760 (2003).

223. Kauraniemi, P. & Kallioniemi, A. Activation of multiple cancer-associated genes at the ERBB2 amplicon in breast cancer. *Endocr. Relat. Cancer* **13,** 39–49 (2006).

224. Kirouac, D. C. *et al.* HER2+ Cancer Cell Dependence on PI3K vs. MAPK Signaling Axes Is Determined by Expression of EGFR, ERBB3 and CDKN1B. *PLOS Comput. Biol.* **12,** e1004827 (2016).

225. Schnitt, S. J. Classification and prognosis of invasive breast cancer: from morphology to molecular taxonomy. *Mod. Pathol.* **23,** S60–S64 (2010).

226. Shi, Y. *et al.* Engagement of immune effector cells by trastuzumab induces HER2/ERBB2 downregulation in cancer cells through STAT1 activation. *Breast Cancer Res.* **16,** 3383 (2014).

227. Kute, T. *et al.* Understanding key assay parameters that affect measurements of trastuzumab-mediated ADCC against Her2 positive breast cancer cells. *Oncoimmunology* **1,** 810–821 (2012).

228. Wilson, F. R. *et al.* Herceptin® (trastuzumab) in HER2-positive early breast cancer: protocol for a systematic review and cumulative network meta-analysis. *Syst. Rev.* **6,** 196 (2017).

229. Harbeck, N. *et al.* HER2 Dimerization Inhibitor Pertuzumab - Mode of Action and Clinical Data in Breast Cancer. *Breast Care* **8,** 49–55 (2013).

230. Tóth, G. *et al.* The combination of trastuzumab and pertuzumab administered at approved doses may delay development of trastuzumab resistance by additively enhancing antibody-dependent cell-mediated cytotoxicity. *MAbs* **8,** 1361–1370 (2016).

231. Blumenthal, G. M. *et al.* First FDA Approval of Dual Anti-HER2 Regimen: Pertuzumab in Combination with Trastuzumab and Docetaxel for HER2-Positive Metastatic Breast Cancer. *Clin. Cancer Res.* **19,** 4911–4916 (2013).

232. Amiri-Kordestani, L. *et al.* First FDA Approval of Neoadjuvant Therapy for Breast Cancer: Pertuzumab for the Treatment of Patients with HER2-Positive Breast Cancer. *Clin. Cancer Res.* **20,** 5359–5364 (2014).

233. Amiri-Kordestani, L. *et al.* FDA Approval: Ado-Trastuzumab Emtansine for the Treatment of Patients with HER2-Positive Metastatic Breast Cancer. *Clin. Cancer Res.* **20,** 4436–4441 (2014).

234. Ryan, Q. *et al.* FDA Drug Approval Summary: Lapatinib in Combination with Capecitabine for Previously Treated Metastatic Breast Cancer That Overexpresses HER-2. *Oncologist* **13,**

1114–1119 (2008).

235. Neratinib Approved for HER2+ Breast Cancer. *Cancer Discov.* **7,** OF1 (2017).

236. Lopez-Albaitero, A. *et al.* Overcoming resistance to HER2-targeted therapy with a novel HER2/CD3 bispecific antibody. *Oncoimmunology* **6,** e1267891 (2017).

237. American Cancer Society. Breast Cancer Survival Rates & Statistics. at <https://www.cancer.org/cancer/breast-cancer/understanding-a-breast-cancer-diagnosis/breast-cancer-survival-rates.html>

238. Ruffell, B. *et al.* Leukocyte composition of human breast cancer. *Proc. Natl. Acad. Sci. U. S. A.* **109,** 2796–801 (2012).

239. Liu, S. *et al.* Role of Cytotoxic Tumor-Infiltrating Lymphocytes in Predicting Outcomes in Metastatic HER2-Positive Breast Cancer: A Secondary Analysis of a Randomized Clinical Trial. *JAMA Oncol.* **3,** e172085 (2017).

240. Kim, A. *et al.* Programmed death-ligand 1 (PD-L1) expression in tumour cell and tumour infiltrating lymphocytes of HER2-positive breast cancer and its prognostic value. *Sci. Rep.* **7,** 11671 (2017).

241. Thomas, A. *et al.* Tumor mutational burden is a determinant of immune-mediated survival in breast cancer. *Oncoimmunology* **7,** e1490854 (2018).

242. Matthews, S. B. & Sartorius, C. A. Steroid Hormone Receptor Positive Breast Cancer Patient-Derived Xenografts. *Horm. Cancer* **8,** 4–15 (2017).

243. Dieci, M. V., Griguolo, G., Miglietta, F. & Guarneri, V. The immune system and hormone-receptor positive breast cancer: Is it really a dead end? *Cancer Treat. Rev.* **46,** 9–19 (2016).

244. Vonderheide, R. H., Domchek, S. M. & Clark, A. S. Immunotherapy for Breast Cancer: What Are We Missing? *Clin. Cancer Res.* **23,** 2640–2646 (2017).

245. Cimino-Mathews, A. *et al.* PD-L1 (B7-H1) expression and the immune tumor microenvironment in primary and metastatic breast carcinomas. *Hum. Pathol.* **47,** 52–63 (2016).

246. Bertucci, F. *et al.* How basal are triple-negative breast cancers? *Int. J. Cancer* **123,** 236–240 (2008).

247. Xu, J., Guo, X., Jing, M. & Sun, T. Prediction of tumor mutation burden in breast cancer based on the expression of ER, PR, HER-2, and Ki-67. *Onco. Targets. Ther.* **11,** 2269–2275 (2018).

248. Nagari, A. & Franco, H. L. Interplay between inflammatory and estrogen signaling in breast

cancer. *Cytokine* **76,** 588–590 (2015).

249. Quigley, D. A. *et al.* Age, estrogen, and immune response in breast adenocarcinoma and adjacent normal tissue. *Oncoimmunology* **6,** e1356142 (2017).

250. Rothenberger, N. J., Somasundaram, A. & Stabile, L. P. The Role of the Estrogen Pathway in the Tumor Microenvironment. *Int. J. Mol. Sci.* **19,** (2018).

251. Nanda, R. *et al.* Pembrolizumab in Patients With Advanced Triple-Negative Breast Cancer: Phase Ib KEYNOTE-012 Study. *J. Clin. Oncol.* **34,** 2460–2467 (2016).

252. Liedtke, C. *et al.* Response to neoadjuvant therapy and long-term survival in patients with triple-negative breast cancer. *J. Clin. Oncol.* **26,** 1275–81 (2008).

253. Adams, S. *et al.* Phase 2 study of pembrolizumab (pembro) monotherapy for previously treated metastatic triple-negative breast cancer (mTNBC): KEYNOTE-086 cohort A. *J. Clin. Oncol.* **35,** 1008–1008 (2017).

254. Adams, S. *et al.* Phase 2 study of pembrolizumab as first-line therapy for PD-L1–positive metastatic triple-negative breast cancer (mTNBC): Preliminary data from KEYNOTE-086 cohort B. *J. Clin. Oncol.* **35,** 1088–1088 (2017).

255. Adams, S. *et al.* Abstract P2-11-06: Safety and clinical activity of atezolizumab (anti-PDL1) in combination with nab-paclitaxel in patients with metastatic triple-negative breast cancer. *Cancer Res.* **76,** P2-11-6-P2-11–6 (2016).

256. Schmid, P. *et al.* Abstract 2986: Atezolizumab in metastatic TNBC (mTNBC): Long-term clinical outcomes and biomarker analyses. *Cancer Res.* **77,** 2986–2986 (2017).

257. Dirix, L. Y. *et al.* Avelumab, an anti-PD-L1 antibody, in patients with locally advanced or metastatic breast cancer: a phase 1b JAVELIN Solid Tumor study. *Breast Cancer Res. Treat.* **167,** 671–686 (2018).

258. Tan, A. R. Checkpoint Inhibitors in Breast Cancer: Changing the Therapeutic Landscape | ASCO Annual Meeting. at <https://am.asco.org/checkpoint-inhibitors-breast-cancer-changing-therapeutic-landscape>

259. Rugo, H. S. *et al.* Safety and Antitumor Activity of Pembrolizumab in Patients with Estrogen Receptor-Positive/Human Epidermal Growth Factor Receptor 2-Negative Advanced Breast Cancer. *Clin. Cancer Res.* **24,** 2804–2811 (2018).

260. Loi, S. *et al.* Abstract GS2-06: Phase Ib/II study evaluating safety and efficacy of pembrolizumab and trastuzumab in patients with trastuzumab-resistant HER2-positive metastatic breast cancer: Results from the PANACEA (IBCSG 45-13/BIG 4-13/KEYNOTE-

014) study. *Cancer Res.* **78,** GS2-06-GS2-06 (2018).

261. Sliwkowski, M. X. *et al.* Nonclinical studies addressing the mechanism of action of trastuzumab (Herceptin). *Semin. Oncol.* **26,** 60–70 (1999).

262. Spiridon, C. I., Guinn, S. & Vitetta, E. S. A Comparison of the in Vitro and in Vivo Activities of IgG and F(ab')2 Fragments of a Mixture of Three Monoclonal Anti-Her-2 Antibodies. *Clin. Cancer Res.* **10,** 3542–3551 (2004).

263. Varchetta, S. *et al.* Elements related to heterogeneity of antibody-dependent cell cytotoxicity in patients under trastuzumab therapy for primary operable breast cancer overexpressing Her2. *Cancer Res.* **67,** 11991–9 (2007).

264. Gennari, R. *et al.* Pilot Study of the Mechanism of Action of Preoperative Trastuzumab in Patients with Primary Operable Breast Tumors Overexpressing HER2. *Clin. Cancer Res.* **10,** 5650–5655 (2004).

265. Beano, A. *et al.* Correlation between NK function and response to trastuzumab in metastatic breast cancer patients. *J. Transl. Med.* **6,** 25 (2008).

266. Musolino, A. *et al.* Immunoglobulin G Fragment C Receptor Polymorphisms and Clinical Efficacy of Trastuzumab-Based Therapy in Patients With HER-2/ *neu* –Positive Metastatic Breast Cancer. *J. Clin. Oncol.* **26,** 1789–1796 (2008).

267. Parsons, M. S. *et al.* NKG2D Acts as a Co-Receptor for Natural Killer Cell-Mediated Anti-HIV-1 Antibody-Dependent Cellular Cytotoxicity. *AIDS Res. Hum. Retroviruses* **32,** 1089–1096

268. Deguine, J., Breart, B., Lemaître, F. & Bousso, P. Cutting edge: tumor-targeting antibodies enhance NKG2D-mediated NK cell cytotoxicity by stabilizing NK cell-tumor cell interactions. *J. Immunol.* **189,** 5493–7 (2012).

269. Di Modica, M. *et al.* Taxanes enhance trastuzumab-mediated ADCC on tumor cells through NKG2D-mediated NK cell recognition. *Oncotarget* **7,** 255–65 (2016).

270. Furue, H. *et al.* Decreased risk of colorectal cancer with the high natural killer cell activity NKG2D genotype in Japanese. *Carcinogenesis* **29,** 316–320 (2008).

271. Espinoza, J. L. *et al.* A functional polymorphism in the NKG2D gene modulates NK-cell cytotoxicity and is associated with susceptibility to Human Papilloma Virus-related cancers. *Sci. Rep.* **6,** 39231 (2016).

272. Lombard, A. P. *et al.* ABCB1 Mediates Cabazitaxel–Docetaxel Cross-Resistance in Advanced Prostate Cancer. *Mol. Cancer Ther.* **16,** 2257–2266 (2017).

273. Madrid-Paredes, A. *et al.* ABCB1 C3435T gene polymorphism as a potential biomarker of clinical outcomes in HER2-positive breast cancer patients. *Pharmacol. Res.* **108,** 111–118 (2016).

274. Kim, J.-W. *et al.* ABCB1, FCGR2A, and FCGR3A polymorphisms in patients with HER2-positive metastatic breast cancer who were treated with first-line taxane plus trastuzumab chemotherapy. *Oncology* **83,** 218–27 (2012).

275. Rimawi, M. F. *et al.* EGFR Expression in Breast Cancer Association with biologic phenotype and clinical outcomes. *Cancer* **116,** 1234 (2010).

276. Changavi, A. A., Shashikala, A. & Ramji, A. S. Epidermal Growth Factor Receptor Expression in Triple Negative and Nontriple Negative Breast Carcinomas. *J. Lab. Physicians* **7,** 79–83 (2015).

277. El Guerrab, A. *et al.* Anti-EGFR monoclonal antibodies and EGFR tyrosine kinase inhibitors as combination therapy for triple-negative breast cancer. *Oncotarget* **7,** 73618–73637 (2016).

278. Ferraro, D. A. *et al.* Inhibition of triple-negative breast cancer models by combinations of antibodies to EGFR. *Proc. Natl. Acad. Sci.* **110,** 1815–1820 (2013).

279. Tang, Y. *et al.* The association between PD-L1 and EGFR status and the prognostic value of PD-L1 in advanced non-small cell lung cancer patients treated with EGFR-TKIs. *Oncotarget* **6,** 14209–19 (2015).

280. D'Incecco, A. *et al.* PD-1 and PD-L1 expression in molecularly selected non-small-cell lung cancer patients. *Br. J. Cancer* **112,** 95–102 (2015).

281. Dynabeads Human T-Activator CD3/CD28 for T Cell Expansion and Activation. at <https://www.thermofisher.com/order/catalog/product/11161D>

282. Collins, D. M. *et al.* Trastuzumab induces antibody-dependent cell-mediated cytotoxicity (ADCC) in HER-2-non-amplified breast cancer cell lines. *Ann. Oncol.* **23,** 1788–95 (2012).

283. Bozic, I. *et al.* Accumulation of driver and passenger mutations during tumor progression. *Proc. Natl. Acad. Sci. U. S. A.* **107,** 18545–50 (2010).

284. Futreal, P. A. *et al.* A census of human cancer genes. *Nat. Rev. Cancer* **4,** 177–83 (2004).

285. Kanehisa, M. & Goto, S. KEGG: kyoto encyclopedia of genes and genomes. *Nucleic Acids Res.* **28,** 27–30 (2000).

286. Kelley, J., de Bono, B. & Trowsdale, J. IRIS: A database surveying known human immune system genes. *Genomics* **85,** 503–511 (2005).

287. Ashburner, M. *et al.* Gene Ontology: tool for the unification of biology. *Nat. Genet.* **25,** 25–29 (2000).

288. Abbas, A. R. *et al.* Immune response in silico (IRIS): immune-specific genes identified from a compendium of microarray expression data. *Genes & Immunity* **6,** 319–331 (2005).

289. Yates, B. *et al.* Genenames.org: the HGNC and VGNC resources in 2017. *Nucleic Acids Res.* **45,** D619–D625 (2017).

290. Zhu, J., He, F., Song, S., Wang, J. & Yu, J. How many human genes can be defined as housekeeping with current expression data? *BMC Genomics* **9,** 172 (2008).

291. Vaquerizas, J. M., Kummerfeld, S. K., Teichmann, S. A. & Luscombe, N. M. A census of human transcription factors: function, expression and evolution. *Nat. Rev. Genet.* **10,** 252–63 (2009).

292. Zhang, Y., Xuan, J., de los Reyes, B. G., Clarke, R. & Ressom, H. W. Reconstruction of gene regulatory modules in cancer cell cycle by multi-source data integration. *PLoS One* **5,** e10268 (2010).

293. Cusanovich, D. A., Pavlovic, B., Pritchard, J. K. & Gilad, Y. The functional consequences of variation in transcription factor binding. *PLoS Genet.* **10,** e1004226 (2014).

294. Zhang, H.-M. *et al.* AnimalTFDB: a comprehensive animal transcription factor database. *Nucleic Acids Res.* **40,** D144–D149 (2012).

295. Piccart-Gebhart, M. J. *et al.* First results from the phase III ALTTO trial (BIG 2-06; NCCTG [Alliance] N063D) comparing one year of anti-HER2 therapy with lapatinib alone (L), trastuzumab alone (T), their sequence (T→L), or their combination (T+L) in the adjuvant treatment of HER2-positive early breast cancer (EBC). *J. Clin. Oncol.* **32,** LBA4-LBA4 (2014).

296. Norton, N. *et al.* Association Studies of Fc Receptor Polymorphisms with Outcome in HER2+ Breast Cancer Patients Treated with Trastuzumab in NCCTG (Alliance) Trial N9831. *Cancer Immunol. Res.* **2,** 962–969 (2014).

297. Winslow, S., Leandersson, K., Edsjö, A. & Larsson, C. Prognostic stromal gene signatures in breast cancer. *Breast Cancer Res.* **17,** 23 (2015).

298. Weinberg, A. *et al.* Viability and functional activity of cryopreserved mononuclear cells. *Clin. Diagn. Lab. Immunol.* **7,** 714–6 (2000).

299. Mata, M. M., Mahmood, F., Sowell, R. T. & Baum, L. L. Effects of cryopreservation on effector cells for antibody dependent cell-mediated cytotoxicity (ADCC) and natural killer

(NK) cell activity in (51)Cr-release and CD107a assays. *J. Immunol. Methods* **406,** 1–9 (2014).

300. Yamashita, M. *et al.* A novel method for evaluating antibody-dependent cell-mediated cytotoxicity by flowcytometry using cryopreserved human peripheral blood mononuclear cells. *Sci. Rep.* **6,** 19772 (2016).

301. Broussas, M., Broyer, L. & Goetsch, L. in *Methods in molecular biology (Clifton, N.J.)* **988,** 305–317 (2013).

302. Petricevic, B. *et al.* Trastuzumab mediates antibody-dependent cell-mediated cytotoxicity and phagocytosis to the same extent in both adjuvant and metastatic HER2/neu breast cancer patients. *J. Transl. Med.* **11,** 307 (2013).

303. Okita, R. *et al.* Lapatinib enhances trastuzumab-mediated antibody-dependent cellular cytotoxicity via upregulation of HER2 in malignant mesothelioma cells. *Oncol. Rep.* **34,** 2864–70 (2015).

304. Beldi-Ferchiou, A. *et al.* PD-1 mediates functional exhaustion of activated NK cells in patients with Kaposi sarcoma. *Oncotarget* **7,** 72961–72977 (2016).

305. Pesce, S. *et al.* Identification of a subset of human natural killer cells expressing high levels of programmed death 1: A phenotypic and functional characterization. *J. Allergy Clin. Immunol.* **139,** 335–346.e3 (2017).

306. Sparano, J. A. *et al.* Adjuvant Chemotherapy Guided by a 21-Gene Expression Assay in Breast Cancer. *N. Engl. J. Med.* **379,** 111–121 (2018).

307. Pagès, F. *et al.* International validation of the consensus Immunoscore for the classification of colon cancer: a prognostic and accuracy study. *Lancet (London, England)* **391,** 2128–2139 (2018).

308. Emens, L. A. & Middleton, G. The interplay of immunotherapy and chemotherapy: harnessing potential synergies. *Cancer Immunol. Res.* **3,** 436–43 (2015).

309. Champiat, S. *et al.* Management of immune checkpoint blockade dysimmune toxicities: a collaborative position paper. *Ann. Oncol.* **27,** 559–574 (2016).

310. Gnjatic, S. *et al.* Identifying baseline immune-related biomarkers to predict clinical outcome of immunotherapy. *J. Immunother. Cancer* **5,** 44 (2017).

311. Rizvi, N. A. *et al.* Mutational landscape determines sensitivity to PD-1 blockade in non-small cell lung cancer. *Science (80-.).* **348,** 124–128 (2015).

312. Hurvitz, S. A. *et al.* Analysis of Fc Receptor IIIa and IIa Polymorphisms: Lack of Correlation

with Outcome in Trastuzumab-Treated Breast Cancer Patients. *Clin. Cancer Res.* **18,** 3478–3486 (2012).

313. Marcus, A. *et al.* Recognition of tumors by the innate immune system and natural killer cells. *Adv. Immunol.* **122,** 91–128 (2014).

314. Raulet, D. H. & Vance, R. E. Self-tolerance of natural killer cells. *Nat. Rev. Immunol.* **6,** 520–531 (2006).

315. Trickett, A. & Kwan, Y. L. T cell stimulation and expansion using anti-CD3/CD28 beads. *J. Immunol. Methods* **275,** 251–5 (2003).

316. Onlamoon, N. *et al.* Influence of cell isolation method on the optimization of CD4+ T cell expansion using anti-CD3/CD28 coated beads. *Asian Pacific J. Allergy Immunol.* **31,** 99–105 (2013).

317. Gasteiger, G. *et al.* IL-2-dependent tuning of NK cell sensitivity for target cells is controlled by regulatory T cells. *J. Exp. Med.* **210,** 1167–78 (2013).

318. O'Brien, N. A. *et al.* Activated phosphoinositide 3-kinase/AKT signaling confers resistance to trastuzumab but not lapatinib. *Mol. Cancer Ther.* **9,** 1489–502 (2010).

319. Martkamchan, S., Onlamoon, N., Wang, S., Pattanapanyasat, K. & Ammaranond, P. The Effects of Anti-CD3/CD28 Coated Beads and IL-2 on Expanded T Cell for Immunotherapy. *Adv. Clin. Exp. Med.* **25,** 821–828

320. Chiang, S. C. C. *et al.* Comparison of primary human cytotoxic T-cell and natural killer cell responses reveal similar molecular requirements for lytic granule exocytosis but differences in cytokine production. *Blood* **121,** 1345–56 (2013).

321. Rentzsch, C. *et al.* Evaluation of pre-existent immunity in patients with primary breast cancer: molecular and cellular assays to quantify antigen-specific T lymphocytes in peripheral blood mononuclear cells. *Clin. Cancer Res.* **9,** 4376–86 (2003).

322. Teschner, D. *et al.* In Vitro Stimulation and Expansion of Human Tumour-Reactive CD8+ Cytotoxic T Lymphocytes by Anti-CD3/CD28/CD137 Magnetic Beads. *Scand. J. Immunol.* **74,** 155–164 (2011).

323. Guillerey, C., Huntington, N. D. & Smyth, M. J. Targeting natural killer cells in cancer immunotherapy. *Nat. Immunol.* **17,** 1025–1036 (2016).

324. Wiesmayr, S. *et al.* Decreased NKp46 and NKG2D and elevated PD-1 are associated with altered NK-cell function in pediatric transplant patients with PTLD. *Eur. J. Immunol.* **42,** 541–550 (2012).

325. Benson, D. M. *et al.* The PD-1/PD-L1 axis modulates the natural killer cell versus multiple myeloma effect: a therapeutic target for CT-011, a novel monoclonal anti-PD-1 antibody. *Blood* **116,** 2286–94 (2010).

326. Grimm Tse-Kuan Yu, A., Caudell, E. G. & Smid, C. MKK1/2/ERK But Not p38 Kinase Pathway IL-2 Activation of NK Cells: Involvement of. *J Immunol Ref.* **164,** 6244–6251 (2018).

327. Lehmann, C., Zeis, M. & Uharek, L. Activation of natural killer cells with interleukin 2 (IL-2) and IL-12 increases perforin binding and subsequent lysis of tumour cells. *Br. J. Haematol.* **114,** 660–5 (2001).

328. Dybkaer, K. *et al.* Genome wide transcriptional analysis of resting and IL2 activated human natural killer cells: gene expression signatures indicative of novel molecular signaling pathways. *BMC Genomics* **8,** 230 (2007).

329. Lehmann, C., Zeis, M. & Uharek, L. Activation of natural killer cells with interleukin 2 (IL-2) and IL-12 increases perforin binding and subsequent lysis of tumour cells. *Br. J. Haematol.* **114,** 660–665 (2001).

330. Sarkar, S. *et al.* Hypoxia Induced Impairment of NK Cell Cytotoxicity against Multiple Myeloma Can Be Overcome by IL-2 Activation of the NK Cells. *PLoS One* **8,** e64835 (2013).

331. Garrido, F., Aptsiauri, N., Doorduijn, E. M., Garcia Lora, A. M. & van Hall, T. The urgent need to recover MHC class I in cancers for effective immunotherapy. *Curr. Opin. Immunol.* **39,** 44–51 (2016).

332. Yamauchi, C. *et al.* E-cadherin expression on human carcinoma cell affects trastuzumab-mediated antibody-dependent cellular cytotoxicity through killer cell lectin-like receptor G1 on natural killer cells. *Int. J. Cancer* **128,** 2125–2137 (2011).

333. Dominguez, C., Tsang, K.-Y. & Palena, C. Short-term EGFR blockade enhances immune-mediated cytotoxicity of EGFR mutant lung cancer cells: rationale for combination therapies. *Cell Death Dis.* **7,** e2380 (2016).

334. Ware, K. E. *et al.* A mechanism of resistance to gefitinib mediated by cellular reprogramming and the acquisition of an FGF2-FGFR1 autocrine growth loop. *Oncogenesis* **2,** e39 (2013).

335. Chang, J. S. *et al.* Comprehensive Analysis of the Incidence and Survival Patterns of Lung Cancer by Histologies, Including Rare Subtypes, in the Era of Molecular Medicine and Targeted Therapy: A Nation-Wide Cancer Registry-Based Study From Taiwan. *Medicine (Baltimore).* **94,** e969 (2015).

336. Zhang, W. *et al.* FCGR2A and FCGR3A polymorphisms associated with clinical outcome of epidermal growth factor receptor expressing metastatic colorectal cancer patients treated with single-agent cetuximab. *J. Clin. Oncol.* **25,** 3712–8 (2007).

337. O'Brien, N. A. *et al.* Activated phosphoinositide 3-kinase/AKT signaling confers resistance to trastuzumab but not lapatinib. *Mol. Cancer Ther.* **9,** 1489–502 (2010).

338. Chen, Y.-N. P. *et al.* Allosteric inhibition of SHP2 phosphatase inhibits cancers driven by receptor tyrosine kinases. *Nature* **535,** 148–152 (2016).

339. Buffière, A. *et al.* Saracatinib impairs maintenance of human T-ALL by targeting the LCK tyrosine kinase in cells displaying high level of lipid rafts. *Leukemia* **32,** 2062–2065 (2018).

340. Wang, C. *et al.* Prognostic Value of PD-L1 in Breast Cancer: A Meta-Analysis. *Breast J.* **23,** 436–443 (2017).

341. Wang, Z.-Q. *et al.* PD-L1 and intratumoral immune response in breast cancer. *Oncotarget* **8,** 51641–51651 (2017).

342. Ali, H. R. *et al.* PD-L1 protein expression in breast cancer is rare, enriched in basal-like tumours and associated with infiltrating lymphocytes. *Ann. Oncol.* **26,** 1488–1493 (2015).

343. Alluri, P. & Newman, L. A. Basal-like and triple-negative breast cancers: searching for positives among many negatives. *Surg. Oncol. Clin. N. Am.* **23,** 567–77 (2014).

344. Rom-Jurek, E.-M. *et al.* Regulation of Programmed Death Ligand 1 (PD-L1) Expression in Breast Cancer Cell Lines In Vitro and in Immunodeficient and Humanized Tumor Mice. *Int. J. Mol. Sci.* **19,** (2018).

345. Soliman, H., Khalil, F. & Antonia, S. PD-L1 expression is increased in a subset of basal type breast cancer cells. *PLoS One* **9,** e88557 (2014).

346. Yu, H., Boyle, T. A., Zhou, C., Rimm, D. L. & Hirsch, F. R. PD-L1 Expression in Lung Cancer. *J. Thorac. Oncol.* **11,** 964–75 (2016).

347. McDermott, M. S. *et al.* PP2A inhibition overcomes acquired resistance to HER2 targeted therapy. *Mol. Cancer* **13,** 157 (2014).

348. Ritter, C. A. *et al.* Human Breast Cancer Cells Selected for Resistance to Trastuzumab In vivo Overexpress Epidermal Growth Factor Receptor and ErbB Ligands and Remain Dependent on the ErbB Receptor Network. *Clin. Cancer Res.* **13,** 4909–4919 (2007).

349. Kakavand, H. *et al.* PD-L1 Expression and Immune Escape in Melanoma Resistance to MAPK Inhibitors. *Clin. Cancer Res.* **23,** 6054–6061 (2017).

350. Sumimoto, H., Takano, A., Teramoto, K. & Daigo, Y. RAS–Mitogen-Activated Protein Kinase Signal Is Required for Enhanced PD-L1 Expression in Human Lung Cancers. *PLoS One* **11,** e0166626 (2016).

351. Lastwika, K. J. *et al.* Control of PD-L1 Expression by Oncogenic Activation of the AKT–mTOR Pathway in Non–Small Cell Lung Cancer. *Cancer Res.* **76,** 227–238 (2016).

352. Monypenny, J. *et al.* ALIX Regulates Tumor-Mediated Immunosuppression by Controlling EGFR Activity and PD-L1 Presentation. *Cell Rep.* **24,** 630–641 (2018).

353. Tung, J.-N. *et al.* PD-L1 confers resistance to EGFR mutation-independent tyrosine kinase inhibitors in non-small cell lung cancer via upregulation of YAP1 expression. *Oncotarget* **9,** 4637–4646 (2018).

354. Liu, Z. *et al.* SHP2 negatively regulates HLA-ABC and PD-L1 expression via STAT1 phosphorylation in prostate cancer cells. *Oncotarget* **8,** 53518–53530 (2017).

355. Han, T. *et al.* PTPN11/Shp2 overexpression enhances liver cancer progression and predicts poor prognosis of patients. *J. Hepatol.* **63,** 651–660 (2015).

356. Shi, M., Cooper, J. C. & Yu, C.-L. A constitutively active Lck kinase promotes cell proliferation and resistance to apoptosis through signal transducer and activator of transcription 5b activation. *Mol. Cancer Res.* **4,** 39–45 (2006).

357. Im, J. S. *et al.* Immune-Modulation by Epidermal Growth Factor Receptor Inhibitors: Implication on Anti-Tumor Immunity in Lung Cancer. *PLoS One* **11,** e0160004 (2016).

358. Ohta, A. A Metabolic Immune Checkpoint: Adenosine in Tumor Microenvironment. *Front. Immunol.* **7,** 109 (2016).

359. Vaupel, P. & Multhoff, G. Commentary: A Metabolic Immune Checkpoint: Adenosine in Tumor Microenvironment. *Front. Immunol.* **7,** 332 (2016).

360. Collins DM, O'Donovan N, Mahgoub T, Gately K, Hughes C, Davies A, O'Byrne KJ, Crown, J. Trastuzumab (T) and pertuzumab (P)-mediated antibody-dependent cell-mediated cytotoxicity (ADCC) in tyrosine kinase inhibitor (TKI)-treated breast cancer (BC) cell lines. *J Clin Oncol* **32:5s,** suppl; abstr 643 (2014).

361. Gaynor, N. *et al.* 14PAlterations to trastuzumab-induced antibody-dependent cell-mediated cytotoxicity (T-ADCC) in a lapatinib-resistant HER2+ breast cancer cell line model. *Ann. Oncol.* **28,** (2017).

362. Cekic, C., Day, Y.-J., Sag, D. & Linden, J. Myeloid Expression of Adenosine A2A Receptor Suppresses T and NK Cell Responses in the Solid Tumor Microenvironment. *Cancer Res.* **74,**

7250–7259 (2014).

363. Young, A. *et al.* Co-inhibition of CD73 and A2AR Adenosine Signaling Improves Anti-tumor Immune Responses. *Cancer Cell* **30,** 391–403 (2016).

364. Turcotte, M. *et al.* CD73 Promotes Resistance to HER2/ErbB2 Antibody Therapy. *Cancer Res.* **77,** 5652–5663 (2017).

365. Koukourakis, M. I. *et al.* Prospective neoadjuvant analysis of PET imaging and mechanisms of resistance to Trastuzumab shows role of HIF1 and autophagy. *Br. J. Cancer* **110,** 2209–16 (2014).

366. Aghazadeh, S. & Yazdanparast, R. Activation of STAT3/HIF-1α/Hes-1 axis promotes trastuzumab resistance in HER2-overexpressing breast cancer cells via down-regulation of PTEN. *Biochim. Biophys. Acta - Gen. Subj.* **1861,** 1970–1980 (2017).

367. Ribas, A. *et al.* Association of Pembrolizumab With Tumor Response and Survival Among Patients With Advanced Melanoma. *JAMA* **315,** 1600 (2016).

368. Maeda, H. & Khatami, M. Analyses of repeated failures in cancer therapy for solid tumors: poor tumor-selective drug delivery, low therapeutic efficacy and unsustainable costs. *Clin. Transl. Med.* **7,** 11 (2018).

369. Ascierto, P. A. *et al.* Sequential treatment with ipilimumab and BRAF inhibitors in patients with metastatic melanoma: data from the Italian cohort of the ipilimumab expanded access program. *Cancer Invest.* **32,** 144–9 (2014).

370. Atefi, M. *et al.* Effects of MAPK and PI3K pathways on PD-L1 expression in melanoma. *Clin. Cancer Res.* **20,** 3446–57 (2014).

371. Krangel, M. S. Mechanics of T cell receptor gene rearrangement. *Curr. Opin. Immunol.* **21,** 133–9 (2009).

372. González, D. *et al.* Immunoglobulin gene rearrangements and the pathogenesis of multiple myeloma. *Blood* **110,** 3112–21 (2007).

373. Trowsdale, J. & Knight, J. C. Major histocompatibility complex genomics and human disease. *Annu. Rev. Genomics Hum. Genet.* **14,** 301–23 (2013).

374. Bosch, F. X., Lorincz, A., Muñoz, N., Meijer, C. J. L. M. & Shah, K. V. The causal relation between human papillomavirus and cervical cancer. *J. Clin. Pathol.* **55,** 244–65 (2002).

375. Xie, X., Yang, M., Ding, Y. & Chen, J. Microbial infection, inflammation and epithelial ovarian cancer. *Oncol. Lett.* **14,** 1911–1919 (2017).

376. Iizasa, H., Nanbo, A., Nishikawa, J., Jinushi, M. & Yoshiyama, H. Epstein-Barr Virus (EBV)-associated gastric carcinoma. *Viruses* **4,** 3420–39 (2012).

377. Lawson, J. S., Salmons, B. & Glenn, W. K. Oncogenic Viruses and Breast Cancer: Mouse Mammary Tumor Virus (MMTV), Bovine Leukemia Virus (BLV), Human Papilloma Virus (HPV), and Epstein-Barr Virus (EBV). *Front. Oncol.* **8,** 1 (2018).

378. Dziurzynski, K. *et al.* Consensus on the role of human cytomegalovirus in glioblastoma. *Neuro. Oncol.* **14,** 246–55 (2012).

379. Marur, S., D'Souza, G., Westra, W. H. & Forastiere, A. A. HPV-associated head and neck cancer: a virus-related cancer epidemic. *Lancet Oncol.* **11,** 781–789 (2010).

380. American Cancer Society. Viruses that can lead to cancer. at <https://www.cancer.org/cancer/cancer-causes/infectious-agents/infections-that-can-lead-to-cancer/viruses.html>

381. Robinson, L. A. *et al.* Molecular evidence of viral DNA in non-small cell lung cancer and non-neoplastic lung. *Br. J. Cancer* **115,** 497–504 (2016).

382. Hassan, M. M. *et al.* Association between hepatitis B virus and pancreatic cancer. *J. Clin. Oncol.* **26,** 4557–62 (2008).

383. Li, N. *et al.* Human papillomavirus infection and bladder cancer risk: a meta-analysis. *J. Infect. Dis.* **204,** 217–23 (2011).

384. Akhtar, S., Vranic, S., Cyprian, F. S. & Al Moustafa, A.-E. Epstein-Barr Virus in Gliomas: Cause, Association, or Artifact? *Front. Oncol.* **8,** 123 (2018).

385. Wang, Z. *et al.* The Landscape of Viral Expression Reveals Clinically Relevant Viruses with Potential Capability of Promoting Malignancy in Lower-Grade Glioma. *Clin. Cancer Res.* **23,** 2177–2185 (2017).

386. Pascale, M. *et al.* Is Human Papillomavirus Associated with Prostate Cancer Survival? *Dis. Markers* **35,** 607–613 (2013).

387. Arzumanyan, A., Reis, H. M. G. P. V. & Feitelson, M. A. Pathogenic mechanisms in HBV- and HCV-associated hepatocellular carcinoma. *Nat. Rev. Cancer* **13,** 123–135 (2013).

388. Xu, W., Liu, Z., Bao, Q. & Qian, Z. Viruses, Other Pathogenic Microorganisms and Esophageal Cancer. *Gastrointest. tumors* **2,** 2–13 (2015).

389. Fiorina, L. *et al.* Systematic analysis of human oncogenic viruses in colon cancer revealed EBV latency in lymphoid infiltrates. *Infect. Agent. Cancer* **9,** 18 (2014).

390. Ralphs, S. & Khan, S. A. The role of the hepatitis viruses in cholangiocarcinoma. *J. Viral Hepat.* **20,** 297–305 (2013).

391. Shimakage, M. *et al.* Expression of Epstein-Barr virus in thyroid carcinoma correlates with tumor progression. *Hum. Pathol.* **34,** 1170–7 (2003).

392. Powles, T. *et al.* Multicenter study of human immunodeficiency virus-related germ cell tumors. *J. Clin. Oncol.* **21,** 1922–7 (2003).

393. Cesarman, E. How do viruses trick B cells into becoming lymphomas? *Curr. Opin. Hematol.* **21,** 358–368 (2014).

394. Rivera, Z. *et al.* The relationship between simian virus 40 and mesothelioma. *Curr. Opin. Pulm. Med.* **14,** 316–321 (2008).

395. Beroukhim, R. *et al.* The landscape of somatic copy-number alteration across human cancers. *Nature* **463,** 899–905 (2010).

396. Slamon, D. J. *et al.* Use of chemotherapy plus a monoclonal antibody against HER2 for metastatic breast cancer that overexpresses HER2. *N. Engl. J. Med.* **344,** 783–92 (2001).

397. Palmberg, C. *et al.* Androgen receptor gene amplification in a recurrent prostate cancer after monotherapy with the nonsteroidal potent antiandrogen Casodex (bicalutamide) with a subsequent favorable response to maximal androgen blockade. *Eur. Urol.* **31,** 216–9 (1997).

398. Gorre, M. E. *et al.* Clinical Resistance to STI-571 Cancer Therapy Caused by BCR-ABL Gene Mutation or Amplification. *Science (80-.).* **293,** 876–880 (2001).

399. Shou, J. *et al.* Mechanisms of tamoxifen resistance: increased estrogen receptor-HER2/neu cross-talk in ER/HER2-positive breast cancer. *J. Natl. Cancer Inst.* **96,** 926–35 (2004).

400. Edwards, S. L. *et al.* Resistance to therapy caused by intragenic deletion in BRCA2. *Nature* **451,** 1111–1115 (2008).

401. Aas, T. *et al.* Specific P53 mutations are associated with de novo resistance to doxorubicin in breast cancer patients. *Nat. Med.* **2,** 811–4 (1996).

402. Oostlander, A., Meijer, G. & Ylstra, B. Microarray-based comparative genomic hybridization and its applications in human genetics. *Clin. Genet.* **66,** 488–495 (2004).

403. Cicchini, M. *et al.* Context-Dependent Effects of Amplified MAPK Signaling during Lung Adenocarcinoma Initiation and Progression. *Cell Rep.* **18,** 1958–1969 (2017).

404. Alsina, J. *et al.* Detection of mutations in the mitogen-activated protein kinase pathway in human melanoma. *Clin. Cancer Res.* **9,** 6419–25 (2003).

405. Reams, A. B. & Roth, J. R. Mechanisms of gene duplication and amplification. *Cold Spring Harb. Perspect. Biol.* **7,** a016592 (2015).

406. Zlotorynski, E. *et al.* Molecular basis for expression of common and rare fragile sites. *Mol. Cell. Biol.* **23,** 7143–51 (2003).

407. Tanaka, H. & Yao, M.-C. Palindromic gene amplification — an evolutionarily conserved role for DNA inverted repeats in the genome. *Nat. Rev. Cancer* **9,** 216–224 (2009).

408. Hastings, P. J., Lupski, J. R., Rosenberg, S. M. & Ira, G. Mechanisms of change in gene copy number. *Nat. Rev. Genet.* **10,** 551–64 (2009).

409. Sun, L. *et al.* Preferential Protection of Genetic Fidelity within Open Chromatin by the Mismatch Repair Machinery. *J. Biol. Chem.* **291,** 17692–705 (2016).

410. Miller, M. L. *et al.* Pan-Cancer Analysis of Mutation Hotspots in Protein Domains. *Cell Syst.* **1,** 197–209 (2015).

411. Chang, M. T. *et al.* Accelerating Discovery of Functional Mutant Alleles in Cancer. *Cancer Discov.* **8,** 174–183 (2018).

412. Chen, T. *et al.* Hotspot mutations delineating diverse mutational signatures and biological utilities across cancer types. *BMC Genomics* **17 Suppl 2,** 394 (2016).

413. Davies, H. *et al.* Mutations of the BRAF gene in human cancer. *Nature* **417,** 949–54 (2002).

414. Sim, E. H., Yang, I. A., Wood-Baker, R., Bowman, R. V & Fong, K. M. Gefitinib for advanced non-small cell lung cancer. *Cochrane Database Syst. Rev.* **1,** CD006847 (2018).

415. Knight, J. C. Genomic modulators of the immune response. *Trends Genet.* **29,** 74–83 (2013).

416. Smith, J. S. *et al.* Human papillomavirus type distribution in invasive cervical cancer and high-grade cervical lesions: A meta-analysis update. *Int. J. Cancer* **121,** 621–632 (2007).

417. Song, D., Li, H., Li, H. & Dai, J. Effect of human papillomavirus infection on the immune system and its role in the course of cervical cancer. *Oncol. Lett.* **10,** 600–606 (2015).

418. Lengyel, E. Ovarian cancer development and metastasis. *Am. J. Pathol.* **177,** 1053–64 (2010).

419. Bell, D. *et al.* Integrated genomic analyses of ovarian carcinoma. *Nature* **474,** 609–615 (2011).

420. Trabert, B. *et al.* Aspirin, Nonaspirin Nonsteroidal Anti-inflammatory Drug, and Acetaminophen Use and Risk of Invasive Epithelial Ovarian Cancer: A Pooled Analysis in the Ovarian Cancer Association Consortium. *JNCI J. Natl. Cancer Inst.* **106,** djt431-djt431 (2014).

421. Al-Shabanah, O. A. *et al.* Human papillomavirus genotyping and integration in ovarian cancer

Saudi patients. *Virol. J.* **10,** 343 (2013).

422. Bilyk, O. O., Pande, N. T., Pejovic, T. & Buchinska, L. G. The frequency of human papilloma virus types 16, 18 in upper genital tract of women at high risk of developing ovarian cancer. *Exp. Oncol.* **36,** 121–4 (2014).

423. Shanmughapriya, S. *et al.* Viral and bacterial aetiologies of epithelial ovarian cancer. *Eur. J. Clin. Microbiol. Infect. Dis.* **31,** 2311–2317 (2012).

424. Arnould, L. *et al.* Trastuzumab-based treatment of HER2-positive breast cancer: an antibody-dependent cellular cytotoxicity mechanism? *Br. J. Cancer* **94,** (2006).

425. Crown, J. *et al.* Abstract P4-12-25: Randomized phase II study of pre-operative docetaxel, carboplatin with trastuzumab (TCH) and/or/lapatinib (L) in HER-2 positive (H+) breast cancer patients (BC pts). ICORG 10-05. *Cancer Res.* **73,** P4-12-25-P4-12–25 (2013).

426. Huober, J. B. *et al.* Survival outcomes of the NeoALTTO study: Updated results of a randomized multicenter phase III neoadjuvant trial. *J. Clin. Oncol.* **35,** 512–512 (2017).

427. Carrillo, M. A., Zhen, A. & Kitchen, S. G. The Use of the Humanized Mouse Model in Gene Therapy and Immunotherapy for HIV and Cancer. *Front. Immunol.* **9,** 746 (2018).

428. Chen, N. *et al.* Upregulation of PD-L1 by EGFR Activation Mediates the Immune Escape in EGFR-Driven NSCLC: Implication for Optional Immune Targeted Therapy for NSCLC Patients with EGFR Mutation. *J. Thorac. Oncol.* **10,** 910–923 (2015).

429. Gainor, J. F. *et al.* EGFR Mutations and ALK Rearrangements Are Associated with Low Response Rates to PD-1 Pathway Blockade in Non-Small Cell Lung Cancer: A Retrospective Analysis. *Clin. Cancer Res.* **22,** 4585–4593 (2016).

430. Ahn, M.-J. *et al. 136O: Osimertinib combined with durvalumab in EGFR-mutant non-small cell lung cancer: Results from the TATTON phase Ib trial*. (2016). doi:10.1016/S1556-0864(16)30246-5

431. Combination Checkpoint Inhibitor Plus Erlotinib or Crizotinib for EGFR or ALK Mutated Stage IV Non-small Cell Lung Cancer - Full Text View - ClinicalTrials.gov. at <https://clinicaltrials.gov/ct2/show/NCT01998126>

432. Ma Brigette. Preliminary safety and clinical activity of erlotinib plus atezolizumab from a Phase Ib study in advanced NSCLC | OncologyPRO. *Ann. Oncol.* **27 (suppl_9),** ix139-ix156 (2016).

433. Groenendijk, F. H. & Bernards, R. Drug resistance to targeted therapies: déjà vu all over again. *Mol. Oncol.* **8,** 1067–83 (2014).

434. Ke, X. & Shen, L. Molecular targeted therapy of cancer: The progress and future prospect. *Front. Lab. Med.* **1,** 69–75 (2017).

435. Huang, M., Shen, A., Ding, J. & Geng, M. Molecularly targeted cancer therapy: some lessons from the past decade. *Trends Pharmacol. Sci.* **35,** 41–50 (2014).

436. Rooney, M. S., Shukla, S. A., Wu, C. J., Getz, G. & Hacohen, N. Molecular and genetic properties of tumors associated with local immune cytolytic activity. *Cell* **160,** 48–61 (2015).

437. O'Donnell, J. S., Long, G. V., Scolyer, R. A., Teng, M. W. L. & Smyth, M. J. Resistance to PD1/PDL1 checkpoint inhibition. *Cancer Treat. Rev.* **52,** 71–81 (2017).

Appendix 1

Document 1: Ethical approval received from SVUH in 2009 for Prof. John Crown to draw blood samples to examine "cell-mediated cytotoxicity in response to trastuzumab in non-HER2 amplified breast cancer cell lines."

Document 2: Ethical approval received from DCU in 2009 for Dr. Norma O'Donovan and Dr. Denis Collins to draw blood samples to examine "cell-mediated cytotoxicity in response to trastuzumab in non-HER2 amplified breast cancer cell lines."

Document 3: Biological safety approval granted July 2017 from DCU biological safety committee for blood samples to be handled as part of the "Human immune cell anti-cancer study" in the NICB by Dr. Denis Collins and Nicola Gaynor.

Document 4: Ethical approval granted to Dr. Denis Collins and Nicola Gaynor, July 2017, from DCU REC committee for blood samples to be drawn for use in the "Human immune cell anti-cancer study".

Document 5: Plain language statement sent to every prospective volunteer for the "Human immune cell anti-cancer study", explaining in lay terms the background, aims and legalities of the study.

Document 6: Informed consent for, which was read, signed, dated and witnessed for every volunteer who donated a blood sample for the "Human immune cell anti-cancer study".

Document 1

St. Vincent's Healthcare GROUP LIMITED

UCD DUBLIN

Ethics and Medical Research Committee
ELM PARK, DUBLIN 4
Tel. (01) 2214117 Fax (01) 2214428 email: joan.mcdonnell@ucd.ie

2nd April 2009

Prof. J. Crown
Consultant Oncologist
St. Vincent's University Hospital
Elm Park
Dublin 4

Re: Cell-mediated cytotoxicity in response to trastuzumab treatment in Non-HER-2 amplified breast cancer cell lines.

Dear Professor Crown,

Thank you for the application to the Ethics Committee dated 30th March 2009.

As Chairman of the Committee I have reviewed the documentation, and have decided that this study does not require full Ethics Committee review and have granted Chairman's approval.

Yours sincerely,

Dr. B. Kirby,
Chairman,
Ethics and Medical Research Committee.

Document 2

DCU

Dublin City University
Ollscoil Chathair Bhaile Átha Cliath

Office of the Vice-President for Research
Dublin 9, Ireland

Dr. Norma O'Donovan
National Institute for Cellular Biotechnology

4th June 2009

REC Reference: DCUREC/2009/063

Proposal Title: **Cell-mediated cytotoxicity in response to trastuzumab exposure in non-Her-2 amplified breast cancer cell lines**

Applicants: Dr. Norma O'Donovan, Dr. Denis Collins

Dear Norma,

This research proposal qualifies under our Notification Procedure, as a low risk project. Therefore, the DCU Research Ethics Committee approves this research proposal. Should substantial modifications to the research protocol be required at a later stage, a further submission should be made to the REC.

Yours sincerely,

Mr. Brian Trench
Chair
DCU Research Ethics Committee

DCU
Office of the Vice-President for Research

Telephone 353 (0)1 700 8000
Facsimile 353 (0)1 700 8002
Email research@dcu.ie
Website www.dcu.ie

Document 3

Faculty of Science & Health

Biological Safety Committee Approval Form

(Submission of Information on GMO & Biological Hazard)

Date of Approval: 3 July 2017
Submission on behalf of: Nicola Gaynor/Denis Collins
Affiliated School/ Centre: NICB

Project Title: Human immune cell anti-cancer study

Decision
On behalf of the Biological Safety Committee, I hereby confirm approval for the project titled above. All amendments and additional information requested from Nicola Gaynor/Denis Collins has been completed and the relevant forms updated.

Dr Sandra O'Neill.

Dr. Sandra O'Neill
Chair of the Biological Safety Committee

Document 4

Ollscoil Chathair Bhaile Átha Cliath
Dublin City University

DCU

Dr Denis Collins
Ms Nicola Gaynor

National Institute for Cellular Biotechnology (NICB)

6th July 2017

REC Reference: **DCUREC/2017/116**

Proposal Title: **Human immune cell anti-cancer study**

Applicant(s): **Dr Denis Collins, Ms Nicola Gaynor**

Dear Nicola, Denis:

Further to expedited review, the DCU Research Ethics Committee approves this research proposal.

Materials used to recruit participants should note that ethical approval for this project has been obtained from the Dublin City University Research Ethics Committee.

Should substantial modifications to the research protocol be required at a later stage, a further amendment submission should be made to the REC.

Yours sincerely,

Donal O'Gorman

Dr Dónal O'Gorman
Chairperson
DCU Research Ethics Committee

DCU
Research & Innovation

Taighde & Nuálaíocht Tacaíocht
Ollscoil Chathair Bhaile Átha Cliath,
Baile Átha Cliath, Éire

Research & Innovation Support
Dublin City University
Dublin 9, Ireland

T +353 1 700 8000
F +353 1 70 0 8002
E research@dcu.ie
www.dcu.ie

Document 5

DUBLIN CITY UNIVERSITY

Plain Language Statement

Study title: Human immune cell anti-cancer study

Research Group: Cancer Biotherapeutics, National Institute for Cellular Biotechnology, School of Biotechnology, Dublin City University.

Principal Investigator: Dr. Denis Collins, Email: denis.collins@dcu.ie Phone: 01 7005647

Co-investigator: Nicola Gaynor, Email: nicola.gaynor4@mail.dcu.ie Phone: 01 7006233

Study requirements: This study requires a once off donation of a 20 ml. blood sample from a healthy volunteer (no acute illness at time of donation e.g. cough, sore throat), information on your sex and age range at time of donation.

Risks: There are minor risks associated with this study. These are the standard risks associated with phlebotomies, such as mild pain and minor bruising at the site at which blood is drawn.

Reason for study: This study aims to identify the best combinations of cancer therapies for increasing the anti-cancer immune response. The long term goal is to provide evidence to support clinical trials of these combinations in the future. The experiments we will be carrying out require white blood cells and plasma which can be isolated from a healthy volunteer blood sample. These white blood cells will be incubated with cancer cells and immune relevant treatments (immune checkpoint inhibitors and monoclonal antibodies). Cancer cell death will then be measured to determine the effectiveness of the treatments at directing the immune cells to kill the cancer cells. The plasma will be used to identify other factors associated with immune cells that are particularly effective at killing cancer cells.

Compensation: There is no remuneration for participation in this study. Participants will not benefit directly from the study but the study will advance knowledge of cancer and the immune system.

CONFIDENTIALITY: BLOOD SAMPLES WILL BE ANONYMISED ONCE TAKEN. PARTICIPANTS WILL NOT RECEIVE INDIVIDUAL RESULTS FROM THIS STUDY. ANONYMISED, AGGREGATED STUDY RESULTS WILL BE INCLUDED IN PEER-REVIEWED PUBLICATIONS, POSTER AND ORAL PRESENTATIONS. CONFIDENTIALITY OF INFORMATION PROVIDED IS SUBJECT TO LEGAL LIMITATIONS. The consent forms are the only data that will be retained for this project. Folders containing consent forms will be stored in secure cabinets in locked offices. Consent forms will be retained for a period and then destroyed. Data will not be held for longer than necessary to fulfill the purpose for which it was originally collected.

Study withdrawal: Participants may withdraw from the research study at any point without giving a reason. Should a participant withdraw consent, all identifiable data and identifiable human biological samples will be destroyed either when the participant withdraws or when the research participant specifically requests that this occur.

If participants have concerns about this study and wish to contact an independent person, please contact: The Secretary, Dublin City University Research Ethics Committee, c/o Research and Innovation Support, Dublin City University, Dublin 9. Tel 01-7008000, E-mail **rec@dcu.ie**

Document 6

DUBLIN CITY UNIVERSITY

Informed Consent Form

Human immune cell anti-cancer study

Cancer Biotherapeutics Research Group

National Institute for Cellular Biotechnology

Dr. Denis Collins

Nicola Gaynor

There has been recent success in a new line of treatments targeting immunosuppression. However, patient response has been limited to undefined subsets.

Response may be boosted by combining different treatments which augment the immune response, such as monoclonal antibodies capable of eliciting antibody dependent cell-mediated cytotoxicity (ADCC) with immune checkpoint inhibitors which can relieve immunosuppression.

The aim of this project is to examine the role of immune-related therapies on immune cell mediated cytotoxicity. Using white blood cells isolated from healthy volunteers' blood, we can then investigate combinations of immune relevant treatments to determine how they affect the immune cells ability to kill cancer cells.

Participant – please complete the following (Circle Yes or No for each question)	
I have read the Plain Language Statement (or had it read to me)	*Yes/No*
I understand the information provided	*Yes/No*
I have had an opportunity to ask questions and discuss this study	*Yes/No*
I have received satisfactory answers to all my questions	*Yes/No*

I understand that I am free to withdraw from the study at any time without giving a reason and without this affecting my future medical care	*Yes/No*
I agree to take part in the study	*Yes/No*

Your identity will remain confidential and your name will not be published or disclosed to anyone. Your blood sample will be identified by a unique number. Confidentiality of information provided is subject to legal limitations.

This study is organised by Prof. John Crown and the cancer biotherapeutics group, National Institute for Cellular Biotechnology, Dublin City University. This research is funded by the clinical cancer research trust. You will not be paid for taking part in this study and any expenses incurred will not be covered for taking part in this study.

Signature:

I have read and understood the information in this form. My questions and concerns have been answered by the researchers, and I have a copy of this consent form. Therefore, I consent to take part in this research project

Participants Signature: _____

Name in Block Capitals: _____

Witness: _____

Date: _____

Appendix 2

Figure 1: Densitometry results for EGFR, pEGFR, AKT, pAKT, MAPK and pMAPK for HCC1954-Par cell line with EGF and lapatinib treatments in HI FBS. Section 5.3.2.1.

Figure 2: Densitometry results for EGFR, pEGFR, AKT, pAKT, MAPK and pMAPK for HCC1954-Lap cell line with EGF and lapatinib treatments in HI FBS. Section 5.3.2.2.

Figure 3: Densitometry results for EGFR, pEGFR, AKT, pAKT, MAPK and pMAPK for SKBR3-Par cell line with EGF and lapatinib treatments in HI FBS. Section 5.3.2.3.

Figure 4: Densitometry results for EGFR, pEGFR, AKT, pAKT, MAPK and pMAPK for SKBR3-Afa cell line with EGF and lapatinib treatments in HI FBS. Section 5.3.2.4.

Figure 5: Densitometry results for EGFR and pEGFR for the HCC1954 cell line treated with EGF and lapatinib, saracatinib and SHP099. Section 5.4.3.2.

Figure 6: Densitometry results for PTPN11 and pPTPN11 for the HCC1954 cell line treated with EGF and lapatinib, saracatinib and SHP099. Section 5.4.3.3.

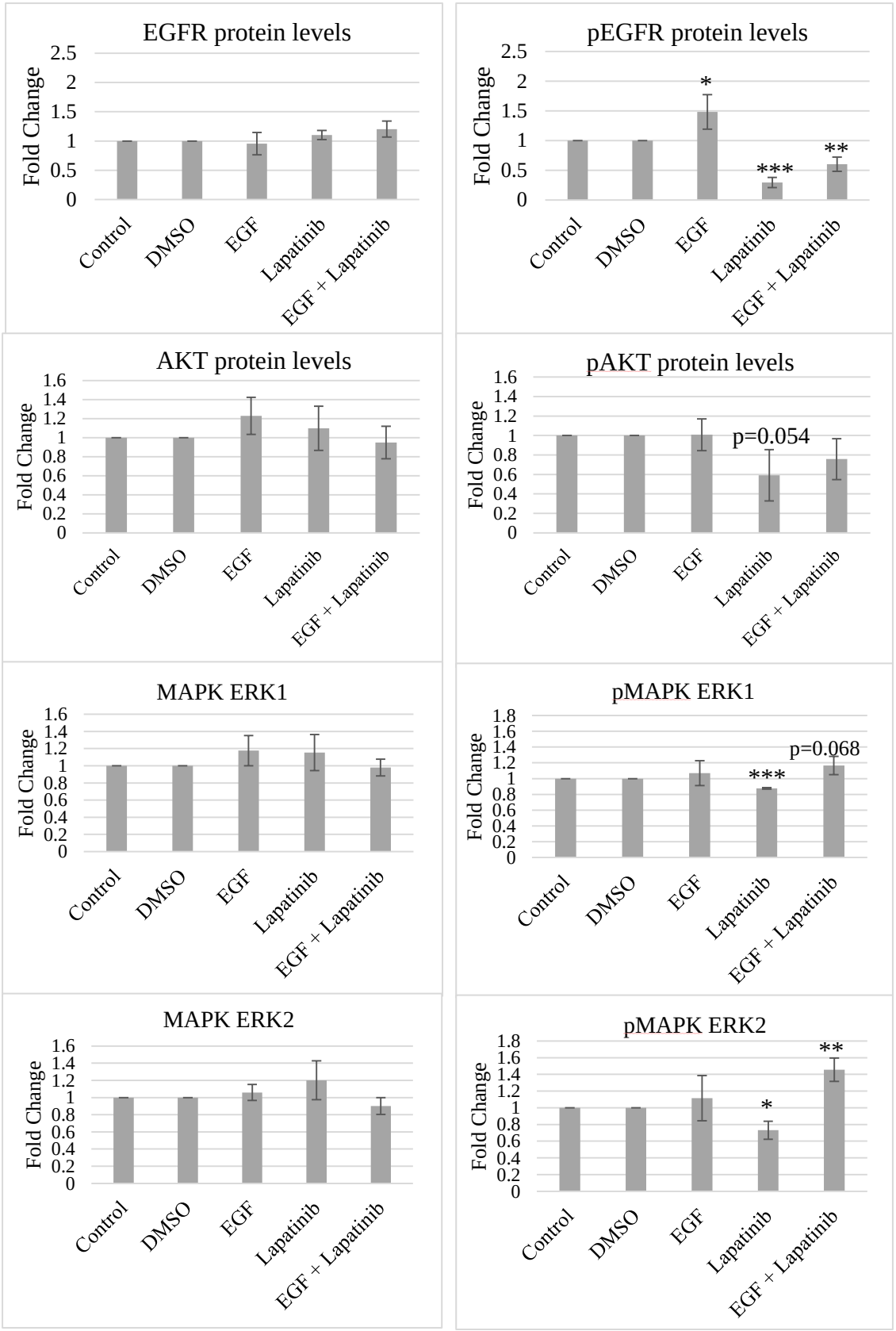

Figure 1: Densitometry analysis of immunoblots of the HCC1954 cell line for EGFR, pEGFR, AKT, pAKT, MAPK and pMAPK protein levels in HI serum conditions. Protein levels are normalised to control protein levels. Error bars represent standard deviation of biological triplicate experiments. The Student's t test was used to determine statistical significance. * $p < 0.05$, ** $p < 0.01$ and *** $p < 0.001$.

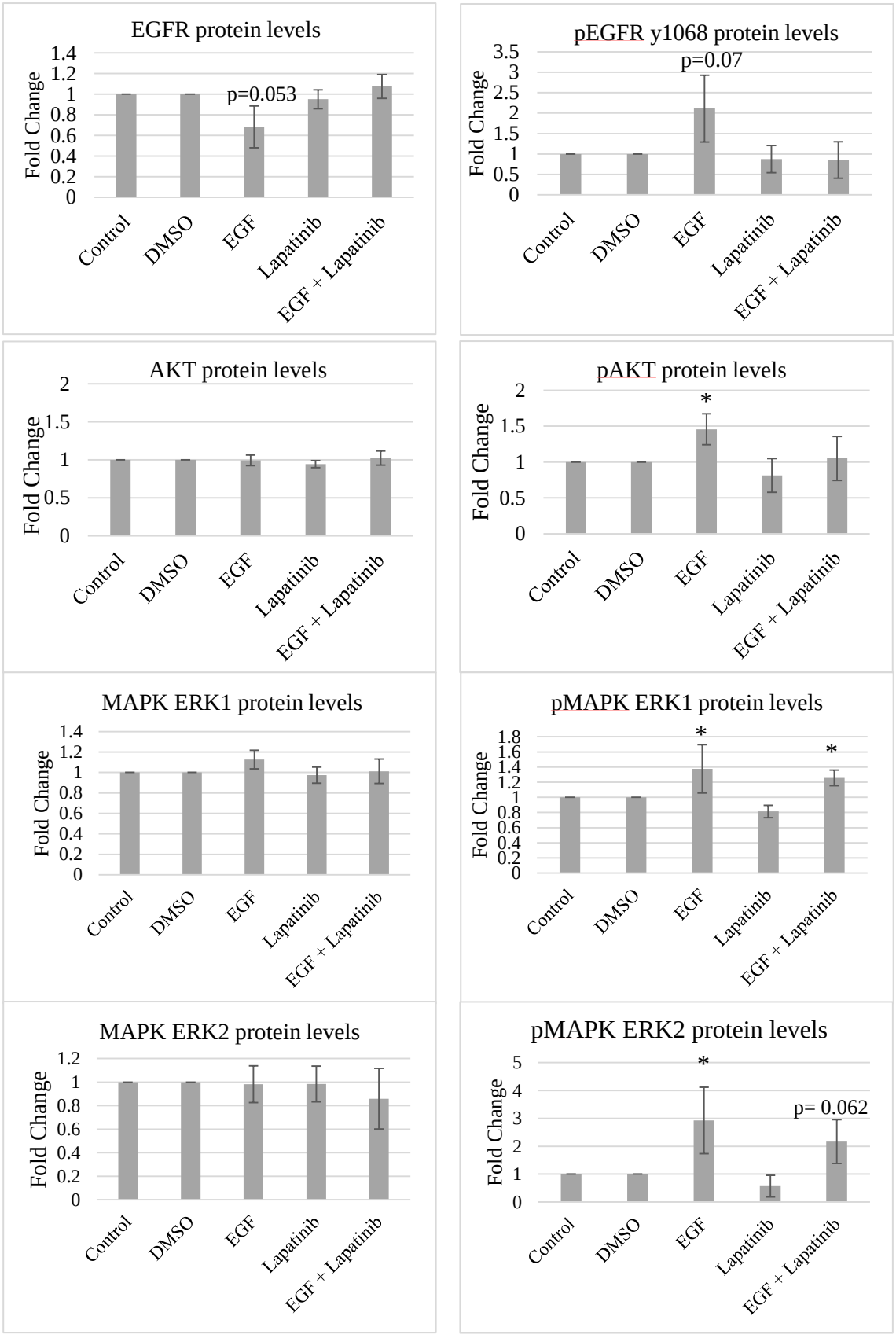

Figure 2: Densitometry analysis of immunoblots of the HCC1954-Lap cell line for EGFR, pEGFR, AKT, pAKT, MAPK and pMAPK protein levels in HI serum conditions. Protein levels are normalised to control protein levels. Error bars represent standard deviation of biological triplicate experiments. The Student's t test was used to determine statistical significance. * $p < 0.05$, ** $p < 0.01$ and *** $p < 0.001$.

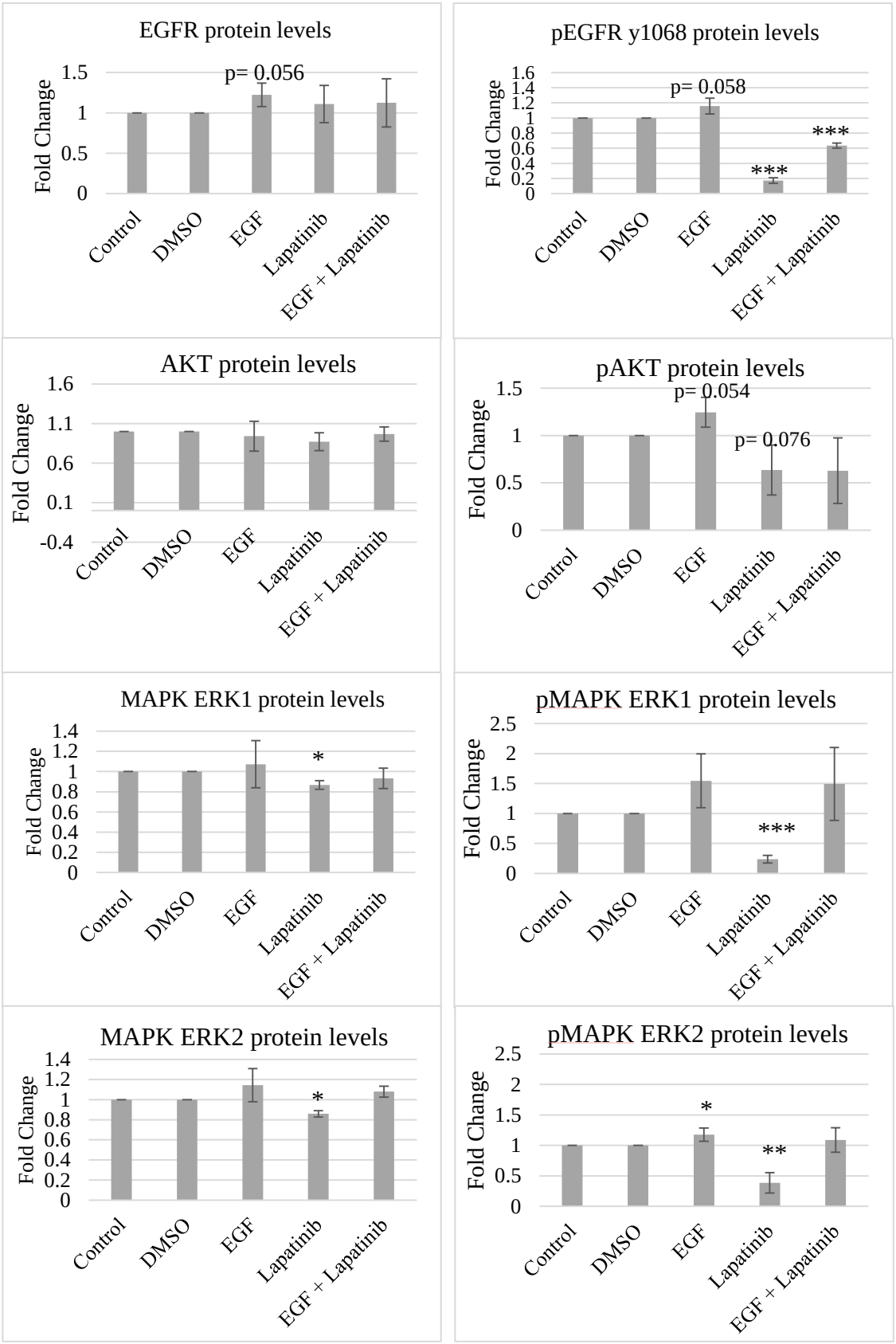

Figure 3: Densitometry analysis of immunoblots of the SKBR3-Par cell line for EGFR, pEGFR, AKT, pAKT, MAPK and pMAPK protein levels in HI serum conditions. Protein levels are normalised to control protein levels. Error bars represent standard deviation of biological triplicate experiments. The Student's t test was used to determine statistical significance. * $p < 0.05$, ** $p < 0.01$ and *** $p < 0.001$.

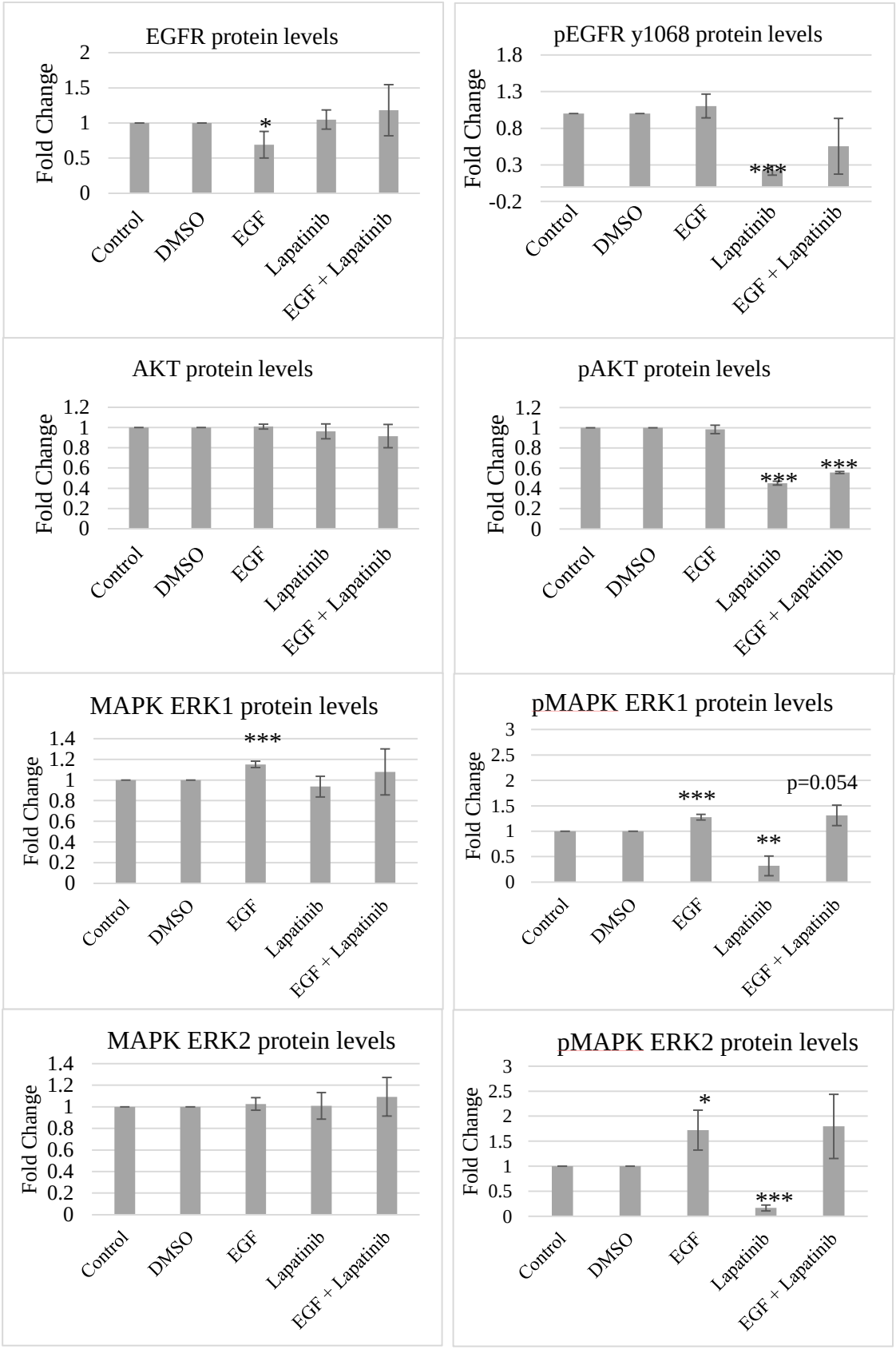

Figure 4: Densitometry analysis of immunoblots of the SKBR3-Afa cell line for EGFR, pEGFR, AKT, pAKT, MAPK and pMAPK protein levels in HI serum conditions. Protein levels are normalised to control protein levels. Error bars represent standard deviation of biological triplicate experiments. The Student's t test was used to determine statistical significance. * $p < 0.05$, ** $p < 0.01$ and *** $p < 0.001$.

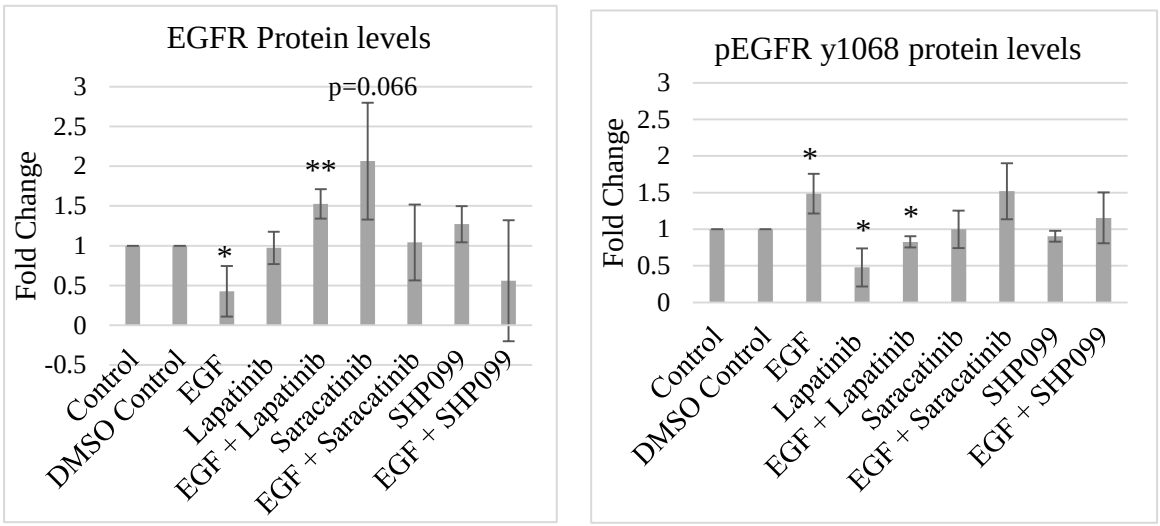

Figure 5: Densitometry analysis of immunoblots of the HCC1954 cell line for EGFR and pEGFR. Protein levels are normalised to control protein levels. Error bars represent standard deviation of biological triplicate experiments. The Student's t test was used to determine statistical significance. * $p < 0.05$, ** $p < 0.01$ and *** $p < 0.001$.

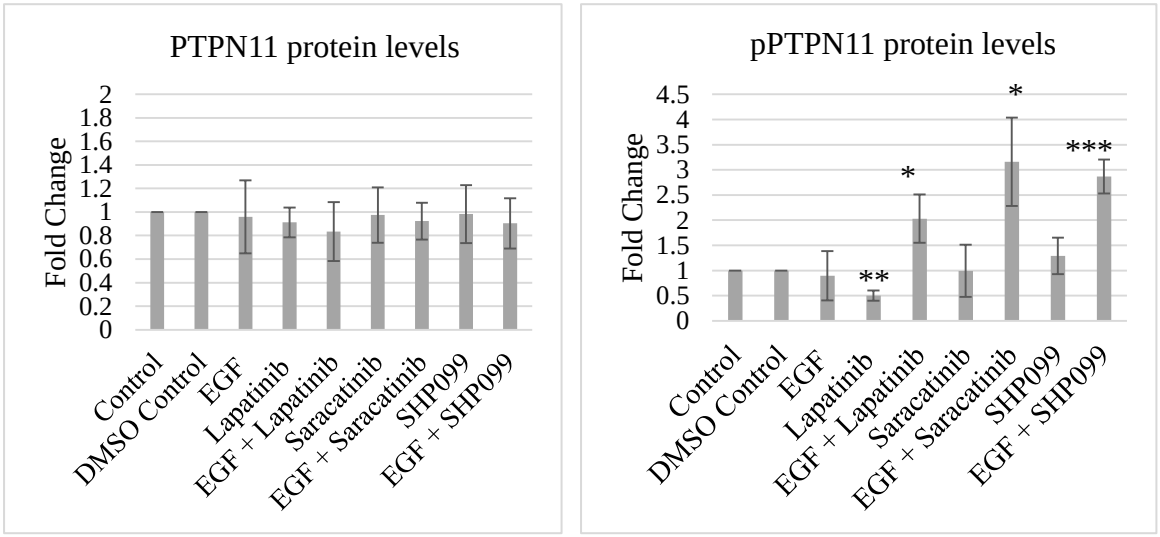

Figure 6: Densitometry analysis of immunoblots of the HCC1954 cell line for PTPN11 and pPTPN11. Protein levels are normalised to control protein levels. Error bars represent standard deviation of biological triplicate experiments. The Student's t test was used to determine statistical significance. * $p < 0.05$, ** $p < 0.01$ and *** $p < 0.001$.